Evaluating Applications of Field Spectroscopy Devices to Fingerprint Commonly Used Construction Materials

DETAILS

71 pages | 8.5 x 11 | PAPERBACK
ISBN 978-0-309-12937-4 | DOI 10.17226/22770

AUTHORS

Zofka, Adam; Chrysochoou, Maria; Yut, Iliya; Johnston, Chad; Shaw, Montgomery; Sun, Shih-Po; Mahoney, James; Farquharson, Stuart; and Donahue, Michael

The Second
STRATEGIC HIGHWAY RESEARCH PROGRAM

SHRP 2 REPORT S2-R06B-RR-1

Evaluating Applications of Field Spectroscopy Devices to Fingerprint Commonly Used Construction Materials

Adam Zofka, Maria Chrysochoou, Iliya Yut, and Chad Johnston
Department of Civil and Environmental Engineering, University of Connecticut

Montgomery Shaw and Shih-Po Sun
Chemical, Materials & Biomolecular Engineering Department, University of Connecticut

James Mahoney
Connecticut Transportation Institute, University of Connecticut

Stuart Farquharson and Michael Donahue
Real-Time Analyzers, Inc.

TRANSPORTATION RESEARCH BOARD

WASHINGTON, D.C.
2013
www.TRB.org

Subscriber Categories

Construction
Highways
Materials

The Second Strategic Highway Research Program

America's highway system is critical to meeting the mobility and economic needs of local communities, regions, and the nation. Developments in research and technology—such as advanced materials, communications technology, new data collection technologies, and human factors science—offer a new opportunity to improve the safety and reliability of this important national resource. Breakthrough resolution of significant transportation problems, however, requires concentrated resources over a short time frame. Reflecting this need, the second Strategic Highway Research Program (SHRP 2) has an intense, large-scale focus; integrates multiple fields of research and technology; and is fundamentally different from the broad, mission-oriented, discipline-based research programs that have been the mainstay of the highway research industry for half a century.

The need for SHRP 2 was identified in *TRB Special Report 260: Strategic Highway Research: Saving Lives, Reducing Congestion, Improving Quality of Life,* published in 2001 and based on a study sponsored by Congress through the Transportation Equity Act for the 21st Century (TEA-21). SHRP 2, modeled after the first Strategic Highway Research Program, is a focused, time-constrained, management-driven program designed to complement existing highway research programs. SHRP 2 focuses on applied research in four areas: Safety, to prevent or reduce the severity of highway crashes by understanding driver behavior; Renewal, to address the aging infrastructure through rapid design and construction methods that cause minimal disruptions and produce lasting facilities; Reliability, to reduce congestion through incident reduction, management, response, and mitigation; and Capacity, to integrate mobility, economic, environmental, and community needs in the planning and designing of new transportation capacity.

SHRP 2 was authorized in August 2005 as part of the Safe, Accountable, Flexible, Efficient Transportation Equity Act: A Legacy for Users (SAFETEA-LU). The program is managed by the Transportation Research Board (TRB) on behalf of the National Research Council (NRC). SHRP 2 is conducted under a memorandum of understanding among the American Association of State Highway and Transportation Officials (AASHTO), the Federal Highway Administration (FHWA), and the National Academy of Sciences, parent organization of TRB and NRC. The program provides for competitive, merit-based selection of research contractors; independent research project oversight; and dissemination of research results.

SHRP 2 Report S2-R06B-RR-1

ISBN: 978-0-309-12937-4
Library of Congress Control Number: 2013931920

Copyright Information

Note: SHRP 2 report numbers convey the program, focus area, project number, and publication format. Report numbers ending in "w" are published as web documents only.

Notice

The project that is the subject of this report was a part of the second Strategic Highway Research Program, conducted by the Transportation Research Board with the approval of the Governing Board of the National Research Council.

The members of the technical committee selected to monitor this project and review this report were chosen for their special competencies and with regard for appropriate balance. The report was reviewed by the technical committee and accepted for publication according to procedures established and overseen by the Transportation Research Board and approved by the Governing Board of the National Research Council.

The opinions and conclusions expressed or implied in this report are those of the researchers who performed the research and are not necessarily those of the Transportation Research Board, the National Research Council, or the program sponsors.

The Transportation Research Board of the National Academies, the National Research Council, and the sponsors of the second Strategic Highway Research Program do not endorse products or manufacturers. Trade or manufacturers' names appear herein solely because they are considered essential to the object of the report.

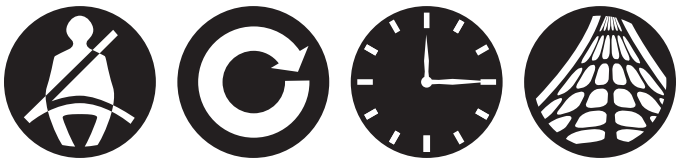

SHRP 2 Reports

Available by subscription and through the TRB online bookstore:
www.TRB.org/bookstore

Contact the TRB Business Office:
202-334-3213

More information about SHRP 2:
www.TRB.org/SHRP2

THE NATIONAL ACADEMIES

Advisers to the Nation on Science, Engineering, and Medicine

The **National Academy of Sciences** is a private, nonprofit, self-perpetuating society of distinguished scholars engaged in scientific and engineering research, dedicated to the furtherance of science and technology and to their use for the general welfare. On the authority of the charter granted to it by Congress in 1863, the Academy has a mandate that requires it to advise the federal government on scientific and technical matters. Dr. Ralph J. Cicerone is president of the National Academy of Sciences.

The **National Academy of Engineering** was established in 1964, under the charter of the National Academy of Sciences, as a parallel organization of outstanding engineers. It is autonomous in its administration and in the selection of its members, sharing with the National Academy of Sciences the responsibility for advising the federal government. The National Academy of Engineering also sponsors engineering programs aimed at meeting national needs, encourages education and research, and recognizes the superior achievements of engineers. Dr. Charles M. Vest is president of the National Academy of Engineering.

The **Institute of Medicine** was established in 1970 by the National Academy of Sciences to secure the services of eminent members of appropriate professions in the examination of policy matters pertaining to the health of the public. The Institute acts under the responsibility given to the National Academy of Sciences by its congressional charter to be an adviser to the federal government and, on its own initiative, to identify issues of medical care, research, and education. Dr. Harvey V. Fineberg is president of the Institute of Medicine.

The **National Research Council** was organized by the National Academy of Sciences in 1916 to associate the broad community of science and technology with the Academy's purposes of furthering knowledge and advising the federal government. Functioning in accordance with general policies determined by the Academy, the Council has become the principal operating agency of both the National Academy of Sciences and the National Academy of Engineering in providing services to the government, the public, and the scientific and engineering communities. The Council is administered jointly by both Academies and the Institute of Medicine. Dr. Ralph J. Cicerone and Dr. Charles M. Vest are chair and vice chair, respectively, of the National Research Council.

The **Transportation Research Board** is one of six major divisions of the National Research Council. The mission of the Transportation Research Board is to provide leadership in transportation innovation and progress through research and information exchange, conducted within a setting that is objective, interdisciplinary, and multimodal. The Board's varied activities annually engage about 7,000 engineers, scientists, and other transportation researchers and practitioners from the public and private sectors and academia, all of whom contribute their expertise in the public interest. The program is supported by state transportation departments, federal agencies including the component administrations of the U.S. Department of Transportation, and other organizations and individuals interested in the development of transportation. **www.TRB.org**

www.national-academies.org

SHRP 2 STAFF

Ann M. Brach, *Director*
Stephen J. Andrle, *Deputy Director*
Neil J. Pedersen, *Deputy Director, Implementation and Communications*
James Bryant, *Senior Program Officer, Renewal*
Kenneth Campbell, *Chief Program Officer, Safety*
JoAnn Coleman, *Senior Program Assistant, Capacity and Reliability*
Eduardo Cusicanqui, *Financial Officer*
Walter Diewald, *Senior Program Officer, Safety*
Jerry DiMaggio, *Implementation Coordinator*
Shantia Douglas, *Senior Financial Assistant*
Charles Fay, *Senior Program Officer, Safety*
Carol Ford, *Senior Program Assistant, Renewal and Safety*
Elizabeth Forney, *Assistant Editor*
Jo Allen Gause, *Senior Program Officer, Capacity*
Rosalind Gomes, *Accounting/Financial Assistant*
Abdelmename Hedhli, *Visiting Professional*
James Hedlund, *Special Consultant, Safety Coordination*
Alyssa Hernandez, *Reports Coordinator*
Ralph Hessian, *Special Consultant, Capacity and Reliability*
Andy Horosko, *Special Consultant, Safety Field Data Collection*
William Hyman, *Senior Program Officer, Reliability*
Michael Marazzi, *Senior Editorial Assistant*
Linda Mason, *Communications Officer*
Reena Mathews, *Senior Program Officer, Capacity and Reliability*
Matthew Miller, *Program Officer, Capacity and Reliability*
Michael Miller, *Senior Program Assistant, Capacity and Reliability*
David Plazak, *Senior Program Officer, Capacity*
Monica Starnes, *Senior Program Officer, Renewal*
Onno Tool, *Visiting Professional*
Dean Trackman, *Managing Editor*
Connie Woldu, *Administrative Coordinator*
Patrick Zelinski, *Communications/Media Associate*

ACKNOWLEDGMENTS

This work was sponsored by the Federal Highway Administration in cooperation with the American Association of State Highway and Transportation Officials. It was conducted in the second Strategic Highway Research Program, which is administered by the Transportation Research Board of the National Academies. The project was managed by Dr. Monica Starnes, Senior Program Officer for SHRP 2 Renewal.

The research reported on herein was performed by the University of Connecticut (UConn), supported by Real-Time Analyzers, Incorporated (RTA, Inc.). Adam Zofka (Assistant Professor, Department of Civil and Environmental Engineering, UConn) was the principal investigator. Maria Chrysochoou (Assistant Professor, Department of Civil and Environmental Engineering, UConn), Montgomery Shaw (Professor of Research, Chemical, Materials & Biomolecular Engineering Department, UConn), James Mahoney (Director, Connecticut Transportation Institute, UConn), Stuart Farquharson (President, RTA, Inc.), and Michael Donahue served as co-principal investigators. Graduate research assistants Iliya Yut and Chad Johnston performed laboratory and field experiments with spectroscopic instruments and also contributed to this report. The authors acknowledge the help of Shi-Po Sun (a former Ph.D. student at the Materials & Biomolecular Engineering Department, UConn) and Xiaolong Zhiang (a former Master's student at the Department of Civil and Environmental Engineering, UConn) for conducting part of the laboratory experiments.

The research team is grateful to Fred Morris with Bruker Optics, Inc., for his assistance with the infrared equipment. Innova X Systems and inXitu, Inc. are acknowledged for their contributions to the analysis of X-ray data. Finally, the research team thanks all manufacturers for voluntarily providing samples of their materials.

FOREWORD

Monica A. Starnes, Ph.D., *SHRP 2 Senior Program Officer, Renewal*

Quality control of materials used during construction is an important issue routinely affecting highway agencies across the United States. Evaluating whether the materials delivered at the construction site agree with those specified can be resolved by existing testing techniques. Spectroscopy technologies have recently been used for typical transportation materials on a limited basis but there is the potential for much broader use of these technologies for quality assurance tests. Furthermore, recent advances in the development of portable equipment could allow evaluation of the materials at the construction site before or during their use.

This report presents the evaluation of portable spectroscopy devices and their capabilities to "fingerprint" typical construction materials. Fingerprinting of typical materials requires developing acceptable spectra of the specific chemical compositions with laboratory-based equipment and then comparing the material being fingerprinted against those spectra. On the basis of this requirement, the project developed a library of reference spectra for common materials used in highway and road construction.

The evaluation of the spectroscopy devices was conducted through laboratory testing and field testing. Field testing verified the feasibility of field quality assurance/quality control procedures for the material–testing method combinations found successful in the laboratory research phase. From this work the project also developed relatively simple and easy-to-use nondestructive testing procedures and protocols that inspectors could use in the field to ensure quality construction.

An additional phase was recently added to this project to develop specifications and pilot them in collaboration with two transportation agencies. Once completed, the results from this additional scope of work will be published as an addendum to this report.

CONTENTS

Executive Summary

One of the goals of the second Strategic Highway Research Program (SHRP 2) is to develop new methods and materials for preserving, rehabilitating, and reconstructing the aging U.S. transportation infrastructure. A growing concern among transportation authorities is that quality assurance/quality control (QA/QC) procedures routinely used in highway construction are time-consuming, expensive, and not always reliable. Accordingly, the SHRP 2 R06B project had as main objective to identify and evaluate handheld spectroscopic equipment for in situ analysis of commonly used construction materials. The first phase to address this objective (Phase 1) was to identify the QA/QC needs for spectroscopic testing among the state highway agencies (SHAs), to determine which spectroscopic techniques can address these needs and to develop appropriate feasibility criteria. To this end a survey was conducted among the SHRP 2 coordinators from 50 states and a workshop was held with experts from both SHAs and industry. As a result, a list of construction materials and desired testing and equipment parameters (e.g., sample preparation, test duration, reliability, training effort, and equipment price) was developed to rank the applicability of the spectroscopic techniques for laboratory and field evaluation. Two potential outcomes of spectroscopic testing were identified: (1) verification of the chemical composition (if provided by the manufacturer) or determination of the signature spectrum for pure materials and compounds and (2) detection and, if possible, quantification of additives and contaminants in a mixture.

The spectroscopic techniques evaluated by the project team in the laboratory included Fourier transform infrared (FTIR) spectroscopy, size-exclusion chromatography (SEC), nuclear magnetic resonance (NMR), X-ray fluorescence (XRF), and X-ray diffraction (XRD). The materials list included epoxy coatings and adhesives, traffic paints, portland cement concrete (PCC) with chemical admixtures and curing compounds, asphalt binders, emulsions, and mixes with polymer additives. The most promising combinations of techniques and materials were evaluated by a comprehensive literature review, in combination with the experience of the research team as well as the survey and workshop results. Accordingly, each combination of material and method was ranked in terms of its probability of success and selected for evaluation under laboratory conditions.

The laboratory testing phase (Phase 2) indicated that three methods were most promising for field application: FTIR, XRF, and Raman. A compact FTIR spectrometer working in the attenuated total reflectance (ATR) mode was the most successful device to fingerprint pure chemical compounds (i.e., epoxies, waterborne paints, polymers, and chemical admixtures) and to detect additives or contaminants in complex mixtures (i.e., PCC, asphalt binders, emulsions, and mixes). ATR analysis requires no special sample preparation and a very small sample amount. This renders the sampling process as the limiting step in ensuring that the collected spectrum is representative of the bulk material. ATR also enables the quantification

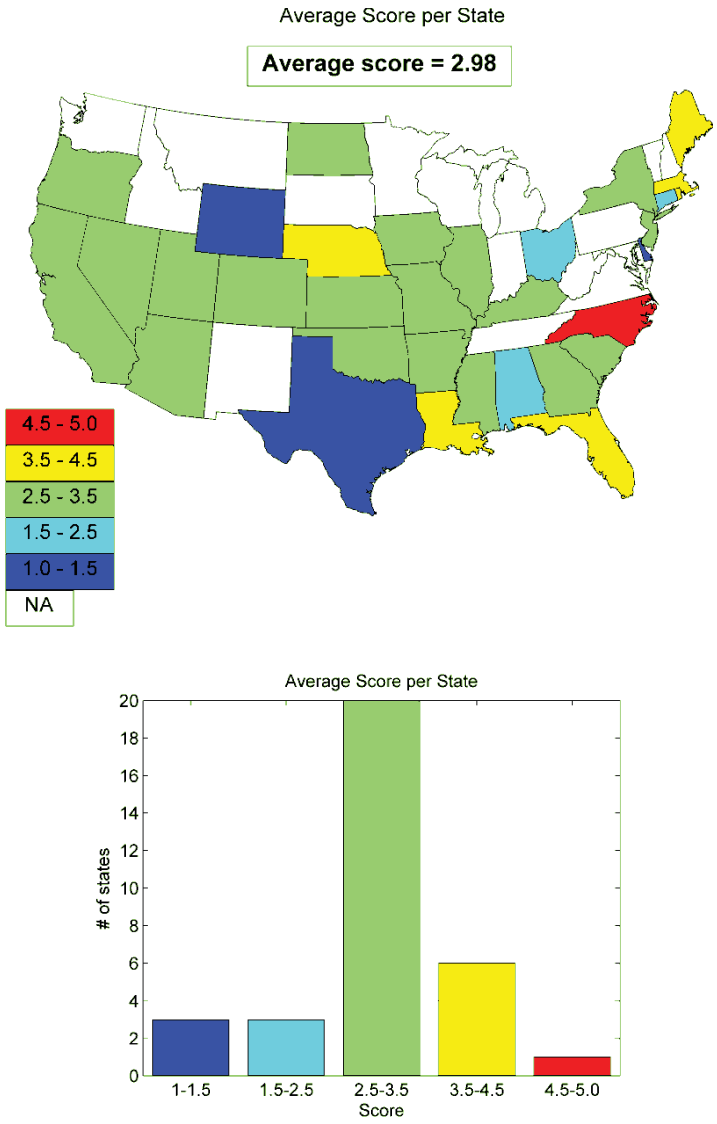

Figure ES.1. Summary of average field need survey scores per SHA.

of polymer additives in asphalt binders and determination of the water or solvent content in paints. Portable XRF was determined to be suitable for QA/QC of paints and epoxies on the basis of their metal content (Ti or Zn). The main factor affecting the accuracy of the XRF method is the calibration method used for analysis, especially for lighter elements (P, S, and Ca). Finally, fingerprinting of paints, curing compounds, and chemical admixtures to PCC was found to be feasible using a portable Raman analyzer developed by Real-Time Analyzers, Inc. (RTA), a member of the research team. Raman analysis is similar to ATR analysis in that it requires a small sample and thus sample variability is the main source of uncertainty associated with both techniques.

Following the completion of the laboratory experiments, an additional survey of the 50 SHAs was conducted to confirm the relevance of the recommended material–method combinations to the needs of material testing professionals. The survey results reflected a strong need (average need ranking score of 3 out of 5 [see Figure ES.1]) for the majority of the proposed field tests (see Table ES.1).

Table ES.1. Summary of SHA Survey for Field Evaluation Needs

Material Category	Spectroscopic Method	Objective	Average Score
Structural coatings and pavement markings	ATR FTIR Raman XRF	Verification of chemical composition	3.05
	ATR FTIR Raman XRF	Verification of presence of solvents/diluents	2.73
Epoxy adhesives	ATR FTIR	Verification of chemical composition	2.68
Chemical admixtures for PCC	ATR FTIR	Verification of presence of admixture in fresh/cured PCC mix	2.65
Curing compounds for PCC	ATR FTIR Raman	Verification of chemical composition/degree of cure (water content)	2.76
Polymer-modified asphalt binders, emulsions, and mixtures	ATR FTIR	Verification of type/class of polymer modifier	3.45
	ATR FTIR	Determination of polymer content	3.52
Antistripping agents	ATR FTIR	Verification of presence/type	3.55
Reclaimed asphalt pavement (RAP)	ATR FTIR	Determination of RAP content in HMA	3.05
Mean average score			**2.97**
SD of mean			**0.40**

A series of field trips to various construction projects was performed in the final phase of the project (Phase 3) to verify the feasibility of field QA/QC procedures for the chosen material–method combinations. Overall, field tests confirmed the applicability of most methods and produced results similar to the laboratory phase. Specifically, the compact ATR FTIR spectrometer, handheld XRF instrument, and RTA's Raman analyzer were employed successfully to analyze the composition of both simple and complex organic compounds, such as epoxy coatings and adhesives, curing compounds, and waterborne traffic paints. Furthermore, ATR allowed for the identification of chemical admixtures in freshly mixed PCC samples and provided their concentrations when they were higher than 0.5 wt%. Verification of polymer presence in asphalt binders and emulsions was also possible using the ATR FTIR spectrometer. Although the identification of polymer in hot-mix asphalt (HMA) presented a challenge, the fast binder extraction procedure in the field using dichloromethane solvent appeared to be a feasible alternative for the direct evaluation of polymer-modified HMA.

Generic testing procedures with sampling and data analysis guidelines were developed during the project for the ATR, Raman, and XRF applications to selected materials. The most successful generic procedures were expanded to draft AASHTO standard specifications as follows: (1) method for fingerprinting chemical admixtures in freshly mixed PCC by portable ATR FTIR and (2) method for determining the metal content in paints by portable XRF.

The target audiences for the AASHTO standards are QA/QC personnel and research and material divisions in SHAs. In addition to the standards, a library of spectra for the tested materials was created, which can be used for the identification of these materials in the field. Finally, field operation manuals were developed for ATR and XRF instruments to supplement the standards. These manuals target the field personnel who will conduct spectroscopic testing; however, the variability in the available instruments requires that the specific technical manual of each instrument should be also consulted.

It should be noted that because of time and budget constraints, a limited range of portable spectroscopic instruments was evaluated in this study. For instance, neither handheld FTIR nor portable time-domain NMR devices were available for the research team. However, the research team believes that the former can be potentially used on construction sites, especially for the analysis of asphalt and concrete products, whereas the latter can allow for the elucidation of practically any organic material structure. In addition, portable gas chromatographs can potentially yield success in evaluation of contaminants and polymer additives in asphalt products. Therefore, further research is suggested with use of handheld FTIR, portable time-domain NMR instruments, and portable gas chromatographs.

Spectroscopic evaluation of construction materials will be always a challenging task, especially when dealing with nonuniform materials or additives at small concentrations. In such cases, more work is needed beyond the scope of this project to develop robust and universal procedures.

CHAPTER 1

Background

Renewal Focus Area

The U.S. highway system is aging and must be rebuilt while we are driving on it and living next to it. Research in the SHRP 2 Renewal focus area addresses the need to develop a consistent, systematic approach to completing highway projects quickly, with minimal disruption to the community, and producing facilities that are long lasting. Identifying new technologies for locating underground utilities; developing procedures to speed the evaluation of designs and the inspection of construction; and applying new methods and materials for preserving, rehabilitating, and reconstructing roadways and bridges are among the goals for this focus area. Alternative strategies for contracting, financing, and managing projects as well as for mitigating institutional barriers also are part of the emphasis on rapid renewal. The renewal scope applies to all classes of roads.

Problem Statement

Several state departments of transportation have reported quality control issues with many of the materials routinely used in highway construction. Fourier transform infrared spectroscopy (FTIR), X-ray fluorescence (XRF), and Raman spectroscopy are material analysis techniques that have recently been used for transportation materials on a limited basis. They have been employed mostly for "fingerprinting" or identifying the presence of mixture components, such as deicing compounds or antistripping agents, and occasionally for quantitative analyses, such as polymer content in asphalt and sulfate content of soils. The potential exists for much broader use of these technologies in quality assurance/quality control (QA/QC), for example, in testing cements, paints, thermoplastics, epoxies, asphalt emulsions, and possibly many others. Using these new technologies, rather than traditional chemical tests, for such applications may allow for faster and accurate QA/QC procedures.

Relatively low-cost ($20,000 to $40,000) portable devices have become available for several of these technologies (FTIR, XRF, Raman, and others) that can be employed in the field to test the chemical composition of the delivered materials. These are point-and-shoot applications that could potentially be used by field technicians with accuracy similar to that obtained by using traditional stationary laboratory equipment. The development of user-friendly software for material analysis and interpretation of results has decreased the need for skilled personnel to use the portable equipment. Therefore, the potential use of portable spectroscopy devices for a wider range of applications has become more practical.

Research Objectives

The primary objective of this project was to identify the most practical applications of portable spectroscopic equipment to a range of materials commonly used in transportation infrastructure. The candidate spectroscopic methods were identified on the basis of a comprehensive review of the related scientific literature and the state-of-practice in spectroscopic equipment. The range of construction materials and desired testing and equipment parameters was identified from a survey of state highway agencies (SHAs).

An additional objective was to develop relatively simple spectroscopic testing procedures and protocols that inspectors and frontline personnel could use in the field to ensure quality construction. Two potential outcomes for spectroscopic testing were identified. They were (1) verification of the chemical composition (if provided by the manufacturer) or determination of the signature spectrum for pure materials and compounds and their components as supplied by manufacturers, and (2) detection, and, if possible, quantification of additives and contaminants in a material.

CHAPTER 2

Methodology

Literature Review

To identify the range of spectroscopic methods applicable to the analysis of transportation infrastructure materials, the research team conducted a comprehensive literature search. The team explored bibliographic databases using the Transportation Research Information Service (TRIS) and then expanded the search to include various Internet bibliographic sources, such as the ASCE Civil Engineering Database, ScienceDirect, and others. This approach did not limit the sources to the fields of transportation and civil engineering but included various journals from the chemistry and petroleum industries. All references were compiled in a computerized bibliographic database using Bibus software.

The literature review was divided into the following topics:

- Underlying principles of the most commonly used spectroscopic methods for material analysis (i.e., infrared and Raman spectroscopy; gas, gel permeation, and liquid chromatography; X-ray diffraction and fluorescence; and nuclear magnetic resonance).
- Practical application of the above methods to identify substances of interest (e.g., paints and coatings, antistripping agents, phosphoric acid additive, air oxidation, polymer additives, asphalt emulsions, water content, curing agents, and portland cement content).
- Evaluation of portable spectroscopic devices and their applicability to on-site analysis of construction materials for availability, applicability, limitations, complexity of usage, sensitivity, and reliability.
- Review of the existing ASTM/AASHTO standards relevant to spectroscopic testing of transportation construction materials.
- On the basis of the findings, potentially promising spectroscopic techniques were recommended for laboratory evaluation with emphasis on portable, yet cost-effective, instruments. The most important review findings are discussed in Chapter 3, while the complete literature review with references can be found in Appendix E.

Surveys and Workshop

To identify the needs for spectroscopic testing among the SHAs and to develop criteria for feasibility and implementability of the field methods, the SHRP 2 coordinators from 50 states were surveyed. The survey questionnaire asked for the most challenging materials in terms of QC in the field, QA/QC procedures used by SHAs, and desirable features of those procedures and related instruments. In addition, a workshop with experts from both SHAs and the industry was held before finalizing the experimental program for Phase 2. The workshop concentrated on qualitative and quantitative requirements for field QA/QC procedures that would be implemented as a result of this project. The workshop addressed sample preparation, test duration, reliability, training effort, and equipment price. On the basis of the workshop feedback, a list of construction materials and desired testing and equipment parameters was compiled. These parameters were used to rank the feasibility of the spectroscopic devices to be chosen for laboratory and field evaluation.

An additional survey of the 50 SHAs was conducted before field implementation of the successful procedures (Phase 3). The survey confirmed the relevance of the compiled material list to the needs of material testing professionals and helped to finalize the list of materials for field testing. The main findings of the two surveys and the workshop are discussed in Chapter 3, and details are provided in Appendices F and G.

Development of Testing Matrix

The testing matrix for "proof-of-concept" laboratory analyses was developed based on the literature review, SHA surveys, input from the workshop participants, and the experience of

the research team. The matrix included portable FTIR, Raman, XRF, and X-ray diffraction (XRD) instruments, as well as stationary (laboratory-based) infrared (IR), XRD, gel permeation chromatography (GPC), and nuclear magnetic resonance (NMR) equipment. This approach ensured that the capabilities of portable equipment would be compared with traditional stationary equipment and methods that are currently immature for field use would be considered in the event of future technological advances. This proved especially true for methods with only few portable instruments available, such as XRD and NMR.

To finalize the list of brands to be tested within each material category, the team conducted a survey of the approved and qualified product lists (APL/QPL) that were available on 34 out of 50 surveyed SHA websites. The top five materials (which appeared most often on APL/QPL) were identified for each group, and one or two were included in the testing matrix. The finalized test matrix and list of materials, along with the details of the material survey, are provided in Appendix A.

Laboratory Analyses

Laboratory experiments were performed in Phase 2 to investigate the applicability of each method to testing selected materials, as summarized in Appendix A, Table A.2. This table also summarizes the specific objectives for each material category and method combination. Two possible outcomes for spectroscopic testing were identified: (1) verification of the chemical composition (if provided by the manufacturer) or determination of the signature spectrum for pure materials and compounds and their components as supplied by manufacturers; and (2) detection and, if possible, quantification of additives and contaminants in a material.

In addition, Phase 2 had the following common objectives for all material categories:

- Compare stationary and portable equipment in terms of detection limit, accuracy, and precision.
- Develop libraries of standard spectra for each material in the testing matrix.
- Identify the material–methods combinations that are most promising for field testing and provide justification for those that are not.
- Develop generic laboratory procedures for the most promising material–method combinations.

On the basis of the results of laboratory experiments in Phase 2, the research team recommended the portable devices that were deemed most suitable for further evaluation in the field (Phase 3). The following criteria guided the selection process (more details on equipment and testing protocols can be found in Appendix A):

- Successful fulfillment of a specific objective for a particular combination of method and material, as stated in Table A.2;
- Specific procedure parameters, such as minimum sample preparation, time, and labor effectiveness (details are provided in Table A.4);
- Specific equipment characteristics, such as accuracy, reliability, and duration of measurement (details are provided in Table A.4); and
- Equipment portability (size and weight) and costs (details are provided in Table A.4).

Field Verification

The main goal of Phase 3 was to test portable equipment identified as successful in Phase 2 under field conditions and to determine whether its use can satisfy the desirable QA/QC criteria. A series of field trips to various construction projects was performed to verify the applicability of laboratory-proven portable spectroscopic devices to the chosen material categories. On-site testing was performed by members of the research team as well as site personnel (field technicians) to evaluate the feasibility of selected devices and to receive feedback on the field procedures. The proposed generic field testing procedures (see Appendix B) were refined based on the experience at the construction sites and test results.

Data Analysis Methods

Two types of data analysis were conducted depending on the material–method combination. They were qualitative analysis and quantitative analysis.

For qualitative analysis, one or more characteristic features of a spectrum are identified (e.g., absorption peaks on an infrared or Raman spectrum) for each material. These characteristic features may then be used to fingerprint a material by matching the experimental spectrum to a typical spectrum for that material that has been saved in a spectral library. The quality of the match can be evaluated visually or by using simple parameters such as a "hit quality index" (HQI) for infrared spectra (see Equation 2.1) (*1*). To compare HQI values of a sample spectrum with a reference spectrum, their spectra were normalized as shown in Equation 2.2 to produce spectral response values (absorbance) between 0 and 1 (*1*).

$$HQI = 1 - \left(\frac{\sqrt{\sum_{i=1}^{n} A_i L_i}}{\sqrt{\sum_{i=1}^{n} A_i^2} \sqrt{\sum_{i=1}^{n} L_i^2}} \right) \quad (2.1)$$

where

A_i = normalized absorbance of the unknown spectrum at ith wavelength (or wave number) and

L_i = absorbance of the unknown spectrum at ith wavelength (or wave number).

$$A_i = \frac{A_i' - A_{\min}}{A_{\max} - A_{\min}} \quad (2.2)$$

where A_i' is the measured absorbance of the infrared incident beam. Note that the vast majority of infrared spectrometers are equipped with customizable software that can automate the HQI calculation and qualitative match to the library spectra. The library can be provided by a vendor or created experimentally by the user. Similar approaches are adopted for qualitative analysis of XRD and Raman spectra.

Fingerprinting of pure materials using XRF was accomplished using quantitative criteria, given that XRF produces the quantitative elemental composition of the analyzed material. In this case, the concentration of critical elements in the material tested in the field (e.g., Ti in paints) can be used as a criterion to match the expected concentration in the pure material that has been established in the lab beforehand.

Special chemometric analysis of the IR spectra was conducted to quantify the composition of complex samples, such as polymer-modified asphalt or a diluted epoxy coating system. Calibration curves were developed by measuring pure samples spiked with incremental and known concentrations of an additive or contaminant (e.g., polymer in asphalt or water in diesel fuel). This approach is based on the Beer-Lambert law, according to which the concentration C of a component is directly proportional to its IR absorbance A at constant path length l, as in Equation 2.3 (*1*):

$$C = \frac{A}{el} \quad (2.3)$$

where e is the molar extinction coefficient, which is constant for a particular component but usually unknown for complex materials.

Finally, certain analyses involved the observation of a relative change in the IR spectra attributable to a physical process, rather than change in composition. Such cases are the determination of oxidation in recycled asphalt pavements (RAP) and the identification of chemical admixtures in PCC. To track spectral changes, the research team employed semiquantitative analysis based on peak-to-peak ratio or valley-to-valley band integration approaches. More details on the semiquantitative approach to spectral analysis are provided in Chapter 3, Appendix N, Appendix O, and elsewhere (*2*).

Repeatability and Reproducibility of Test Results

The repeatability and reproducibility of test results on the most successful material–method combinations were evaluated in both laboratory and field phases of the project. The evaluation of repeatability concerned the variation in measurements taken by a single operator or instrument on the same item and under the same conditions. The reproducibility of test results was judged by the level of variability in the results measured by independent operators on the same equipment. It should be noted that because of schedule constraints, only a limited number of materials were included in the repeatability and reproducibility study, as summarized in Chapter 3 and detailed in Appendix P. Finally, the spectra or quantities obtained in the field for a specific material were compared with the spectra or quantities measured in the laboratory. This comparison facilitated conclusions on precision and accuracy of a particular material–method combination.

Project Deliverables

Spectral Library

A library of reference spectra for pure materials analyzed in Phase 2 was created that can be used for fingerprinting of these materials in the field. The database consists of a series of files with fingerprinting number values and key to the material labels. It will supplement the standards developed under this project and can be used by QA/QC specialists. The electronic copy of the spectral library is located at www.trb.org/Main/Blurbs/167279.aspx.

Provisional AASHTO Standards

Generic testing procedures with sampling and data processing guidelines were developed for the attenuated total reflectance (ATR) FTIR, Raman, and XRF analysis of liquid and solid samples (see Appendix B). On the basis of Phase 3, field verification, the most successful spectroscopic testing procedures were expanded to draft AASHTO standard specifications. These specifications cover the analysis of titanium content in traffic paints by XRF and identification of chemical admixtures by ATR (see Appendix C). The target audiences

for these AASHTO standards are QA/QC personnel at the research and material divisions of SHAs.

Field Operation Manuals

Field operation manuals were developed for the most successful spectroscopic devices (i.e., ATR and XRF instruments). These manuals target technical personnel designated by a transportation agency for the spectroscopic testing. They are expected to facilitate understanding of the somewhat sophisticated documents provided with the spectroscopic devices that are usually designated for a researcher. The field manuals are included in Appendix D.

References

1. Duckworth, J. H. Spectroscopic Quantitative Analysis. In *Applied Spectroscopy: A Compact Reference for Practitioners,* Academic Press, Chestnut Hill, Mass., 1998, pp. 93–107.
2. Yut, I., and A. Zofka. Attenuated Total Reflection Fourier Transform Infrared Spectroscopy of Oxidized Polymer-Modified Bitumens. *Applied Spectroscopy,* Vol. 65, No. 7, 2011, pp. 765–770.

CHAPTER 3

Findings and Applications

Review of Spectroscopic Applications to Construction Materials

This chapter presents the major findings from the literature search on the state-of-the-art theory and practice for fingerprinting the most common materials used in highway construction. The full literature review of the principles of several spectroscopic techniques and a discussion on their applicability to testing highway construction materials is provided in Appendix E. The chapter also compares the laboratory and field testing devices in terms of their applicability, complexity of usage, sensitivity, and reliability. A detailed description of each device can be found in Appendix E as well.

Overview of Spectroscopic Techniques

Spectroscopy generally relies on the interaction of light with matter. Electromagnetic waves of different wavelengths interact with atoms and molecules in different ways that are governed by physical laws. Each material has a unique chemical composition and structure, consisting of elements combined in predictable amounts and, for most crystalline materials, spatial configurations. The type and physical arrangement of elements in a compound dictate the outcome of its interaction with light at different wavelengths. Targeting a material with radiation of known wavelength and observing the outgoing signal can be used to infer the chemical properties of the material and potentially its amount within a mixture. Figure 3.1 shows different regions of electromagnetic spectra employed by the spectroscopy methods covered in this study. Each method is briefly presented below.

Infrared spectroscopy relies on the absorption of IR radiation (0.78 to 1,000 μm) by vibrating molecular bonds of different atoms (e.g., C–H, C–O, N–H, S–H, S–O, and so forth). The chemistry and molecular bonds in a compound dictate the characteristic wavelengths of IR absorption and the degree of absorption, which can be used to fingerprint the material. Raman spectroscopy also relies on the interaction of light (near infrared, visible, or ultraviolet range) with molecular vibrations, exploiting the effect named after C. V. Raman, which refers to the shift in energy of a laser beam as it interacts with different modes of vibration in a system. Similar to IR, interpretation of Raman spectrum relies on the comparison of characteristic frequencies and intensities of pure compounds with the experimental spectrum. Both IR and Raman spectroscopy are suitable to analyzing materials with molecular bonds that vibrate in the desired frequencies, typically organic compounds and inorganic compounds with covalent bonds.

NMR spectroscopy employs the radio frequency range (60 to 800 MHz for hydrogen nuclei) to measure the energy of photons. The difference between the resonance frequency of the nucleus and a standard (usually, carbon-13 or hydrogen-1) is called the chemical shift of a nucleus, which is measured in parts per million (ppm) and denoted by δ. Measuring the chemical shift enables the identification of chemical elements.

XRF is the emission of characteristic "secondary" (or fluorescent) X-rays from a material excited by high-energy X-rays (wavelength 0.01 to 10 nm) or gamma rays (wavelength <0.01 nm). The energy and intensity of the emitted X-rays depend on the type and concentration of elements in a sample; thus XRF is used to quantify the elemental composition of a sample. Stationary XRF can quantify elements with $Z > 11$ (Na), while portable XRFs such as the one owned by the research team can quantify elements with $Z > 15$ (P).

X-ray diffraction relies on the interaction of X-rays of a certain wavelength with crystalline materials (i.e., materials that have a periodic, predictable physical structure). The reflected (or diffracted) X-ray beam has a direction and intensity that is a function of the interatomic distances in the material and the chemical composition. Interpretation of XRD patterns thus relies on the comparison of diffracted angles and intensities of pure materials with the observed peaks in the pattern. XRD is typically used to analyze inorganic solid materials, including cements, soils, aggregates, and mineral ores.

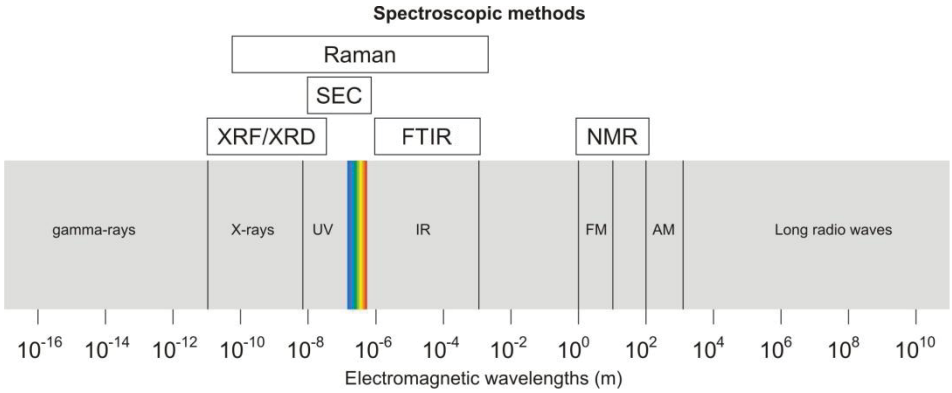

Figure 3.1. Electromagnetic frequencies employed by spectroscopic methods.

Chromatographic methods physically separate the components of a mixture and distribute them between two phases. One phase remains stationary (a solid, a gel, or a liquid solvent), while the other phase (a liquid or a gas) moves in a definite direction. The separation principle in size-exclusion chromatography (SEC) is determined by the selective permeation of the polymers into and out of the mobile-phase filled pores of the column packing. The separated compounds can be detected by coupling the chromatographic column with a detector that identifies each compound separately.

A summary of the specifications of the respective devices for each method can be found in Appendix E, Table E.2. On the basis of the review of the spectroscopic equipment, the following preliminary conclusions were drawn:

- GPC, high-performance liquid chromatography (HPLC), and gas chromatography (GC) are useful for separation and qualitative analysis before further identification by other spectroscopic methods. Portable chromatographs are available for use in field and mobile laboratories.
- Infrared and Raman analyzers can be used for the analysis of a range of materials in the liquid, solid, or gas phase (mid-IR only). Several field portable systems are available.
- The handheld XRF systems are available for the identification of chemical composition of metal-containing materials, while compact XRD instruments have been developed for testing mineral aggregates. Both can be operated in outdoor conditions at temperatures above freezing.
- Most of the NMR equipment for analyzing solid-state matter is laboratory-based and cannot be used in the field. However, benchtop (or semiportable) time-domain NMR analyzers are available that appear to be useful for the analysis of liquid-state substances, such as fractionated asphalts.

Summary of Spectroscopic Applications to Construction Materials

A quantitative analysis of the bibliographic database that includes 240 references was conducted to determine the most commonly used spectroscopic method as applied to specific material categories. The pie chart in Figure 3.2 shows the distribution of the publications by spectroscopic method. Many studies reported more than one method of material analysis, because none of the spectroscopic methods could provide full characterization of a material (i.e., both chemical composition and physical properties). For example, most asphalt studies used chromatography as a preparation method for further evaluation of asphalt fractions by FTIR or NMR. The pie chart in Figure 3.2 indicates that most studies employed FTIR and SEC (41% and 22%, respectively) for chemical characterization of materials. XRF spectroscopy was least used for construction materials, presumably because of their predominantly organic nature.

The distribution of bibliographic sources by materials and methods is provided in Figure 3.3. FTIR and chromatography were most often used for research on asphalt materials. Among the other categories of construction materials, PCC and aggregates were more often reported to be evaluated by XRD, XRF, Raman, and FTIR. The absence of NMR studies for epoxies, paints, and soils can be explained by the high cost

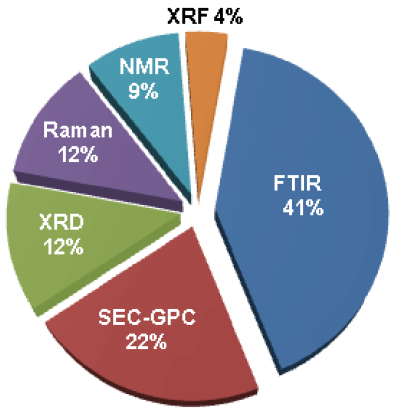

Figure 3.2. Distribution of bibliographic sources by spectroscopic methods.

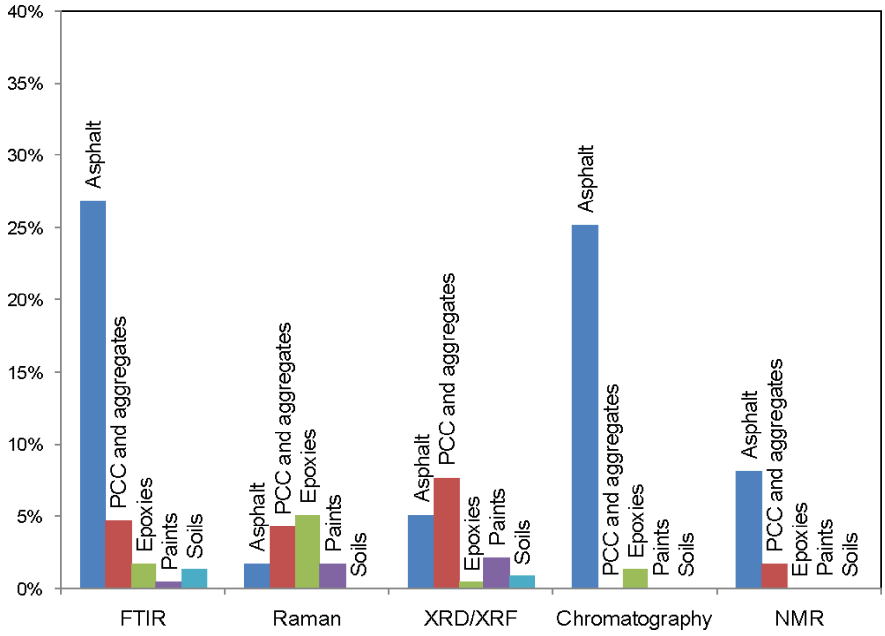

Figure 3.3. Distribution of bibliographic sources by material and method.

of NMR equipment. Another important observation from the literature review is that researchers have been more successful in the qualitative rather than the quantitative analysis of chemicals compounds, because the quantification of components in construction materials requires the development of calibration curves using pure compounds.

Spectroscopic methods are used primarily by academic and industrial researchers because of equipment availability and resources required for these analyses. Nevertheless, a few ASTM and AASHTO standards exist for the FTIR and XRF testing of paints and polymers in construction and they are used by some transportation agencies in the United States (e.g., Virginia and Texas). It is plausible to assume that with advances in the manufacturing of reliable portable devices (e.g., portable FTIR, XRF, XRD, Raman, and NMR), more agencies will be interested in the future in using fast and nondestructive spectroscopic methods for QA/QC purposes.

Federal and Local Standards for Spectroscopic Testing in the United States

The literature review included the ASTM and AASHTO standards relevant to spectroscopic testing of transportation construction materials. Additionally, the research team identified several local specifications developed by SHAs. Out of 26 standards summarized in Appendix E, Table E.3, only seven are used by SHAs to test highway construction materials, primarily portland cement and its products and paint coatings. Two procedures were developed by FHWA for asphalt-related materials. A search of all 50 SHAs websites revealed that nine states share their locally developed (or modified ASTM and AASHTO) standards, including Arizona, California, Kentucky, Louisiana, Maryland, Washington, and West Virginia (see Appendix E, Table E.4).

Summary of Literature Review

The objective of this project was to evaluate the suitability of various spectroscopic techniques for fingerprinting transportation construction materials in the field. Effectively, the literature review covered the underlying principles of the most commonly used spectroscopic methods, as well as the current practice of their application to the analysis of asphalt, portland cement, and other construction materials. In addition, the research team prepared an overview of the available equipment with emphasis on portable devices for the feasibility study. Tables E.5 and E.6 in Appendix E show the universality ranking of the methods most applicable to transportation construction materials. On the basis of the quantitative comparison, it appears that the methods that can be applied to most materials are FTIR, XRF, Raman, NMR, and SEC-HPLC. The quantitative comparison though does not exclude other discussed methods that can be very productive in some particular applications.

The literature also indicates that some techniques are more favorable for the analysis of particular materials than others. FTIR was successfully used to determine fundamental

properties of both asphaltic materials and portland cement. XRD has been traditionally used to investigate the portland cement composition rather than for the analysis of asphalt components. The suitability of Raman technology for the asphalt analysis should be evaluated further in this study, because literature references were not adequate to establish this. In the majority of published studies, the researchers succeeded in the qualitative rather than quantitative analysis of chemical compounds. Finally, a number of portable devices (GPC, HPLC, and GC chromatographs, FTIR and Raman spectrometers, and XRD-XRF analyzers) were identified as potential candidates for the feasibility study in Phase 2.

Analysis of the national standards for spectroscopic testing indicated that several procedures developed by the ASTM and AASHTO were used by the SHAs to test highway construction materials, primarily portland cement and its products and paint coatings. A search through the 50 SHAs websites revealed that nine states share their locally developed (or modified ASTM and AASHTO) standards online. The search indicated the need for developing new procedures that could replace the often complicated and time-consuming chemical tests and thus allow faster and more accurate measurements.

Survey and Workshop Results

Preliminary Survey Results

The preliminary survey included a questionnaire that was sent to the SHRP 2 coordinators in 50 SHAs and 16 responses were received. The survey included questions on three fundamental issues:

- What materials are the most challenging in terms of their quality control in the field?
- What analytical procedures are currently used by state agencies?
- What testing constraints are common under field conditions, and what features of the QA/QC procedures and related devices are desirable to address these requirements?

The complete answers on the questionnaire and analysis of the preliminary survey are provided in Appendix F. Overall, the survey indicated that

- Some departments of transportation are familiar with spectroscopy methods;
- Asphalt- and portland cement-related materials and paints are the most challenging in terms of QA/QC; and
- Test duration, personnel training, and equipment cost are the biggest concerns when implementing new procedures.

Workshop Results

In addition to the preliminary survey, a workshop with experts from both SHAs and industry was held before finalizing the experimental protocol for this project. The workshop concentrated on both qualitative and quantitative requirements for the field QA/QC procedures that would be implemented as a result of this project. Table F.3 in Appendix F presents a summary of findings from the workshop. On the basis of the results of the workshop, a set of desired testing and equipment parameters, such as sample preparation, test duration, reliability, training effort, and equipment price, was developed. It helped to rank practicality of the spectroscopic devices to be chosen for laboratory and field evaluation. More details on the discussion during the workshop are provided in Appendix F.

Finalizing Design of Experiment for Proof of Concept

The literature review, SHAs' responses to the questionnaire, input from the workshop participants, and the experience of the research team contributed to the design of the experimental matrix, as shown in Figure 3.4. Table A.2 in Appendix A

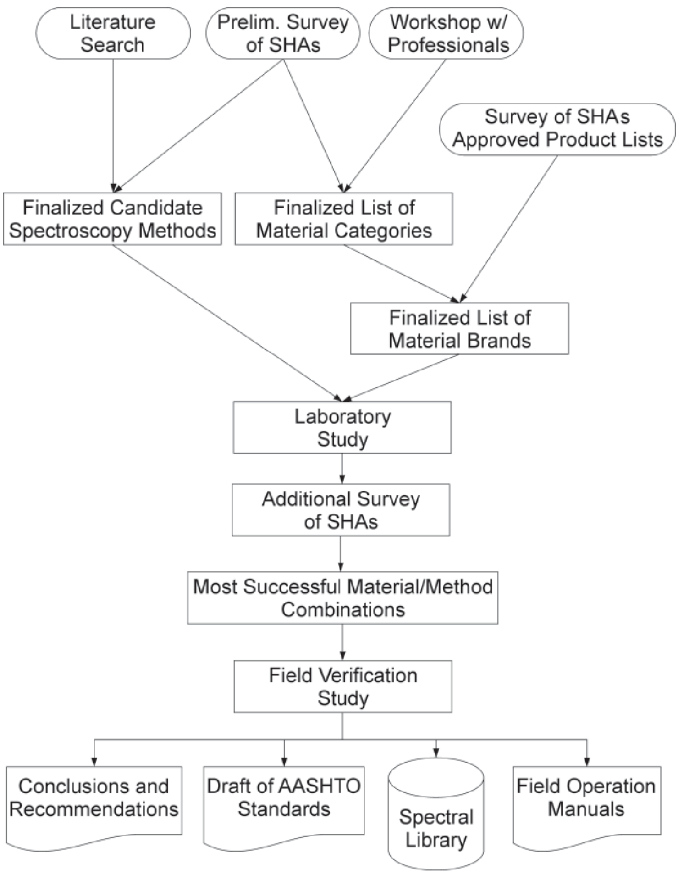

Figure 3.4. Flowchart for the experimental design.

lists the spectroscopic devices chosen for the proof-of-concept experiments in Phase 2. Both portable and stationary equipment were included in the experimental protocol to compare detection limits, accuracy, and precision. Although it was expected that the stationary equipment in the laboratory would be accurate and robust, technological improvements may allow for the use of portable equipment now or in the future. Appendix A provides detailed descriptions of the materials, equipment, and testing protocols evaluated in Phase 2. Table A.4 in Appendix A summarizes the results of the evaluation of spectroscopic equipment in terms of compliance with suitability criteria.

The list of material categories and spectroscopic methods for proof-of-concept testing is summarized in Appendix A, Table A.2. The individual testing objectives for each material–method combination were established on the basis of the input from the workshop participants. For each type of material, at least two brands were chosen for the final test matrix shown in Table A.1. The brands included in Table A.1 were obtained by surveying the APL/QPLs that were available on 34 out of 50 SHA websites. Figures A.8 through A.17 in Appendix A summarize the findings from the APL/QPL survey.

The most successful pairs of material–method combinations identified in the laboratory phase were proposed for field testing. The following guidelines were established for the selection process:

- Fulfillment of a specific objective for a particular combination of method and material, as stated in Table A.2;
- Full compliance with specific procedure parameters, such as minimum sample preparation, time, and labor effectiveness (details are provided in Table A.4);
- Full compliance with specific equipment characteristics, such as accuracy, reliability, duration of measurement (details are provided in Table A.4); and
- Equipment portability (size and weight) and costs (details are provided in Table A.4).

Concurrently, generic laboratory testing protocols were developed for each spectroscopic method to be further refined under real-time field conditions (see Appendix B).

Field Needs Survey Results

To verify the relevance of the testing matrix to the needs of transportation construction professionals, an additional survey of the 50 SHAs was conducted before the final phase of the project, field verification, was initiated. Participants were asked to rank the need for a particular material QC objective from 1 (low) to 5 (high). The research team used survey outcomes to finalize the scope of work for the field phase of the project, as summarized in Table 3.1. The detailed results of the survey can be found in Appendix G.

Figure 3.5 summarizes the distribution of average field need scores between SHAs, where the average score is calculated as the average score from a given state to all 10 material categories listed in Table 3.1. Twenty-seven out of 33 surveyed respondents assigned the score of 3 or higher to the proposed

Table 3.1. Scope of Work for Field Phase with SHA Ranks

Material Category	Objective	Average Score	Rank
Structural coatings and pavement markings	Verification of chemical composition	3.05	2
	Verification of presence of solvents/ diluents	2.73	3
Epoxy adhesives	Verification of chemical composition	2.68	3
PCC	Verification of presence of admixture in fresh/cured PCC mix	2.65	3
Curing compounds for PCC	Verification of chemical composition/ degree of cure (water content)	2.76	3
Polymer-modified asphalt Binders, emulsions, and mixtures	Verification of type/class of polymer modifier	3.45	1
	Determination of polymer content	3.52	1
Antistripping agents	Verification of presence/type	3.55	1
RAP	Verification of RAP presence in mixture	2.30	4
	Determination of RAP content in HMA	3.05	2
Mean average score		**3.0**	
SD of mean		**0.4**	

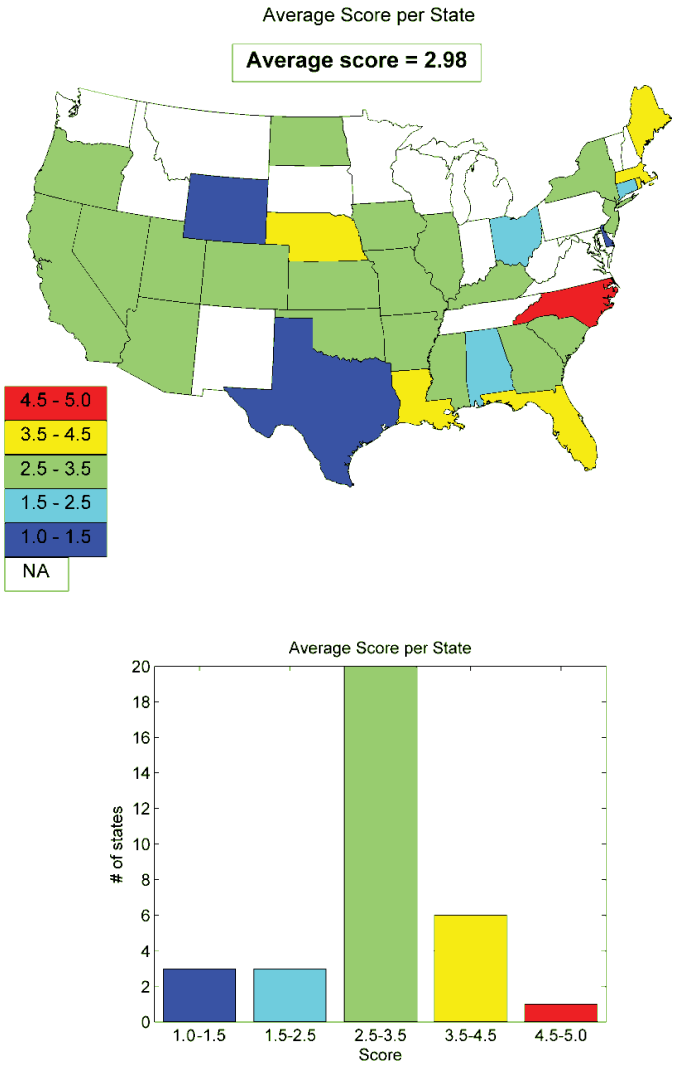

Figure 3.5. Summary of average field need survey scores per SHA.

field tests. The overall scores varied from 1.0 (Texas) to 4.8 (North Carolina), with an average value of 3.0 ± 0.4 (standard deviation).

Table 3.1 provides the averages and standard deviations for each field test objective as assigned by all states. It shows that scores varied between materials from 2.3 to 3.55, with an average value of 3.0 ± 0.4. The ranks in Table 3.1 were assigned by dividing the test objectives into four distinctive groups. The first group (rank = 1) includes verification of the presence and determination of content of polymer additives and antistripping agents in asphalt binders, emulsions, and mixtures, with the scores around 3.5. The second group (rank = 2) contains fingerprinting of structural coatings and pavement markings and determination of RAP content in asphalt mixes with the score around 3.0. The third group (rank = 3) comprises scores within 1 SD below the mean (score > 2.6). This group includes fingerprinting of PCC-related materials (chemical admixtures, curing compounds, epoxy adhesives) and verification of presence of water, solvents, or diluents in liquids. The only item that fell below the threshold of 2.6 is verification of presence of RAP with a score of 2.3.

Fingerprinting of Pure Materials

Verification of chemical composition was pursued for the materials with known chemical structures provided by the manufacturers. If such information was not available, the signature spectra were obtained for comparison with unknown samples or mixtures. As shown in Table 3.2, analysis using a portable ATR FTIR instrument either verified the structure or provided unique spectra for all materials. The characteristic IR absorption peaks for pure additives (i.e., chemical admixtures, curing compounds, and polymers) served as an indicator of their presence in complex materials, such as PCC and polymer-modified asphalts.

The portable Raman analyzer was only successfully used to evaluate the composition of liquid materials that did not fluoresce. Analysis of traffic paints and epoxies with the portable XRF device provided the concentration of the primary metals in pigments and fillers (Ti or Zn) that can be used as indicators for QA/QC of these materials. The stationary GPC system was suitable to fingerprint the materials with molecular weights higher than 1,000 Da. All organic materials in which phase separation did not occur were successfully evaluated by the stationary NMR system. The GPC chromatograms and NMR spectra of pure materials can be found in Appendices L and M, respectively.

The following text provides expanded discussion on the characteristic spectral features of the materials in Table 3.2 for each method. The ATR and Raman signature spectra can be found in Appendices I and J, while the XRF numerical results are provided in Appendix K. In addition, an electronic version of spectral data was provided to SHRP 2 administration and is located at www.trb.org/Main/Blurbs/167279.aspx.

Epoxy Paints and Adhesives

Epoxy Structural Coatings and Pavement Markings

Typical epoxy-based coating systems consist of epoxy resin, solvent, pigment, and sometimes metal filler (e.g., zinc powder). The product may be supplied in separate components. As the paint dries, the solvent evaporates and the hardened (oxidized) epoxy creates a thin film on the surface.

Two brands of structural coatings—Carbozinc 859 and Scotchkote—were tested with FTIR. The former is a three-part organic zinc-rich epoxy coating, whereas the latter is a fusion-bonded epoxy. The epoxy pavement marking brands were Epoplex LS50 for white and yellow lane markings. The

Table 3.2. Summary of Success in Spectroscopic Fingerprinting of Pure Materials

Material Category	Portable Methods				Stationary Methods	
	ATR FTIR	Raman	XRF	XRD	GPC	NMR
Structural coatings and pavement markings	Yes[a]	Yes[b]	Yes	na	Yes[a]	Yes
Epoxy adhesives	Yes	Yes[b]	na	na	No	Yes
Chemical admixtures for PCC	Yes	Yes	No	na	No	Yes[c]
Curing compounds for PCC	Yes	Yes	na	na	Yes	Yes[c]
Polymer additives for asphalt binders	Yes	Yes	na	na	Yes	Yes
Antistripping agents in asphalt concrete	Yes	Yes	na	na	No	Yes

Note: na = not applicable.

[a] Organic constituents only.

[b] Not applicable for solids and fluorescing constituents.

[c] In some cases, phase separation is expected.

signature spectra of individual material components (Parts A and B) were obtained (see Appendix I). Next, a sample of each product was prepared following the mixing directions provided in their material safety data sheets (MSDS) (see Appendix H). The spectra of mixed samples were collected in liquid state (from the container and after surface application) by the spectroscopic methods listed in Table 3.2. Although all methods except XRD were applicable for identification of epoxy paints, only portable ATR, Raman, and XRF could test dried paint in both laboratory and field environments. These three techniques yielded highly repeatable results that could be interpreted qualitatively (absorption peaks by ATR and Raman) or quantitatively (metal content by XRF).

The presence of epoxy resin in a coating material is easily detected by FTIR because of the triple absorption in the region between 1,530 and 1,680 cm^{-1}. An aliphatic solvent yields very strong IR absorption peaks located between 650 and 900 cm^{-1} that decrease while paint is drying. Oxidative hardening of an epoxy can be tracked by the increase in carbonyl absorption around 1,650 to 1,750 cm^{-1}. The signature spectra of dried paint may vary in the intensity of peaks but not in their location (see Figures I.1 through I.4 in Appendix I). RTA's Raman analyzer can be used to characterize components of a structural coating by a maximum intensity Raman shift peak as listed in Appendix J, Table J.1, provided the signal-to-noise ratio is sufficiently high (i.e., normally greater than 10).

XRF analysis was successful to differentiate between different epoxies and paints based on their metal content. An average of 74 ± 2 wt% for Zn was found to be a typical concentration for Carbozinc 859 and Scotchkote had 6 to 7 wt% concentration of titanium dioxide. Last, a consistently different Ti content was found in Epoplex LS50 white and yellow paints (30.4 ± 0.4 wt% and 5.2 ± 0.09 wt%, respectively). More details on the epoxy and paint evaluation by XRF can be found in Appendix K.

Epoxy Adhesives

Two-component epoxy adhesives are typically used in PCC for bonding, patching, and crack repairs. Part A is typically an epoxy resin, whereas Part B is an amine-based hardener. Besides the hardener component, the chemical structure and hence spectra of epoxy adhesives are similar to those of epoxy paints.

The ready-mixed product hardens in a very short time (about 11 min), and the process is accompanied by heating up to 60°C. Therefore, spectroscopic evaluation of the mixed product presents a challenge, because portable equipment typically does not operate under these conditions. In this study, portable ATR and Raman instruments were successfully used to fingerprint components of Ultrabond 1100 and Sikadur 31 (see links to MSDS in Appendix H). The signature ATR and Raman spectra of the components can be found in Appendices I and J, respectively. The evaluation of dried Ultrabond 1100 was implemented in the field phase of the project, as discussed in the section on field verification of laboratory results.

Waterborne Paints

Waterborne traffic paints typically have several components: polymer binder, pigment, filler, water, organic solvent, and other minor additives. Pigments often consist of transition metal elements, such as Ti, Cr, and Fe. The organic paint components can be identified by FTIR, Raman, and NMR spectroscopy, whereas metals can be quantified by XRF. This study evaluated two brands of polyacrylic waterborne paints: (1) 3M All Weather (see link to MSDS in Appendix H) and (2) Ennis FAST DRY (no MSDS available). Both products were supplied with white and yellow pigment. The signature ATR and Raman spectra of these products can be found in Appendices I and J, respectively, while typical metal content as measured by XRF is provided in Appendix K.

Figures I.5 through I.7 show example spectra of a polyacrylic waterborne paint. The structure of liquid paints sample can be identified on a FTIR spectrum by the medium-wide water-associated OH band (~3,400, ~3,250, and ~1,640 cm^{-1}) and strong sharp carboxylate-associated (~1,730 and ~875 cm^{-1}) absorption bands. The evaporation of water can be tracked by observing the reduction in the intensity of the OH vibrations in a freshly painted marking line (about 15 to 30 min after application). According to ATR FTIR analysis, the 3M and Ennis paints had similar compositions.

The white and yellow polyacrylic paints could be differentiated by XRF using their Ti content as a criterion. For example, Ennis white paint in the liquid form had an average Ti concentration of 4.92 ± 0.05 wt%, while Ennis yellow paint sample yielded a Ti content of 2.12 ± 0.04 wt%.

Chemical Admixtures in Concrete

Four chemical admixtures typically used in the United States were evaluated: W. R. Grace's ADVA 190 (superplasticizer), Euclid's AIR MIX 200 (air entrainer), Accelguard 80 (set accelerator), and Eucon Retarder 75 (set retarder). The technical and chemical information on these products can be found in the corresponding MSDS using links provided in Appendix H. For the purpose of fingerprinting, all admixtures were tested as aqueous solutions. As shown in Table 3.2, only ATR and Raman analyses yielded meaningful spectra for all admixtures. NMR samples were prone to phase separation during analysis because of the high water content.

The main challenge with identifying concrete admixtures by ATR and Raman is their relatively close chemical composition (i.e., abundance of C–H, C–O, and O–H bonds in their structure). Nevertheless, the ATR signature spectra were distinguished as follows (see corresponding spectra in Figures I.10 through I.13 in Appendix I):

- ADVA 190 has a strong and wide absorption band at ~1,090 cm^{-1} attributable to CH_2–O vibrations of polyether.
- AIR MIX 200 differs from ADVA 190 and Eucon Retarder 75 by the absence of the band around ~1,080 to 1,050 cm^{-1} and by distinctive shoulders at ~1,780 cm^{-1} and ~1,540 cm^{-1} attributable to carbonyl and C–N components of tall oil (a mixture of mainly acidic compounds like turpentine found in pine trees).
- Retarder 75 has a prominent terminal carboxylate in its structure, and it yields a characteristic split of the water band (~1,650 and ~1,600 cm^{-1}) and a strong split band at ~1,080 and ~1,040 cm^{-1} because of vibrations of the multiple hydroxide (OH) groups.
- Accelguard 80 is characterized by a strong and wide band at ~1,331 cm^{-1} attributable to nitrogen dioxide (NO_2) and two medium and sharp peaks at ~1,050 and ~830 cm^{-1} associated with nitrate (NO_3^-) as well as by the absence of hydrocarbons.

The Raman spectra of the admixtures in the discussion are provided in Appendix J. The typical Raman shift peaks and corresponding signal-to-noise ratios are listed in Table J.1 It appears that Accelguard 80 can be identified by Raman with higher probability because of its much higher signal-to-noise ratio as compared with the rest of the considered admixtures.

Curing Compounds

Curing compounds are applied to concrete surfaces to create a film that retains water in the concrete to ensure full hydration of the cement. The curing compounds are typically water-based wax emulsions. Consequently, water and the organic wax component can be identified by ATR FTIR and Raman spectroscopy. The wide and strong IR absorption band in the region between 3,200 and 3,400 cm^{-1} coupled with a single peak at ~1,640 cm^{-1} wave numbers is usually associated with the hydrogen-bonded OH group in water. The multiple peaks between 2,800 and 3,000 cm^{-1}, as well as a double peak at ~1,455 and ~1,375 cm^{-1}, indicate the presence of aliphatic hydrocarbons (wax). Measuring the ratio of wax-related peak intensities to water-related ones (e.g., A_{1455}/A_{1640}) can be used to track the water content in a curing compound.

Raman analysis is similar to ATR analysis in that it indicated the presence of wax in curing compounds by a triple Raman-shift peak between 2,800 and 3,000 cm^{-1} as well as by two single peaks at ~1,440 and ~1,300 cm^{-1}. Raman analysis was more sensitive to the hydrocarbon component and less sensitive to water than ATR.

Two brands were evaluated in Phase 2: (1) WR Meadows's Sealtight 1100 Clear and (2) ChemMasters' Safe-Cure 1200. Their ATR and Raman fingerprint spectra can be found in Appendix I (Figures I.14 and I.15) and Appendix J (Figures J.15 and J.19), respectively. In addition, field ATR measurements were performed on a PCC surface with TAMMSCURE applied,

as described in the section on field verification of laboratory results.

Polymer Additives to Asphalt

Polymer additives have been increasingly used to improve asphalt durability and resistance to rutting. The following three polymer products commonly used for asphalt modification were included in the experimental design: DuPont Elvaloy 4170, Kraton D1101 styrene–butadiene–styrene (SBS), and BASF's Butonal styrene–butadiene (SB) latex. The Elvaloy is a vinyl acetate/carbon monoxide/ethylene copolymer, while Kraton and Butonal products are manufactured from styrene–butadiene polymer. More details about these products can be found in the MSDS (see link in Appendix H). The pure polymer samples were scanned by portable ATR and Raman to obtain the "signature" spectra (see Appendices I and J, respectively). The major IR absorption peaks were used to identify the presence of a polymer and determine its concentration in the polymer-modified asphalt binders and HMA mixtures, as discussed in the next section. Raman could not be used for the evaluation of polymer-modified asphalts because of the high opacity of asphalt binders.

A typical ATR FTIR spectrum of Elvaloy exhibits several distinctive absorption peaks. The polyethylene chain is characterized by sharp peaks at 2,920, 2,850, and 724 cm^{-1}. The carbonyl peak at 1,735 cm^{-1} coupled with a double peak at 1,240 to 1,270 cm^{-1} represents the acetic component in Elvaloy. Finally, two peaks at ~1,640 and ~1,560 cm^{-1} are associated with vinyl vibrations. When added to asphalt binder, Elvaloy 4170 still shows two distinctive peaks at ~1,240 and 1,735 cm^{-1}, which can be used for positive identification of this additive.

The most distinctive chemical bonds in a typical SB-based polymer are aromatic C–H bonds in polystyrene (PS) and trans-alkene (vinyl) C–H bonds in polybutadiene (PB). The out-of-plane vibrations yield prominent IR peaks at ~700 and ~965 to 970 cm^{-1} for PS and PB, respectively. The PS and PB peaks can be easily identified on both Kraton's and Butonal's spectra in Figures I.18 and I.19, respectively, in Appendix I. The obvious difference between those two polymers is the presence of emulsifier in Butonal, which is characterized by strong bands associated with OH vibrations at ~3,400 and ~1,645 cm^{-1}.

The double peak at 2,850 to 2,880 cm^{-1} on a typical Raman spectrum of Elvaloy is associated with the ethylene functional group and yields the highest intensity (see Figure J.22 in Appendix J). The two single peaks at ~1,440 and ~1,300 cm^{-1} are also attributed to aliphatic hydrocarbon chains. The other pronounced peaks at ~1,120 and ~1,060 cm^{-1} are associated with stretching vibrations of the carbon skeleton in Elvaloy. The Kraton and Butonal polymers have a common SB component, which is identified by strong and narrow peaks at ~1,000 and ~1,670 cm^{-1} (see Figures J.21 and J.23). Butonal can be differentiated from Kraton by the peak at ~470 cm^{-1}, which is most likely due to the carboxylic emulsifier.

Antistripping Agents for Asphalt Applications

Antistripping agents in asphalt mixtures increase the adhesion of asphalt binder to aggregate and reduce moisture damage. The antistripping agents tested in this project were Akzo Nobel's Kling Beta and ArrMaz's AD-here, both amido amine-based concentrated liquids. Highly repeatable signature spectra were obtained for both materials using the portable ATR FTIR, as shown in Figures I.20 and I.21 in Appendix I. The ATR analysis indicated that Kling Beta and Ad-here differed in aromaticity (note the difference in the region around 800 cm^{-1}). This difference affected their viscosity; hence there are slightly different applications (see links to MSDS in Appendix H for more information).

The two chemicals appeared to have similar chemical structure. Thus aliphatic hydrocarbons were identified by the ATR at 2,924, 2,854, ~1,460, and ~725 cm^{-1}, whereas double peaks at ~1,650 to 1,550 and 1,130 to 1,070 cm^{-1} were assigned to amido and amino groups, respectively (see Figure I.22). The ATR FTIR spectrum of an Ad-here sample obtained from the manufacturer (lab sample) is compared in Figure I.22 with a sample obtained from a storage facility. One can observe stronger absorption bands for the aliphatic hydrocarbons along with significantly lower absorption for amido-amino functional groups. This suggests that the field sample may be contaminated with asphalt binder or, alternatively, diluted by an aliphatic solvent to reduce the viscosity of the antistripping agent.

Raman analysis yielded a representative spectrum for Kling Beta (see Figure J.13 in Appendix J). However, the high opacity of AD-here additive precluded Raman analysis.

Identification and Quantification of Additives and Contaminants in Complex Materials

One of the main objectives of spectroscopic investigations in this project was the identification and quantification of additives and contaminants in mixtures. Specifically, the presence of water in waterborne paints, chemical admixtures in PCC, polymer modifiers, antistripping agents, RAP, and contaminants in asphalt products were of interest. Table 3.3 compares the spectroscopic methods in terms of their success for each mixture. ATR FTIR analysis performed well for all cases except to detect diesel contamination in asphalts. The stationary GPC and NMR systems were successful in the detection of all additives in asphalt products except antistripping agents

Table 3.3. Summary of Success in Spectroscopic Identification and Quantification of Additives and Contaminants

Material Category	Objective	Portable Methods				Stationary Methods	
		FTIR	Raman	XRF	XRD	GPC	NMR
Epoxy coatings, paints, and adhesives	Presence of solvents	Yes	na	na	na	No	Yes
Waterborne paints	Presence of water	Yes	na	na	na	na	na
PCC	Identification of admixture in PCC mix	Yes[a]	na	No	na	na	na
	Quantification of content	No	na	No	Yes[b]	na	na
Curing Compounds for PCC	Identification of curing membrane on PCC surface	Yes	na	na	na	Yes	na
Polymer-modified asphalt binders, emulsions, and mixtures	Identification of polymer and water in product	Yes[b]	No[c]	na	na	Yes	Yes
	Quantification of content	Yes	na	na	na	Yes	na
HMA concrete	Detection of contaminants (e.g., motor oil, diesel fuel)	No	No[c]	na	na	Yes	Yes
Antistripping agents in binders and mixtures	Identification of antistripping in product	No	No	na	na	No	Yes
	Quantification of content	No	No[c]	na	na	No	na
Oxidation in RAP	Verification of presence in mixture	Yes	No[c]	na	na	Yes	Yes
	Quantification of content	Yes[c]	na	na	na	Yes[c]	na

Note: na = not applicable.

[a] For concentrations greater than 0.4%.

[b] High variability in results is expected.

[c] Not applicable for solids and fluorescing constituents.

(most likely because of their extremely low concentration in the mixtures).

Quantification of chemical admixtures in PCC and antistripping agents in asphalts by ATR was not found practical because of the low concentrations prescribed by the manufacturers. In addition, diesel fuel contamination in asphalt binder could not be identified using FTIR because of the overlapping bands of the two materials. However, a quantitative analysis of the FTIR spectra obtained for polymer-modified binders and RAP-containing asphalt products yielded reasonable results. The same level of success was achieved by the quantitative analysis of GPC chromatograms and NMR spectra for these materials, as described in the Appendix O. The next sections summarize the results of the most successful ATR quantitative analyses.

Curing of Epoxies

Three types of epoxies were evaluated by the Bruker ALPHA ATR FTIR spectrometer to investigate the feasibility of tracking changes in their chemical composition in situ: (1) three-part, organic, zinc-rich epoxy coating system (Carbozinc 859); (2) fusion-bonded epoxy (Scotchkote); and (3) two-part high-strength epoxy bonding adhesive (Ultrabond 1100). The signature spectra of those materials were previously obtained in the laboratory. Next, the testing specimens were fabricated by mixing ingredients in accordance with manufacturer's instructions and applying the coating to a metal plate. The probes for ATR testing of Carbozinc and Scotchkote systems were taken by scrapping a small amount of an epoxy from the plate immediately and after 20 to 60 min of the air curing. The Ultrabond adhesive was probed after 10 min of curing because of rapid hardening. The results of spectral analysis for cured epoxies are discussed next.

The three spectra shown in Figure 3.6 indicate the evaporation of toluene solvent by a drastic decrease in the IR absorbance at 738 and 698 cm^{-1}, and the hardening and oxidation of the epoxy base by an increase in the absorbance at 1,728 and 1,276 cm^{-1}. Nevertheless, the presence of epoxy resin can be tracked even after an hour of air-curing, as evident by

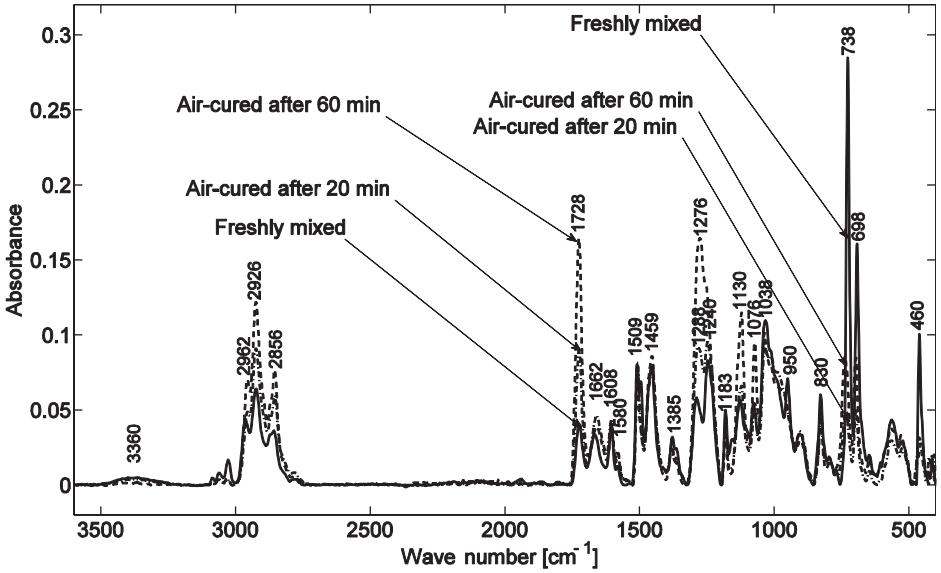

Figure 3.6. Changes in the ATR FTIR spectra caused by curing of Carbozinc 859 epoxy coating system.

the IR absorption peaks at 1,662, 1,608, and 1,580 cm^{-1}. Figure 3.7 tracks changes in the ATR FTIR spectrum of Ultrabond 1100 adhesive after 10-min curing. It shows that virtually all characteristic absorption peaks of the adhesive can be positively identified within 10 min (onset time) from the time of application. Curing process is characterized by the evaporation of solvent as evident by a reduced intensity of the associated peaks between 2,800 and 3,000 cm^{-1} at ~830 cm^{-1}. Also, consolidation of the adhesive can be tracked by the increase in amino-related absorption of hardener at 1,130 to 1,070 cm^{-1} wave numbers.

Waterborne Paints and Curing Compounds

An ATR study of Ennis FAST DRY white paint was performed on samples taken from a storage tank before application, from newly painted pavement marking, from an old white lane at the same facility. The ATR FTIR spectra of the three

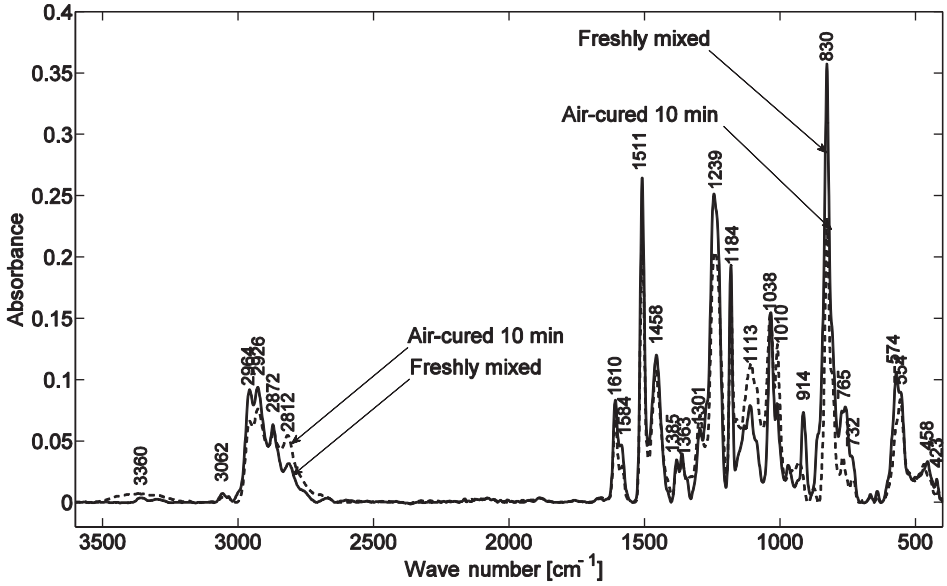

Figure 3.7. Changes in the ATR FTIR spectra caused by curing of Ultrabond 1100 epoxy adhesive.

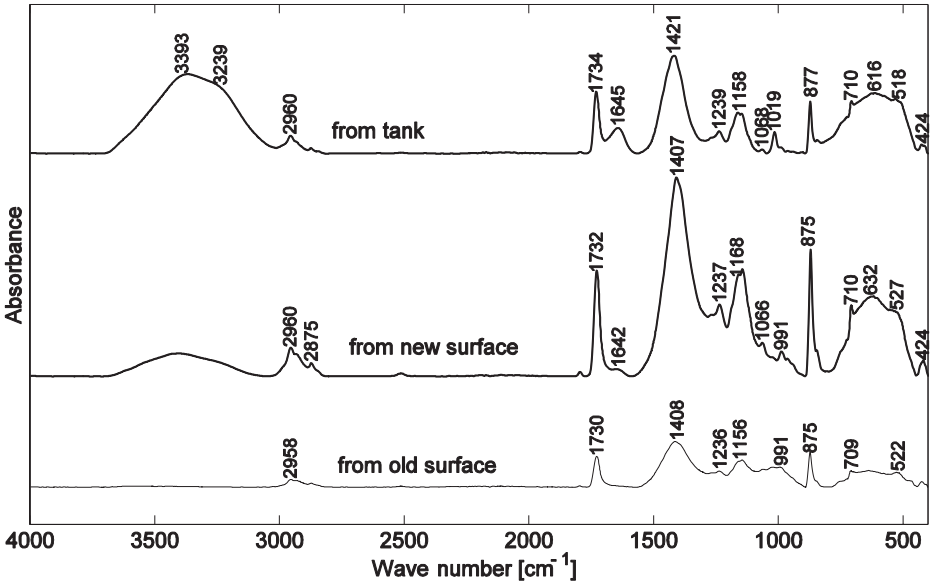

Figure 3.8. Comparison of the ATR FTIR spectra of Ennis FAST DRY white paint sampled from tank, freshly applied white marking, and old white line surface.

samples are compared in Figure 3.8. The waterborne vinyl acrylate structure of a liquid sample from a tank can be easily identified by the medium-wide water-associated (~3,400, ~3,250, and ~1,640 cm^{-1}) and strong sharp carboxylate-associated (~1,730 and ~875 cm^{-1}) absorption bands. Note that the evaporation of water can be tracked by observing significant reduction in the intensity of the OH vibrations in the freshly painted white line (about 15 to 30 min after application). Consequently, no water can be detected in the old paint several months after application.

Figure 3.9 superimposes the ATR FTIR spectra of the pure chemical (TAMMSCURE curing compound), the sample scratched from the freshly covered PCC surface, and the sample of the dried PCC surface. Each spectrum represents an average of three replicate probes from each sample. It is obvious from Figure 3.9 that characteristic peaks (2,938, 2,856,

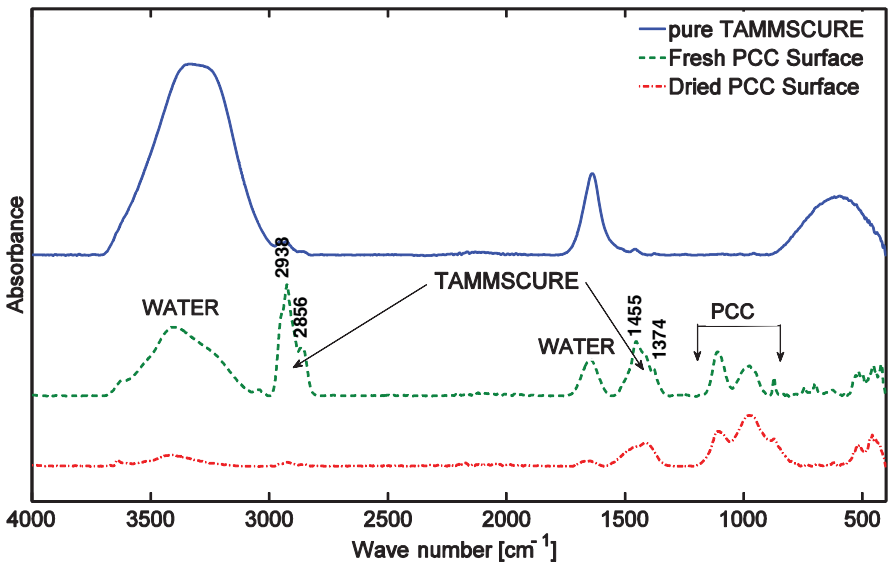

Figure 3.9. ATR FTIR spectra of TAMMSCURE curing compound before and after application to a PCC surface.

Table 3.4. Chemical Composition of Admixtures

Admixture Type	Product Name	Manufacturer	Chemical Components (wt%)	Chemical Functionalities
Superplasticizer (high-range water reducer)	ADVA 190	W. R. Grace & Co.	Water (90–99) Carboxylated polyether (1–10)	H_2O;–COO–;–CH_2–O–CH_2
Air entrainer	AIR MIX 200 (AIR 200)	Euclid Chemical	Water (>60) Tall oil, sodium salt (10–30) 4-Chloro-3-methylphenol (<1)	H_2O; –CONaO–; –C_6H_3OH;–CH_3; –Cl
Set accelerator	Accelguard 80	Euclid Chemical	Water (40–70) Calcium nitrate (40–70)	H_2O; $Ca(NO_3)_2$
Set retarder	Eucon Retarder 75	Euclid Chemical	Water (>60) Sodium gluconate (30–60) 4-Chloro-3-methylphenol (<1)	H_2O; –CHOH–;CH_2OH; CONaO; –C_6H_3OH; –CH_3; –Cl

1,455, and 1,374 cm^{-1}) associated with hydrocarbon resin and aliphatic naphtha components of TAMMSCURE (see MSDS) can be tracked on the ATR FTIR spectra of both freshly covered and dried PCC surfaces to which the curing compound have been applied.

Chemical Admixtures in Fresh Concrete

This study employed four chemical admixtures that are typically used in the United States: W. R. Grace's ADVA 190 (superplasticizer), Euclid's AIR MIX 200 (air entrainer), Accelguard 80 (set accelerator), and Eucon Retarder 75 (set retarder). Table 3.4 summarizes technical and chemical information on these products. All admixtures were supplied as aqueous solutions. The PCC batches (2 kg each) were prepared using Type 2 portland cement supplied by Lafarge North America and local fine and coarse aggregates of nominal maximum aggregate size of 4 and 12.5 mm, respectively. Five PCC batches, one control with no admixtures and one for each admixture from Table 3.4, were mixed in proportions shown in Table 3.5 with total weight of about 1.8 kg per batch. The admixtures were first mixed with batch water in proportions recommended by their manufacturers and then added to the dry batch mix. To obtain the IR spectra of PCC samples modified with a chemical admixture, about 1 g of fine PCC fraction (cement–sand–water–admixture) was placed directly on the internal reflection element (IRE) and a fixed load was applied to a sample to ensure its full contact with the IRE.

The fingerprint ATR FTIR spectra of the admixtures in discussion were obtained in the laboratory as discussed earlier in this report. Identifying the characteristic IR absorption bands of the admixtures in the ATR FTIR spectra of their corresponding PCC mixes is a challenging task. Only ADVA 190 and Accelguard 80 could be positively identified as additives by the characteristic IR absorption bands shown in Figures 3.10 and 3.11. An apparent reason for that is a much higher concentration of those admixtures (0.4 and

Table 3.5. Summary of PCC Batch Proportions

Batch	1[a]	2	3	4	5
Admixture type	None	ADVA 190	AIR 200	Eucon Retarder 75	Accelguard 80
Water–cement ratio	0.5	0.45	0.45	0.45	0.45
Design water	8.3%	7.60%	8.30%	8.30%	8.20%
Type 2 cement	16.6%	23.70%	18.40%	18.40%	18.30%
Batch water	8.7%	7.90%	8.70%	8.70%	8.60%
Stone	34.7%	41.10%	34.60%	34.60%	34.40%
Sand	40.0%	26.80%	38.20%	38.20%	37.90%
Admixture	0.0%	0.43%	0.070%	0.13%	0.72%
Total	100.00%	100.00%	100.00%	100.00%	100.00%

[a] Batch one is the control.

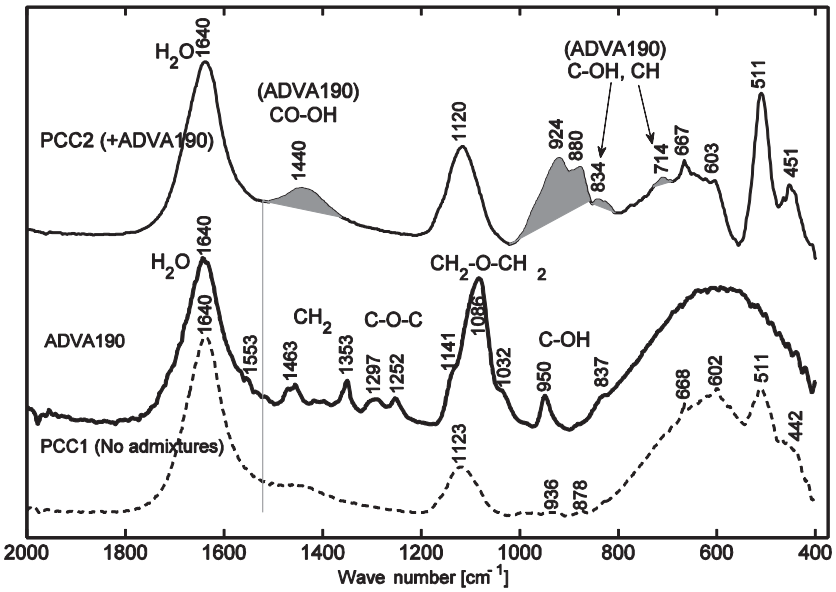

Figure 3.10. Composition of the ATR FTIR spectrum of PCC sample modified with ADVA 190.

0.7 wt% of the batch weight for ADVA 190 and Accelguard 80, respectively) as compared with AIR 200 and Eucon Retarder 75 with 0.07 and 0.13 wt%, respectively (see Table 3.5).

The ATR testing of fresh PCC mix samples verified feasibility of identification of the presence of high-range water reducers (HRWR) and nonchloride (NCL) set accelerators in fresh PCC mixes. In knowing that HRWR chemicals preserve rate of hydration, the presence of HRWR can be verified by the relatively strong IR absorption peaks at 933, 874, and 828 cm^{-1} associated with formation of the primary hydration product [calcium–silicate–hydrate (C–S–H)], as shown in Figure 3.12. Furthermore, a closer look at the zoomed-in spectra in the region between 1,500 and 1,300 cm^{-1} reveals relatively weak but visible peaks associated with admixtures. For instance, the three peaks at 1,455, 1,280, and 1,250 cm^{-1} can be related to the presence of HRWR, while the two peaks at 1,410 and 1,330 cm^{-1} indicate the presence of NCL accelerator.

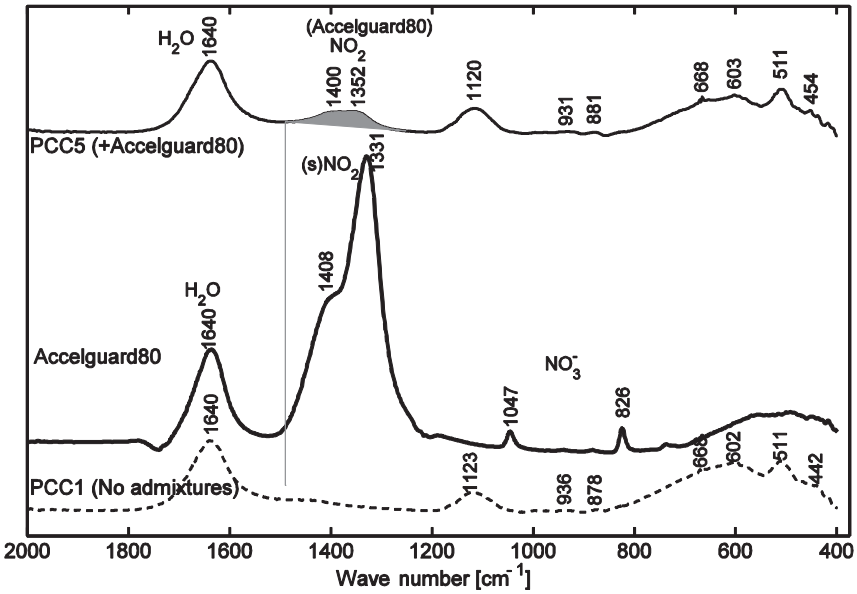

Figure 3.11. Composition of the ATR FTIR spectrum of PCC sample modified with Accelguard 80.

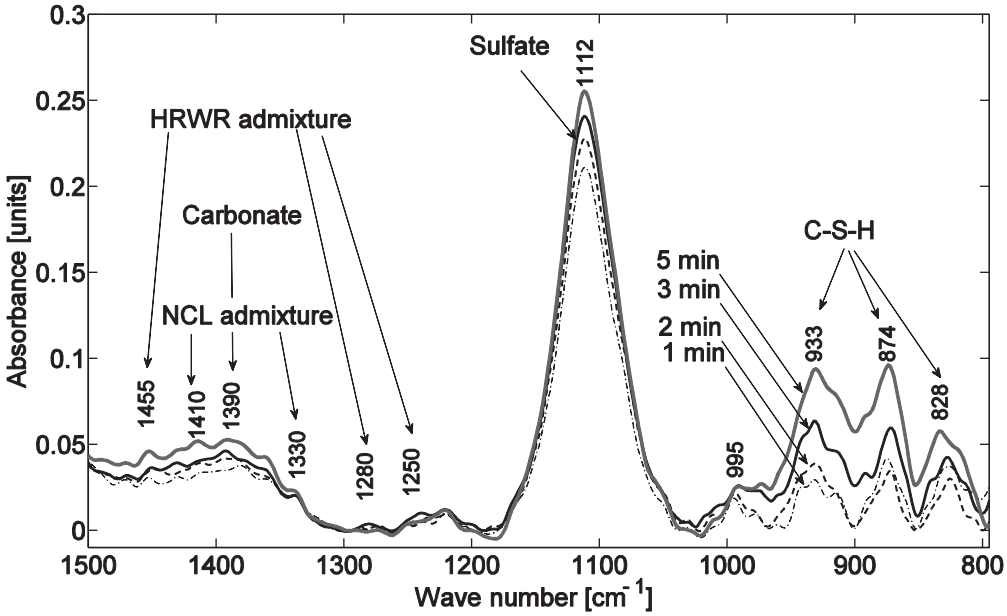

Figure 3.12. ATR FTIR spectra of hydrated PCC sample with HRWR and NCL admixtures.

Polymers in Asphalt Products

The major objective for spectroscopic evaluation of polymer-modified asphalt products was identification of polymer type and, if possible, determination of polymer content in asphalt binders, emulsions, and HMA mixtures. Two SB-based polymers—Kraton SBS and BASF's Butonal NX1138—were used in this study to produce polymer-modified binders in the laboratory. In addition, two styrene–butadiene rubber (SBR) latex-modified binders (of different performance grades [PG]) as well as the SB-modified cationic rapid setting emulsion CRS-1P were supplied by a refinery and evaluated in the laboratory. The spectra of polymer-modified emulsions, polymer-modified binders (PMB), and polymer-modified asphalt mixtures collected in the laboratory were compared with those obtained in the field setting from the real paving projects. The results of spectral analysis of these materials are discussed separately in the next two subsections.

Styrene–Butadiene-Modified Emulsions

Figure 3.13 superimposes the ATR FTIR spectra of the polymer-modified emulsion CRS-2 in two states: (1) sampled from the tank and (2) applied to stone aggregate (Novachip seal technology). The two main emulsion components are easily identified by strong and wide water bands centered around 3,300 and 1,640 cm^{-1} and doubled aliphatic binder peaks at about 2,920, 2,850, 1,455, and 1,375 cm^{-1}. The SBS additive can be detected by two characteristic peaks at 967 and 700 cm^{-1} associated with polybutadiene and polystyrene, respectively. The spectra of the Novachip stone coated by the CRS-2 emulsion clearly indicate the absence of water after the emulsion breaks on the aggregate. Note that the wide band at 1,600 cm^{-1} is associated with the aromatic carbon skeleton of the binder. For the polymer, the polybutadiene peak is obscured by the signal from silicate component of the aggregate at ~990 cm^{-1}. However, the SBS presence can still be verified by a weak yet distinctive peak at about 695 cm^{-1}.

Figure 3.14 compares the ATR FTIR spectra of two polymer-modified asphalt emulsions tested in the laboratory and in the field by two separate Bruker ALPHA ATR FTIR spectrometers. Note that practically no difference in chemical composition of the two samples is indicated. However, the higher water content in CRS-1P relative to CRS-2 can be deduced by the significantly lower intensity of the absorption bands associated with the aliphatic binder. Nevertheless, the presence of polymer is clearly indicated by the SBS-related peaks at 966 and 695 cm^{-1}.

Because asphalt emulsions are chemically stabilized systems, their balance can be easily disturbed with exposure to air. Therefore, sampling and scanning of those products with the ATR FTIR was a challenging task. During storage, the bitumen can segregate from the water. Figure 3.15 presents three spectra for CRS-1P: the agitated emulsion and the water-segregated and binder-segregated components of the same product. The presence of the SB polymer is easily indicated by a distinctive peak at ~965 cm^{-1}. The absorbance peak at ~1,640 cm^{-1} is assigned to water while the two peaks at ~1,460 cm^{-1} and ~1,380 cm^{-1} correspond to the stretch-

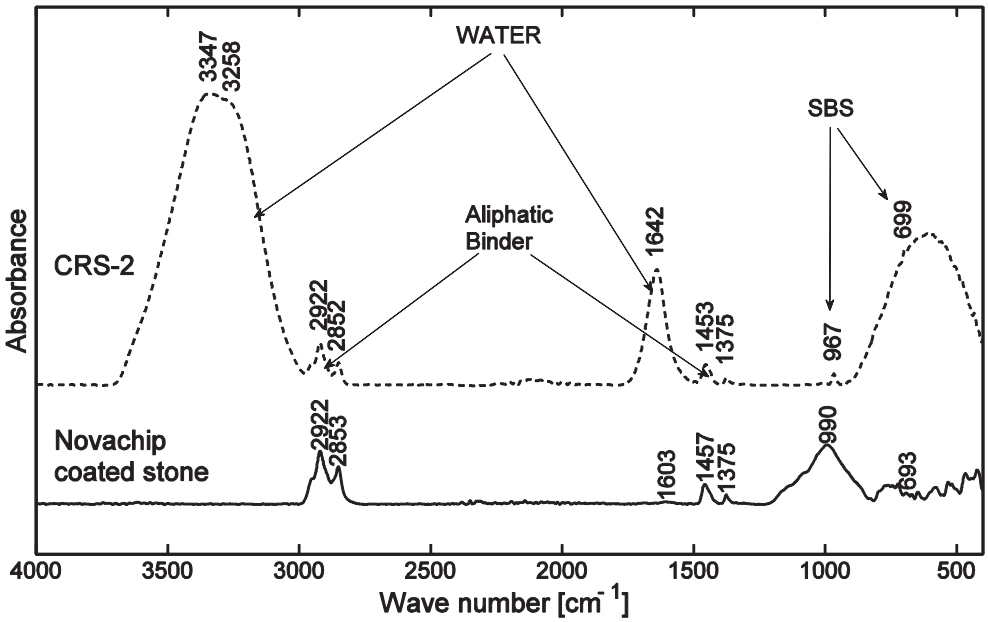

Figure 3.13. ATR FTIR spectra of pure emulsion from tank (CRS-2) and Novachip coated aggregate.

ing vibrations of aliphatic hydrocarbons in asphalt binder. Last, one can notice that spectra of both stirred emulsion and its binder-segregated portion show highly intensive absorbance at ~1,740 and ~1,250 cm^{-1}, which indicates presence of carboxylate emulsifier in the polymer-modified emulsions. In conclusion, although segregation of the asphalt emulsion is most likely to preclude the quantitative analysis of its spectra during FTIR testing, it is still possible to identify its major components (i.e., water, binder, and polymer additive).

Styrene–Butadiene-Modified Binders

This study employed various original asphalt binders modified with SBS and SBR polymers. The PMB samples were mixed in the laboratory as well as supplied by a refinery. Table 3.6

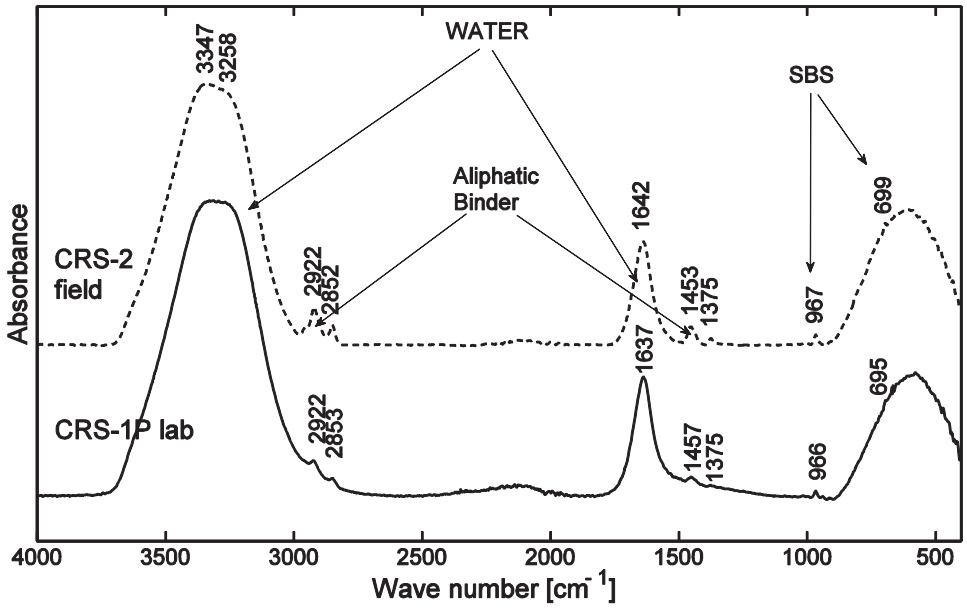

Figure 3.14. ATR FTIR spectra of polymer-modified emulsions.

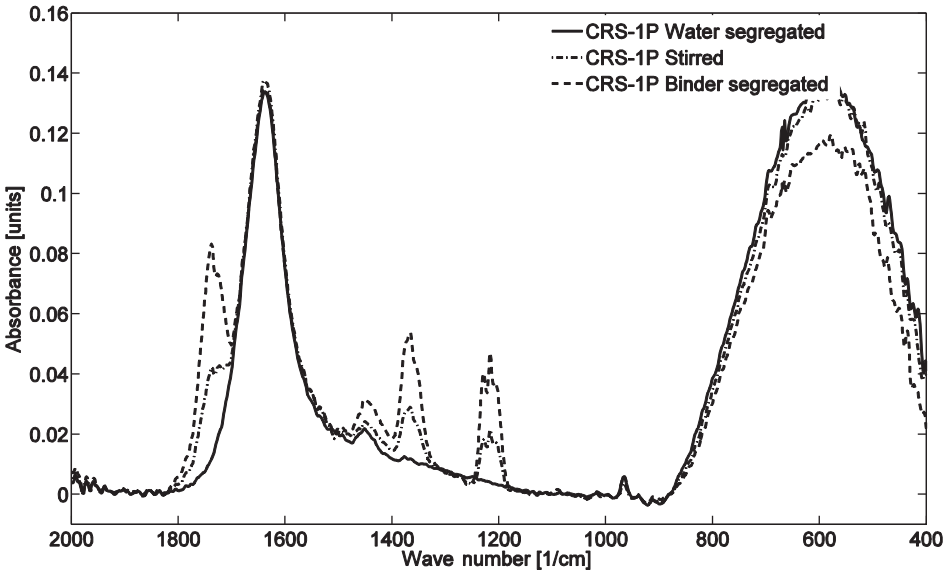

Figure 3.15. ATR FTIR spectra of CRS-1P asphalt emulsion.

summarizes the asphalt binders and the modifiers used for aging experiments. The PG of asphalt binders ranged from PG 52-34 to PG 64-28. Note that the virgin binders PG 58-28 and PG 64-22 were obtained from two different refineries: Nu Star in Rhode Island and West State Asphalt from Washington State. Two types of polymer—Kraton SBS D1101 and BASF Butonal NX1138—were added to the original asphalt binders in proportions ranging between approximately 1 and 3 wt%. The SBR latex-modified and neat asphalt binders were supplied by Hudson Asphalt Group, Providence, Rhode Island. The SBS- and Butonal-modified asphalt binders were prepared in the laboratory, as described in the following text.

To prepare the SBS-modified samples in the laboratory, about 400 g of base bitumen (PG 64-22 or PG 58-28) was preheated in an oven to a temperature of 160°C for about 1.5 h. Then the sample in a stainless steel flask was put in a heating jacket and stirred at 175°C ± 5°C using a high-shear mixer for about 2 h. The Kraton SBS pellets were added gradually within 5 min after stirring started. The liquid Butonal latex was added to the preheated bitumen sample at 135°C ± 5°C and stirred at lower speed (about 1,000 rpm) for 1 h. For both polymers, a sample was taken from the flask every 0.5 h and the ATR FTIR spectrum was measured to track the dispersion of the polymer. Three different replicate batches were prepared for each laboratory combination of bitumen and polymer concentration. Finally, each produced PMB batch was divided into three 6-oz cans for sampling and ATR FTIR spectrometry.

To evaluate the effect of the temperature and pressure on the chemical composition of PMB, two accelerated aging methods were used in this study: rolling thin film oven–aged (RTFO) air blowing and pressure aging vessel (PAV) conditioning. The aging cycle for each sample included RTFO for 85 min followed by PAV for 20 h. Each sample was scanned by the ATR FTIR spectrometer before and after every step in the aging cycle. The spectra of virgin and aged samples for each PMB with maximum polymer concentration are superimposed in Figures I.27 through I.30 in Appendix I.

The primary objective of spectral analysis was to identify a polymer type by the characteristic IR absorption peak. In addition, calibration equations for the quantification of polymer content in binders listed in Table 3.5 were developed based on the Beer-Lambert law (Equation 2.3 in Chapter 2). The molar

Table 3.6. Summary of Polymer-Modified Binders

Bitumen PG Grade	Modifier Name	Modifier Amount Added	Preparation
PG 64-22	Kraton SBS D1101	0, 1, and 3 wt%	Laboratory
PG 58-28	BASF Butonal NX1138 (SB latex)	0, 1.5, and 3.3 wt%	Laboratory
PG 52-34	SB latex (source unknown)	1.5 wt%	Refinery
PG 64-28	SB latex (source unknown)	3.3 wt%	Refinery

extinction coefficients (or coefficient of absorptivity, *e*) for polystyrene and polybutadiene were determined as a ratio of IR absorbance value, *A*, at ~965 and ~700 cm^{-1}, correspondingly, over the polymer content, *c*, multiplied by the IR light path length, *l*, as shown in Equation 3.1. The path length was calculated as 0.25 power of wavelength (1/wave number).

$$e = \frac{A}{cl} \tag{3.1}$$

Figure 3.16 graphically compares the calibration slopes for SBS-modified PMBs between different binder sources (east versus west) and different polymers. It can be seen that calibration slopes for polystyrene peak (A700) do not differ between east and west. This suggests that in this study, no dependence of absorptivity on the binder source was observed.

It should be noted that other quantitative methods of spectral analysis were evaluated in this study to establish reliable calibration equations. One was peak-to-peak ratio. This method correlates the normalization of PB or PS absorption peak intensity to that associated with aliphatic CH stretching or bending vibrations that did not change with increase in polymer concentration (e.g., A966/A1377 and A700/A2920). Another so-called semiquantitative method involved normalization of valley-to-valley integrated absorption bands centered at ~965 and ~700 cm^{-1} for PB and PS, respectively. The two methods are described in Appendix N and can be applied to any complex material or compound.

Using peak-to-peak ratio rather than direct peak values as measured by ATR did not noticeably improve the goodness of fit for calibration equations (see Figure N.1 in Appendix N). Therefore, it is recommended that directly measured A966

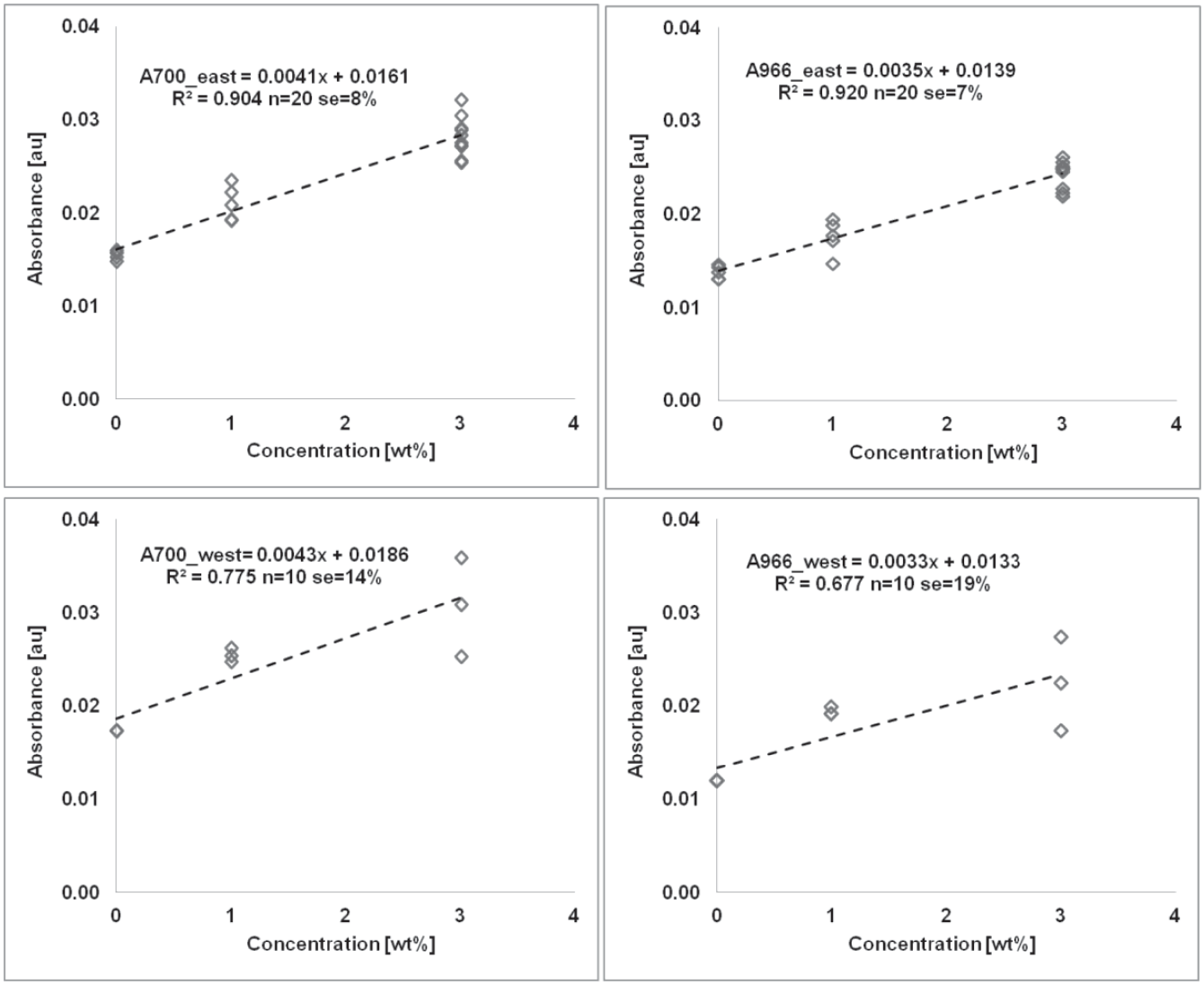

Figure 3.16. Calibration equations for SBS-modified PMB based on polybutadiene and polystyrene absorption.

and A700 peaks be interchangeably used for quantification of SB polymers in PMBs. When the team studied the effect of oxidative hardening on PMBs, no noticeable change in polymer content resulting from oxidation was found for PMBs with the SB content up to 3.5 wt% (see Figure K.5 in Appendix K).

Styrene–Butadiene-Modified Hot-Mix Asphalt Mixtures

An attempt to identify polymer modifiers in HMA mixtures from the analysis of FTIR spectra was done using HMA mixtures produced in the laboratory with polymer-modified binders. The PG 64-22 east binder modified with 1, 3, and 6 wt% SBS was preheated to 163°C and mixed with aggregates to produce the HMA mixtures. The FTIR spectra were obtained for each mix a week later at about 20°C. The two IR absorption peaks at ~965 and ~700 cm^{-1} were expected to serve as indicators of the presence of PB and PS in the mix. However, no PB peak could be extracted from the ATR FTIR spectra of the mix samples and no correlation between peaks at ~695 to 700 cm^{-1} and SBS concentration was found. Further investigation was conducted by means of two-dimensional correlation spectroscopy to allow a closer look at the chemical composition of the HMA samples. Figure 3.17 presents the two-dimensional correlation spectroscopy plot for SBS-modified HMA samples. Note that, on the one hand, there is no correlation observed between absorption bands at 965 and 695 cm^{-1}. On the other hand, strong correlation between two peaks at 695 and 793 cm^{-1} indicates the presence of quartz in either siliceous limestone or granite aggregate.

Field evaluation of HMA samples was conducted during paving operations on I-84 near Farmington, Connecticut. The mix including PG 76-22 SBS-modified binder was sampled from two separated trucks immediately after unloading. Figure 3.18 presents the normalized (to 2,920 cm^{-1} peak value) ATR FTIR spectra of two samples taken from the paver within 15 min of each other. One can see that absorption peaks of the two samples are matching, which suggests they have identical chemical composition. The peak at about 2,180 cm^{-1} indicates the presence of carbon dioxide from entrapped hot air. In addition, minor oxidative hardening caused by mixing and placement of the HMA can be detected by the peak at about 1,700 cm^{-1}. The rest of the peaks are associated with the binder (2,961, 2,921, 2,853, ~1,600, 1,455, and 1,375 cm^{-1}) and filler and aggregates (~1,000, 793, 637, 585, 530, and 467 cm^{-1}).

Figure 3.19 presents a closer look at two SBS-modified HMA samples: (1) prepared in the laboratory and (2) obtained from the field. There are two small but not negligible peaks at ~967 and ~695 cm^{-1}, which can be associated with the presence of SBS polymer in the PG 76-22 binder. The spectrum of the field sample, however, does not positively indicate the

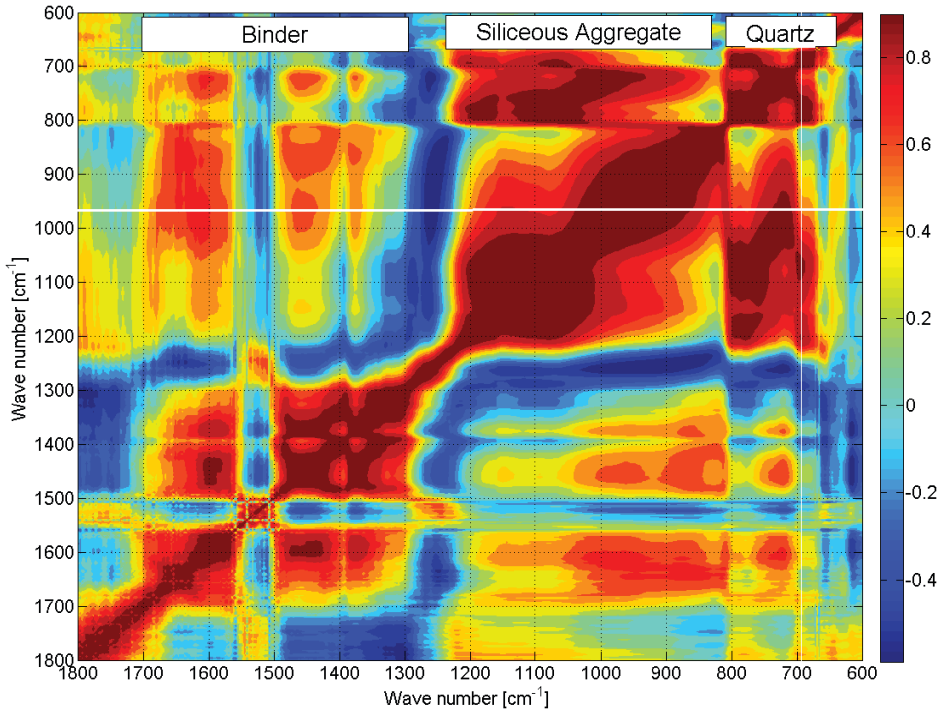

Figure 3.17. Two-dimensional correlation spectroscopy plot for SBS-modified HMA samples.

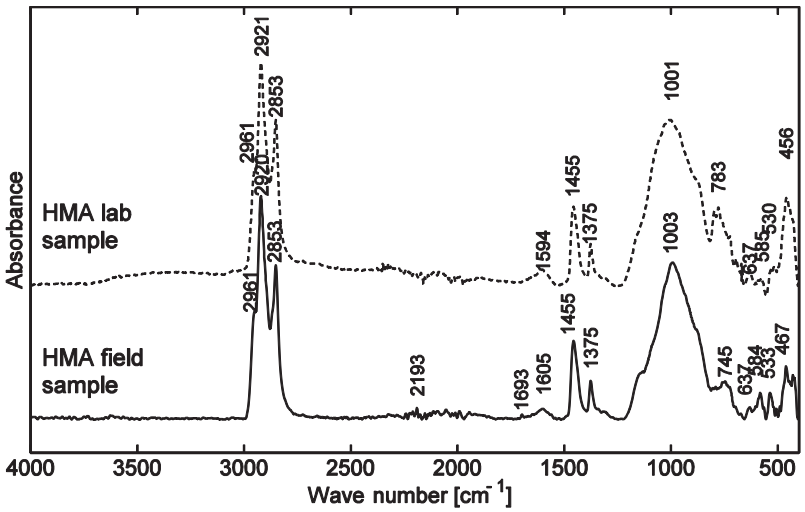

Figure 3.18. ATR FTIR spectra of HMA field samples.

presence of SBS. It should be noted that polybutadiene peak at 967 cm^{-1} is likely to be obscured by the strong and wide band centered around 1,000 cm^{-1} that is associated with the silicate component of the aggregates. Furthermore, the peak near 700 cm^{-1} can be associated with the presence of quartz in siliceous aggregates rather than with polystyrene-related IR absorptions.

The direct ATR measurements on HMA samples showed that quantification of SBS content in the fresh mix appears impractical for two reasons. First, the weight percent content of the polymer compared with the mix sample weight is extremely low (around 0.002 wt%), which makes identifying the SBS peaks a challenging task. Second, the polymer content is usually governed by a binder grade specification. Therefore, it appeared logical to verify polymer content in an extracted binder sample as discussed in the next section.

Polymer-Modified Binder Extracted from Hot-Mix Asphalt

The experiment on quick extraction of PMB was conducted on Novachip street paving project in Rocky Hill, Connecticut. About 5 g of HMA passing No. 16 (1.18 mm) sieve size was added to 15 mL of stabilized dichloromethane (DCM) for spectroscopic applications, manually shaken for 2 min, and then left for 15 min to allow sedimentation of suspended filler particles. The liquid phase of the solution

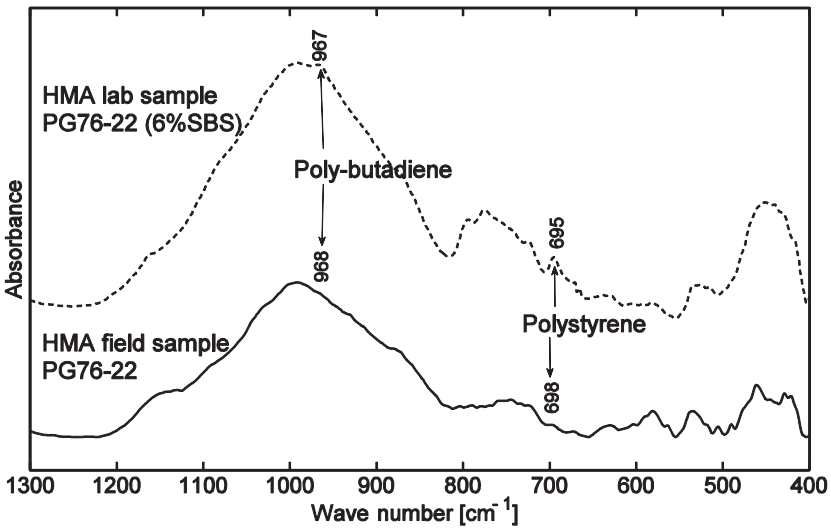

Figure 3.19. Zoom-in on SBS-associated absorption bands in laboratory and field samples of polymer-modified HMA.

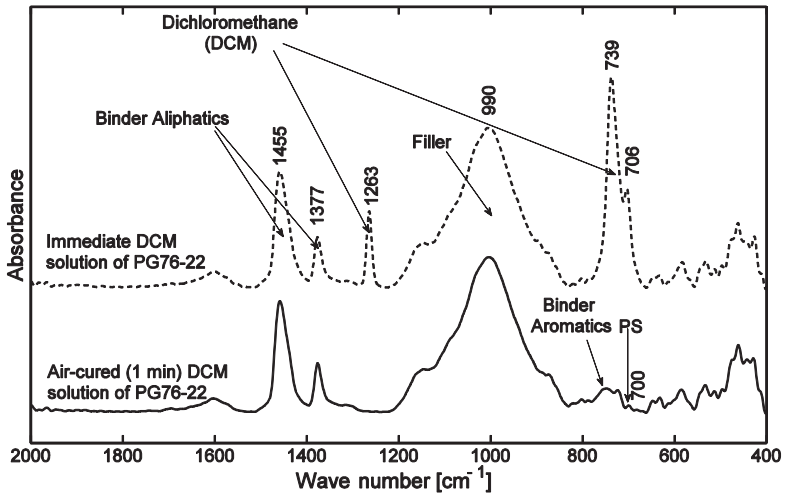

Figure 3.20. Identification of SBS polymer in asphalt binder PG 76-22 extracted from HMA.

was probed by pipetting two to three drops on the ATR sampling plate. The ATR FTIR spectra of the sample were collected twice: immediately and within 1 to 2 min from the moment of placement.

Figure 3.20 compares the ATR FTIR spectra in the fingerprinting region (1,800 to 400 cm^{-1}) of a DCM-extracted PG 76-22 binder sample obtained immediately and 1 min after placing the sample on the ATR plate. It is shown that the only three characteristic absorption peaks attributed to DCM, which are at 1,263, 739, and 706 cm^{-1}, do not interfere with characteristic peaks of the aliphatic component of the binder (1,455 and 1,377 cm^{-1}) or with the absorption of filler particles. However, the DCM solvent peaks do obscure the signal from the aromatic hydrocarbons (860 to 725 cm^{-1}) and, if present, from the polystyrene component of the SBS polymer (expected around 700 cm^{-1}). When the sample is allowed to cure for 1 min, the solvent evaporates completely, making it possible to identify both binder aromatics and the SBS-related peak.

Oxidation in Recycled Asphalt

This study targeted the following two objectives related to recycled asphalt pavements:

- Feasibility of the identification of elevated oxidation level in the RAP-modified binder blends and HMA mixes by means of a portable infrared spectrometer, and
- Possibility of the determination of RAP content in binder blend–HMA mix based on the concentration of the oxidized chemical functionalities.

Two types of samples were prepared in the laboratory (see Table 3.7): (1) binder blends containing 15 to 40 wt% RAP

Table 3.7. Summary of RAP-Modified Materials

Material Category	Brand/Material Name	Composition
Neat asphalt binders mixed with RAP binders	Virgin PG 64-22 West (VB) RAP Tilcon Waterbury (RAP1)/Manchester (RAP2)	60% VB : 40% RAP1 70% VB : 30% RAP1 80% VB : 20% RAP1 70% VB : 30% RAP2 80% VB : 20% RAP2 85% VB : 15% RAP2
RAP-containing HMA mixes	Virgin PG 64-22 West (VB) Virgin aggregate (VAGG) RAP Tilcon North Brantford (RAP)	5.0% VB : 95.0%VAGG : 0.0% RAP 4.6% VB : 85.8%VAGG : 9.6% RAP 4.3% VB : 76.6%VAGG : 19.1% RAP 3.9% VB : 67.3%VAGG : 28.8% RAP 2.8% VB : 38.9%VAGG : 58.3% RAP 2.0% VB : 19.6%VAGG : 78.4% RAP

binder and (2) loose HMA samples modified by up to 80 wt% RAP. The infrared spectra were collected using a Bruker ALPHA FTIR spectrometer equipped with a single reflection diamond ATR accessory. About 0.1 g of a RAP-modified sample (binder blend or HMA mix) was put directly on the ATR prism and a fixed load was applied to a sample to ensure its full contact with the diamond. Twenty-four scans were averaged for each sample within the wave number range of 4,000 to 400 cm^{-1} at a resolution of 4 cm^{-1}, and the resultant averaged spectrum was recorded. Three replicate probes from each sample were scanned to establish standard deviation of the method.

To track the changes in chemical composition of the RAP-modified binder blends and HMA mixes attributable to an increase in RAP content, the ATR FTIR spectrum of each sample was analyzed both qualitatively and quantitatively. The qualitative analysis involved identifying characteristic IR absorption bands for the functional groups typically present in binders. Beside the aliphatic (CH, $[CH_2]_n$, and CH_3) and aromatic (C=C and arCH) binder components, the oxidation products such as hydroxyls (OH), dicarboxylic anhydrides (O=C–O–C=O), ketones (C=O), and sulfoxides (S=O) were identified in both binder blends and HMA. Last, the characteristic absorption bands associated with mineral aggregate component were determined. Figures 3.21 and 3.22 provide detailed spectra for a 40 wt% RAP-modified binder blend and a 80 wt% RAP-modified HMA, respectively. Of particular interest was an increase in the IR absorption for the oxidized functional groups, such as phenolics hydroxyl, carbonyl, and sulfoxide, as shown in Figure 3.23.

To quantify spectral changes attributable to RAP presence in binder blends, bands area for OH, C=O, and S=O functionalities were first valley-to-valley integrated within the limits

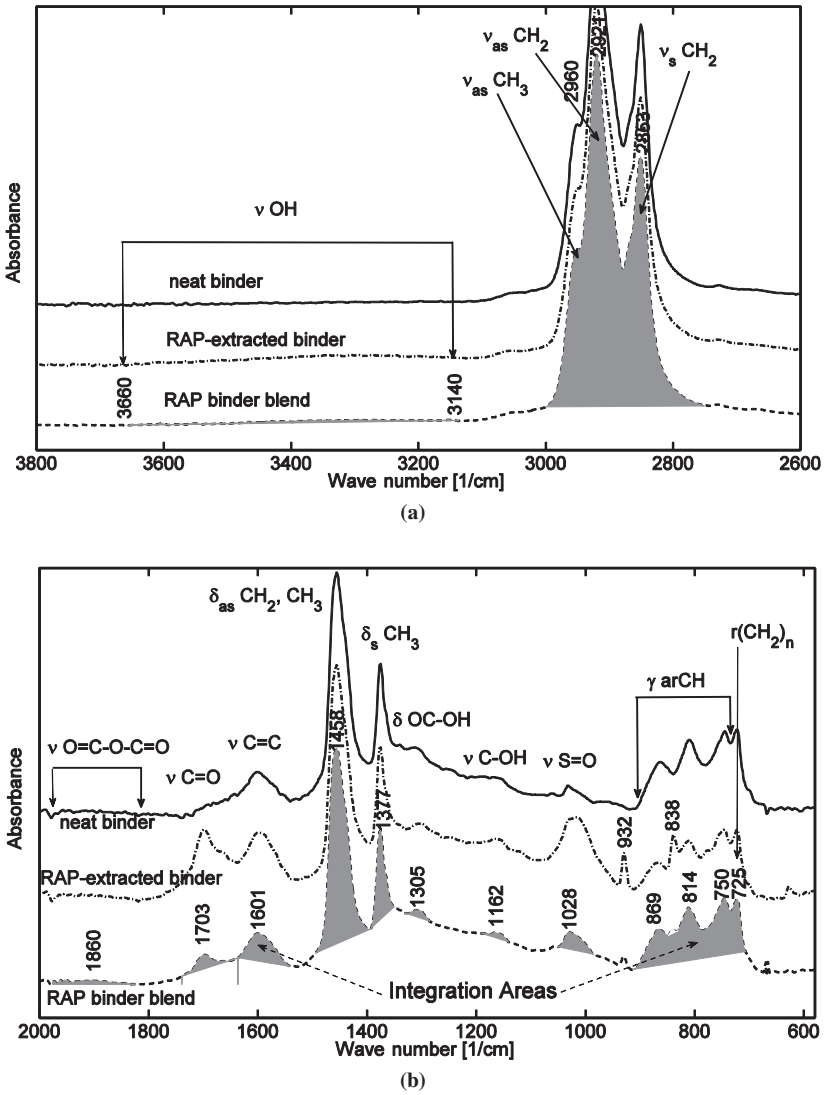

Figure 3.21. Comparison of ATR FTIR spectra of neat and RAP-extracted binders and their 60/40 blend (1).

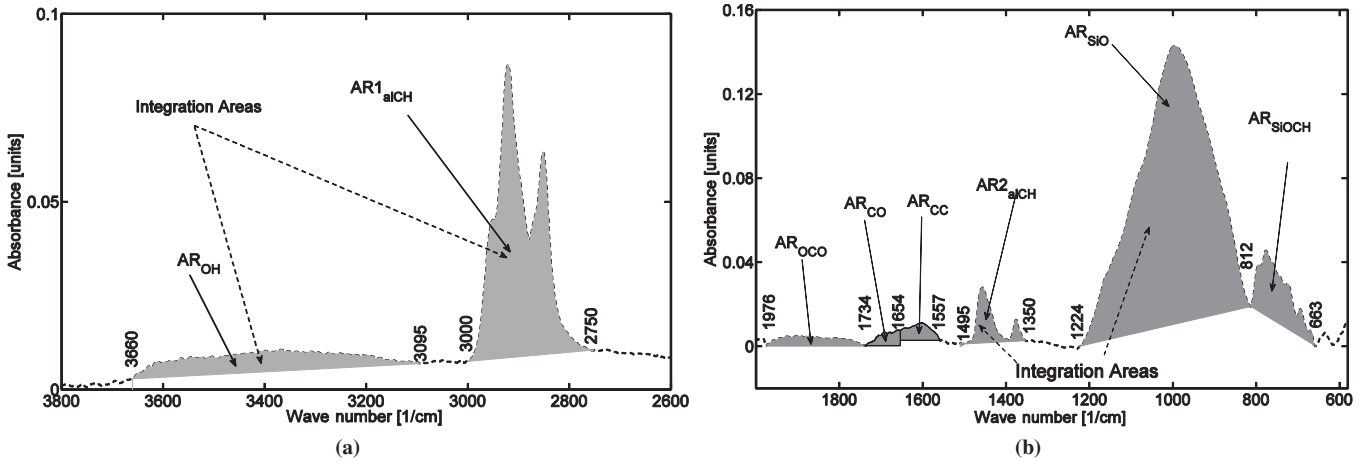

Figure 3.22. Typical ATR FTIR spectra of 80 wt% RAP-modified HMA mix (1).

shown in Figure 3.23. The individual integrated areas of the oxidized functionalities were then normalized to the sum of all band areas to calculate individual oxidation indices (*1*). A similar approach was implemented to a quantitative analysis of the RAP-modified HMAs. The only difference was associated with using SiO absorption band instead of S=O band because of their large overlap. Figure 3.23 supports justification of such an approach by showing a steady increase in OH, C=O, and SiO absorption intensity with an increasing RAP content in HMA.

On the basis of the multiple correlation analysis of the oxidation indices against RAP content (C_RAP), two best-fit linear models with a similar goodness of fit (R^2 of 0.97 to 0.98) were developed. The first model (Equation 3.2) where only the sulfoxide index (I_{SO}) is used for prediction yields slightly better standard error, while the second model (Equation 3.3) accounts for all major oxidation products using sum of hydroxyl, carbonyl, and sulfoxides indices (I_{OH}+ I_{CO}+ I_{SO}) as a predictor. The two models produced similar standard error of 5% to 7%.

$$C\_RAP = -0.236 + 0.400 I_{SO} \quad (3.2)$$

$$C\_RAP = -0.095 + 0.190\left(I_{OH} + I_{CO} + I_{SO}\right) \quad (3.3)$$

The evaluation of the effect of RAP content on the oxidation level in RAP-modified HMA samples revealed significant deviation from the linearity and higher variability for carbonyl index. Nevertheless, the correlation analysis suggested both carbonyl index and its combination with silicate index as an independent variable being the best candidates for predicting RAP content in HMA. The linear prediction models in Equations 3.4 and 3.5 yielded R^2 values of 0.72 and 0.86 with standard errors of 15% and 11%, respectively.

$$C\_RAP = -0.191 + 1.117 I_{CO} \quad (3.4)$$

$$C\_RAP = -1.48 + 0.76 I_{CO} + 0.025 I_{SiO} \quad (3.5)$$

Two reasons would explain a lower agreement in prediction models in HMA. First, a much higher standard error for HMA data as compared with binders' data is mostly governed by nonuniformity of replicate samples because of variation in particle size. Second, there can be a lack of interaction between binder adsorbed to RAP particles and the virgin binder.

In summary, it can be recommended to use ATR measurements of the IR absorption oxidized functional groups in RAP binder blends to predict RAP content in the field samples using the following step-by-step procedure:

Step 1. Extract binder from a representative pure RAP sample.
Step 2. Obtain a representative sample of a virgin binder.
Step 3. Perform ATR measurement and calculate OH, CO, and SO indices for both virgin and pure RAP binder samples as described above and elsewhere (*1*).
Step 4. Determine intercept and slope of the calibration line from the plot of sum of oxidation indices versus 0% and 100% RAP content.

It should be noted that it is necessary to have a pure RAP sample for developing concentration model. Furthermore, it is understood that a given model is applicable only for a given RAP source. Finally, it is found to be feasible to detect elevated oxidation level in RAP-modified HMAs; however, the quantification of RAP in HMA based on the ATR measurements appears to be impractical.

Reliability of Portable Spectroscopic Measurements

The repeatability and reproducibility of test results or the most successful material–method combinations were evaluated in both laboratory and field environment. The evaluation of

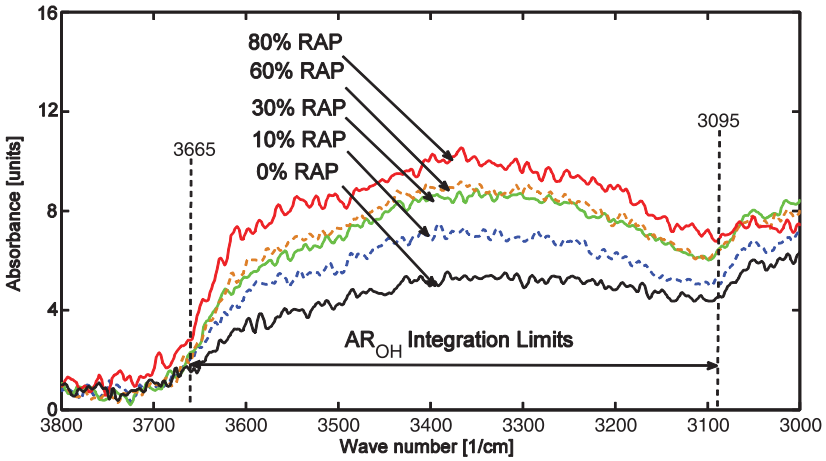

(a)

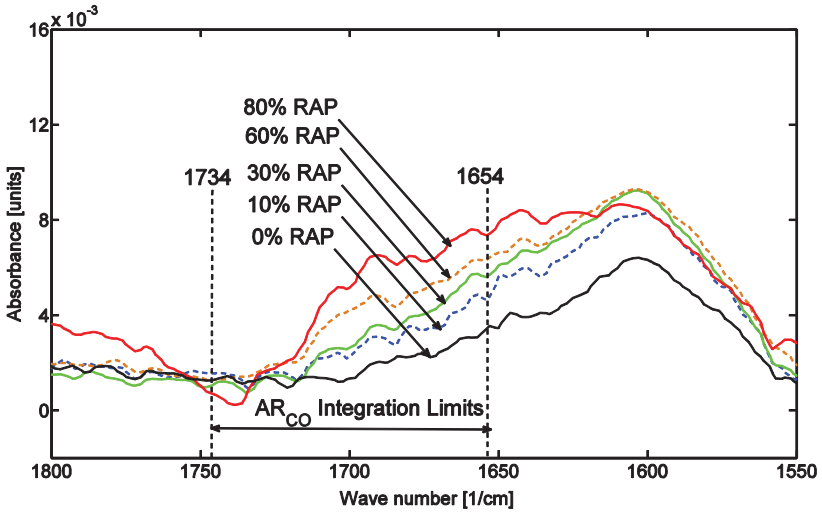

(b)

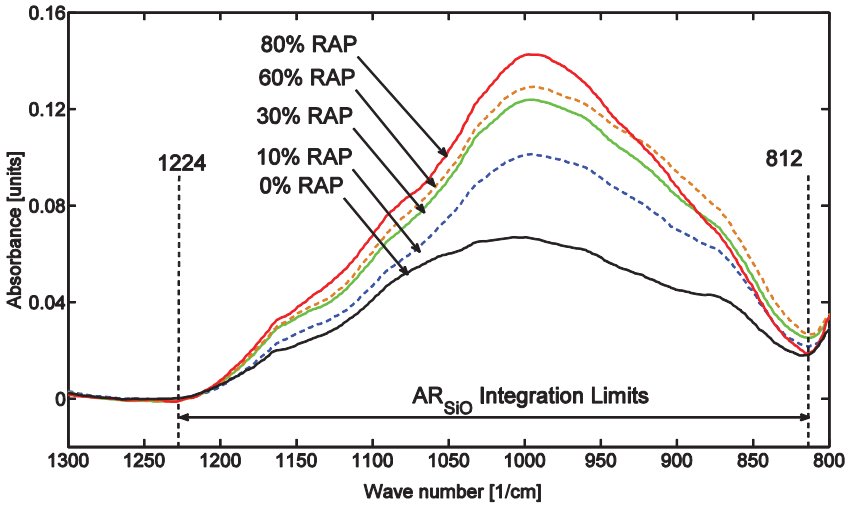

(c)

Figure 3.23. Integration limits for (a) hydroxyl (AR_{OH}), (b) carbonyl (AR_{CO}), and (c) silicate/sulfoxide (AR_{SiO}) absorption bands (1).

repeatability concerned the variation in measurements taken by a single operator or instrument on the same item and under the same conditions. The reproducibility of test results was judged by the level of variability in the results measured by independent operators on the same equipment. The repeatability was measured by the coefficient of variation (COV) in the absorbance of the primary components (major peaks) between the probes produced by one operator. The reproducibility was evaluated by COV in mean absorbance between the independent operators who tested the same material. It should be noted that because of the schedule constraints, only a limited number of materials were included in the repeatability and reproducibility study, as summarized below. The main findings of the variability study are separately discussed for portable ATR and XRF/XRD instruments, while the details are provided in Appendix P.

Variability in Attenuated Total Reflectance Results

The first round of ATR testing indicated that repeatability of FTIR results for pure materials and components and simple compounds (i.e., those materials that can be easily fingerprinted) was not an issue. The repeatability of the FTIR results for the materials and components of known composition was high, with variation not exceeding 5% of the absorption peak intensity. This did not apply to complex mixtures where phase separation was possible or the concentration of additive was extremely low. The effect of difference in sample preparation was also a concern. Therefore, the second round of testing in the repeatability and reproducibility study concerned composite materials, such as structural coating systems, pavement markings, portland cement concrete with admixtures, and polymer-modified binders. All those products were prepared in the lab according to the proportions as summarized in Table 3.8. More details on the variability in ATR measurements on particular materials are provided in Appendix P. The conclusions from the variability study follow.

Epoxy Paints

On the one hand, as shown in Tables P.2 and P.3 in Appendix P, repeatability (within-variation) of the ATR results for epoxy paints was comparable with their reproducibility (between-variation) and remained within 3% to 10% for major paint components. On the other hand, the within-variation in solvent-associated IR absorption could reach 25%. Furthermore, no difference between within-variations and between-variations suggested that no operator dependence was a factor of variability in the ATR measurements on liquid paint sample. It was noted, however, that the variation in the pressure applied to a sample placed on the ATR crystal before scanning significantly affected the absorbance values obtained for spectra of hardened epoxy-based pavement markings. This could be explained by the stiffness of the epoxy film preventing full contact between the sample and ATR crystal, thus reducing the

Table 3.8. List of Materials Tested by ATR FTIR in the Reproducibility and Repeatability Study

Material Category	Brand/Material Name	Composition	Material State	Test Objective
Structural coatings	Carbozinc 859	2 PartA:1 PartB: 10 Filler	Powder	Reproducibility study
	Scotchkote	1 PartA:1 PartB	Solid	Reproducibility study
Pavement markings	3M White	100% Ready	Liquid	Reproducibility study
	Epoplex LS50 Yellow	2:PartA:1 PartB	Solid	Reproducibility study
PCC with admixtures	Lafarge Type 2 cement/local aggregates/AIR 200/Eucon Retarder 75	8.0% water 17.0% cement 31.9% stone 35.2% sand 0.2% AIR 200	Wet mix	Repeatability study
	Lafarge Type 2 cement/local aggregates/Eucon Retarder 75	8.0% water 17.0% cement 31.9% stone 35.2% sand 0.3% AIR 200	Wet mix	Repeatability study Reproducibility study
Polymer-modified asphalt binders	PG 64-22 modified by Kraton SBS	PG 64-22 East + 1% SBS PG 64-22 East + 3% SBS PG 64-22 East + 6% SBS PG 64-22 West + 1% SBS PG 64-22 West + 3% SBS PG 64-22 West + 6% SBS	Viscous solid	Repeatability study

signal intensity. This observation was reflected in developing a test procedure for pavement markings by recommending of the use of pressure applicator with solid samples as a general rule for ATR testing.

Portland Cement Concrete with Chemical Admixtures

The coefficient of variation for three replicates of air-entrained PCC prepared in the same proportions varied between 10% and 40%, as shown in Tables P.4 and P.5 in Appendix P. This was eventually attributed to the nonuniform water content in the samples, nonhomogeneity of PCC in general, and extremely low (0.4 to 0.5 wt%) concentration of an additive within a sample. It was also found that the variability in the concentration of major absorption bands was inversely proportional to the concentration level. In spite of a similarly high level of variability in ATR measurements on the field samples, the identification of presence of high-range water reducer and nonchloride set accelerator in the fresh PCC samples still was possible.

Polymer-Modified Asphalt Binders

The case of polymer-modified binders represented more homogeneous mixtures. Consequently, the variation in the concentration of the major component (binder) as measured by the ATR FTIR did not exceed 5%. However, the variation in oxygen content (ketones and sulfoxides) and polymer content (SBS) reached 30% (see Table P.6 in Appendix P). It was also found that the variability in the signal associated with additives and functional groups increased proportionally to their concentration in a sample. This phenomenon can be attributed to the nonuniform oxidation during the storage of binder samples. Another reason could be a nonuniform distribution of the polymer network within the binder phase, which may occur because of differences in sample preparation.

On the basis of the analysis of variability in ATR measurements in this study, it can be concluded that repeatability of the results within the same batch or sample of a simple compound is not a concern. However, sample preparation and handling are the main factors of the variability in the ATR results obtained from different samples of a complex mixture. Therefore, while definitely being suitable for fingerprinting pure materials and simple compounds, the ATR FTIR spectrometer cannot be positively recommended for quantitative analysis under the field conditions.

Variability in X-Ray Fluorescence Results

A two-step approach was adopted for the analysis of variability in XRF measurements. Single measurements were first employed to establish proof-of-concept that XRF can yield measurable results for each material. When an element was detected in prominent concentrations that would not likely have interferences from other field materials and were significantly higher than the method detection limit, XRF was considered a promising QA/QC method. In the next step, 10 measurements were obtained for each material to determine the precision of the method. Because the portable XRF device owned by the research team was deemed to be successful to different extents in the evaluation of epoxy structural coating systems and pavement markings, only the results for these materials are summarized below. A more elaborate discussion of the XRF results is provided in Appendix P.

Several replicates of each mix were investigated for both the error associated with preparing different mixes and the variability within a single mix. The mixtures were prepared in the laboratory in accordance with manufacturer guidelines (see Tables P.7, P.9, and P.11 in Appendix P). Next, 10 probes from a sample batch were compared to establish mean and standard deviation in concentration of major metal oxides. Both soil and mining modes produced highly repeatable measurements (within 5% variation of mean), of Ti for epoxy paints as shown in Tables P.10, P.12, and P.13 in Appendix P. Field measurements on white and yellow pavement markings prepainted on the asphalt surface yielded slightly higher but still acceptable standard deviation of about 11% of the mean Ti content (see Tables P.2 through P.5 in Appendix P). In conclusion, the portable XRF owned by the team produced highly reliable results for heavy metal content in metal-based paints.

Portable Versus Stationary Results

One objective of the laboratory phase of the experiments in this project targeted the comparison between portable and stationary spectroscopic instruments. The instruments were compared for detection limits and method precision. Two spectroscopic methods for which both portable and stationary equipment was available were infrared spectroscopy and X-ray diffraction technique. The most important findings follow, while more details on the comparison between portable and stationary IR and XRD measurements are provided in Appendix P.

Portable Versus Stationary Infrared

A direct quantitative comparison of the FTIR spectra produced by the portable ATR FTIR and stationary transmission IR spectrometers was not possible because of the differences in technology and sample preparation. Nevertheless, the qualitative assessment of the absorbance spectra produced by both methods revealed that both devices identified major absorption

bands for a given material at the same wavelength (see Figures P.1 and P.2 in Appendix P). Note that two types of samples, liquid paint and solid binder, were evaluated. Therefore, it was concluded that the portable ATR FTIR spectrometer is capable of producing at least the same quality of IR spectra as the stationary IR spectrometer.

Portable Versus Stationary X-Ray Diffraction

Samples of crystalline materials such as portland cement, mineral aggregates, and ready-mixed concrete were tested by portable and stationary XRD instruments. The spectra of these samples are compared in Appendix P in Figures P.3 through P.8, while the quantitative results are summarized in Tables P.16 through P.21. It appeared that the stationary XRD equipment provided better results for resolution then the portable XRD, especially when longer scanning times were employed. Nonetheless, the portable instrument was successful in identifying all major phases qualitatively. The quantitative analyses yielded some discrepancy between the stationary and portable equipment but remained within reasonable error. The largest obstacle would be that the software statistics showed that the portable XRD equipment had a signal-to-noise ratio too low to trust the numerical goodness of fit. Therefore, the investigation of heterogeneous materials, such as natural aggregates and concrete, showed that it is not practical to apply the XRD method in the field for QA/QC purposes.

Field Verification of Laboratory Results

This section briefly summarizes the outcomes of the final phase (Phase 3) of this project: field verification of the laboratory results. It describes the scope of work and provides the conclusions. The full report of the field verification phase can be found in Appendix Q.

Objectives and Scope

The main goal of field experiments was to verify the applicability of portable equipment identified as successful in laboratory to the testing of construction materials in field conditions at a level of quality that satisfies current QA/QC criteria. Effectively, the following were the objectives for field experiments in Phase 3:

- Conduct field testing to demonstrate that the spectroscopic techniques recommended in Phase 2 can be transferred to field application.
- Document all test procedures and protocols for the successful techniques and applications.
- Recommend reasonable modifications to the equipment for improved implementation of the technologies.

Table Q.1 in Appendix Q summarizes project types, locations, and labor and equipment details for the field experiments conducted in Phase 3.

Field Experimental Protocol

The portable devices recommended for field verification were the Bruker ALPHA spectrometer with a single-reflection diamond ATR accessory, the Innov-X Alpha XRF analyzer, and RTA's Fourier transform Raman spectrometer. These instruments are described in detail in Appendix A. The field setup for the three devices included using an independent power source (built-in for Raman and XRF and external battery for ATR). The Raman analyzer was equipped with an extended 5-m-long probe, which allowed for taking measurements directly from the surface if needed. Typically, the ATR and Raman spectrometers were set in the trunk of a minivan and connected to a laptop and an external battery. The XRF instrument with a built-in personal digital assistant was used in the handheld mode by attaching the scanner to the tested surface.

As a rule, no sample preparation was necessary for any material except using DCM solvent to extract PMB from HMA. The ATR sampling mode was used for substances in liquid, thin film, or powder form, such as paints, chemical admixtures to PCC, asphalt binders and emulsions, and cement mortars. To obtain spectra for those materials, several drops of a liquid or approximately 0.5 g of a solid were placed on the ATR sampling plate and 24 co-averaged scans were collected at a resolution of 4 cm^{-1}. In the case of thin films and powders, pressure was applied to the sample to ensure full contact with the ATR prism surface.

The portable Innov-X Alpha XRF analyzer owned by the team was used for testing traffic paints in field applications. Exchangeable alloy, soil, and mining measurement modes allowed for the detection of typical heavy metal concentrations in both liquid (laboratory tested) and solid (in situ tested) paint samples. To obtain concentration quantities, cured pavement markings were tested by applying the XRF instrument to the surface and collecting data over 90-s time intervals. Liquid paint samples were collected from the tank and tested in the laboratory (on arrival from the field) in their as-received state by placing 15 to 30 g of each sample in an XRF sample holder.

Field measurements of Raman spectra of traffic paints, curing compounds, and chemical admixtures to PCC were recorded using RTA's Fourier transform Raman spectrometer operating at 1,064-nm laser excitation at 500 mW. Resolution was set at eight wave numbers (cm^{-1}) for all collections. Collection was performed using RTA's FTIR software operating in continuous collection mode. A 5-m, steel-jacketed, fiber-optic probe was used for collection. Given the potential interference of ambient light, spectral analysis consisted

Table 3.9. Summary of Portable Equipment Evaluation

Feature[a]		Target Value	FTIR	Raman	XRF	XRD
Accuracy	Minimum	1%	<0.5%	<2%	<1%	<1%
	Goal	<0.5%				
Duration of measurement	Maximum	1 h	~1 min	~1 min	6–12 min	15 min
	Goal	~5 min				
Effort involved	Maximum	1 person	1 person	1 person	1 person	1 person
	Goal	1 person				
Amount of prior training	Maximum	1 day	1 h	1 h	1 h	1 h
	Goal	0.5 day				
Reliability	Minimum	Depends on material (90%)	99% (software failure)	Depends on material[c]	99% (software failure)	99% (software failure)
	Goal	95%				
Time to get results	Maximum	Depends on construction process (1 h)	~5 min	~5 min	~5 min	~5 min
	Goal	~5 min				
Price range	Maximum	$50,000	~$25,000	~$60,000	~$37,000	$45,000
	Goal	<$20,000				
Device weight	Maximum	50 lb	~16 lb	~20 lb	~4 lb (handheld) ~15 lb (benchtop)	~27 lb
	Goal	<20 lb				
Sample preparation	Maximum	Solvent	As is[b]	As is[b]	As is (liquids) pulverization (solids)[b]	Crushing (solids)
	Goal	As is[b]				

[a] *Accuracy:* Agreement between a measurement and the true or correct value.
Duration of measurement: Time between start and end of testing cycle.
Effort involved: Personnel required to perform the test.
Amount of prior training: Time required to make personnel familiar with a testing procedure.
Reliability: Unlikelihood of equipment failure during the test.
Time to get results: Time between the beginning of the sample preparation and the end of the analysis of the test results.
Price range: Cost of the equipment.
Device weight: Mass of the equipment including the case or enclosure.
Best time for QA/QC: Stage of the manufacturing and application process when the test is most timely.
Sample preparation: Processing and manipulating the material before the test.
Minimum and maximum: Acceptable threshold value from the user perspective that given equipment should produce.
Goal: Desirable target value from the user perspective that given equipment should produce.
[b] Pulverization of granular materials (aggregates) is required for better quality.
[c] Failure to get the signal for fluorescent materials or because of thermal emission.

of first evaluating those contributions and determining the appropriate background removal techniques to yield spectra consistent with those of controlled laboratory conditions.

Summary of Field Results

A summary of the field results follows.

1. On the basis of the results of the field verification experiments, it can be concluded that, predominantly, the experiments conducted in the field phase of this project verified the methodology and reproduced the results similar to those in the laboratory phase.
2. Specifically, the compact ATR FTIR spectrometer, handheld XRF instrument, and RTA's Raman analyzer were successful in the identification of chemical structure, or fingerprinting, of both simple and complex organic compounds, such as epoxy coatings and adhesives, curing compounds, and waterborne traffic paints.
3. Furthermore, such complex composite material as PCC yielded meaningful ATR absorbance spectra, which allowed for the identification of chemical admixtures in fresh mix samples, provided their concentrations were higher than 0.5 wt%.
4. Verification of polymer presence in asphalt binders and emulsions was possible using the ATR FTIR spectrometer. While identification of polymer in an HMA mix presented a challenge, the fast binder extraction procedure in the field with using DCM solvent appeared to be a feasible alternative to direct evaluation of polymer-modified HMA.
5. Although successful in fingerprinting pure materials, RTA's Raman analyzer demonstrated some safety issues, due to potential damage to the operator's eye by open laser light beam and issues with handling the Raman probe when not in the collecting mode.

Summary of Technical Performance of Portable Instruments

This section summarizes the results of the technical evaluation of the portable spectroscopic devices. The evaluation concerned the ability of portable FTIR, Raman, XRF, and XRD devices to comply with qualitative and quantitative requirements of field QA/QC procedures. The qualitative and quantitative requirements were accuracy, time, and labor involved in testing; level of training required; and other parameters. These requirements were established in the preliminary phase of the project based on the feedback of the professionals who participated in the workshop organized by the team. Table 3.9 compares the actual parameters achieved in the laboratory and in the field with the target values. As shown in Table 3.9, all devices evaluated in this study comply with the previously established technical criteria, suggesting that the team chose the equipment correctly. However, final recommendations for the use of these instruments are based on their success in producing reliable and interpretable results that can be used for QA/QC purposes on a daily basis.

Reference

1. Yut, I., and A. Zofka. Spectroscopic Evaluation of Recycled Asphalt Pavement Materials. Presented at 91st Annual Meeting of the Transportation Research Board, Washington, D.C., 2012.

CHAPTER 4

Conclusions and Suggested Research

This chapter presents conclusions on the applicability of portable spectroscopic devices to conducting QA/QC for common construction materials. In addition, the chapter briefly discusses the deliverables of the project, followed by suggestions for further research.

Applicability of Portable Spectroscopic Equipment to Field Evaluation of Construction Materials

The primary objective of this project was to identify the most practical applications of spectroscopic techniques to a wide range of materials commonly used in transportation infrastructure. To identify the needs for spectroscopic testing among the SHAs and to develop feasibility criteria, the SHRP 2 coordinators from 50 states were surveyed and a workshop with experts from both SHAs and the industry was held. A list of construction materials and desired testing and equipment parameters were developed to rank the feasibility of the spectroscopic techniques for laboratory and field evaluation.

Two potential outcomes for spectroscopic testing were identified: (1) verification of the chemical composition (if provided by the manufacturer) or determination of the signature spectrum for pure materials and compounds and their components, and (2) detection and, if possible, quantification of additives and contaminants in a material. The spectroscopic techniques evaluated by the project team in the laboratory testing phase (Phase 2) included ATR FTIR spectroscopy; size-exclusion GPC; NMR; XRF; and XRD. The materials analyzed were epoxy coatings and adhesives, traffic paints, portland cement concrete with chemical admixtures and curing membranes, asphalt binders, emulsions, and mixes with polymer additives. On the basis of the laboratory experiments, portable ATR, XRF and Raman instruments were recommended for field evaluation.

The field phase of the project confirmed that a compact ATR FTIR spectrometer was the most successful device to fingerprint all pure chemical compounds (i.e., epoxies, waterborne paints, polymers, and chemical admixtures) and to detect additives or contaminants with concentration of 0.4 wt% and higher in complex mixtures (i.e., portland cement concrete, asphalt binders, emulsions, and mixes). In addition, ATR was successful in quantifying polymer additives in asphalt binders and water–solvent content in paints at concentrations >0.5 wt%, based on developed calibration curves. ATR generally did not require sample preparation and the major source of error was sample heterogeneity, given the very small amount of material used for analysis. Thus sampling procedures should ensure that the chosen sample and the surface exposed to the infrared beam are representative of the bulk material.

On the basis of the field results, the project team found that a handheld XRF instrument may be used to conduct QA/QC of epoxy coatings and traffic paints based on the concentration of major metals in the pigment (Ti or Zn). In other words, the Ti content may be used as an indicator to determine the purity and quality of the paint, whether it has been thinned out with solvent or mixed with other materials. XRF results are a function of the water content of the material, which needs to be taken into account when establishing QC criteria under lab settings. It is recommended that QC criteria for approved material brands are developed by state laboratories, given that manufacturer specifications are typically too broad and not specific to the physical state of the material.

Raman analysis was successful in fingerprinting pure, nonopaque liquid samples both in the lab and in the field. However, some safety issues were identified, specifically potential damage to the operator's eye by open laser light. In addition, the price of the Raman instruments available on the market considerably exceeds the target cost established in this project ($75,000 as compared with the maximum target cost of $25,000). Therefore, portable Raman instruments are not recommended for use at field conditions.

Finally, spectroscopic evaluation of construction materials is a challenging task, especially when dealing with non-uniform materials or additives at small concentrations. In such cases, more work is needed beyond this project to develop robust and universal procedures.

Project Deliverables

Electronic Spectral Library

A library of spectra for pure materials was created. This library can be used for the identification of those materials in the field. The database will supplement the standards developed under this project and can be potentially available online for QA/QC specialists. The electronic copy of the spectral library is located at www.trb.org/Main/Blurbs/167279.aspx.

Draft AASHTO Standards

During the laboratory and field spectroscopic experiments, generic testing procedures with sampling and data analysis guidelines were developed for the ATR, Raman, and XRF applications to liquid and solid material samples. The most successful generic procedures were expanded to the draft AASHTO standard specifications as follows:

- Identification of water-reducing, -accelerating, and -retarding chemical admixtures in fresh portland cement concrete by attenuated total reflection infrared spectrometer; and
- Standard method of test for determination of titanium content in traffic paints by field-portable X-ray fluorescence spectroscopy.

The AASHTO standards provided in Appendix C are designated for the QA/QC personnel and research and material divisions in the SHAs. They can be added to their special provisions or construction specifications.

Field Operation Manuals

On the basis of the experience collected throughout this project as well as the feedback received during the field phase, the research team prepared two separate field operation manuals for ATR and XRF instruments. These manuals target technical personnel designated by a transportation agency for the spectroscopic testing. The manuals will help the testing personnel to undertake correct steps during spectroscopic testing and will provide more concise instructions as opposed to typical generic manuals provided by the manufacturers.

Further Research

A limited range of portable spectroscopic instruments was evaluated in this study because of time and budget constraints. For instance, neither truly handheld FTIR nor portable time-domain NMR devices were available to the research team. However, the research team believes that the former device can be potentially used on construction sites, especially for the analysis of asphalt and concrete products, while the latter device can allow for the elucidation of practically any organic material structure. In addition, portable gas chromatographs can potentially yield success in evaluation of contaminants and polymer additives in asphalt products. Therefore, further research is suggested with use of handheld FTIR, portable time-domain NMR instruments, and portable gas chromatographs, especially when their costs become more affordable to SHAs. Finally, the research team anticipates that Raman instruments will be upgraded to prevent thermal emission and operator hazard, which will facilitate their use in construction applications.

APPENDIX A

Laboratory Equipment and Testing Protocols

This appendix describes the spectroscopic equipment and testing protocols used in the laboratory testing portion of this project. The testing protocols include procedures for the preparation of samples, acquisition of data, and interpretation of results. The following spectroscopic methods were included in the laboratory evaluation:

- Fourier transform infrared (FTIR) spectroscopy;
- Raman spectroscopy;
- X-ray fluorescent (XRF) spectroscopy;
- X-ray diffraction (XRD) spectroscopy;
- Gel permeation chromatography (GPC) with evaporative light-scattering detectors (ELSD) and ultraviolet (UV) detectors; and
- Nuclear magnetic resonance (NMR).

The following is a detailed discussion of these methods and their corresponding experimental protocols.

Fourier Transform Infrared Spectroscopy

A comprehensive literature search conducted in Phase 1 of the project identified FTIR spectroscopy as one of the most promising spectroscopic methods for "fingerprinting" construction materials. Therefore, a careful evaluation of FTIR spectrometers was included in the laboratory phase. The team employed two different FTIR devices in its testing. The first device, a portable Bruker ALPHA attenuated total reflectance (ATR) FTIR spectrometer owned by the research team, tested all of the materials and material components listed in Table A.1. Concurrently, the team used a stationary Nicolet Magna 560 FTIR spectrometer located in the Institute of Material Science (IMS) of the University of Connecticut (UCONN) to examine the same materials. A comparison of the results from the portable and stationary FTIR equipment allowed the team to verify the reliability of the former device and recommend it for further evaluation in the field phase of the project. More details on both devices are given below.

Portable Bruker ALPHA Attenuated Total Reflectance Fourier Transform Infrared Spectrometer

Equipment Setup

The ALPHA FTIR device by Bruker Optics (Figure A.1) has dimensions of 22 × 30 × 25 cm and weighs about 7 kg. It is able to analyze a spectral range from 7,500 cm^{-1} to 375 cm^{-1} with a spectral resolution of at least 2 cm^{-1} (0.9 cm^{-1} is optional) and an accuracy of 0.01 cm^{-1}. The device is designed to operate at 18°C to 35°C and is powered by 100 to 240 V AC or by a high-capacity battery. Software, including a comprehensive library of chemical components, is provided with this device. The exchangeable measurement modules include transmission, ATR, and reflection, making it possible to analyze a range of materials (liquid, solid, or gas). The team used the following settings in their laboratory testing:

- A laptop PC with OPUS 6.5 infrared (IR) spectroscopy software was provided by Bruker Optics.
- The ATR mode was used to acquire the infrared spectra for all materials and their components.
- The spectra for each material and component were obtained in the range from 4,000 to 400 cm^{-1}, where most of the chemical components yield detectable absorbance.
- The spectral resolution was set to 1.5 cm^{-1}.
- Twenty-four scans were run for each sample.
- Ambient temperatures during testing ranged between 20°C and 23°C.

The team decided to use the ATR cell because, in most cases, it does not require any special sample preparation and also allows for a quick determination of the sample's spectra

Table A.1. Finalized List of Materials to Be Tested in Phase 2

Material Category	Brand	Manufacturer	Number of States Approving the Material	Original State (Liquid, Solid, Powder, Other)	Information on Chemical Composition Available (Yes/No)
Structural coatings	Scotchkote	3M	19	Epoxy	Yes
	Carbozinc 859	RPM International Inc.	18	Epoxy + powder	Yes
Traffic paints	LS50	Epoplex	19	Epoxy	Yes
	All Weather HB-R1	3M	12	Liquid	Yes
Epoxy adhesives for concrete repair	Sikadur	Sika Construction	20	Epoxy + liquid	Yes
	Ultrabond 1100	Adhesives Technology Corporation	14	Epoxy + powder	Yes
Portland cement	Type 1, 2, and 3 cement	Lafarge North America	25	Powder	Yes
	Type 1, 2, and 3 cement	LeHigh	23	Powder	Yes
Portland cement concrete (PCC)	Local	Tilcon	5	Solid	Yes
Air-entraining admixtures for PCC	Air Mix 200	Euclid Chemical	25	Liquid	Yes
Accelerating/retarding admixtures for PCC	Eucon Retarder 75	Euclid Chemical	26	Liquid	Yes
	Accelguard 80	Euclid Chemical	14	Liquid	Yes
Water reducers/plasticizers for PCC	ADVA 190	W. R. Grace	23	Liquid	Yes
Curing compounds for PCC	Sealtight 1100-CLEAR	W. R. Meadows	13	Liquid	Yes
	Safe-Cure 1200	ChemMasters	9	Liquid	Yes
Hot-mix asphalt concrete	Local	Tilcon–Oldcastle Company	5	Solid	No
Asphalt binders	PG 58-28	NuStar	NA	Viscous liquid	No
	PG 64-22	NuStar	NA	Viscous liquid	No
	PG 64-28	NuStar	NA	Viscous liquid	No
	PG 70-28	NuStar	NA	Viscous liquid	No
	PG 76-22	NuStar	NA	Viscous liquid	No
	PG 76-34CR	NuStar	NA	Viscous liquid	No
	PG 64-28PPA	NuStar	NA	Viscous liquid	No
Polymer modifiers for binders	Elvaloy 4170	DuPont	NA	Granules	Yes
	D1101 (SBS)	Kraton	NA	Granules	Yes
	Butonal NX1138 (SB Latex)	BASF	NA	Liquid	Yes
Asphalt emulsions	CRS-1	All States Asphalt Group	18	Liquid	No
	CRS-1P	All States Asphalt Group	18	Liquid	No
Antistripping agents for asphalt concrete	Kling Beta 2912	Akzo Nobel	11	Liquid	Yes
	AD-here LOF 65	ArrMaz	12	Liquid	Yes
Reclaimed asphalt pavement	Local	Tilcon	50	Solid	No
Aggregate minerals	Local	Local quarry—Tilcon	NA	Solid	No

Note: NA = not available.

Figure A.1. Image of ALPHA ATR FTIR portable spectrometer.

without sacrificing the quality of spectrum resolution. The OPUS software accompanying the device is also user friendly and platform independent.

Test Sample Preparation

The research team tested the materials and components included in Phase 2 in their original physical state (as provided by manufacturer) (i.e., liquid, paste and emulsion, and solid state) (Table A.1). For the vast majority of materials, the samples required no special preparation. Liquid materials, such as structural and traffic paints, portland cement concrete (PCC) curing compounds, PCC chemical admixtures, and anti-stripping agents, were sampled using pipettes or syringes. A spatula was used to sample viscous liquids, such as epoxy pastes for concrete repair and asphalt emulsions, and viscous solids, such as asphalt binders and finely ground powders (e.g., portland cement and zinc filler for Carbozinc 859 structural coating system). A sample of each material and component was placed on the ATR diamond surface in an amount sufficient to cover the surface (several drops of liquid or approximately 1 g of solid). The following samples required a different preparation procedure: pellet samples [asphalt polymer modifiers, Kraton styrene–butadiene–styrene (SBS), and Elvaloy], granular materials (such as mineral aggregates and hot-mix asphalt mixes), and dry solid samples of epoxy-based paints. In these cases, pressure was applied to ensure full contact between the sample and the ATR diamond surface. Finally, in the case of rigid solid pavement markings (Epoplex LS), the sample size had to be reduced to fit the size of the ATR window.

Control Sample Preparation

The control is a sample of material with a controlled chemical composition that serves as a reference for the test samples. In cases where the quantification of a specific component's concentration in the designated mixture or solution was an objective (see Table A.2), several control samples were prepared by mixing the component of interest with the neat or original material in different proportions. The mixing procedures complied with the original procedure provided by the manufacturers to produce the designated material.

Testing Procedure

A typical FTIR testing procedure for any material included the following routines:

- Prepare control sample, if required.
- Obtain infrared spectrum of the control sample.
- Prepare test sample as explained above.
- Obtain infrared spectrum of the test sample.
- Compare the test sample spectrum with that of the control sample by using an appropriate method of analysis, as discussed in Chapter 2.

Nicolet Magna 560 FTIR Spectrometer

Equipment Setup

The Nicolet Magna 560 FTIR spectrometer (Figure A.2) is a research-grade benchtop size device operating in a wavelength range between 6,500 and 100 cm^{-1}. It provides a spectral resolution of 0.35 cm^{-1} with a sensitivity of 0.125 cm^{-1}. The device operates at room temperature in the ATR and transmission mode. The objective of using the stationary FTIR spectrometer was to verify the IR spectra acquired by the portable FTIR device. The following settings were used for Nicolet Magna 560 testing:

- The IR transmission window mode to obtain spectra for all material and components.
- The OMNIC software to analyze the signal.

Table A.2. Summary of Phase 2 Objectives for Material–Method Combinations

Material Category	Method	Objective
Structural coatings	FTIR, Raman, XRF, NMR, GPC	Verification of chemical composition Presence of solvents/diluents
Traffic paints	FTIR, Raman, XRF, NMR, GPC	Verification of chemical composition Presence of solvents/diluents
Epoxy adhesives	FTIR, Raman, XRF, NMR, GPC	Verification of chemical composition
Portland cement	FTIR, Raman, XRF, NMR	Verification of cement quality and type
PCC	FTIR, Raman, XRF, XRD	Verification of presence of admixture in PCC mix Quantification of content
Chemical admixtures for PCC	FTIR, Raman, XRF, NMR, GPC	Verification of chemical composition
Curing compounds for PCC	FTIR, Raman, XRF, NMR, GPC	Verification of chemical composition
Polymer additives for asphalt binders	FTIR, Raman, XRF, NMR, GPC	Verification of chemical composition
Polymer-modified asphalt binders	FTIR, Raman, NMR, GPC	Verification of chemical composition Quantification of content
Hot-mix asphalt concrete	FTIR, NMR, GPC	Detection of prohibited chemicals/modifiers (such as motor oil, diesel fuel)
Asphalt emulsions	FTIR, Raman, NMR, GPC	Type and water content
Antistripping agents in asphalt concrete	FTIR, Raman, NMR	Verification of presence in mixture Quantification of content
Oxidation in reclaimed asphalt pavement	FTIR, NMR, GPC	Verification of presence in mixture Quantification of content
Aggregate minerals	FTIR, XRF, XRD	Metal contamination Organic content

- The spectra for each material and component were obtained in the range of 4,000 to 400 cm^{-1} (the same as for the portable ATR FTIR).
- The spectral resolution was set at 2 cm^{-1}.
- Sixteen scans were performed on each sample.
- All spectra were acquired at room temperature.

Test Sample Preparation

The sample preparation procedures for the stationary IR transmission spectrometer differed from those of the ATR device (portable device). The transmission mode requires either putting the sample between two 25-mm-diameter potassium bromide (KBr) disks or mixing the sample with KBr powder. Accordingly, the following three alternative sample preparation methods were used:

1. Liquid and viscous solid–liquid samples (which include all materials except those mentioned below) were prepared by placing 100 μg of material between two 25-mm-diameter KBr disks.
2. Pellet samples (Kraton SBS and Elvaloy) were dissolved in 1 mL of tetrahydrofuran (THF) solvent as a 10 wt% solution and then dried on a 25-mm-diameter KBr disk.
3. Cured epoxy adhesive samples (Ultrabond 1100 and Sikadur 31) were prepared by mixing ground epoxy powder with KBr powder as a 5 wt% mixture. The mixture was then pressed as a KBr disk.

Control Sample Preparation

The control sample preparation procedure was the same as for the portable ATR FTIR device.

Testing Procedure

The testing procedure was the same as for the portable ATR FTIR device.

Raman Spectroscopy

The search conducted in Phase 1 identified Raman spectroscopy as a relatively promising spectroscopic method for evaluating construction materials. Although it was found that Raman technology has primarily been used on a narrower range of construction materials than the FTIR (mostly for portland cement–related products), it was decided that this method should be pursued for all materials

Figure A.2. Image of Nicolet Magna 560 FTIR spectrometer.

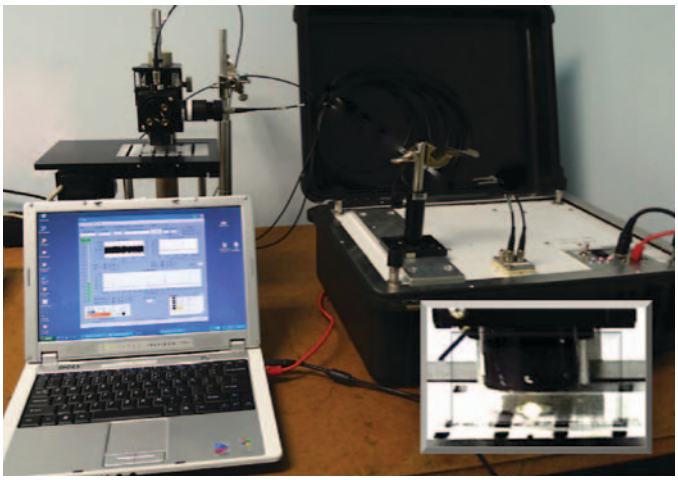

Figure A.3. Image of RTA's portable Raman analyzer.

included in the scope of this project. The reasoning behind this was to eliminate the least successful materials and focus on the feasible materials in Raman field testing in Phase 3. Therefore, samples of all materials were shipped to Real-Time Analyzers (RTA) for evaluation in their laboratory facilities. The following segments describe the equipment, sample preparation, and testing protocols used in Raman evaluation.

Real-Time Analyzers' Portable Raman Analyzer

Equipment Setup

RTA's portable Raman analyzer (Figure A.3) measures the entire Raman spectrum in each scan, from 3,350 cm^{-1} to 150 cm^{-1}, with a selectable spectral resolution between 2 and 32 cm^{-1}. According to the manufacturer's specifications, the device is capable of analyzing any solid or liquid in a very short amount of time (about 10 s) and comes equipped with software installed on a laptop computer. Additionally, it does not require any sample preparation or calibration. The portable Raman analyzer operates at temperatures from 2°C to 37°C and uses a 5-h rechargeable battery. This analyzer employs interferometry to generate the Raman spectrum, which eliminates the need for analyzer recalibrations. In Phase 2 of the project, the following settings were used in Raman testing:

- All spectra were collected using a 1,064-nm excitation source featuring a 500 mW IR laser.
- A default range was set in the IR region between 4,500 and 100 cm^{-1} with a spectral resolution of 3 cm^{-1}.
- Raman spectra were collected at room temperature using the laboratory bench probe (Figure A.3).
- RTA's RamanVista software was used for the analysis of spectra.

Test Sample Preparation

No sample preparation or conditioning was required for most of the materials. Samples were divided into small aliquots of a reasonable size for each material (i.e., drops for liquids and a small spatula for powders). Each aliquot was then placed on a microscope slide for Raman analysis. In some instances, an additional microscope slide was placed on top of the sample to minimize the evaporation of volatiles and provide a uniform upper surface for analysis by the downward-facing Raman probe (Figure A.3). The upper surface of glass also helped to conduct heat away from the sample, which was helpful when thermal emission from the laser heating became an issue. For asphalt binders, asphalt emulsions, and gels (e.g., Ultrabond 1100 Part B, Scotchkote Part B), solvent extractions (with hexane and methylene chloride) were performed to avoid the detrimental effects of heating or fluorescence excitation.

X-Ray Fluorescence Spectroscopy

A review of the applications of XRF spectroscopy to highway materials revealed that portable XRF devices have been available since the early 1990s for the analysis of the heavy metal concentration in certain substances (e.g., paints and soils). Therefore, the portable XRF device was included in the laboratory testing of metal-containing materials. The equipment setup and testing procedures are described in detail.

Innov-X Alpha XRF Analyzer

Equipment Setup

The portable Innov-X Alpha XRF analyzer (Figure A.4) owned by the team measures the concentration of the following

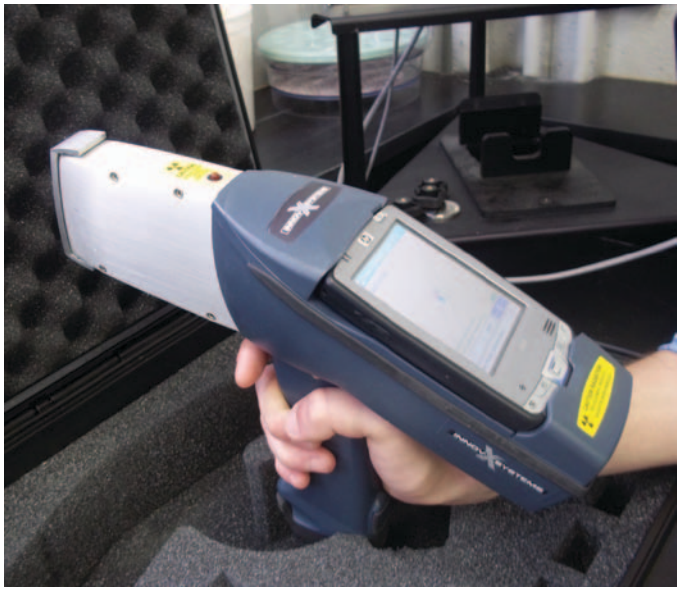

Figure A.4. Image of Innov-X Alpha XRF analyzer.

elements: P, S, Cl, K, Ca, Ti, Cr, Mn, Fe, Co, Ni, Cu, Zn, As, Se, Sr, Zr, Mo, Ag, Cd, Sn, I, Ba, W, Hg, and Pb. There are two separate calibration modes for this particular XRF: one mode for trace elements in soils (concentrations up to 8% to 10% by weight) and one mode for alloys and ores that have concentrations >1% by weight. However, the alloy mode can only measure elements heavier than Ti, so Ca, K, and other lighter elements can only be measured in relatively low concentrations using this equipment. Other portable XRF devices are available that can measure light elements in higher concentrations as well as capture Mg, Si, and Al, but the cost of these devices is higher (around $85,000).

Test Sample Preparation

The general sample preparation method for the XRF was as follows:

- Liquid samples, emulsions, and portland cement were tested in their as-received state by placing a 15 to 30 g of the sample in an XRF sample holder.
- Aggregates and solids were crushed and pulverized to pass through a U.S. No. 60 screen, in accordance with U.S. Environmental Protection Agency Method 6200.

X-Ray Diffraction Spectroscopy

In Phase 1, numerous studies were found to present XRD analysis as a good quantitative method for analyzing portland cement and its supplements. In addition, XRD was mentioned as a suitable technique for identifying the mineral components of aggregates. Therefore, XRD was included in the scope of laboratory testing in Phase 2 with the objective of evaluating the applicability of portable XRD devices. XRD was used to analyze PCC-related products and aggregates and to compare the performance of portable and stationary XRD systems. The following is a description of the XRD equipment and testing protocols used by the team in Phase 2.

Stationary Bruker-AXS (Siemens) D5005 Diffractometer

Equipment Setup

For stationary XRD analysis, the team used the Bruker-AXS (Siemens) D5005 diffractometer (Figure A.5) located in the facilities of IMS at UCONN. The diffractometer was equipped with a Cu source ($\lambda = 1.5418$ Å) and the X-ray tube was operated at 40 kV and 40 mA using a diffracted beam graphite-monochromator. The data were collected for scattering angles (2θ) ranging from 5° to 65° with a step size of 0.02° and variable counting times. The counting time affects the signal-to-noise ratio and the overall quality of the data. High counting times are desirable to lower the XRD detection limit and obtain good quantitative data, but the scanning time may become prohibitive for field applications. The required scanning time will also vary with the instrument type and the age of the X-ray tube. The scanning times varied between 2 s per step and 14 s per step. Samples were marked as LR (low resolution) when scanning times were less than 5 s per step and HR (high resolution) when the scanning time was more than 5 s per step. This enabled a comparison between the data quality of LR and HR samples. LR corresponds to approxi-

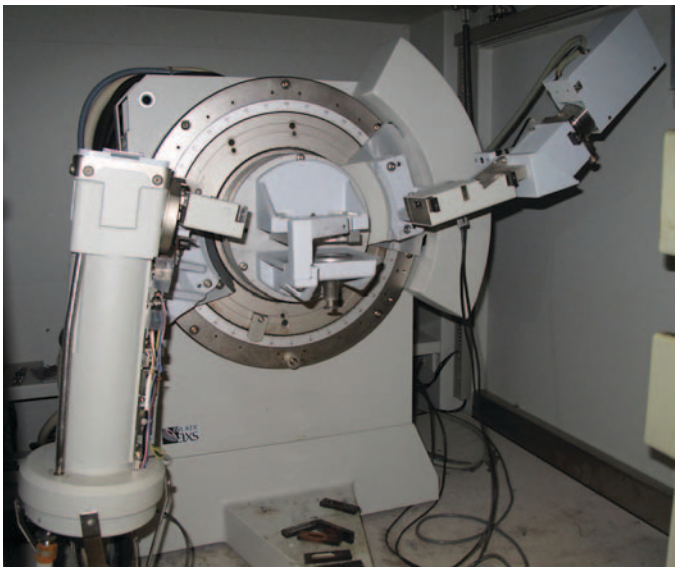

Figure A.5. Image of Bruker-AXS (Siemens) D5005 diffractometer.

mately 2 to 4 h of scanning time, while HR required 8 to 12 h of scanning time.

Qualitative and quantitative analysis of the XRD data was performed using Jade software, Version 8.5 (MDI, 2008), with reference to the patterns of the International Centre for Diffraction Data database (PDF-2, 2002) and the American Mineralogist Crystal Structure database (http://rruff.geo.arizona.edu/AMS/amcsd.php). The Rietveld method, using the whole pattern fitting function of Jade, yielded quantitative phase analysis (relative amounts of each substance).

Test Sample Preparation

For stationary XRD analyses, a subsample of 10 to 20 g was obtained from the material containers, placed in a Petri dish, and air-dried for 24 h as needed. The sample was pulverized to pass a U.S. 40 (0.425 mm) sieve. The pulverized sample was then manually homogenized and 1 g of the whole sample was pulverized to pass the U.S. 400 (38 μm) sieve. An aliquot of 0.8 g of the finely pulverized sample was mixed with 0.2 g of corundum (α-Al_2O_3), which was used as the internal standard for quantitative analysis. The corundum obtained from Sawyer was previously found to be 93% crystalline by comparing it with a National Institute of Standards and Technology ZnO standard (*1*). The Rietveld method provides a relative quantification of the identified crystalline compounds in an XRD sample. If a compound is either low in content, or disordered or amorphous, it will not be detected and thus the compound will not be quantified. In that case, the sum of the phases that cannot be detected in the XRD pattern are termed "amorphous" or "sample amorphicity." This leads to an overestimation of the observed crystalline compounds. By spiking the sample with a known amount of a crystalline material, it is possible to backcalculate the amorphous content, *A,* using Equation A.1:

$$A = \frac{I_R - I}{I_R(1 - I)} \qquad (A.1)$$

where I_R is the Rietveld-estimated quantity and I is the actual amount of the spiked mineral. A 20% corundum was used as the known spike.

Portable Terra XRD/XRF Analyzer

Equipment Setup

The portable XRD and XRF Terra analyzer is approximately the size of a briefcase (about 49 × 40 × 20 cm in dimensions and 14.5 kg by weight). The company inXitu developed this device for the identification of minerals and aggregate mixtures. According to the manufacturer, the system requires minimal sample preparation and detects single minerals or simple mixtures within minutes. The Terra analyzer provides an XRD resolution of 0.25° over the 2θ range of 5° to 55° and XRF resolution of 230 eV (at 5.9 keV) over the range of 2 to 25 keV. The device can operate in an autonomous mode for at least 4 h. A laptop computer allows the user to configure the analysis, preview live data, explore archive files, and download data for pattern matching with a mineral database using commercial software.

Test Sample Preparation

For the analysis of the portable XRD, the same samples were used as for the stationary XRD. The samples were shipped to inXitu headquarters in Campbell, California.

Gel Permeation Chromatography

Although GPC (with UV detectors and ELSD) was not identified as a portable spectroscopic method, it was found to be a successful analytical procedure for a range of materials, especially for asphalt-related products. Assuming that the benchtop device can potentially be fitted into a mobile laboratory, the team decided to include GPC in Phase 2 testing and evaluate its applicability to fingerprinting the construction materials within the scope of this project. The Waters 410 GPC system located in IMS at UCONN was used for the evaluation, as discussed below.

Waters GPC System

Equipment Setup

Waters GPC has a horizontally placed column (Figure A.6) with the stationary phase (gel) placed in a cylindrical tube. The sample (diluted in solvent) is injected into the column, and a UV or light-scattering detector measures the change in the absorption of light as the fractionated material exits the column. The separated components of the material can then be further analyzed by coupling the chromatographic column with a detector that identifies each compound separately. The system is able to resolve over a molecular weight range of 100 to 250,000 Da, with a precision of 1% to 3%. The following GPC procedural settings were used in laboratory testing:

- THF was used as the eluent with a flow rate of 1 mL/min at 35°C.
- Typical test lasted for 35 min.
- Both a PL-ELS100 (evaporative light-scattering) detector and a Waters 2487 dual wavelength absorbance (UV) detector were used.
- Signals were recorded and analyzed with Millennium software.

Figure A.6. Image of Waters GPC system.

- Polystyrene standards with molecular weights of 2,000,000, 900,000, 824,000, 400,000, 200,000, 110,000, 43,000, 30,000, 17,600, 6,930, 2,610, 982, and 450 were used to establish the calibration curve.
- Peak molecular weights were identified and labeled on the spectra.

Test Sample Preparation

Three different types of samples were prepared for the GPC experiments as follows:

1. Structural coatings, traffic paints, and epoxy adhesives were dissolved in 5 mL of THF solvent as a 1 wt% solution. The solution was then transferred to a syringe and forced through a 0.45-μm filter. The filtered solution was then transferred into a GPC vial.
2. The other materials, with the exception of recycled asphalt pavement (RAP)-containing binders, were dissolved in 5 mL of THF as a 1 wt% solution and then transferred into a GPC vial without filtering.
3. The RAP-containing binders were first extracted by placing 5 g of mix in a 20-mL vial with 10 mL of methylene chloride, stirring for 5 min, filtering the solution, and vacuum drying the filtrate into a clean vial. The resulting binder extract was then dissolved in 10 mL of THF as the GPC solvent and then transferred into a GPC vial.

Nuclear Magnetic Resonance

The literature search conducted in Phase 1 of this project revealed that, since the 1980s, laboratory NMR systems have been mostly used by university-based researchers for the analysis of petroleum products. However, knowing that NMR spectroscopy is extremely helpful in identifying the chemical structure of virtually any organic compound, the team decided to include this method in the laboratory testing program. Despite the team's having no access to portable NMR equipment by the time this report was finalized, the results obtained from the NMR testing in laboratory conditions may be useful in the future.

Bruker DRX-400 NMR Spectrometer

Equipment Setup

Figure A.7 shows the setup of the Bruker DRX-400 NMR spectrometer located in the IMS facilities at UCONN. The device uses time-domain analysis for solutions and frequency-domain analysis for solids in a ^{1}H, ^{13}C, ^{31}P, or ^{19}F environment. In Phase 2, ^{1}H proton NMR spectra were recorded and analyzed as follows:

- Sixteen scans were performed for each run.
- D-chloroform was used as the lock solvent.
- TopSpin software was used to collect the signal.
- MestReNova software was used to analyze the signal and prepare the report.
- The peaks were identified from the known constituents and a table of NMR chemical shifts.

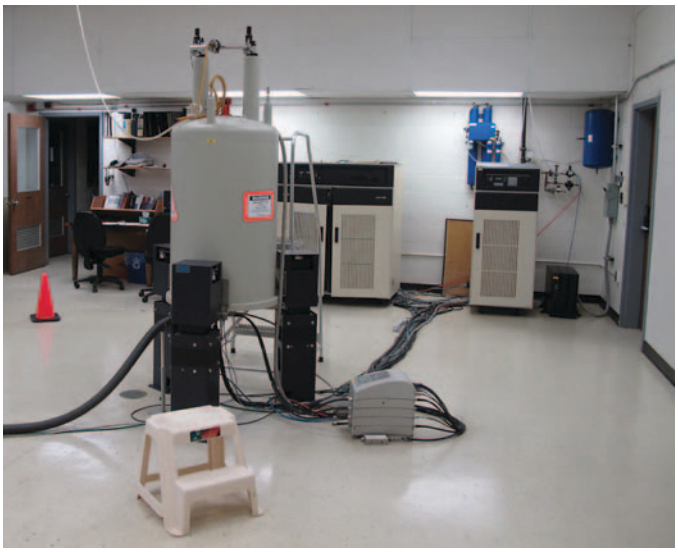

Figure A.7. Image of Bruker DRX-400 NMR system.

Test Sample Preparation

Because the NMR requires material to be in the liquid state, the following preparation methods were used:

1. Structural coatings, traffic paints, and epoxy adhesives were dissolved in 2 mL of $CDCl_3$ (D-chloroform) solvent as a 2 wt% solution. The solution was then transferred to a syringe and forced through a 0.45-μm filter. The filtered solution was loaded into the NMR tube.
2. The rest of the materials, with the exception of RAP-containing binders and hot-mix asphalt mixes, were dissolved in 2 mL of $CDCl_3$ solvent as a 1 wt% solution and transferred directly into the NMR tube.
3. The RAP-containing binders were first extracted by placing 5 g of mix in a 20-mL vial with 10 mL of methylene chloride, stirring the suspension for 5 min, filtering the solution, and vacuum drying the filtrate in a fresh vial. The resulting binder extract was then dissolved in 1 mL of D-chloroform and diluted to 2 wt% solution.

Summary of Equipment

This section summarizes the results of the evaluation of the portable spectroscopic devices in Phase 2. Table A.3 lists the spectroscopic devices chosen for the "proof of concept" in the laboratory phase of the project. The evaluation concerned the ability of portable FTIR, Raman, XRF, and XRD devices to comply with qualitative and quantitative requirements of field quality assurance/quality control procedures, such as accuracy, time and labor involved in testing, level of training required, and other parameters. These requirements were established in Phase 1 based on the feedback of the professionals who participated in the workshop organized by the team and held at UCONN. Table A.4 compares the actual parameters achieved in the laboratory conditions with the target values.

As shown in Table A.4, all devices evaluated in Phase 2 comply with the previously established criteria, suggesting that the team chose the equipment correctly. However, final recommendations for the further evaluation of these devices in Phase 3 (field experiments) were based on the success of the portable equipment to produce interpretable results for the materials included in experimental design of Phase 2. These recommendations are summarized in Chapter 4.

Summary of Survey of Approved and Qualified Product Lists

Figures A.8 to A.17 summarize the results of the survey of approved and qualified product lists.

Reference

1. Dermatas, D., M. Chrysochoou, S. Sarra Pardali, and D. G. Grubb. Influence of X-Ray Diffraction Sample Preparation on Quantitative Mineralogy: Implications for Chromate Waste Treatment. *Journal of Environmental Quality,* Vol. 36, 2007, pp. 487–497.

Table A.3. Finalized List of Spectroscopic Devices for "Proof of Concept" in the Laboratory

Spectroscopic Method	Brand/Manufacturer	Model	Portability
FTIR	Nicolet	Magna 560	Stationary
	Bruker	ALPHA II ATR	Portable (benchtop)
	RTA, Inc.	RamanID	Portable (trunk size)
XRD	Bruker-AXS (Siemens)	D5005	Stationary
	inXitu, Inc.	Terra	Portable (trunk size)
XRF	Innov-X Systems, Inc.	Alpha	Portable (handheld)
NMR	Bruker	DRX-400	Stationary
GPC	Viscotec	Waters	Stationary

Table A.4. Summary of Portable Equipment Evaluation in Phase 2

Feature[a]		Value	FTIR	Raman	XRF	XRD
Accuracy	Minimum	1%	<0.5%	<2%	<1%	<1%
	Goal	<0.5%				
Duration of measurement	Maximum	1 h	~1 min	~1 min	6–12 min	15 min
	Goal	~5 min				
Effort involved	Maximum	1 person	1 person	1 person	1 person	1 person
	Goal	1 person				
Amount of prior training	Maximum	1 day	1 h	1 h	1 h	1 h
	Goal	0.5 day				
Reliability	Minimum	Depends on material (90%)	99% (software failure)	Depends on material[c]	99% (software failure)	99% (software failure)
	Goal	95%				
Time to get results	Maximum	Depends on construction process (1 h)	~5 min	~5 min	~5 min	~5 min
	Goal	~5 min				
Price range	Maximum	$50,000	~$25,000	~$60,000	~$37,000	$45,000
	Goal	<$20,000				
Device weight	Maximum	50 lb	~16 lb	~20 lb	~4 lb (handheld) ~15 (benchtop)	~27 lb
	Goal	<20 lb				
Sample preparation	Maximum	Solvent	As is[b]	As is[b]	As is (liquids) pulverization (solids)	Crushing (solids)
	Goal	As is				

[a] *Accuracy:* Agreement between a measurement and the true or correct value.
Duration of measurement: Time between start and end of testing cycle.
Effort involved: Personnel required to perform the test.
Amount of prior training: Time required to make personnel familiar with a testing procedure.
Reliability: Unlikelihood of equipment failure during the test.
Time to get results: Time between beginning of the sample preparation and the end of the analysis of the test results.
Price range: Cost of the equipment.
Device weight: Mass of the equipment including the case or enclosure.
Best time for QA/QC: Stage of the manufacturing or application process when the test is most timely.
Sample preparation: Processing/manipulating the material before the test.
Minimum/maximum: Acceptable threshold value from the user perspective that given equipment should produce.
Goal: Desirable target value from the user perspective that given equipment should produce.
[b] Pulverization of granular materials (aggregates) is required for better quality.
[c] Failure to get the signal for fluorescent materials or because of thermal emission.

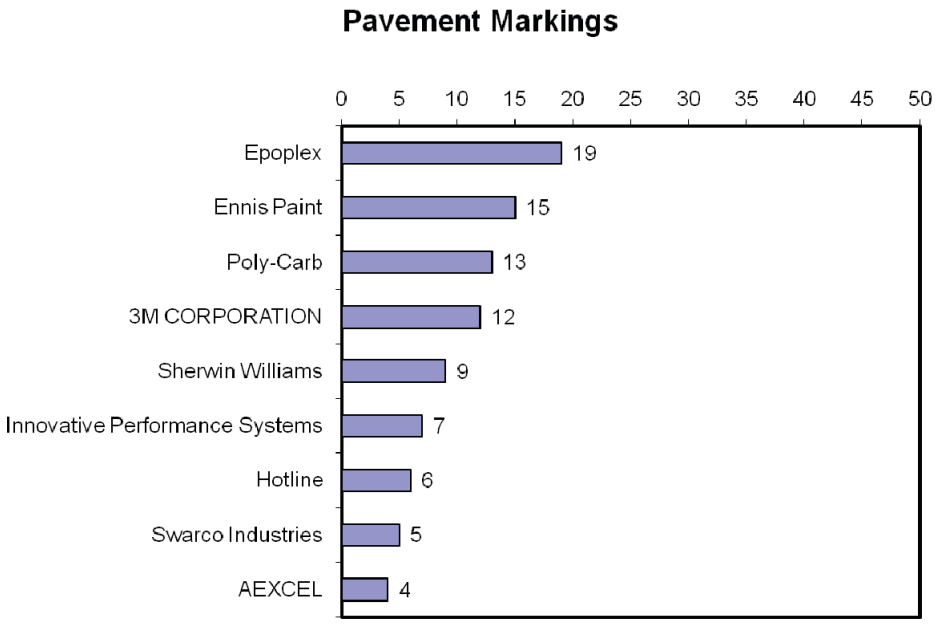

Figure A.8. Distribution of pavement marking brands approved by state highway agencies (SHAs).

Figure A.9. Distribution of structural coating brands approved by SHAs.

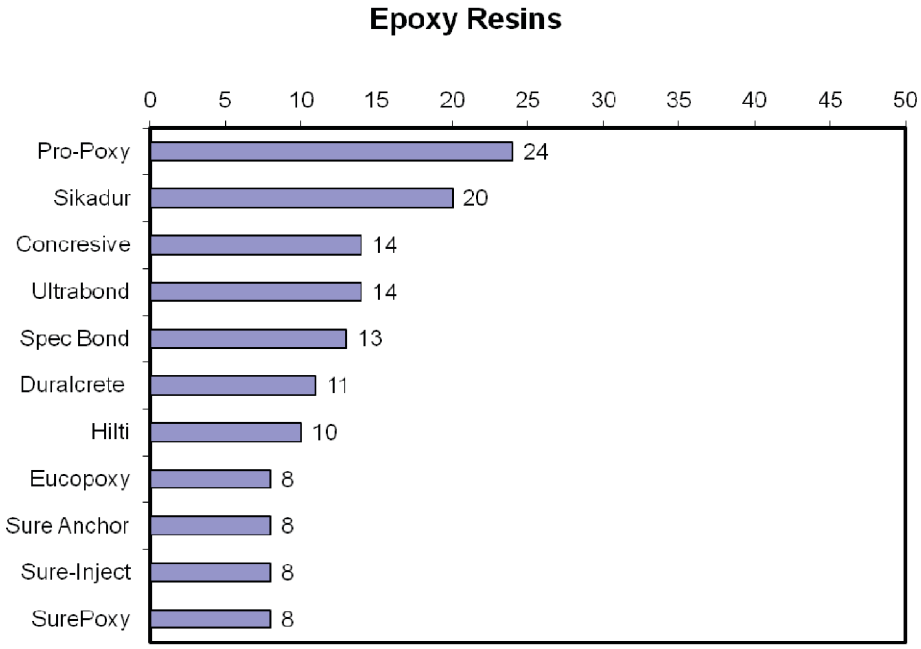

Figure A.10. Distribution of epoxy resin brands approved by SHAs.

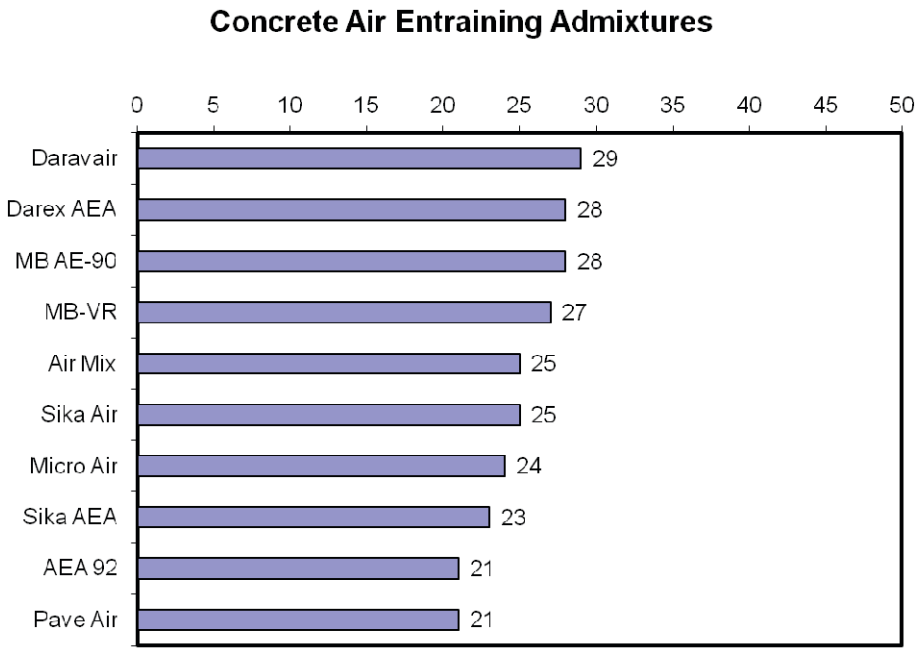

Figure A.11. Distribution of air-entraining admixture brands approved by SHAs.

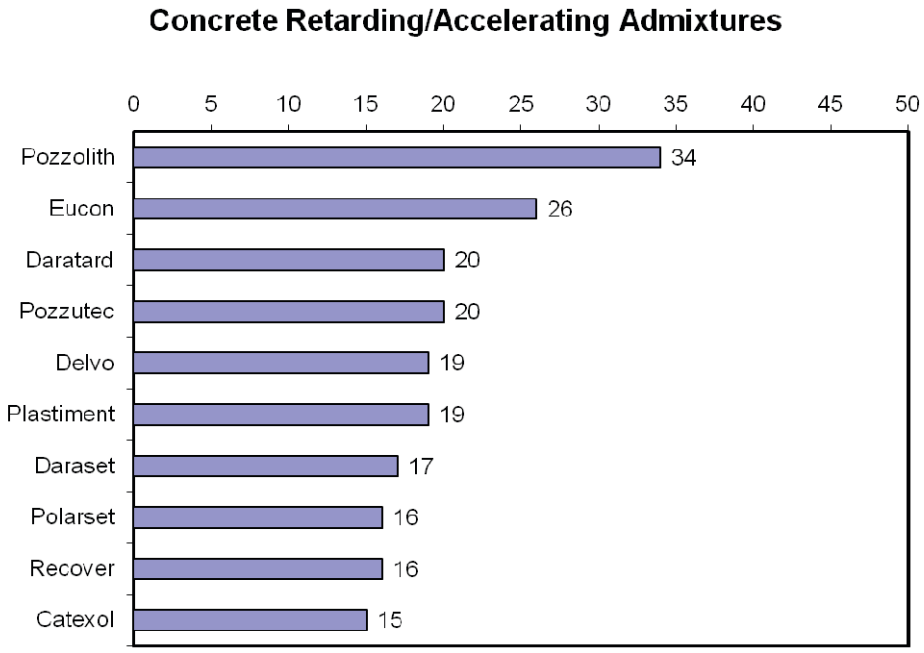

Figure A.12. Distribution of PCC set retarder and accelerator brands approved by SHAs.

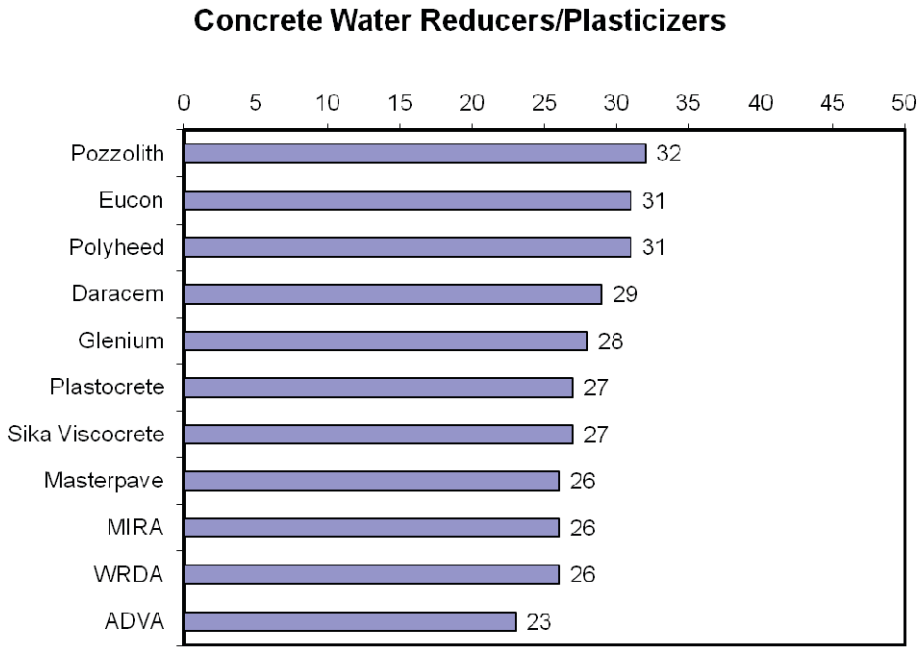

Figure A.13. Distribution of water reducer and plasticizer brands approved by SHAs.

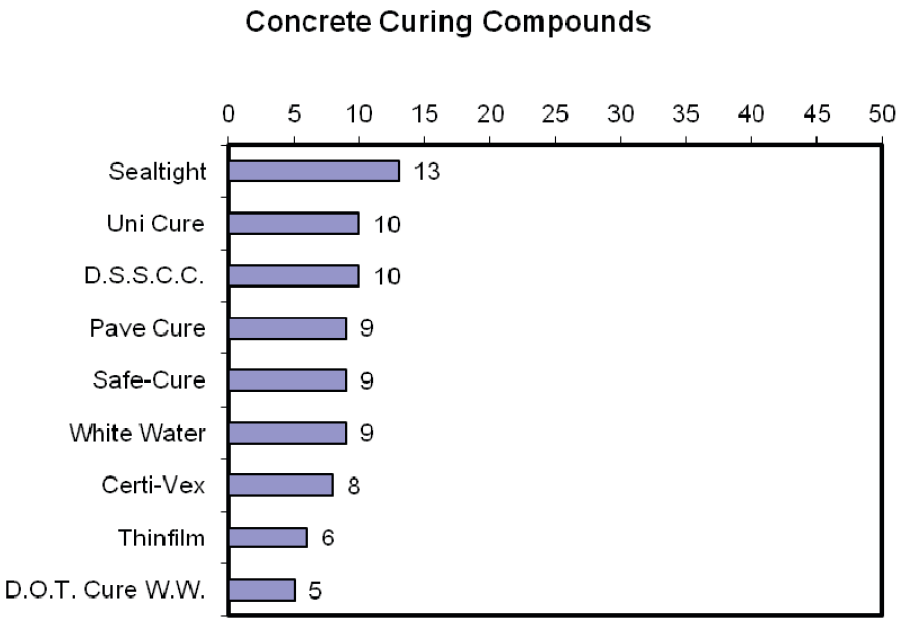

Figure A.14. Distribution of PCC curing compound brands approved by SHAs.

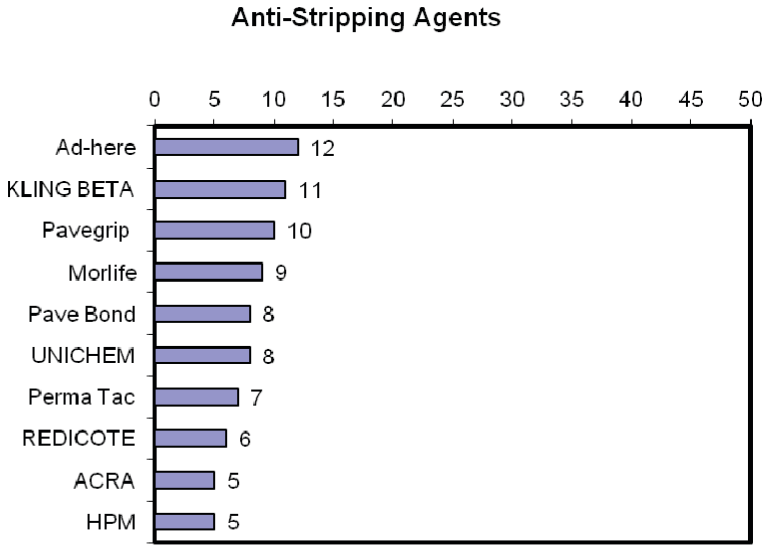

Figure A.15. Distribution of asphalt antistripping brands approved by SHAs.

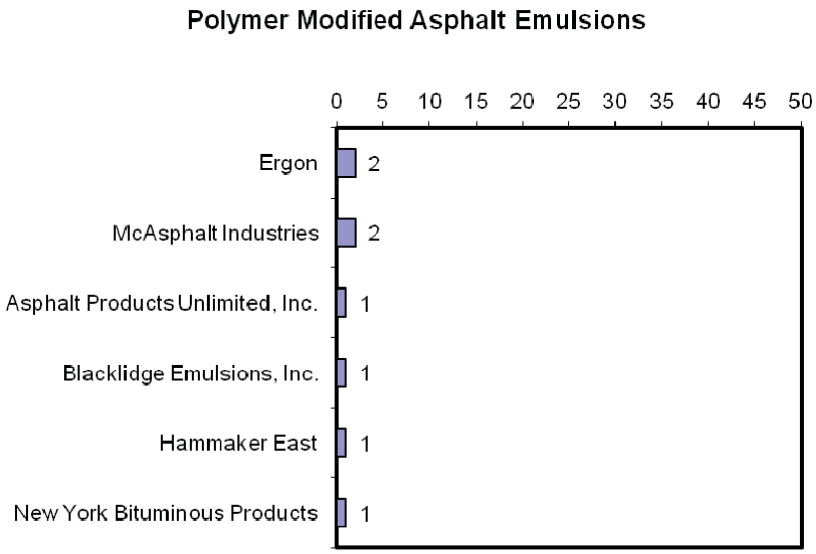

Figure A.16. Distribution of polymer-modified emulsion vendors approved by SHAs.

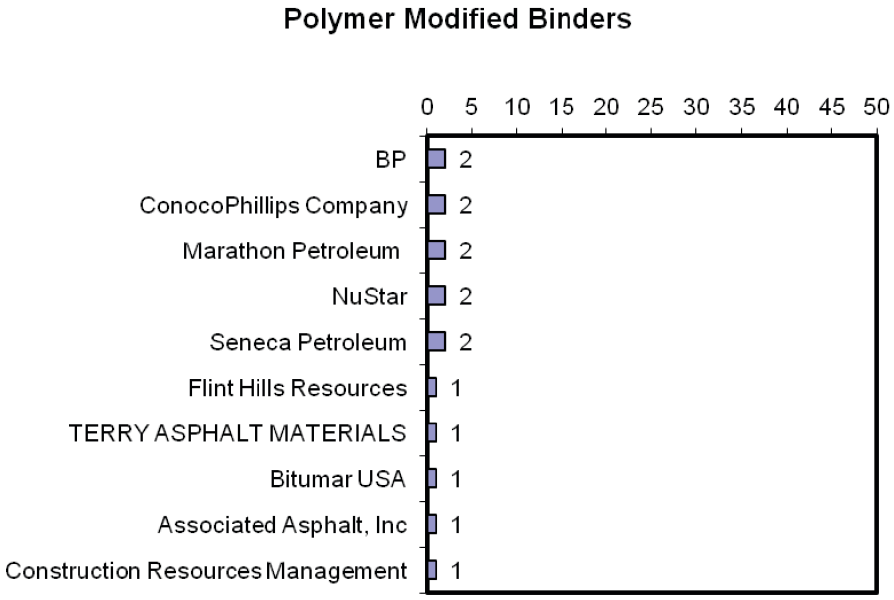

Figure A.17. Distribution of polymer-modified binder suppliers approved by SHAs.

APPENDIX B

Generic Spectroscopic Testing Procedures

This appendix presents generic procedures for the proposed spectroscopic methods. Those procedures were first implemented in the laboratory and then re-evaluated under field conditions. As a result, field operation manuals for the most successful spectroscopic methods, attenuated total reflectance (ATR) and X-ray fluorescence (XRF), were developed (see Appendix D).

Generic FTIR Testing Procedure

Scope

This test method covers sample preparation, acquisition of infrared (IR) spectra, and comparison of the sample IR spectra with reference (standard) spectra. The concentration of each chemical component is determined by analyzing IR spectra on the basis of the Beer-Lambert law.

Apparatus

The apparatus includes the following:

- Spatula (for solids and extremely viscous liquids) and pipette (for mobile liquids);
- ATR gas cell (for volatile liquids) (optional);
- Solvent (for solutions);
- Acetone (for removal of test material from the ATR crystal surface);
- Fourier transform infrared (FTIR) spectrometer with IR transmission window or horizontal ATR module; and
- Personal computer (desktop or laptop) with MS Excel or similar spreadsheet analysis software (optional).

Sample Preparation

Liquid Sample

The following methods are used:

- *IR Transmission Method.* Use sealed or semipermanent transmission cell for nonvolatile or semivolatile liquids. Use gas cell for volatile liquids. Use salt optic (e.g., KBr or NaCl) windows for viscous liquids. Do not use salt optics when water is present in a sample.
- *ATR Method.* Use pipette to draw the mobile liquid into and put enough material to cover the entire ATR diamond surface. Use a sealed ATR cell for volatile liquids and solutions with volatile solvent. The heated ATR gas cell is optional for extremely volatile liquids. Use small spatula or screwdriver for extremely viscous materials (e.g., asphalt binder) to place enough material to cover the entire ATR diamond surface.

It should be noted that the transmission method will be used over the ATR method only for material–method combinations that do not yield useful results using the ATR method, which is more amenable to field use. This applies to all sample types.

Paste, Emulsion, and Slurry Sample

The following methods are used:

- *IR Transmission Method.* Use KBr or NaCl optics, as done for viscous liquids.
- *ATR Method.* Use small spatula or screwdriver to place enough material to cover the entire ATR diamond surface.

Solid Sample Preparation

The following methods are used:

- *IR Transmission Method.* For grindable powders, prepare a compressed KBr or KCl pellet or a mineral oil mull. For coarse or hard organic powders, mix sample with KBr/KCl in 1:10 proportion (use 1:50 proportion for inorganic samples). For amorphous solids, mold or hot-press the sample to prepare self-supporting film. Minimize the thickness of sample for highly absorptive materials.
- *ATR Method.* For grindable powders and fibrous and elastomeric materials, place enough material to cover the

entire ATR diamond surface and apply pressure to ensure full contact between the sample and the ATR diamond surface. For moldable materials, prepare self-supporting film before placing sample on the ATR diamond surface. For soluble solids, use volatile solvent for soluble materials to cast the material into a film. Heat the sample to remove all residual solvent. Be sure to record the solvent used in the preparation in case residual solvent remains.

Control Sample Preparation

The control sample is a sample of material with the designated chemical composition that is to serve as a reference for comparison to test samples. If the concentration of a chosen component in the designated mixture or solution is analyzed, several control samples should be prepared by mixing the component of interest with the neat/original material in different proportions. The mixing procedure should comply with the original procedure used by a manufacturer to produce the designated material. In some cases, it may be necessary to dissolve a solid (or liquid) sample in a solvent to obtain a satisfactory spectrum. Common solvents, such as acetone, methanol, *n*-hexane, or water, will be used as necessary.

Testing Procedure

The testing procedure is as follows:

- Prepare control sample, if required.
- Obtain infrared spectrum of the control sample as specified by the FTIR equipment user manual.
- Collect test material according to an ASTM/AASHTO procedure, if applicable.
- Prepare test sample as specified above.
- Obtain infrared spectrum as specified in the FTIR equipment user's manual.
- Compare the test sample spectrum with that of the control sample by using an appropriate method of analysis, as described below.

Data Reduction and Analysis

The data for the FTIR spectroscopic analysis are collected in absorbance units over the typical wavelength number range (4,000 cm^{-1} to 400 cm^{-1} for FTIR spectroscopes). The tabulated data may be plotted for graphical representation (absorbance on the *y*-axis versus wavelength number on the *x*-axis). Several methods of analysis are available depending on the objectives of the test. Confirmation of a known chemical composition is a primary objective of the quality control procedure. For this purpose, the infrared spectrum of a test sample can be compared with that of a control sample in terms of correlation (R^2) or in terms of significance of the difference (Student's *t*-test). To analyze an unknown material, other statistical methods, such as multiple regression and principle component analysis, can be used concurrently with spectra libraries available in the literature.

Generic Raman Testing Procedure

Scope

This test method covers preparing samples of the designated material, obtaining Raman spectra of the samples, and comparing the spectra to reference (standard) spectra of the material and components of the material. The concentrations of specific chemical components are determined from the analysis of Raman spectra of each pure (100%) component using the same measurement conditions.

Apparatus

The apparatus includes the following:

- Spatula (for solids and extremely viscous liquids) and pipette (for mobile liquids);
- Mortar and pestle to grind course solids;
- Disposable 2-mL glass vials or 1-in. × 3-in. glass slides;
- Solvents (for preparing solutions or performing simple extractions);
- Portable Raman analyzers with 785-, 976-, and 1,064-nm laser excitation; and
- Laptop computer with Raman VISTA spectral analysis software.

Sample Preparation

Liquid Sample

For liquids, a pipette sample is prepared in 2-mL glass vials.

Paste, Emulsion, and Slurry Sample

For the paste, emulsion, and slurry samples, use a small spatula to cover ~½-in. square glass slides.

Solid Sample Preparation

The solid sample preparation includes the following:

- *Fine Powders.* Use small spatula to place samples into 2-mL glass vials.
- *Course Powders.* Use mortar and pestle to grind to reasonable powder, then small spatula to place into 2-mL glass vials.

Control Sample Preparation

The control sample is a sample of material with the designated chemical composition that is to serve as a reference for comparison to test samples. If the concentration of a chosen component in the designated mixture or solution is analyzed, several control samples should be prepared by mixing the component of interest with the neat (original) material in different proportions. The mixing procedure should comply with the original procedure used by a manufacturer to produce the designated material. In some cases, it may be necessary to dissolve a solid (or liquid) sample in a solvent to obtain a satisfactory spectrum. Common solvents, such as acetone, methanol, *n*-hexane, or water, will be used as necessary.

Testing Procedure

The testing procedure is as follows:

- Prepare control sample, if required.
- Place the glass vial or slide containing the control sample onto the Raman sample holder.
- Measure the Raman spectrum as specified in the user's manual (e.g., set laser to 400 maw and acquisition time to 1 min).
- Collect test material according to an ASTM/AASHTO procedure, if applicable.
- Prepare test sample as specified above.
- Place the glass vial or slide containing the test sample onto the Raman sample holder.
- Measure the Raman spectrum as specified in the user's manual.
- Compare the test sample spectrum to the control sample using the ChemID software described below.

Data Reduction and Analysis

Raman spectra typically consist of peaks distributed between 0 and 4,000 cm^{-1} shifted from the laser excitation wavelength, which are attributable to molecular vibrations. The peak position corresponds to the energy of the vibration, while the peak intensity corresponds to the concentration of the vibration (or the chemical).

Material Identification

Real-Time Analyzers' (RTA's) ChemID software employs four different library search algorithms to identify an unknown chemical. In essence, the measured spectrum is subtracted from all of the spectra in a stored library (database), where a perfect match equals zero. After subtraction, all of the library spectra are ranked with the lowest value (closest to zero) representing a match. Successful analysis requires populating the library with spectra of chemicals or materials likely to be analyzed. Consequently, highway materials must be measured as references.

Material Quantification

RTA's S-Quant software can be used to quantify up to five components in a mixture. If the components are known, their spectra are loaded and weighted by percent until the measured spectrum is recreated (based on peak intensities). If the components are unknown, they can be identified using the ChemID program.

Generic XRD/XRF Testing Procedure

Scope

This test method covers preparing a sample of the designated material (the sample) and performing X-ray diffraction (XRD) and X-ray fluorescence (XRF) analysis of the sample. XRD analysis is used to identify chemical structure of the sample on the basis of the comparison of the diffraction peaks against a library of known crystalline materials. XRF analysis is used to quantify sample components on the basis of the intensity of their characteristic fluorescent radiation.

Apparatus

The apparatus used includes the following:

- Bruker D5005 X-ray diffractometer,
- inXitu XRD/XRF Terra analyzer and laptop computer with custom software, and
- Innov-X Systems portable XRF analyzer with custom software and personal digital assistant.

Sample Preparation

The methods of sample preparation are as follows:

- *XRF Method.* No sample preparation is required. This method can be conducted on any surface and type of material.
- *XRD Method.* Oven-dry or air-dry liquid sample. Grind or pulverize solid, powder, and extracted pigments samples to reduce particle size. If only qualitative evaluation of material components is required, samples may remain wet.

There are no control samples required for XRD and XRF analyses.

XRD Testing Procedure

The XRD testing procedure is as follows:

- Prepare test sample as specified above.
- Place sample into a sample holder. Alternatively, smear uniformly onto a glass slide, assuring a flat upper surface, pack into a sample container, or sprinkle on double sticky tape.
- Place sample holder or container into an X-ray diffractometer.
- Obtain diffractogram of the sample as specified in the equipment user's manual.
- Reduce and analyze the data, as described below.

XRD Data Reduction and Analysis

Qualitative and quantitative analysis of the diffractograms will be performed using the Jade v.8.5 software with reference to the International Centre for Diffraction Data database and the American Mineralogist Crystal Structure Database.

XRF Testing Procedure

The XRF testing procedure is as follows:

- Turn on portable XRF device.
- Attach the X-ray tube of the device to the sample surface.
- Obtain the fluorescence energy spectrum of the test sample.
- Reduce and analyze the data, as described below.

XRF Data Reduction and Analysis

The software provided with the Innov-X portable analyzer automatically reduces the data and provides a list of metal concentrations that can be downloaded in Excel format.

APPENDIX C

Proposed AASHTO Standards of Practice

Standard Practice for

Identification of Water Reducing, Accelerating, and Retarding Chemical Admixtures in Fresh Portland Cement Concrete by Attenuated Total Reflection Infrared Spectrometer

AASHTO Designation SP XX-12

1. SCOPE

1.1 This method covers the qualitative identification of the type of a chemical admixture for portland cement concrete (PCC). The method is based on the qualitative analysis of the infrared absorbance spectra of a pure admixture sample. A pure admixture sample is obtained from the storage or feeding tank in a concrete plant. A pure admixture sample is scanned by attenuated total reflection (ATR) infrared spectrometer to obtain its absorbance spectrum. Next, the type of admixture is determined based on characteristic absorption bands associated with particular admixture type. Last, a fresh PCC sample is scanned by the ATR spectrometer, and the absorption bands associated with presence of the admixture are identified.

1.2 It is desired to perform ATR testing of an admixture sample immediately after sampling. Long exposure of an admixture to air can result in the evaporation of water or oxidation of an organic content of the admixture, which would alter its chemical composition.

1.3 It is required that PCC sample be tested by the ATR spectrometer within 5 minutes after its removal from framework. Furthermore, the ATR scanning should occur within 2 minutes after its placement on the ATR sampling plate. This is to avoid the damage to the testing apparatus due to fast drying of a thin PCC paste sample.

1.4 This procedure may involve hazardous materials, operation, and equipment. This procedure does not purport to address all of the safety concerns associated with its use. It is the responsibility of the user of this procedure to consult and establish appropriate safety and health practices and to determine the applicability of regulatory limitation before use.

2. REFERENCED DOCUMENTS

2.1 *ASTM Standards:*

- C494, Standard Specification for Chemical Admixtures for Concrete
- C1017, Standard Specification for Chemical Admixtures for Use in Producing Flowing Concrete
- C260, Standard Specification for Air-Entraining Admixtures for Concrete

3. APPARATUS

3.1 Sampling equipment

3.2 Pipette for sampling liquid admixture

3.3 Spoon for sampling PCC

3.4 Spectroscopic equipment

3.5 Infrared spectrometer equipped with diamond single reflection ATR accessory and load applicator

3.6 Cleaning tools

3.7 99% Acetone for cleaning ATR sampling plate after sample is removed.

3.8 Soft cloth or tissue for sample removal

4. SAMPLE PREPARATION

4.1 **Pure chemical admixtures.** Normally, no sample preparation is required for liquefied chemicals when the horizontal ATR sampling plate is used.

4.2 **Fresh PCC.** A PCC sample with maximum particle size of 1 mm is collected from a mixer or from the formwork with using a sampling spoon. Special care should be taken to avoid particles bigger than 2 mm and to preserve representative moisture content in a PCC sample.

5. SPECTROSCOPIC EQUIPMENT SETUP

5.1 The ATR spectrometer should be placed on a firm horizontal surface to avoid any vibrational interference with the instrument signal.

5.2 A reliable source of electric power (AC or DC) should be provided to ensure no interference with the spectrometer signal.

5.3 It is recommended to follow the instrument manual in regards to the ambient temperature and moisture.

5.4 The ATR spectrometer should be connected to a data acquisition system (normally, a computer with an accompanying software) all the time during a test.

6. PROCEDURE

6.1 **ATR Testing of Pure Admixture Sample**

6.1.1 Clean up the surface of the ATR sampling plate by applying soft tissue wetted in 99% acetone.

6.1.2 Collect and store the background spectrum in accordance with the ATR spectrometer manual.

6.1.3 Collect admixture sample using a pipette and place 3 to 5 drops of a sample on the ATR sampling plate.

6.1.4 Operate ATR spectrometer in accordance to the instrument manual to obtain infrared absorbance spectrum of a sample. Use accompanied data acquisition software to subtract background spectrum, correct baseline, and remove

atmosphere- and water vapor-related absorption bands from the sample spectrum. Store the ATR absorbance spectrum in numerical format for further processing as needed.

6.1.5 Repeat steps described in 6.1.1 through 6.1.4 two more times to establish standard deviation, as explained in Section 8.X of this standard.

6.1.6 Interpret the absorbance spectrum of the admixture sample and determine the type of admixture as explained in Sections 7.XX and 7.XXX of this standard.

6.2 **ATR Testing of Fresh PCC Sample**

6.2.1 Clean up the surface of the ATR sampling plate by applying soft tissue wetted in 99% acetone.

6.2.2 Collect and store the background spectrum in accordance with the ATR spectrometer manual.

6.2.3 Collect PCC sample using a sampling spoon and place enough of a sample to entirely cover ATR sampling plate. Ensure sample to be as explained in Section 4.2. Apply pressure to a sample using load applicator supplied with an instrument.

Note: If no load applicator is supplied with the ATR instrument, it is recommended to: (a) ensure sample particle size is not larger than 0.3 mm to avoid increased variability in results, and (b) apply pressure to a sample through the flat surface of a sampling spoon.

6.3 Operate ATR spectrometer in accordance to the instrument manual to obtain infrared absorbance spectrum of a sample. Use accompanied data acquisition software to subtract background spectrum, correct baseline, and remove atmosphere- and water vapor-related absorption bands from the sample spectrum. Store the ATR absorbance spectrum in numerical format for further processing as needed.

6.4 Repeat steps described in 6.2.1 through 6.2.3 four more times to establish standard deviation, as explained in Section 8.XX of this standard.

6.5 Interpret the absorbance spectrum of the admixture sample and verify presence of the admixture as explained in Sections 7.XXXX and 7.XXXXX of this standard.

7. SPECTRAL DATA PROCESSING

7.1 Identification of absorption bands in simple compounds such as chemical admixtures to PCC is normally done using software supplied with an infrared spectrometer by a manufacturer. The software generates an output in both tabular and graphic formats. In both formats, the reciprocal wavelength, or wave number, at the center of an identified band is reported along with the corresponding intensity of infrared absorption at that wave number. Alternatively, user can identify the absorption peaks from visual analysis of a spectrum.

7.2 The absorbance is directly proportional to the concentration of particular component of a compound or a mixture. The concentration of the admixtures in a PCC sample is expected to range between as low as 0.05% to 1%, which may make visual analysis of its spectrum difficult. In addition, the default sensitivity of the instrument software may not be sufficient to identify weak but narrow absorption bands associated with the admixture. However, a relatively simple mathematical manipulation of a spectrum using second-derivative method may be used for extraction of absorption peaks of any intensity. This method is documented elsewhere and it is beyond the scope of this standard practice.

8. INTERPRETATION OF RESULTS

This section provides guidelines for the interpretation of the absorbance spectra of a pure admixture and a PCC sample. The class of admixture is determined based on the characteristic infrared absorption bands on a spectrum. The unique absorption bands are attributed to specific chemical components (functional groups) within an admixture. Those characteristic spectral features are used to verify the presence of the admixture in a resultant PCC mix sample. Appendix E briefly discusses classification of chemical admixtures to PCC and provides an example list of characteristic spectral features for the admixtures along with spectral graphs.

8.1 Identification of the Type of Admixture by Infrared Absorption Bands

8.1.1 *Nonchloride Accelerators (ASTM C494, Type C).*

8.1.1.1 **Sodium thiocyanate** is identified by the weak to medium band centered on 2,070 ±5 cm^{-1} wave numbers. When in aqueous solution, it can additionally give rise to strong and wide band centered around 1,330 ± 5 cm^{-1} with distinctive shoulder at 1,410 ± 5 cm^{-1}.

8.1.1.2 **Calcium nitrate** is identified by a strong and wide band at 1,330 ± 5 cm^{-1} with distinctive shoulder at 1,410 ± 5 cm^{-1} attributable to NO_2 and two medium and sharp peaks at 1,047 ± 5 cm^{-1} and 826 ± 5 cm^{-1} associated with nitrate anion NO_3.

8.1.2 *Water Reducers (ASTM C494, Types A and D).*

8.1.2.1 **Polycarboxylate ether** is identified by a very strong absorption band centered around 1,086 ± 5 cm^{-1} with distinctive shoulder at about 1,140 cm^{-1} associated with polyether backbone.

8.1.2.2 **Carbohydrates** are typically identified by the coupled C–O–C vibrations yielding medium peaks at 1,300 and 1,250 cm^{-1} as well as by C–OH vibrations with a strong corresponding peak at 950 cm^{-1}.

8.1.3 *Retarders (ASTM C494, Type B).*

8.1.3.1 **Sodium gluconate** is identified by a prominent terminal carboxylate in its structure, which yields characteristic split of the water band (1,649 and 1,592 cm^{-1}) and a strong band split at 1,084 and 1,038 cm^{-1} because of vibrations of the multiple OH groups.

8.1.3.2 **Carbohydrates**—See 8.1.2.2.

8.2 Verification of Presence and Type of Admixture in Fresh PCC Sample

8.2.1 On the spectrum of a fresh PCC sample, identify characteristic peaks described in 8.1.

8.2.2 Assign characteristic peaks in accordance with 8.1.

Note: Positive verification of the presence of a particular admixture is limited to those added in minimum 0.5% of the total PCC batch weight or 2% of the cement weight.

9. PRECISION

9.1 This method is based on the qualitative evaluation of the ATR spectra in regards to location of characteristic infrared absorption bands. It cannot be used for quantitative assessment of the admixture content in PCC.

9.2 Location of the characteristic peaks on an ATR spectrum can vary within ±10 cm^{-1} from the values given in this method.

Standard Practice for

Standard Method of Test for Determination of Titanium Content in Traffic Paints by Field-Portable X-Ray Fluorescence Spectroscopy

AASHTO Designation SP XX-12

1. SCOPE AND OVERVIEW

1.1 This guide covers the use of field-portable X-ray fluorescence (XRF) spectroscopy for the determination of titanium content traffic paints and pavement markings.

1.2 XRF spectroscopy is a proven analytical technique for measuring elemental concentrations. Increased sophistication of XRF technology has led to the development of field-portable devices that can be used for rapid, nondestructive analyses for on-site quality control in a variety of industrial settings.

1.3 The XRF spectrometer determines the concentrations of metals by measuring the intensity of the fluorescent radiation emitted by atoms at their characteristic energies upon bombardment by high-energy X-rays.

1.4 Because the specific operation varies greatly among the available XRF devices, no specific instructions are provided herein, and the user should refer to the operating instructions provided by the manufacturer.

1.5 The specific elements able to be detected by XRF depend on the type and calibration of the analyzer. In general, organic compounds cannot be detected using XRF and so this guide is applicable only for inorganic substances.

2. REFERENCED DOCUMENTS

2.1 *ASTM Standards:*

- D3925, Sampling of Liquid Paints and Pigment Coatings
- D4764, Titanium Dioxide Content in Paint by XRF
- D5381, XRF of Pigments and Extenders

3. SIGNIFICANCE AND USE

3.1 The method described herein is effective for the rapid, nondestructive, on-site determination of titanium in traffic paints and related coatings by XRF for quality control purposes.

3.2 The method is suitable for measurements of liquid paint samples and in situ measurements of pavement markings.

4. SAFETY

4.1 XRF spectrometers produce ionizing radiation, which can damage biological tissue. Thus, necessary precautions must be followed to ensure safety and minimize exposure.

4.2 XRF spectrometers should be used only by trained operators in accordance with the instructions issued by the manufacturer and applicable occupational safety regulations.

4.3 Engineered safety features, such as trigger locking mechanisms and sample proximity sensors, are specific to the device. Consult the technical manual supplied by the manufacturer for device-specific safety practices and operating instructions.

4.4 The dangers involved with X-ray devices, and mitigation thereof, are well documented and, as such, this manual is not intended to be a reference to all the hazards associated with X-ray devices.

5. APPARATUS

5.1 *Portable XRF Spectrometer*—This is typically designed as a handheld device that is easily transported to and from field sites and measurement locations therein. The detectable elements depend on the instrument and manufacturer. Typical accessories include batteries, charging adapters, and a personal digital assistant (PDA) installed with the necessary measurement software.

5.2 *Sampling Containers*—Containers should be selected based on manufacturer recommendations. These are required when the material of interest must be sampled before analysis (i.e., for ex situ XRF measurements).

5.3 *X-Ray Transparent Tape or Film*—The sample containers should be covered by an X-ray transparent tape or film, such that X-rays can penetrate the sample in close proximity without damaging the instrument.

6. SAMPLE

6.1 Sampling of liquid paints should be conducted in accordance with ASTM Method D3925.

7. POTENTIAL INTERFERENCES

7.1 *Moisture Effects*—Caution must be exercised when analyzing and comparing XRF results obtained for paints that have variable moisture content. Titanium in the paint is necessarily concentrated as paint dries.

7.2 *Sample Preparation*—Steps should be taken to ensure that samples are uniform, homogenous, and randomly sampled, such that the results obtained are representative of the bulk of the material.

7.3 *Spectral Overlap*—When interpreting XRF results, one must be aware of potential overlap of signals from different elements with similar characteristic energies. This phenomenon is well documented and is likely addressed by the manufacturer.

7.4 *Penetration Depth*—X-rays penetration depth is usually on the order of micrometers to millimeters and is a complicated function of X-ray energy and the properties of the material. If the sample is thinner than the depth of X-ray penetration, the results will include contribution from the substrate.

8. STANDARDIZATION

8.1 Follow the instructions for device start-up and standardization as described by the manufacturer.

8.2 Typically, this is performed using a standardization material (e.g., Alloy 316) after a specified instrument warm-up period. Most devices have a digital screen or PDA that will prompt the user to perform the specific method for internal standardization.

9. PROCEDURE

9.1 For in situ measurements of pavement coatings:

9.1.1 Select a coated pavement surface that is smooth, clean, and of representative thickness.

9.1.2 Gently apply the XRF spectrometer directly to the clean coating, such that it is flush against the device and away from the adjacent exposed pavement.

9.2 For ex situ measurements:

9.2.1 Place a uniform, homogenized, and representative amount of the liquid paint into a sample container such that it is at least halfway filled.

9.2.2 Cover the opening of the container with X-ray transparent film and fasten into place.

9.3 Perform the measurement in accordance with the operating instructions for the device. Typically, data are collected on a continuously averaged basis for 1 to 2 minutes and repeated as necessary to obtain a sufficient sample size.

9.4 The results will be displayed in the form in concentration units.

9.5 Quality assurance can be addressed by periodically re-standardizing the instrument, verifying the standardization by measuring a known standard, and performing a blank measurement. If necessary and possible, collect a sample for laboratory analysis to verify measurement accuracy or identify possible matrix effects, or both.

10. REPORT

10.1 The report shall include the following:

10.1.1 The titanium content in units of percent concentration or parts per million by mass.

10.1.2 The mean and standard deviation associated with each sample.

10.1.3 Proof of verified instrument calibration (e.g., by ASTM Method D4764) if absolute concentration is reported.

10.1.4 Limits of detection.

APPENDIX D

Field Operation Manuals

Field Operation Manual for Portable Attenuated Total Reflectance Fourier Transform Infrared Spectroscopy

1. Scope and Overview

1.1 This manual covers the use of field-portable attenuated total reflectance Fourier transform infrared (ATR-FTIR) spectroscopy for on-site characterization of construction materials.

1.2 Field-portable ATR-FTIR is a useful technique for on-site characterization of materials with little or no sample preparation. An ATR-FTIR spectrometer measures the infrared spectrum of a material, which can be used to identify or quantify the compounds present in a material, or both.

1.3 Given the variety of ATR-FTIR spectrometers available, this guide is not a sufficient substitute for the instruction manual issued by the manufacturer.

2. Apparatus

2.1 *Portable ATR-FTIR Spectrometer*—Portable ATR-FTIR spectrometers are designed to be compact, battery-powered units that can be easily transported to field sites. The main components of the spectrometer include housing for the laser source and optics, and a sampling plate. The sampling plate contains an optically dense crystal called an internal reflection element (IRE) on which the material is placed during measurements.

2.2 *Accessories*—A laptop computer with measurement software is typically required to perform measurements. A rechargeable battery pack will be required to power the spectrometer on site, as well as a crossover cable to interface the spectrometer and the computer.

3. Sampling

3.1 Use precaution to ensure that sample selection is random and that measurements are an accurate representation of the true composition of the entire quantity of material in question.

4. Potential Interferences

4.1 *Poor Sample Contact*—Inadequate contact of a sample with the IRE will result in a noisy spectrum with bands of low intensity, if any. Recall that an ATR spectrum is the result of the interaction between the sample and the IR radiation

that protrudes a very small distance (on the order of microns) above the IRE; thus close contact of the sample with the IRE is required to obtain a high-quality spectrum. This can present a challenge when testing solids and powders. Many modern spectrometers have addressed this issue by incorporating a clamp mechanism that applies pressure on the sample.

4.2 *Residue on the IRE*—Potential spectral interference may arise from an unclean IRE surface, which may be attributable to residue from a previously tested sample, a leftover quantity of the chemical used to clean the IRE, or even fingerprints. Therefore it is necessary to ensure that the IRE is sufficiently clean before measurements. Rapidly evaporating solvents such as acetone and ethanol are typically used as cleaning agents. Modern spectroscopy programs often include functions for determining if the IRE is sufficiently clean.

4.3 *Spectral Overlap*—ATR spectra represent contributions from all detectable compounds present in the sample, creating the potential for spectral overlap, in which case the IR bands of interest may be obscured. This is a common occurrence in samples that contain water, which strongly absorbs IR radiation. Often in such cases, subtraction of the interfering spectrum (e.g., a spectrum of pure water) can isolate the IR bands from the compound of interest.

5. Procedure

5.1 Follow the instructions for device start-up as described in the instruction manual of the spectrometer. Make sure that the proper environmental operating requirements, such as ambient temperature and humidity, are met. For example, on a hot and humid day, the ambient temperature may exceed the recommended limit set by the manufacturer.

5.2 Select values for resolution and number of scans to be averaged per measurement. Typically, 24 scans are collected at resolution of 4 cm^{-1}.

5.3 Collect a background spectrum (i.e., a spectrum of the bare IRE). The software uses this spectrum to eliminate atmospheric contributions and produce the sample spectrum.

5.4 Place a portion of the material onto the sampling plate such that sufficient coverage of the IRE is achieved. Take note of the following nuances associated with different sample types (in order of increasing difficulty):

5.4.1 *Liquids*—Place enough of the liquid sample on the sampling plate to cover the IRE using a pipette, or a spatula for more viscous samples. Use caution to avoid spillage, which can damage components of the spectrometer and the computer.

5.4.2 *Particulate Solids*—After covering the IRE with the powdered material, use the pressure clamp (if available) to hold the sample in place and maintain close contact the IRE.

5.4.3 *Bulk Solids/Mixes*—Materials containing larger particles, such as aggregates, asphalt mixtures, and coatings on larger particles, require more effort to achieve good IRE contact and obtain meaningful results because of their bulkiness and inherent nonuniformity. Portions of the sample with flat surfaces should be selected for measurement, and the pressure clamp should be used. The number of samples may need to be increased to obtain an accurate representation of the bulk material.

5.5 Collect a sample spectrum with the same measurement parameters (number of scans and resolutions) used for the background spectrum. Perform multiple measurements as need (e.g., to obtain a less noisy average spectrum or to evaluate changes in sample composition over time).

5.6 Evaluate the quality of the spectrum by visual inspection (e.g., to determine if IRE contact was sufficient) and perform an additional measurement, if needed, starting from Step 5.3.

5.7 Perform spectral processing as needed. Such tasks can be completed on most spectroscopy programs and typically include baseline subtraction, conversion of ATR units to absorbance units, and atmospheric correction, which involves removal of bands associated with water vapor and carbon dioxide.

5.8 The resulting spectra can then be used for quantitative analysis or to fingerprint the material with the aid of a spectral database, or both.

Field Operation Manual for Field-Portable X-Ray Fluorescence Spectroscopy

1. Scope and Overview

1.1 This manual covers the use of field portable X-ray fluorescence (XRF) spectroscopy for on-site characterization of construction materials.

1.2 Field-portable XRF is a quick and inexpensive technique for on-site elemental analysis with little to no sample preparation. XRF spectrometry is based on the characteristic energies of elements, of which the intensities are measured by a detector and translated into elemental concentrations.

1.3 Despite having a common scientific basis, the specific method of operation varies among the multitude of field-portable XRF devices available on the market, and thus this guide is not a sufficient substitute for the instruction manual issued by the manufacturer.

2. Safety

2.1 XRF spectrometers produce ionizing radiation, which can damage biological tissue. Thus, necessary precautions must be followed to ensure safety and minimize exposure.

2.2 XRF spectrometers should be used only by trained operators in accordance with the instructions issued by the manufacturer and applicable occupational safety regulations.

2.3 Engineered safety features, such as trigger locking mechanisms and sample proximity sensors, are specific to the device. Consult the technical manual supplied by the manufacturer for device-specific safety practices and operating instructions.

2.4 The dangers involved with X-ray devices, and mitigation thereof, are well documented and, as such, this manual is not intended to be a reference to all the hazards associated with X-ray devices.

3. Apparatus

3.1 *Portable XRF Spectrometer*—This is typically designed as a handheld device that is easily transported to and from field sites and measurement locations therein. The detectable elements depend on the instrument and manufacturer. Typical accessories include batteries, charging adapters, and a personal digital assistant (PDA) installed with the necessary measurement software.

3.2 *Sampling Containers*—Containers should be selected based on manufacturer recommendations. These are required when the material of interest must be sampled before analysis (i.e., for ex situ XRF measurements).

3.3 *X-Ray Transparent Tape or Film*—The sample containers should be covered by an X-ray transparent tape or film, such that X-rays can penetrate the sample in close proximity without damaging the instrument.

4. Sampling

4.1 Use precaution to ensure that sample selection is random and that measurements are an accurate representation of the true composition of the entire quantity of material in question.

5. Potential Interferences

5.1 *Moisture Effects*—Caution must be exercised when analyzing and comparing XRF results obtained for materials that have variable moisture content. For example, a drying paint layer or freshly mixed cement may experience dilution effects that skew the results towards lower and higher relative concentrations when wetter or dryer, respectively.

5.2 *Sample Preparation*—Steps should be taken to ensure that samples are uniform, homogenous, and randomly sampled, such that the results obtained are representative of the bulk of the material.

5.3 *Spectral Overlap*—When interpreting XRF results, one must be aware of potential overlap of signals from different elements with similar characteristic energies. This phenomenon is well documented and is likely addressed by the manufacturer.

5.4 *Penetration Depth*—If the sample is thinner than the depth of X-ray penetration, the results will include contribution from the substrate.

6. Procedure

6.1 Follow the instructions for device start-up and calibration as described by the manufacturer. Typically, calibration is performed using a standardization material (e.g., Alloy 316) after a specified instrument warm-up period. Most devices have a digital screen or PDA that will prompt the user to perform the specific calibration method for internal standardization.

6.2 For in situ measurements, gently apply the XRF device directly to a clean, uniform surface, such that it is flush against the device. For ex situ measurements, place a uniform, homogenized, and representative amount of the material into the sample container and cover with X-ray transparent film.

6.3 Perform the measurement in accordance with the operating instructions for the device. Typically, data are collected on a continuously averaged basis for 1 to 2 minutes.

6.4 Repeat as necessary to obtain a sufficient sample size.

6.5 Quality assurance can be addressed by periodically restandardizing the instrument, verifying the internal calibration by measuring a known standard, and performing a blank measurement. If necessary and possible, collect a sample for laboratory analysis to verify measurement accuracy or identify possible matrix effects, or both.

APPENDIX E

Literature Review

This appendix presents the results of the literature search on the state-of-the-art theory and practice for "fingerprinting" the most common materials used in highway construction. The appendix includes a review of the theory behind several spectroscopic techniques and a discussion on their applicability to highway construction materials. Finally, the most promising laboratory and field testing devices are compared in terms of their applicability, complexity of usage, sensitivity, and reliability.

Introduction

The research team explored bibliographic databases using the Transportation Research Information Service (TRIS) and then expanded the search to include various Internet bibliographic sources, such as the ASCE Civil Engineering database, ScienceDirect, and others. This approach did not limit the sources to those directly related to the fields of transportation or civil engineering but included various journals on chemistry and the petroleum industry where asphalt-related materials were widely discussed. On the basis of the results of the literature search, the research team created a computerized bibliographic database in specialized software called Bibus.

The literature analysis was divided into the following topics:

- Underlying principles of the most commonly used spectroscopic methods of material analysis (i.e., infrared and Raman spectroscopy; gas, gel permeation, and liquid chromatography; X-ray diffraction and fluorescence; and nuclear magnetic resonance);
- Practical application of the above methods to identify substances of interest (e.g., paints and coatings, antistripping agents, phosphoric acid additive, air oxidation, polymer additives, asphalt emulsions, water content, curing agents, portland cement content);
- Evaluation of spectroscopic devices and their applicability to the on-site analysis of construction materials versus laboratory analysis in terms of availability, applicability, limitations, complexity of usage, sensitivity, and reliability; and
- Review of the ASTM and AASHTO standards relevant to spectroscopic testing of the transportation construction materials.

Overview of Instrumental Techniques of Material Analysis

Most spectroscopic techniques described here (with the exception of chromatography) rely on the interaction of light with matter. Electromagnetic waves of different wavelengths interact with atoms and molecules in different ways that are dictated by physical laws. Each material has a unique chemical structure, consisting of chemical elements that combine in predictable amounts and spatial configurations. The type and chemical arrangement of elements in a compound dictate the outcome of its interaction with light of different wavelengths. Targeting a material with radiation of known wavelength and observing the outgoing signal can be used to infer the chemical properties of the material and potentially its amount within a mixture of different compounds. This section discusses theoretical aspects of chromatographic and spectroscopic techniques of interest for transportation materials.

Chromatography

Chromatographic methods physically separate the components of a mixture and distribute them between two phases. One phase remains stationary (a solid, a gel, or a liquid solvent), while the other phase (a liquid or a gas) moves in a definite direction (*1*). The separated compounds can then be

detected by coupling the chromatographic column with a detector that identifies each compound separately.

The stationary phase can be placed in two shapes of apparatus, the column and the planar chromatograph. In the column chromatograph, the stationary phase is placed in a cylindrical tube. In the planar chromatograph, a thin layer of solid particles spread on a glass plate or a paper saturated by a liquid may serve as the stationary phase (*1*). The classification of the separation techniques according to the physical state of mobile and stationary phases include gas–liquid chromatography (GLC), gas–solid chromatography (GSC), liquid–liquid chromatography (LLC), and liquid–solid chromatography (LSC) (*1*). Finally, four different separation mechanisms can be used in chromatography: adsorption, partition (gas or liquid chromatography), ion-exchange chromatography, and size-exclusion chromatography (*1*). Each separation methods exploits a different attribute of the mixture components: affinity to sorb on the stationary phase, affinity to dissolve in a particular medium, ability to occupy anionic or cationic sites, and size, respectively. Figure E.1 schematically summarizes the classification of chromatographic methods. The separation results are typically presented in the form of a chromatogram, where the concentration of each component in the mobile phase is graphed versus the mobile phase volume or over time. The detailed description of chromatographic techniques can be found elsewhere (*1, 2*).

The research team identified the following methods as most commonly used for highway construction materials: (a) gel permeation chromatography (GPC), (b) size-exclusion chromatography (SEC), (c) GLC, and (d) high-performance liquid chromatography (HPLC). These methods are further discussed in the section on the current practice of material analysis in transportation, whereas the feasibility of using portable chromatographic devices is analyzed in the section on the overview of spectroscopic equipment.

Infrared Spectroscopy

Infrared (IR) spectroscopy is based on the energy absorption of IR electromagnetic waves by molecules. The IR radiation spectrum covers a range of wavelengths from 0.78 to 1,000 μm, which corresponds to the red end of the visible region at high frequencies and the microwave region at low frequencies (*3*). The IR range is usually subdivided into three regions: (a) near-infrared (NIR) spectra (0.78- to 2.5-μm wavelength), (b) mid-infrared (now referred to as IR) spectra (2.5-μm to 50-μm wavelength), and (c) far-infrared (50-μm to 1,000-μm wavelength) spectra (*3*).

Photon energies associated with this part of the infrared spectrum (from 1 to 15 kcal/mole) are not large enough to excite electrons but may induce vibrational excitation of covalently bonded atoms and groups, for example –OH, C–C, or –COOH. Because organic compounds mostly comprise covalently bonded atoms, IR spectroscopy is primarily applied to fingerprint organic materials (even though inorganic compounds with covalent bonds are also amenable to IR analysis). IR spectrometers record the lattice's absorption of electromagnetic energy as a function of wavelength of specific groups of atoms in molecules. Each group has a unique absorption band at specific wavelengths regardless of the composition of the remaining molecular structure. The absorbance at these specific wavelengths can be used to quantify a particular functional group in the analyzed substance (*4*). The specific absorption peaks are easily identified on a spectrogram and can be used to identify a compound in a mixture once its IR peaks are known from the analysis in a pure state.

Two types of IR spectrometers—dispersive and Fourier transform—are available for obtaining IR spectra. Dispersive IR spectrometers have been in use since the 1940s, whereas Fourier transform IR (FTIR) devices were introduced in the 1980s. Because FTIR spectrometers are faster and can analyze multiple spectra simultaneously, they gradually replaced dispersive spectrometers. The FTIR devices employ an inert solid that is electrically heated to a temperature of 1,000°C to 1,800°C to produce infrared radiation. The other important component of FTIR spectrometers is the interferometer. The interferometer produces a unique type of signal, which has all of the infrared frequencies "encoded" into it. The signal can be measured quickly, usually on the order of 1 s or so. Thus, the time element per sample is reduced to a matter of a few seconds rather than several minutes. Most interferometers employ a beam splitter, which takes the incoming infrared beam and divides it into two optical beams. The two beams reflect off their respective mirrors

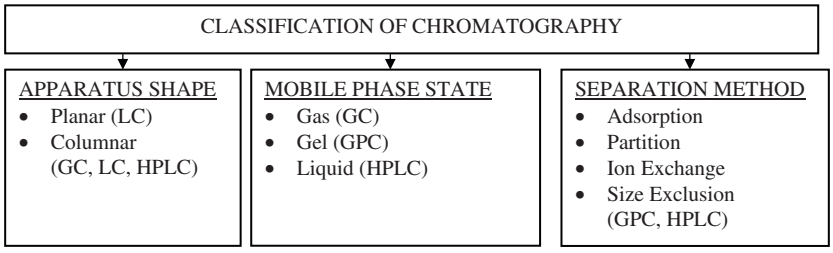

Figure E.1. Classifications of chromatographic techniques.

and are recombined when they meet back at the beam splitter. Because the path that one beam travels is a fixed length and the other is constantly changing as its mirror moves, the signal, which exits the interferometer, is the result of these two beams "interfering" with each other. The resulting signal is called an interferogram. An interferogram has the unique property that every data point (a function of the moving mirror position) making up the signal has information about every infrared frequency, which comes from the source. FTIR is the most commonly used IR method. Attenuated total reflectance (ATR) accessories have recently become available for obtaining IR spectra of highly absorbing samples that cannot be readily examined by the normal transmission method (*3*).

X-Ray Fluorescence Spectroscopy

X-ray fluorescence spectroscopy (XRF) is the emission of characteristic "secondary" (or fluorescent) X-rays from a material that has been excited by a bombardment of high-energy X-rays or gamma rays (*5*). When materials are exposed to short-wavelength X-rays or gamma rays, their component atoms may ionize. As a result, the material emits radiation at energy characteristic of the atoms present. The term fluorescence is applied to phenomena in which the absorption of higher-energy radiation results in the re-emission of lower-energy radiation (*5*). The wavelength of this fluorescent radiation can be calculated and analyzed either by sorting the energies of the photons (energy-dispersive analysis) or by separating the wavelengths of the radiation (wavelength-dispersive analysis). Once sorted, the intensity of each characteristic radiation is directly related to the amount of each element in the material.

The XRF method is widely used to determine the elemental composition of materials. Because this method is fast and nondestructive to the sample, it is often used in field and industrial applications for quality control of materials.

X-Ray Diffraction Spectroscopy

X-ray diffraction (XRD) spectrometry is one of the most powerful analytical tools available for identifying crystalline substances in complex mixtures (*6*). All crystals are composed of regular, repeating planes of atoms that form a lattice. When coherent X-rays are directed at a crystal, the X-rays interact with each atom in the crystal, exciting their electrons and causing them to vibrate with the frequency of the incoming radiation. The electrons become secondary sources of X-rays, reradiating this energy and creating interference patterns that depend on the distance between atomic layers, chemical composition, and the angle between the X-ray beam and the atomic plane (*6*).

The diffraction pattern created by constructive interference is recorded by a beam detector as the X-ray tube and the detector are rotated around the sample. The relationship between the angle at which diffraction peaks occur (2θ) and the interatomic spacing of a crystalline lattice (d-spacing) is expressed by Bragg's law: $n_l = 2d\sin u$. Traditionally XRD traces, or diffractograms, are expressed in units of two theta degrees (2θ). Because each crystalline structure is unique, the angles of constructive interference form a unique pattern. By comparing the positions and intensities of the diffraction peaks against a library of known crystalline materials, samples of unknown composition can be identified (*6*).

Raman Spectroscopy

Raman spectroscopy is named after C. V. Raman, who discovered the photon-scattering effect. The Raman method exploits the effect of the inelastic scattering of light from laser in NIR visible or ultraviolet (UV) range. Light interacts with phonons (quantized modes of vibration) or other excitations in the system, resulting in a shift of the laser photons' energy (*7*). The difference between the incident and scattered frequencies corresponds to an excitation of the molecular system. A Raman spectrum is obtained by measuring the intensity of the scattered light as a function of the frequency difference. This spectrum reveals information about the chemical structure and physical state of the sample (*8*).

A Raman instrument comprises three basic components: (a) a laser to excite the sample, (b) a spectrograph that channels the light and separates the component frequencies, and (c) a detector that measures the energy, or intensity, of each component frequency. Many complete Raman systems also include operating software for instrument control, data acquisition, data processing, and analysis (*8*).

The Raman method can be applied to solid, liquid, or gaseous samples (transparent or nontransparent) of a wide size range (from 1 m^2 to a few square centimeters) with different surface textures (i.e., Raman spectroscopy can be applied to any optically accessible sample, where a pretreatment of the sample is not necessary) (*9*). The main drawback of Raman reported in the literature is its poor sensitivity, which precludes the detection of substances at very low concentrations (*9*). However, two special techniques—the resonance Raman effect and surface-enhanced Raman scattering—can be used to enhance the intensity of the inherently weak Raman signals by several orders of magnitude (*9*).

A detailed description of Raman spectroscopy can be found in the literature (*7–10*). Applications of Raman spectroscopy to highway materials and specific Raman devices are discussed later in this report.

Nuclear Magnetic Resonance

Nuclear magnetic resonance (NMR) is a phenomenon that occurs when the nuclei of certain atoms are immersed in a static

magnetic field and exposed to a second oscillating magnetic field. Only the nuclei with spin (a fundamental particle property produced by the rotation of nucleons, protons, or electrons around their own axis) exhibit the NMR phenomenon (*11*). Time-domain NMR is used to probe molecular dynamics in solutions, whereas solid-state NMR is used to determine the molecular structure of solids in the frequency domain (*11*).

NMR spectroscopy employs the radio frequency (RF) range (60 to 800 MHz for hydrogen nuclei) to measure the energy of photons (*11*). The NMR signal results from the difference between the energy absorbed by the spins making a transition from a lower to a higher energy state and the energy emitted by the spins simultaneously making a transition from a higher to a lower energy state (*11*). The signal is thus proportional to the population difference between the states. NMR is a rather sensitive spectroscopy because it is capable of detecting these very small population differences by measuring resonance, or exchange of energy, at a specific frequency between the spins and the spectrometer (*11*). The difference between the resonance frequency of the nucleus and a standard (usually, carbon-13 or hydrogen-1) is called the chemical shift of a nucleus, which is measured in parts per million (ppm) and denoted by δ (*11*). Measuring the chemical shift enables the identification of chemical elements.

Figure E.2 shows a schematic diagram of the NMR hardware (*11*). Within the bore of the magnet are the shim coils for homogenizing the produced magnetic field. The probe placed within the shim coils contains the RF coils, which in turn produce the magnetic field necessary to rotate the spins by 90° or 180° and detect the signal from the spins (*11*). A computer controls all of the spectrometer components, including the RF frequency source and pulse programmer, which control the pulse sequences and frequencies.

Current Practice of Material Analysis in Transportation

This section presents a review of current applications of spectroscopic techniques for identifying transportation-related materials and their components. The review includes the techniques applied by researchers and material engineers in the laboratory as well as in the field conditions. Table E.1 provides a summary of references grouped by materials and methods.

Applications of Chromatography

For the past two decades, material engineers have used different chromatographic methods to study the properties of various asphalt additives and, recently, of portland cement. The most commonly used methods are SEC/GPC, liquid chromatography (LC), ion-exchange chromatography (IEC), and gas chromatography (GC). Below is a brief review of the relevant studies.

Size Exclusion and Gel Permeation Chromatography

This method showed success in characterizing asphalt components and predicting asphalt behavior in the field (*12–14*). The aromatic fractions of asphalt were analyzed by GPC to study the process of crystallization (*12, 13*). In the early 1990s, a strong correlation was found between GPC profiles and rheological properties of asphalt, such as viscosity and resistance to oxidation (*14, 15*).

The U.S. Army Corps of Engineers used GPC to investigate the aging of asphalt- and coal tar-based joint sealants (*16, 17*).

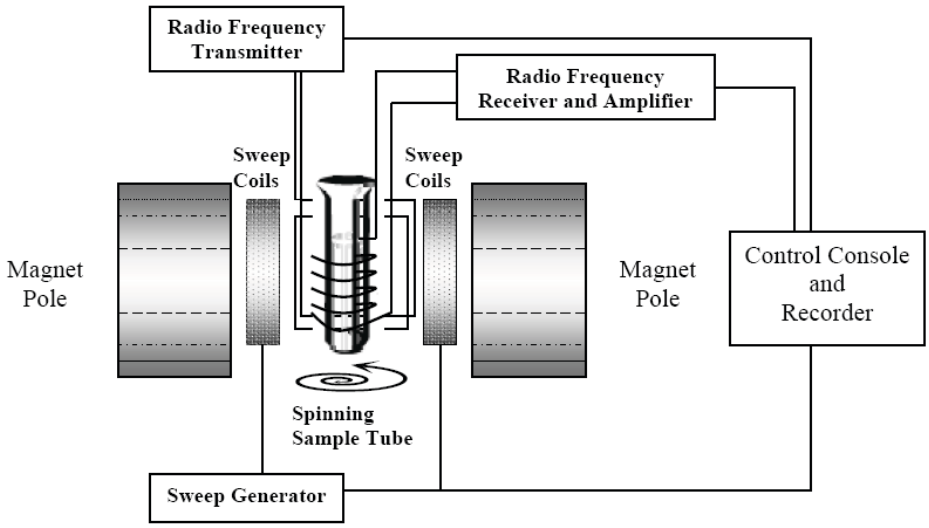

Figure E.2. Diagram of the major systems of an NMR spectrometer.

Table E.1. Summary of References by Materials and Methods

			Methods									
			NMR	Raman	FTIR	NIR	XRD	XRF	GC	LC/HPLC	SEC/GPC	IEC
		Reference	*13, 55, 70, 79, 88–92*	*50, 63–73*	*19, 24, 34–59*	*60–62*	*69, 70, 74–83*	*81, 84–87*	*33–35*	*20, 29, 30*	*12–25,26–28*	*28, 31, 32*
Materials	Coatings	Epoxy coatings			*59*							
	Asphalt-Related Materials and Properties	Hydrated lime										*32*
		Antistripping agents			*45, 46*							
		Asphalt contaminants			*34, 35*				*34, 35*			
		Phosphoric acid additives									*27*	
		Aging and antioxidants	*91*		*19, 38–44*					*20*	*18–20, 22–25*	
		Polymer additives		*71*	*24, 47–49*				*33*		*24–26, 31*	
		Asphalt emulsions			*42, 43*							
		Air-blown asphalt									*21*	
		Physical properties	*13, 88–90, 92*	*72,73*		*60*	*74*				*12–14, 28*	
	Sealants	Joint sealants									*16, 17*	
	Portland Cement Concrete-Related Materials	Sulfate–magnesium reactions			*54, 55*							
		Fly ash and aggregates		*67*			*81, 82*					
		Portland cement	*55,70, 79*	*50, 63–66, 68–70*	*50–53*		*69, 70, 75–80*					
		Admixtures			*56–58*						*29*	
	Reinforcement/corrosion						*83*					
	Soil stabilization/compaction					*62*						
	Wood structures					*61*						
	Detection of metals in air and soils						*78, 83*	*84–87*				

The study showed that GPC could be successfully used to identify sealants that have been exposed to prolonged heating in the laboratory or to natural weathering in the field. However, the researchers failed to correlate the changes in the molecular size distribution of the sealants to their physical properties (*16, 17*).

The GPC method was also successfully used to study the effect of aging on asphalt behavior (*18–20*). Using GPC allowed for the identification of air-blown asphalts, which are prohibited for use in some states because of preoxidation that occurs during production (*21*). GPC results also reflected well the compositional changes in rejuvenated binders (*22, 23*). The foregoing studies agreed that the distribution of molecular sizes was affected by the age of asphalt (i.e., the amount of large-sized molecules increased with the time as the amount of the medium- and small-sized molecules decreased).

Additionally, a number of studies used GPC to evaluate polymer-modified binders and emulsions (*24–26*). For example, the GPC chromatograms of styrene–butadiene–styrene (SBS) polymer indicated that the considerable degradation of polymer over time contributed to the binder aging (*24, 25*). However, others reported that GPC merely indicated the presence of a polymer in the binder, but failed to identify its chemical structure (*26*). Similarly, a study investigating the effect of polyphosphoric acid (PPA) addition in binders succeeded in identifying the presence of PPA in the binder using GPC (*27*). To facilitate the process of defining the asphalt fractions, a multiple-column SEC/GPC was developed under a FHWA study in 2001 (*28*). SEC/GPC was employed not only for asphalt but also for portland cement concrete-related research, such as the evaluation of the performance of a plasticizer–water reducer (*29*). GPC is a reliable technique to determine molecular weight of different components in a mixture.

Liquid Chromatography

When using a high-performance liquid (e.g., helium-sparged *n*-hexan, methanol, and toluene), the separation technique is referred to as high-performance liquid chromatography (*20, 28, 30*). HPLC was employed to quantify the aromatic fraction of aged recycled asphalts using the refractive index response factor (*20*). An FHWA study indicated that excessively large molecules can be slowed inside the column during the SEC/GPC separation and may thus be unaccounted for (*28*). Using HPLC also allowed for the prediction of pavement service life based on differences in the molecular size distribution of individual asphalts (*28*).

Ion-Exchange Chromatography

The IEC separation method uses an activated anion or cation resin as a mobile phase. A detailed description of the method can be found elsewhere (*1, 28, 31*). This method is less commonly used in the asphalt industry because of the high costs and the complexity of sample preparation (*32*). Nevertheless, it was effectively used for determining the concentration of hydrated lime in asphalt (*32*).

Gas Chromatography

GC was successfully used in Canada to measure the initial boiling point of low-fuming SBS-modified asphalt (*33*). It allowed hot-mix plant operators and paving contractors to minimize fumes and odors from mix plants and paving job sites (*33*). Purdue University researchers used GC to detect the presence of contamination (alternative fuel) in asphalt (*34, 35*).

Chromatographic methods are particularly applicable to fractionate asphalt binders in order to identify individual chemicals. Most of the chromatographic separation methods require stationary laboratory equipment, which may not be readily available to departments of transportation and contractors. However, attempts have been made recently to develop portable chromatographic devices (e.g., handheld GC and table-size HPLC equipment). The feasibility of using those devices for transportation-related materials analysis is discussed later in this report.

Applications of Infrared Spectroscopy

IR spectroscopy is the most commonly used method to determine the chemical composition of various construction materials, including portland cement, asphalt, and epoxy coatings. Below is a review of the research conducted and documented during the past 15 years.

Fourier Transform Infrared Spectroscopy

Various studies employed FTIR to investigate aging of asphalt. For instance, FTIR was used to quantify the extent of oxidation based on the area under the carbonyl absorption band (*19, 36–44*). The mechanism of rejuvenator diffusion into the recycled binder was also qualitatively evaluated using FTIR (*39*). The researchers found FTIR suitable for monitoring the diffusion process involved in bituminous binder mixing if a difference between IR absorption exists between the two components (*39*). Contaminant residues (decomposed tars and fuel) were effectively identified by FTIR in South Dakota (*34, 35*). FTIR has also been used to detect the presence of a stripping agent (*45, 46*).

AASHTO T302-05 standardized the FTIR method to identify polymer-modified binders (PMB) procedures (*47*). The Virginia Department of Transportation established this test as a first-level indicator for quality assurance of the PMBs (*48*). SBS polymers were successfully identified using FTIR spectra (peaks at 966 cm^{-1} and 700 cm^{-1}) instead of a traditionally used softening point test (*24, 49*). Similar results were obtained in studies of emulsified binders (*42, 43*). The presence of antioxidants, such as zinc dialkyldithiophosphate and

zinc dibutyl dithiocarbamate, was effectively tracked using FTIR even at very low concentrations (*41*).

FTIR has been successfully used in the portland cement industry for more than three decades. Since the 1970s, clinker constituents (alite, belite, tricalcium aluminate, and brownmillerite) have been quantified with FTIR (*50–53*). The behavior of PCC exposed to magnesium- and sulfate-aggressive environments has also been studied (*54, 55*). FTIR studies were recently conducted on the effect of different admixtures (pozzolanic, polymeric, and air-entraining additives) on portland cement properties (*56–58*).

Another example of a material successfully studied with FTIR is protective coating of steel structures (*59*). Analysis of FTIR spectra identified a low degree of curing as the reason for premature failure of the coating.

Near-Infrared Spectroscopy

Although most studies found in the literature were conducted in the mid-infrared region (2.5-μm to 25-μm wavelength), some researchers exploited the near-infrared region (0.75-μm to 2.5-μm wavelength) to investigate a range of construction materials. For example, a good correlation was reported between NIR spectra and asphalt properties, such as penetration, viscosity, and flash point (*60*). The NIR absorbance spectra showed very strong correlation ($R^2 = 0.9$) with the weathering behavior of in-service wood structures (*61*). The NIR method, though, was not recommended for use in monitoring compaction of soils because of high sensitivity to nonmoisture factors that harm the accuracy of results (*62*).

FTIR technology became the most common method of material analysis because of the equipment's compact size and the relatively easy interpretation of absorbance spectra. This makes the FTIR spectroscopy a good candidate for further evaluation because of its applicability to on-site identification of different chemicals. A detailed discussion of the FTIR equipment as compared to other spectroscopic methods is provided later in this report.

Applications of Raman Spectrometry

Raman has been used primarily for the analysis of substances with low light absorptivity, such as white portland cement and its supplements. Additionally, the hard X-ray Raman spectra have been used to characterize light elements in petroleum products.

Infrared Raman Spectroscopy

Raman was first used in the late 1970s for the chemical analysis of portland cement (*50, 63*). At that time, the application of Raman to gray cement was limited by the low laser power, though it was successful in studying white cement (*64*). Recently, researchers conducted a comprehensive Raman analysis of portland cement, slag, and fly ash, and they concluded that structural fluorescence can be overcome by using a 785-nm NIR laser (*65, 66*). In another study, the chemical composition of fly ash was established using Raman (*67*). Raman also appeared to be useful to characterize hydraulic lime (*68, 69*) as well as various forms of gypsum using a 514.5-nm excitation wavelength (*66*). Despite these successful applications, some researchers still question the usefulness of IR Raman, compared to other spectroscopic methods (e.g., XRD and NMR), to analyze cement mineralogy (*70*).

Over the past decade, multiple attempts were made to develop reliable portable Raman devices. For instance, the prototype of a portable FTIR Raman spectrometer was reported to be used successfully to correlate Raman kinetic data with rheological properties of cured polymers (*71*).

X-Ray Raman Spectroscopy

The literature search yielded few studies on the use of Raman for asphalt analysis. One study found that X-ray Raman energy peaks were correlated with the macroscopic properties of polycyclic aromatic hydrocarbons and asphaltenes (*72, 73*). In conclusion, while some promising results have been shown and documented in applying Raman technology to the analysis of cement-based materials, further research is needed to establish the feasibility of using Raman for fingerprinting asphalt-based products.

Applications of X-Ray Spectroscopy

X-ray spectroscopy is the oldest spectroscopic method for material analysis. Over the past two decades, it has been frequently used to study physical material properties and to identify the chemical components of many transportation-related materials, including aggregates, asphalt binders, emulsions, portland cements, and coatings. The three most commonly used X-ray methods are X-ray tomography (imaging), XRD, and XRF. Traditionally, X-ray technology required room-size equipment to generate X-rays, which made it inapplicable for field use. Recently, however, portable XRF and XRD devices have become available. Because on-site fingerprinting of target chemicals concerns this project, the XRD and XRF spectroscopic methods are discussed below.

X-Ray Diffraction

XRD has been rarely employed for the analysis of asphalt materials as compared with chromatography and FTIR spectroscopy (Table E.1). Only one study employed XRD in conjunction with GPC and NMR to compare asphalt binders with different rheological properties (*74*). On the contrary, numerous studies present XRD analysis as a good quantitative

method for analyzing portland cement and its supplements (*69, 70, 75–79*). In general, XRD is more appropriate for crystalline organic compounds and only finds application in organics analysis in the pharmaceutical industry. Recently, an ASTM method was developed for quantitative X-ray diffraction testing of portland cement using the Rietveld method (*80*). However, the technique is only used to quantify clinker minerals in dry cement, which are well-defined crystalline compounds. Testing the composition of hydrated portland cement and concrete is a more complicated task.

The NCHRP *Research Results Digest 281* pointed at XRD as a suitable technique for identifying the mineral components of aggregates (*81*). In India, an XRD test was conducted to study the crystalline phases present in fly ash (*82*). In a study of potential soil stabilization options, XRD analysis yielded the quantitative composition of the soil with reasonable accuracy (*78*). Because X-rays are extremely sensitive to the presence of heavy metals, XRD was successfully used to study corroded reinforcement (*83*).

X-Ray Fluorescence

XRF was used to assess the durability of carbonate aggregates (*81*). Portable XRF devices have been available since the early 1990s, which, in conjunction with their ability to quantify the concentration of heavy metals, facilitates their use in air and soil analysis (*84–87*). This also makes XRF a good candidate for asphalt applications concerning metals.

Application of Nuclear Magnetic Resonance

Among various spectroscopic techniques, NMR appears to be the most powerful tool to quantitatively describe the atomic and molecular structure of materials. In the transportation field, researchers have been successfully using NMR spectroscopy and NMR imaging to analyze asphalt- and portland cement-related materials since the 1990s. The carboxylic acid and phenol content of a variety of asphalts (first fractionated by SEC) were measured using carbon-13 and hydrogen-1 NMR spectra (*13, 88–90*). In another study, NMR imaging facilitated assessing the degree of aging and asphalt compatibility in aged asphalt (*91*). NMR imaging was recently used to evaluate moisture-induced damage in asphalt layers by measuring the interfacial properties of asphalt components (*92*). For cement-based materials, NMR was used to investigate the structural organization of portland cement and its phases using silica-29 spectra (*55, 70, 79*).

NMR has traditionally required a laboratory environment because of the high magnetic fields required. Recently, however, portable NMR devices have become available (*93*), creating an excellent opportunity to explore their application in field conditions as part of this study.

Summary of Applications Review

Table E.1 summarizes the references used in this section in the form of a material–method matrix. On the basis of the number of references related to a specific method or material, one can reasonably conclude that some techniques were used for the analysis of particular materials more often than others. For example, it appears that FTIR has been successfully used for the analysis of fundamental properties of asphalt and its additives as well as for the analysis of portland cement and its admixtures. XRD has been used more often to determine the composition of portland cement with almost no asphalt-related applications. All types of chromatography appeared necessary to separate asphalt components to enable the interpretation of FTIR or Raman spectra. NMR spectroscopy and imaging have been reported to be robust quantitative methods for both asphalt and portland cement. The suitability of Raman technology for asphalt analysis should be evaluated further in this study.

Another important observation from the literature review is that researchers have been more successful in the qualitative analysis of chemicals components compared to quantitative analysis. Quantification of the components or phases in construction materials requires comprehensive spectra libraries and precise analytical procedures. These issues, along with the availability of the portable equipment, the limitations, and complexity of device usage, analysis time, sensitivity, and reliability are discussed in the next section.

Overview of Spectroscopic Equipment

Spectroscopic methods are compared in terms of the size of the apparatus (i.e., room size, table size, portable, or handheld), sample preparation requirements, limitations and complexity of usage, analysis time, sensitivity, and reliability. The following types of equipment are discussed: SEC/GPC, HPLC, GC, FTIR, Raman, XRD, and NMR. Typical features and images are provided for each device type.

Size-Exclusion Chromatography and Gel Permeation Chromatography

The SEC/GPC apparatus developed in the 2001 FHWA study includes the following main components: a refraction column (usually 5 cm in diameter and 100 cm long) filled with reagent (e.g., toluene, methanol, or dichloromethane), two flasks filled with sample of asphalt solution, several graduated cylinders, about 10 m of tubing, and a laboratory pump (*28*). A sample of asphalt to be separated is relatively small (16 g) (*28*). FHWA reported that the precision of the method depends on the sharpness of the onset of fluorescence in the

SEC Fraction-II eluates. The method is very precise when the same asphalt dependent cut point for SEC Fraction-I is used for each run (*28*). One drawback of the setup is that a large amount of toluene is necessary for the separation, although the toluene is typically distilled and is reused (*28*). For portability of the proposed setup laboratory, room conditions are essential for the process, making on-site use difficult. An image of a Waters GPC system can be found elsewhere (*94*).

Size-Exclusion Chromatography and High-Performance Liquid Chromatography Chromatographs

Concurrently with the GPC setup, the fast SEC/HPLC experimental protocol was developed in the FHWA study (*28*). Although the main components of the apparatus remained the same, a modern and compact device was added, the Hewlett Packard (HP) Series II 1090 liquid chromatograph (*95*), along with a laptop computer with the HPLC analysis software (*28*). This HPLC device uses liquid-grade toluene as a reagent. The sample size (weighed, dissolved, and centrifuged) is about 24 mg contained in 220-mL solution (*28*). A very high level of precision (1% standard deviation from the average for the largest fractions) was reported by the developers of this experimental setup, though some calibration was still required (*28*). Another example of a portable HPLC chromatograph is the SRI Model 210D with specifications similar to those of HP Series II 1090 liquid chromatograph (*96*). The portability of HPLC devices can be described as low, because they cannot be carried by the operator. However, installation of such devices in a mobile laboratory (e.g., truck-based) is possible.

Gas Chromatographs

GC was reported to be successful for detection of asphalt contaminants and polymer additives. Therefore, the use of portable GC devices could facilitate on-site quality control. One example of such a device is a Photovac's Voyager portable chromatograph (*97*). According to its manufacturer, the device is capable of detecting a range of chemicals, including petrochemicals, latex polymers, and volatile organic compounds when an appropriate compound library is used with the device. The Voyager portable GC is 39 cm long, 27 cm wide, and 15 cm high and weighs about 7.2 kg. It is also equipped with a NiCd battery that has an 8-h life (*97*). These characteristics make the Voyager a good candidate for a feasibility study.

Fourier Transform Infrared Spectrometers

FTIR spectrometers have been used in the analysis of a wide range of transportation-related materials. These devices have seen dramatic improvements in portability, precision, reliability, and time efficiency in the past two decades. Only the most recently developed devices are compared here as relevant to this project and available to the research team.

ALPHA FTIR device by Bruker Optics is 22 × 30 × 25 cm in dimensions and weighs about 7 kg (*98*). It has a spectral range from 7,500 cm^{-1} to 375 cm^{-1} with a resolution of at least 2 cm^{-1} (0.9 cm^{-1} is optional) and an accuracy of 0.01 cm^{-1} (*98*). The device is designed to operate at 18°C to 35°C and is powered by 100 to 240 volts AC power or by a high-capacity battery. Software, including a comprehensive library of chemical components, is provided with this device (*98*). The exchangeable measurement modules include transmission, ATR, and reflection, making it possible to analyze a range of materials (liquid, solid, or gas) (*98*). The research team has already acquired an ALPHA FTIR device that will be used in the experimental phase of the project in both laboratory and field conditions.

A handheld Exoscan ATR FTIR spectrometer has been developed by A_2 Technologies (*99*). It has dimensions of 17 × 12 × 23 cm and weighs about 3 kg (*99*). The spectral range of Exoscan (4,000 cm^{-1} to 650 cm^{-1}) is narrower than that of Bruker's ALPHA. The device operates at any positive outside temperature (0°C to 50°C) and has a lithium battery life of 3.2 h, which makes it valuable for on-site analyses of large samples that cannot be brought to the laboratory (*99*). A personal digital assistant attached to the Exoscan device facilitates the analysis of the sample, practically, on the spot. The operational modes include ATR and reflection, which, according to the manufacturer, make Exoscan useful in a range of applications, such as evaluation of coatings, glues, and cured polymers, and capable of sampling liquids, solids, gels, and gases (*99*). A similar device, the HazMatID Ranger, uses ATR FTIR principles of operations (*100*). It is able to operate at a slightly wider range of temperatures (–7°C to 50°C). The library of identifiable chemicals includes up to 32,000 materials (*100*).

Raman Analyzers

One example of briefcase-size Raman spectrometers is the Real-Time Analyzers' RamanID (*101*). The analyzer measures the entire Raman spectrum in each scan, from 150 to 3,350 cm^{-1}, with a spectral resolution selectable from 2 cm^{-1} to 32 cm^{-1}. Both 785- and 1,064-nm laser excitation are offered (Class 3B lasers). Fiber optic probes and enclosed sample compartments (for added eye safety) are also available. According to the manufacturer's specifications, the device is capable of analyzing any solid or liquid in a very short (about 10 s) time and is equipped with software installed on a laptop computer (*101*). Additionally, it does not require any sample preparation or calibration, although sample preparation is a function of the measurement objective (for example, asphalt binders may be too complex to analyze

without any sample preparation). The RamanID operates at 2°C to 37°C and has a 5-h rechargeable battery (*101*). The analyzer employs interferometry to generate the Raman spectrum, which eliminates need for recalibrations (*101*).

The handheld lightweight (about 2 kg) Raman detectors have been reported to be used for verifying chemical identities of pharmaceutical and other industrial materials (e.g., raw materials, oils, coating) (*102, 103*). The two examples of such equipment are Ahura Scientific's TruScan (*102*) and DeltaNu's Inspector Raman (*103*). Both devices provide a common, but truncated, spectral range (about 250 cm^{-1} to 2,000 cm^{-1}) with resolution of 7 cm^{-1} to 10 cm^{-1} across the range (*102, 103*).

X-Ray Diffraction and X-Ray Fluorescence Systems

High-resolution laboratory X-ray equipment occupies a space comparable to a medium-size room. Because this project is focused on the devices suitable for field operations, only portable X-ray equipment is discussed in this section.

The portable XRD/XRF Terra analyzer (*104*) is briefcase size (about 49 × 40 × 20 cm in dimensions and 14.5 kg by weight). This device was developed by inXitu (*104*) for the identification of minerals and aggregate mixtures. According to the manufacturer, the system requires only minimum sample preparation and, within minutes, detects single minerals or simple mixtures. The Terra analyzer provides XRD resolution of 0.25° 2θ over the range of 5° to 55° 2θ and XRF resolution of 230 eV (at 5.9 keV) over the range of 2 to 25 keV (*104*). The device can operate in autonomic mode for at least 4 h and a laptop computer allows the user to configure the analysis, preview live data, explore archive files, and download data for pattern matching with a mineral database using commercial software (*104*).

Handheld XRF devices are available for the analysis of metals in soils and lead in air, such as Innov-X Alpha (*105*), Thermo Scientific NITON XL3t, and Skyray Instruments EDX Pocket-II analyzers (*106, 107*). They usually contain a miniature X-ray tube and a built-in screen (*106, 107*). As reported by the manufacturers, the portable X-ray devices are capable of identifying a wide range of metallic elements with varied detection limits (e.g., 15 ppm for Cd; 8 ppm for Pb, Hg, and Br; and 25 ppm for Cr) (*106, 107*). The research team already owns an Innov-X portable XRF analyzer.

Nuclear Magnetic Resonance Analyzers

Since the 1980s, laboratory-based NMR systems have been used for the analysis of petroleum products, mostly by university-based researchers. For example, a Bruker AV300/1 NMR spectrometer uses time-domain analysis of solutions or frequency-domain analysis of solids in ^{1}H, ^{13}C, ^{31}P, or ^{19}F environments (*108*). Such equipment may weigh up to 1,500 to 2,000 lb. This time-domain or low-resolution NMR (TD-NMR) has been used for quality assurance/quality control in the petrochemical and polymer industry (*93*). A portable high-resolution spin track NMR spectrometer has been developed by Process NMR Associates LLC (*109*). A laptop computer with software containing many standard NMR relaxation routines and applications is provided with this device (*109*).

Summary of Spectroscopic Devices Overview

The spectroscopic devices discussed above were identified as potential candidates for a feasibility study for on-site fingerprinting of transportation-related construction materials. Table E.2 summarizes the specifications of these devices. On

Table E.2. Summary of Spectroscopic Equipment Specifications

Feature	Devices							
	SEC/GPC	**SEC/HPLC**	**GC**	**FTIR**	**Raman**	**XRD**	**XRF**	**NMR**
Sample type	Liquid	Liquid	Liquid	Solid, liquid, gas	Solid, liquid	Solid	Solid, gas	Solid, liquid
Detection range	100–250,000 Da (*28*)	300–100,000 Da (*28*)	5–50 ppb (*97*)	7,500–375 cm^{-1} (*98*) 4,000–600 cm^{-1} (*99*)	3,350–150 cm^{-1} (*101*) 2,000–250 cm^{-1} (*103*)	5°–55° 2θ (*104*)	3–25 keV (*104*)	100–800 MHz (Stationary) (*93,108*) 5–60 MHz (Spin Track) (*109*)
Precision	1%–3% (*113*)	0.40‰–1.90‰ (*114*)	0.20‰–1.00‰ (*116*)	0.01 cm^{1} (*98*)	0.05 cm^{1} (*101*)	0.25 2θ (*104*)	230 eV (*104*)	±2% (*110*)
Accuracy	±3% (*113*)	3%–7% (*115*)	−1.11 ± 3.16‰ (*116*)	2–0.9 cm^{-1} (*98*)	32–2 cm^{-1} (*101*)	±3% (*112*)	1%–20% (*111*)	2%–9% (*110*)

the basis of the review of the spectroscopic equipment, the following preliminary conclusions can be drawn:

- The GPC, HLPC, and GC chromatographs are useful for separation and qualitative analysis before further identification by other spectroscopic methods. Portable chromatographs are available for use in the field and mobile laboratories.
- Infrared and Raman analyzers can be used for the analysis of a wide range of materials in the liquid, solid, or gas phase (mid-IR only). Several field-portable systems are available.
- The handheld XRD and XRF systems are available for the identification of a wide range of metals. They can be operated in outdoor conditions at temperatures above freezing.
- Most of the NMR equipment for analyzing solid-state matter is laboratory-based and cannot be used in the field. However, bench-top (or semiportable) time-domain NMR analyzers are available that appear to be useful for the analysis of liquid-state substances, such as fractionated asphalts.

Spectroscopy Standards in State Transportation Agencies in the United States

This part of the literature review covers the ASTM/AASHTO standards relevant to spectroscopic testing of transportation construction materials. Additionally, it describes local specifications developed by the state highway agencies (SHAs) throughout the United States.

ASTM/AASHTO Standards

Twenty-six national standards were found to be relevant to the objective of this study (Table E.3). Three spectroscopic methods appear to be the best documented: (a) FTIR, (b) XRF, and (c) chromatography (liquid, gas, and ion). Out of 26 standards summarized in Table E.3, only seven were found to be used by SHAs for testing highway construction materials, primarily portland cement and its products and paint coatings. Two procedures were developed by FHWA for asphalt-related materials.

State Highway Agencies' Spectroscopic Testing Procedures

A search of all 50 SHAs' websites revealed that nine states share their locally developed (or modified ASTM/AASHTO) standards, including Arizona, California, Kentucky, Louisiana, Maryland, Washington, and West Virginia. Table E.4 contains the spectroscopic procedures available for download from each department of transportation website.

Summary of Literature Review

The objective of this project is to evaluate the suitability of various spectroscopic techniques for fingerprinting transportation construction materials in the field. Task 1 of this study focused on the comprehensive search of literature available from transportation-related sources (e.g., TRIS), as well as from multidisciplinary bibliographic databases, such as the ASCE Civil Engineering Database and ScienceDirect. The literature review covered the underlying principles of the most commonly used spectroscopic methods, as well as the current practice of their application to the analysis of asphalt, portland cement, and other construction materials. Finally, the research team prepared an overview of the available equipment with emphasis on portable devices for the feasibility study.

Tables E.5 and E.6 show universality rankings of methods most applicable to transportation construction materials. On the basis of the quantitative comparison, it appears that the methods that can be applied to most materials are FTIR, XRF, Raman, NMR, and SEC/HPLC. This does not exclude though other discussed methods that can be very productive in some particular applications.

Table E.3. ASTM/AASHTO Spectroscopic Testing Standards

Designation	Title
Most Relevant Standards	
ASTM C25-06	Standard Test Methods for Chemical Analysis of Limestone, Quicklime, and Hydrated Lime
AASHTO T260	Standard Method of Test for Sampling and Testing for Chloride Ion in Concrete and Concrete Raw Materials
ASTM C114-09	Standard Test Methods for Chemical Analysis of Hydraulic Cement
ASTM C311-07	Standard Test Methods for Sampling and Testing Fly Ash or Natural Pozzolans for Use in Portland-Cement Concrete
ASTM D2621-87 (2005)	Standard Test Method for Infrared Identification of Vehicle Solids from Solvent-Reducible Paints
ASTM D4326-04	Standard Test Method for Major and Minor Elements in Coal and Coke Ash by X-Ray Fluorescence
ASTM D5380 93 (2009)	Standard Test Method for Identification of Crystalline Pigments and Extenders in Paint by X-Ray Diffraction Analysis

(continued on next page)

Table E.3. ASTM/AASHTO Spectroscopic Testing Standards (continued)

Designation	Title
Other Standards	
ASTM E1151 93 (2006)	Standard Practice for Ion Chromatography Terms and Relationships
ASTM E682–92 (2006)	Standard Practice for Liquid Chromatography Terms and Relationships
ASTM D3016–97 (2003)	Standard Practice for Use of Liquid Exclusion Chromatography Terms and Relationships
ASTM E355–96 (2007)	Standard Practice for Gas Chromatography Terms and Relationships
ASTM E1840–6 (2007)	Standard Guide for Raman Shift Standards for Spectrometer Calibration
ASTM E1683–2 (2007)	Standard Practice for Testing the Performance of Scanning Raman Spectrometers
ASTM D2124–99 (2004)	Standard Test Method for Analysis of Components in Poly(Vinyl Chloride) Compounds Using an Infrared Spectrophotometric Technique
ASTM D3124–8 (2003)	Standard Test Method for Vinylidene Unsaturation in Polyethylene by Infrared Spectrophotometry
ASTM E275-08	Standard Practice for Describing and Measuring Performance of Ultraviolet, Visible, and Near-Infrared Spectrophotometers
ASTM D5477-02	Standard Practice for Identification of Polymer Layers or Inclusions by Fourier Transform Infrared Microspectroscopy (FTIR)
ASTM D5576–00 (2006)	Standard Practice for Determination of Structural Features in Polyolefins and Polyolefin Copolymers by Infrared Spectrophotometry (FTIR)
ASTM D5594–98 (2004)	Standard Test Method for Determination of the Vinyl Acetate Content of Ethylene-Vinyl Acetate (EVA) Copolymers by Fourier Transform Infrared Spectroscopy (FTIR)
ASTM D6247–8 (2004)	Standard Test Method for Analysis of Elemental Content in Polyolefins by X-Ray Fluorescence Spectrometry
ASTM E1621-05	Standard Guide for X-Ray Emission Spectrometric Analysis
ASTM D6248–8 (2004)	Standard Test Method for Vinyl and Trans Unsaturation in Polyethylene by Infrared Spectrophotometry
ASTM C1118-07	Standard Guide for Selecting Components for Wavelength-Dispersive X-Ray Fluorescence (XRF) Systems
ASTM D6645-01	Standard Test Method for Methyl (Comonomer) Content in Polyethylene by Infrared Spectrophotometry
ASTM E1421–99 (2004)	Standard Practice for Describing and Measuring Performance of Fourier Transform Mid-Infrared (FTMIR) Spectrometers: Level Zero and Level One Tests
ASTM E1944–98 (2007)	Standard Practice for Describing and Measuring Performance of Laboratory Fourier Transform Near-Infrared (FTNIR) Spectrometers: Level Zero and Level One Tests
FHWA	
FHWA	Susan P. Needham Test Method for Detecting the Presence of Phosphoric Acid in Asphalt
FHWA	Laboratory Procedure for the Determination of Lime in Hot-Mix Asphalt

Table E.4. SHA Spectroscopic Testing Procedures

State	Material	Spectroscopic Method
Arizona	Exchangeable sodium in topsoil	Spectrophotometry
	Chloride in concrete admixtures	Ion meter
California	Portland cement, fly ash, pozzolan	XRF
	Chloride in soils and waters	Ion chromatography
	Portland cement concrete admixtures	FTIR
	Pigments and extenders in paints and coatings	XRD
Kentucky	Hydrated lime, fly ash, portland cement	XRF
Louisiana	Portland cement concrete admixtures	FTIR
Maryland	Sulfur fungicide products	FTIR
Washington State	Coatings (pigmented sealers) on concrete structures	FTIR
West Virginia	Hydraulic cement	XRF

Table E.5. Universality Rank of Spectroscopic Devices

Material Category	Method								Objective
	SEC/GPC	SEC/HPLC	GC	FTIR	Raman	XRD	XRF	NMR	
Structural coatings (epoxy and polyurethane based)	0	0	0	2	1	1	1	1	Formula verification Presence of solvents/diluents
Pavement markings (such as epoxy markings)	0	2	1	2	2	1	0	1	Formula verification Presence of solvents/diluents
Epoxies (for concrete repair)	0	2	0	2	1	0	0	1	Formula verification (proper proportioning for two components)
Portland cement	0	0	0	2	2	2	2	1	Cement quality and type
Portland cement concrete (PCC)	0	0	0	0	0	2	2	0	Cement/water/additives content in PCC Detection of prohibited chemicals/modifiers
Admixtures for PCC	1	0	0	2	2	2	0	1	Formula and type verification
Curing Compounds for PCC	0	0	0	2	2	1	1	1	Formula and type verification
Modified asphalt (SBS, Elvaloy, EVA, PPA)	1	2	1	2	1	1	0	1	Type and content verification
Asphalt concrete	0	2	0	1	1	0	1	0	Detection of prohibited chemical/modifiers (such as motor oil, diesel fuel)
Asphalt emulsions	0	0	0	1	1	0	0	1	Type and water content
Antistripping agents in asphalt concrete	0	0	0	2	1	0	0	1	Type and content verification
Oxidation in asphalt concrete	2	2	0	2	1	0	0	1	Presence and amount verification
Structural steel	0	0	0	0	0	0	2	1	Quality and type verification
Aggregate minerals	0	0	0	1	1	1	0	0	Amount of noncarbonate aggregate Evaluation of the resistance to a hydrochloric acid solution
Universality score (total sum)	**4**	**10**	**2**	**21**	**16**	**11**	**9**	**11**	
Universality rank	**1**	**2**	**1**	**4**	**3**	**2**	**2**	**2**	

Note: 0 = will not work. There is no evidence in the literature review; it is not possible according to trial testing and the experience of the research team.
1 = could work. There is some evidence in the literature, based on the research team's experience.
2 = very promising. This is based on an example found in the literature.

Table E.6. General Ranking of Spectroscopic Devices

Feature	Weighting Factor	SEC/GPC	SEC/ HPLC	GC	FTIR	Raman	XRD	XRF	NMR
Analysis time	**0.8**	8–12 h (*29*)	0.5–1 h (*29*)	0.5–1 h (*29*)	1 min (5 min pretest) (*97*)	10 s (2 min warm-up) (*100*)	0.5–2 h	1–5 s (*105*)	10 min
		1	**3**	**3**	**4**	**4**	**2**	**4**	**4**
Portability	**0.5**	No	Low	Low	Medium	Medium	Medium	High	Medium
		0	**1**	**1**	**2–3**[a]	**2–3**[a]	**2**	**3**	**2**
Ambient temperature range	**0.5**	Room (*29*)	0°–55°C (*94*)	5°–40°C (*96*)	18°–35°C Benchtop (*97*) 0°–50°C-Handheld (*99*)	2°–37°C (*100*)	0°–50°C (*103*)	–30°–40°C (*103*)	Room (*107*)
		1	**1**	**1**	**1**	**1**	**1**	**1**	**1**
Ease of use	**0.8**	Medium to difficult	Difficult	Difficult	Easy to medium	Easy to medium	Medium to difficult	Easy	Medium
		1	**1**	**1**	**2–3**	**2–3**	**1–2**	**3**	**1**
Price	**0.8**	$30,000	$30,000	$27,000	<$20,000	$60,000	$65,000	$35,000–40,000	<$16,000
		2	**2**	**2**	**2**	**1**	**1**	**2**	**3**
On-site calibration required	**0.8**				No	No	No	No	
		1	**1**	**1**	**1**	**1**	**1**	**1**	**1**
Sample preparation (As it is, solution, separation, enrichment, heated/cooled)	**0.8**	None to complex	None to complex	None to complex	None to complex	None to complex	Crushing	None	None to complex
		1–3	**1–3**	**1–3**	**1–3**	**1–3**	**2**	**3**	**1–3**
Universality rank (From Table E.5)	**1**	1	2	1	4	3	2	2	2
Final rank		**7.1**	**10.2**	**9.2**	**14.7**	**12.9**	**9.1**	**14.4**	**12.3**

Note: *Analysis time:* >5 h = 1, 1–5 h = 2, <1 h = 3, <10 min = 4.
Portability: No = 0 (no portable device available), Low = 1 (heavy tabletop device), Medium = 2 (light tabletop device), High = 3 (handheld).
Temperature range: Does not work in common field conditions = 0, works in common field conditions = 1.
Ease of use: Difficult with extensive training = 1, medium with light training = 2, easy with minimal training = 3.
Price: >$50,000 = 1, $30,000–50,000 = 2, $15,000–30,000 = 3, <$15,000 = 4.
On-site calibration required: 0 = Yes, 1 = No.
Sample preparation: Complex = 1 (enrichment, separation required), simple = 2 (crushing), none = 3. This preparation may vary by material.
Universality ranking: 1–6 = 1, 7–12 = 2, 13–18 = 3, 19–23 = 4, 24–28 = 5.
Weighting factors: Established based on the responses to the workshop questionnaire (see Chapter 3).
[a] Both FTIR and Raman have handheld and light tabletop equipment available, but the latter equipment is more suitable for most materials in this project.

The literature search indicated that, because of the complexity of asphalt-related materials, chromatography is typically used first to separate the components of interest, and then a spectroscopic analysis is performed to verify the identity and quantity of the components. The literature also indicates that some techniques are more favorable for the analysis of particular materials than others are. FTIR was successfully used to determine fundamental properties of both asphaltic materials and portland cement. XRD has been traditionally used to investigate the portland cement composition rather than for the analysis of asphalt components. The suitability of Raman technology for the asphalt analysis should be evaluated further in this study, because literature references were not adequate to establish this. In the majority of published studies, the researchers succeeded in the qualitative rather than quantitative analysis of chemical compounds.

A number of portable devices such as GPC, HPLC, and GC chromatographs, FTIR and Raman spectrometers, and XRD/XRF analyzers were identified as potential candidates for the feasibility study in Phase 2. Analysis of the national standards for spectroscopic testing indicated that several procedures developed by the ASTM and AASHTO were used by the SHAs to test highway construction materials, primarily portland cement and its products and paint coatings. A search through the 50 SHA websites revealed that nine states share their locally developed (or modified ASTM/AASHTO) standards online. The search indicated the need for developing new procedures that could replace the often complicated and time-consuming chemical tests and thus allow faster and more accurate measurements.

References

1. Ettre, L. S. Nomenclature for Chromatography (IUPAC Recommendations). *Pure and Applied Chemistry,* Vol. 65, No. 4, 1993, pp. 819–872.
2. Settle, F. *Handbook of Instrumental Techniques for Analytical Chemistry.* Prentice Hall, Upper Saddle River, N.J., 1997.
3. Hsu, C-P. S. Infrared Spectroscopy. In *Handbook of Instrumental Techniques for Analytical Chemistry,* Prentice Hall, Upper Saddle River, N.J., 1997, pp. 247–283.
4. Houston, W. N., M. W. Mirza, C. E. Zapata, and S. Raghavendra. *Environmental Effects in Pavement Mix and Structural Design Systems,* NCHRP Web-Only Document 113, Transportation Research Board of the National Academies, Washington, D.C., 2005, 281 pp.
5. Jenkins, R. *X-Ray Fluorescence Spectrometry.* John Wiley & Sons, Inc., Hoboken, N.J., 1988.
6. Jenkins, R., and R. L. Snyder. *Introduction to X-Ray Powder Diffractometry.* John Wiley & Sons, Inc., New York, 1996.
7. Gardiner, D. J. *Practical Raman Spectroscopy.* Springer-Verlag, Heidelberg, Germany, 1989.
8. Lambda Solutions, Inc. www.lambdasolutions.com. Accessed August 28, 2008.
9. Schmitt, M., and J. Popp. Raman Spectroscopy at the Beginning of Twenty First Century. *Journal of Raman Spectroscopy,* Vol. 37, 2006, pp. 20–28.
10. Real-Time Analyzers, Inc. www.rta.biz. Accessed March 31, 2009.
11. Hornak, J. P. *The Basics of NMR.* http://www.cis.rit.edu/htbooks/nmr/. J. P. Hornak. 1997–2000.
12. Jennings, P. W., J. A. S. Pribanic, M. A. Desando, and M. F. Raub. Characteristics of Asphalt by NMR Spectroscopy and High Performance Gel Permeation Chromatography. *Proc., Conference on Strategic Highway Research Program and Traffic Safety on Two Continents, Part Four,* Gothenburg, Sweden, 1991, pp. 91–103.
13. Jennings, P., J. Pribanic, T. M. Mendes, and J. A. Smith. High Performance Gel Permeation Chromatography in the Characterization of Self-Assemblies in Asphalt. *Proc., American Chemical Society Symposium on Chemistry and Characterization of Asphalts,* Washington, D.C., 1992, pp. 1312–1321.
14. Garrick, N. W. Use of Gel Permeation Chromatography in Predicting Properties of Asphalt, *Journal of Materials in Civil Engineering,* Vol. 6, No. 3, 1994, pp. 376–389.
15. Kim, K. W., and J. L. Burati. Use of GPC Chromatograms to Characterize Aged Asphalt Cements. *Journal of Materials in Civil Engineering,* Vol. 5, No. 1, 1993, pp. 41–52.
16. Graham, R. T., and L. N. Lynch. *Gel Permeation Chromatography Analysis of Asphalt-Based Joint Sealants.* Technical Report AD-A268 314, U.S. Army Waterways Experiment Station, Vicksburg, Miss., 1994.
17. Graham, R. T., and L. N. Lynch. 1994b. *Gel Permeation Chromatography Analysis of Coal Tar-Based Joint Sealants.* Report GL-94-20. Federal Aviation Administration, Washington, D.C., 1994, 104 pp.
18. Churchill, E. V., S. N. Amirkhanian, and J. L. Burati. HP-GPC Characterization of Asphalt Aging and Selected Properties. *Journal of Materials in Civil Engineering,* Vol. 7, No. 1, 1995, pp. 41–49.
19. Jemison, H. B., R. R. Davison, C. J. Glover, and J. A. Bullin. Fractionation of Asphalt Materials by Using Supercritical Cyclohexane and Pentane. *Fuel Science and Technology International,* Vol. 13, 1995, pp. 605–638.
20. Chaffin, J. M., M. Liu, R. R. Davison, C. J. Glover, and J. A. Bullin. Supercritical Fractions as Asphalt Recycling Agents and Preliminary Aging Studies on Recycled Asphalts. *Industrial & Engineering Chemistry Research,* Vol. 36, 1997, pp. 656–666.
21. Hardee, J. R. *Physical and Chemical Characteristics of Superpave Binders Containing Air-Blown Asphalt from Two Different Feedstocks.* Final Report MBTC 2076. Arkansas State Highway and Transportation Department, Little Rock, Ark., 2004, 27 pp.
22. Shen, J., S. Amirkhanian, S. Lee, and B. Putman. Recycling of Laboratory-Prepared Reclaimed Asphalt Pavement Mixtures Containing Crumb Rubber-Modified Binders in Hot-Mix Asphalt. In *Transportation Research Record: Journal of the Transportation Research Board, No. 1962,* Transportation Research Board of the National Academies, Washington, D.C., 2006, pp. 71–78.
23. Shen, J., S. Amirkhanian, and S. Lee. HP-GPC Characterization of Rejuvenated Aged CRM Binders. *Journal of Materials in Civil Engineering,* Vol. 19, 2007, pp. 515–522.
24. Lu, X., and U. Isacsson. Chemical and Rheological Evaluation of Aging Properties of SBS Polymer Modified Bitumens. *Fuel,* Vol. 77, 1998, pp. 961–972.
25. Wahhab, H., I. M. Asi, F. M. Ali, and I. A. Al-Dubabi. Prediction of Asphalt Rheological Properties Using HP-GPC. *Journal of Materials in Civil Engineering,* Vol. 11, No. 1, 1999, pp. 6–14.
26. Molenaar, J. M. M., E. T. Hagos, M. F. C. Van De Ven, and R. Hofman. An Investigation into the Analysis of Polymer Modified Bitumen. *Proc., 3rd Eurasphalt & Eurobitume Congress,* Vienna, Austria, Book I, 2004, pp. 666–682.

27. Baumgardner, G. L., J. F. Masson, J. R. Hardee, A. M. Menapace, and A. G. Williams. Polyphosphoric Acid Modified Asphalt: Proposed Mechanisms. *Proc., Association of Asphalt Paving Technologists,* Long Beach, Calif., 2005, pp. 283–305.
28. Robertson, R. E., J. F. Branthaver, P. M. Harnsberger, J. C. Petersen, S. M. Dorrence, J. F. Mckay, T. F. Turner, A. T. Pauli, S. Huang, J. Huh, J. E. Tauer, K. P. Thomas, D. A. Netzel, F. P. Miknis, and T. Williams. *Fundamental Properties of Asphalts and Modified Asphalts, Volume II: Final Report, New Methods.* Report FHWA-RD-99-013. FHWA, McLean, Va., 2001, 266 pp.
29. Kamoun, A., A. Jelidi, and M. Chaabouni. Evaluation of the Performance of Sulfonated Esparto Grass Lignin as a Plasticizer-Water Reducer for Cement. *Cement and Concrete Research,* Vol. 33, 2003, pp. 995–1003.
30. Levin, S. *High Performance Liquid Chromatography.* www.forumsci.co.il/HPLC. 2002.
31. Holleran, G., and J. R. Reed, *Analysis of Emulsion Stability and Asphalt Compatibility.* Asphalt Emulsions Manufacturers Association, www.aema.org, 1999.
32. Arnold, T. S. Determination of Lime in Hot-Mix Asphalt. In *Transportation Research Record: Journal of the Transportation Research Board, No. 1962,* Transportation Research Board of the National Academies, Washington, D.C., 2006, pp. 113–120.
33. Klen, D. S. Unmasking the Problem: BP Amoco Cleans Industry with Low Fuming Asphalt. *Roads & Bridges,* Vol. 39, 2001, pp. 32–34.
34. McDaniel, R. S., and J. Haddock. *Effects of Hot Plant Fuel Characteristics and Combustion on Asphalt Concrete Quality (Final Report).* Report SD2001-13-F. South Dakota Department of Transportation, Pierre, S.D., 2004, 76 pp.
35. McDaniel, R. S., and J. Haddock. *Effects of Hot Plant Fuel Characteristics and Combustion on Asphalt Concrete Quality (Appendices).* Report SD2001-13-A. South Dakota Department of Transportation, Pierre, S.D., 2004, 121 pp.
36. www.thermonicolet.com. Accessed March 31, 2009.
37. PerkinElmer. www.perkinelmer.com. Accessed August 29, 2008.
38. Liu, M., M. A. Ferry, R. R. Davison, C. J. Glover, and J. A. Bullin. Oxygen Uptake as Correlated to Carbonyl Growth in Aged Asphalts and Asphalt Corbett Fractions. *Industrial Engineering Chemistry Research,* Vol. 37, 1998, pp. 4669–4674.
39. Karlsson, R., and U. Isacsson. Investigations on Bitumen Rejuvenator Diffusion and Structural Stability (with Discussion). *Journal of the Association of Asphalt Paving Technologists,* Vol. 72, 2003, pp. 463–501.
40. Yamaguchi, K., I. Sasaki, and S. Meiarashi. Photodegradation Test of Asphalt Binder Using Pressed Thin Film Samples. *Canadian Journal of Civil Engineering,* Vol. 32, 2005, pp. 1166–1169.
41. Ouyang, C., S. Wang, Y. Zhang, and Y. Zhang. Improving the Aging Resistance of Styrene-Butadiene-Styrene Tri-Block Copolymer Modified Asphalt by Addition of Antioxidants. *Polymer Degradation and Stability,* Vol. 91, 2006, pp. 795–804.
42. Gueit, C., M. Robert, and G. Durand. *Transportation Research Circular E-C122: Characterization of the Different Phases in the Life Cycle of the Binder in a Bitumen Emulsion: Recovery Methods.* Transportation Research Board of the National Academies, Washington, D.C., 2007, pp. 1–10.
43. Hazlett, D. *Transportation Research Circular E-C122: Emulsion Residue Recovery Techniques: How Do We Get Emulsion Residue Representative of In-Service Binder?* Transportation Research Board of the National Academies, Washington, D.C., 2007, pp. 15–23.
44. Michalica, P., P. Daucik, and L. Zanaotto. Monitoring of Compositional Changes Occurring During the Oxidative Aging of Two Selected Asphalts from Different Sources. *Petroleum & Coal,* Vol. 50, 2008, pp. 1–10.
45. Zuyu, L. *Study on Preparation of Asphalt Antistrip Additives from Amines and Aldehydes.* ARRB Transport Research Ltd., Australia, 2000, 4 pp.
46. Bagampadde, U. Laboratory Studies on Stripping at Bitumen/Substrate Interfaces Using FTIR-ATR. *Journal of Material Science,* Vol. 42, 2007, pp. 3197–3206.
47. American Association of State Highway Transportation Officials (AASHTO). *AASHTO T302-05: Standard Method of Test for Polymer Content of Polymer-Modified Emulsified Asphalt Residue and Asphalt Binders,* AASHTO, Washington, D.C., 2005.
48. Diefenderfer, S. *Detection of Polymer Modifiers in Asphalt Binder.* Report FHWA/VTRC 06-R18. Virginia Department of Transportation, Richmond, Va., 2006, 18 pp.
49. Lu, X., U. Isacsson, and J. Ekblad. Phase Separation of SBS Polymer Modified Bitumens. *Journal of Materials in Civil Engineering,* Vol. 11, 1999, pp. 51–57.
50. Ghosh, S. N., and S. K. Handoo. Infrared and Raman Spectral Studies in Cement and Concrete (Review). *Cement and Concrete Research,* Vol. 10, 1980, pp. 771–782.
51. Yu, P., R. J. Kirkpatrick, B. Poe, P. F. McMillan, and X. Cong. Structure of Calcium Silicate Hydrate (C-S-H): Near-, Mid-, and Far-Infrared Spectroscopy. *Journal of American Ceramic Society,* Vol. 82, 1999, pp. 742–748.
52. Rodrigues, F. A. Low-Temperature Synthesis of Cements from Rice Hull Ash. *Cement and Concrete Research,* Vol. 33, No. 5, 2003, pp. 1525–1529.
53. Whiting, N., and M. B. Snyder. Effectiveness of Portland Cement Concrete Curing Compounds. In *Transportation Research Record: Journal of the Transportation Research Board, No. 1834,* Transportation Research Board of the National Academies, Washington, D.C., 2003, pp. 59–69.
54. Fernon, V., A. Vichot, N. Legoanvic, P. Columbet, F. Corazza, and U. Costa. Interaction Between Portland Cement Hydrates and Polynaphthalene Sulfonates. *Proc., 5th CANMET/ACI Internal Conference on Superplasticizers and Other Chemical Admixtures in Concrete,* Rome, 1997, pp. 225–248.
55. Brew, D., and F. P. Glasser. Synthesis and Characterization of Magnesium Silicate Hydrate Gels. *Cement and Concrete Research,* Vol. 35, 2005, pp. 85–98.
56. Paya, J., J. Monzo, M. V. Borrachero, S. Velazquez, and M. Bonilla. Determination of the Pozzolanic Activity of Fluid Catalytic Cracking Residue. Thermogravimetric Analysis Studies on FC3R-Lime Pastes. *Cement and Concrete Research,* Vol. 33, 2003, pp. 1085–1091.
57. Gomes, C. M., O. P. Ferreira, and M. R. Fernandes. Influence of Vinyl Acetate-Versatic Vinylester Copolymer on the Microstructural Characteristics of Cement Pastes. *Materials Research,* Vol. 8, 2005, pp. 51–56.
58. Nagi, M. A., P. A. Okamoto, and R. L. Kozikowski. *NCHRP Report 578: Evaluating Air-Entraining Admixtures for Highway Concrete.* Transportation Research Board of the National Academies, Washington, D.C., 2007, 60 pp.
59. Weldon, D. G. Failure Analysis and Degree of Cure. *Journal of Protective Coatings & Linings,* Vol. 22, 2005, pp. 48–55.
60. Lima, F. S., and L. F. Leite. Determination of Asphalt Cement Properties by Near Infrared Spectroscopy and Chemometrics. *Petroleum Science and Technology,* Vol. 22, 2004, pp. 589–600.

61. Zanetti, M., T. G. Rials, and D. Rammer. NIR-Monitoring of In-Service Wood Structures. *Proc., Conference on Metropolis and Beyond,* American Society of Civil Engineers, 2005, 9 pp.
62. Veenstra, M., D. J. White, and V. R. Schaefer. *Synthesis of Nondestructive Testing Technologies for Geomaterial Applications.* CTRE Project 03-146. Iowa Department of Transportation, Ames, 2005, 132 pp.
63. Bensted, J. Uses of Raman Spectroscopy in Cement Chemistry. *Journal of the American Ceramic Society,* Vol. 59, 1976, pp. 140–144.
64. Newman, S. P., S. J. Clifford, P. V. Coveney, V. Gupta, J. D. Blanchard, F. Serafin, D. Ben-Amotz, and S. Diamond. Anomalous Fluorescence in Near-Infrared Raman Spectroscopy of Cementitious Materials. *Cement and Concrete Research,* Vol. 35, 2005, pp. 1620–1628.
65. Potgieter-Vermaak, S. S., J. H. Potgieter, and R. Van Grieken. The Application of Raman Spectrometry to Investigate and Characterize Cement, Part I: A Review. *Cement and Concrete Research,* Vol. 36, 2006, pp. 656–662.
66. Potgieter-Vermaak, S. S., J. H. Potgieter, M. Belleil, F. DeWeerdt, and R. V. Van Grieken. The Application of Raman Spectrometry to the Investigation of Cement. Part II: A Micro-Raman Study of OPC, Slag and Fly Ash. *Cement and Concrete Research,* Vol. 36, 2006, pp. 663–670.
67. Bumrongjaroen, W., S. Swatekititham, R. A. Livingston, and J. J. Schweitzer. Synthetic Glass Models for Investigating Fly Ash Reactivity. *American Concrete Institute Special Publications,* Vol. 242, 2007, pp. 227–242.
68. Martinez-Ramirez, S., S. Sanchez-Cortes, J. V. Garcia-Ramos, C. Domingo, C. Fortes, and M. T. Blanco-Varela. Micro-Raman Spectroscopy Applied to Depth Profiles of Carbonates Formed in Lime Mortar. *Cement and Concrete Research,* Vol. 33, 2003, pp. 2063–2068.
69. El-Turki, A., R. J. Ball, and G. C. Allen. The Influence of Relative Humidity on Structural and Chemical Changes During Carbonation of Hydraulic Lime. *Cement and Concrete Research,* Vol. 37, 2007, pp. 1233–1240.
70. Skibsted, J., and C. Hall. Characterization of Cement Minerals, Cements and Their Reaction Products at the Atomic and Nano Scale. *Cement and Concrete Research,* Vol. 38, 2008, pp. 205–225.
71. Farquharson, S., W. Smith, J. Rose, and M. Shaw. Correlations Between Molecular (Raman) and Macroscopic (Rheology) Data for Process Monitoring of Thermoset Composites. *Journal of Process Analytical Chemistry,* 2001, pp. 45–53.
72. Bergmann, U., O. C. Mullins, and S. P. Cramer. X-ray Raman Spectroscopy of Carbon in Asphaltenes: Light Element Characterization with Bulk Sensitivity. *Analytical Chemistry,* Vol. 72, 2000, pp. 2609–2612.
73. Bergmann, U., H. Groening, O. C. Mullins, P. Glatzel, J. Fetzer, and S. P. Cramer. X-Ray Raman Spectroscopy—A New Tool to Study Local Structure of Aromatic Hydrocarbons and Asphaltenes. *Petroleum Science and Technology,* Vol. 22, 2004, pp. 863–875.
74. Enustun, B. V., S. S. Kim, and D. Y. Lee. *Correlation of Locally-Based Performance of Asphalts with Their Physicochemical Parameters.* Project HR-298 Final Report. Iowa Department of Transportation, Ames, 1990, 112 pp.
75. De la Torre, A. G., and M. A. Aranda. Accuracy in Rietveld Quantitative Phase Analysis of Portland Cements. *Journal of Applied Crystallography,* Vol. 36, 2003, pp. 1169–1176.
76. Hong, H., Z. Fu, and X. Min. Quantitative XRD Analysis of Cement Clinker by the Multiphase Rietveld Method. *Journal of Wuhan University of Technology,* Vol. 18, No. 3, 2003, pp. 56–59.
77. Brew, D., and F. P. Glasser. Synthesis and Characterization of Magnesium Silicate Hydrate Gels. *Cement and Concrete Research,* Vol. 35, 2005, pp. 85–98.
78. Dermatas, D., M. Chrysochoou, S. Sarra Pardali, and D. G. Grubb. Influence of X-Ray Diffraction Sample Preparation on Quantitative Mineralogy: Implications for Chromate Waste Treatment. *Journal of Environmental Quality,* Vol. 36, 2007, pp. 487–497.
79. Raupp-Pereira, F., R. J. Ball, J. Rocha, J. A. Labrincha, and G. C. Allen. New Waste Based Clinkers: Belite and Lime Formulations. *Cement and Concrete Research,* Vol. 38, 2008, pp. 511–521.
80. American Society for Testing and Materials (ASTM). *ASTM C1365-06 Standard Test Method for Determination of the Proportion of Phases in Portland Cement and Portland-Cement Clinker Using X-Ray Powder Diffraction Analysis,* ASTM International, West Conshohocken, Pa., 2005.
81. National Cooperative Highway Research Program. *Aggregate Tests for Portland Cement Concrete Pavements: Review and Recommendations, Research Results Digest No. 281,* Transportation Research Board of the National Academies, Washington, D.C., Sept. 2003, 28 pp.
82. Kaniraj, S. R., and V. Gayathri. Permeability and Consolidation Characteristics of Compacted Fly Ash. *Journal of Energy Engineering,* Vol. 130, 2004, pp. 18–43.
83. Poupard, O., L. V. Hostis, S. Catinaud, and I. Petre-Lazar. Corrosion Damage Diagnosis of a Reinforced Concrete Beam After 40 Years Natural Exposure in Marine Environment. *Cement and Concrete Research,* Vol. 36, 2006, pp. 504–520.
84. McCain, R. G. *Qualitative Evaluation of Heavy Metals in Soils Using Portable XRF Instruments.* Westinghouse Hanford Company, Richland, Wash., 1993, 10 pp.
85. Zamurs, J., J. Bass, B. Williams, R. Fritsch, D. Sackett, and R. Heman. Real-Time Measurement of Lead in Ambient Air During Bridge Paint Removal. In *Transportation Research Record 1641,* TRB National Research Council, Washington, D.C., 1998, pp. 29–38.
86. Walsh, A. M. *Field-Portable X-Ray Fluorescence (FP-XRF) Determinations of Metals in Post-Blast Ordnance Residues.* TR-04-5 ERDC/CRREL Report. U.S. Army Environmental Center, Aberdeen, Md., 2004, 26 pp.
87. Uda, M., A. Ishizaki, R. Saoh, K. Okada, Y. Nakajima, D. Yamashita, K. Ohashi, Y. Sakuraba, A. Shimono, and D. Kojima. Portable X-Ray Diffractometer Equipped with XRF for Archaeometry. *Nuclear Instruments and Methods in Physics Research,* Vol. B239, 2005, pp. 77–84.
88. Gawel, I., and F. Czechowski. Study of Saturated Components in Asphalt. *Petroleum Science and Technology,* Vol. 15, No. 7–8, 1997, pp. 729–742.
89. Khanna, S. K., H. U. Khan, S. P. Nantiyal, K. M. Agarwal, M. Kaloopwan, and O. S. Tyagi. IR and HNMR Analysis of Asphaltic Materials Present in Some Indian Crude Oils of Gujarat Region. *Petroleum Science and Technology,* Vol. 24, 2006, pp. 23–30.
90. Netzel, D. A., and T. F. Turner. NMR Characterization of Size Exclusion Chromatographic Fractions from Asphalt. *Petroleum Science and Technology,* Vol. 26, 2008, pp. 1369–1380.
91. Miknis, F. P., A. T. Pauli, L. C. Michon, and D. A. Netzel. NMR Imaging Studies of Asphaltene Precipitation in Asphalts. *Fuel,* Vol. 77, No. 5, 1998, pp. 399–405.
92. Miknis, F. P., A. T. Pauli, A. Beemer, and B. Wilde. Use of NMR Imaging to Measure Interfacial Properties of Asphalts. *Fuel,* Vol. 84, 2005, pp. 1041–1051.

93. Bruker. www.bruker.com/products/infrared-and-raman-spectroscopy.html. Accessed Jan. 31, 2013.
94. http://blog.umd.edu/fml/equipment/gpc/. Accessed Feb. 28, 2012.
95. Labequip. New and Used Laboratory Equipment. www.labequip.com/hewlett-packard-1090-series-ii-uvvisible-hplc-system.html. Accessed Feb. 28, 2012.
96. www.srigc.com/210Dman.pdf. Accessed Feb. 28, 2012.
97. www.photovac.com/Voyager.aspx. Accessed Feb. 28, 2012.
98. Bruker. www.brukeroptics.com/alpha.html. Accessed Feb. 28, 2012.
99. SelectScience. Exoscan Hand-Held FTIR Spectrometer. www.selectscience.net/products/exoscan-hand-held-ftir-spectrometer/?prodID=85774&techBID=249. Accessed Feb. 28, 2012.
100. Smiths Detection. HazMatID Ranger. www.smithsdetection.com/hazmatid_ranger.php. Accessed Feb. 28, 2012.
101. Real-Time Analyzers, Inc. RamanID. www.rta.biz/images/customer-files//RamanIDSS2009-01.pdf. Accessed Feb. 28, 2012.
102. Thermo Scientific. TruScan. www.wetool.se/produkter/Ahura/truscan.htm. Accessed Feb. 28, 2012.
103. Intevac. DeltaNu. www.intevac.com/intevacphotonics/deltanu. Accessed Feb. 28, 2012.
104. inXitu. Terra: Rock and Mineral Analyzer. www.inxitu.com/html/Terra.html. Accessed Feb. 28, 2012.
105. Olympus. XRF and XRD Analyzers. www.olympus-ims.com/en/innovx-xrf-xrd/. Accessed Feb. 28, 2012.
106. www.niton.com/Niton-Analyzers-Products/xl3.aspx?sflang=en. Accessed Feb. 28, 2012.
107. www.skyray-instrument.com/en/product/productshow.aspx?bookid=84ee1fe7-2f38-48ef-a214-addf050872c5. Accessed Feb. 28, 2012.
108. www.southampton.ac.uk/nmr/spectroscopy/instrumentation/index.htmlr. Accessed Feb. 28, 2012.
109. Process NMR Associates, LLC. Portable Low-Resolution NMR Analyzer–Spin Track. www.process-nmr.com/portable_lowfield_nmr.htm. Accessed Feb. 28, 2012.
110. Hatada, K., and T. Kitayama. *NMR Spectroscopy of Polymers.* Springer, New York, 2004, 222 pp.
111. Spijker, J. *Geochemical Patterns in the Soils of Zeeland,* Job Spijker, 2005. www.spkr.nl/research/thesisonline/node24.html. Accessed April 19, 2009.
112. Bruker. www.bruker-axs.com/uploads/tx_linkselectorforpdfpool/Lab_Report_XRD_34_Quantification_of_Clinker_and_Cement_Phases_-_with_the_Highest_Speed_and_Accuracy_L88-E00033.pdf. Accessed Feb. 28, 2012.
113. Karmarkar, S., R. Garber, J. Kluza, and M. Koberda. Gel Permeation Chromatography of Dextrans in Parenteral Solutions: Calibration Procedure Development and Method Validation. *Journal of Pharmaceutical and Biomedical Analysis,* Vol. 41, 2006, pp. 1260–1267.
114. Caimi, R. J., and J. T. Brenna. High-Precision Liquid Chromatography-Combustion Isotope Ratio Mass Spectrometry. *Analytical Chemistry,* Vol. 65, 1993, pp. 3497–3500.
115. De Beer, T. R. M., W. R. G. Baeyens, A. Vermeire, D. Broes, J. P. Remonc, and C. Vervaet. Raman Spectroscopic Method for the Determination of Medroxyprogesterone Acetate in a Pharmaceutical Suspension: Validation of Quantifying Abilities, Uncertainty Assessment and Comparison with the High Performance Liquid Chromatography Reference Method. *Analytica Chimica Acta,* Vol. 589, 2007, pp. 192–199.
116. Wong, W. W., D. L. Hachey, S. Zhang, and L. L. Clarke. Accuracy and Precision of Gas Chromatography/Combustion Isotope Ratio Mass Spectrometry for Stable Carbon Isotope Ratio Measurements. *Rapid Communications in Mass Spectrometry,* Vol. 9, No. 11, 1995, pp. 1007–1011.

APPENDIX F

Summary of Preliminary Survey and Workshop

Summary of Preliminary Survey

A questionnaire (see Table F.1) was sent to the SHRP 2 coordinators in all 50 states. This was the first action. Sixteen SHAs responded to the questionnaire.

It contained a series of questions regarding three fundamental issues:

- What materials are the most challenging regarding their quality control in the field?
- What analytical procedures are currently used in the state agencies?
- What testing constraints are common under field conditions, and what features of the quality assurance/quality control (QA/QC) procedures and related devices are desirable to address these requirements?

Figures F.1 through F.4 present a summary of findings from the questionnaire. It can be concluded that some department of transportation (DOT) agencies are familiar with spectroscopy methods, that asphalt- and cement-related materials and paints are the most challenging in terms of QA/QC, and finally that time, training and, costs are the biggest concerns when implementing new procedures.

Summary of Workshop

The second action was to organize a workshop with several experts in materials and construction from both industry and transportation agencies. Before the workshop, all participants received the same questionnaire as the SHRP 2 coordinators and a short up-to-date summary of findings. The workshop took place at the University of Connecticut on May 6, 2009. Table F.2 lists the industries and government agencies of the participants.

Table F.3 presents a summary of findings from the questionnaire and the workshop. On the basis of the responses and the discussion during the workshop, the following comments can be made:

- Materials and construction professionals were concerned that spectroscopy devices require extensive training in preparation for testing and interpreting their results. State representatives were also concerned about budget restrictions hindering their ability to provide the necessary extra training activities and about the qualification of their personnel.
- Current specifications for many construction materials are based on their mechanical performance in the lab or field testing. The participants were concerned that, in order to successfully implement spectroscopy methods, AASHTO procedures must be developed and adopted by the DOTs in their QA/QC specifications.
- Correct timing of QA/QC testing during the construction process is very important. The timing depends on several factors, including what material is tested, whether the testing is done on the components or the mix, the amount of material and the importance of the job, who is performing the testing (DOT or contractor), and the construction sequence (if timing is too late, then tons of materials will be wasted or lost).
- Equipment cost must be justified by its capabilities because most practitioners do not foresee an everyday use of spectroscopic techniques. They envision spectroscopy devices as potentially applicable to larger construction jobs if the quality of the materials is in question. Some professionals, however, mentioned that if the device is highly reliable and accurate, the cost could be offset by potential savings in ensuring the quality and durability of the materials.
- Several participants expressed the need for checking the physical parameters of materials (such as air content and aggregate gradation). To the best knowledge of the research team, this cannot be directly achieved by spectroscopy

(continued on page 93)

Table F.1. Summary of Questionnaire for Preliminary Survey and Workshop

No.	Question	Answer
1	What materials or their compounds cause the largest quality control issues?	
2	What materials or their compounds are the most crucial for the safety, durability, and reliability of the highway facilities?	
3	What materials or their compounds are the most challenging to control in terms of the uniformity during handling and delivery?	
4	What analytical procedures for QA/QC of construction materials are you familiar with?	
5	What constraints (e.g., time, cost, personnel training) would you place on the analytical QA/QC procedures in the field?	
6	How would you rank the importance of the following features for the QA/QC field devices? (5–important, 1–not important): • Accuracy • Precision • Reliability • Speed of testing • Reproducibility • Ease of interpreting the results • Ease of use in the field	

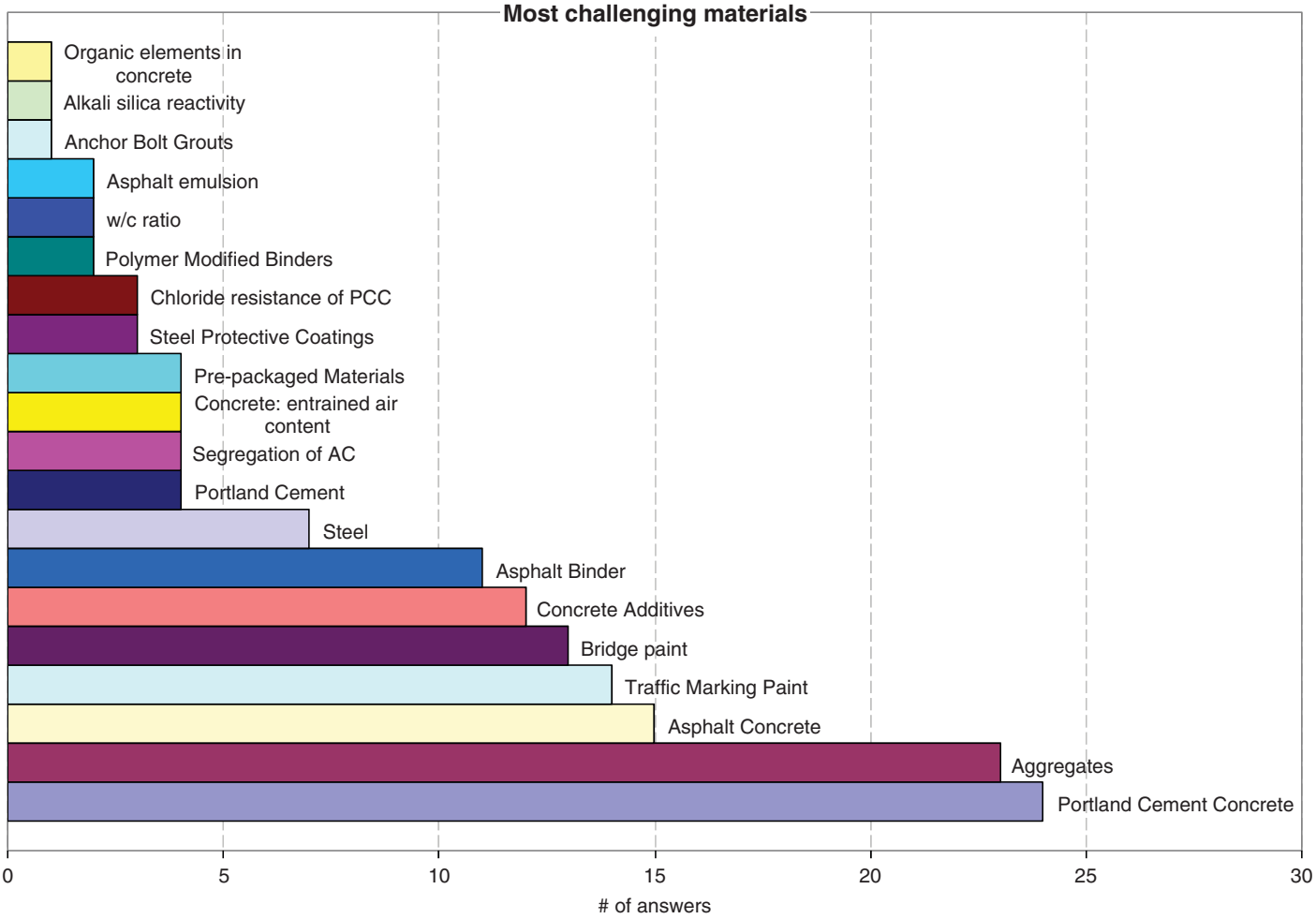

Figure F.1. Most challenging construction materials in terms of their QA/QC.

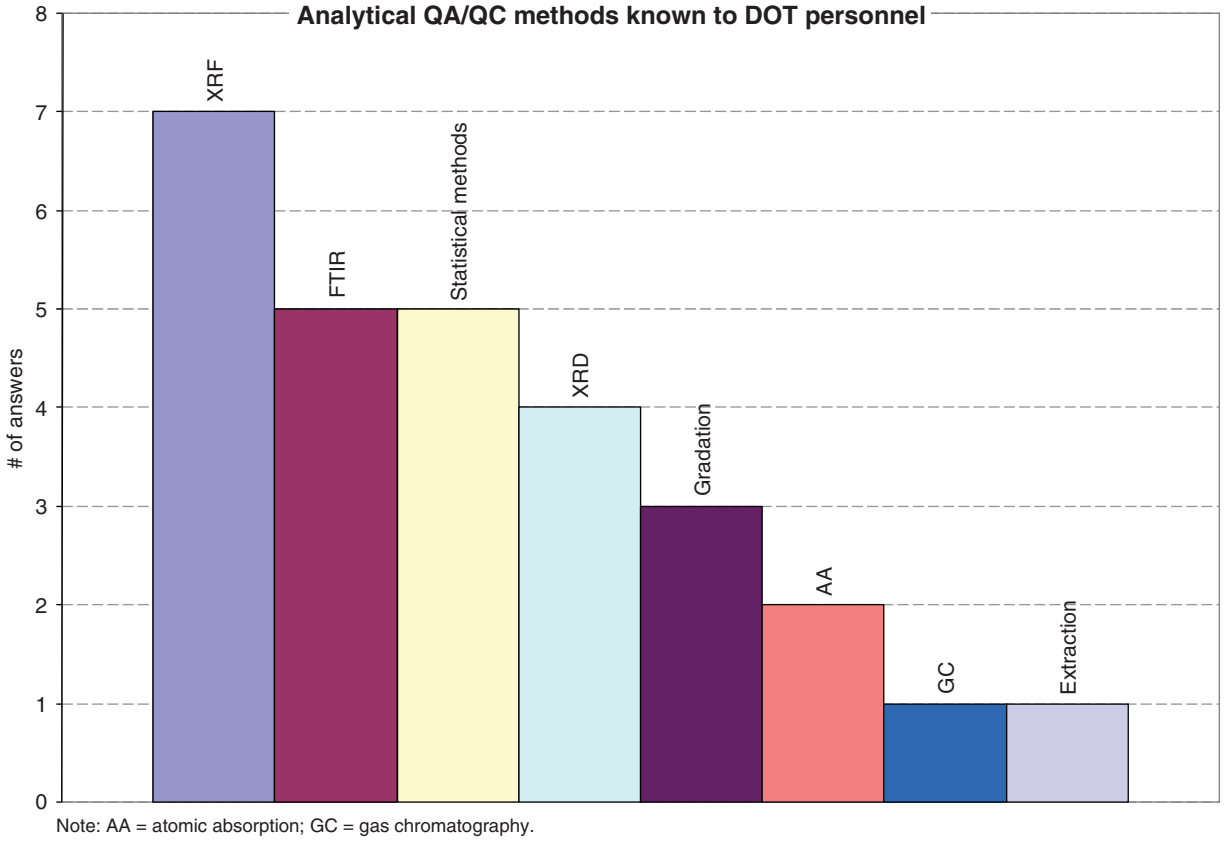

Figure F.2. Analytical QA/QC procedures used in the state agencies.

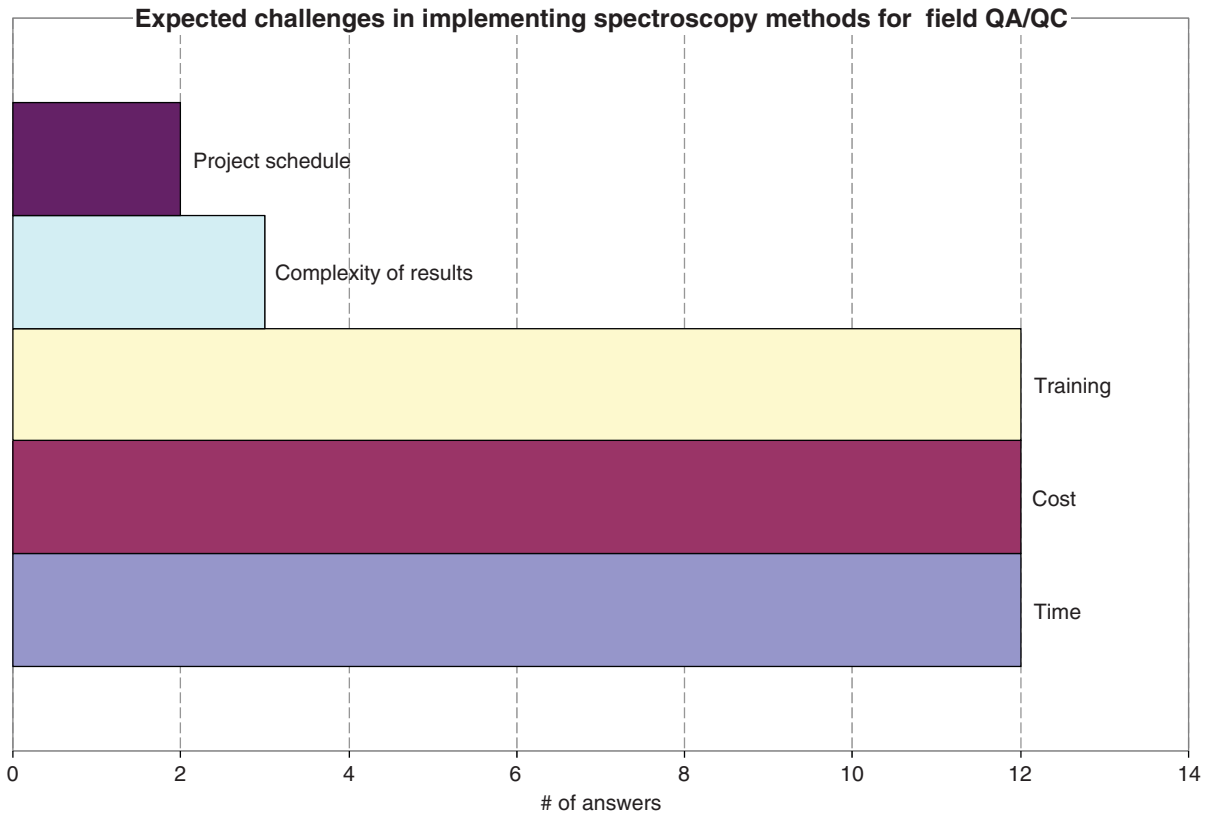

Figure F.3. Challenges in implementing spectroscopy procedures as field QA/QC methods.

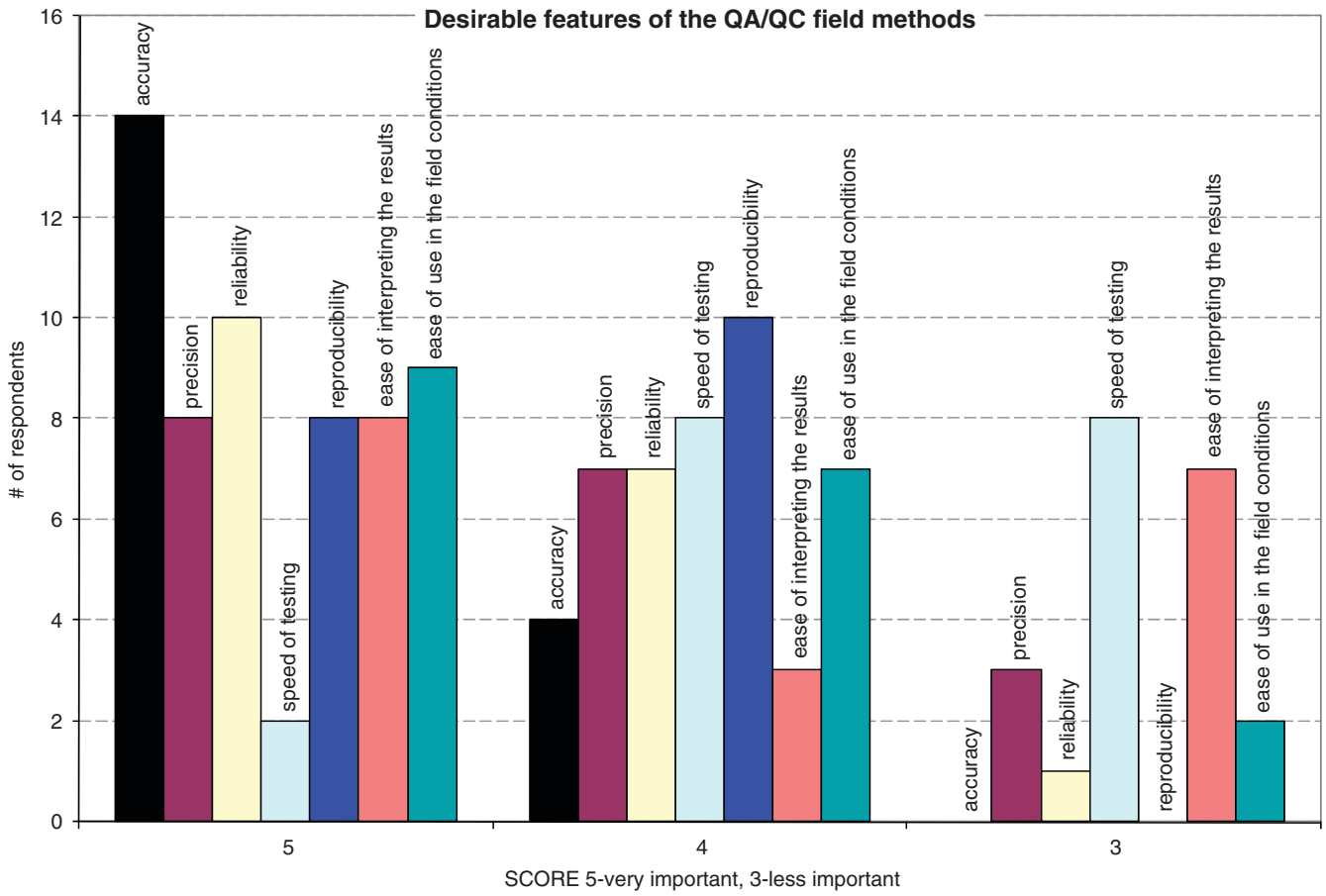

Figure F.4. Desirable features of the QA/QC methods in the field.

Table F.2. Workshop Participants

Area of Expertise	Industry	Government Agency
Materials	Lafarge North America Cementitious & CKD Projects Manager	Connecticut DOT, Division of Research Transportation Engineer
Construction	Pike Industries, Inc. Corporate Quality Control Manager Tilcon Connecticut Inc. Managers, Asphalt Division	New York State DOT Materials Bureau

Table F.3. Qualitative and Quantitative Requirements for Field QA/QC Methods

Feature[a]		Value
Accuracy	Minimum	1%
	Goal	<0.5%
Duration of measurement	Maximum	1 h
	Goal	~5 min
Effort involved	Maximum	1 person
	Goal	1 person
Amount of prior training	Maximum	1 day
	Goal	0.5 day
Reliability	Minimum	Depends on material (90%)
	Goal	95%
Time to get results	Maximum	Depends on construction process (1 h)
	Goal	~5 min
Price range	Maximum	$50,000
	Goal	<$20,000
Device weight	Maximum	50 lb
	Goal	<20 lb
Best time for QA/QC? (tank/plant/truck before/after placing?)	Maximum	Depends on material[b]
	Goal	Depends on material[b]
Sample preparation	Maximum	Solvent
	Goal	As is

[a] *Accuracy:* Agreement between a measurement and the true or correct value.
Duration of measurement: Time between start and end of testing cycle.
Effort involved: Personnel required to perform the test.
Amount of prior training: Time required to make personnel familiar with a testing procedure.
Reliability: Unlikelihood of equipment failure during the test.
Time to get results: Time between beginning of the sample preparation and the end of the analysis of the test results.
Price range: Cost of the equipment.
Device weight: Mass of the equipment including the case or enclosure.
Best time for QA/QC: Stage of the manufacturing and application process when the test is most timely.
Sample preparation: Processing and manipulating the material before the test.
Minimum/maximum: Acceptable threshold value from the user perspective that given equipment should produce.
Goal: Desirable target value from the user perspective that given equipment should produce.
[b] See Tables A.3 and A.4 in Appendix A.

(continued from page 89)

devices. It could potentially be investigated in some larger study.

- The physical weight of the field device is important. However, if the device is highly reliable and accurate, then it can be truck-mounted and used during the construction process.
- Under no circumstances should developed procedures for spectroscopy methods impose any licensing or security issues. This would create significant obstacles for the successful implementation of these procedures.
- The qualitative and quantitative requirements for the QA/QC methods in the field were identified during the workshop (Table F.3). These features will be considered in the selection process for specific spectroscopy field devices for Phase 3.

APPENDIX G

Field Needs Survey

Table G.1. Fill-Out Form for Ranking the Objectives for Spectroscopic Evaluation in the Field

Category	Material Category	Objectives	Score[a]
C1	Structural coatings and pavement markings	Verification of chemical composition ("fingerprinting")	
C2		Verification of the presence of solvents/diluents	
C3	Epoxy adhesives	Verification of chemical composition ("fingerprinting")	
C4	Portland cement concrete (PCC)	Verification of presence of chemical admixtures (plasticizer, air-entrainer, retarder, etc.) in fresh/cured PCC mix	
C5	Curing compounds for PCC	Verification of chemical composition/degree of cure (water content)	
C6	Polymer-modified asphalt Binders, emulsions, and mixtures	Verification of type/class of polymer modifier	
C7		Determination of polymer content	
C8	Antistripping agents in asphalt binders and mixtures	Verification of presence/type	
C9	Reclaimed asphalt pavement (RAP)	Verification of RAP presence in asphalt mixture	
C10		Determination of RAP content in asphalt mixture	

[a] 5 = Significant need; 1 = no need.

Table G.2. Summary of Scores per Category from Fill-Out Form

State	Category[a]										Per State	
	C1	C2	C3	C4	C5	C6	C7	C8	C9	C10	Mean	SD
Alabama	1	1	1	3	2	3	2	4	1	2	2.0	1.1
Alaska	4	1.5	4	1	1	2	3	3	3	3.5	2.6	1.1
Arizona	2	3	2	4	3	3	4	4	1	4	3.0	1.1
Arkansas	2	2	1	4	4	4	4	4	1	1	2.7	1.4
California	1	1	5	2	5	3	4	3	2	4	3.0	1.5
Colorado	3	3	3	4	4	4	4	3	3	3	3.4	0.5
Connecticut	1	1	1	1	1	4	4	4	1	1	1.9	1.4
Delaware	1	1	1	1	1	1	1	1	1	1	1.0	0.0
Florida	4	4	4	2	5	5	5	5	5	5	4.4	1.0
Georgia	2	2	2	2	2	4	4	4	2	4	2.8	1.0
Hawaii	NA	NA	NA	NA	NA	NA	NA	NA	NA	NA	NA	NA
Idaho	NA	NA	NA	NA	NA	NA	NA	NA	NA	NA	NA	NA
Illinois	4	3	3	2	3	2	4	4	1	3	2.9	1.0
Indiana	NA	NA	NA	NA	NA	NA	NA	NA	NA	NA	NA	NA
Iowa	3	3	2	4	5	4	1	4	1	1	2.8	1.5
Kansas	2	2	2	5	2	5	5	5	2	2	3.2	1.5
Kentucky	2	4	4	2	2	3	3	3	2	3	2.8	0.8
Louisiana	5	5	4	4	3	5	5	4	3	5	4.3	0.8
Maine	4	3	3	3	2	4	5	5	5	5	3.9	1.1
Maryland	3	3	3	1	1	4	4	3	5	4	3.1	1.3
Massachusetts	5	3	3	3	3	5	5	3	3	5	3.8	1.0
Michigan	NA	NA	NA	NA	NA	NA	NA	NA	NA	NA	NA	NA
Minnesota	NA	NA	NA	NA	NA	NA	NA	NA	NA	NA	NA	NA
Mississippi	4	5	2	1	3	5	3	3	1	1	2.8	1.5
Missouri	3.5	3.5	3.5	4	3.5	3	3	3.3	2.3	3	3.3	0.5
Montana	NA	NA	NA	NA	NA	NA	NA	NA	NA	NA	NA	NA
Nebraska	4	4	4	3	4	5	5	5	1	2	3.7	1.3
Nevada	2	2	2	4	3	3	5	3	5	5	3.4	1.3
New Hampshire	NA	NA	NA	NA	NA	NA	NA	NA	NA	NA	NA	NA
New Jersey	4	3	3	3	2	4	4	2	3	5	3.3	0.9
New Mexico	NA	NA	NA	NA	NA	NA	NA	NA	NA	NA	NA	NA
New York	4	4	3	3	5	3	3	4	2	3	3.4	0.8
North Carolina	5	5	5	5	5	5	5	5	3	5	4.8	0.6
North Dakota	5	5	2	3	3	4	4	2	2	2	3.2	1.2
Ohio	1	1	1	1	1	3	3	3	1	1	1.6	1.0
Oklahoma	4	1	3	3	3	2	2	5	2	4	2.9	1.2
Oregon	3	1	3	1	1	4	4	4	4	4	2.9	1.4

(continued on next page)

Table G.2. Summary of Scores per Category from Fill-Out Form (continued)

State	Category[a]										Per State	
	C1	C2	C3	C4	C5	C6	C7	C8	C9	C10	Mean	SD
Pennsylvania	NA	NA	NA	NA	NA	NA	NA	NA	NA	NA	NA	NA
Rhode Island	5	5	5	3.5	3.5	4	4	4	4.5	5	4.4	0.6
South Carolina	3	3	3	3	3	3	3	4	2	2	2.9	0.6
South Dakota	NA	NA	NA	NA	NA	NA	NA	NA	NA	NA	NA	NA
Tennessee	NA	NA	NA	NA	NA	NA	NA	NA	NA	NA	NA	NA
Texas	2	1	1	1	1	1	1	1	1	1	1.1	0.3
Utah	4	3	2	1	1	3	3	1	4	4	2.6	1.3
Vermont	NA	NA	NA	NA	NA	NA	NA	NA	NA	NA	NA	NA
Virginia	NA	NA	NA	NA	NA	NA	NA	NA	NA	NA	NA	NA
Washington	NA	NA	NA	NA	NA	NA	NA	NA	NA	NA	NA	NA
West Virginia	NA	NA	NA	NA	NA	NA	NA	NA	NA	NA	NA	NA
Wisconsin	NA	NA	NA	NA	NA	NA	NA	NA	NA	NA	NA	NA
Wyoming	1	1	1	1	1	1	1	5	1	1	1.4	1.3
District of Columbia	NA	NA	NA	NA	NA	NA	NA	NA	NA	NA	NA	NA
Mean	3.0	2.7	2.7	2.6	2.7	3.5	3.5	3.5	2.4	3.1		
SD	1.4	1.4	1.2	1.3	1.4	1.2	1.3	1.2	1.4	1.5		

Note: NA = not available.

[a] See Figure G.1.

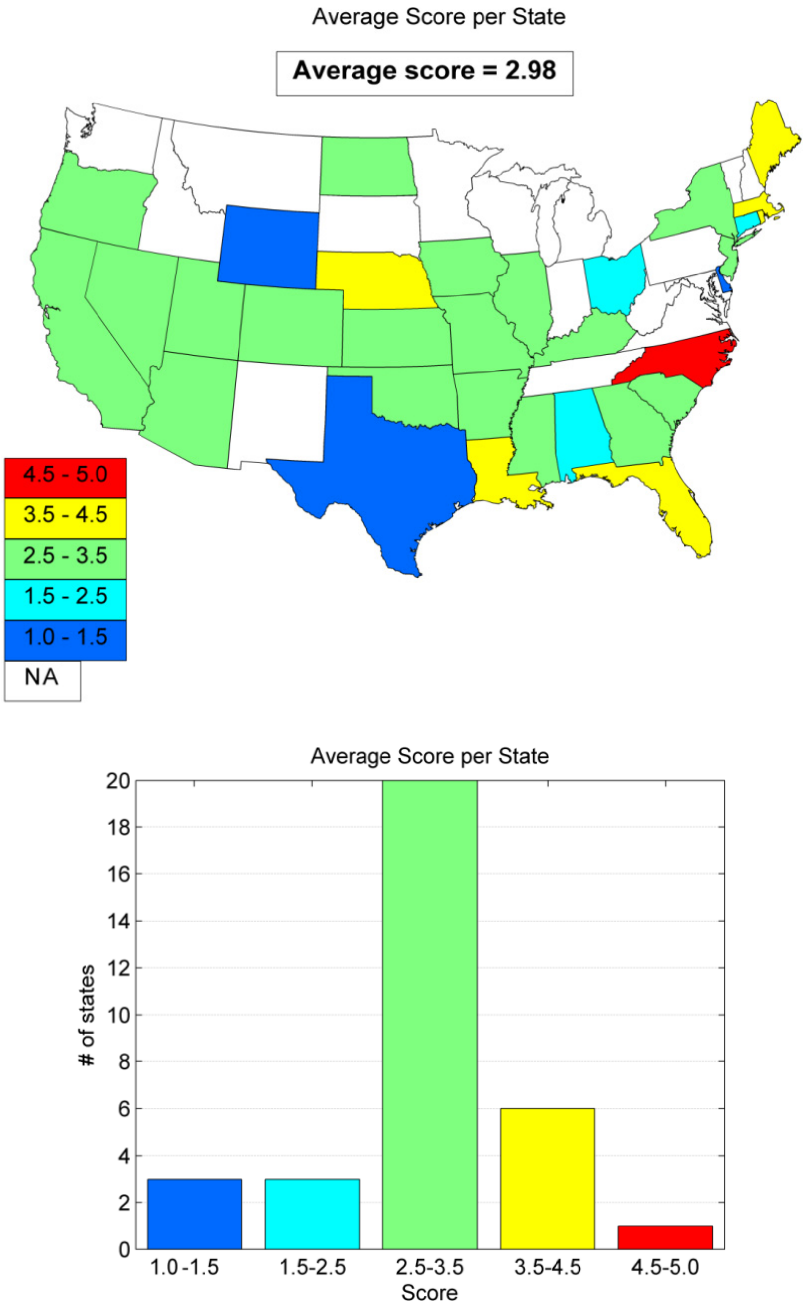

Figure G.1. Distribution of average score per state.

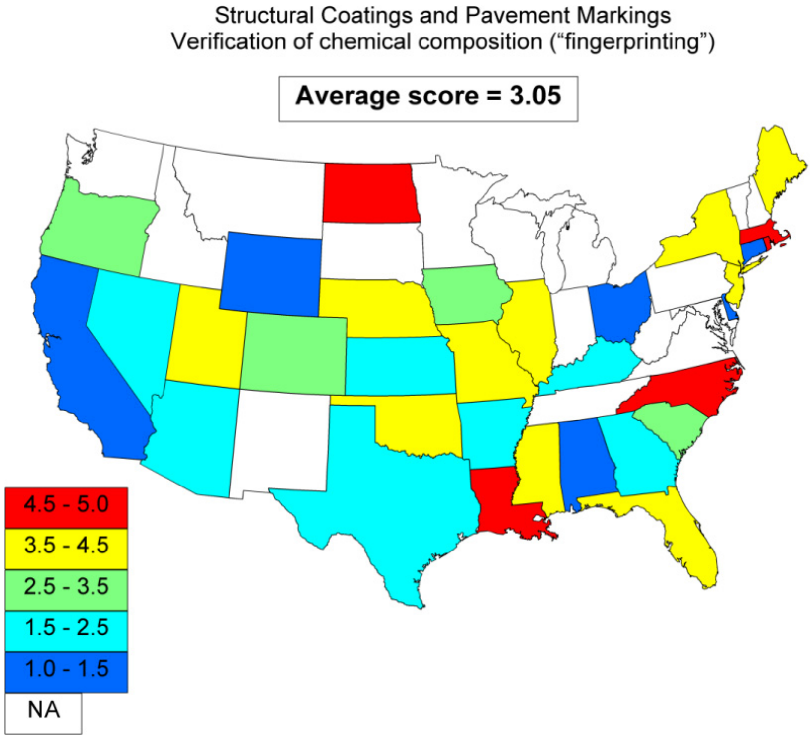

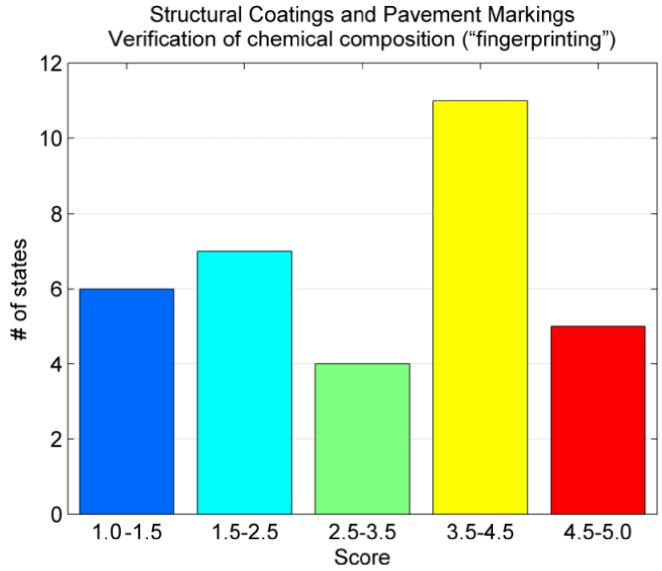

Figure G.2. Distribution of scores for verification of chemical composition (fingerprinting) of structural coatings and pavement markings.

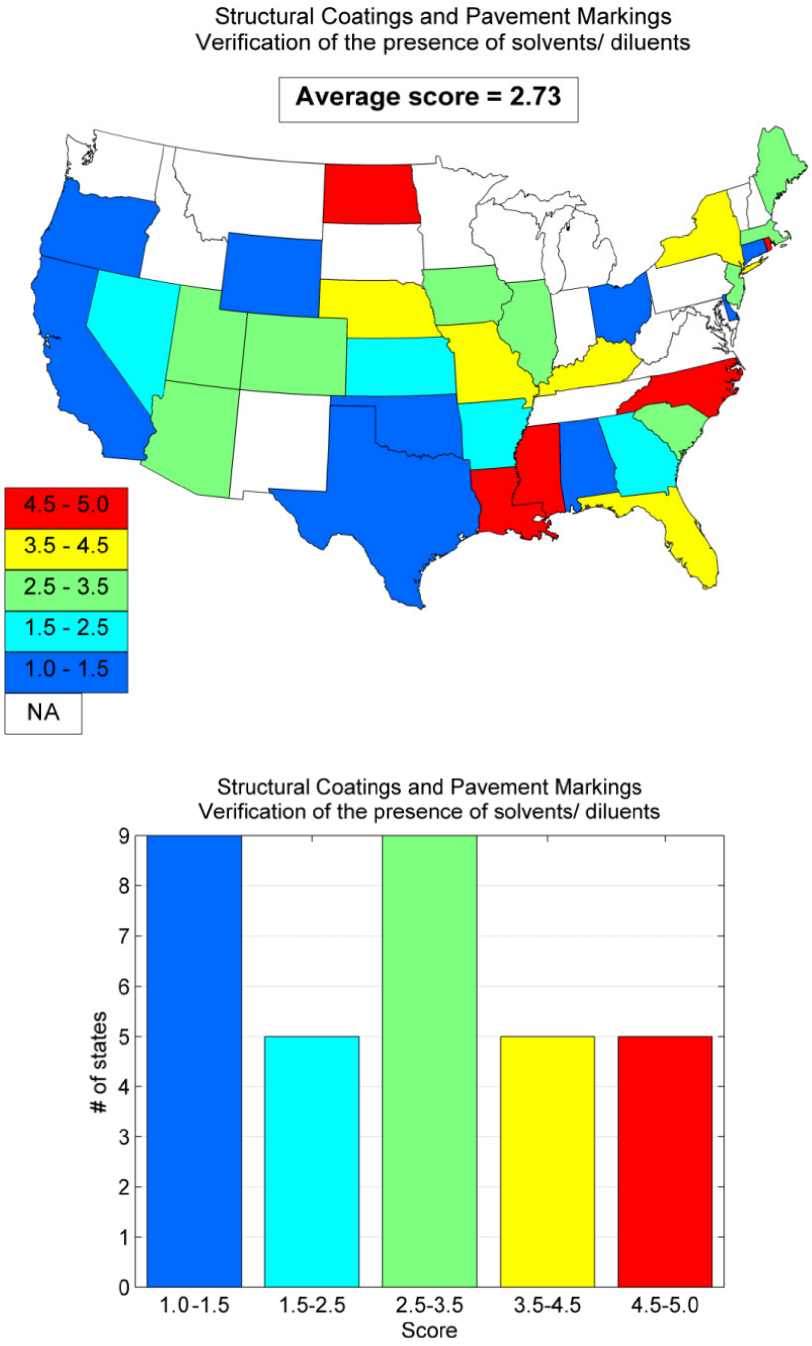

Figure G.3. Distribution of scores for verification of presence of solvents and diluents in structural coatings and pavement markings.

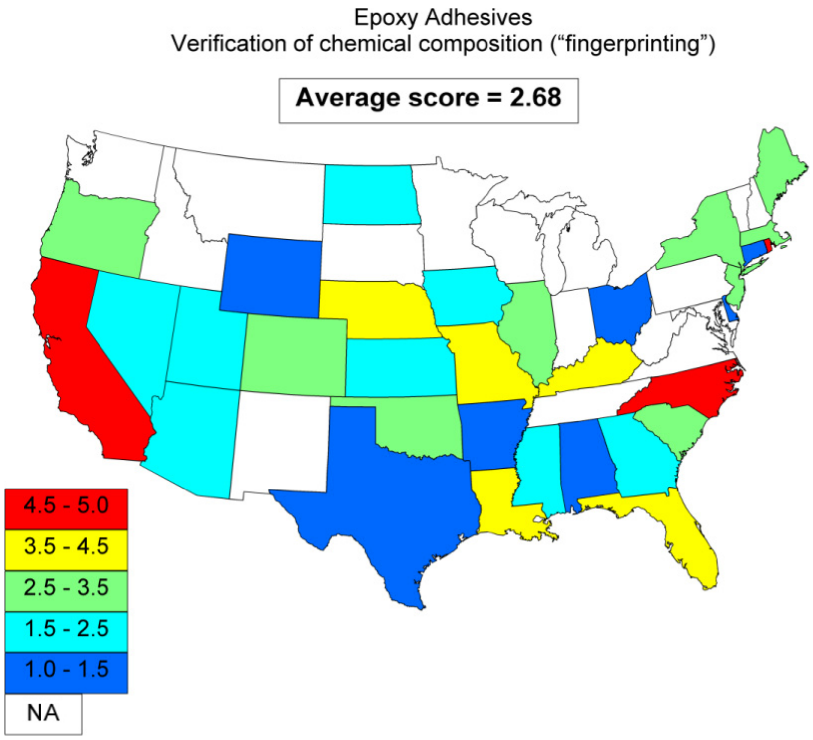

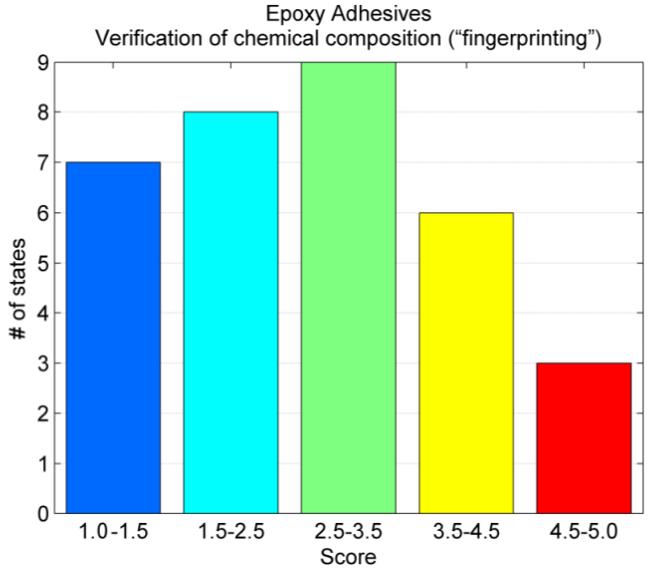

Figure G.4. Distribution of scores for verification of chemical composition of epoxy adhesives.

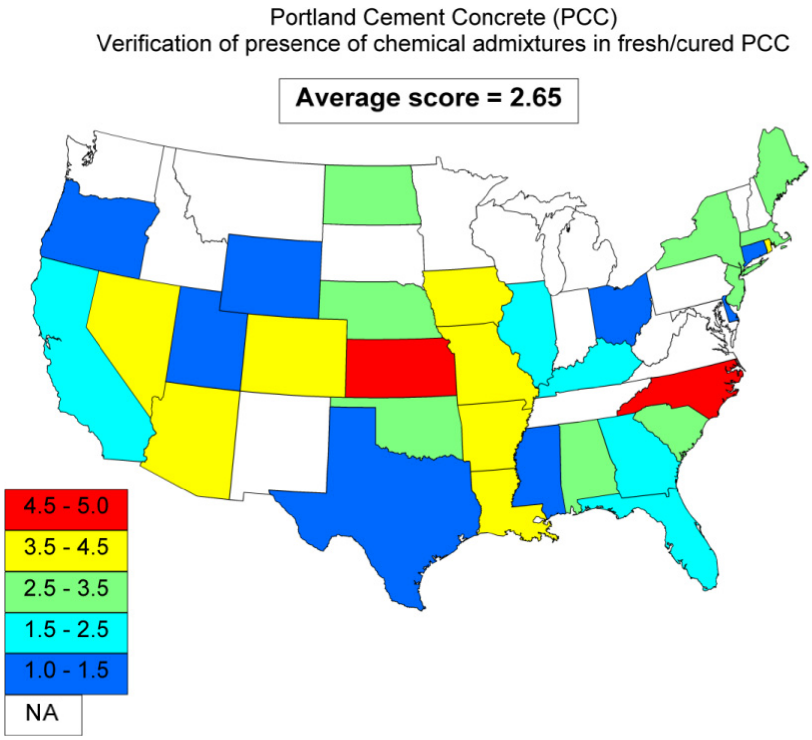

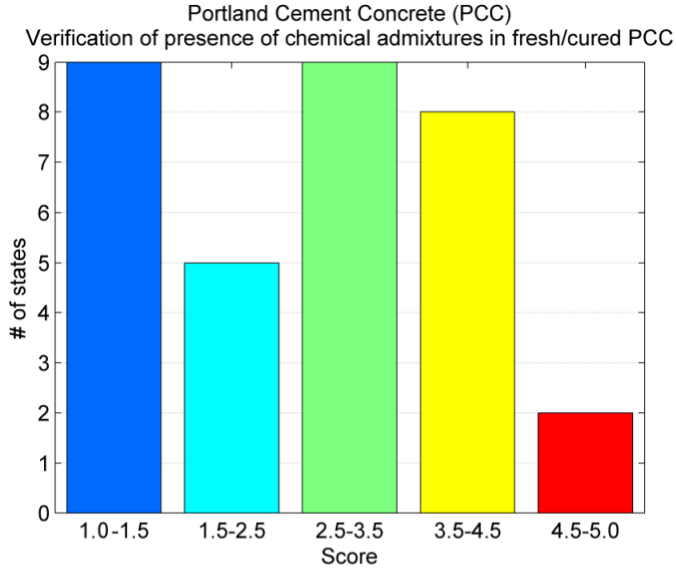

Figure G.5. Distribution of scores for verification of the presence of chemical admixtures in fresh or cured PCC.

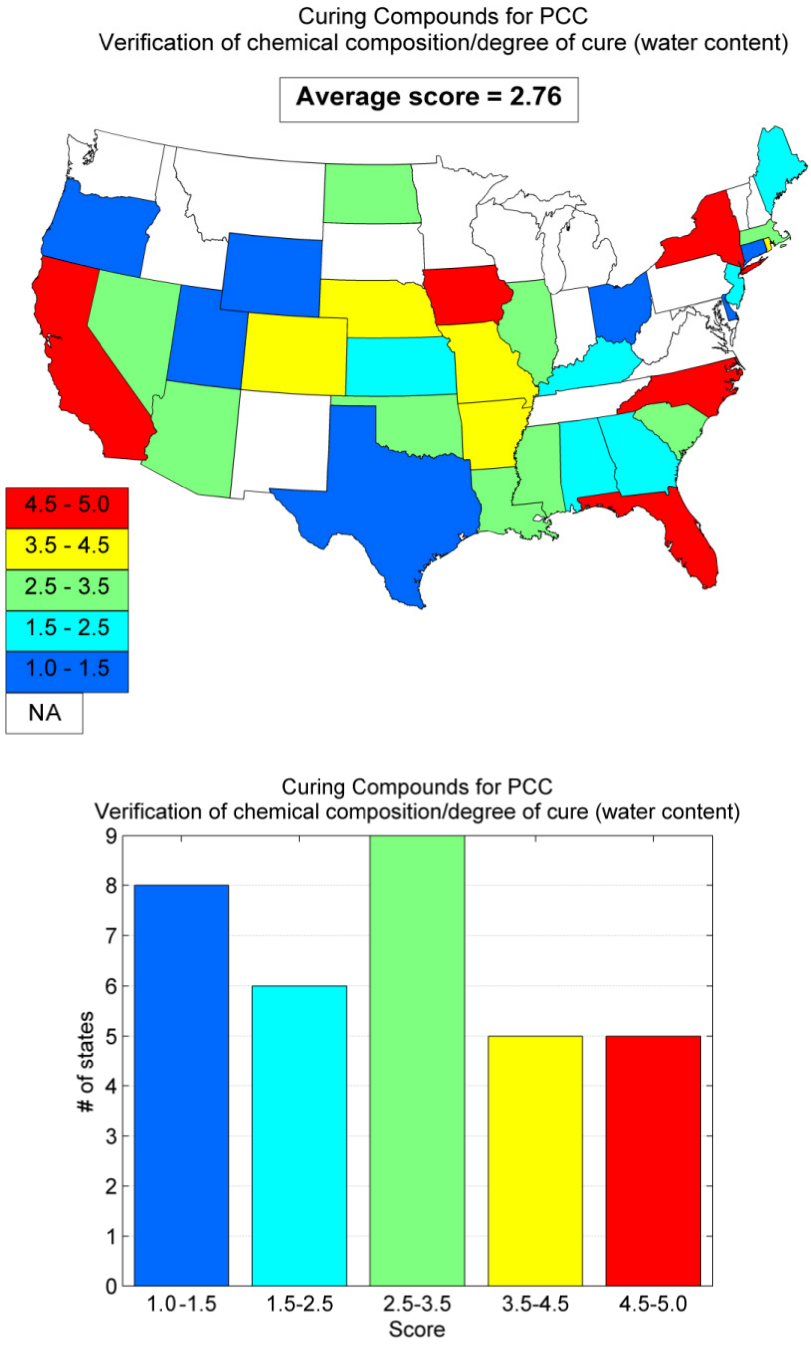

Figure G.6. Distribution of scores for verification of chemical composition and degree of cure (water content) in curing compounds for PCC.

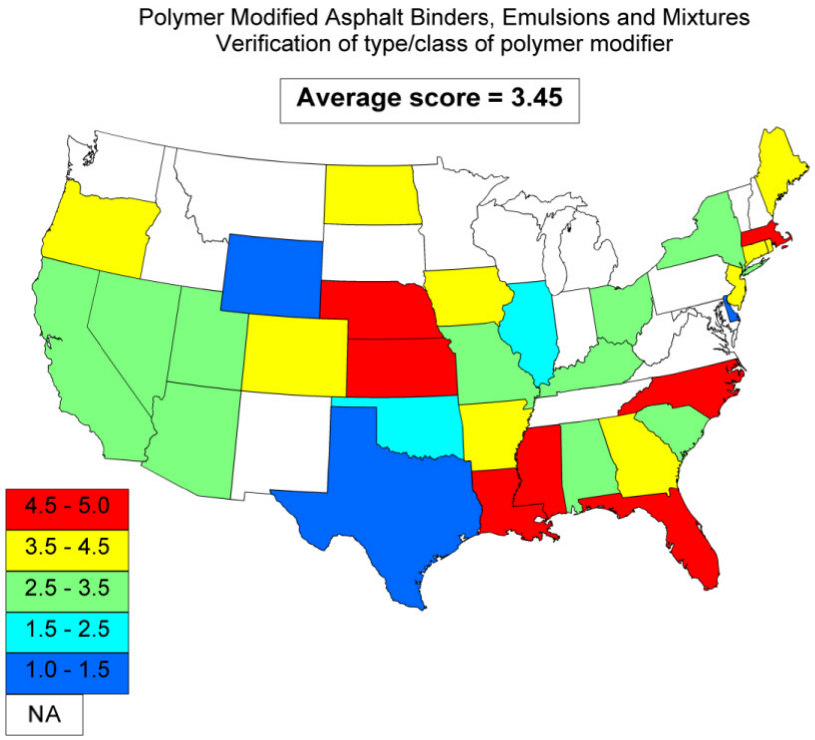

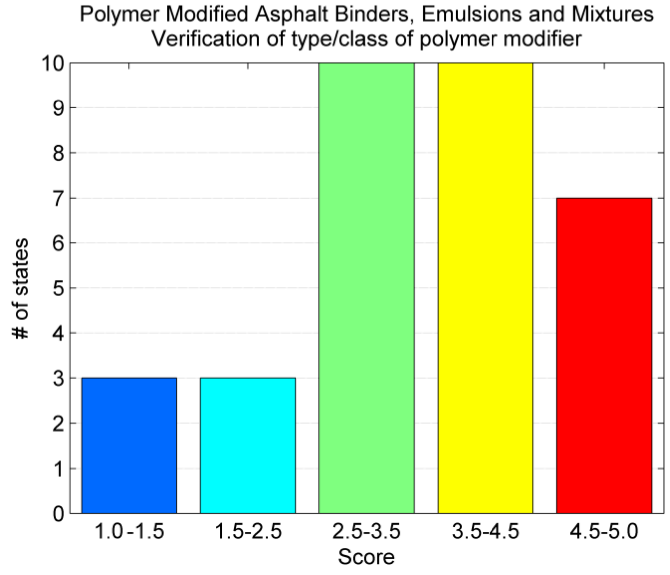

Figure G.7. Distribution of scores for verification of type and class of polymer additives in asphalt products.

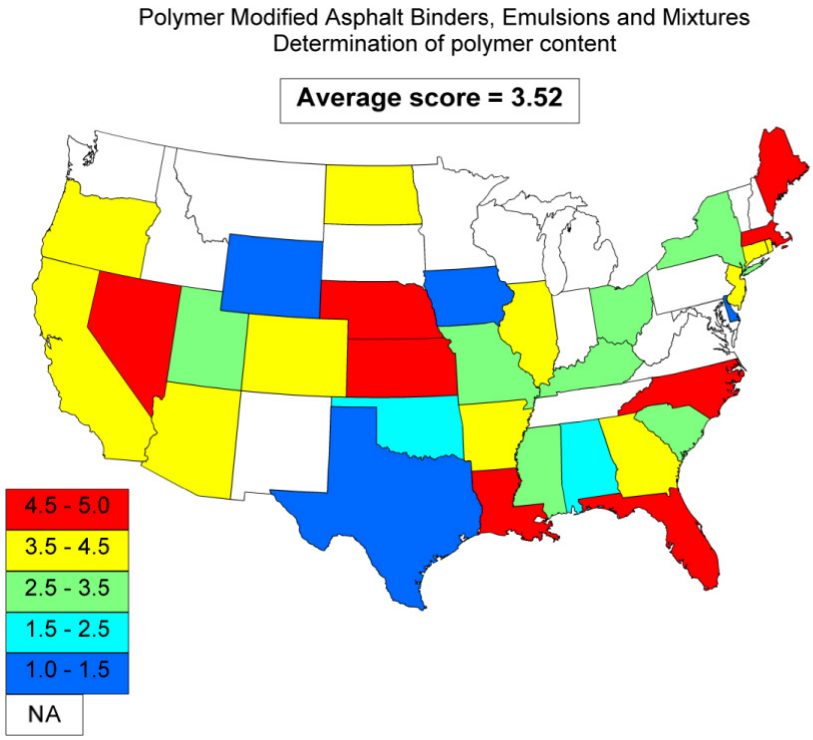

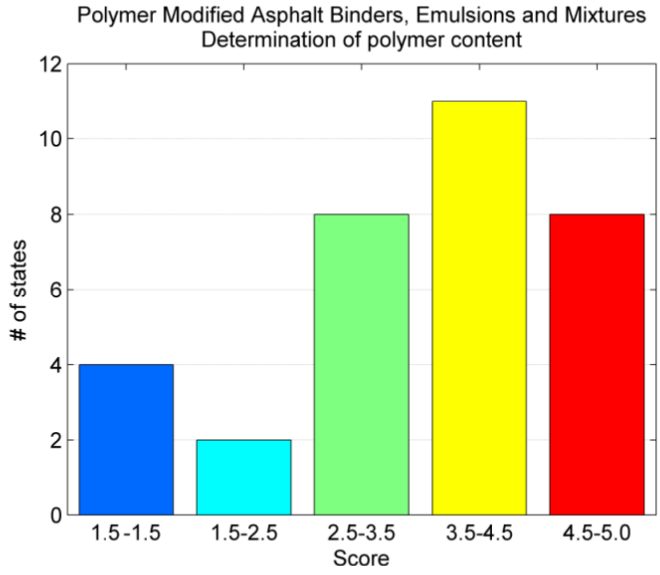

Figure G.8. Distribution of scores for determination of polymer content in asphalt products.

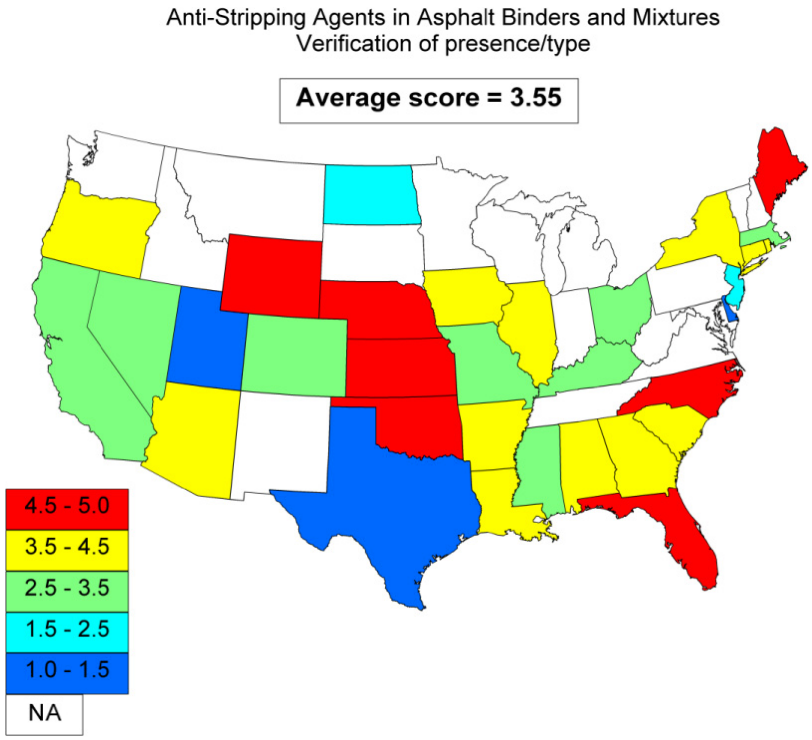

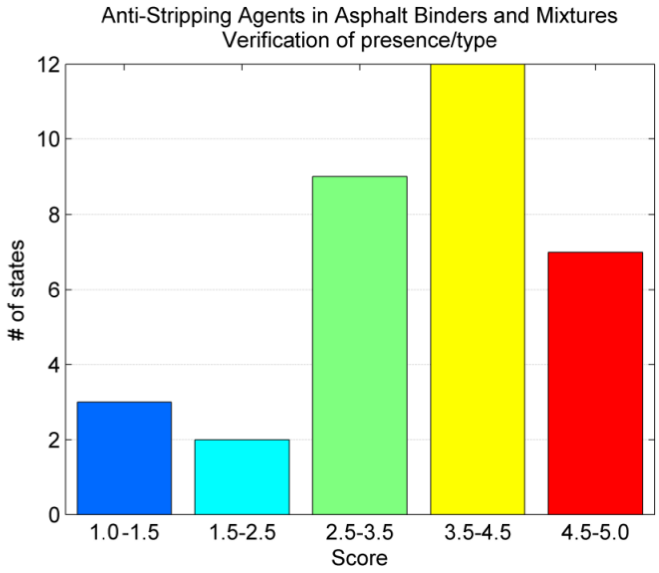

Figure G.9. Distribution of scores for verification of presence/type of antistripping agents in asphalt binders and mixtures.

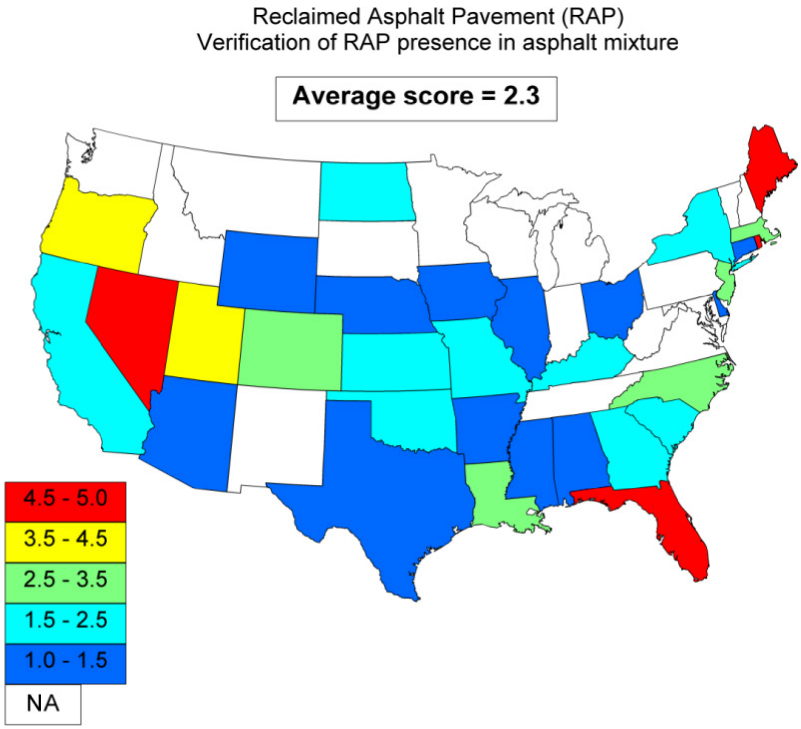

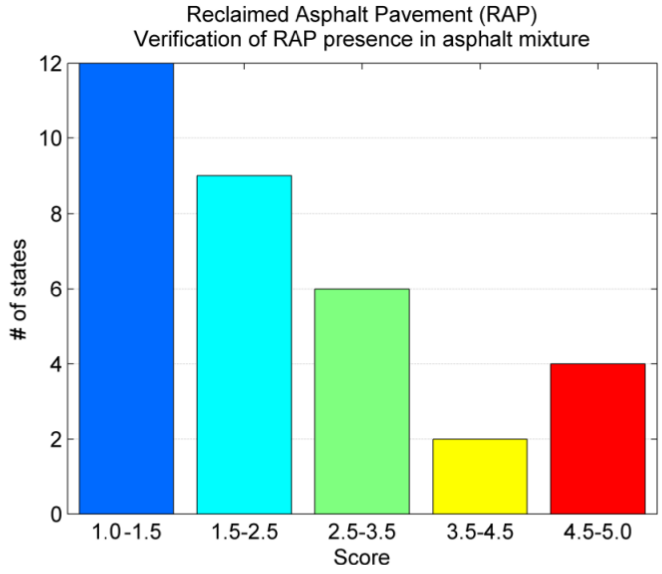

Figure G.10. Distribution of scores for verification of RAP presence in asphalt mixtures.

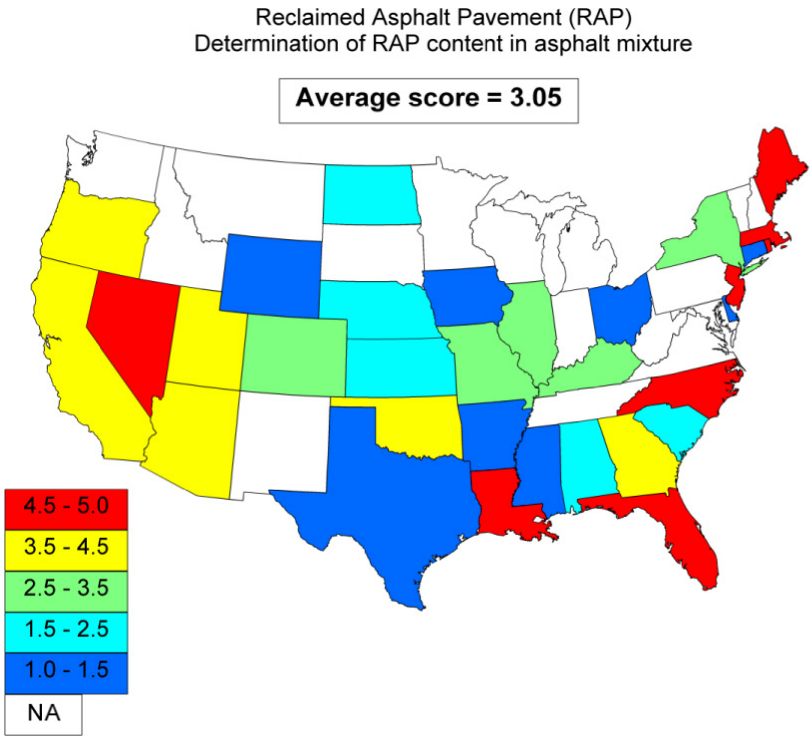

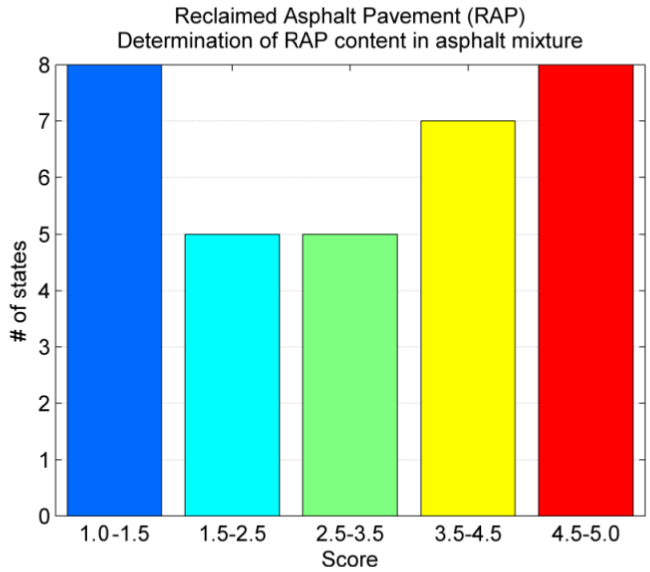

Figure G.11. Distribution of scores for determination of RAP content in asphalt mixtures.

Table G.3. Summary of Rankings of Material Categories per Objective by Spectroscopic Testing

Material Category	Objective	Mean Score	SD	Rank
Structural coatings and pavement markings	Verification of chemical composition	3.05	1.38	2
	Verification of the presence of solvents/diluents	2.73	1.41	3
Epoxy adhesives	Verification of chemical composition	2.68	1.25	3
Portland cement concrete (PCC)	Verification of presence of chemical admixtures in fresh/cured PCC mix	2.65	1.28	3
Curing compounds for PCC	Verification of chemical composition/degree of cure (water content)	2.76	1.36	3
Polymer-modified asphalt binders, emulsions, and mixtures	Verification of type/class of polymer modifier	3.45	1.20	1
	Determination of polymer content	3.52	1.28	1
Antistripping agents	Verification of presence/type	3.55	1.17	1
Reclaimed asphalt pavement (RAP)	Verification of RAP presence in HMA	2.30	1.33	4
	Determination of RAP content in HMA	3.05	1.53	2

APPENDIX H

Links to Material Safety Data Sheet

Brand	Description	Link to Material Safety Data Sheet
1100-CLEAR	Resin-based, water-based concrete curing compound	www.wrmeadows.com/data/370.pdf
3M All Weather Paint White	Pavement marking	http://multimedia.3m.com/mws/mediawebserver?mwsId=SSSSSuUn_zu8l00x4YtGN82vnv70k17zHvu9lxtD7SSSSSS—
3M All Weather Paint Yellow	Pavement marking	http://multimedia.3m.com/mws/mediawebserver?SSSSSuUn_zu8l00xMxtZlx_U4v70k17zHvu9lxtD7SSSSSS—
Accelguard 80	Portland cement concrete set-accelerating admixture	www.euclidchemical.com/fileshare/ProductFiles/msds/019_99_C.pdf
AD-here LOF 65-00 LS	Amido-amine-derived asphalt antistripping agent	www.am-cc.com/pdfs/ArrMaz_Asphalt_Additives.pdf
ADVA 190	High-range water-reducing admixture	www.na.graceconstruction.com/concrete/download/ADVA%20190%20D-06621%20_Q_.pdf
Air Mix 200	Air-entraining admixture	www.rwsidley.com/MSDS/euclid%20air%20mix.pdf
Butonal NX1138	Cationic styrene butadiene polymer additive to asphalt	http://worldaccount.basf.com/wa/NAFTA/Catalog/FunctionalPolymers/doc4/BASF/PRD/30239910/.pdf?title=&asset_type=msds/pdf&language=EN&validArea=US&urn=urn:documentum:ProductBase_EU:09007af8800903ee.pdf
Carbozinc 859 Part A	Organic zinc-rich epoxy	http://msds.carboline.com/website/carbmsds.nsf/(all)/E17F4AD2BED198E98525704200517184/$file/0486a1nl_2_usansi.pdf
Carbozinc 859 Part B	Organic zinc-rich epoxy	https://www.dot.ny.gov/divisions/engineering/technical-services/technical-services-repository/details/cz859_msdsb.pdf
Carbozinc 859 zinc filler	Organic zinc-rich epoxy	http://msds.carboline.com/website/carbmsds.nsf/(all)/EF6A6C613ADE8659852570420051702B/$file/0229b1nl_2_usansi.pdf
CRS-1	Cationic emulsion	www.trinidadlakeasphalt.com/home/images/stories/pdfs/msds-crs-1.pdf
Kraton D1101	Styrene–butadiene–styrene block copolymer additive to asphalt	http://docs.kraton.com/tl_warehouse/technical_literature/docs/SBS-D%20Series%20(02-25-11).pdf
DuPont Elvaloy 4170	Ethylene-acrylate copolymer additive to asphalt	http://msds.dupont.com/msds/pdfs/EN/PEN_09004a358049f142.pdf
Epoplex LS50 White	Epoxy traffic paint	http://docs.stonhard.com/website/Epoplex.nsf/docids/BD959318F531DF8E8525741A0057029B/$FILE/513B+EPOPLEX+LS50+WHITE+EPOPLEX+English+COMMERCIAL.pdf

(continued on next page)

Brand	Description	Link to Material Safety Data Sheet
Epoplex LS50 Yellow	Epoxy traffic paint	http://docs.stonhard.com/WebSite/Epoplex.nsf/docids/3A976EB208F2E83A852574190064133D/$FILE/ATTPKUAA.pdf
Epoplex LS50 hardener	Epoxy traffic paint	http://docs.stonhard.com/WebSite/Epoplex.nsf/docids/267C1F33F6441CAB8525741A005772BB/$FILE/ATTMVRLY.pdf
Eucon Retarder 75	Concrete set-retarding admixture	www.rwsidley.com/MSDS/euclid%20eucon%20retarder.pdf
Kling Beta 2700	Liquid antistrip for hot-mix asphalt pavements	www.e-asphalt.com/ingles/akzo/adhesion_data/kb2700.pdf
Kling Beta 2912	Liquid antistrip for hot-mix asphalt pavements	www.e-asphalt.com/ingles/akzo/adhesion_data/kb2912.pdf
Safe-Cure 1000	Concrete curing compound	www.chemmasters.net/Products/Cures/MSDS/SafeCure1000CN.pdf
Safe-Cure 1200 Clear	Concrete curing compound	www.chemmasters.net/Products/Cures/MSDS/SafeCure1200Clear.pdf
Scotchkote 323 Part A	Corrosion protection coating	www.farwestcorrosion.com/ccp/msds/3M_Scotchkote323_A.pdf
Scotchkote 323 Part B	Corrosion protection coating	www.farwestcorrosion.com/ccp/msds/3M_Scotchkote323_B.pdf
Sikadur 31 Part A	Thixotropic epoxy resin adhesive for concrete repair	http://us01.webdms.sika.com/fileshow.do?documentID=644
Sikadur 31 Part B	Thixotropic epoxy resin adhesive for concrete repair	http://us01.webdms.sika.com/fileshow.do?documentID=645
Ultrabond 1100	Fast set, medium viscosity bonding system for concrete repair	www.atc.ws/PDF/TDS%20&%20MSDS%20by%20Formula/Ultrabond%201100/MSDS_UB1100.pdf
TAMMSCURE WB 30D	Concrete curing compound	www.buildsite.com/dbderived/euclid/derived_files/derived383317.pdf

APPENDIX I

ATR FTIR Spectra

Structural Coatings

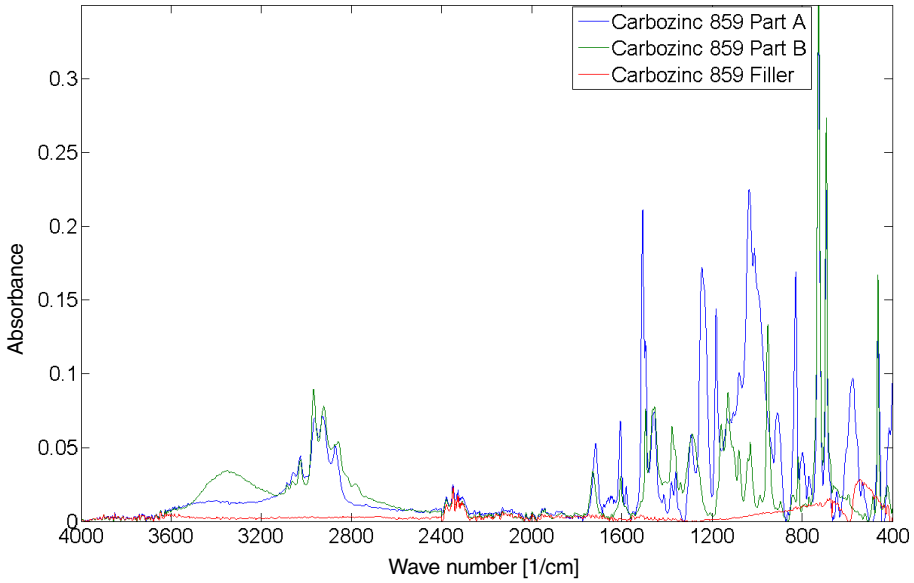

Figure I.1. Baseline-corrected attenuated total reflectance (ATR) Fourier transform infrared (FTIR) spectra of Carbozinc 859 components.

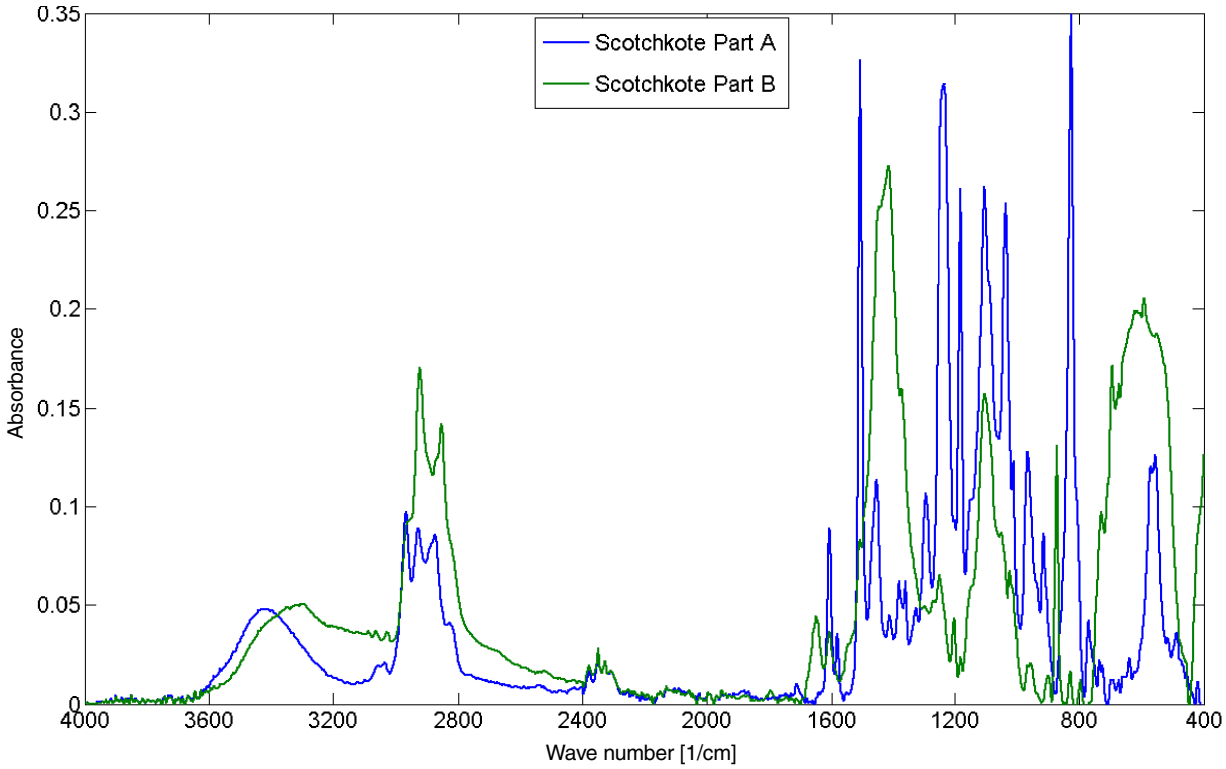

Figure I.2. Baseline-corrected ATR FTIR spectra of Scotchkote components.

Epoxy Pavement Markings

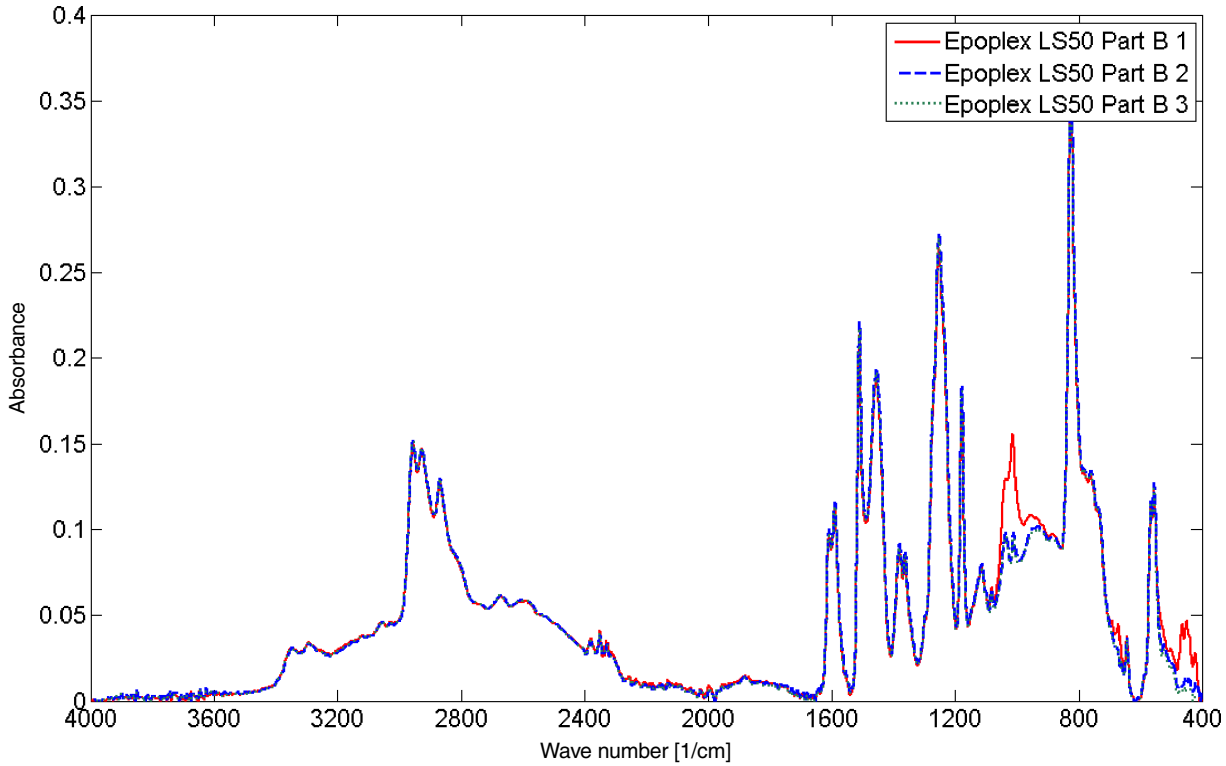

Figure I.3. Baseline-corrected ATR FTIR spectra of Epoplex LS50 Part B.

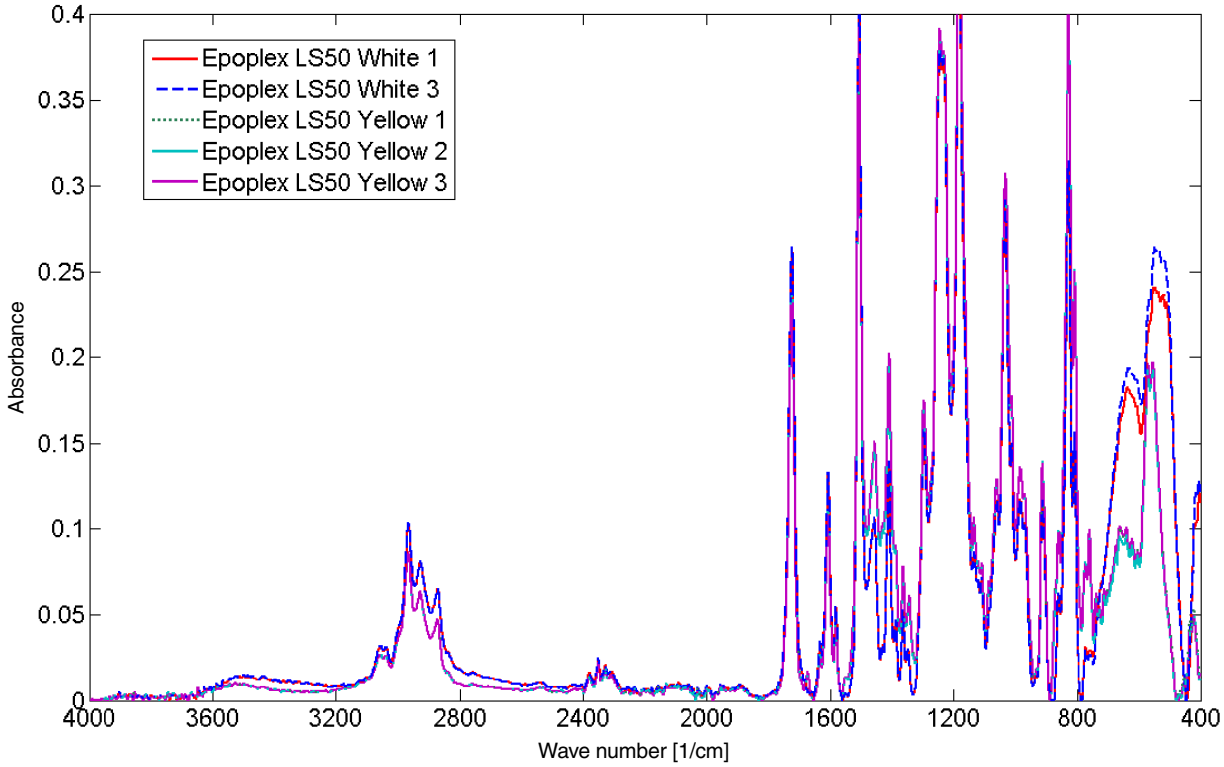

Figure I.4. Baseline-corrected ATR FTIR spectra of ready-mixed white and yellow Epoplex LS50 pavement marking.

Waterborne Traffic Paints

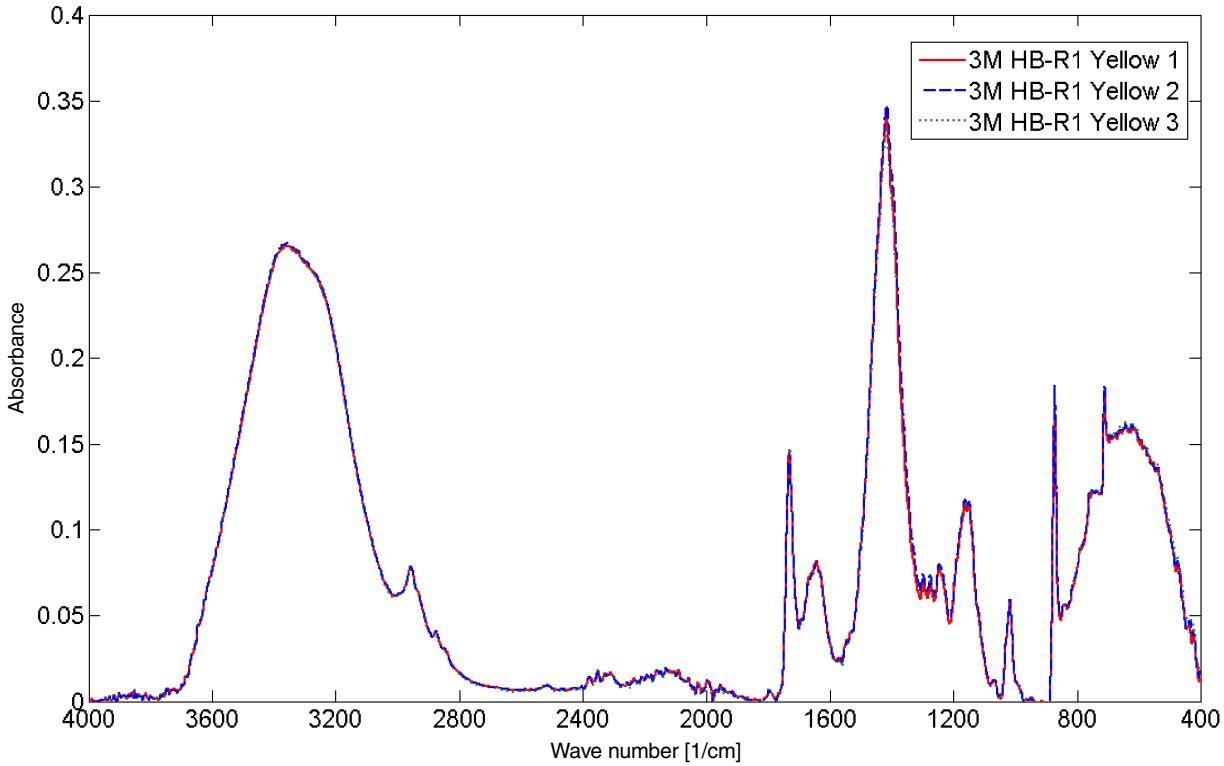

Figure I.5. Baseline-corrected ATR FTIR spectra of 3M All Weather yellow paint.

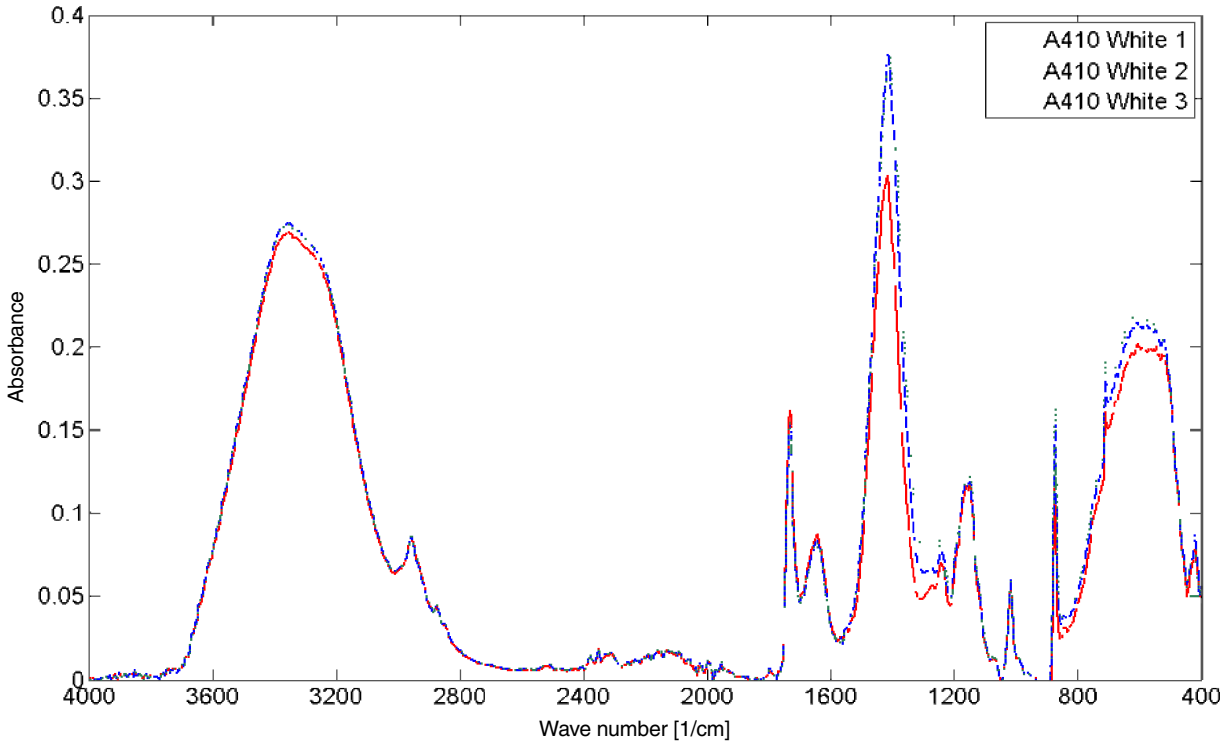

Figure I.6. Baseline-corrected ATR FTIR spectra of Aquaspar waterborne white paint.

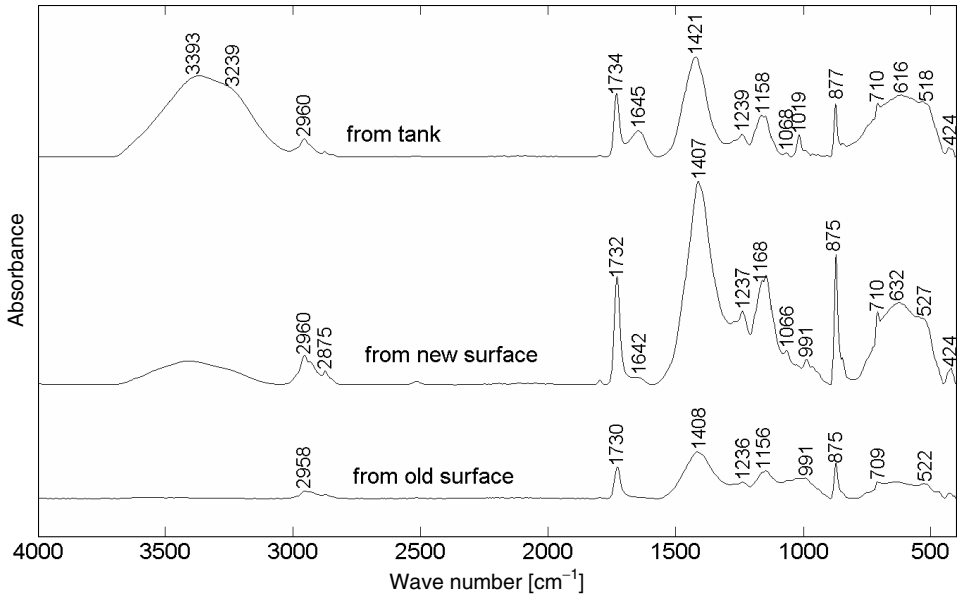

Figure I.7. Baseline-corrected ATR FTIR spectra of polyacrylic waterborne Ennis white paint.

Epoxy Adhesives

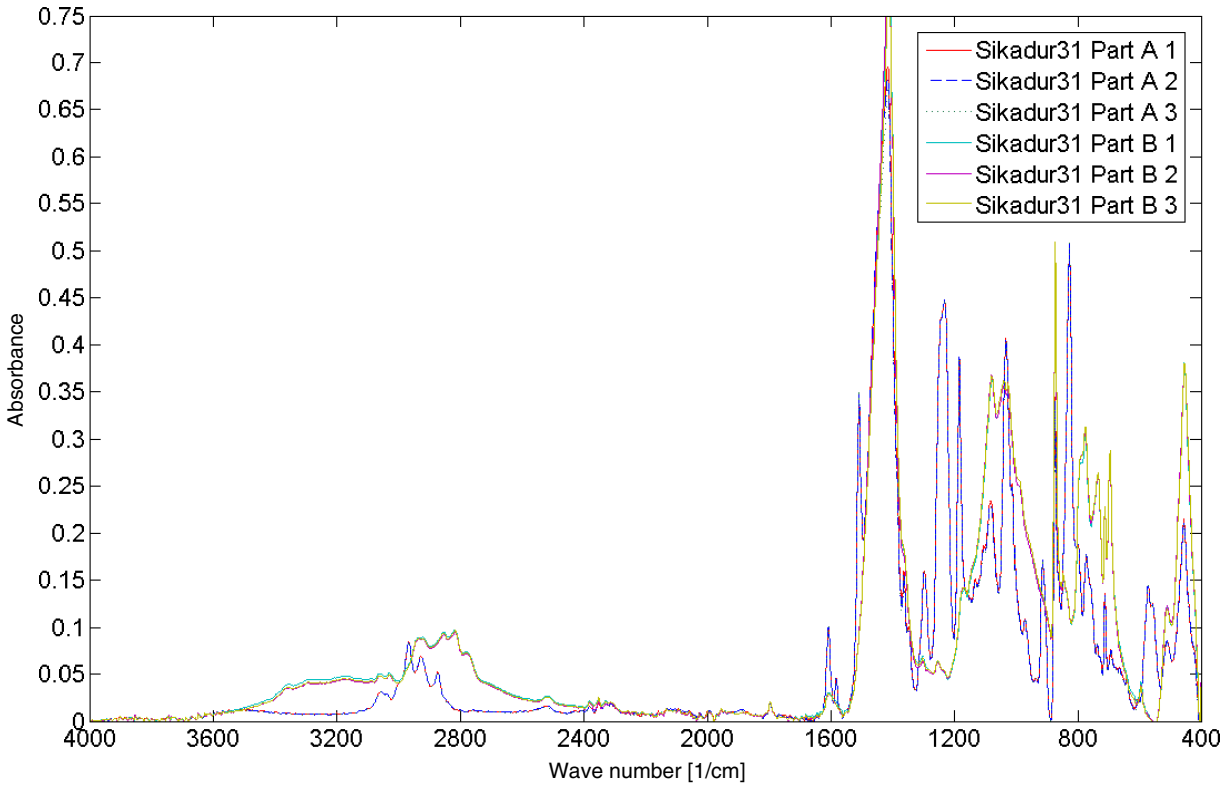

Figure I.8. Baseline-corrected ATR FTIR spectra of Sikadur31 components.

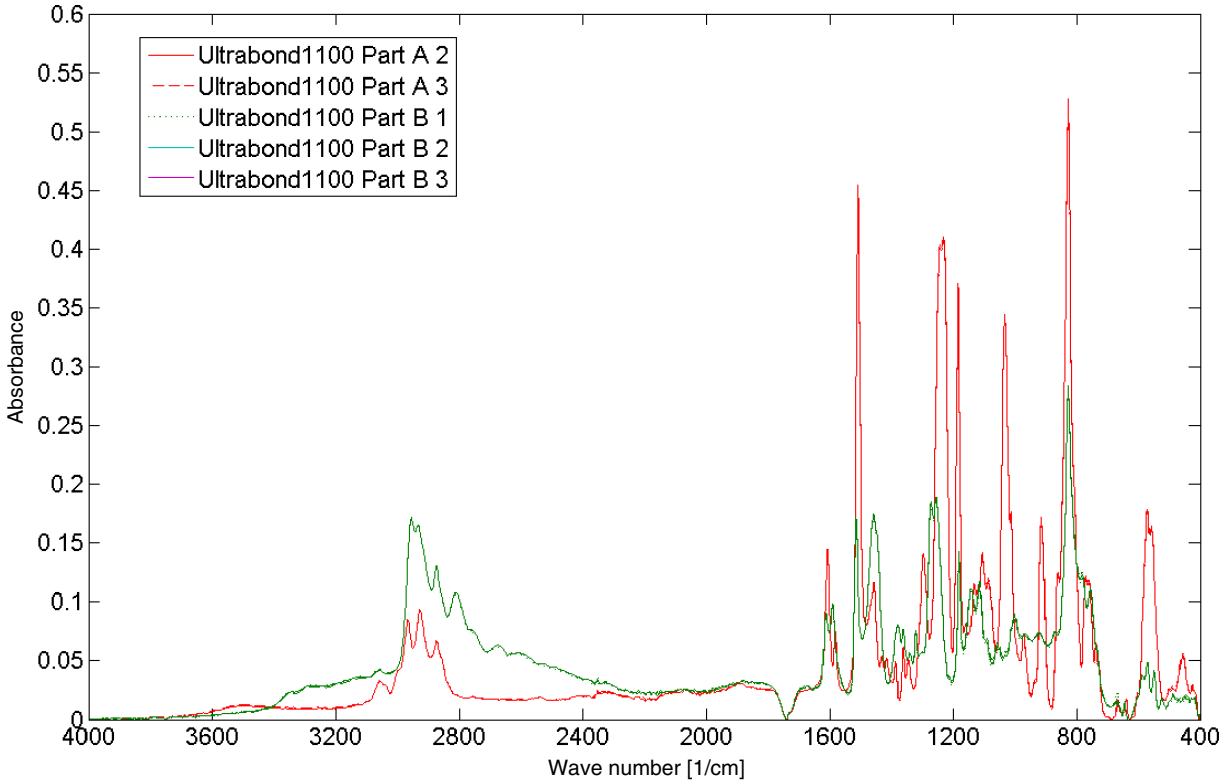

Figure I.9. Baseline-corrected ATR FTIR spectra of Ultrabond1100 components.

Chemical Admixtures for PCC

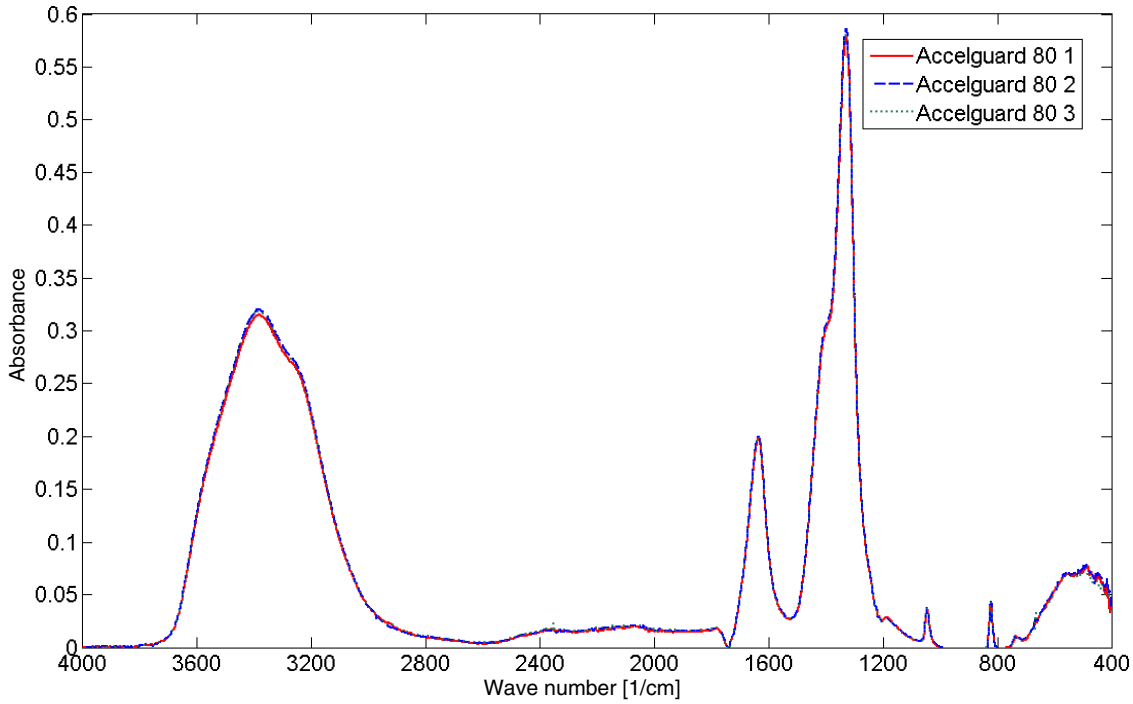

Figure I.10. Baseline-corrected ATR FTIR spectra of Accelguard 80 set accelerator.

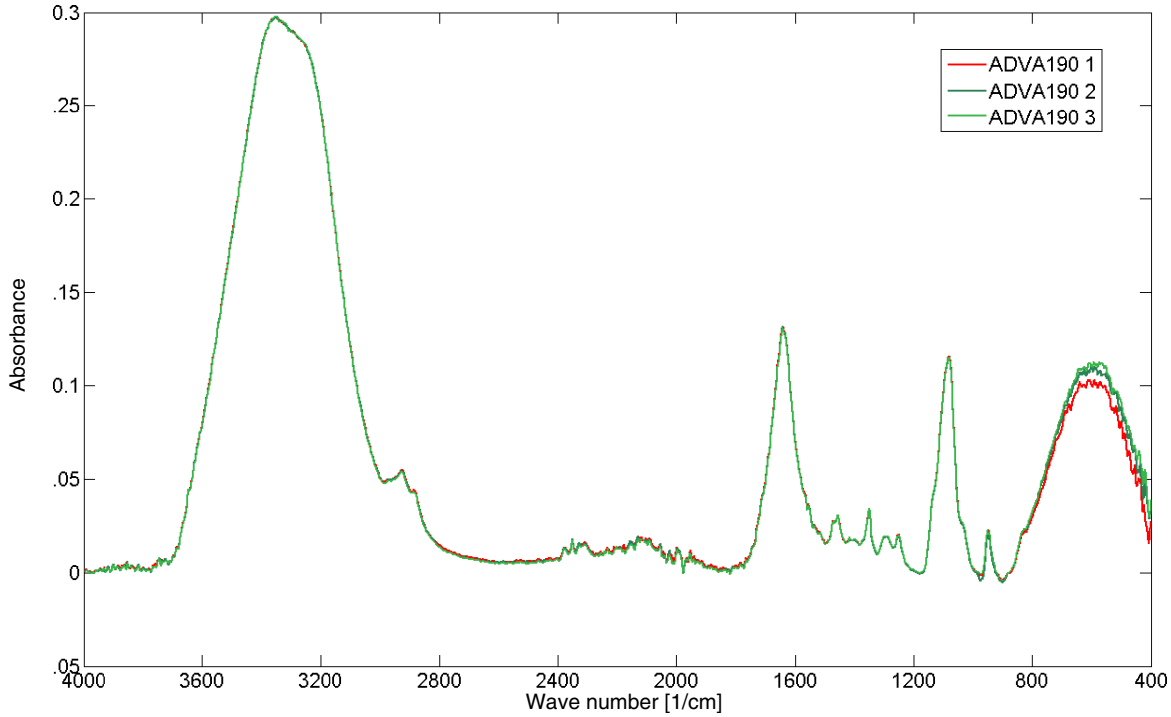

Figure I.11. Baseline-corrected ATR FTIR spectra of ADVA 190 superplasticizer.

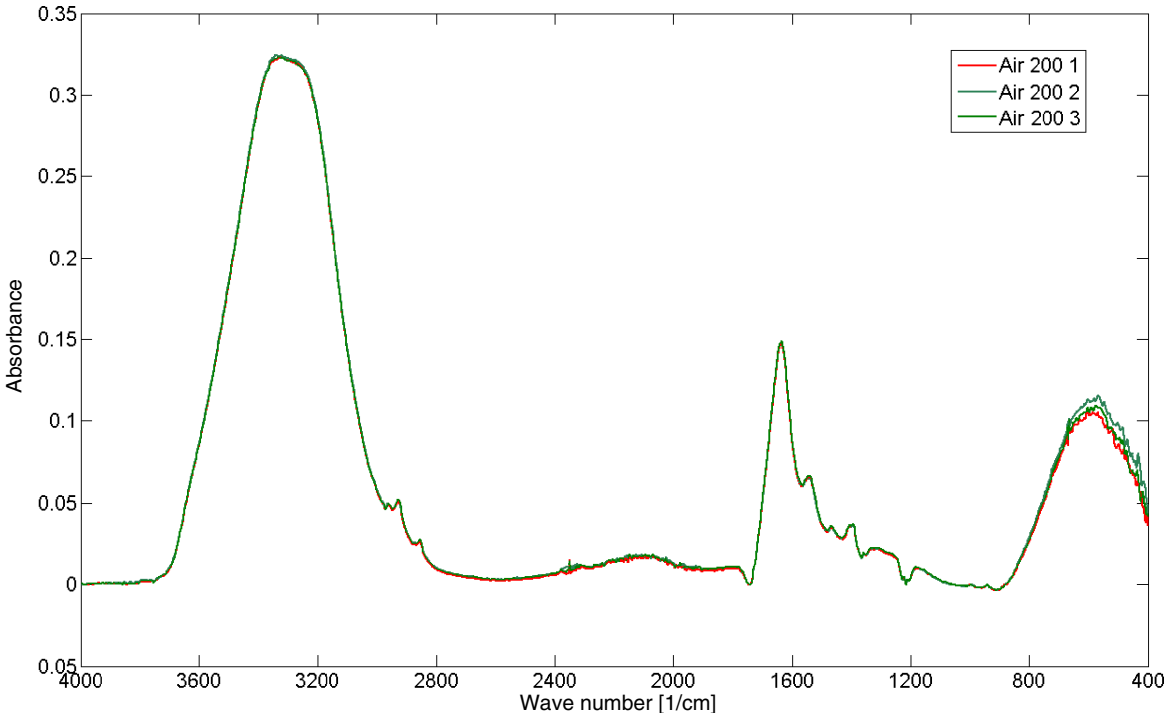

Figure I.12. Baseline-corrected ATR FTIR spectra of Air 200 air entrainer.

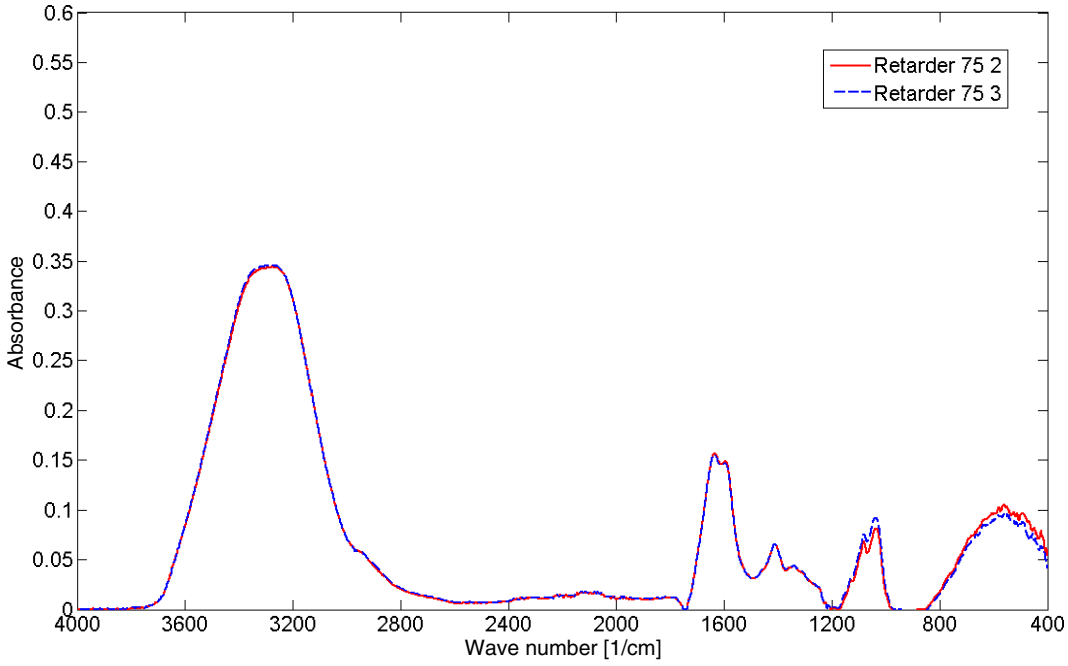

Figure I.13. Baseline-corrected ATR FTIR spectra of Retarder 75 set retarder.

Curing Compounds for PCC

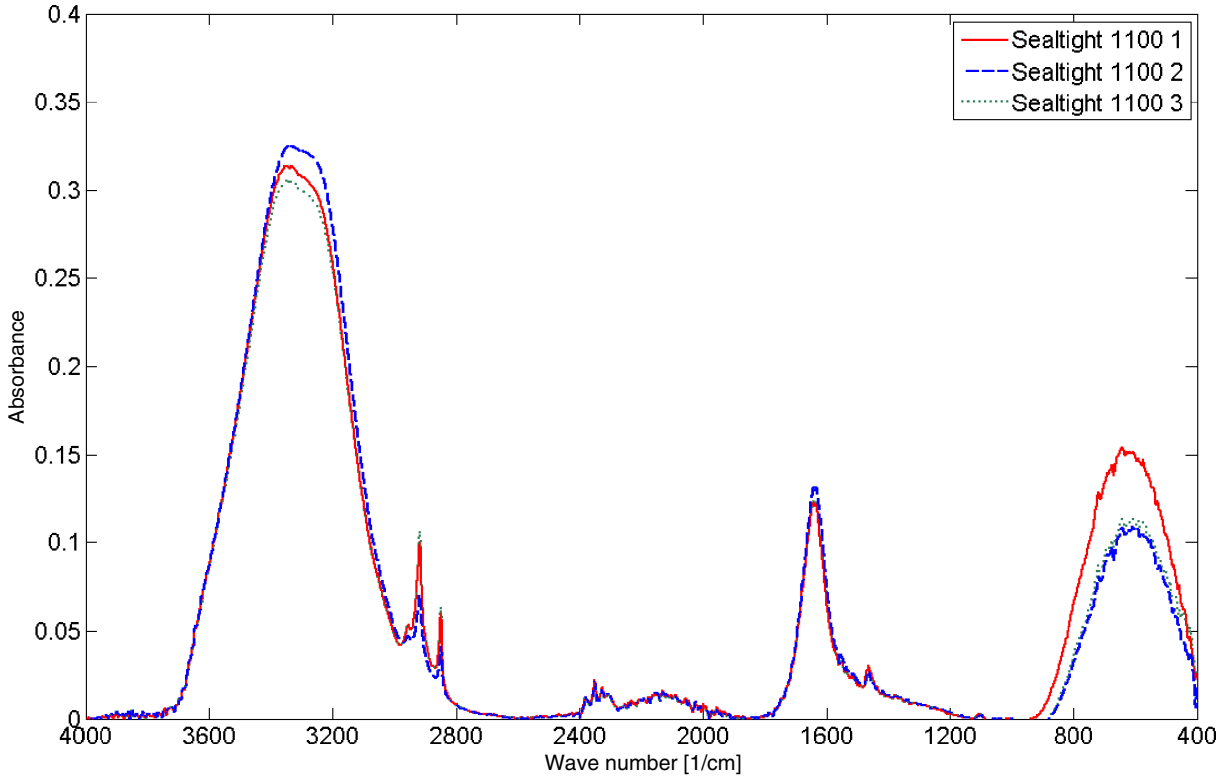

Figure I.14. Baseline-corrected ATR FTIR spectra of W. R. Meadows's Sealtight 1100-CLEAR.

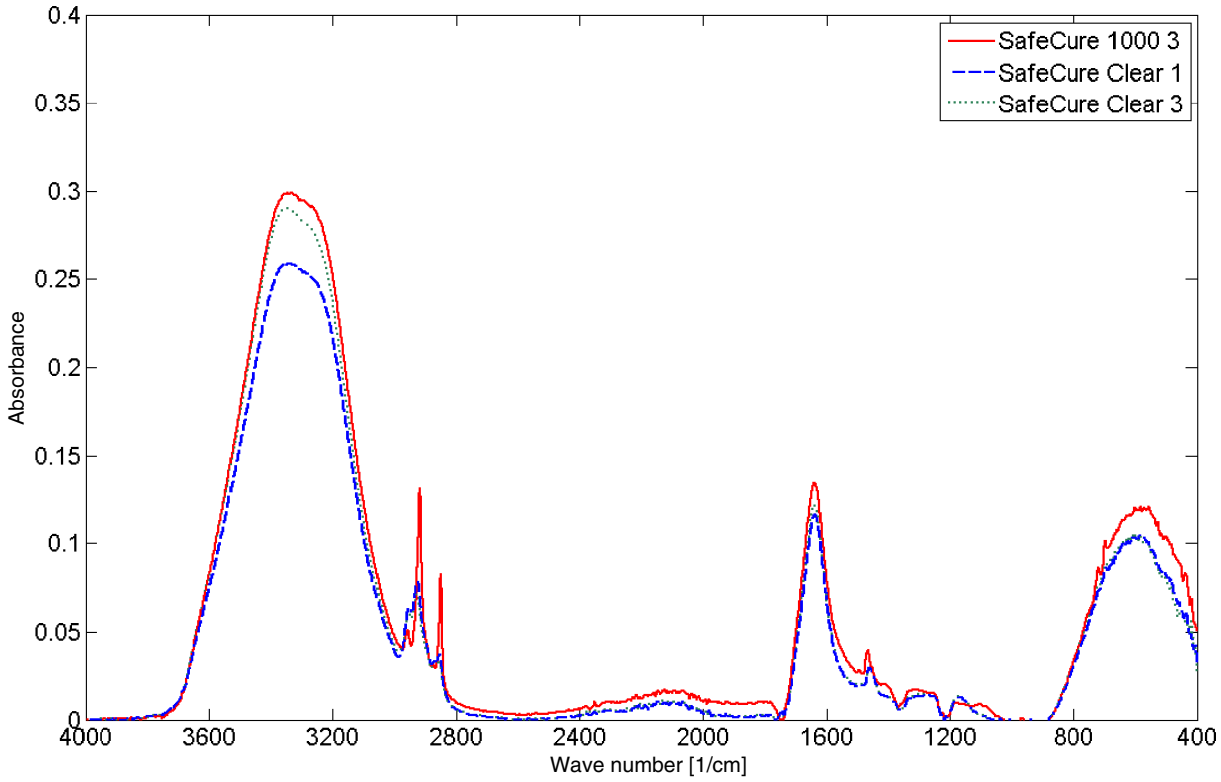

Figure I.15. Baseline-corrected ATR FTIR spectra of ChemMaster's Safe-Cure 1000.

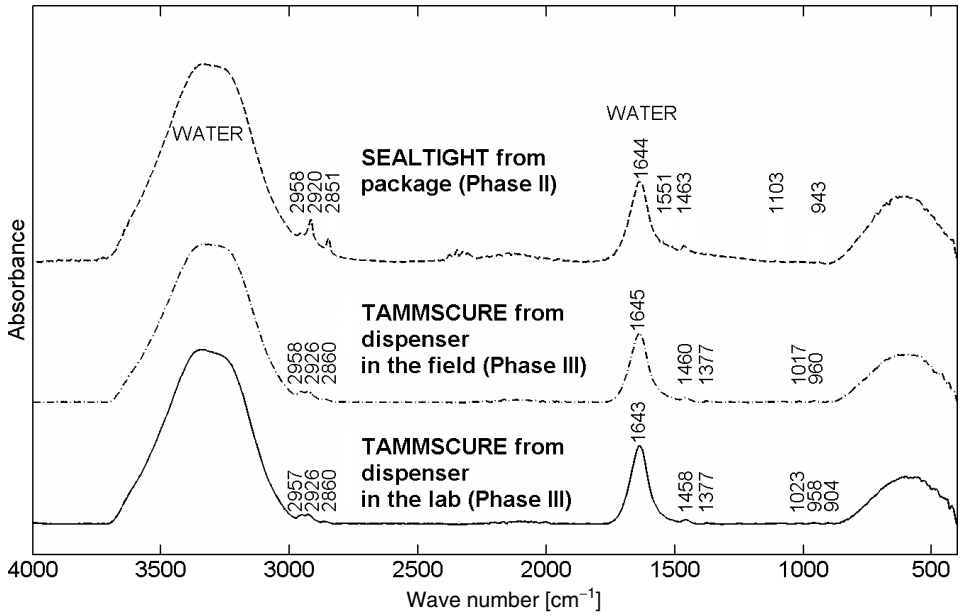

Figure I.16. Baseline-corrected lab and field ATR FTIR spectra of TAMMSCURE compared with Sealtight.

Polymer Modifiers for Asphalt Binders

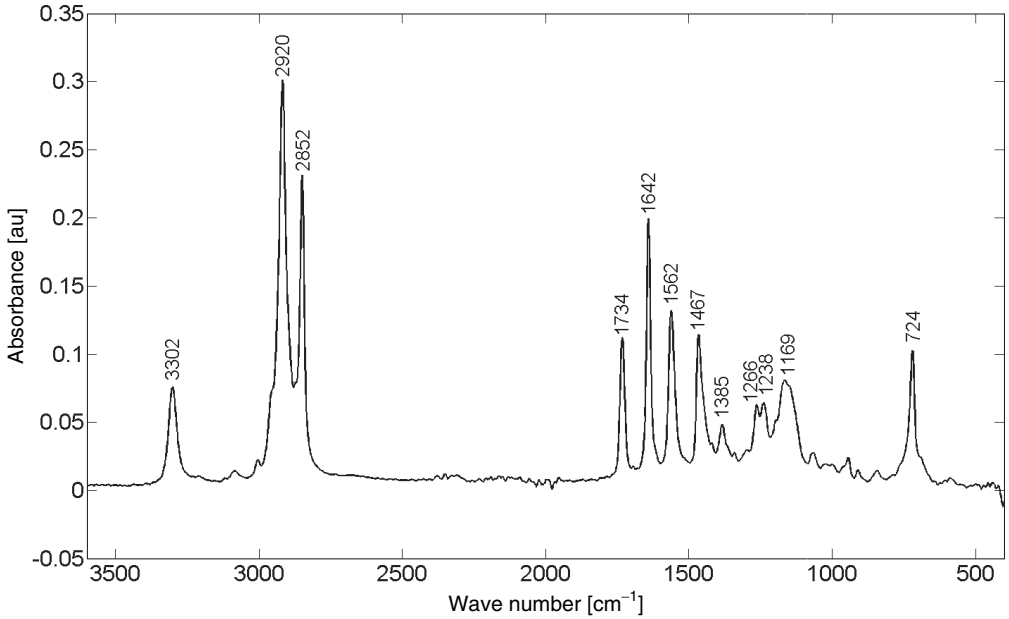

Figure I.17. Baseline-corrected ATR FTIR spectrum of DuPont Elvaloy 4170 polymer.

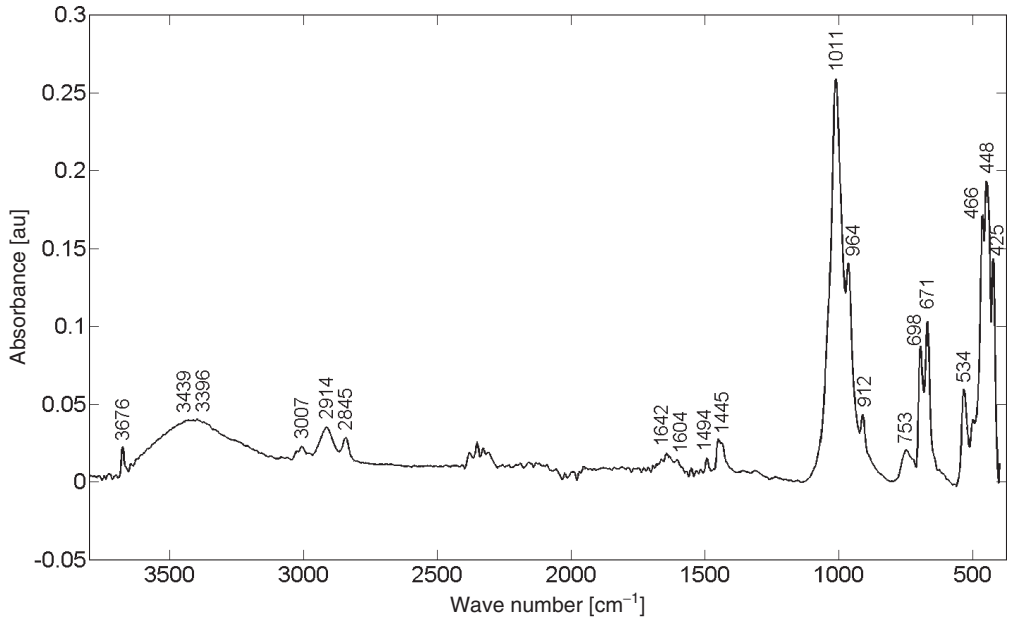

Figure I.18. Baseline-corrected ATR FTIR spectrum of Kraton D1101 SBS polymer.

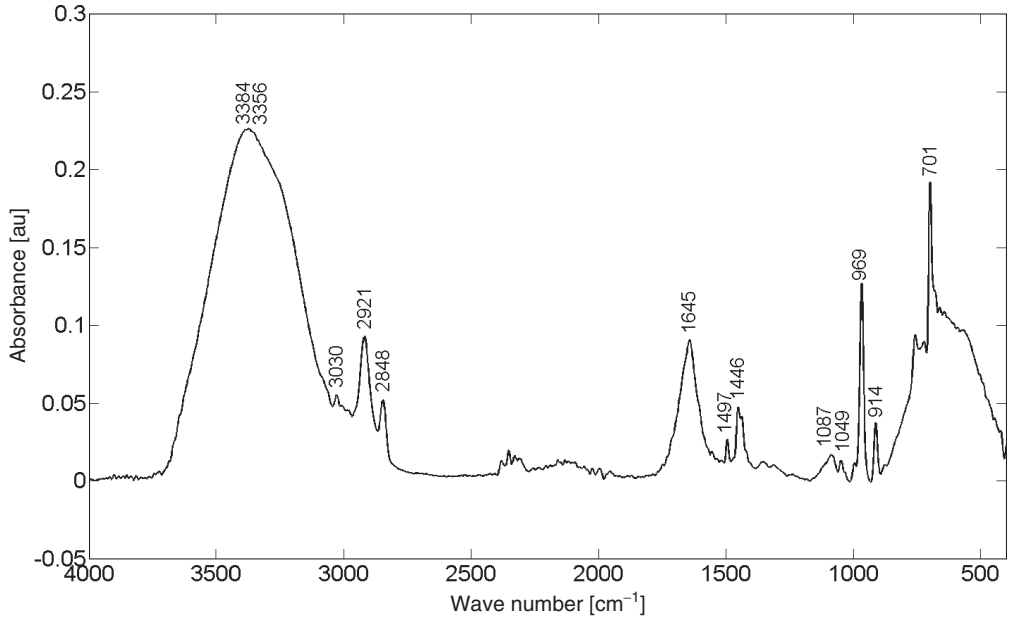

Figure I.19. Baseline-corrected ATR FTIR spectrum of BASF's Butonal SB latex polymer.

Antistripping Agents for Asphalt

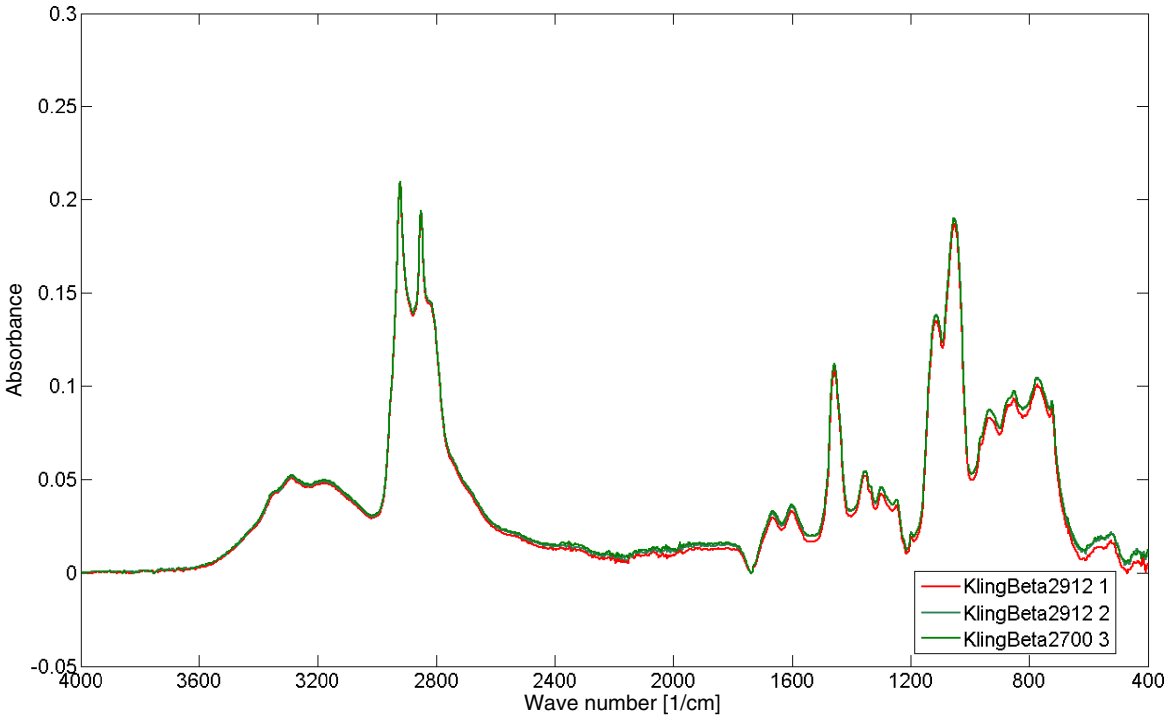

Figure I.20. Baseline-corrected ATR FTIR spectra of Akzo Nobel's Kling Beta.

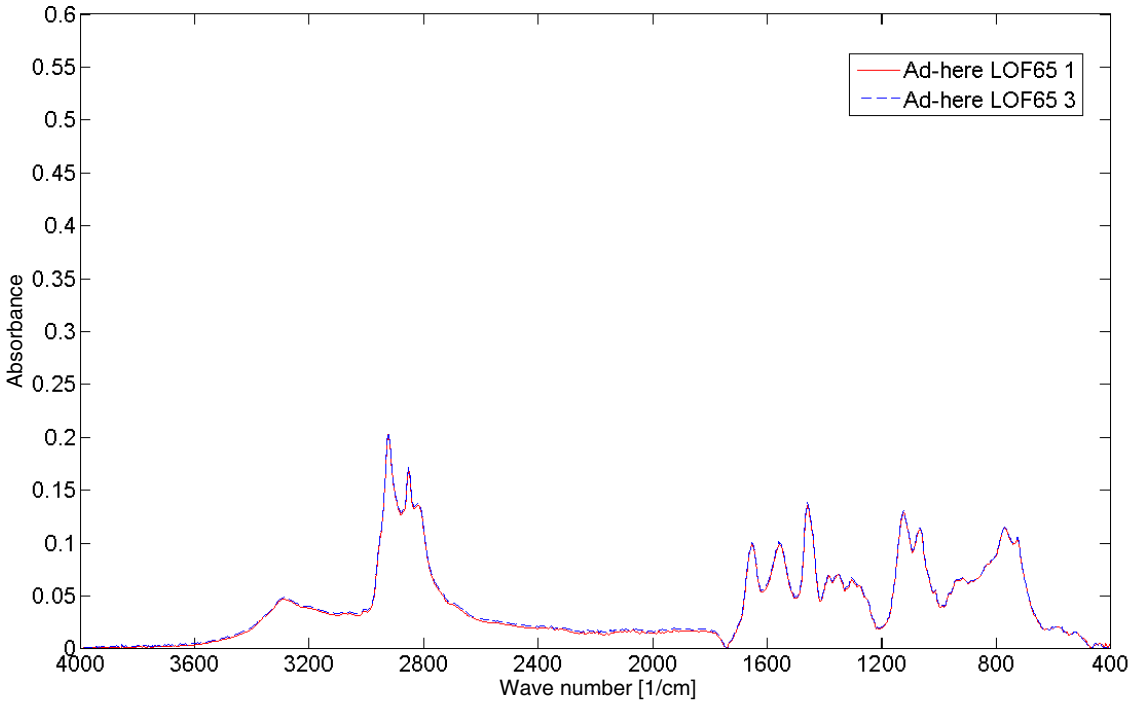

Figure I.21. Baseline-corrected ATR FTIR spectra of ArrMaz's AD-here.

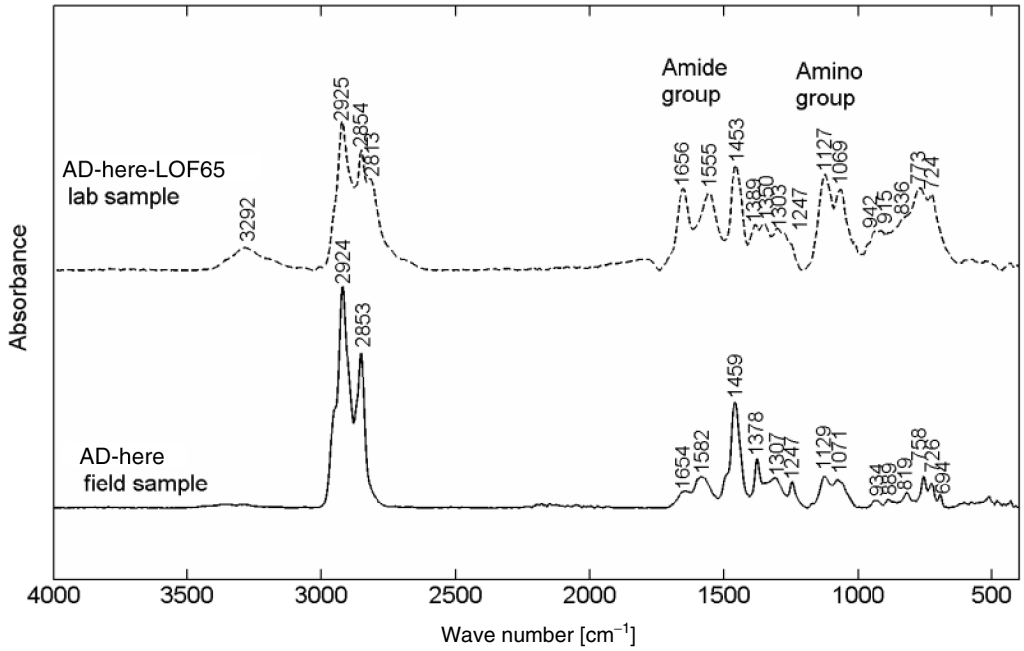

Figure I.22. Comparison of the lab and field ATR FTIR spectra of ArrMaz's AD-here.

Unmodified Asphalt Binders

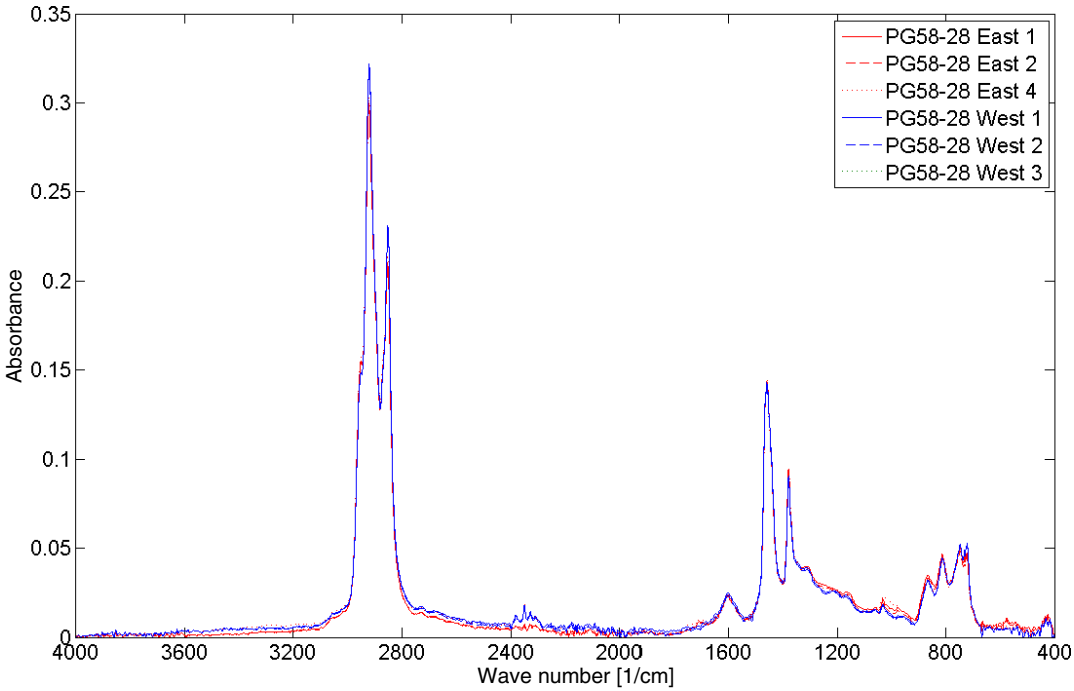

Figure I.23. Comparison of ATR FTIR spectra of PG 58-28 binders from different refineries.

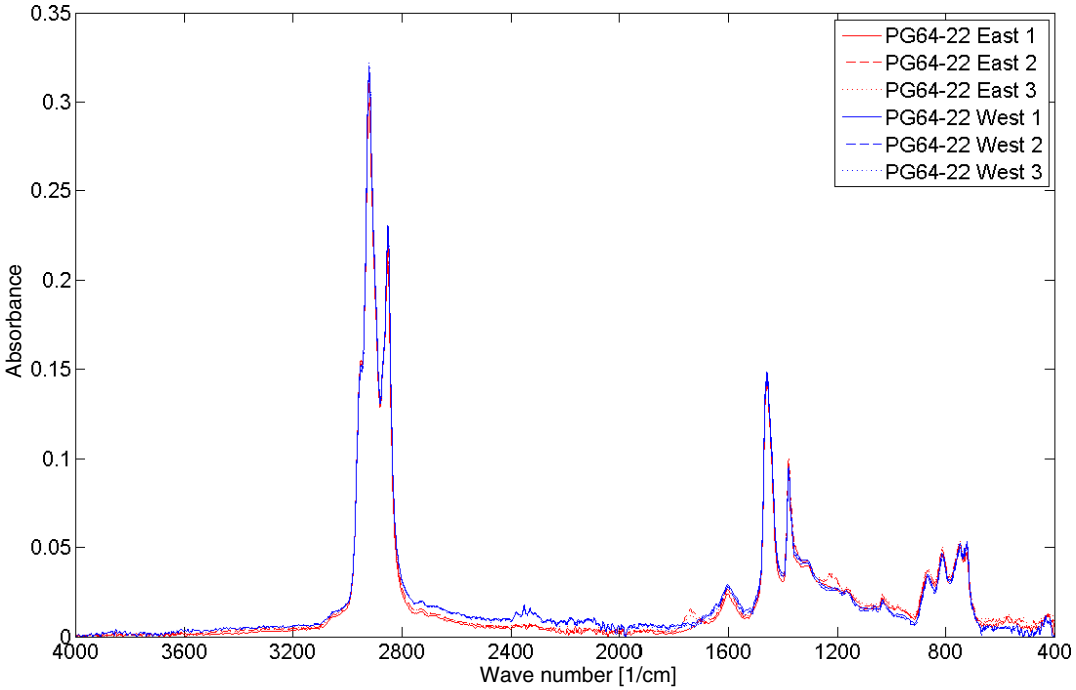

Figure I.24. Comparison of ATR FTIR spectra of PG 64-22 binders from different refineries.

Polymer-Modified Binders

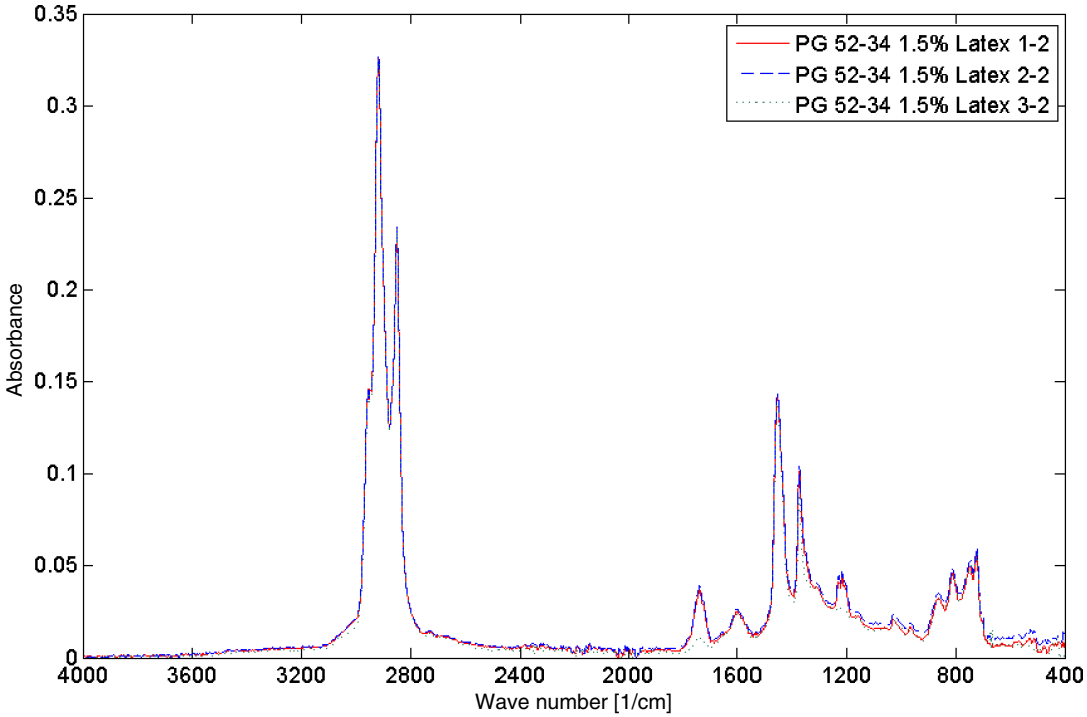

Figure I.25. Typical ATR FTIR spectrum for PG 52-34 binder modified with 1.5 wt% styrene–butadiene rubber latex.

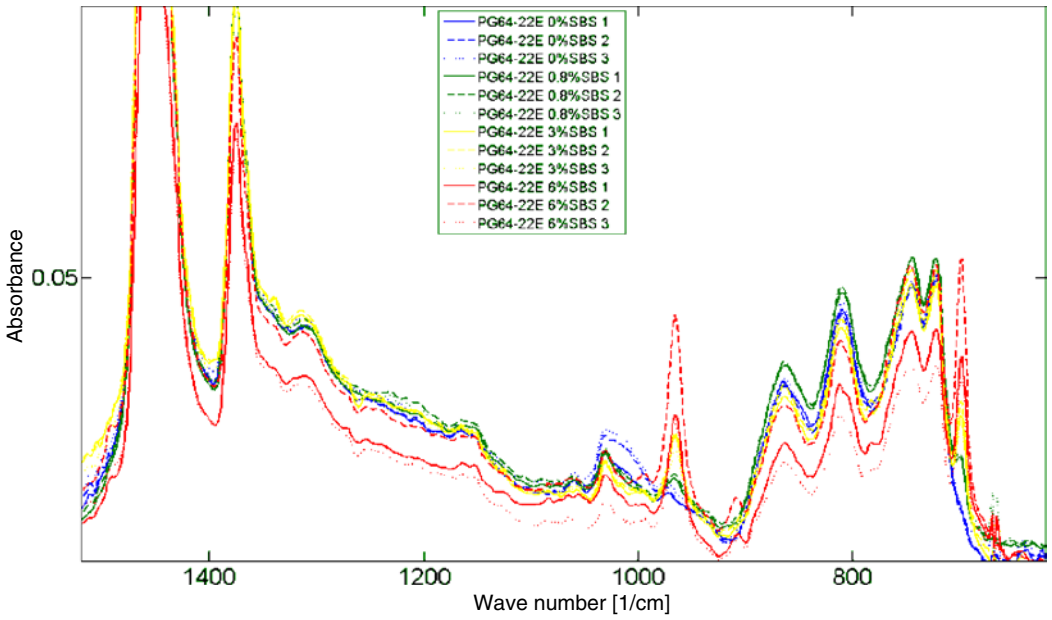

Figure I.26. Comparison of the ATR FTIR spectra for PG 64-22 binders modified with 1, 3, and 6 wt% Kraton SBS.

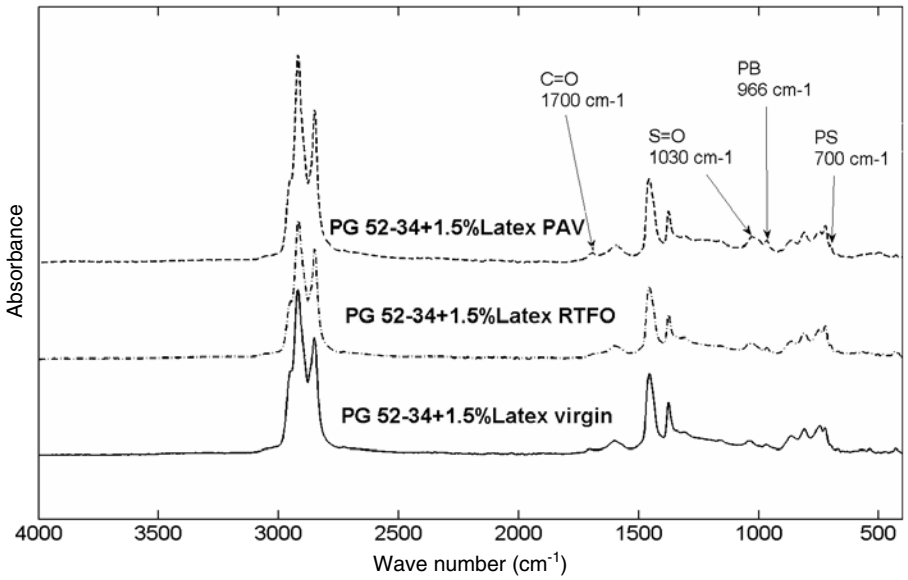

Figure I.27. Comparison of the ATR spectra for virgin, RTFO-aged, and PAV-aged PG52-34 binder modified with 1.5 wt% SBR Latex.

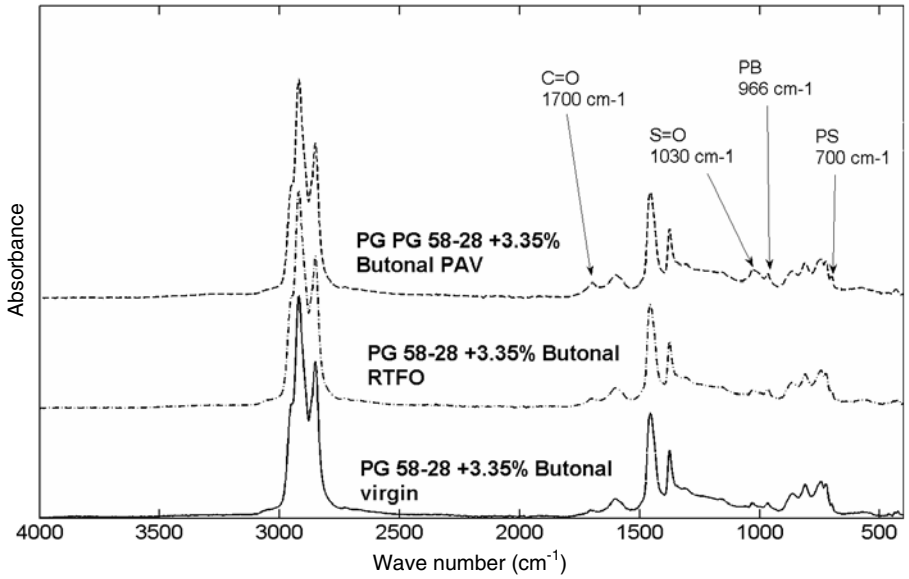

Figure I.28. Comparison of the ATR spectra for virgin, RTFO-aged, and PAV-aged PG58-28 binder modified with 3.3 wt% BASF Butonal.

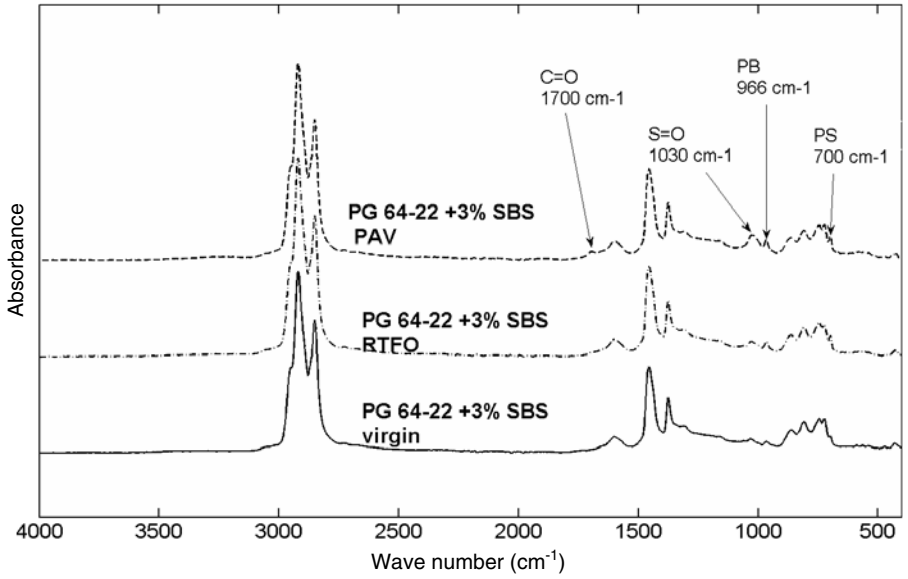

Figure I.29. Comparison of the ATR spectra for virgin, RTFO-aged, and PAV-aged PG64-22 binder modified with 3 wt% Kraton SBS.

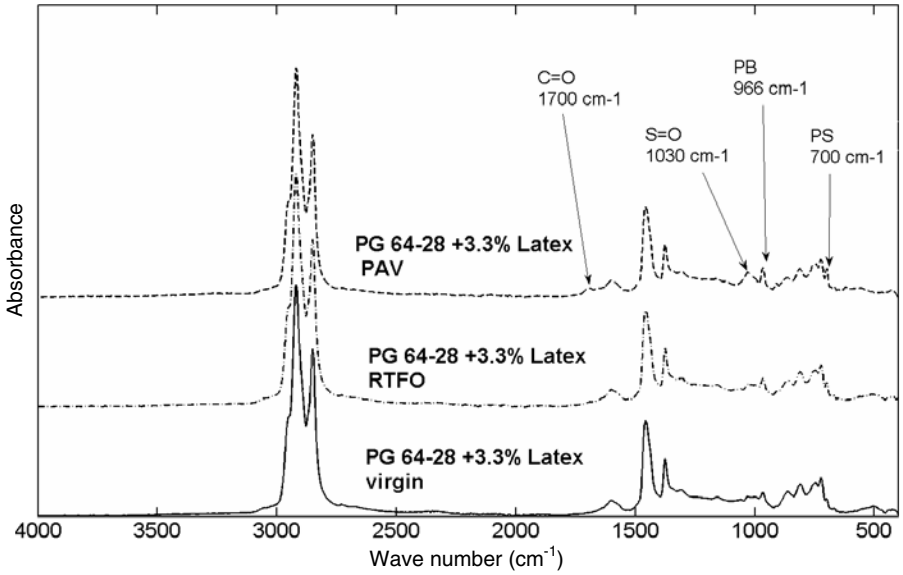

Figure I.30. Comparison of the ATR spectra for virgin, RTFO-aged, and PAV-aged 64-28 binder modified with 3.3 wt% SBR Latex.

APPENDIX J

Raman Spectra

Laboratory Results

For Raman spectroscopy using 1,064 excitation, a National Institute of Standards and Technology (NIST) standard reference material (SRM) 2244 has become available to remove instrument effects as well as obtain a spectrum that does not include the variability associated with the use of alternative laser sources (and thus detectors with varying response functions, see Figure J.1). The 3M MBR9 yellow sample spectra are displayed as an example of the processing that can be done to enhance Raman spectra (compare Figures J.2 and J.3). Figure J.2 depicts the raw spectrum for the 3M MBR9; notice the waviness from 1,800 to 2,800 cm^{-1}. In Figure J.3 the spectrum is corrected for variability in the instrument response, and the underlying fluorescence background is better represented. Subsequently, a better pure Raman spectrum can be produced by fluorescence removal with inclusion of the proper number of factors and fit to the appropriate polynomial (Figure J.4). However, band shape variability artifacts do persist as a result of this processing. Ideally, sampling conditions would be optimized to reduce the necessity of significant postprocessing of data. Additional corrected spectra are attached as well for AD-here, ADVA 190, Air 200, Aquaspar, Epoplex LS50 pB, Epoplex LS50 White, Epoplex LSS Yellow, Kling Beta 2700, Kling Beta 2912, Eucon Retarder 75 IL, Sealtight 1100, Sikadur Part A, Sikadur Part B, Ultrabond 1100 Part A, Safe-Cure 1000, and Safe-Cure Clear.

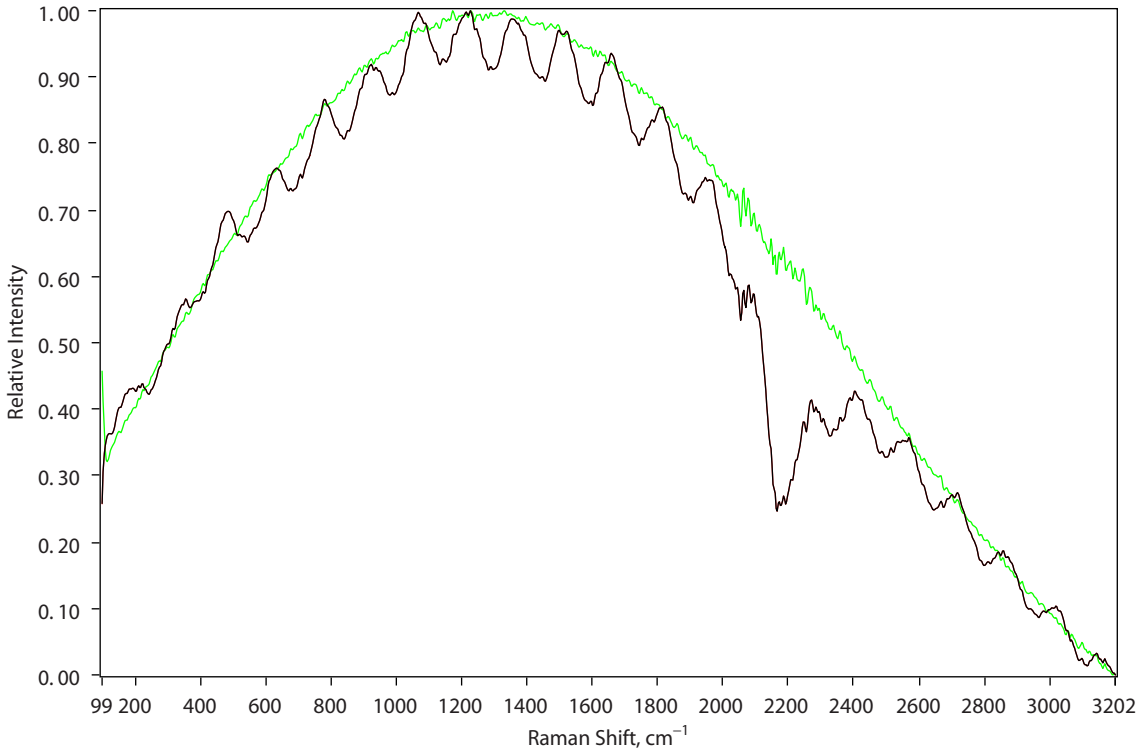

Figure J.1. NIST SRM raw (black trace) and corrected (green trace).

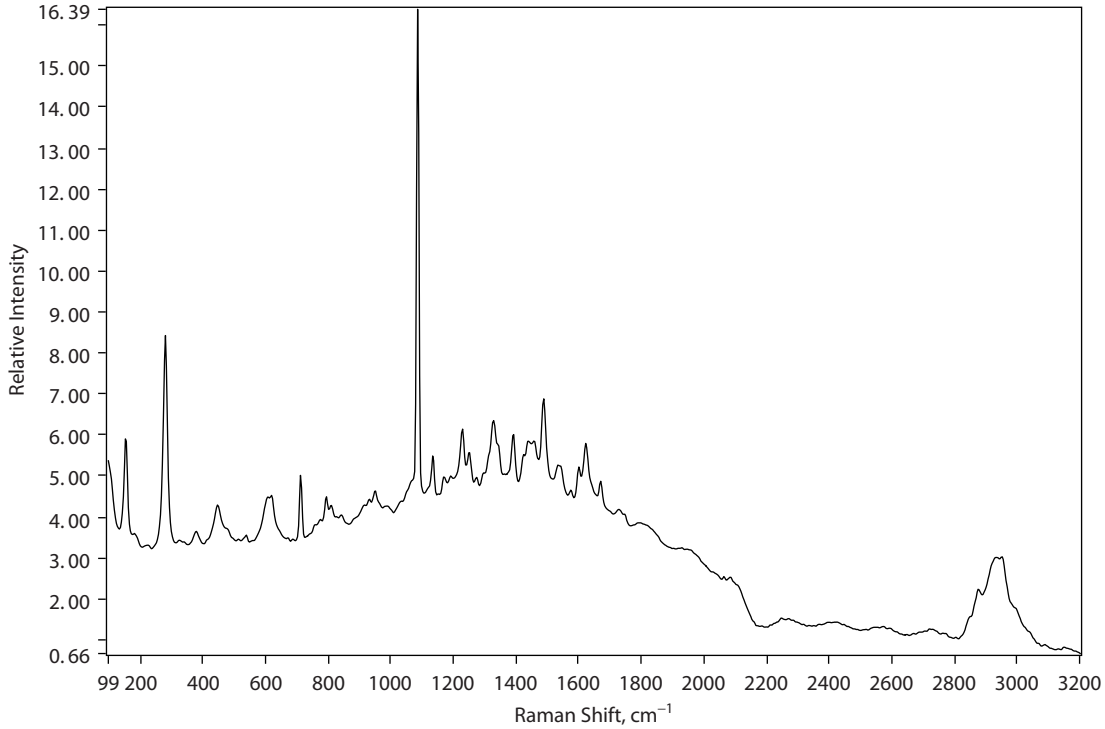

Figure J.2. Raw spectra for 3M MBR9 yellow.

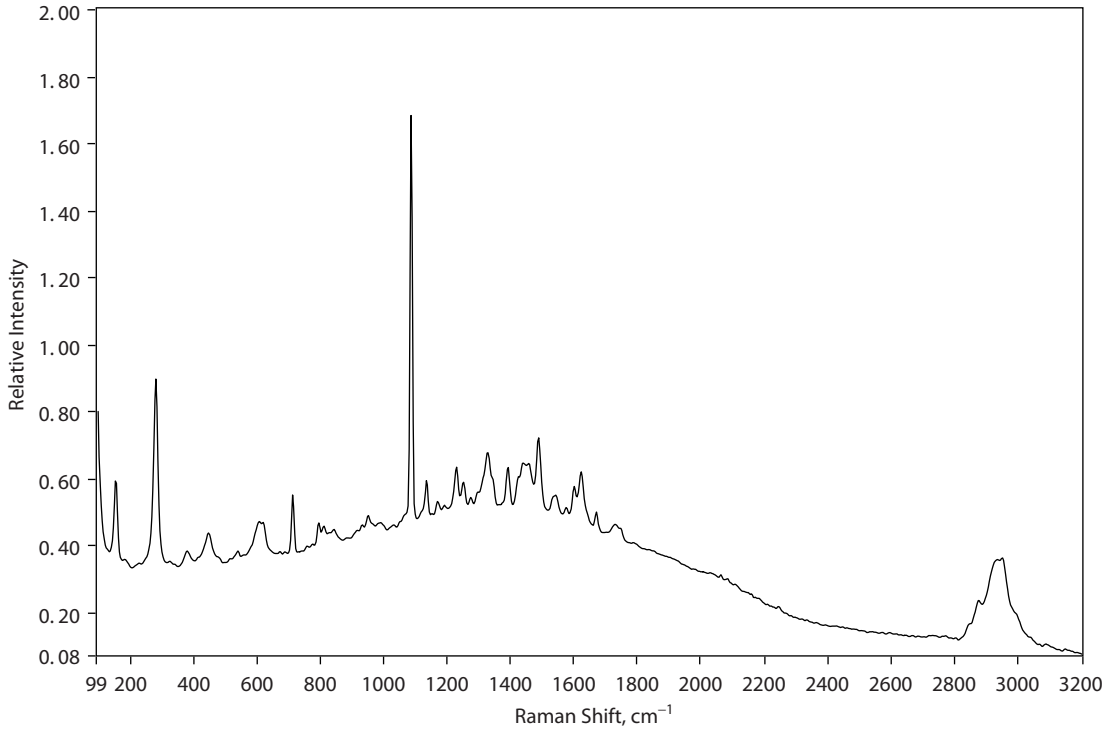

Figure J.3. SRM 2244 corrected spectrum of 3M MBR9 yellow. Note the removal of wavy baseline present in Figure J.2.

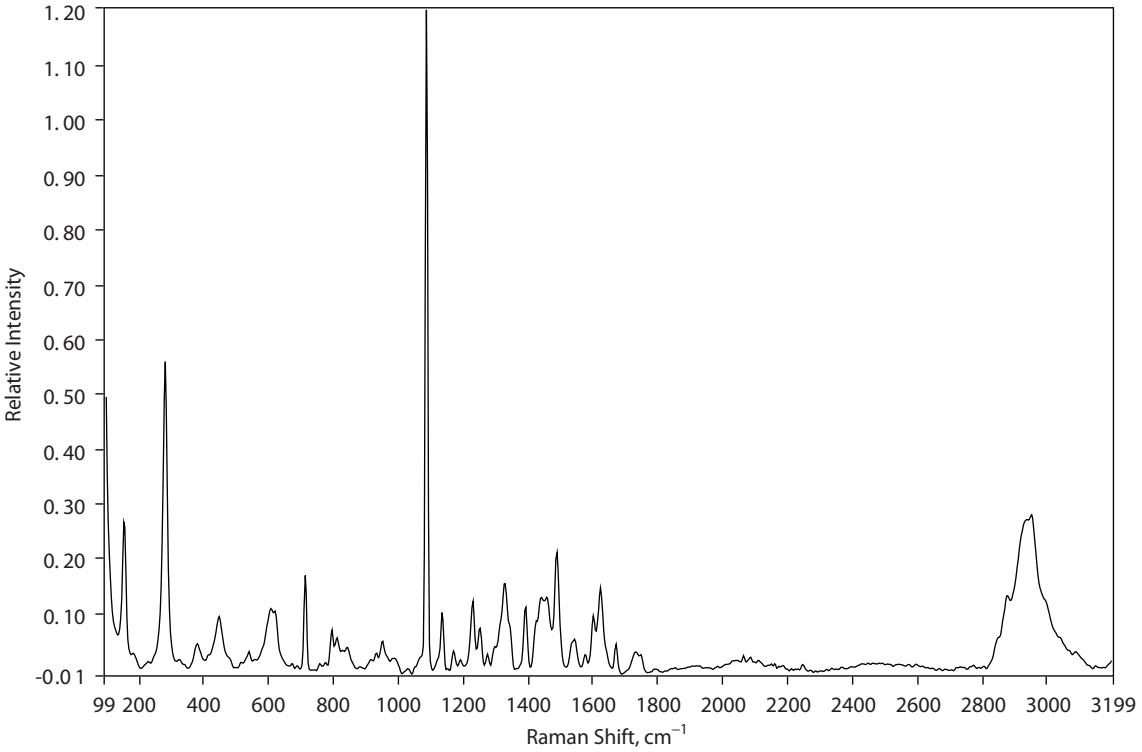

Figure J.4. Fluorescence background removed based on a seven-group LU decomposition for 3M MBR9 yellow. The prominent sharp band at 1,085 cm^{-1} is typical of the carbonate anion $-CO_3$.

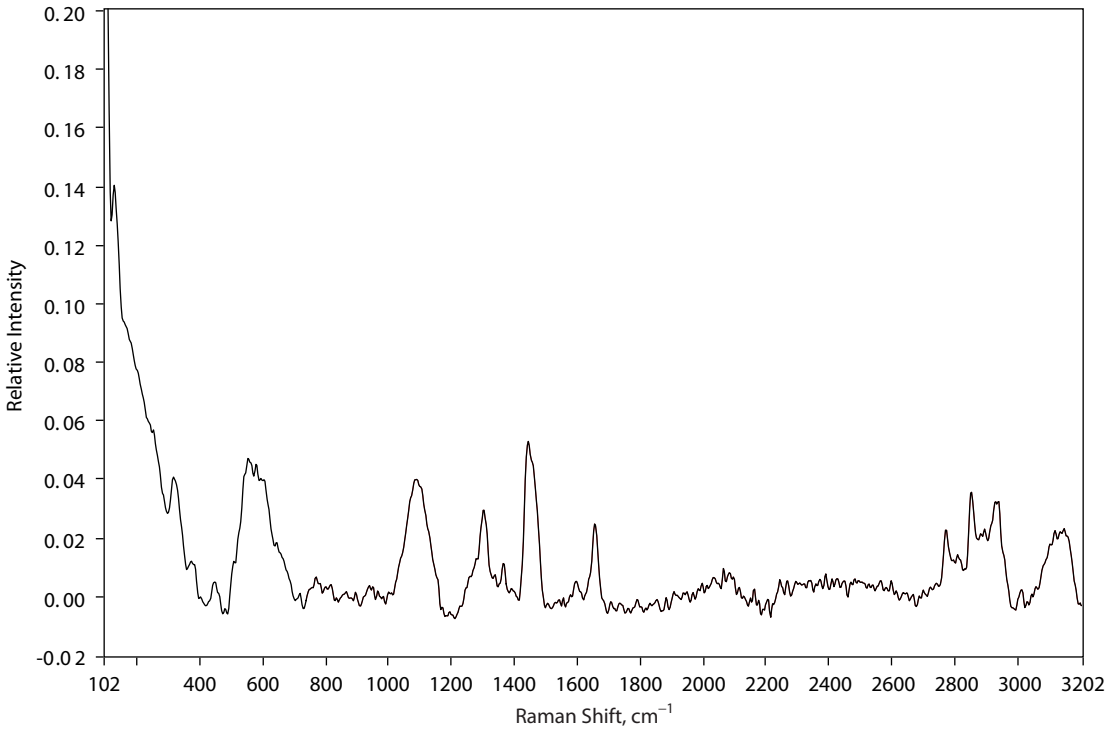

Figure J.5. AD-here SRM 2244 fluorescence corrected. Peaks at 1,450 and 2,800 to 2,970 cm^{-1} are representative of C–H modes.

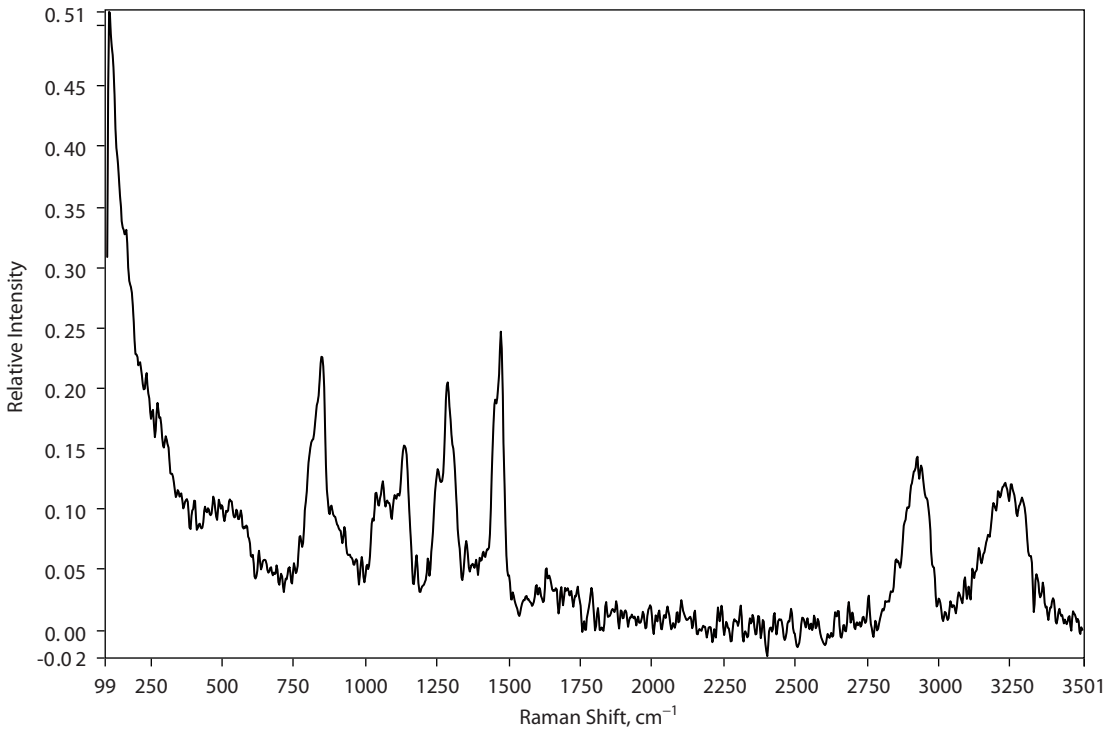

Figure J.6. ADVA 190 SRM 2244 fluorescence corrected. Note similarity to AD-here, with water peak at 3,250 cm⁻¹.

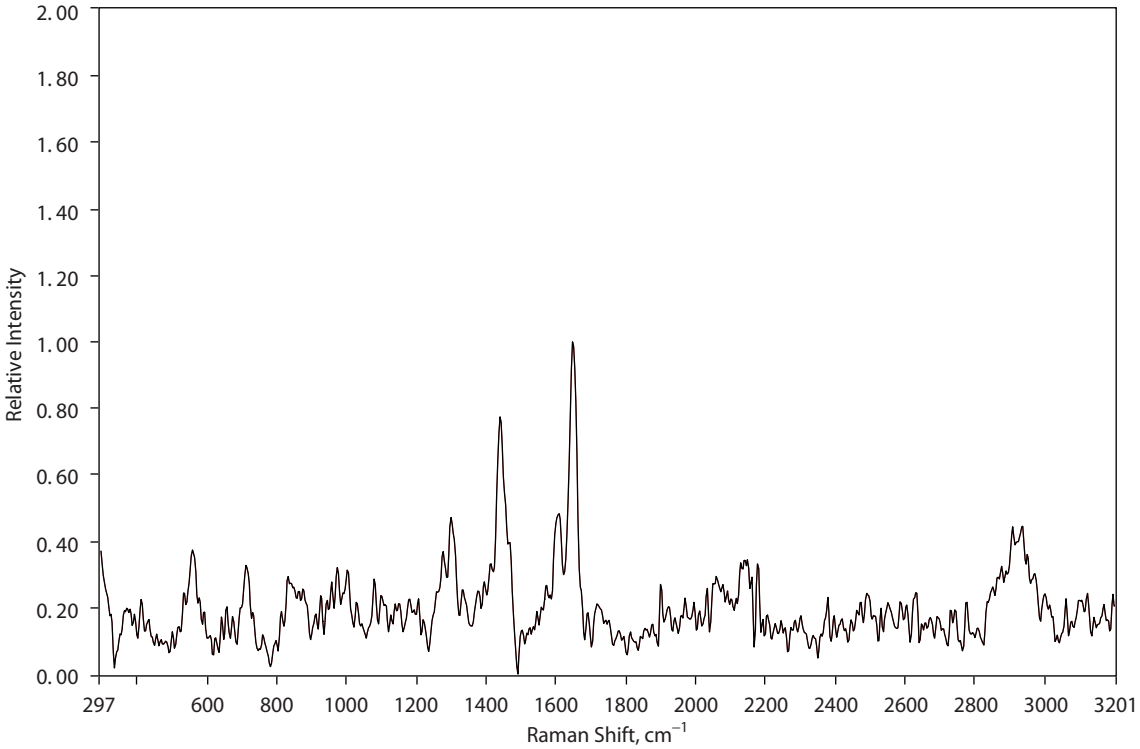

Figure J.7. Air 200 SRM 2244 fluorescence corrected. The 1,680 cm⁻¹ peak is typical of alkenes. Note similarities to ADVA 190.

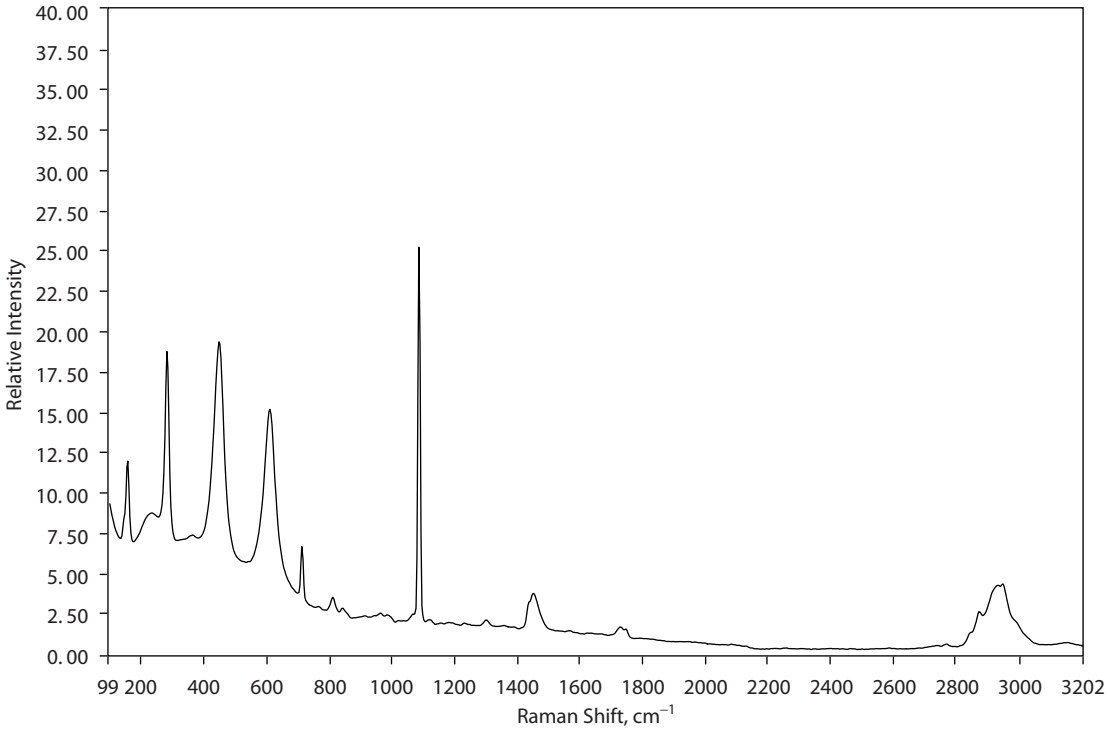

Figure J.8. Aquaspar SRM 2244 baseline corrected. Note similarities to 3M MBR9 yellow. The prominent sharp band at 1,085 cm^{-1} is typical of the carbonate anion $-CO_3$, with additional peaks at lower wave numbers typical of salts.

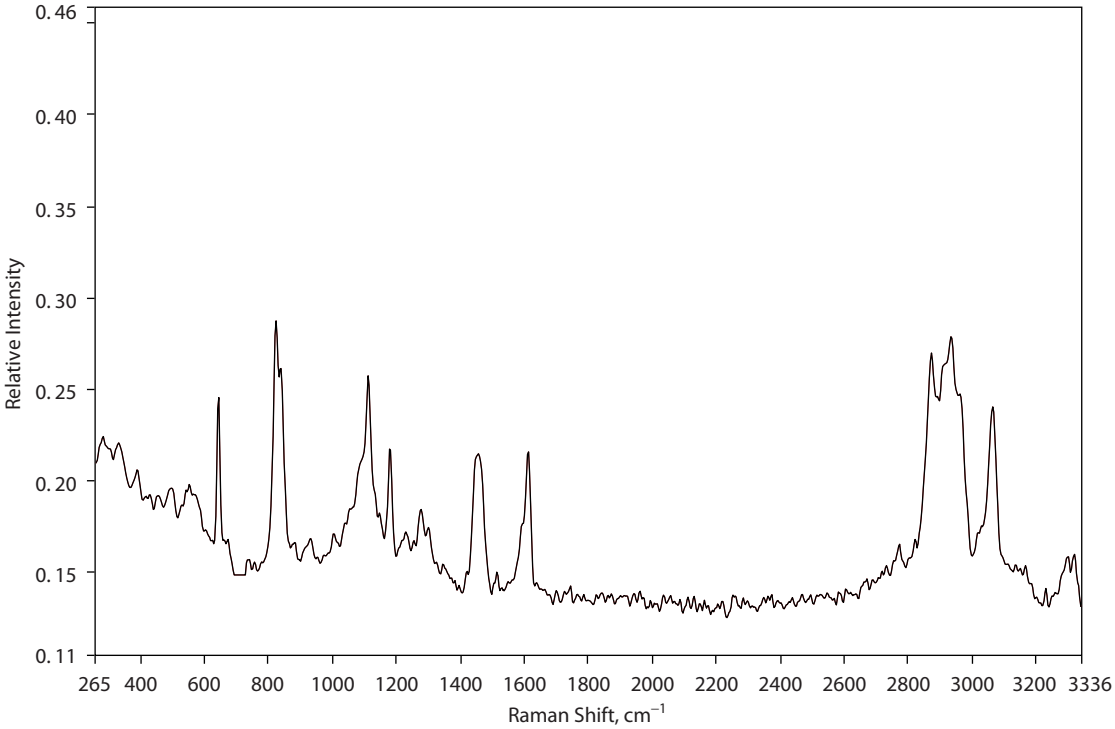

Figure J.9. Epoplex LS50 pB SRM 2244 corrected. This overall spectrum is typical for epoxy. Note aromatic C–H stretch at 3,100 cm^{-1}.

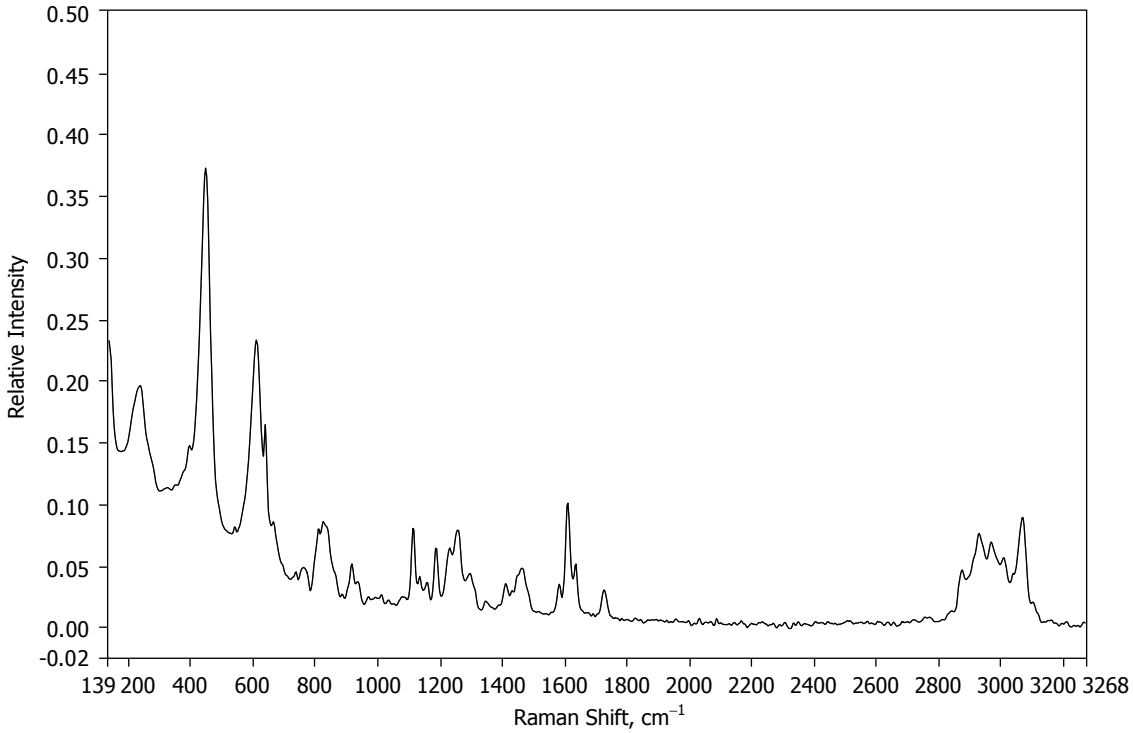

Figure J.10. Epoplex LS50 White SRM 2244 corrected. Note similarity to Aquaspar, although the epoxy may be interfering with the carbonate band.

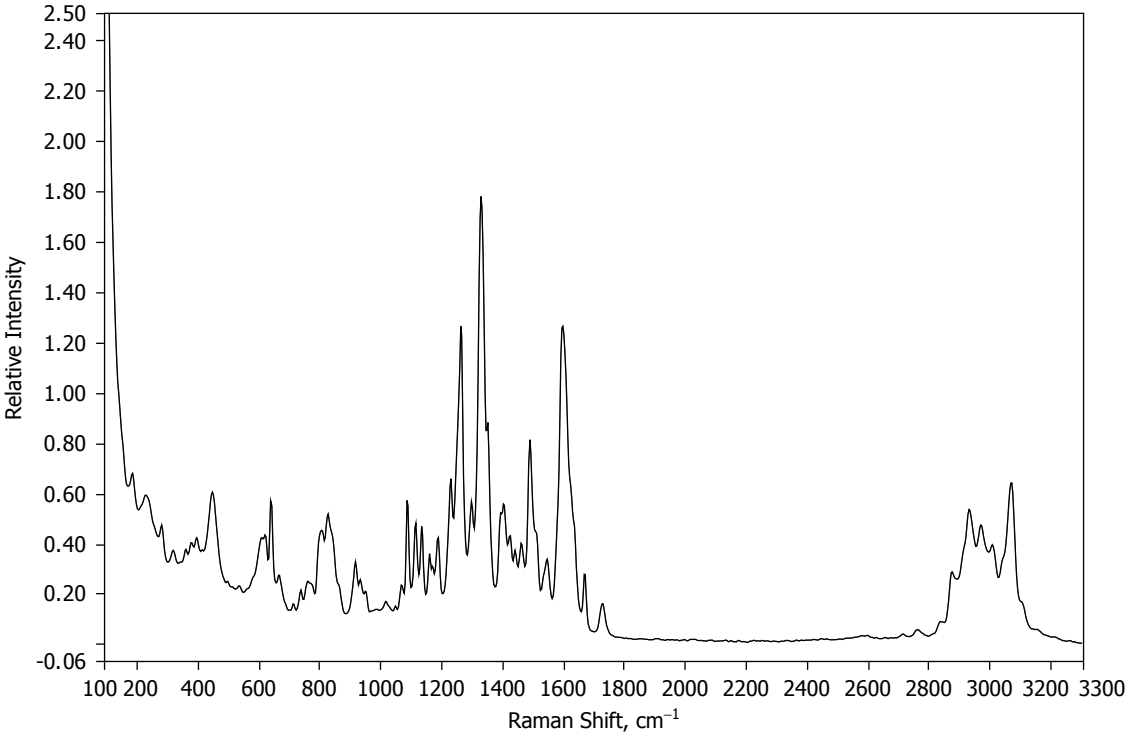

Figure J.11. Epoplex LSS Yellow SRM 2244 corrected. Note additional fine structure from the presence of the organic yellow dye.

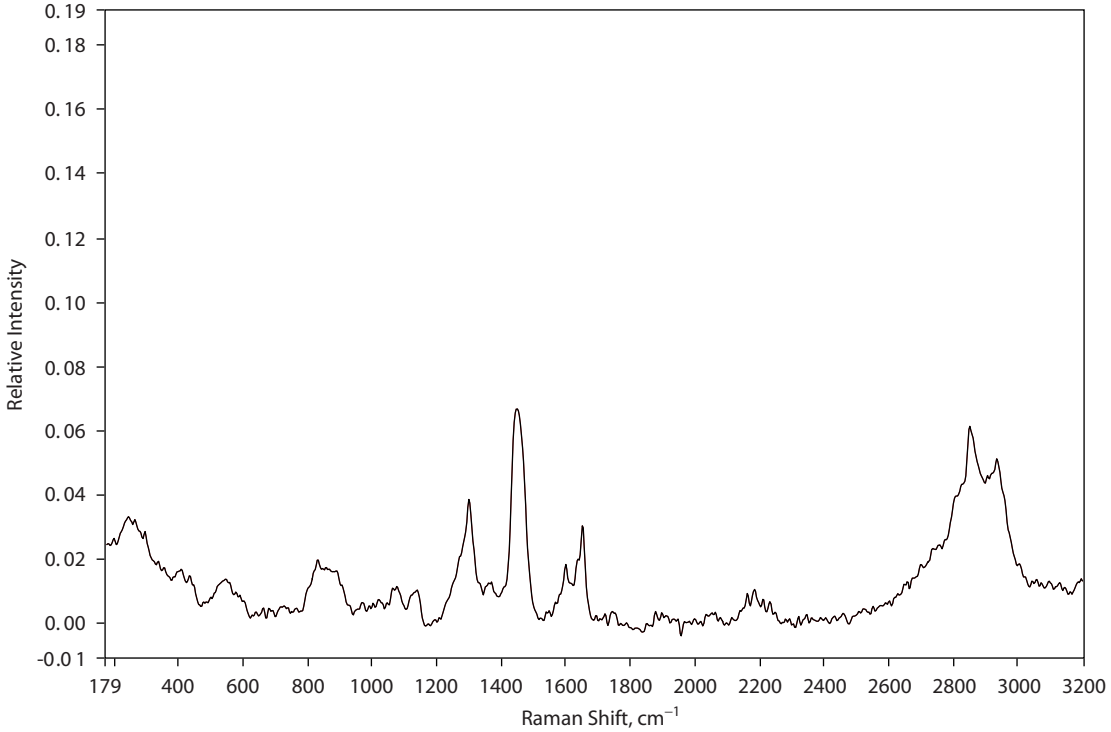

Figure J.12. Kling Beta 2700 SRM 2244 baseline corrected. Note amine C–H band at 1,300 cm⁻¹.

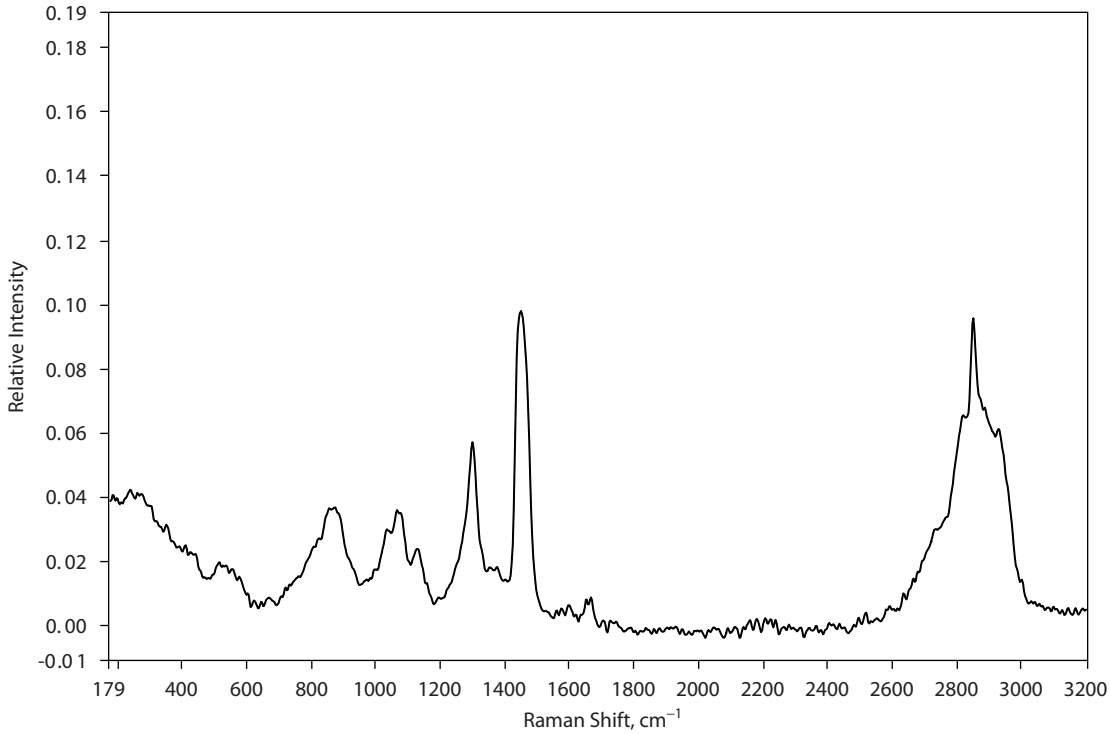

Figure J.13. Kling Beta 2912 SRM 2244 baseline corrected, similar to 2,700 cm⁻¹ with pronounced alkane stretch at 2,850 cm⁻¹.

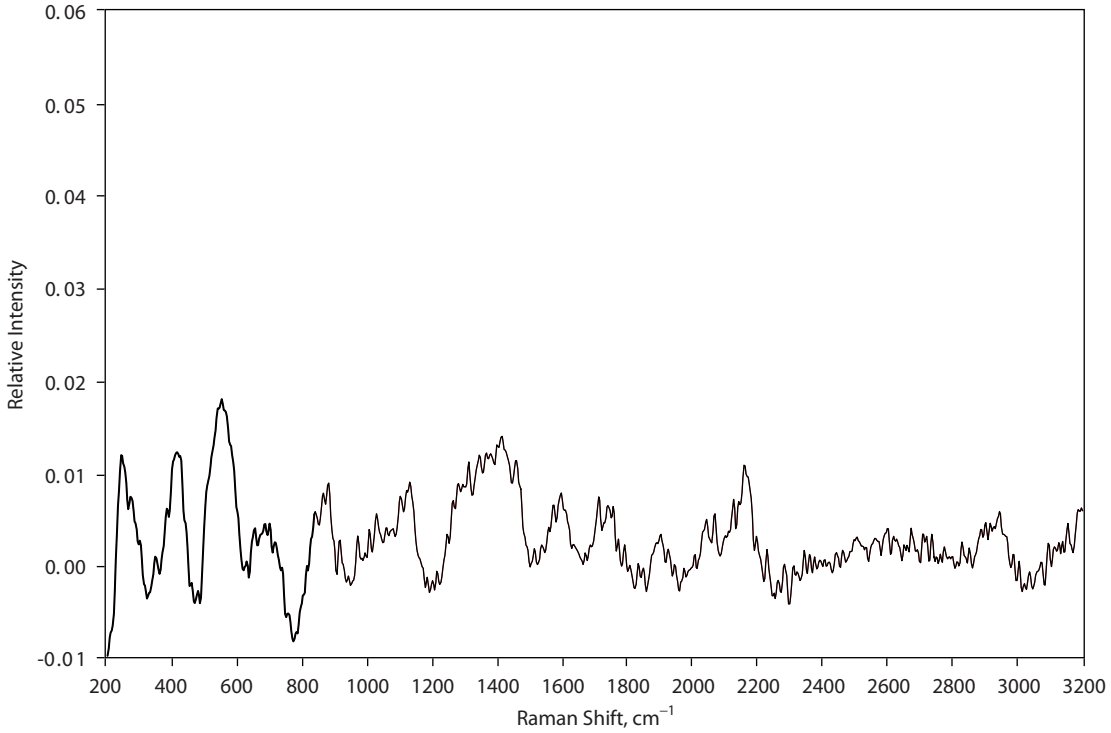

Figure J.14. Eucon Retarder 75 IL SRM 224 baseline corrected, with possible nitrile peak at 2,150 cm⁻¹.

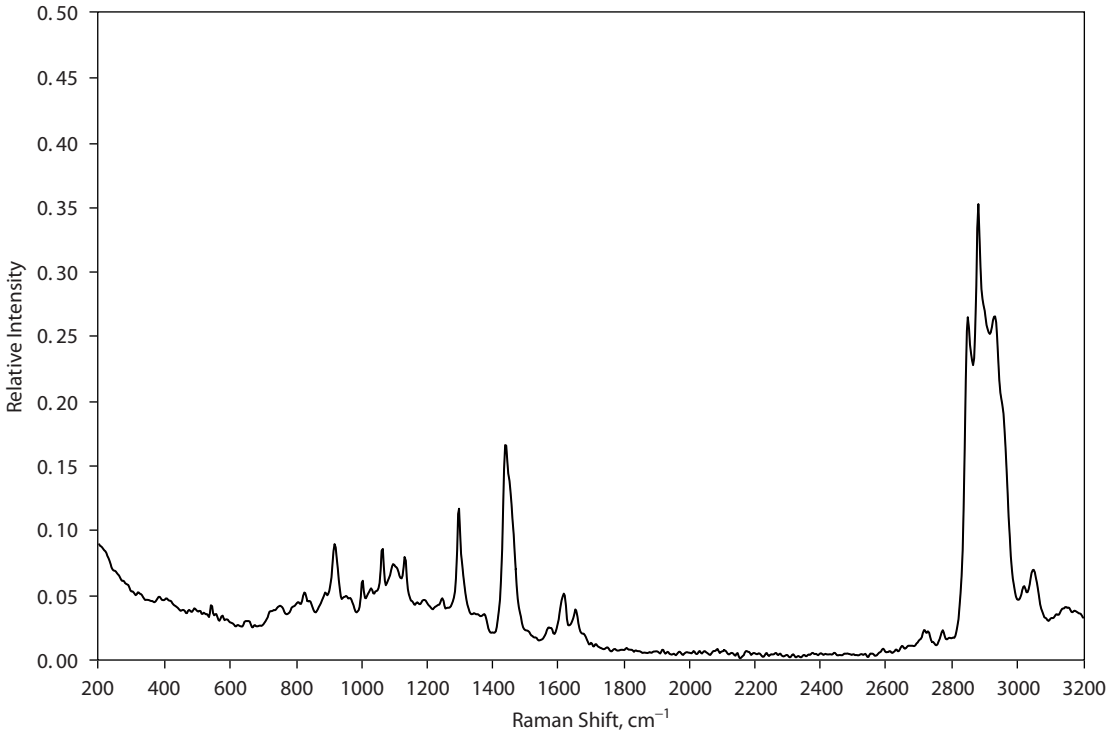

Figure J.15. Sealtight 1100 SRM 2244 corrected, a typical hydrocarbon spectrum.

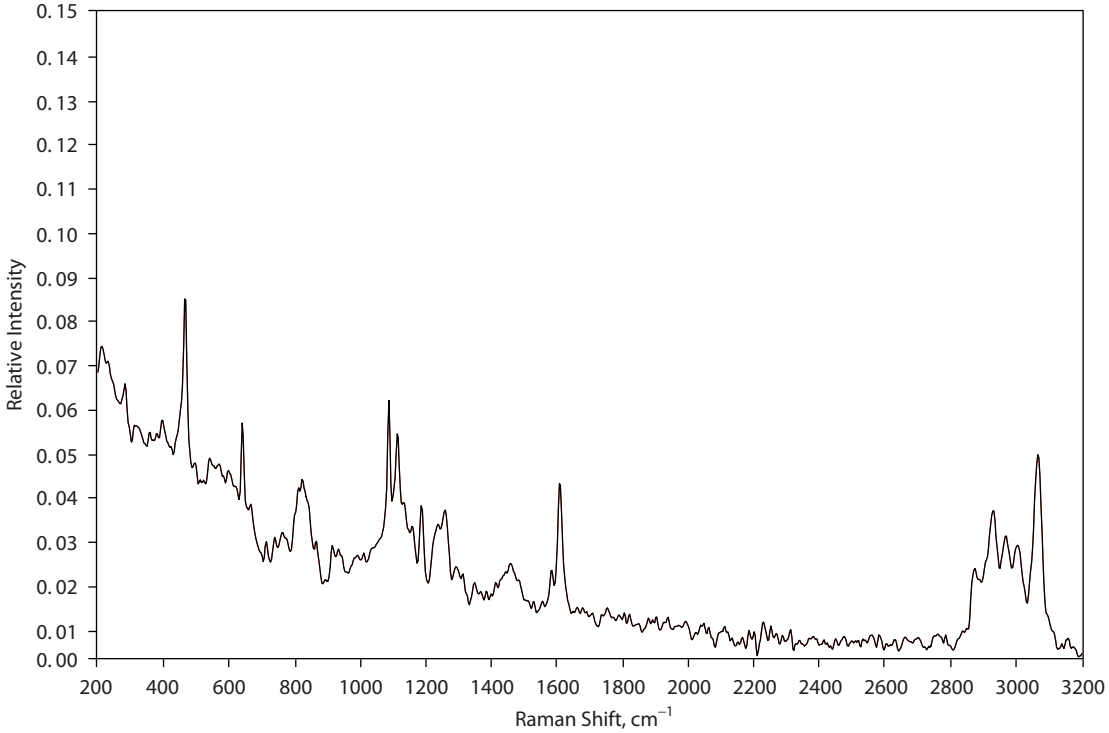

Figure J.16. Sikadur pA SRM 2244 corrected. Although a weak spectrum overall, numerous unique peaks are present, consistent with ceramics.

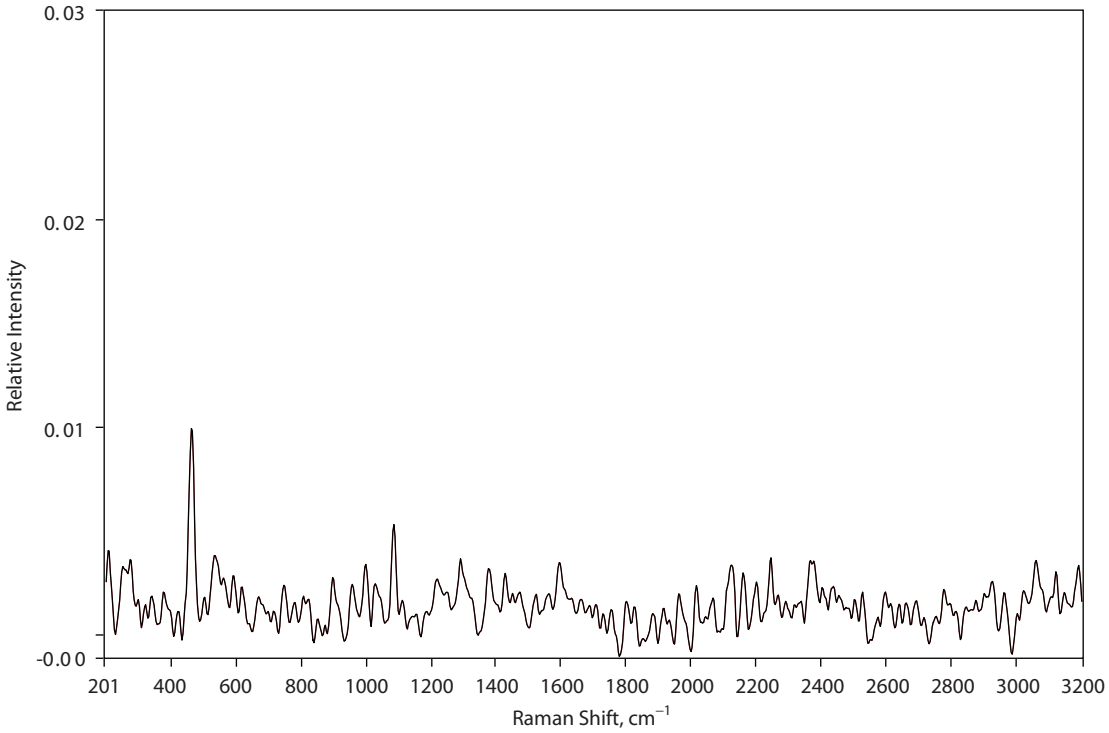

Figure J.17. Sikadur pB SRM 2244 corrected. Although weak, the peak at 450 cm^{-1} (potential oxide) is quite sharp.

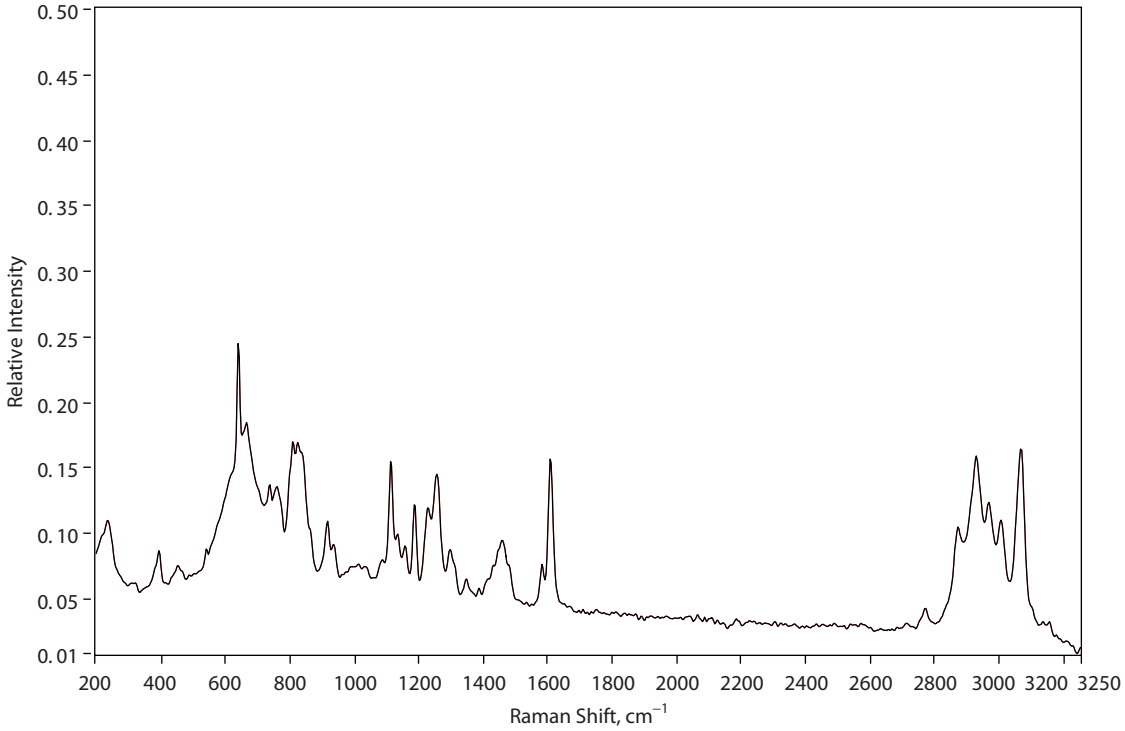

Figure J.18. Ultrabond 1100 pA SRM 2244 corrected, another typical epoxide spectrum.

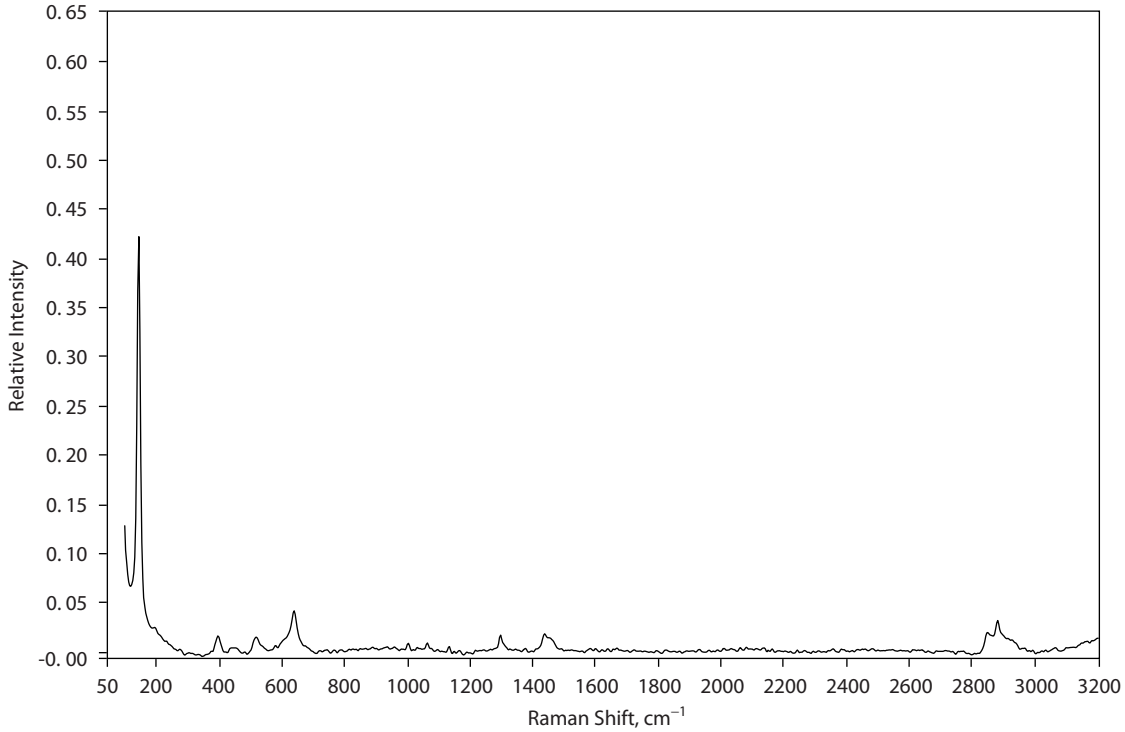

Figure J.19. Safe-Cure 1000 SRM fluorescence corrected. Note that the single low-frequency mode is typical for heavier elements.

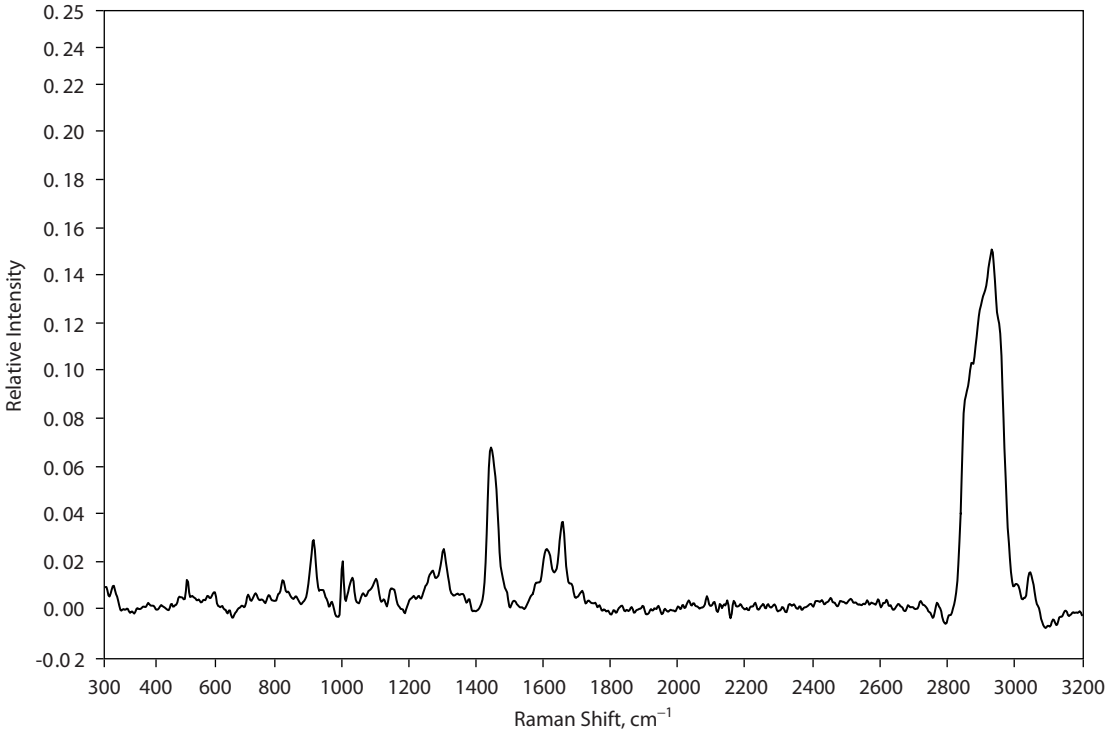

Figure J.20. Safe-Cure Clear SRM 2244 corrected, typical hydrocarbon with unique C–H stretch features (2,800 to 3,000 cm^{-1}).

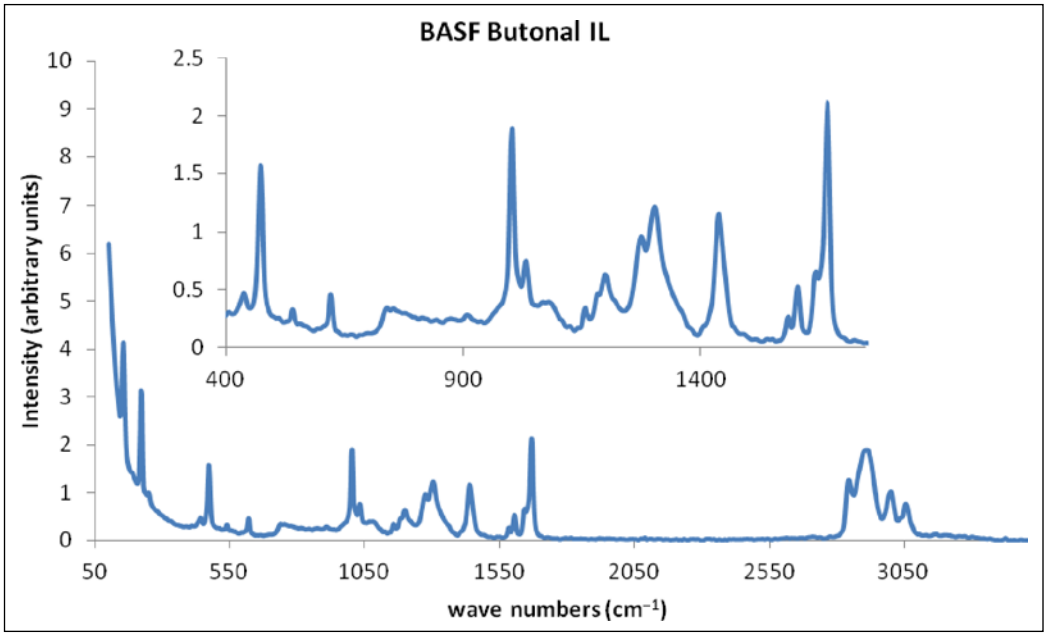

Figure J.21. Butonal NX1138 corrected Raman spectrum.

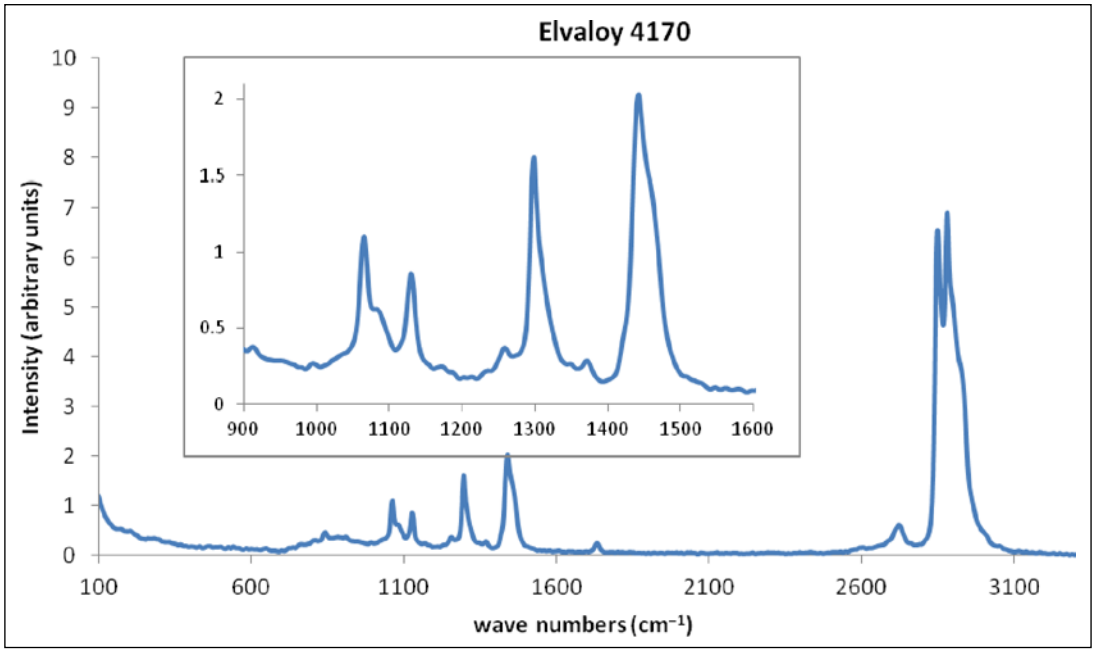

Figure J.22. Elvaloy 4170 corrected Raman spectrum.

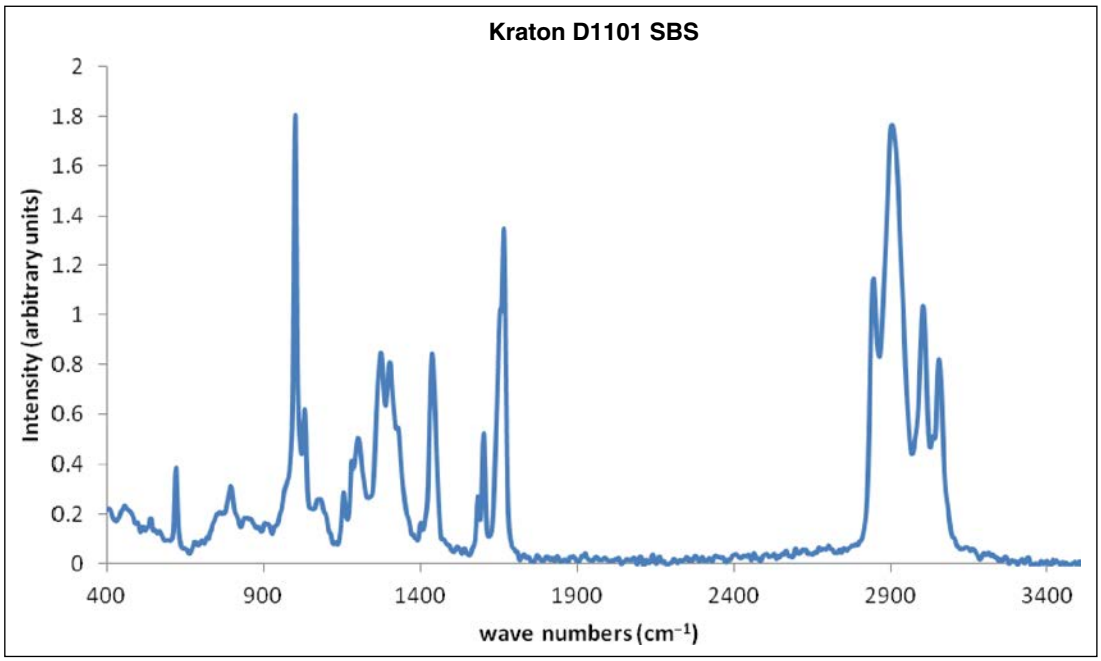

Figure J.23. Kraton D1101 SBS corrected Raman spectrum.

Table J.1. Summary of Laboratory Raman Testing Results

Material Category	Sample ID	Success (Yes/No)	Relative Signal Intensity	Wave Number Peak[b] (cm^{-1})	Noise (SD)	Signal-to-Noise Ratio
Structural coatings	Carbozinc 859 Part A	Yes	16.42	1,086.5	0.001	1,500
	Carbozinc 859 Part B	Yes	2.305	1,000	0.0125	209
	Carbozinc 859 Zinc Filler	Yes	1.195	1,110[a]	0.0116	8
	3M Scotchkote Part A	Yes	3.824	2,930	0.01160	351
	3M Scotchkote Part B	No	NA	NA	NA	NA
Pavement markings	3M All Weather HB-R1 White	Yes	25.33	1,090	0.00895	2,820
	Epoplex LS50 Part B	Yes	0.6963	824	0.00895	79.4
	Epoplex LS50 White	Yes	3.641	448	0.00717	508
	Epoplex LS50 Yellow	Yes	16.66	1,330	0.0216	989
Epoxy adhesives for concrete repair	Sikadur Part A	Yes	0.8661	465	0.00708	129
	Sikadur Part B	Yes	0.4408	465	0.00718	75.8
	Ultrabond 1100 Part A	Yes	1.864	640	0.101	75.9
	Ultrabond 1100 Part B	No	NA	NA	NA	NA
Portland cement	Lehigh cement	No	NA	NA	NA	NA
	Lafarge cement	No	NA	NA	NA	NA
Chemical admixtures for PCC	Accelguard 80	Yes	1.776	1,050	0.00945	188
	ADVA 190	Yes	0.2468	1,470	0.00749	33
	Air Mix 200	Yes	0.4061	1,650	0.00762	56
	Retarder 75	Yes	0.1408	3,230	0.00509	27.6
Curing compounds for PCC	Safe-Cure 1000	Yes	4.437	143	0.00792	561
	Safe-Cure clear	Yes	1.472	2,930	0.00751	196
	Sealtight 1100	Yes	1.518	1,440	0.00814	186
Polymer additives to asphalt binder	Elvaloy 4170	Yes	6.919	2,880	0.00899	782
	Kraton SBS	Yes	1.82	1,000	0.00758	240
	BASF Butonal II	Yes	2.126	1,670	0.00844	257
Neat asphalt binders	PG 58-28	No	NA	NA	NA	NA
	PG 64-22	No	NA	NA	NA	NA
Polymer-modified asphalt binders	PG 52-34 1.5% SBR Latex	No	NA	NA	NA	NA
	PG 64-28 3.3% SBR Latex	No	NA	NA	NA	NA
Asphalt emulsions	CRS-IP	No	NA	NA	NA	NA
	CRS-1	No	NA	NA	NA	NA
Antistripping agents for asphalt	AD-here LOF 65	Yes	2.421	1,470	0.00749	33
	Kling Beta 2700	Yes	0.9226	1,450	0.00673	147
	Kling Beta 2912	Yes	1.01	1,450	0.00787	133
Mineral aggregates	Stone aggregate	No	NA	NA	NA	NA

Note: NA = not available; PCC = portland cement concrete.

[a] Thermal emission.

[b] Not baseline adjusted.

Field Results

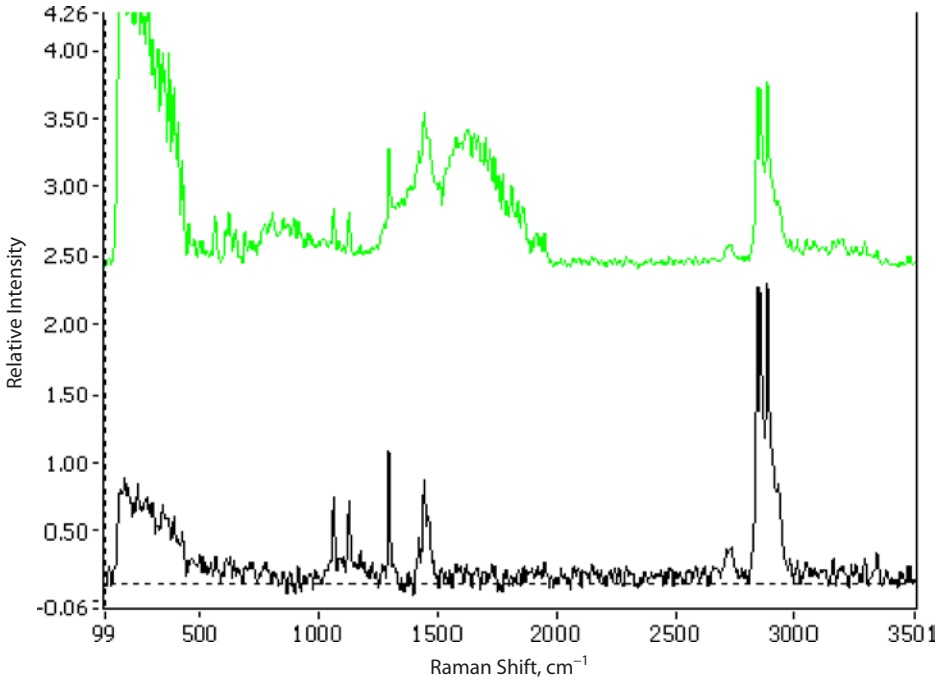

Figure J.24. (Top) Real-Time Analyzers' (RTA's) portable Raman analyzer. (Bottom) TAMMSCURE Raman spectrum recorded in the field (top green trace) showing contributions from ambient light (broad band from 1,400 to 2,000 cm⁻¹). The bottom trace shows the corrected spectrum calculated using RTA's Raman Vista advanced calculator and subtraction of background.

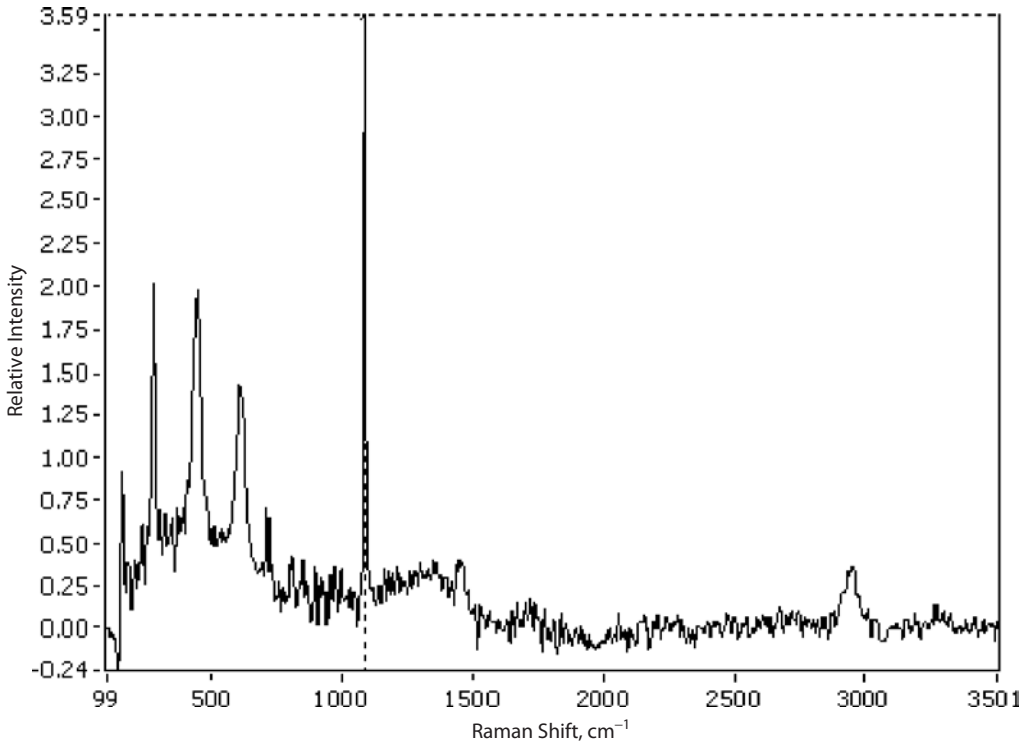

Figure J.25. White paint measured on glass corrected to remove fluorescence and ambient light contributions.

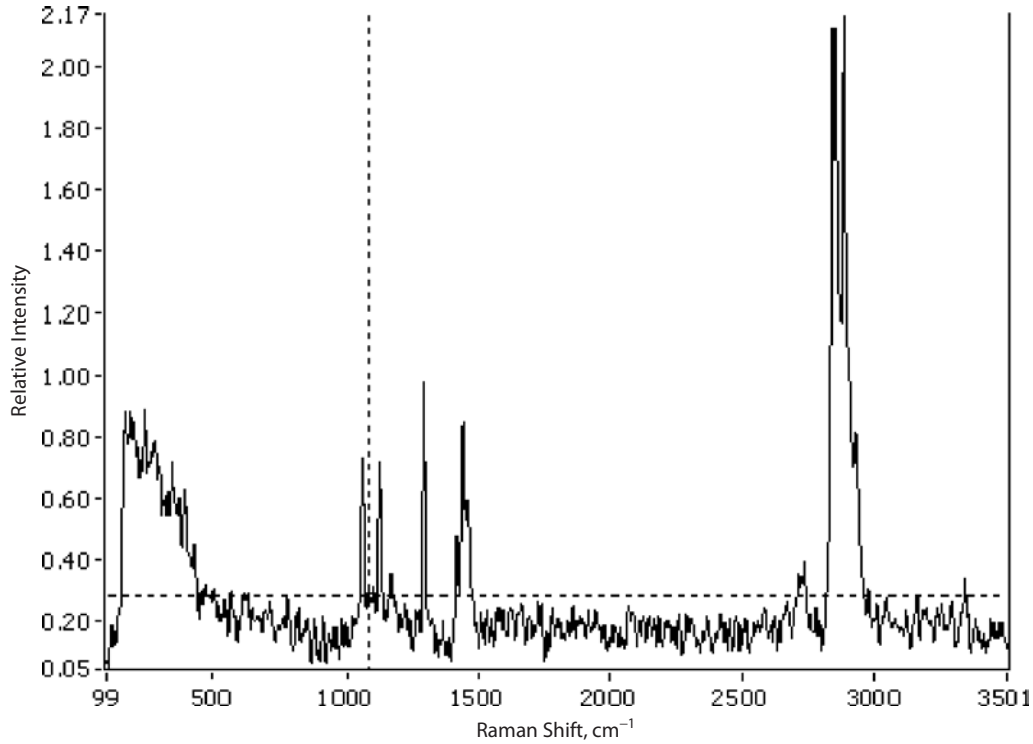

Figure J.26. Yellow paint measured on glass corrected to remove fluorescence and ambient light contributions.

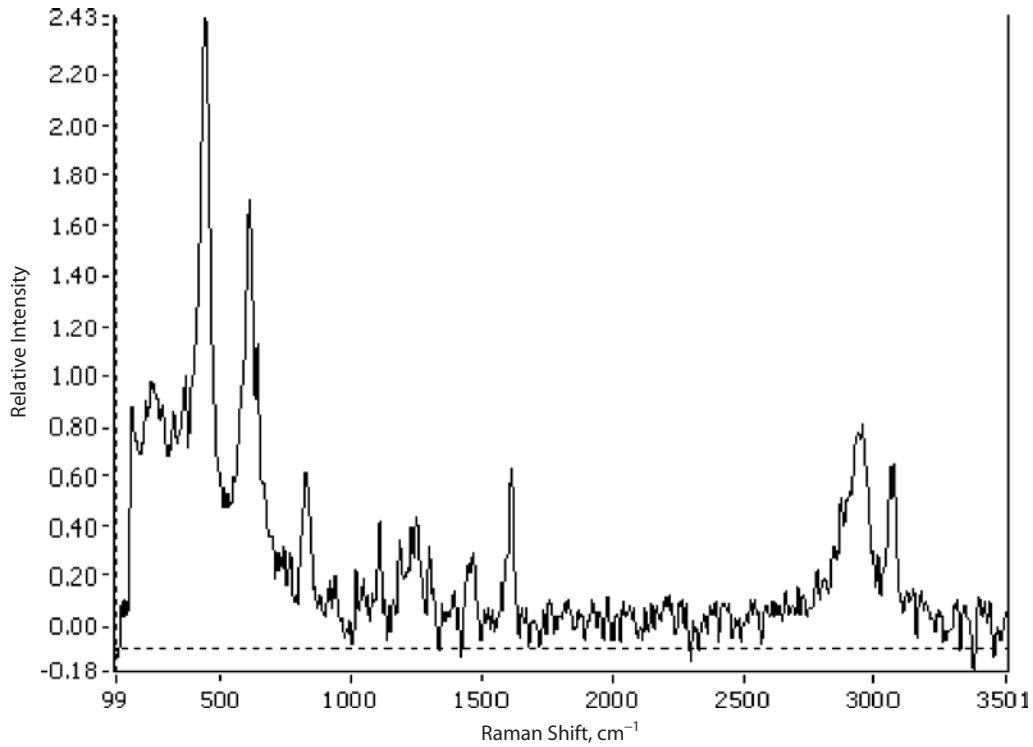

Figure J.27. White paint (old) corrected to remove fluorescence and ambient light contributions.

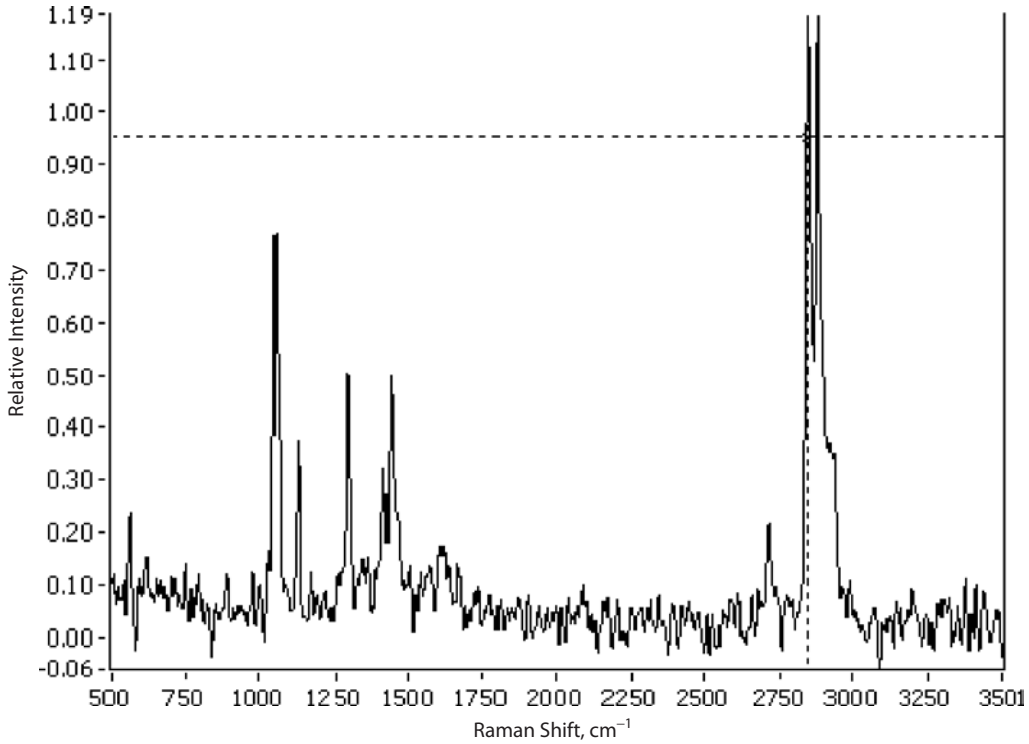

Figure J.28. A-80 spectrum averaged for three collections (12 equivalent scans, no background subtraction necessary).

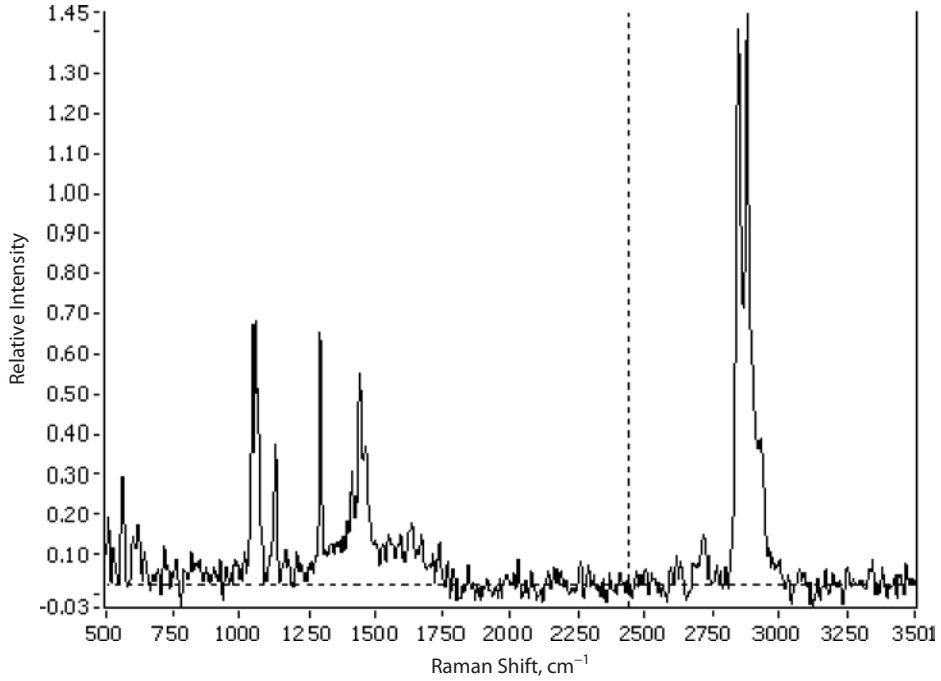

Figure J.29. Air 200 spectrum averaged for 20 scans (five spectra measured at four scans, no background subtraction necessary).

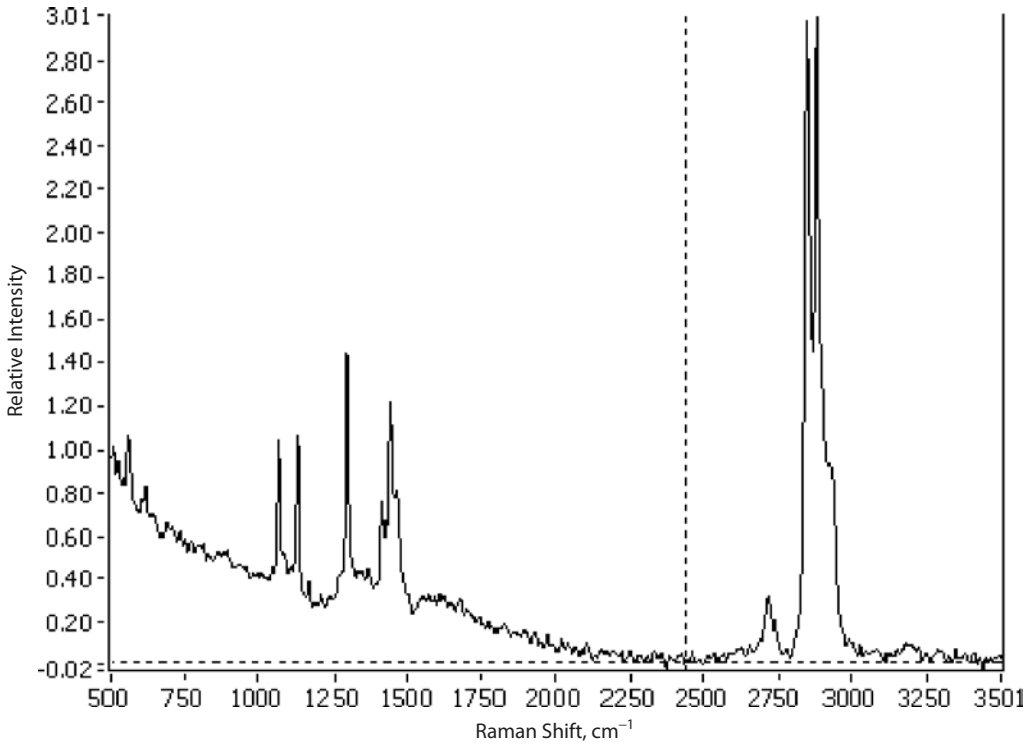

Figure J.30. R-75 spectrum averaged for 40 scans (10 spectra measured at four scans, no background subtraction necessary).

Table J.2. Field Raman Spectral Results and Signal-to-Noise Ratio Calculations

Material Category	Sample ID	Success (Yes/No)	Relative Signal Intensity	Wave Number Peak (cm^{-1})	Noise (SD)	Signal-to-Noise Ratio
Field-tested materials	White paint	Yes	4.00	1,086	0.0435	85
	Yellow paint	Yes	1.00	1,295	0.036	27
	TAMMSCURE	Yes	1.19	1,110	0.0116	8
	A-80	Yes	1.29	2,843	0.040	0.71
	Air 200	No	NA	NA	NA	NA
	R-75	No	NA	NA	NA	NA
	White paint strip (old)	Yes	2.43	443.4	0.058	46

Note: NA = not available.

APPENDIX K

XRF Data

Table K.1. X-Ray Fluorescence (XRF) Data for Carbozinc 859

Reading	P	S	Cl	K	Ca	Ti	Cr	Mn	Zn	Sr	Mo	I	Ba	Fe	Co
Carbozinc 1-1#	166,059 ± 23,928	54,732 ± 6,849	9,587 ± 1,726	14,940 ± 1,043	13,284 ± 736	1,673 ± 355	499 ± 45	1,009 ± 62	2,885,995 ± 108,934	82 ± 12	939 ± 42	1,253 ± 343	1,359 ± 118	45,224 ± 1,636	2,128 ± 626
Carbozinc 2-1#	146,466 ± 22,857	56,682 ± 6,843	9,895 ± 1,692	15,814 ± 1,050	12,979 ± 715	2,202 ± 365	556 ± 46	1,047 ± 63	2,628,019 ± 91,690	62 ± 11	926 ± 39	1,556 ± 350	1,314 ± 117	51,174 ± 1,810	2,383 ± 589
Carbozinc 2-2#	140,070 ± 22,680	60,740 ± 7,022	9,799 ± 1,690	16,722 ± 1,080	12,203 ± 690	1,800 ± 368	477 ± 44	1,043 ± 63	2,696,883 ± 97,454	76 ± 12	912 ± 40	1,944 ± 361	1,517 ± 123	50,483 ± 1,784	3,255 ± 620
Carbozinc 3-1#	197,098 ± 25,351	55,998 ± 6,930	9,434 ± 1,717	15,835 ± 1,071	12,281 ± 703	2,125 ± 373	529 ± 46	1,007 ± 63	2,808,377 ± 103,796	83 ± 13	988 ± 43	1,609 ± 356	1,373 ± 121	52,200 ± 1,879	2,785 ± 638
Carbozinc 3-2#	140,611 ± 22,934	64,049 ± 7,226	12,074 ± 1,769	16,370 ± 1,071	13,163 ± 722	2,039 ± 361	568 ± 47	1,061 ± 64	2,816,805 ± 104,304	48 ± 12	984 ± 43	1,266 ± 343	1,318 ± 117	51,825 ± 1,835	2,592 ± 637
Carbozinc 3-3#	176,390 ± 24,204	57,293 ± 6,871	7,272 ± 1,624	18,285 ± 1,141	12,510 ± 705	2,031 ± 361	533 ± 45	1064 ± 64	2,720,854 ± 96,669	53 ± 12	999 ± 42	1,953 ± 358	1,291 ± 116	49,941 ± 1,776	2,722 ± 607
Carbozinc 3-4#	142,800 ± 22,558	56,546 ± 6,784	9,539 ± 1,666	16,429 ± 1,063	13,354 ± 723	2,397 ± 370	578 ± 47	1,022 ± 62	2,685,529 ± 95,080	59 ± 12	982 ± 41	1,517 ± 351	1,346 ± 118	52,192 ± 1,830	2,611 ± 611
Carbozinc 3-5#	169,759 ± 23,535	49,537 ± 6,506	10,816 ± 1,713	15,828 ± 1,048	12,139 ± 685	1,910 ± 358	554 ± 46	1,000 ± 61	2,757,497 ± 100,693	63 ± 12	936 ± 41	1,674 ± 347	1,311 ± 116	51,542 ± 1,818	<LOD ± 1,839
Mean	159,907 ± 23,506	56,947 ± 6,879	9,802 ± 1,670	16,278 ± 1,071	12,739 ± 710	2,022 ± 364	537 ± 46	10,325 ± 63	2,749,995 ± 99,828	66 ± 12	958 ± 41	1,597 ± 351	1,354 ± 118	50,573 ± 1,796	2,639 ± 7,715
SD	20,802 ± 956	4,241 ± 205	1,355 ± 43	975 ± 31	510 ± 17	229 ± 6	35 ± 1	25 ± 1	83,776 ± 5,655	13 ± 0.5	33 ± 1	264 ± 7	71 ± 2	2,304 ± 72	351 ± 432

Note: LOD = limit of detection.

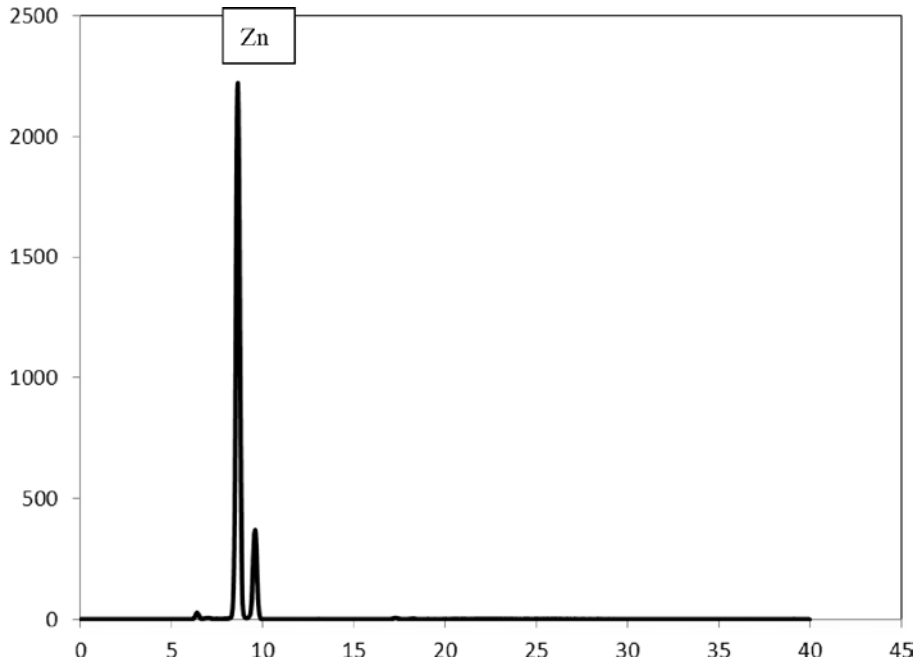

Figure K.1. XRF spectrum for Carbozinc 859.

Table K.2. XRF Data for Epoplex White

Reading	Ca	Ti	Zr	Ba
Epoplex White 1#	2,091 ± 126	322,067 ± 2,747	622 ± 4	3,776 ± 115
Epoplex White 2#	1,730 ± 124	314,771 ± 2,709	606 ± 4	3,757 ± 115
Epoplex White 3#	1,739 ± 126	317,454 ± 2,736	626 ± 4	3,745 ± 116
Epoplex White 4#	1,751 ± 126	322,173 ± 2,765	631 ± 4	3,772 ± 116
Epoplex White 5#	1,488 ± 126	318,065 ± 2,743	626 ± 4	3,602 ± 115
Epoplex White 6#	1,468 ± 124	314,469 ± 2,696	609 ± 4	3,585 ± 114
Epoplex White 7#	1,392 ± 125	319,508 ± 2,748	633 ± 4	3,541 ± 115
Epoplex White 8#	1,555 ± 125	321,046 ± 2,737	619 ± 4	3,696 ± 115
Epoplex White 9#	1,488 ± 126	321,437 ± 2,753	630 ± 4	3,755 ± 116
Epoplex White 10#	1,527 ± 124	319,176 ± 2,716	616 ± 4	3,709 ± 115
Mean	1,623 ± 125	319,017 ± 2,735	622 ± 4	3,694 ± 115
SD	2,082 ± 1	2,820 ± 22	9 ± 0	86 ± 0.6

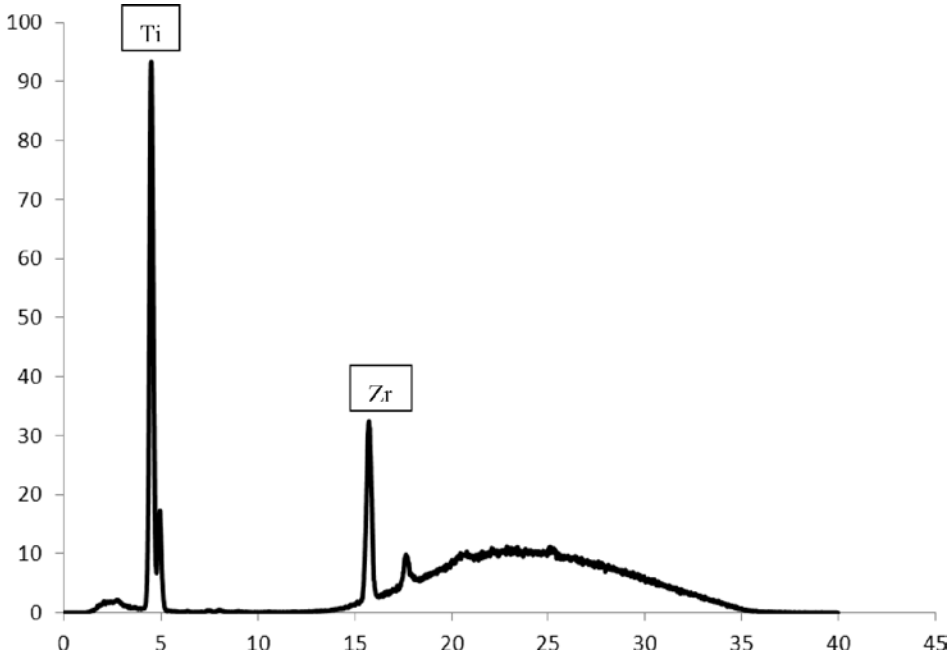

Figure K.2. XRF spectrum for Epoplex White.

Table K.3. XRF Data for Epoplex Yellow

Reading	Cl	K	Ca	Ti	Fe	Sr	Zr	Mo	Ba
Epoplex Yellow 1#	1,193 ± 203	352 ± 77	98,004 ± 691	38,973 ± 296	35 ± 3	36 ± 1	10 ± 1	12 ± 1	574 ± 31
Epoplex Yellow 2#	1,399 ± 205	284 ± 77	99,329 ± 700	39,103 ± 297	30 ± 3	35 ± 1	10 ± 1	13 ± 1	560 ± 31
Epoplex Yellow 3#	1,209 ± 207	246 ± 78	99,033 ± 709	38,788 ± 300	36 ± 3	35 ± 1	9 ± 1	12 ± 1	574 ± 31
Epoplex Yellow 4#	1,023 ± 204	606 ± 81	97,799 ± 698	38,770 ± 298	35 ± 3	36 ± 1	10 ± 1	13 ± 1	567 ± 31
Epoplex Yellow 5#	1,230 ± 202	357 ± 77	97,667 ± 689	38,462 ± 293	33 ± 3	34 ± 1	10 ± 1	13 ± 1	557 ± 31
Epoplex Yellow 6#	713 ± 200	254 ± 77	104,364 ± 729	39,849 ± 300	27 ± 3	34 ± 1	9 ± 1	11 ± 1	534 ± 31
Epoplex Yellow 7#	1,059 ± 203	358 ± 78	102,522 ± 718	39,504 ± 298	29 ± 3	35 ± 1	10 ± 1	12 ± 1	513 ± 31
Epoplex Yellow 8#	1,033 ± 203	344 ± 78	102,670 ± 718	39,618 ± 299	29 ± 3	34 ± 1	11 ± 1	12 ± 1	511 ± 31
Epoplex Yellow 9#	1,214 ± 209	266 ± 79	106,533 ± 753	40,082 ± 306	28 ± 3	34 ± 1	9 ± 1	8 ± 1	538 ± 31
Epoplex Yellow 10#	806 ± 200	244 ± 77	102,958 ± 719	39,095 ± 295	32 ± 3	34 ± 1	11 ± 1	11 ± 1	566 ± 31
Mean	1,088 ± 204	331 ± 78	101,088 ± 712	39,224 ± 298	31 ± 3	35 ± 1	10 ± 1	12 ± 1	549 ± 31
SD	207 ± 3	108 ± 1	3,123 ± 19	520 ± 4	3 ± 0	0.8 ± 0	0.7 ± 0	1.5 ± 0	24 ± 0.3

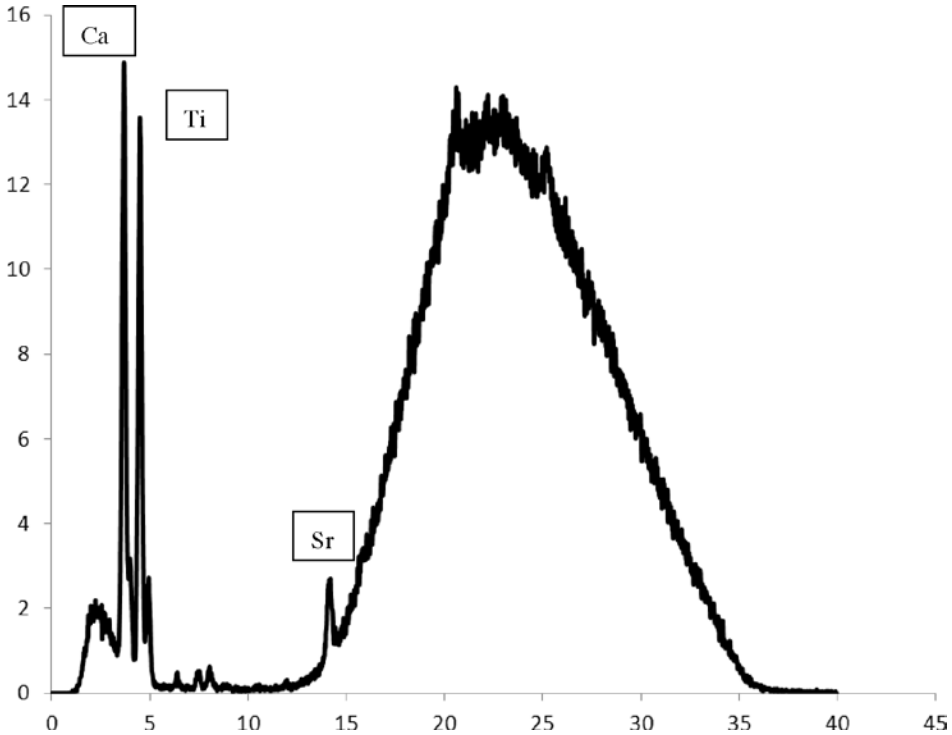

Figure K.3. XRF spectrum for Epoplex Yellow.

Table K.4. XRF Data for Lafarge Cement

Reading	S	K	Ca	Ti	Cr	Mn	Fe	Co	Ni	Cu	Zn	As	Se	Rb	Sr	Zr	Mo	I	Hg
Lafarge 1	41,985 ± 3,318	12,148 ± 420	781,235 ± 9,667	620 ± 105	57 ± 7	327 ± 12	15,700 ± 199	115 ± 38	68 ± 13	39 ± 7	98 ± 5	10 ± 2	4 ± 1	16 ± 1	645 ± 7	79 ± 3	7 ± 2	2,275 ± 493	<LOD
Lafarge 2	41,902 ± 3,355	12,798 ± 429	788,725 ± 9,807	640 ± 106	48 ± 7	308 ± 12	16,022 ± 204	155 ± 37	45 ± 12	27 ± 6	113 ± 5	8 ± 2	5 ± 1	16 ± 1	639 ± 7	73 ± 3	11 ± 2	2,772 ± 499	18 ± 4
Lafarge 3	44,072 ± 3,349	12,658 ± 425	784,434 ± 9,695	740 ± 107	57 ± 7	293 ± 11	15,810 ± 200	152 ± 38	54 ± 12	47 ± 7	125 ± 6	7 ± 2	6 ± 1	18 ± 1	640 ± 7	76 ± 3	9 ± 2	2,336 ± 494	18 ± 4
Lafarge 4	38,552 ± 3,237	12,684 ± 419	764,639 ± 9,381	437 ± 104	50 ± 7	328 ± 12	15,623 ± 196	169 ± 38	60 ± 13	37 ± 7	108 ± 5	9 ± 2	5 ± 1	17 ± 1	629 ± 7	74 ± 3	11 ± 2	3,239 ± 487	15 ± 4
Lafarge 5	40,068 ± 3,321	12,079 ± 422	772,236 ± 9,665	740 ± 107	46 ± 7	319 ± 12	15,678 ± 201	153 ± 38	42 ± 12	36 ± 7	106 ± 5	7 ± 2	<LOD	17 ± 1	632 ± 7	79 ± 3	10 ± 2	2,445 ± 496	12 ± 4
Lafarge 7	42,795 ± 3,370	12,435 ± 428	767,523 ± 9,670	784 ± 107	42 ± 7	325 ± 12	15,627 ± 202	155 ± 38	46 ± 12	49 ± 7	103 ± 5	<LOD	3 ± 1	15 ± 1	631 ± 7	78 ± 3	10 ± 2	1,876 ± 495	16 ± 4
Lafarge 8	44,384 ± 3,409	12,998 ± 435	781,059 ± 9,826	624 ± 107	52 ± 7	314 ± 12	15,732 ± 203	<LOD	61 ± 13	45 ± 7	108 ± 5	7 ± 2	7 ± 1	16 ± 1	635 ± 7	72 ± 3	13 ± 2	3,359 ± 503	13 ± 4
Lafarge 9	48,107 ± 3,483	12,290 ± 431	790,632 ± 10,002	662 ± 108	53 ± 7	315 ± 12	16,036 ± 208	117 ± 38	70 ± 13	35 ± 7	114 ± 6	<LOD	4 ± 1	16 ± 1	649 ± 7	72 ± 3	11 ± 2	3,078 ± 508	16 ± 4
Lafarge 10	46,344 ± 3,394	12,600 ± 427	766,286 ± 9,585	654 ± 106	44 ± 7	302 ± 12	15,444 ± 198	<LOD	59 ± 12	44 ± 7	111 ± 5	9 ± 2	5 ± 1	15 ± 1	639 ± 7	73 ± 3	11 ± 2	2,398 ± 494	12 ± 4
Lafarge 11	48,247 ± 3,392	12,033 ± 417	767,323 ± 9,504	590 ± 105	56 ± 7	315 ± 12	15,542 ± 197	<LOD	71 ± 13	45 ± 7	112 ± 5	7 ± 2	6 ± 1	16 ± 1	632 ± 7	75 ± 3	7 ± 2	3,161 ± 492	15 ± 4
Mean	43,645. 6 ± 3,362.8	12,472 ± 425	776,409 ± 9,680	649 ± 106	51 ± 7	315 ± 12	15,721 ± 201	145 ± 60	58 ± 13	40 ± 7	110 ± 5	8 ± 3	5 ± 1	16 ± 1	637 ± 7	75 ± 3	10 ± 2	2,694 ± 496	15 ± 4
SD	3,238 ± 65	328 ± 6	9,906 ± 174	97 ± 1	5 ± 0	11 ± 0.3	191 ± 3.6	21 ± 36	10.6 ± 0.5	6.8 ± 0.3	7 ± 0.4	1 ± 2	1 ± 0.6	0.9 ± 0	6.5 ± 0	2.8 ± 0	1.9 ± 0	498 ± 6	2.3 ± 0

Note: LOD = limit of detection.

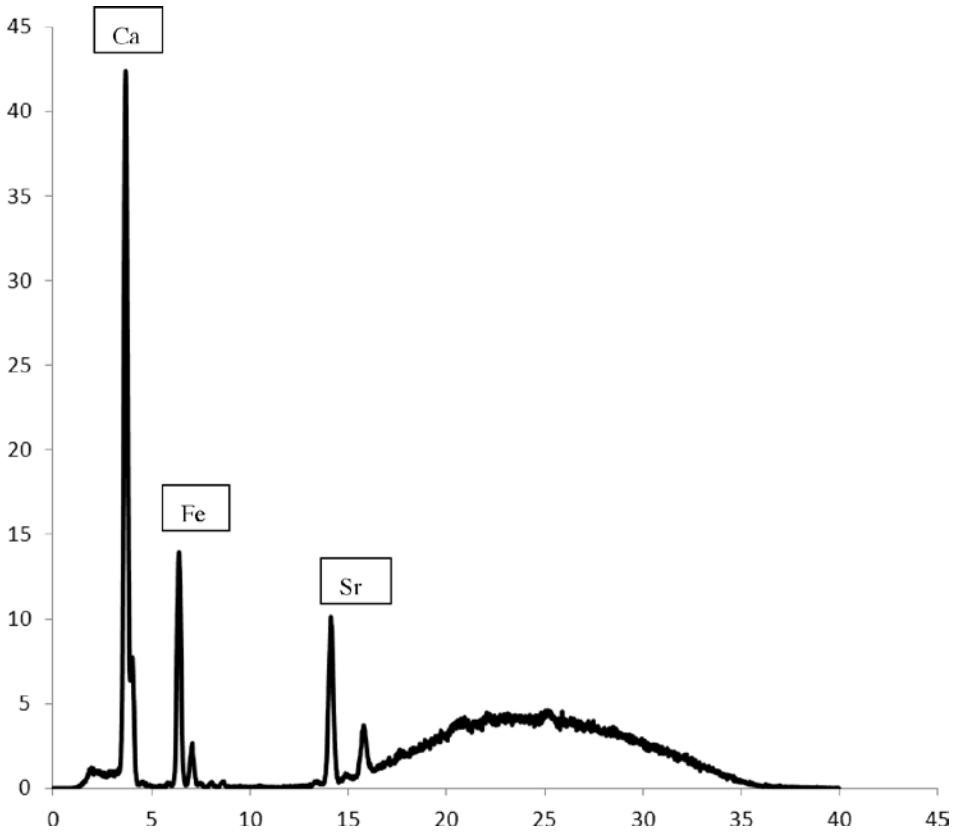

Figure K.4. XRF spectrum for Lafarge cement.

Table K.5. XRF Data for Lehigh Cement

Reading	S	K	Ca	Ti	Cr	Mn	Fe	Co	Ni	Cu	Zn	Se	Rb	Sr	Zr	I	Ba
Lehigh cement 1	42,920 ± 3,378	23,470 ± 545	764,145 ± 9,616	1,187 ± 117	23 ± 7	286 ± 12	15,585 ± 201	194 ± 39	42 ± 13	38 ± 7	46 ± 4	6 ± 1	38 ± 2	1,864 ± 17	73 ± 3	3,070 ± 498	214 ± 23
Lehigh cement 2	43,473 ± 3,360	22,265 ± 526	767,588 ± 9,556	888 ± 115	32 ± 7	277 ± 11	15,650 ± 200	146 ± 38	39 ± 13	36 ± 7	40 ± 4	<LOD	40 ± 2	1,858 ± 17	73 ± 3	4,254 ± 498	206 ± 23
Lehigh cement 3	41,915 ± 3,337	22,770 ± 533	760,344 ± 9,513	918 ± 116	<LOD	255 ± 11	15,373 ± 197	135 ± 38	41 ± 13	21 ± 7	42 ± 4	5 ± 1	40 ± 2	1,830 ± 17	71 ± 3	3,369 ± 495	265 ± 23
Lehigh cement 4	44,384 ± 3,328	22,553 ± 525	746,943 ± 9,248	722 ± 113	34 ± 7	252 ± 11	15,297 ± 194	<LOD	38 ± 12	22 ± 7	41 ± 4	6 ± 1	37 ± 2	1,815 ± 17	68 ± 3	4,584 ± 491	218 ± 22
Lehigh cement 5	39,755 ± 3,274	23,060 ± 532	745,056 ± 9,274	1,210 ± 114	22 ± 7	242 ± 11	15,140 ± 193	187 ± 39	<LOD	45 ± 7	53 ± 4	5 ± 1	39 ± 2	1,862 ± 17	74 ± 3	2,254 ± 485	228 ± 23
Lehigh cement 6	53,535 ± 3,445	23,272 ± 533	756,323 ± 9,360	1,353 ± 115	29 ± 7	249 ± 11	15,341 ± 195	151 ± 39	41 ± 13	34 ± 7	51 ± 4	6 ± 1	41 ± 2	1,859 ± 17	74 ± 3	1,936 ± 486	207 ± 22
Lehigh cement 7	46,616 ± 3,406	22,453 ± 531	761,928 ± 9,552	1,230 ± 116	28 ± 7	283 ± 11	15,461 ± 199	<LOD	49 ± 20	29 ± 7	46 ± 4	3 ± 1	41 ± 2	1,857 ± 17	74 ± 3	2,047 ± 493	237 ± 23
Lehigh cement 8	44,407 ± 3329	21,811 ± 517	742,662 ± 9,218	1,274 ± 114	30 ± 7	259 ± 11	15,124 ± 192	184 ± 39	<LOD	31 ± 7	46 ± 4	4 ± 1	40 ± 2	1,867 ± 17	72 ± 3	2,321 ± 484	209 ± 22
Lehigh cement 9	39,109 ± 3304	22,713 ± 533	756,683 ± 9,475	1,196 ± 116	33 ± 7	268 ± 11	15,472 ± 198	149 ± 38	<LOD	24 ± 7	50 ± 4	7 ± 1	38 ± 2	1,840 ± 17	67 ± 3	2,469 ± 492	220 ± 23
Lehigh cement 10	45,207 ± 3438	25,147 ± 566	783,918 ± 9,883	1,047 ± 118	29 ± 7	280 ± 12	15,925 ± 206	134 ± 39	42 ± 13	26 ± 7	45 ± 4	5 ± 1	38 ± 2	1,886 ± 17	70 ± 3	2,290 ± 504	291 ± 24
Mean	44,132 ± 3,360	22,951 ± 534	758,559 ± 9,470	1,103 ± 115	29 ± 7	265 ± 11	15,437 ± 198	160 ± 38	42 ± 20	31 ± 7	46 ± 4	5 ± 1	39.2 ± 2	1,854 ± 17	72 ± 6	2,859 ± 493	230 ± 23
SD	4,043 ± 57	911 ± 13	12,242 ± 203	201 ± 1.5	4 ± 0	15.8 ± 0.4	242 ± 4	24 ± 0	3.5 ± 0	7.7 ± 0	4 ± 0	1.2 ± 0	1.42 ± 0	20 ± 0	2.5 ± 0	935 ± 6.4	28 ± 0.6

Note: LOD = limit of detection.

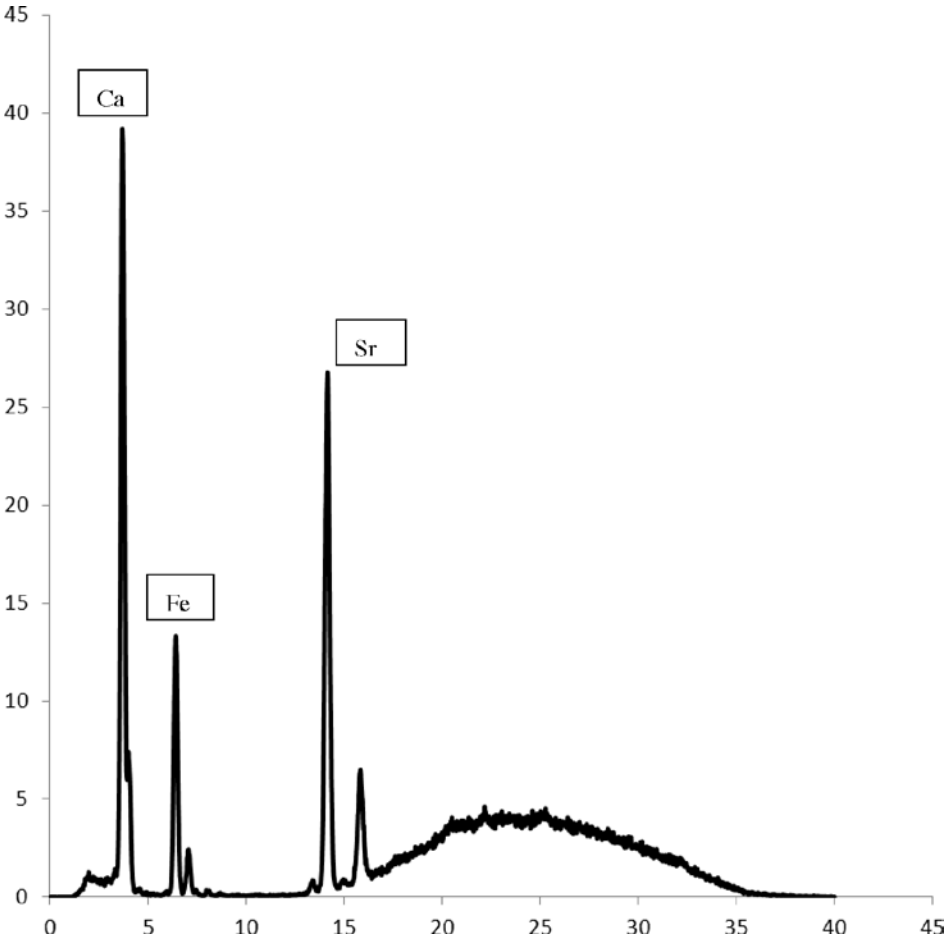

Figure K.5. XRF spectrum for Lehigh cement.

Table K.6. XRF Data for Sand Aggregate

Reading	K	Ca	Ti	Cr	Mn	Fe	Co	Zn	Rb	Sr	Zr	Ba	Pb
Sand 1#	16,956 ± 272	11,239 ± 170	1,732 ± 61	26 ± 5	473 ± 10	17,110 ± 157	<LOD	30 ± 3	55 ± 1	182 ± 2	145 ± 2	212 ± 16	17 ± 2
Sand 2#	8,528 ± 207	23,249 ± 302	2,881 ± 84	30 ± 6	933 ± 16	33,035 ± 324	193 ± 49	32 ± 3	29 ± 1	184 ± 2	305 ± 3	192 ± 20	15 ± 2
Sand 3#	13,163 ± 244	8,612 ± 151	1,131 ± 60	31 ± 6	591 ± 12	27,295 ± 258	148 ± 39	32 ± 3	45 ± 1	214 ± 2	62 ± 2	195 ± 17	15 ± 2
Sand 4#	8,745 ± 205	15,310 ± 220	2,771 ± 81	35 ± 6	1,461 ± 21	34,968 ± 337	<LOD	42 ± 3	28 ± 1	179 ± 2	77 ± 2	184 ± 20	12 ± 2
Sand 5#	9,317 ± 212	23,739 ± 303	4,394 ± 99	37 ± 6	979 ± 16	31,065 ± 300	301 ± 45	27 ± 3	27 ± 1	190 ± 2	192 ± 2	238 ± 22	9 ± 2
Sand 6#	11,134 ± 226	18,984 ± 251	3,757 ± 89	33 ± 6	1,040 ± 16	29,787 ± 282	217 ± 42	25 ± 3	37 ± 1	177 ± 2	74 ± 2	221 ± 20	15 ± 2
Mean	11,307 ± 228	16,856 ± 233	2,778 ± 79	32 ± 6	913 ± 15	28,877 ± 276	215 ± 43	31 ± 3	37 ± 1	188 ± 2	143 ± 2	207 ± 19	14 ± 2
SD	3,275 ± 26	6,240 ± 65	1,216 ± 16	4 ± 0.4	352 ± 3.8	6,340 ± 65	64 ± 10	6 ± 0	11 ± 0	13.7 ± 0	94 ± 0.4	20 ± 2	2.9 ± 0

Note: LOD = limit of detection.

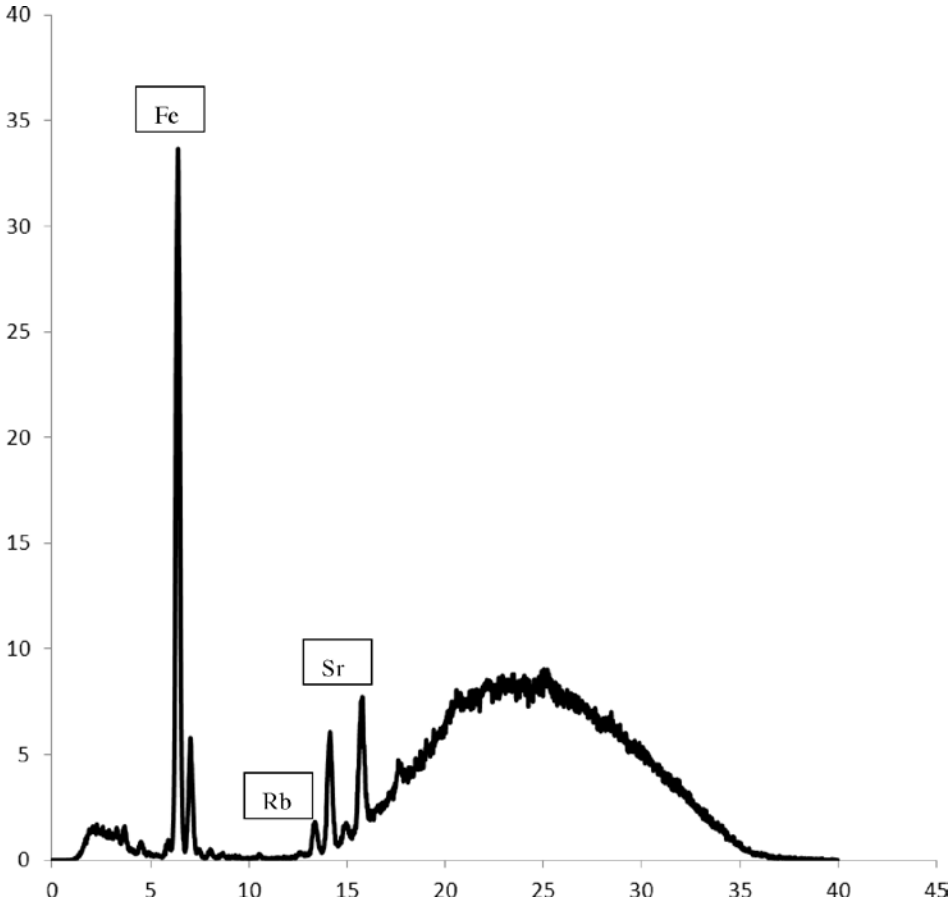

Figure K.6. XRF spectrum for sand aggregate.

Table K.7. XRF Data for Stone Aggregate

Reading	K	Ca	Ti	Cr	Mn	Fe	Ni	Zn	Rb	Sr	Zr	Ba	Pb
Stone 1#	17,410 ± 325	16,749 ± 257	4,363 ± 105	56 ± 7	259 ± 10	19,340 ± 207	75 ± 10	33 ± 3	69 ± 1	121 ± 2	224 ± 3	285 ± 23	8 ± 2
Stone 2#	26,295 ± 422	9,782 ± 185	3,768 ± 99	41 ± 7	336 ± 11	23,522 ± 251	46 ± 10	46 ± 3	117 ± 2	199 ± 3	343 ± 3	293 ± 23	7 ± 2
Stone 3#	20,854 ± 485	59,757 ± 926	2,830 ± 133	42 ± 11	884 ± 23	51,288 ± 710	<LOD	51 ± 4	54 ± 2	284 ± 4	46 ± 2	544 ± 36	<LOD
Stone 5#	16,765 ± 290	10,996 ± 180	3,493 ± 85	29 ± 5	166 ± 7	12,571 ± 126	27 ± 8	23 ± 2	38 ± 1	227 ± 3	222 ± 3	246 ± 19	9 ± 2
Stone 6#	14,063 ± 276	20,480 ± 285	3,002 ± 84	28 ± 6	354 ± 10	18,143 ± 187	29 ± 9	29 ± 3	33 ± 1	307 ± 3	112 ± 2	210 ± 19	6 ± 2
Stone 7#	14,556 ± 274	26,061 ± 332	3,916 ± 100	99 ± 8	1,048 ± 18	42,451 ± 416	61 ± 11	67 ± 4	26 ± 1	163 ± 2	238 ± 3	323 ± 24	9 ± 2
Mean	17,867 ± 331	22,087 ± 332	3,138 ± 92	44 ± 7	446 ± 12	24,483 ± 277	47.6 ± 9	37 ± 3	53 ± 1	219 ± 3	172 ± 2.4	297 ± 22	7.8 ± 2
SD	4,365 ± 89	17,645 ± 270	1,238 ± 28	27 ± 2	370 ± 6	16,671 ± 224	20 ± 1	20 ± 0.8	32 ± 0.5	65 ± 0.8	117 ± 0.8	120 ± 7.5	1.30384 ± 0

Note: LOD = limit of detection.

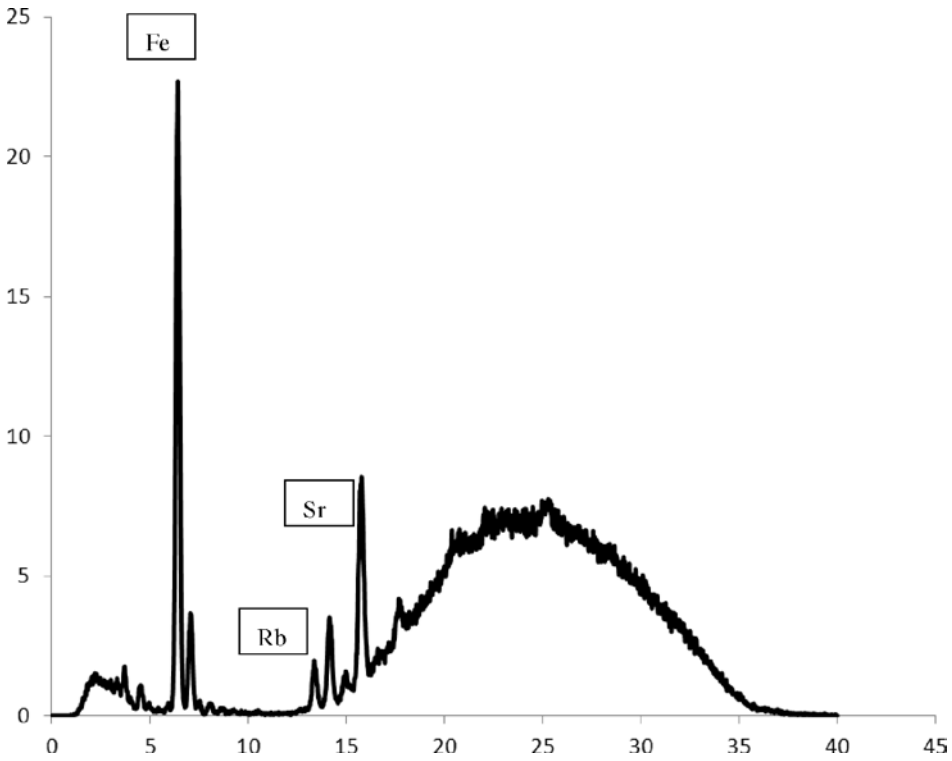

Figure K.7. XRF spectrum for stone aggregate.

Table K.8. XRF Data for Scotchkote

Reading	K	Ca	Ti	Fe	Co	Cu	Sr	Zr	Mo	Ba
Scotchkote 20-1#	484 ± 109	134,115 ± 1,096	62,209 ± 530	11,206 ± 90	86 ± 18	53 ± 4	34 ± 1	7 ± 1	6 ± 1	883 ± 47
Scotchkote 20-2#	<LOD	137,183 ± 1,114	63,812 ± 540	11,372 ± 91	59 ± 18	52 ± 4	34 ± 1	7 ± 1	4 ± 1	829 ± 47
Scotchkote 20-3#	<LOD	137,684 ± 1,134	63,627 ± 546	11,402 ± 93	93 ± 18	44 ± 4	34 ± 1	7 ± 1	6 ± 1	887 ± 47
Scotchkote 20-4#	<LOD	133,303 ± 1,082	61,642 ± 522	10,999 ± 88	86 ± 18	41 ± 4	34 ± 1	7 ± 1	4 ± 1	835 ± 46
Scotchkote 20-5#	417 ± 109	138,639 ± 1,129	64,091 ± 543	11,405 ± 92	76 ± 18	54 ± 4	32 ± 1	7 ± 1	7 ± 1	854 ± 47
Scotchkote 10-1#	529 ± 109	136,325 ± 1,111	62,860 ± 534	11,242 ± 91	<LOD	47 ± 4	34 ± 1	7 ± 1	5 ± 1	884 ± 47
Scotchkote 10-2#	388 ± 106	134,688 ± 1,085	62,232 ± 523	11,160 ± 89	56 ± 18	47 ± 4	34 ± 1	6 ± 1	5 ± 1	934 ± 46
Scotchkote 10-3#	646 ± 110	136,432 ± 1,107	63,546 ± 537	11,226 ± 90	71 ± 18	50 ± 4	35 ± 1	6 ± 1	<LOD	820 ± 46
Scotchkote 5-1#	444 ± 111	141,321 ± 1,160	65,039 ± 556	11,631 ± 94	110 ± 18	45 ± 4	34 ± 1	7 ± 1	7 ± 1	932 ± 48
Scotchkote 5-2#	606 ± 110	137,357 ± 1,113	63,574 ± 537	11,252 ± 90	62 ± 18	48 ± 4	37 ± 1	8 ± 1	9 ± 1	816 ± 46
Mean	502 ± 109	136,705 ± 1,113	63,263 ± 537	11,290 ± 91	78 ± 18	48 ± 4	34 ± 1	6.9 ± 1	5.9 ± 1	867 ± 47
SD	97 ± 4	2,339 ± 24	1,023 ± 10	172 ± 2	18 ± 0	4 ± 0	1.2 ± 0	0.6 ± 0	1.6 ± 0	43.6 ± 0.7

Note: LOD = limit of detection.

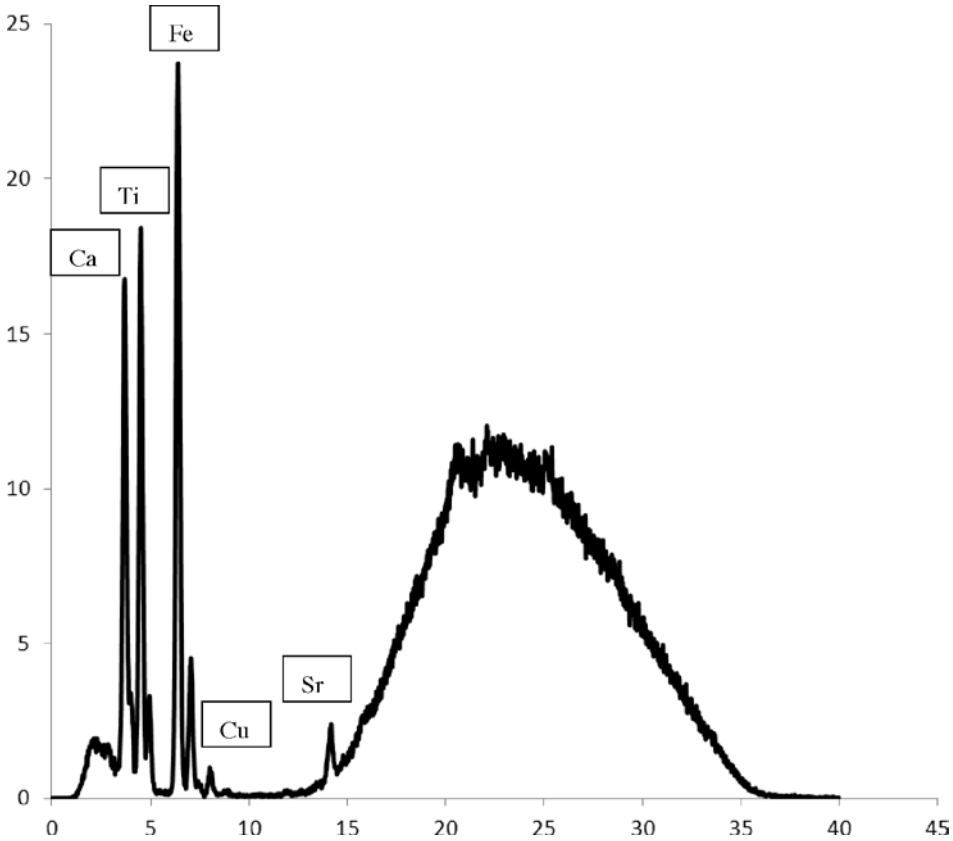

Figure K.8. XRF spectrum for Scotchkote.

Table K.9. XRF Data for Air 200

Cl	486 ± 55
K	295 ± 22
Fe	32 ± 2
Rb	5 ± 0
Sr	13 ± 1
Zr	35 ± 1
Mo	38 ± 1
Pb	4 ± 1

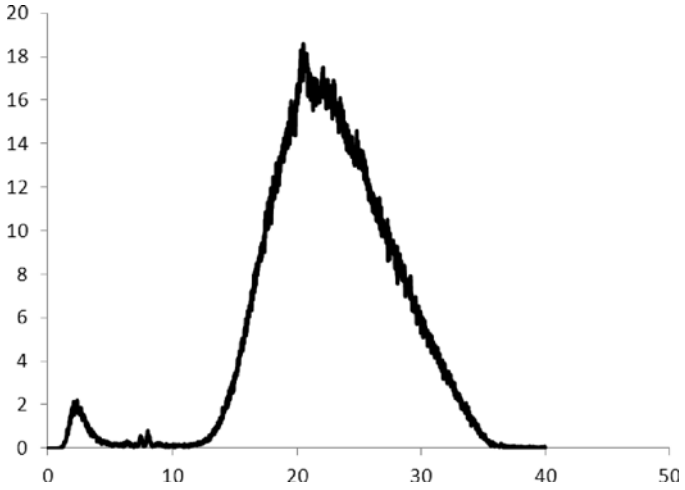

Figure K.9. XRF spectrum for Air 200.

Table K.10. XRF Data for ADVA 190

Cl	416 ± 53
K	172 ± 20
Rb	5 ± 0
Sr	13 ± 1
Zr	35 ± 1
Mo	39 ± 1
Pb	3 ± 1

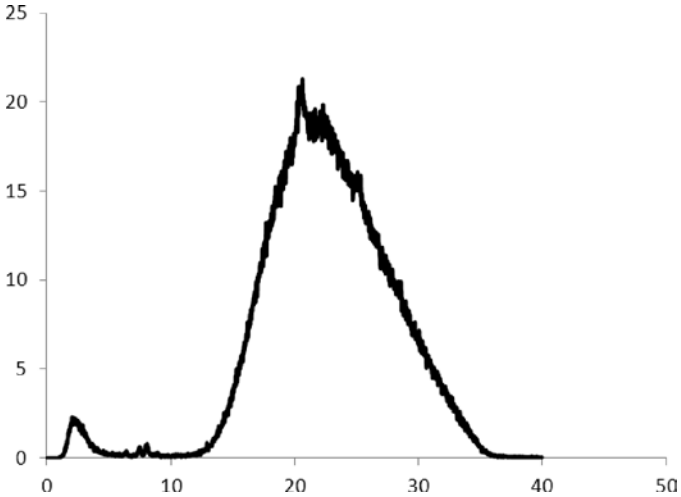

Figure K.10. XRF spectrum for ADVA 190.

Table K.11. XRF Data for Sealtight 1100-CLEAR

Cl	398 ± 46
K	207 ± 18
Rb	5 ± 0
Zr	34 ± 1
Mo	40 ± 1
Pb	3 ± 1

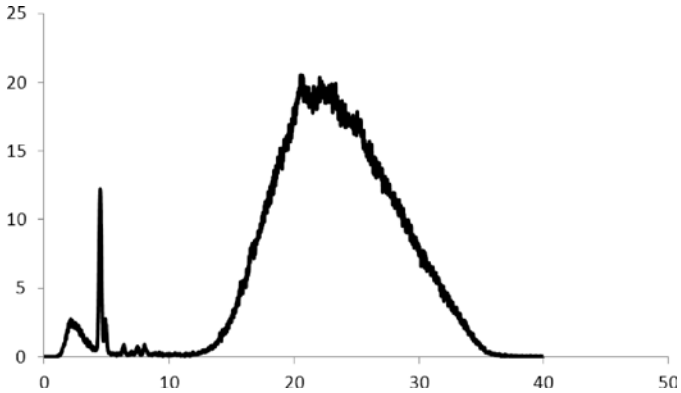

Figure K.11. XRF spectrum for Sealtight 1100-CLEAR.

Table K.12. XRF Data for Elvaloy 4170

Cl	472 ± 38
K	211 ± 14
Mn	4 ± 1
Rb	9 ± 0
Sr	18 ± 1
Zr	47 ± 1
Mo	50 ± 1
Pb	9 ± 1

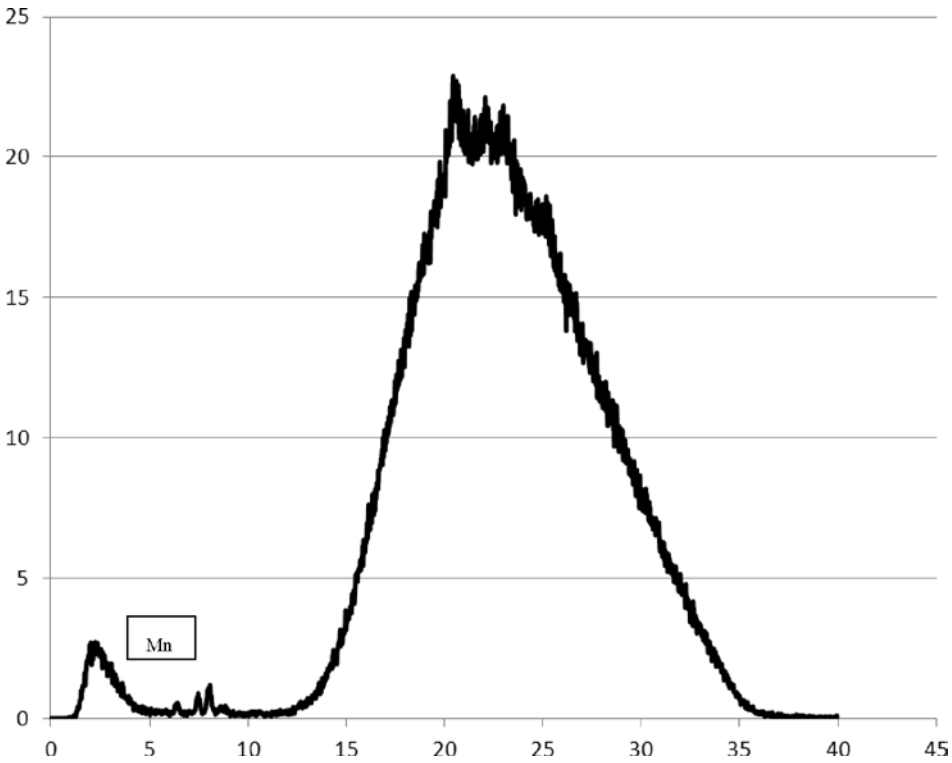

Figure K.12. XRF spectrum for Elvaloy 4170.

Table K.13. XRF Data for Kraton D1101

Cl	483 ± 49
K	198 ± 18
Mn	17 ± 2
Fe	34 ± 2
Se	45 ± 1
Rb	210 ± 2
Sr	19 ± 1
Zr	49 ± 1
Mo	50 ± 1
Hg	7 ± 2
Pb	46 ± 2

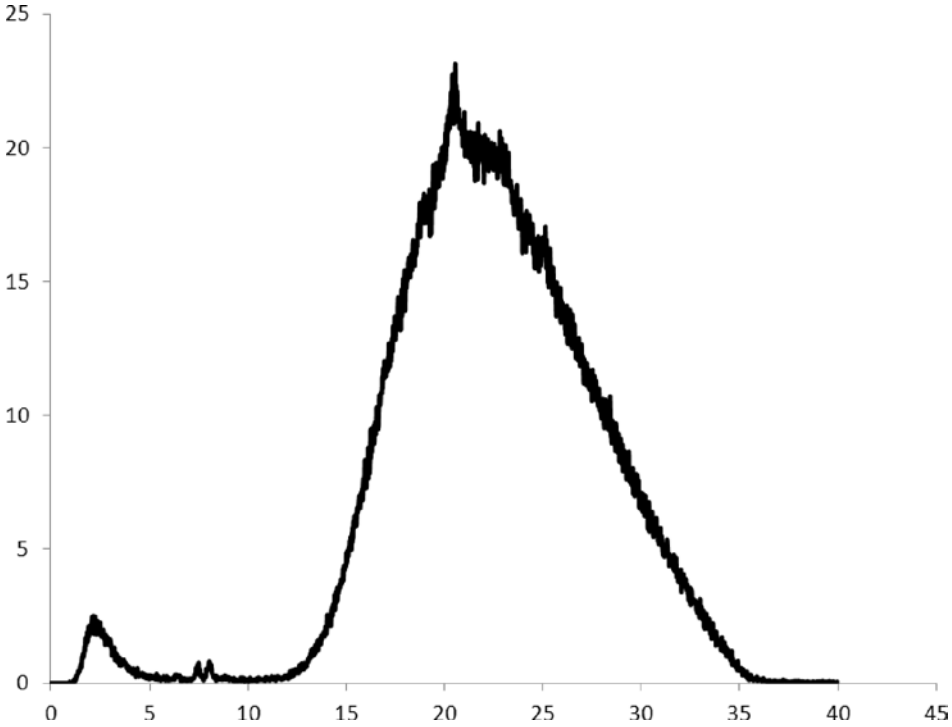

Figure K.13. XRF spectrum for Kraton D1101.

Table K.14. XRF Data for Eucon Retarder 75

Cl	527 ± 54
K	293 ± 22
Fe	21 ± 2
Zn	6 ± 1
Rb	2 ± 0
Sr	8 ± 1
Zr	24 ± 1
Mo	28 ± 1
Hg	3 ± 1

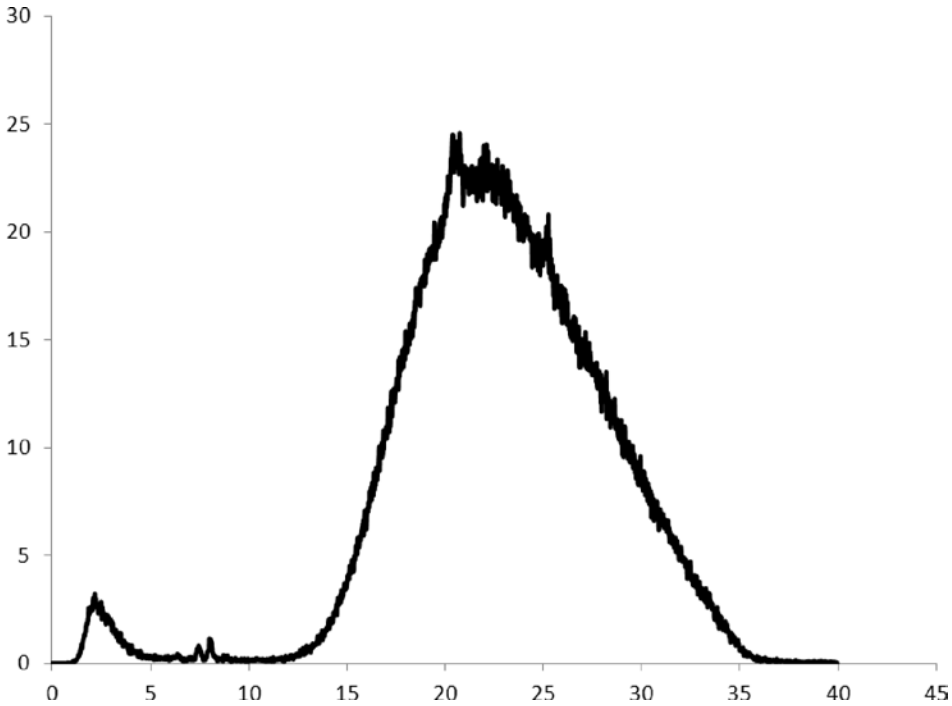

Figure K.14. XRF spectrum for Eucon Retarder 75.

Table K.15. XRF Data for Accelguard 80

Ca	155,496 ± 1,172
Rb	3 ± 1
Sr	1,471 ± 8
Mo	5 ± 1
I	1,390 ± 138

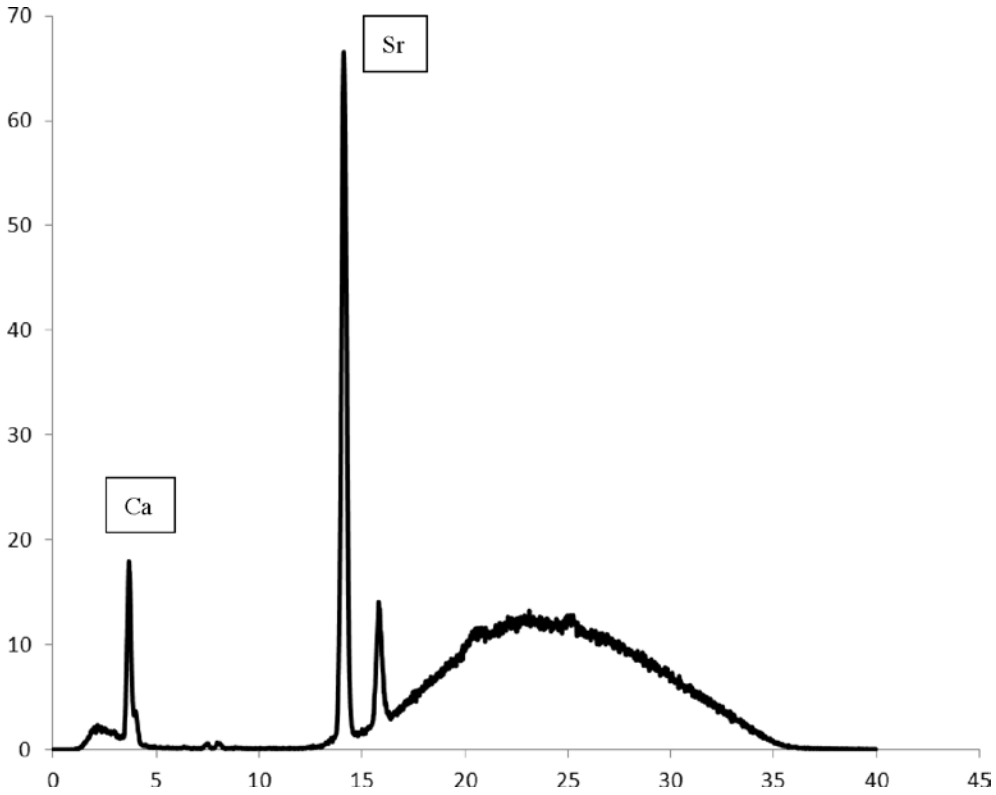

Figure K.15. XRF spectrum for Accelguard 80.

Table K.16. XRF Data for 3M All Weather Traffic Paint

K	705 ± 182
Ca	416,493 ± 3,859
Ti	8,153 ± 134
Fe	1,701 ± 21
Sr	43 ± 1
Zr	25 ± 1
I	2,466 ± 287
Ba	105 ± 21

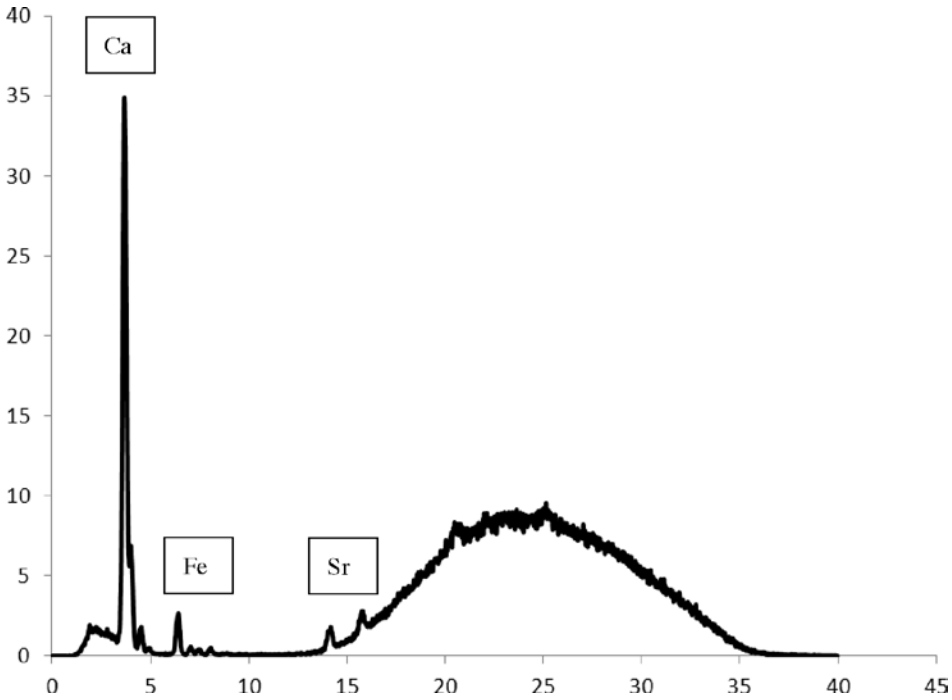

Figure K.16. XRF spectrum for 3M All Weather traffic paint.

APPENDIX L

GPC Chromatograms

Size-exclusion gel permeation chromatography (GPC) is one of the spectroscopic methods included in the Phase 2 laboratory effort. To obtain a chromatogram, GPC was coupled with ultraviolet (UV) detectors and evaporative light-scattering detectors (ELSDs). In the first round, the chromatograms of pure compounds and components (as supplied by manufacturers) were obtained to verify the overall applicability of GPC. The team focused only on the qualitative analysis of the chromatograms of pure compounds (e.g., structural coatings, pavement markings, and chemical admixtures), which translated into the identification of materials and components based on their characteristic peaks. The meaningful chromatograms were obtained for all pure materials with molecular weights higher than 1,000 Da (see Table L.1). For that reason, GPC was an unsuitable method for the solvent parts of structural coatings (Part B of Carbozinc 859 and Scotchkote), epoxy-based pavement markings (Epoplex LS50), and epoxy adhesives for concrete repair. Another reason for the failure to evaluate GPC results was a total absence of both UV and ELSD signals for liquids that do not absorb UV and scatter light, such as some chemical admixtures for portland cement concrete (PCC) (Eucon Retarder 75 and Accelguard 80) and all antistripping agents. All successful GPC chromatograms can be found in this appendix.

A comprehensive literature search in Phase 1 showed that GPC had been successfully used for the evaluation of asphalt products. Therefore, a special evaluation of asphalt-related products, such as polymer-, antistripping- and recycled asphalt pavement (RAP)-modified asphalt binders and hot-mix asphalt (HMA) mixtures, was conducted in the laboratory, as discussed in Appendix O.

Table L.1. Summary of GPC Applicability

Material Category	Brand Name	Applicability (Yes/No)	Reason not Applicable
Structural coatings	Carbozinc 859 Part A	Yes	
	Carbozinc 859 Part B	No	Low molecular weight (<1,000)
	Scotchkote 413 Part A	Yes	
	Scotchkote 413 Part B	No	Low molecular weight (<1,000)
Pavement markings	All Weather paint white	Yes	
	LS 50 White	No	Low molecular weight (<1,000)
	LS 50 Yellow	No	Low molecular weight (<1,000)
	LS 50 Hardener	No	Low molecular weight (<1,000)
Epoxy adhesives for concrete repair	Ultrabond 1100 Part A	No	Low molecular weight (<1,000)
	Ultrabond 1100 Part B	Yes	
	Sikadur 31 Part A	No	Low molecular weight (<1,000)
	Sikadur 31 Part B	No	Low molecular weight (<1,000)
Chemical admixtures for PCC	Air Mix 200	No	Low molecular weight (<1,000)
	Retarder 75	No	No UV and ELSD signal
	Accelguard 80	No	No UV and ELSD signal
	ADVA 190	No	Low molecular weight (<1,000)
Curing compounds for PCC	Sealtight 1100	Yes	
	Safe-Cure 1200	Yes	
	Safe-Cure Clear	Yes	
Neat asphalt binders	PG 58-28	Yes	
	PG 64-22	Yes	
Polymer modifiers for asphalt binders	Elvaloy 4170	Yes	
	Kraton	Yes	
	Butonal	No	No UV and ELSD signal
Asphalt emulsions	CRS-1	Yes	
	CRS-1P	Yes	
Antistripping agents	Kling Beta 2912	No	No UV and ELSD signal
	Kling Beta 2700	No	No UV and ELSD signal
	AD-here 65	No	No UV and ELSD signal
Polymer-modified asphalt binders	PG 52-34 1.5% SBR latex	Yes	
	PG 64-28 3.3% SBR latex	Yes	
	PG 64-22E + 1%–6% SBS	Yes	
RAP-modified asphalt binders	PG 64-22W + RAP	Yes	
Oxidation in RAP	RAP mixes extracted from aggregate	Yes	
RAP-modified HMA	HMA + RAP + 1%–6% SBS	Yes	
Antistripping-modified asphalt binders	PG 64-22W + AD-here 65, Kling Beta 2912	No	No UV and ELSD signal
Cured epoxy adhesives for concrete repair	Cured Ultrabond 1100	No	Unable to dissolve
	Cured Sikadur 31	No	Unable to dissolve

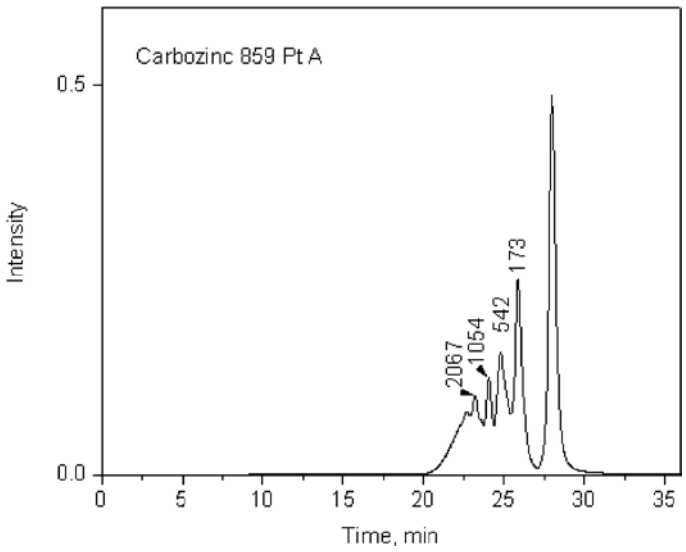

Figure L.1. GPC profile for Carbozinc 859 Part A (UV detector).

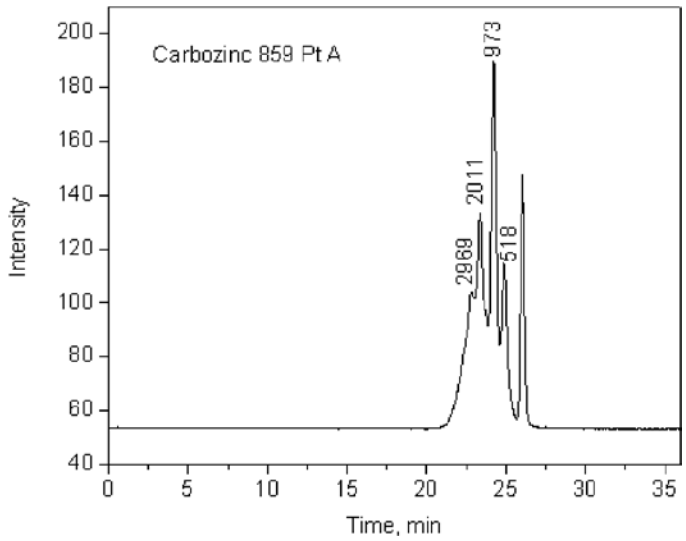

Figure L.2. GPC profile for Carbozinc 859 Part A (ELSD).

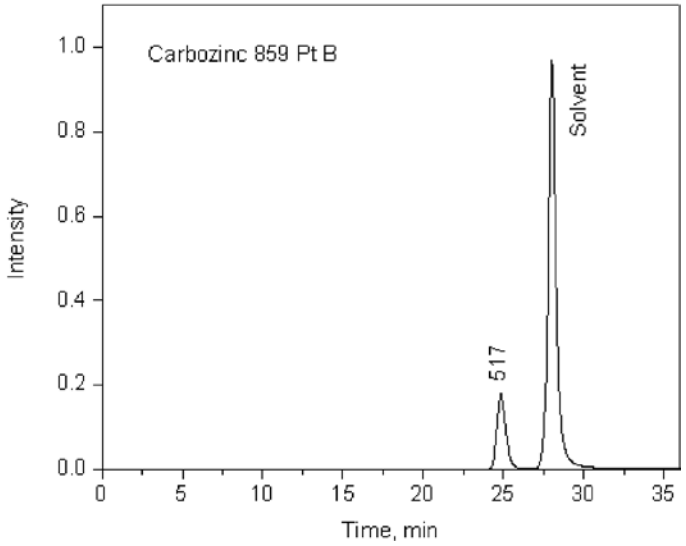

Figure L.3. GPC profile for Carbozinc 859 Part B (UV detector).

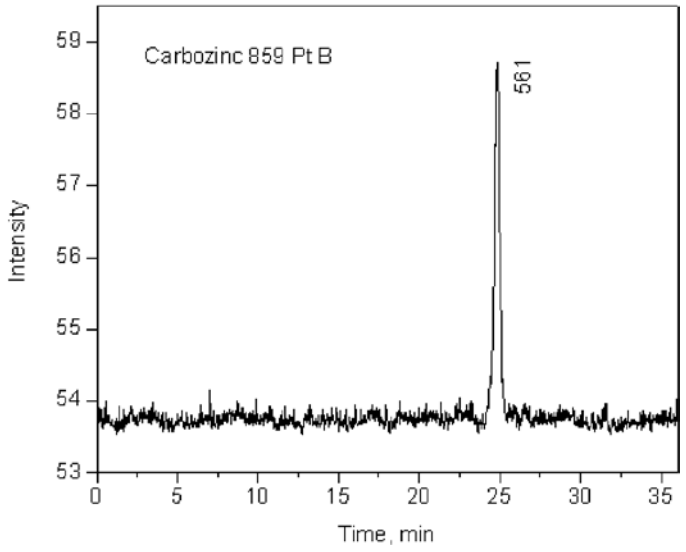

Figure L.4. GPC profile for Carbozinc 859 Part B (ELSD).

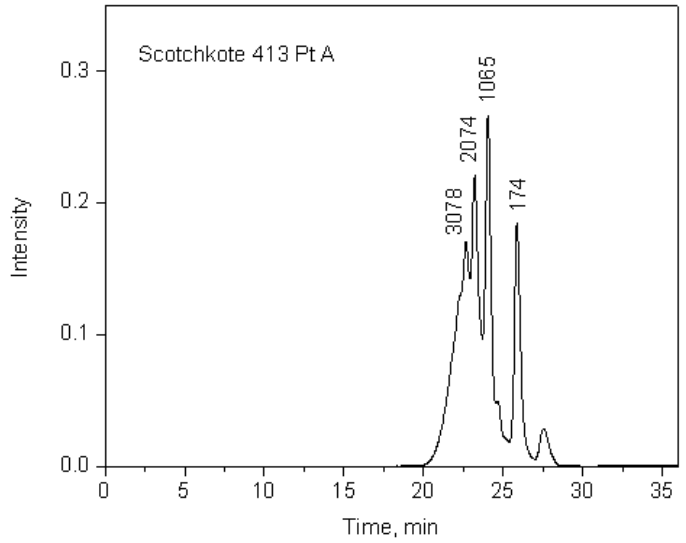

Figure L.5. GPC profile for Scotchkote 413 Part A (UV detector).

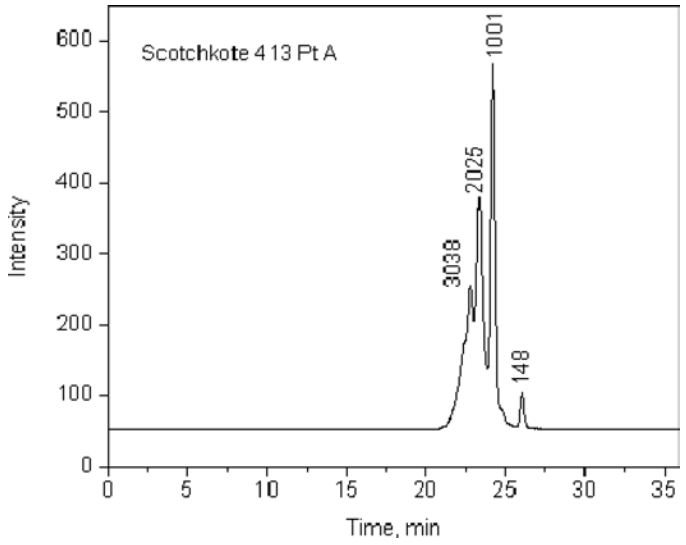

Figure L.6. GPC profile for Scotchkote 413 Part A (ELSD).

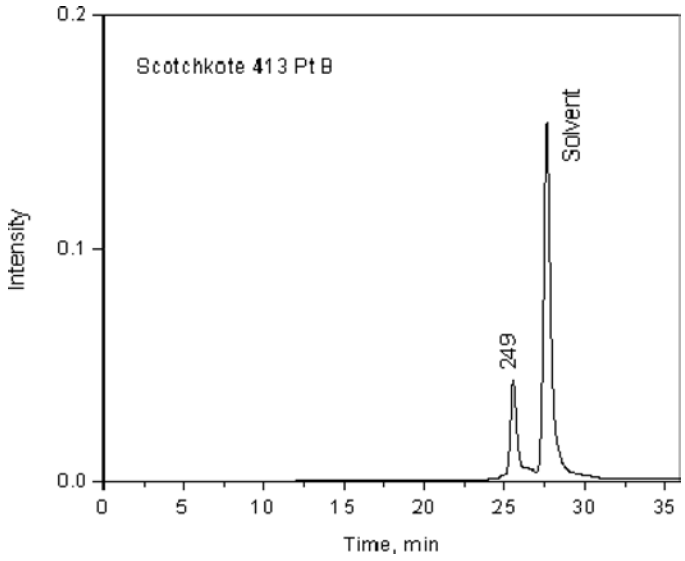

Figure L.7. GPC profile for Scotchkote 413 Part B (UV detector).

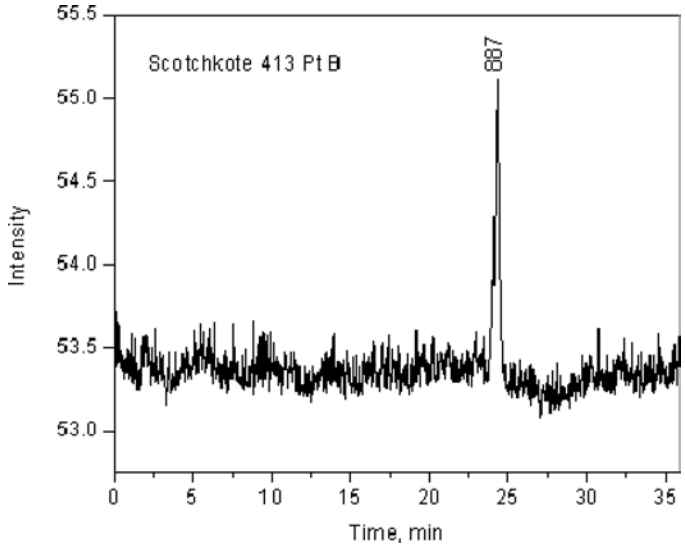

Figure L.8. GPC profile for Scotchkote 413 Part B (ELSD).

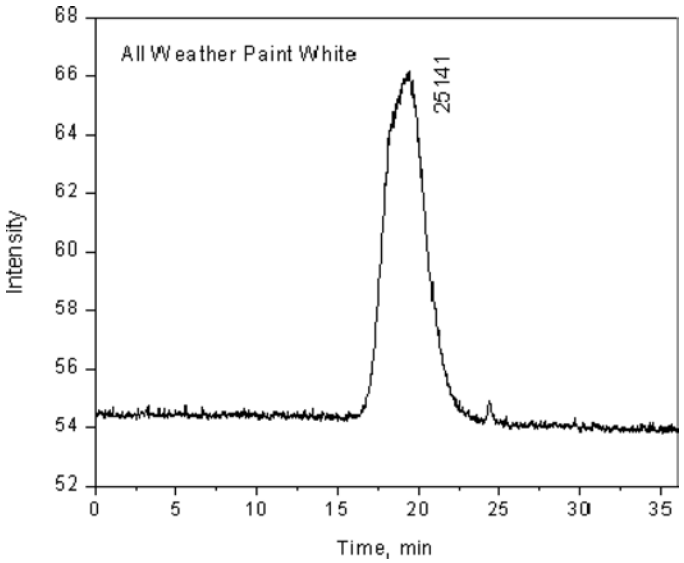

Figure L.9. GPC profile for All Weather White traffic paint (UV detector).

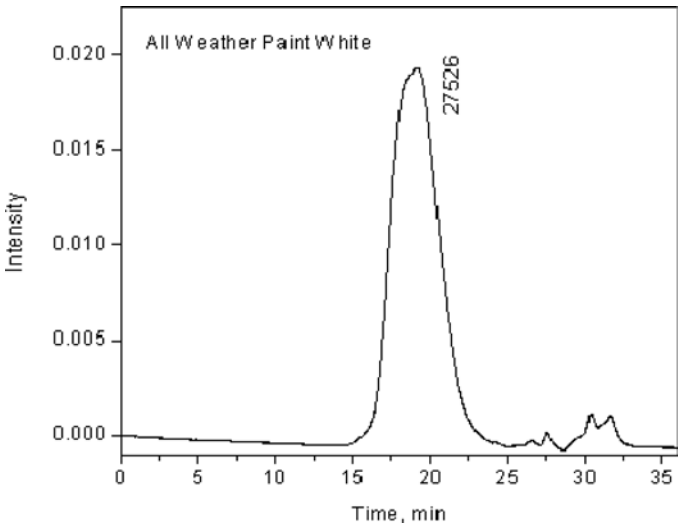

Figure L.10. GPC profile for All Weather White traffic paint (ELSD).

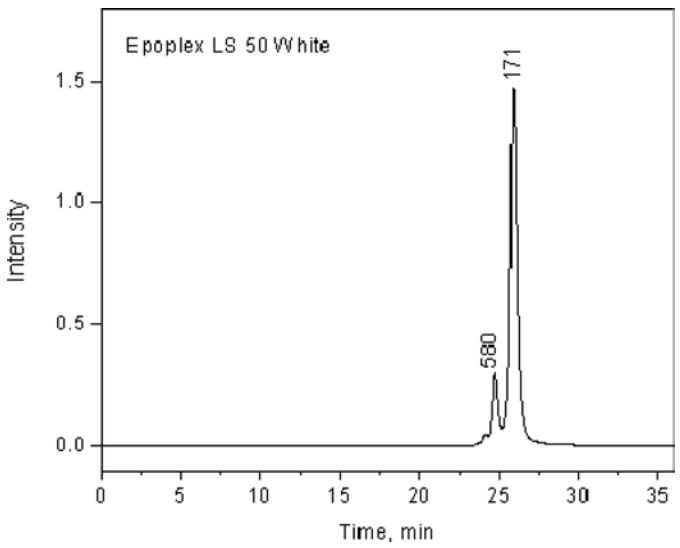

Figure L.11. GPC profile for Epoplex LS50 White traffic paint (UV detector).

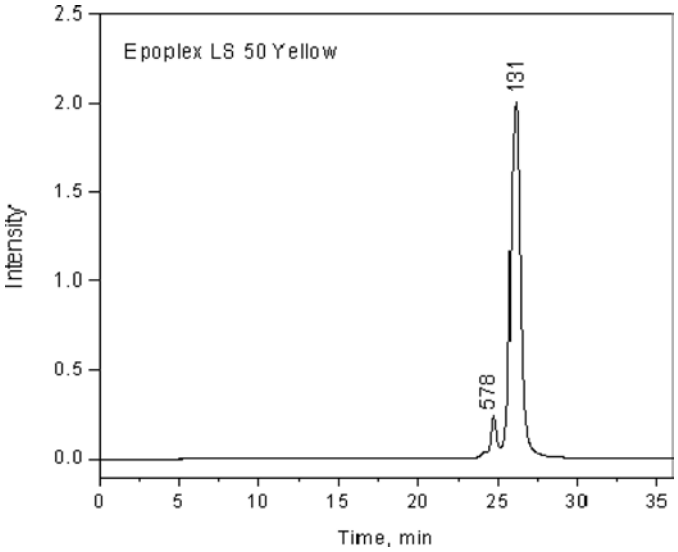

Figure L.13. GPC profile for Epoplex LS50 Yellow traffic paint (UV detector).

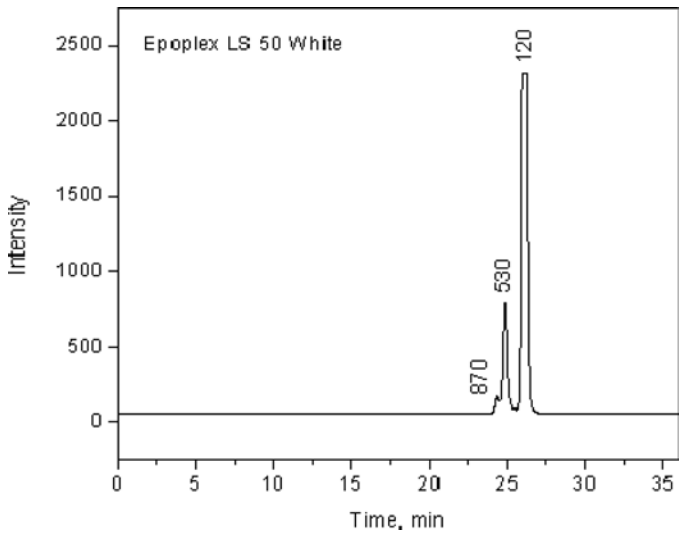

Figure L.12. GPC profile for Epoplex LS50 White traffic paint (ELSD).

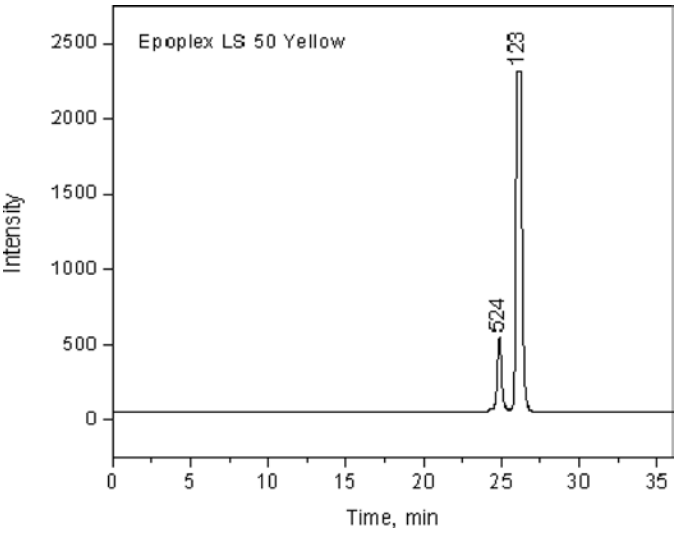

Figure L.14. GPC profile for Epoplex LS50 Yellow traffic paint (ELSD).

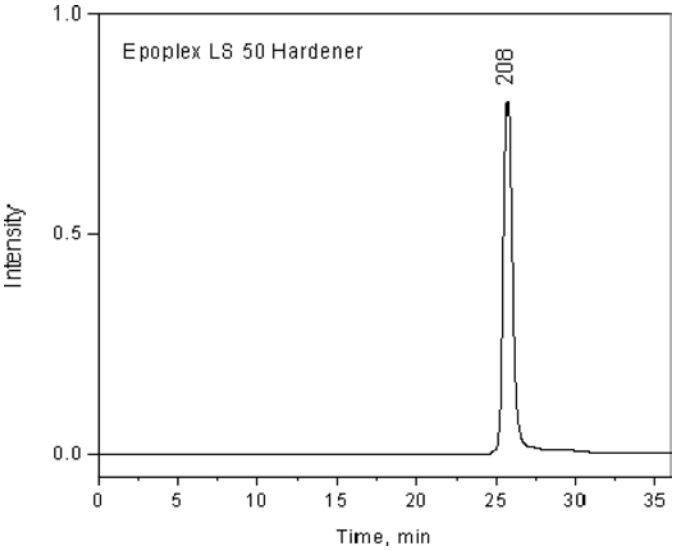

Figure L.15. GPC profile for Epoplex LS50 hardener (UV detector).

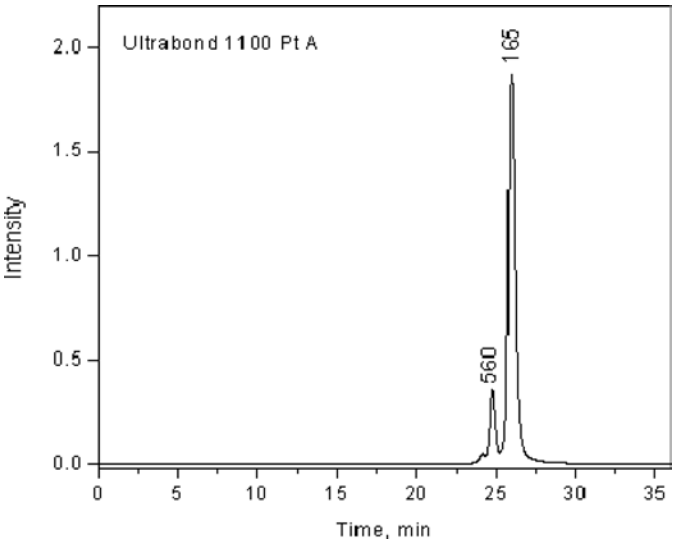

Figure L.17. GPC profile for Ultrabond 1100 Part A (UV detector).

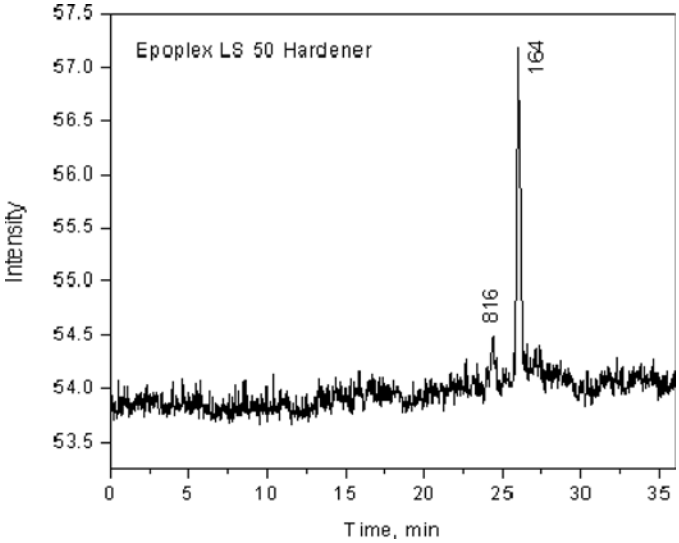

Figure L.16. GPC profile for Epoplex LS50 hardener (ELSD).

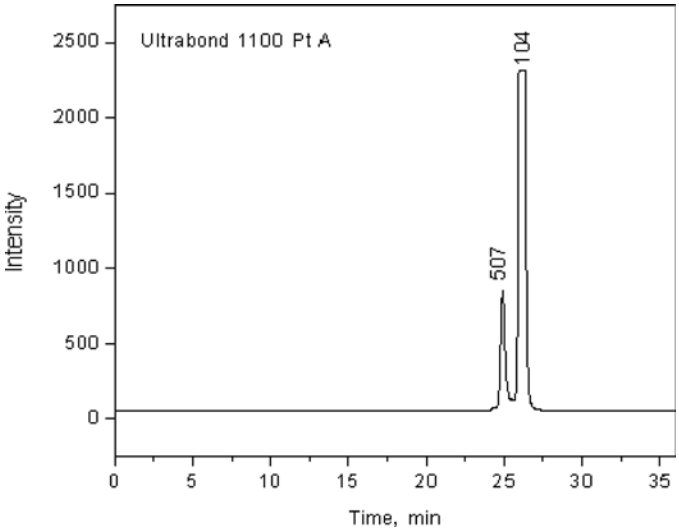

Figure L.18. GPC profile for Ultrabond 1100 Part A (ELSD).

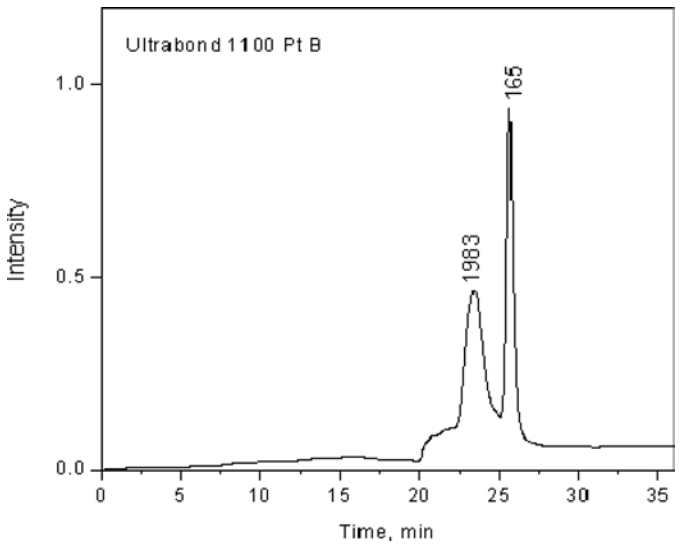

Figure L.19. GPC profile for Ultrabond 1100 Part B (UV detector).

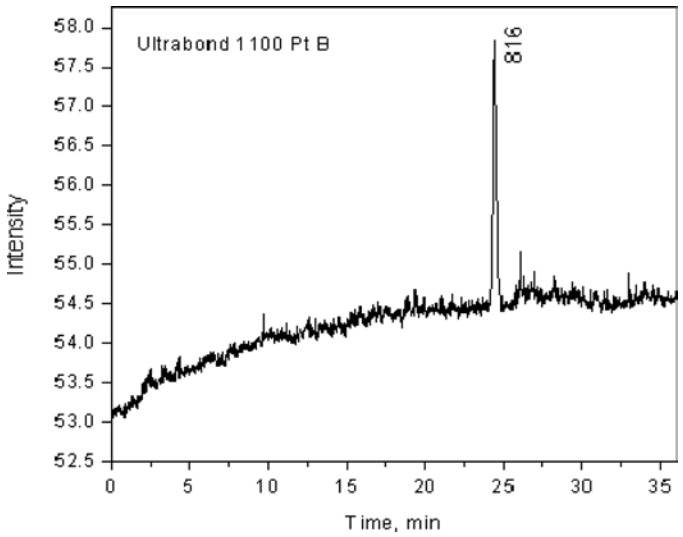

Figure L.20. GPC profile for Ultrabond 1100 Part B (ELSD).

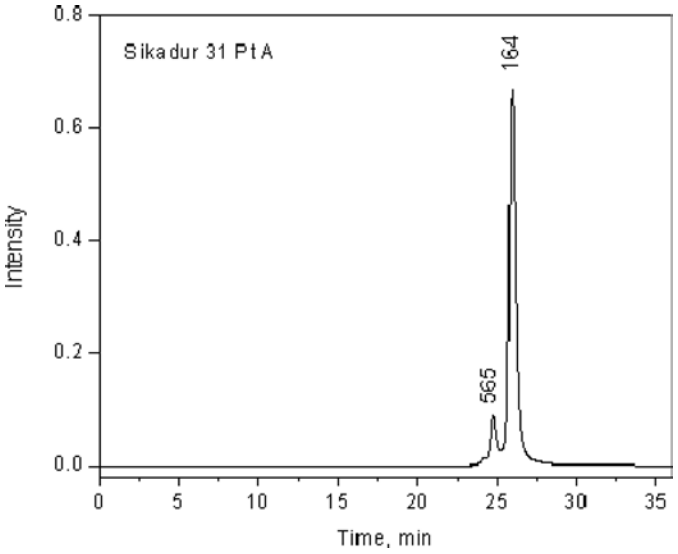

Figure L.21. GPC profile for Sikadur 31 Part A (UV detector).

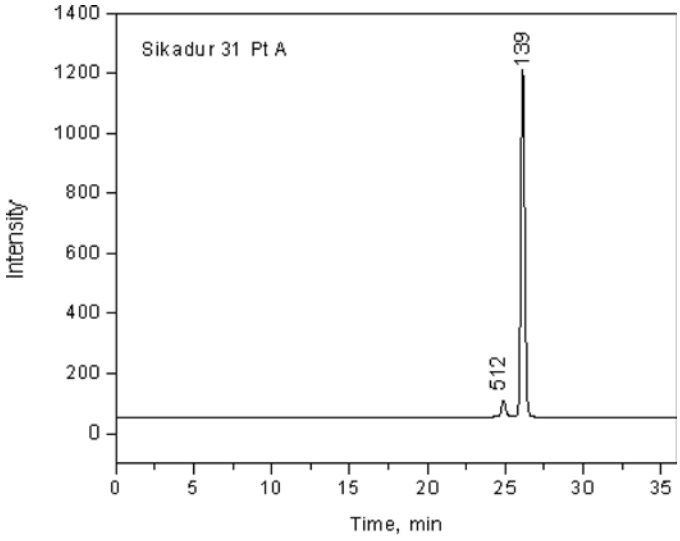

Figure L.22. GPC profile for Sikadur 31 Part A (ELSD).

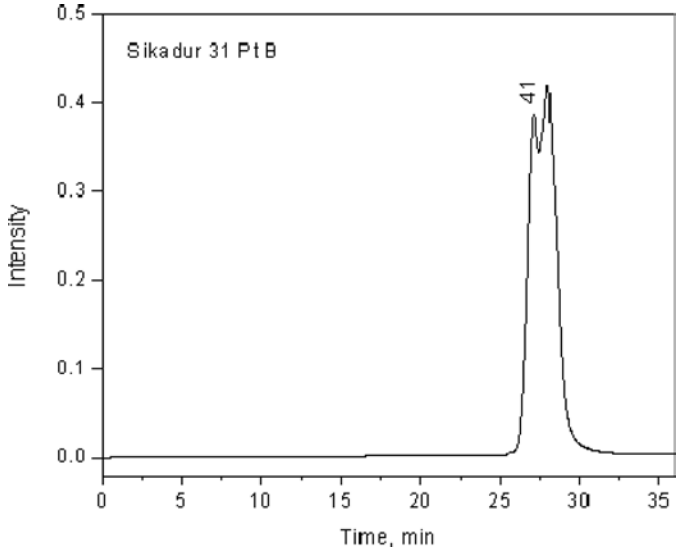

Figure L.23. GPC profile for Sikadur 31 Part B (UV detector).

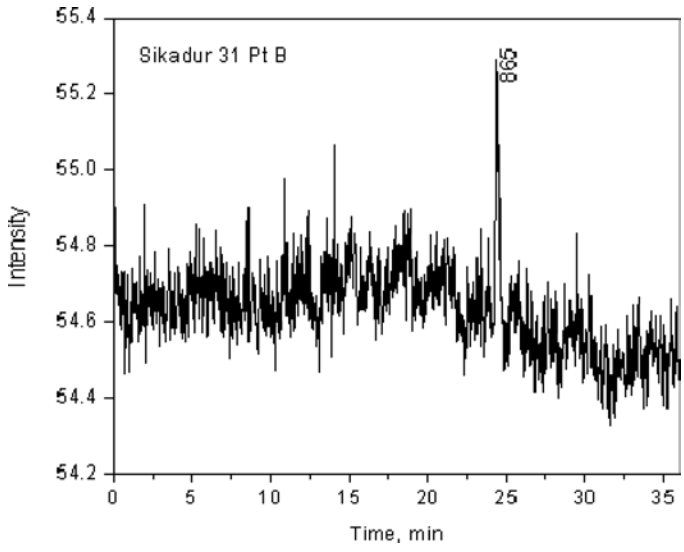

Figure L.24. GPC profile for Sikadur 31 Part B (ELSD).

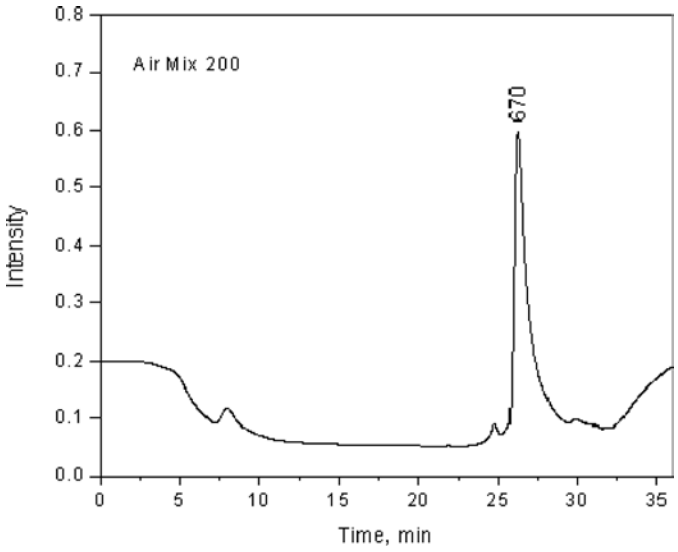

Figure L.25. GPC profile for Air Mix 200 (UV detector).

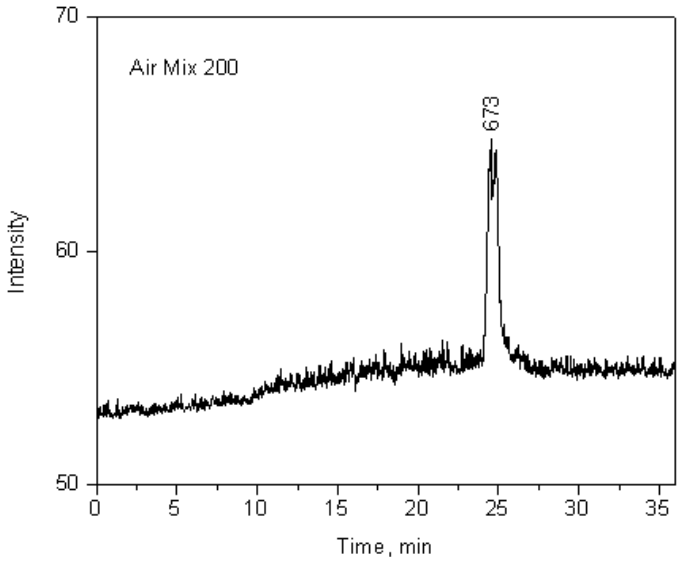

Figure L.26. GPC profile for Air Mix 200 (ELSD).

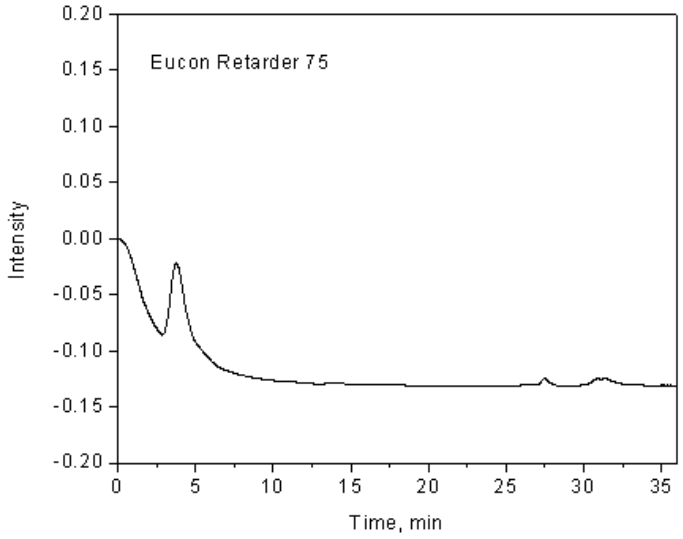

Figure L.27. GPC profile for Eucon Retarder 75 (UV detector).

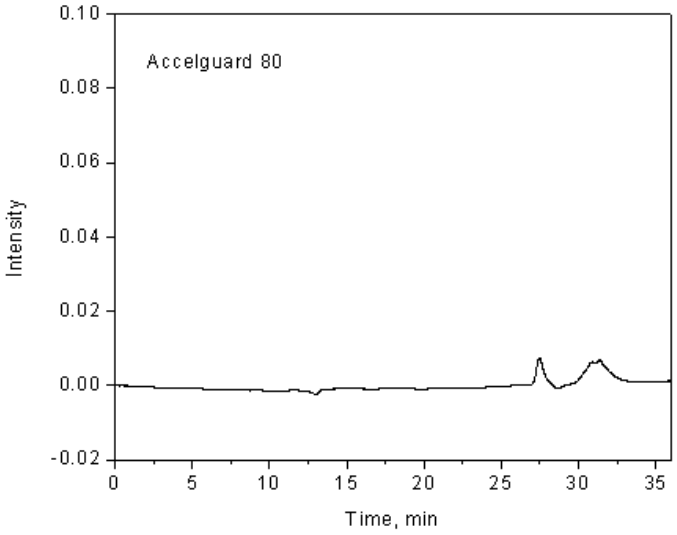

Figure L.29. GPC profile for Accelguard 80 (UV detector).

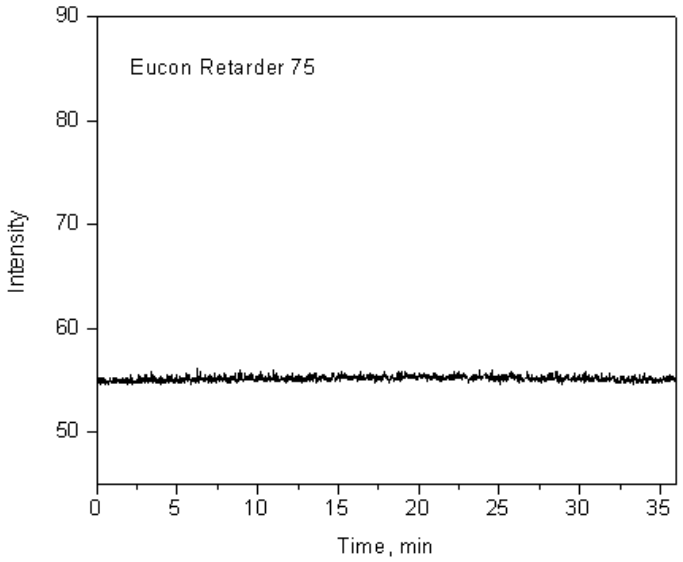

Figure L.28. GPC profile for Eucon Retarder 75 (ELSD).

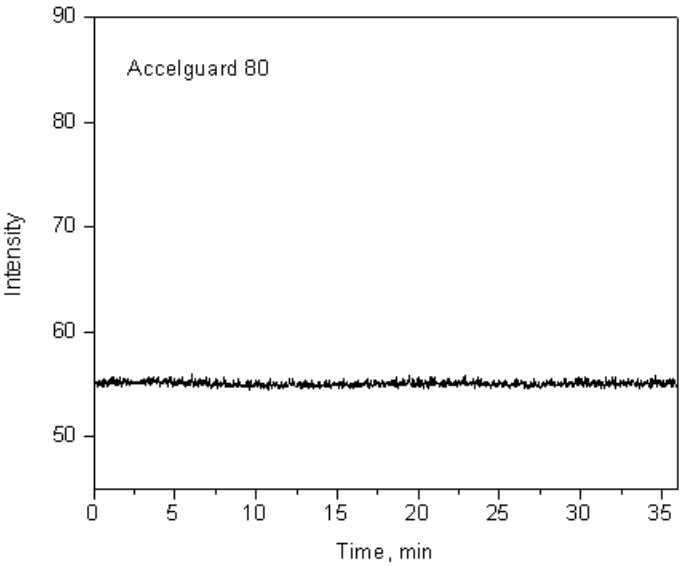

Figure L.30. GPC profile for Accelguard 80 (ELSD).

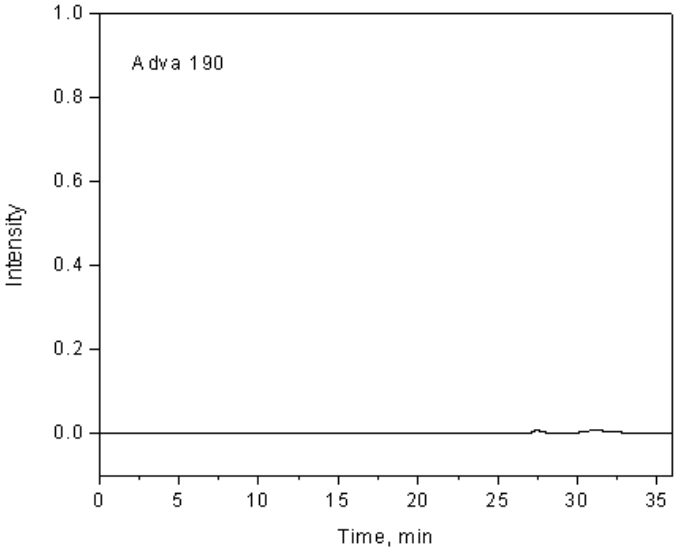

Figure L.31. GPC profile for ADVA 190 (UV detector).

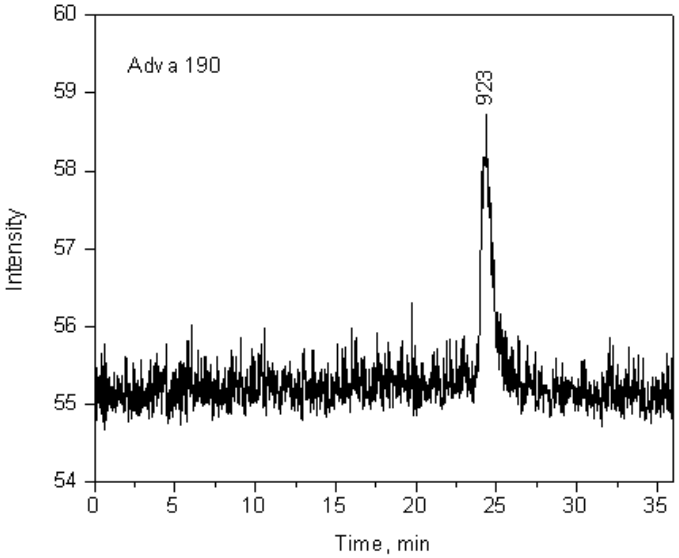

Figure L.32. GPC profile for ADVA 190 (ELSD).

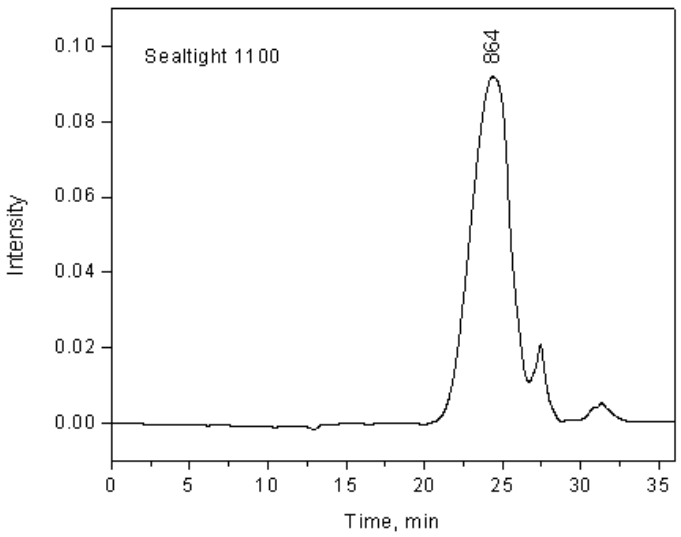

Figure L.33. GPC profile for Sealtight 1100 (UV detector).

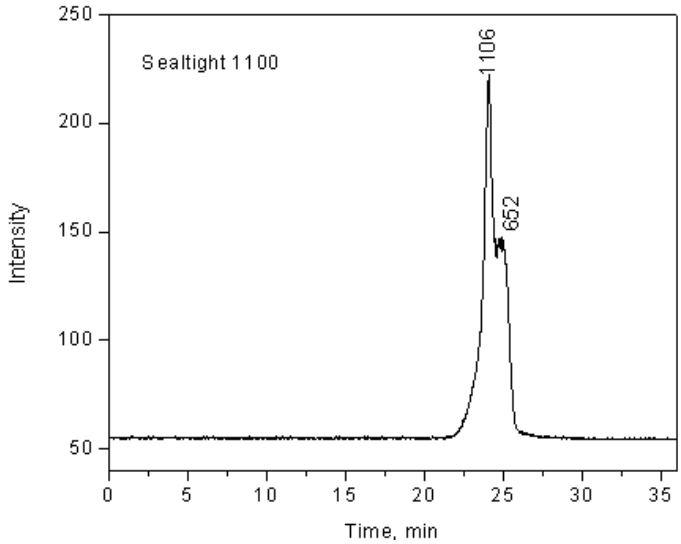

Figure L.34. GPC profile for Sealtight 1100 (ELSD).

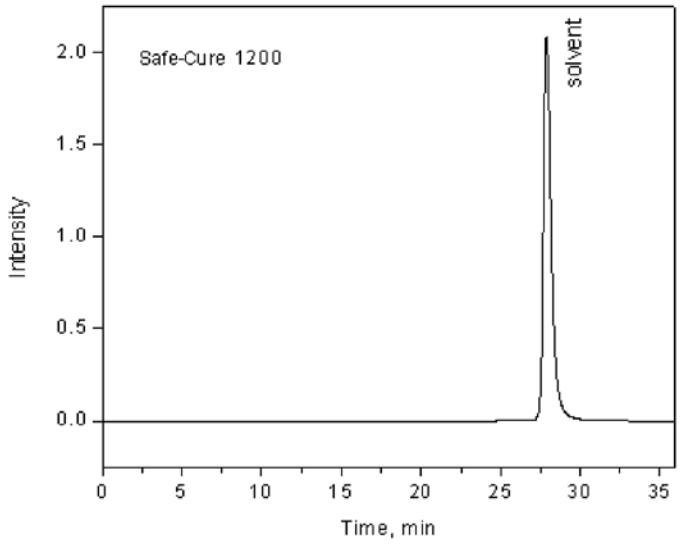

Figure L.35. GPC profile for Safe-Cure 1200 (UV detector).

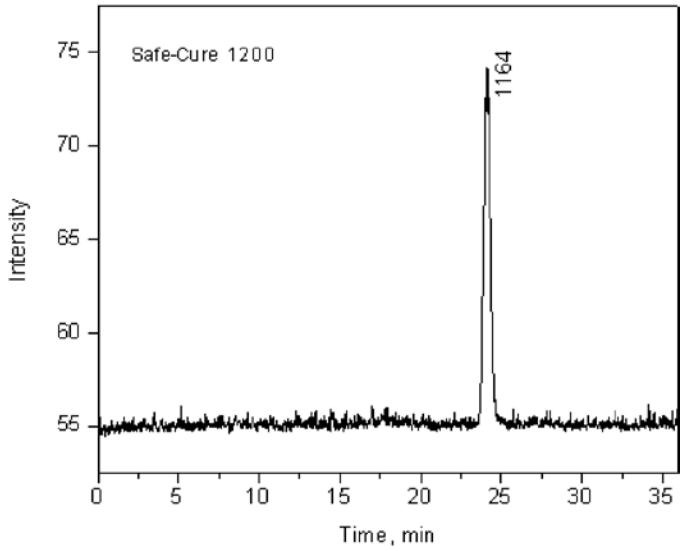

Figure L.36. GPC profile for Safe-Cure 1200 (ELSD).

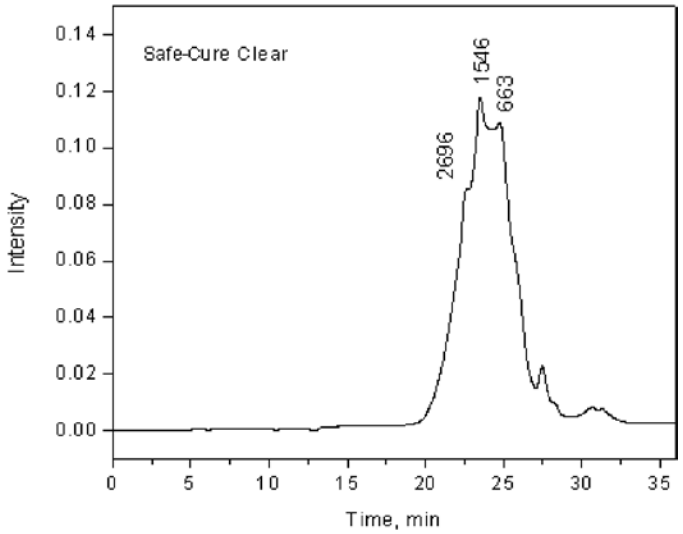

Figure L.37. GPC profile for Safe-Cure Clear (UV detector).

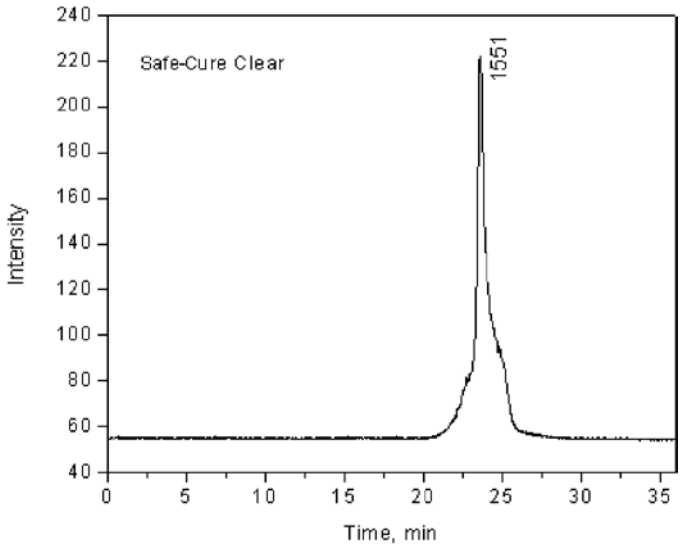

Figure L.38. GPC profile for Safe-Cure Clear (ELSD).

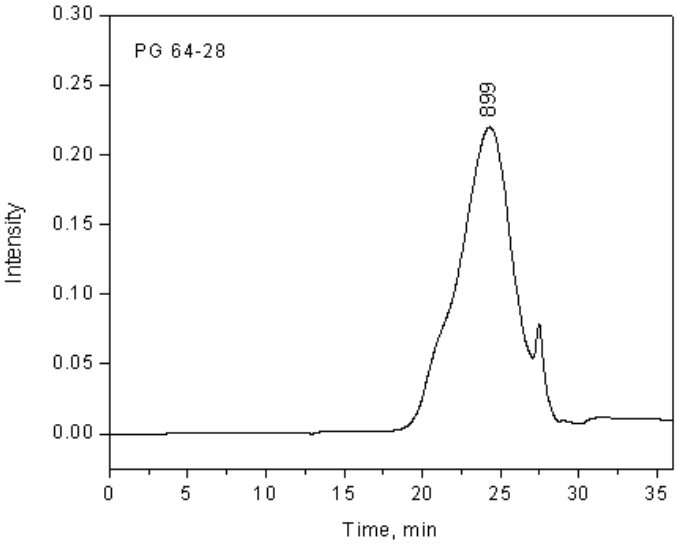

Figure L.39. GPC profile for PG 64-28 asphalt binder (UV detector).

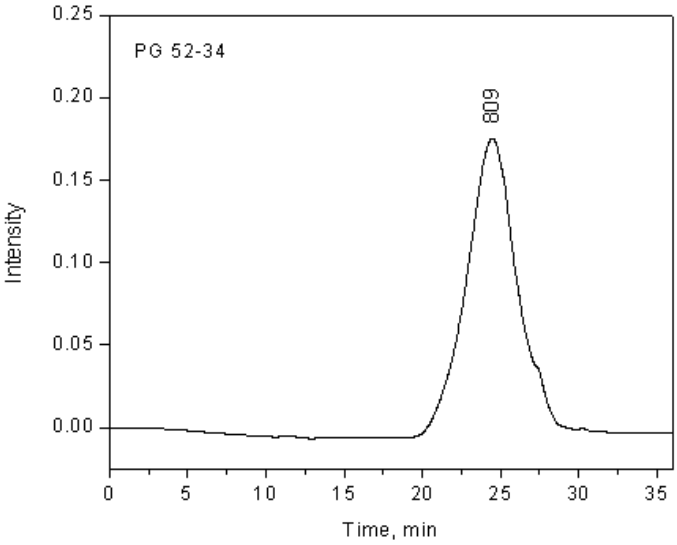

Figure L.41. GPC profile for PG 52-34 asphalt binder (UV detector).

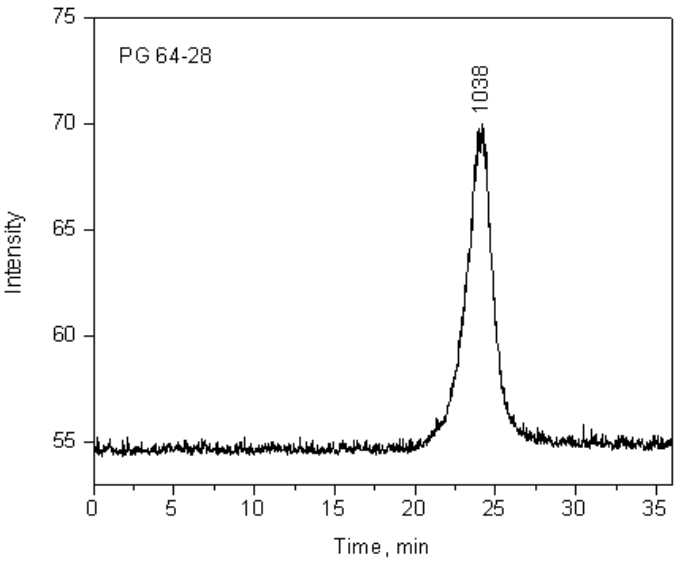

Figure L.40. GPC profile for PG 64-28 asphalt binder (ELSD).

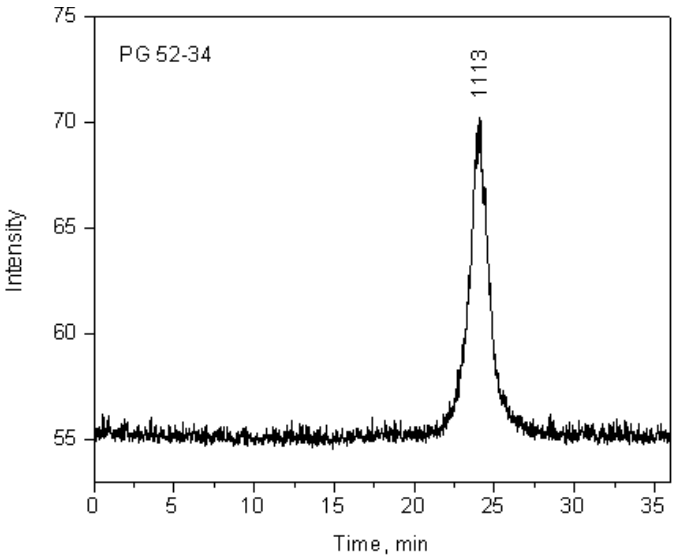

Figure L.42. GPC profile for PG 52-34 asphalt binder (ELSD).

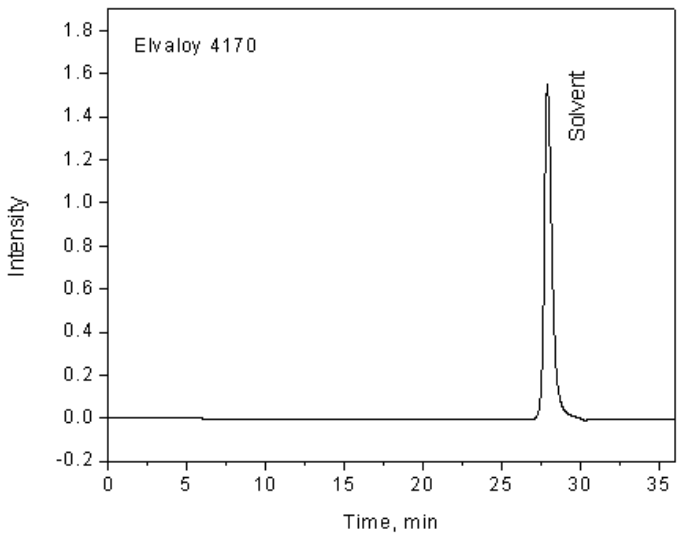

Figure L.43. GPC profile for Elvaloy 4170 (UV detector).

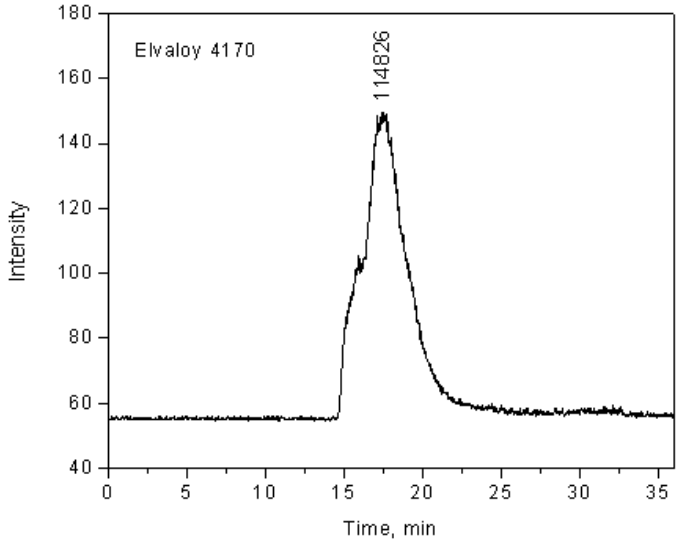

Figure L.44. GPC profile for Elvaloy 4170 (ELSD).

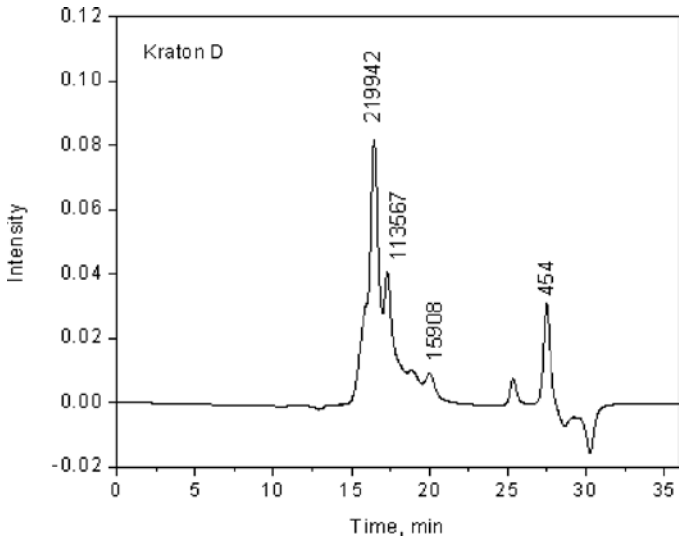

Figure L.45. GPC profile for Kraton D1101 (UV detector).

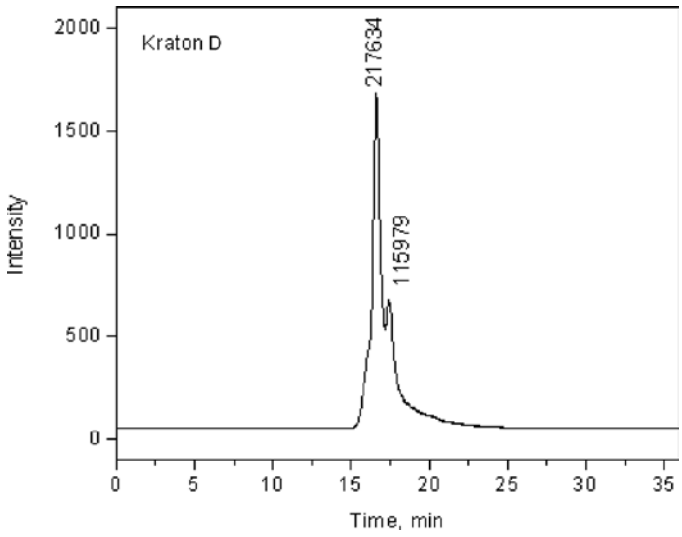

Figure L.46. GPC profile for Kraton D1101 (ELSD).

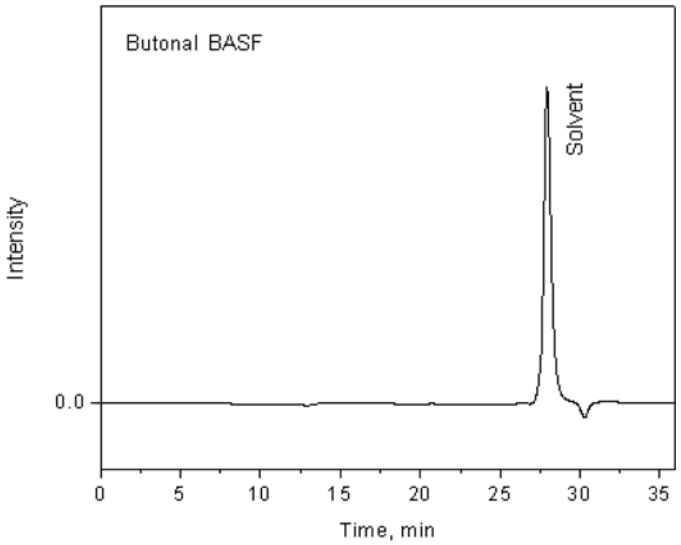

Figure L.47. GPC profile for BASF Butonal NX1138 (UV detector).

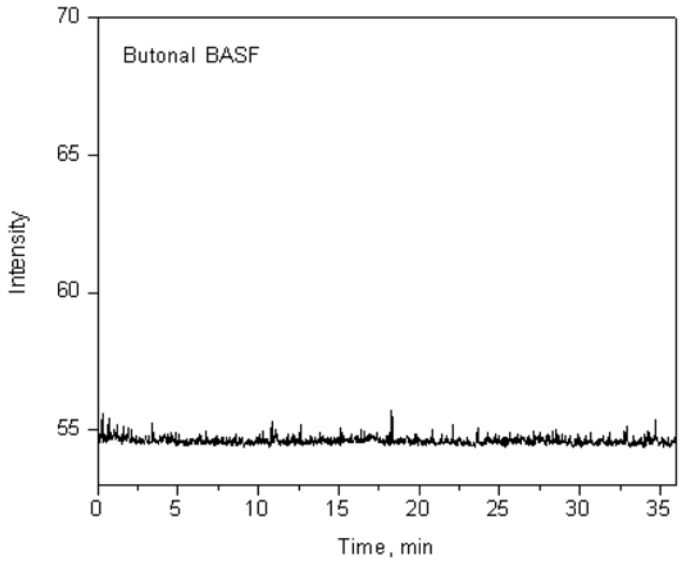

Figure L.48. GPC profile for BASF Butonal NX1138 (ELSD).

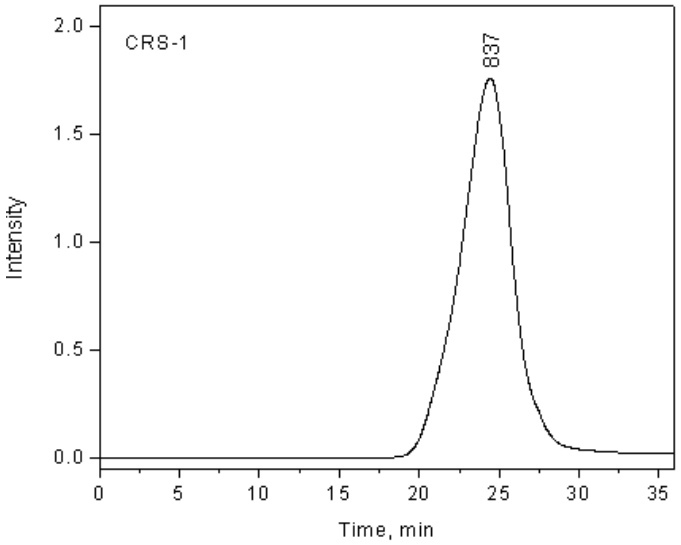

Figure L.49. GPC profile for CRS-1 asphalt emulsion (UV detector).

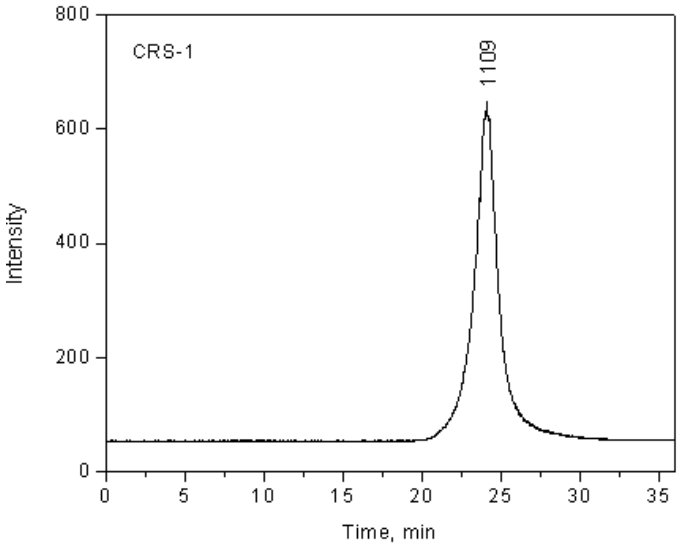

Figure L.50. GPC profile for CRS-1 asphalt emulsion (ELSD).

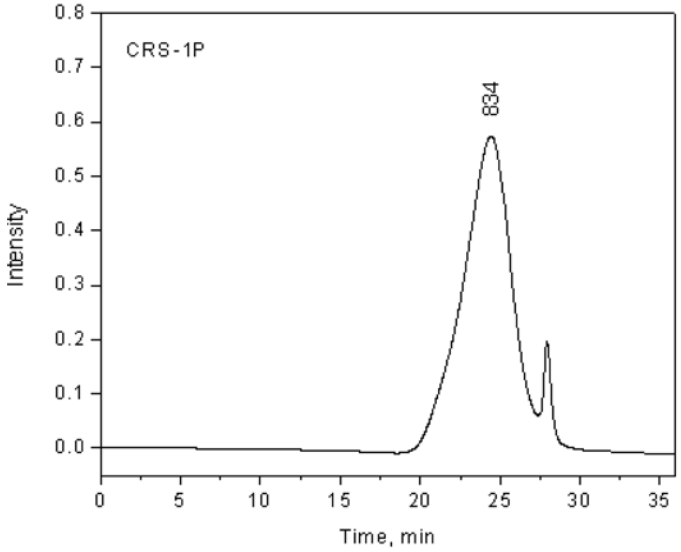

Figure L.51. GPC profile for CRS-1P asphalt emulsion (UV detector).

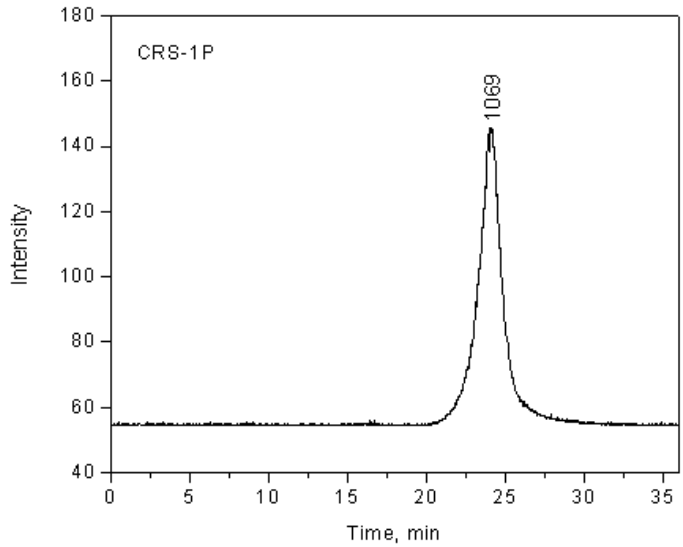

Figure L.52. GPC profile for CRS-1P asphalt emulsion (ELSD).

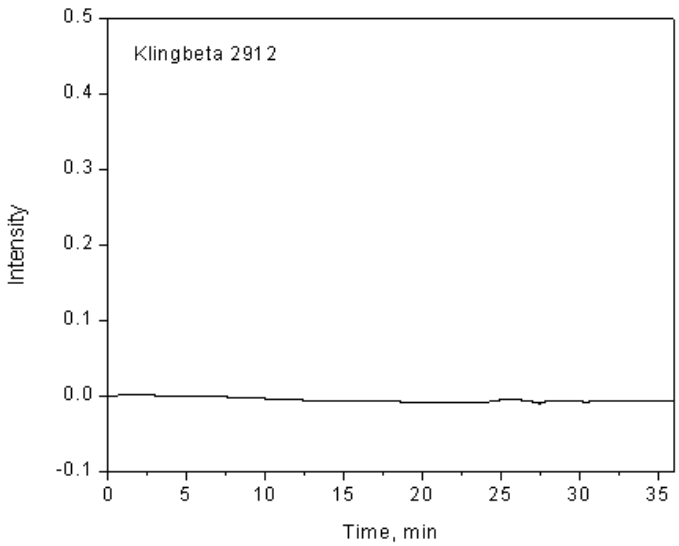

Figure L.53. GPC profile for Kling Beta 2912 antistripping agent (UV detector).

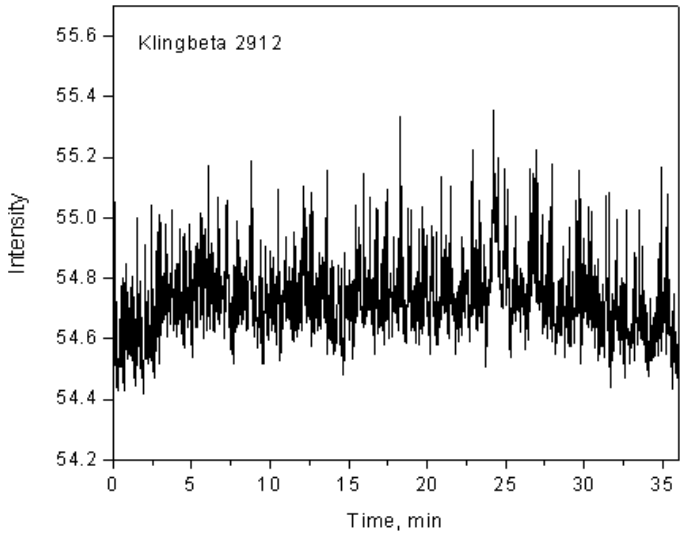

Figure L.54. GPC profile for Kling Beta 2912 antistripping agent (ELSD).

APPENDIX M

NMR Spectra

Nuclear magnetic resonance (NMR) spectroscopy was applied to all materials included in Phase 2 experiments to verify the feasibility of identifying these materials and their components under laboratory conditions. NMR is known for its high effectiveness in identifying organic compounds, including hydrocarbons and compounds with heteroatoms, such as oxygen, nitrogen, sulfur, silicon, halogens, and others. For that reason, all materials that were soluble with no phase separation in D-chloroform (the solvent used for sample preparation) yielded meaningful NMR spectra. In most cases, the exact chemical formula of the matter was revealed (see Appendix H). Table M.1 summarizes the applicability of the NMR method to all materials included in the laboratory phase of experiments.

Once the feasibility of NMR spectroscopy was confirmed, especially for researching petroleum products, the team evaluated the applicability of NMR to identifying the presence of modifiers, contaminants, and recycled asphalt pavement (RAP) in asphalt binders and hot-mix asphalt (HMA) mixes. In addition, an attempt was made to quantify the amount of modifiers and RAP based on NMR data. The results of these experiments are presented in Appendix O.

Table M.1. Summary of NMR Applicability

Material Category	Brand Name	Applicability (Yes/No)	Reason not Applicable
Structural coatings	Carbozinc 859 Part A	Yes	
	Carbozinc 859 Part B	Yes	
	Scotchkote 413 Part A	Yes	
	Scotchkote 413 Part B	Yes	
Pavement markings	All Weather paint white	Yes	
	LS 50 White	Yes	
	LS 50 Yellow	Yes	
	LS 50 Hardener	Yes	
Epoxy adhesives for concrete repair	Ultrabond 1100 Part A	Yes	
	Ultrabond 1100 Part B	Yes	
	Sikadur 31 Part A	Yes	
	Sikadur 31 Part B	Yes	
Chemical admixtures for portland cement concrete (PCC)	Air Mix 200	No	Phase separation
	Retarder 75	Yes	
	Accelguard 80	No	Phase separation
	ADVA 190	Yes	
Curing compounds for PCC	Sealtight 1100	Yes	
	Safe-Cure 1200	Yes	
	Safe-Cure Clear	Yes	
Neat asphalt binders	PG 58-28	Yes	
	PG 64-22	Yes	
Polymer modifiers for asphalt binders	Elvaloy 4170	Yes	
	Kraton	Yes	
	Butonal	Yes	
Asphalt emulsions	CRS-1	Yes	
	CRS-1P	Yes	
Antistripping agents	Kling Beta 2912	Yes	
	Kling Beta 2700	Yes	
	AD-here 65	Yes	
Polymer-modified asphalt binders	PG 52-34 1.5% SBR Latex	Yes	
	PG 64-28 3.3% SBR Latex	Yes	
	PG 64-22E + 1%–6% SBS	Yes	
RAP-modified asphalt binders	PG 64-22W + RAP	Yes	
Oxidation in RAP	RAP mixes extracted from aggregate	Yes	
RAP-modified HMA	HMA + RAP + 1%–6% SBS	Yes	
Antistripping-modified asphalt binders	PG 64-22W + AD-here 65, Kling Beta 2912	Yes	
Cured epoxy adhesives for concrete repair	Cured Ultrabond 1100	No	Unable to dissolve
	Cured Sikadur 31	No	Unable to dissolve

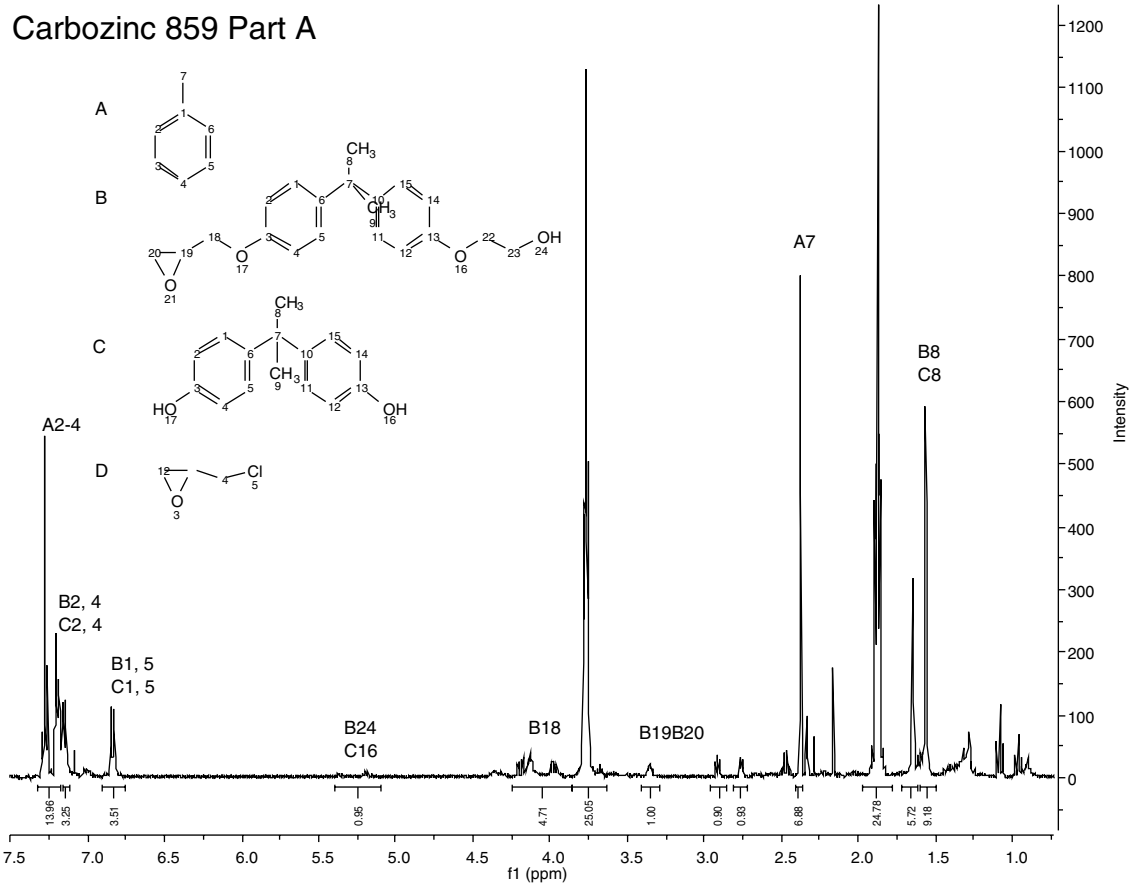

Figure M.1. NMR spectrum for Carbozinc 859 Part A.

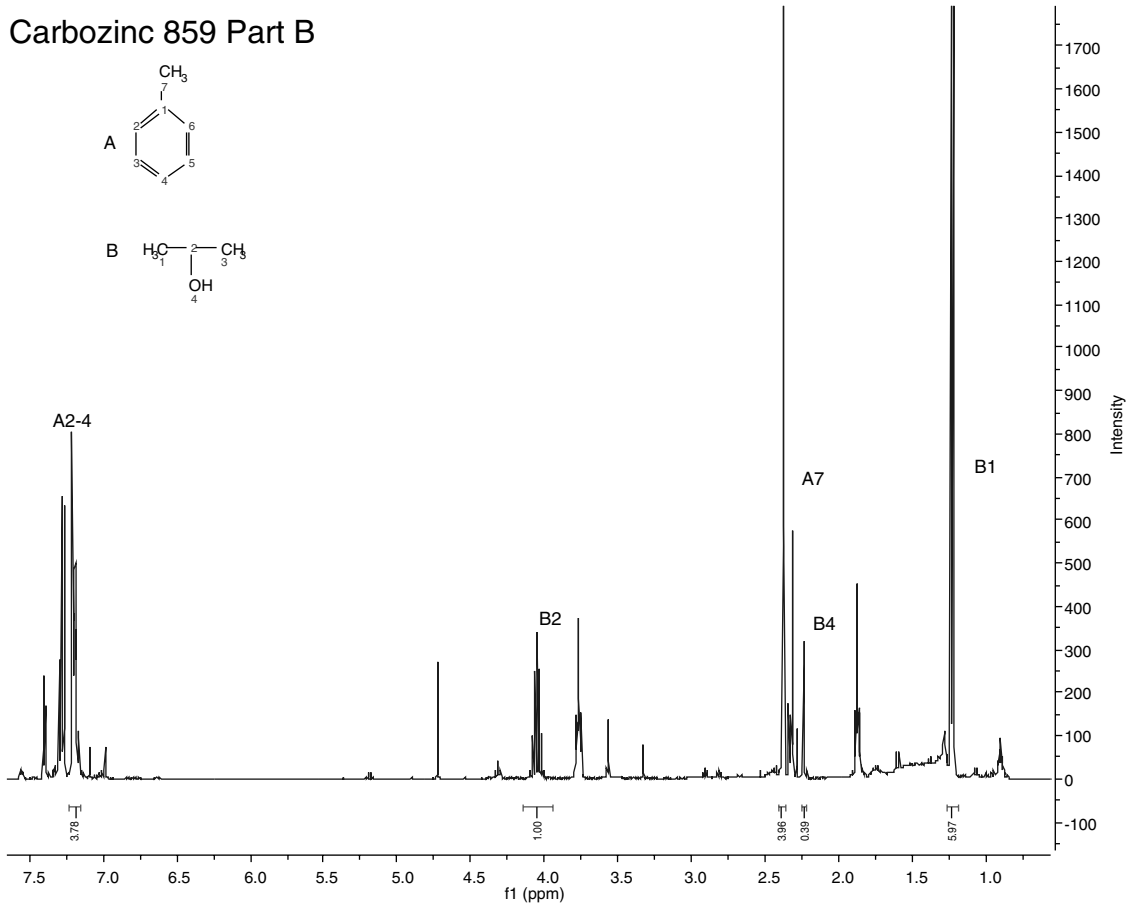

Figure M.2. NMR spectrum for Carbozinc 859 Part B.

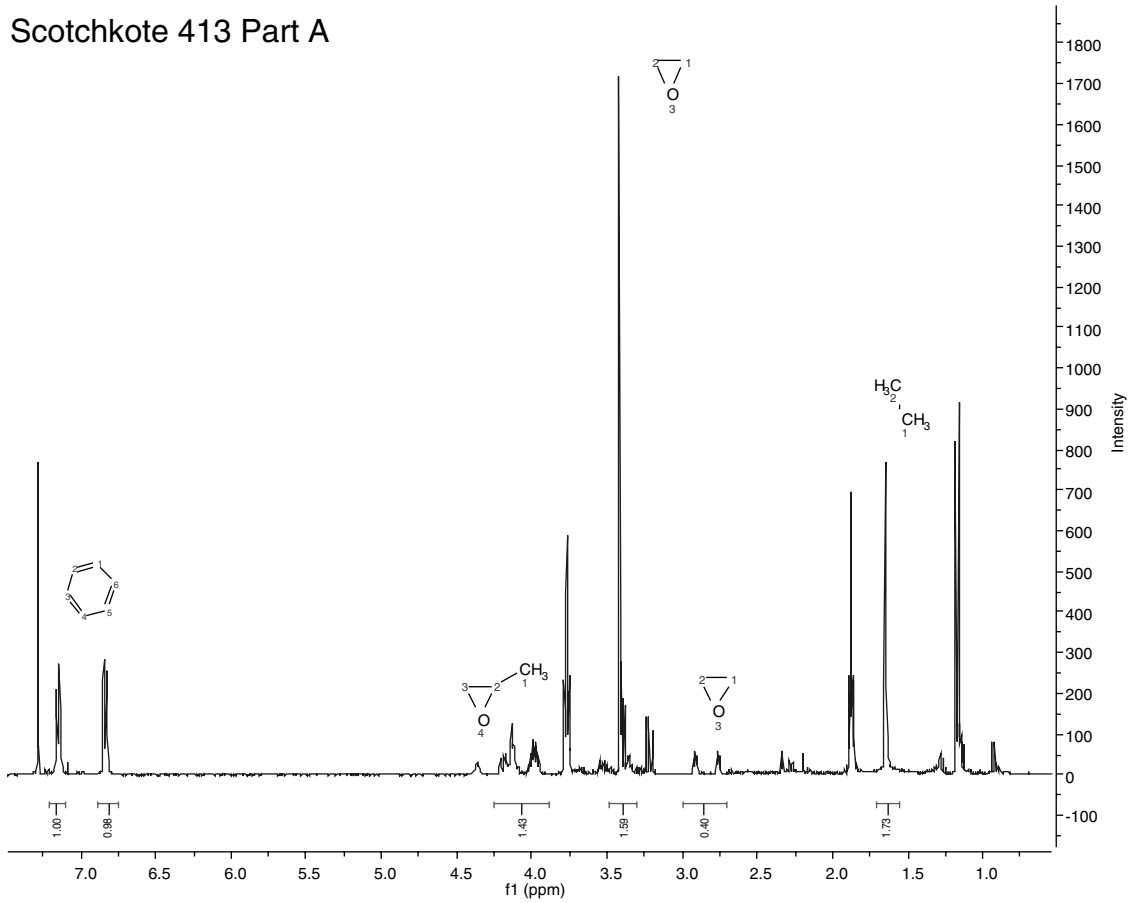

Figure M.3. NMR spectrum for Scotchkote 413 Part A.

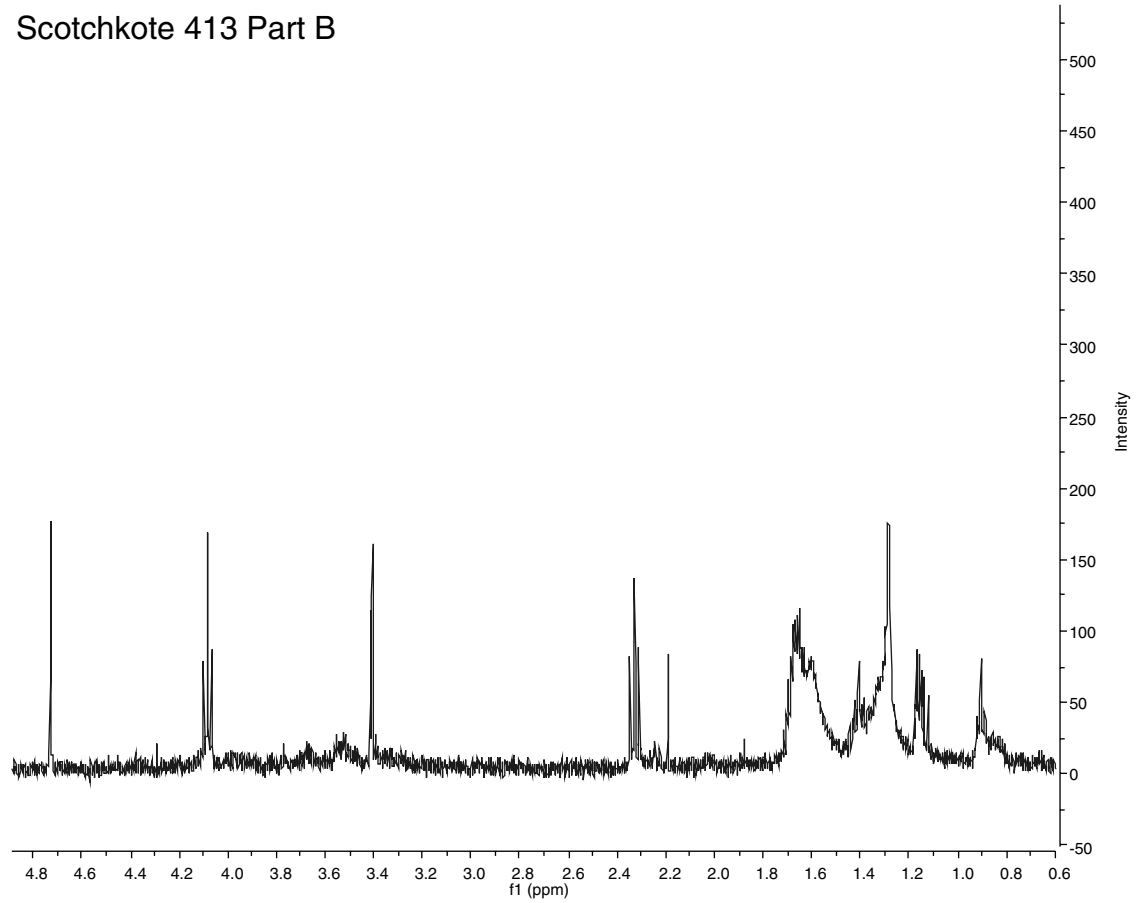

Figure M.4. NMR spectrum for Scotchkote 413 Part B.

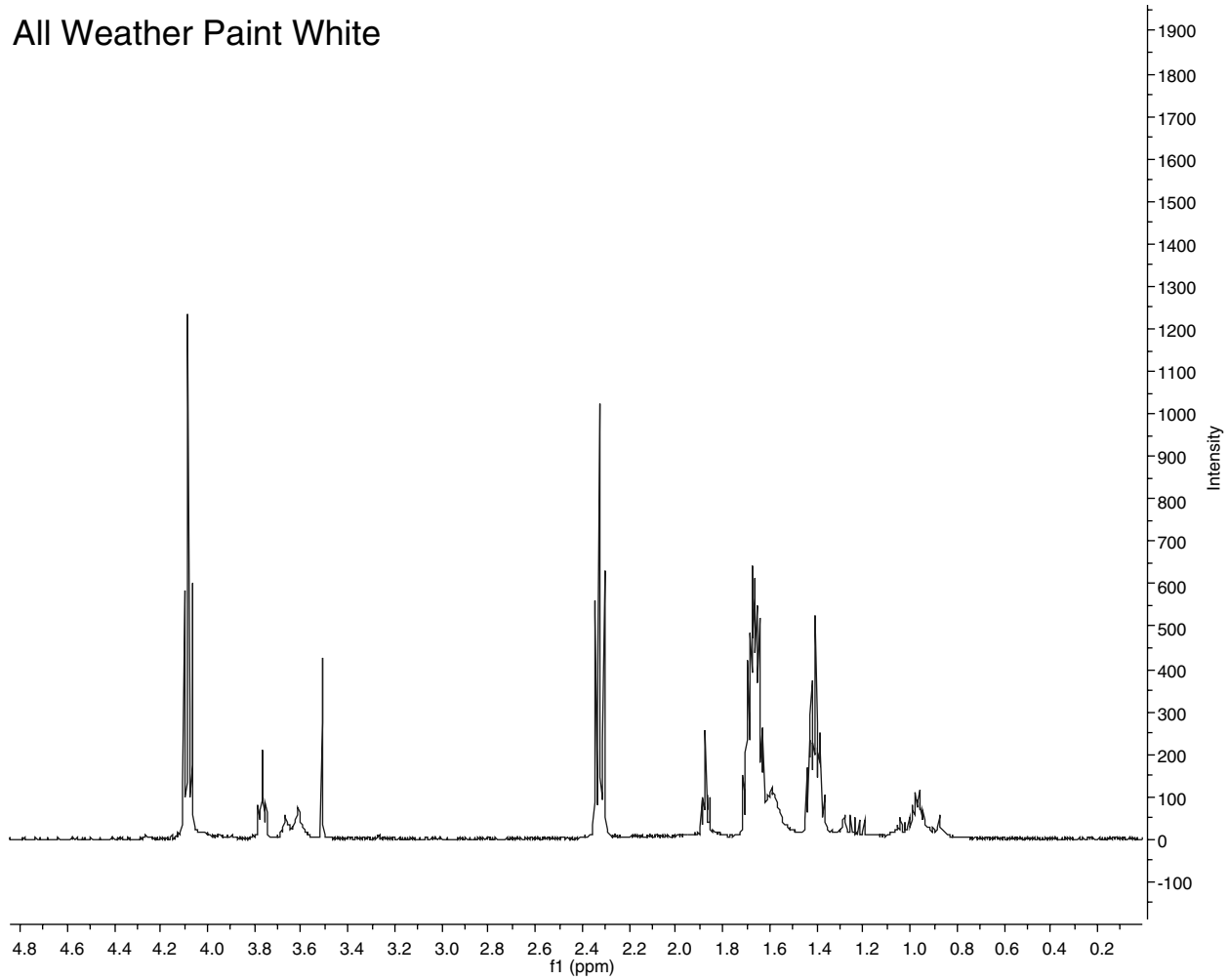

Figure M.5. NMR spectrum for 3M All Weather white paint.

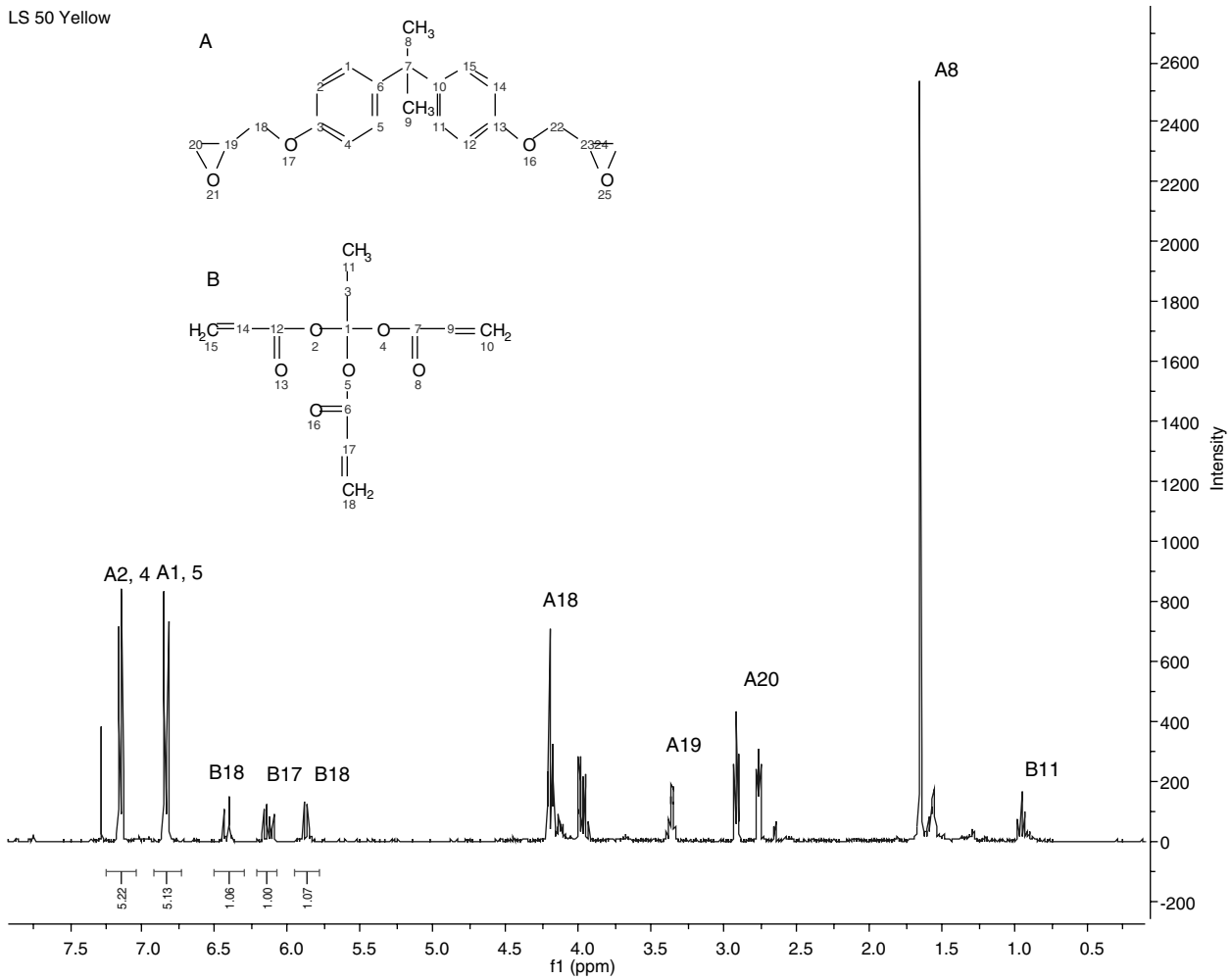

Figure M.6. NMR spectrum for Epoplex LS50 yellow paint.

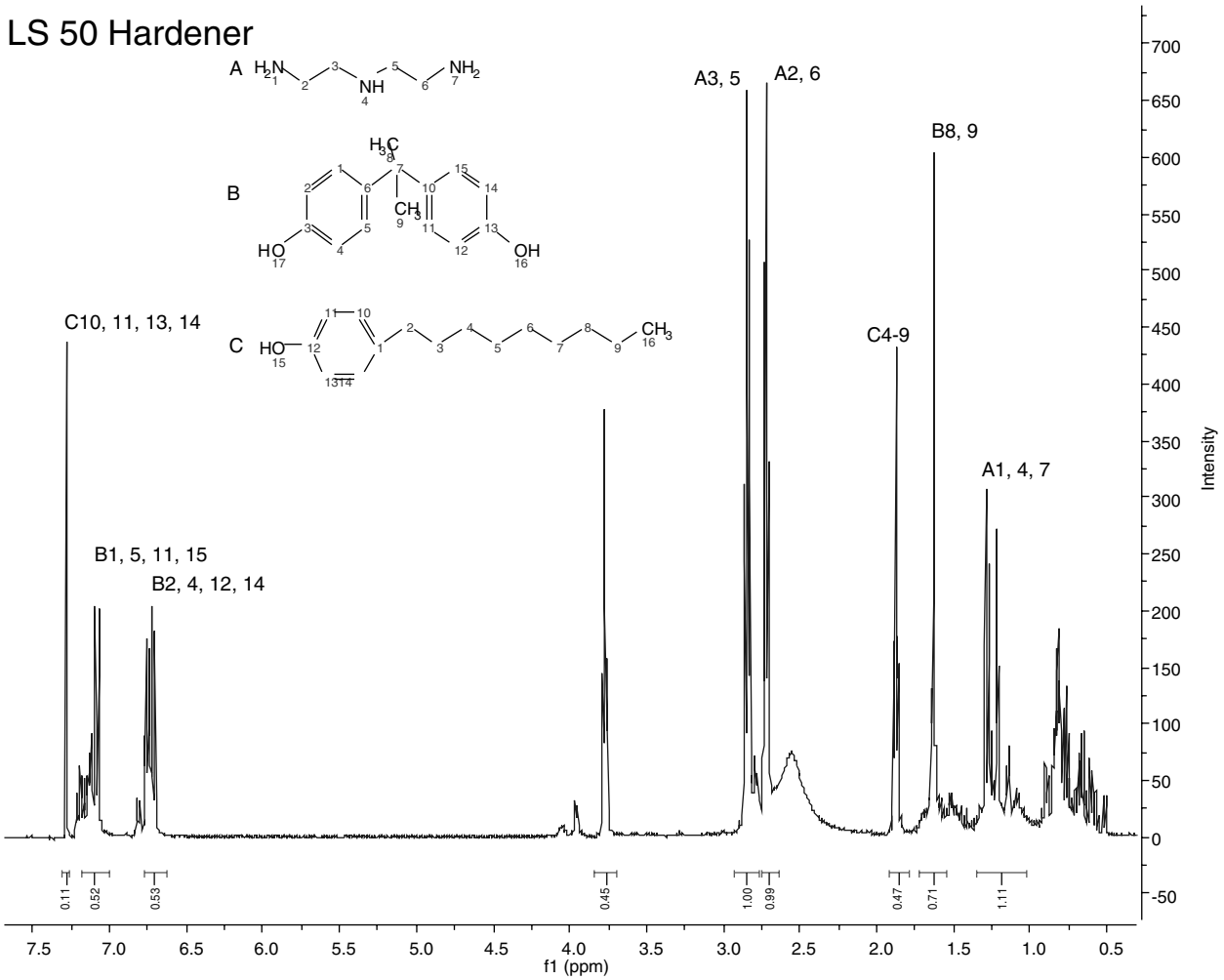

Figure M.7. NMR spectrum for Epoplex LS50 hardener.

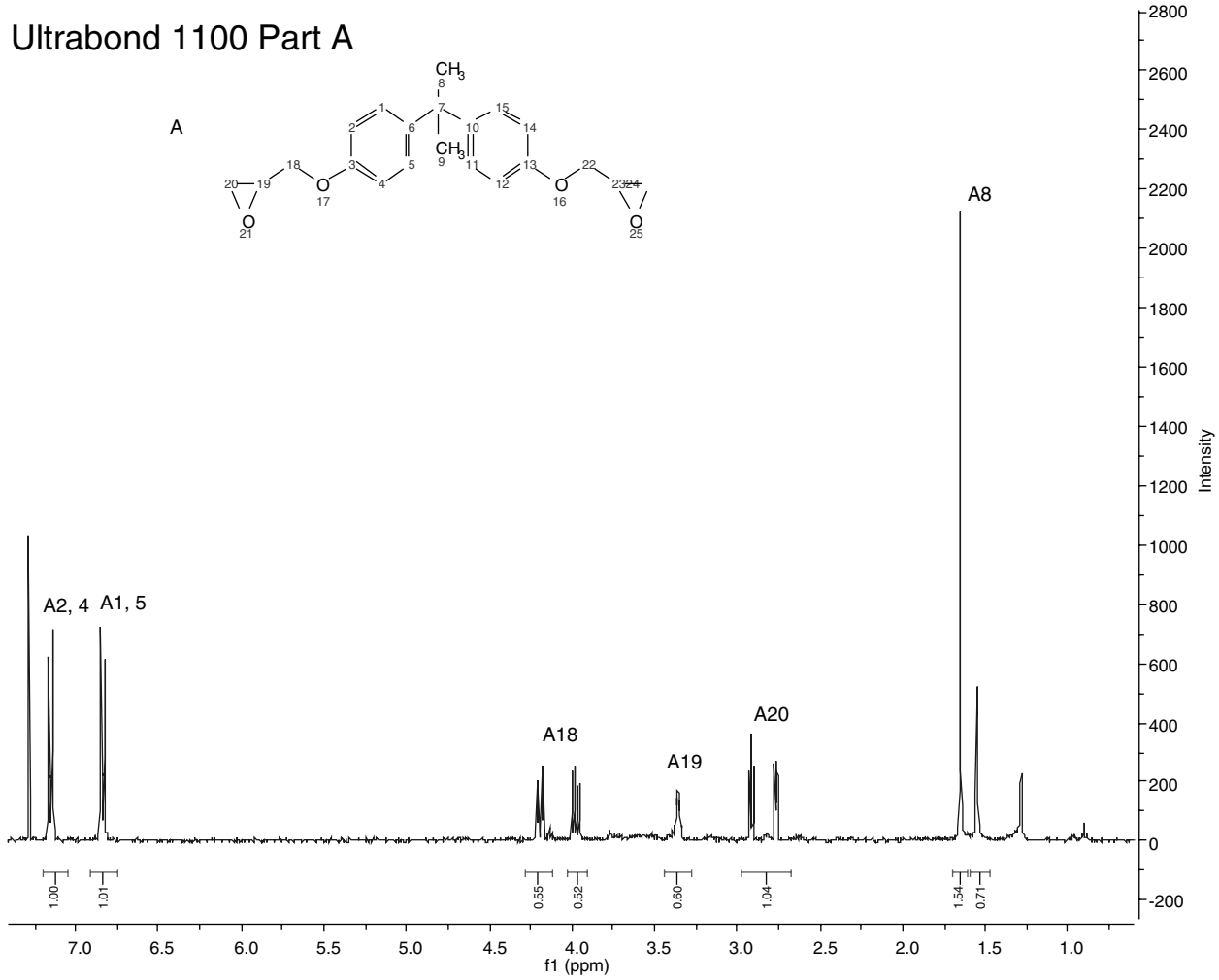

Figure M.8. NMR spectrum for Ultrabond 1100 Part A.

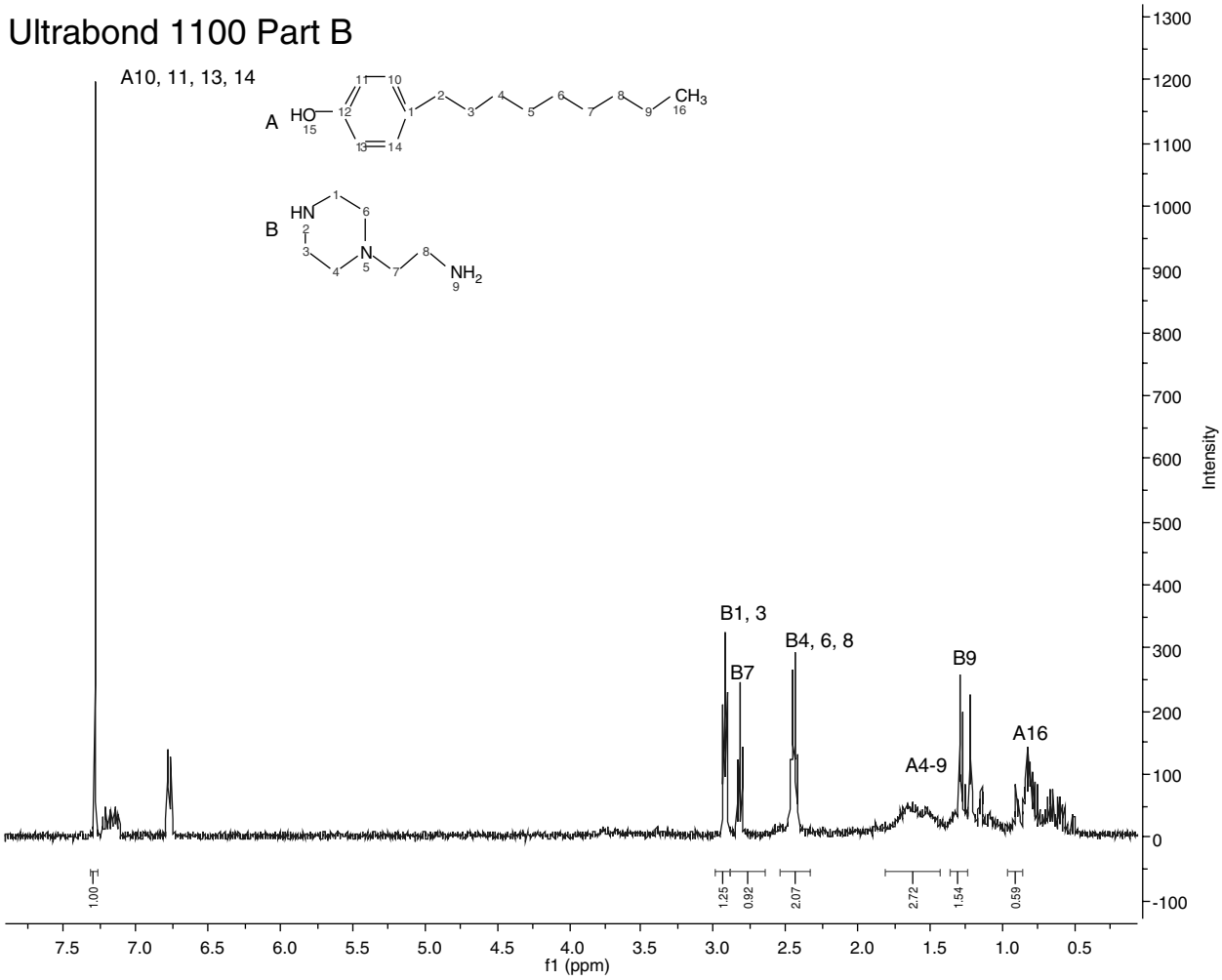

Figure M.9. NMR spectrum for Ultrabond 1100 Part B.

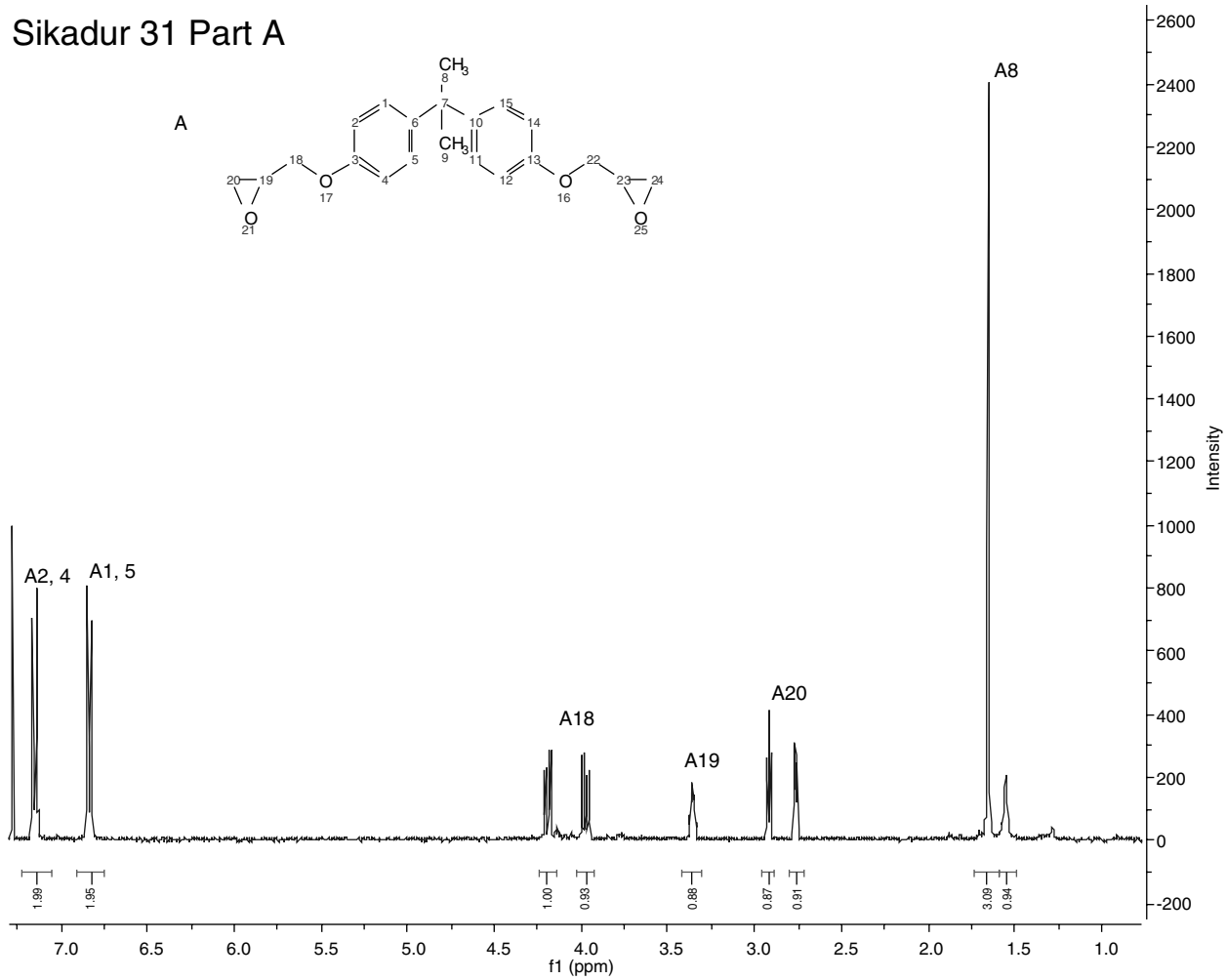

Figure M.10. NMR spectrum for Sikadur 31 Part A.

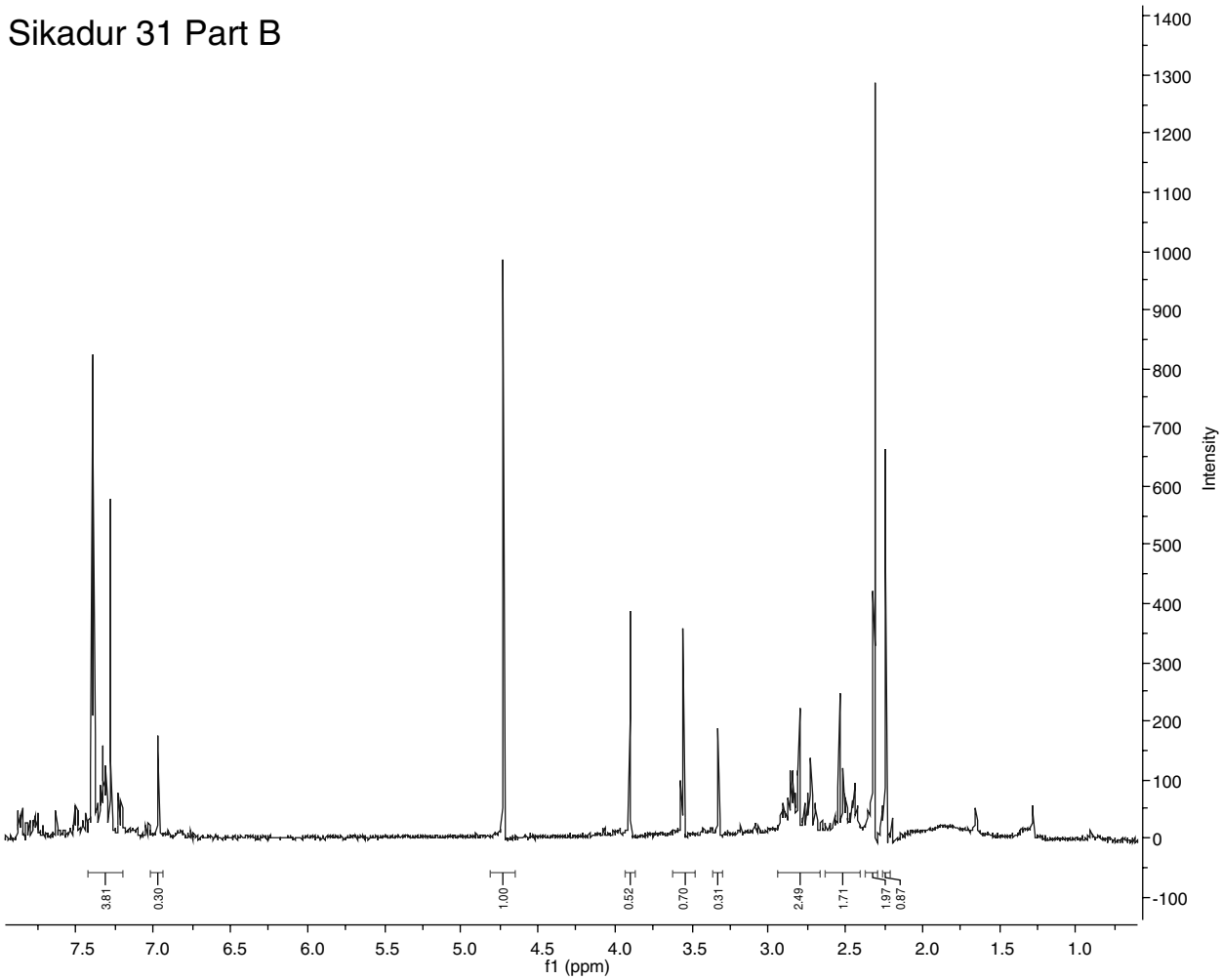

Figure M.11. NMR spectrum for Sikadur 31 Part B.

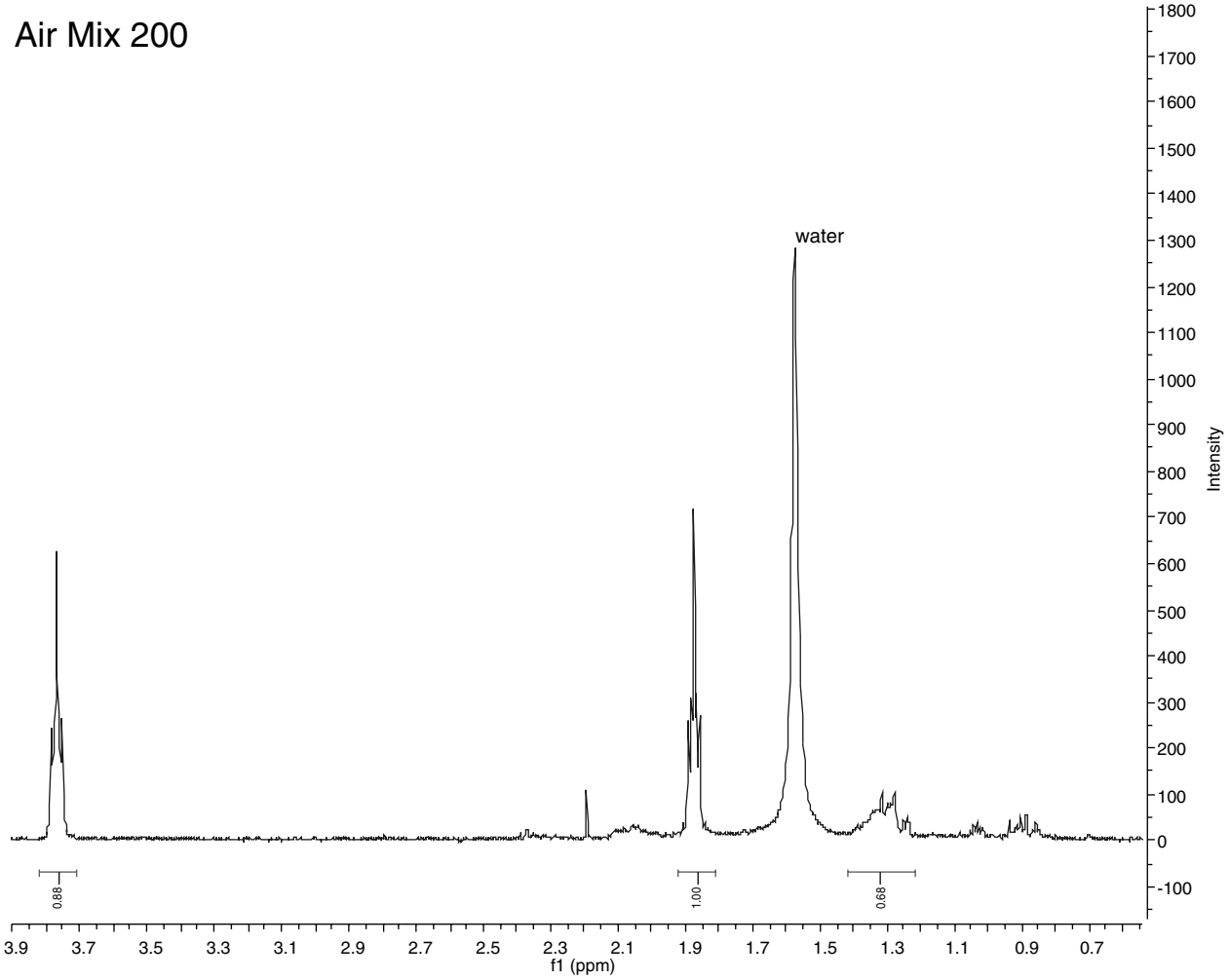

Figure M.12. NMR spectrum for Air Mix 200.

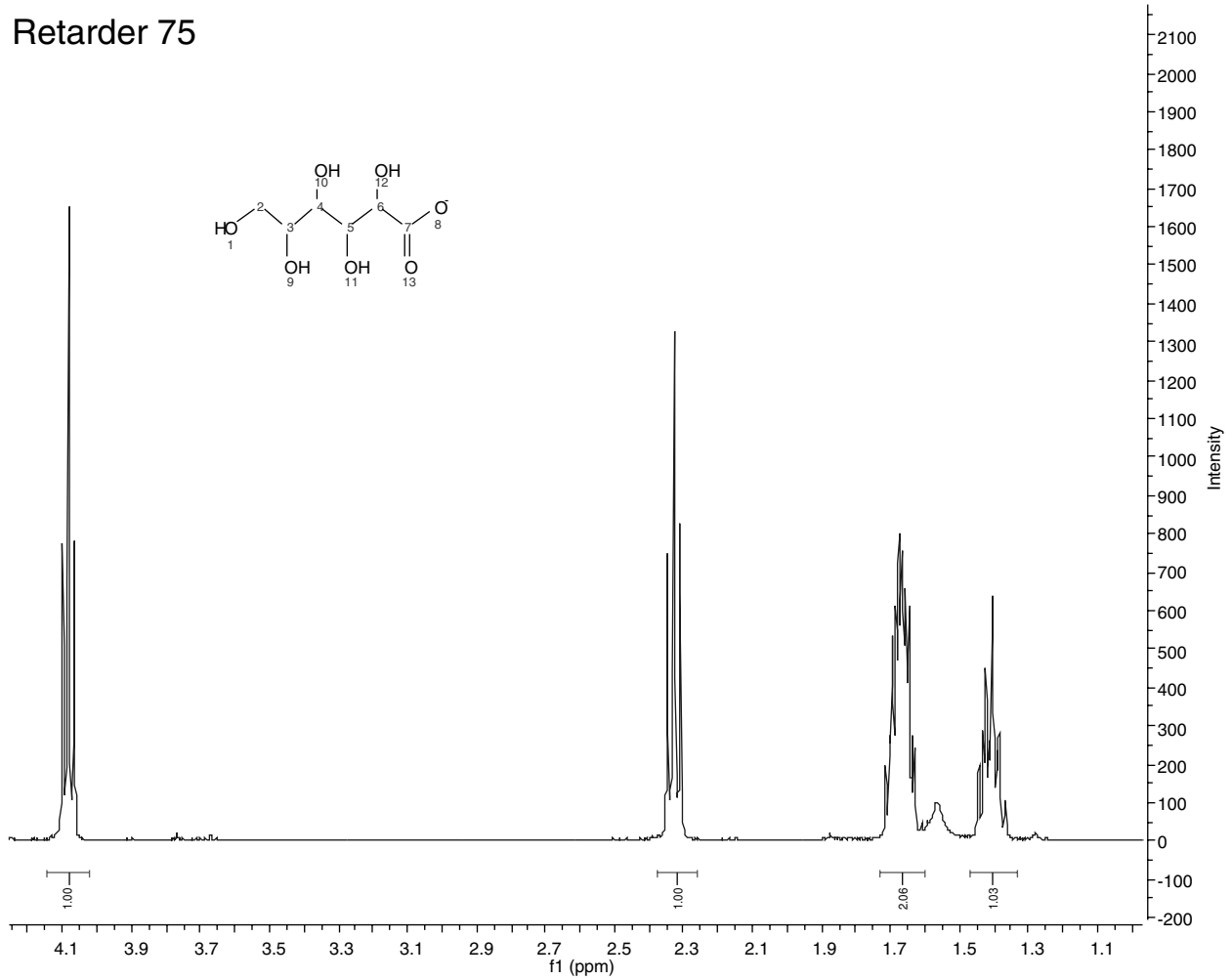

Figure M.13. NMR spectrum for Eucon Retarder 75.

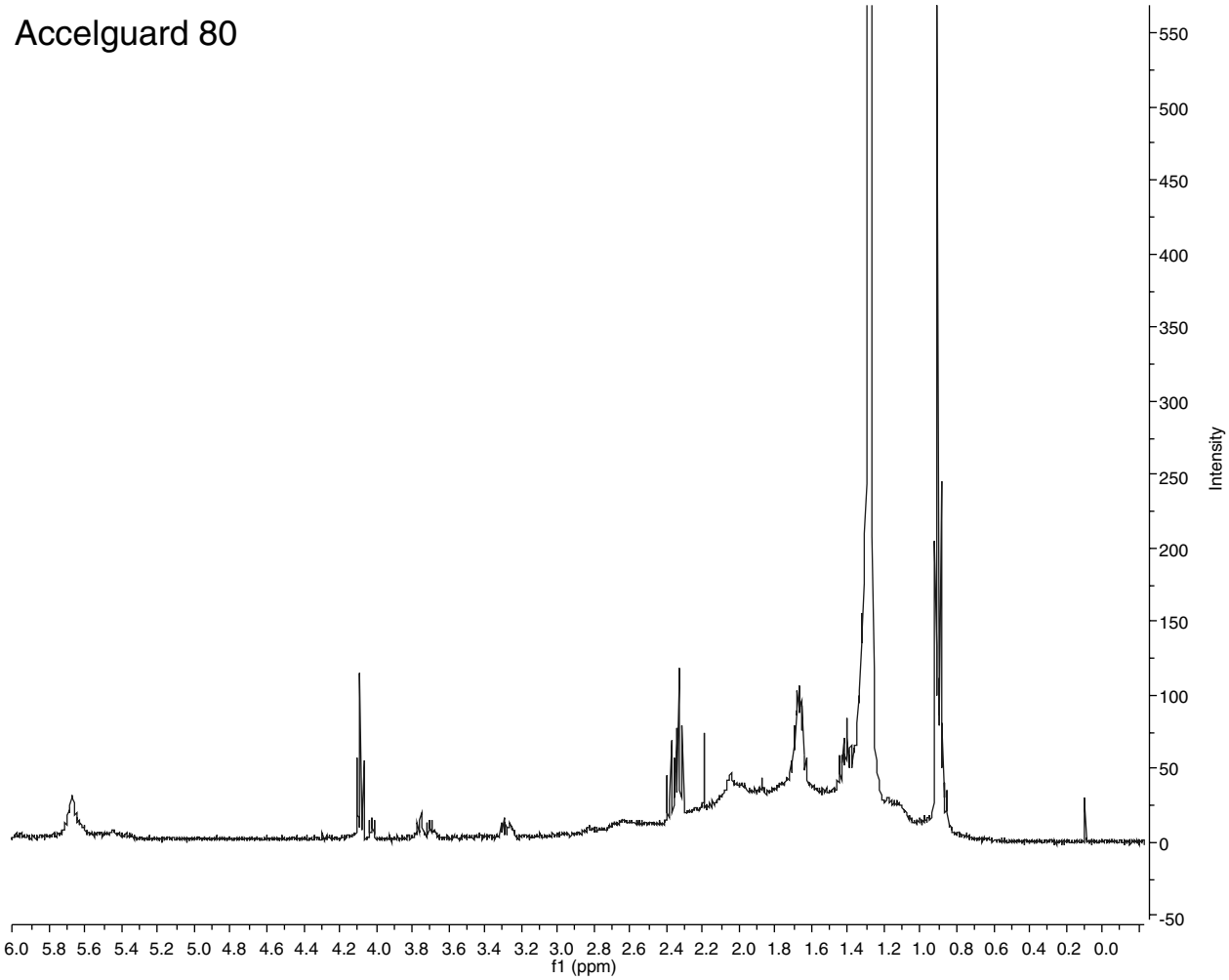

Figure M.14. NMR spectrum for Accelguard 80.

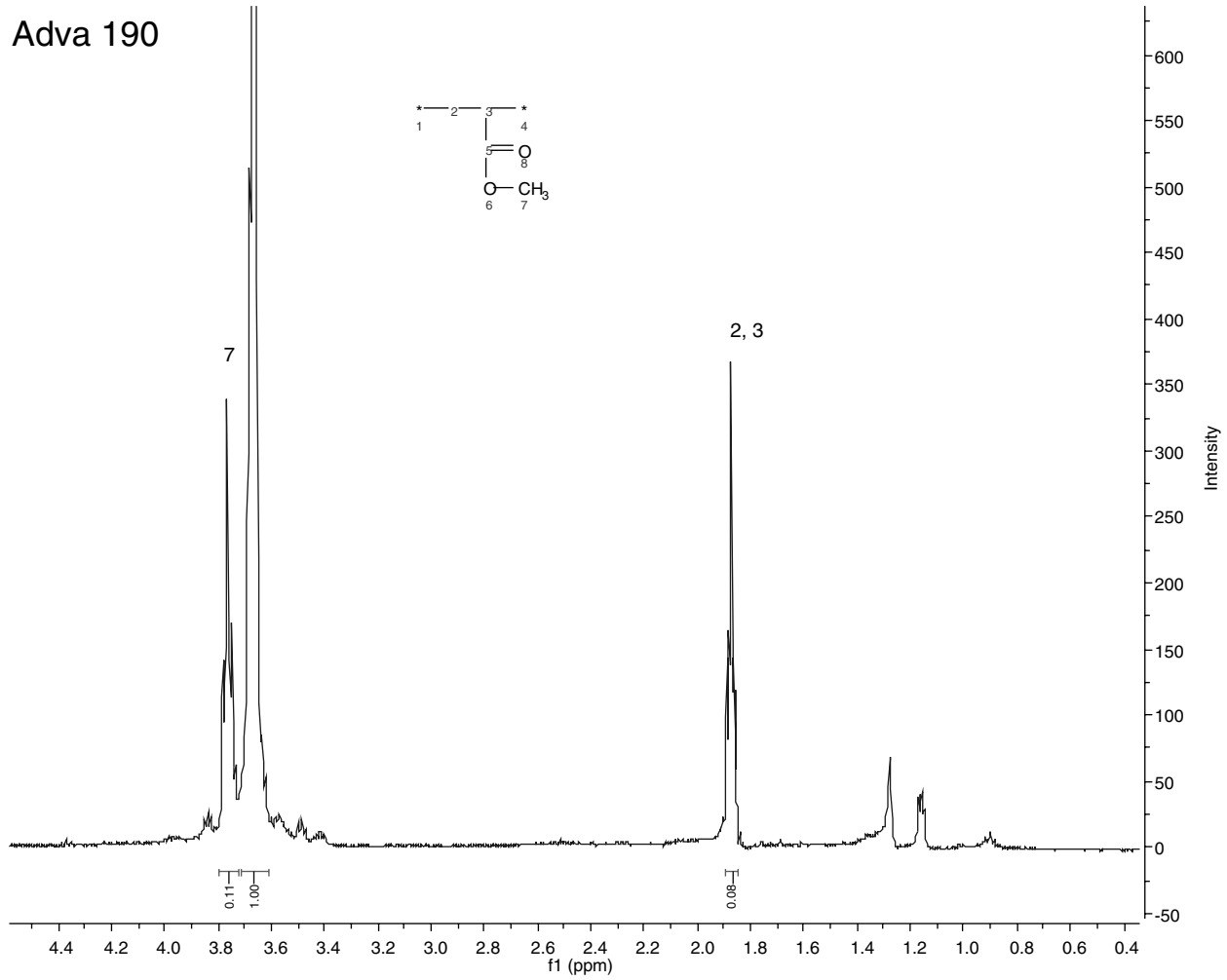

Figure M.15. NMR spectrum for ADVA 190.

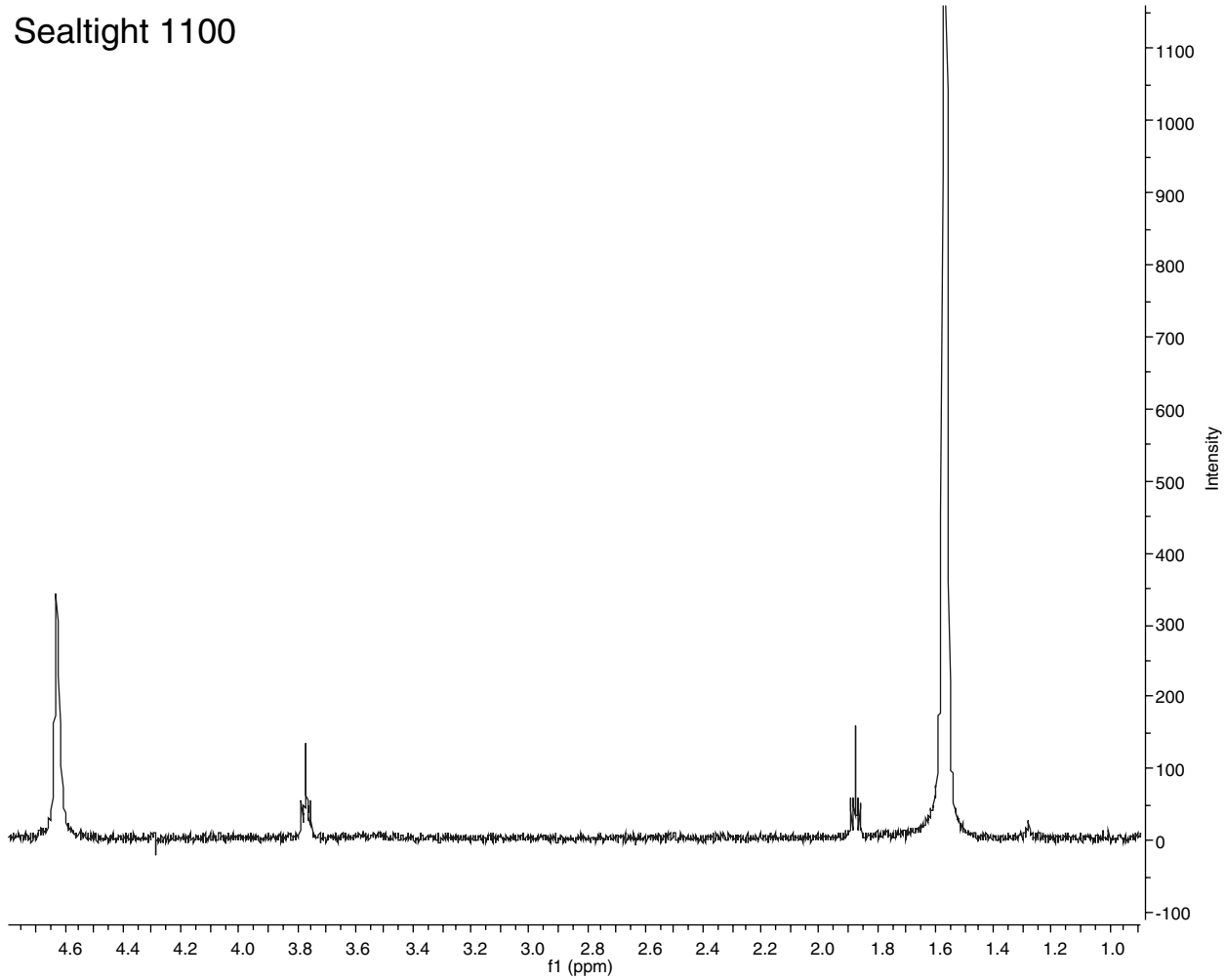

Figure M.16. NMR spectrum for Sealtight 1100.

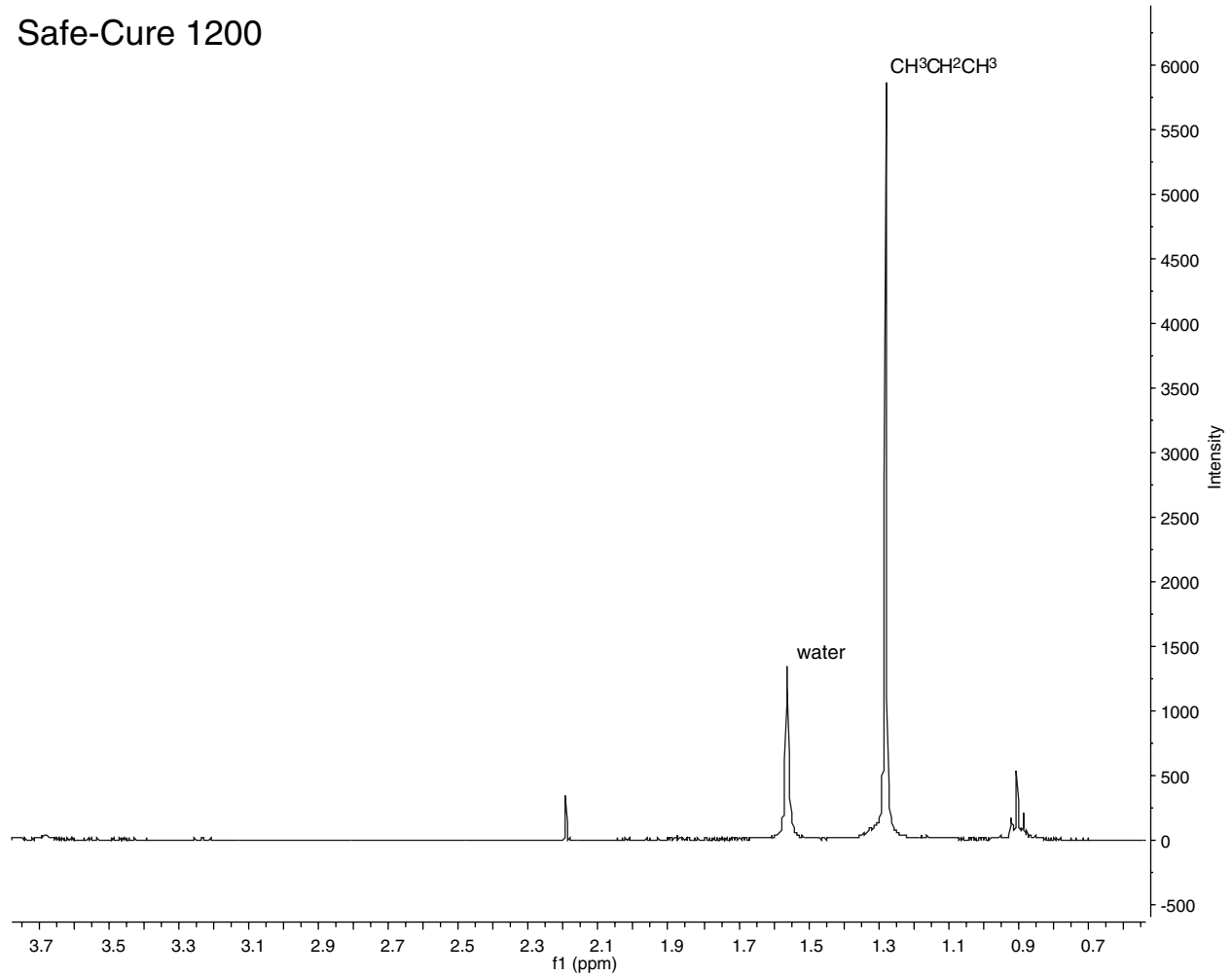

Figure M.17. NMR spectrum for Safe-Cure 1200.

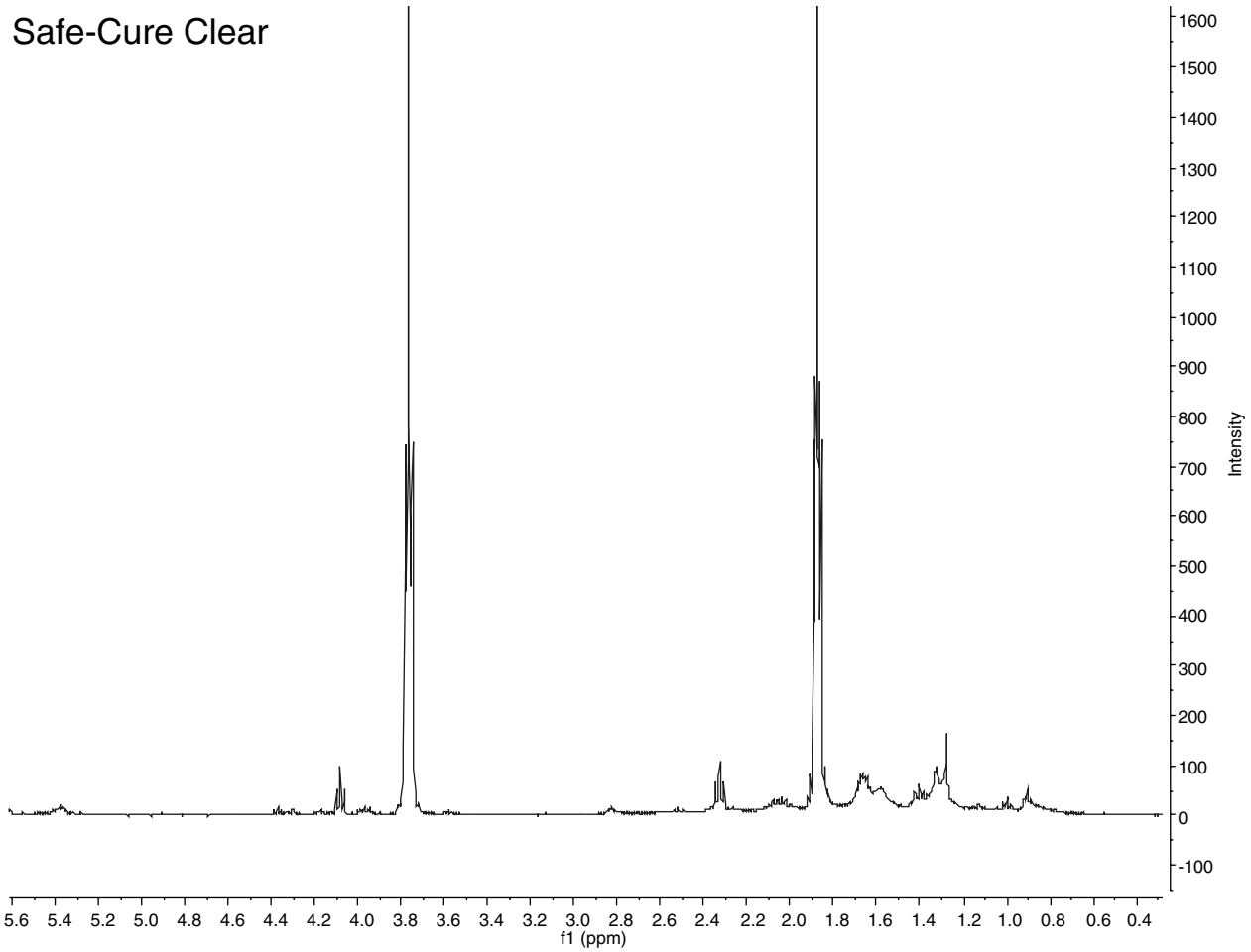

Figure M.18. NMR spectrum for Safe-Cure Clear.

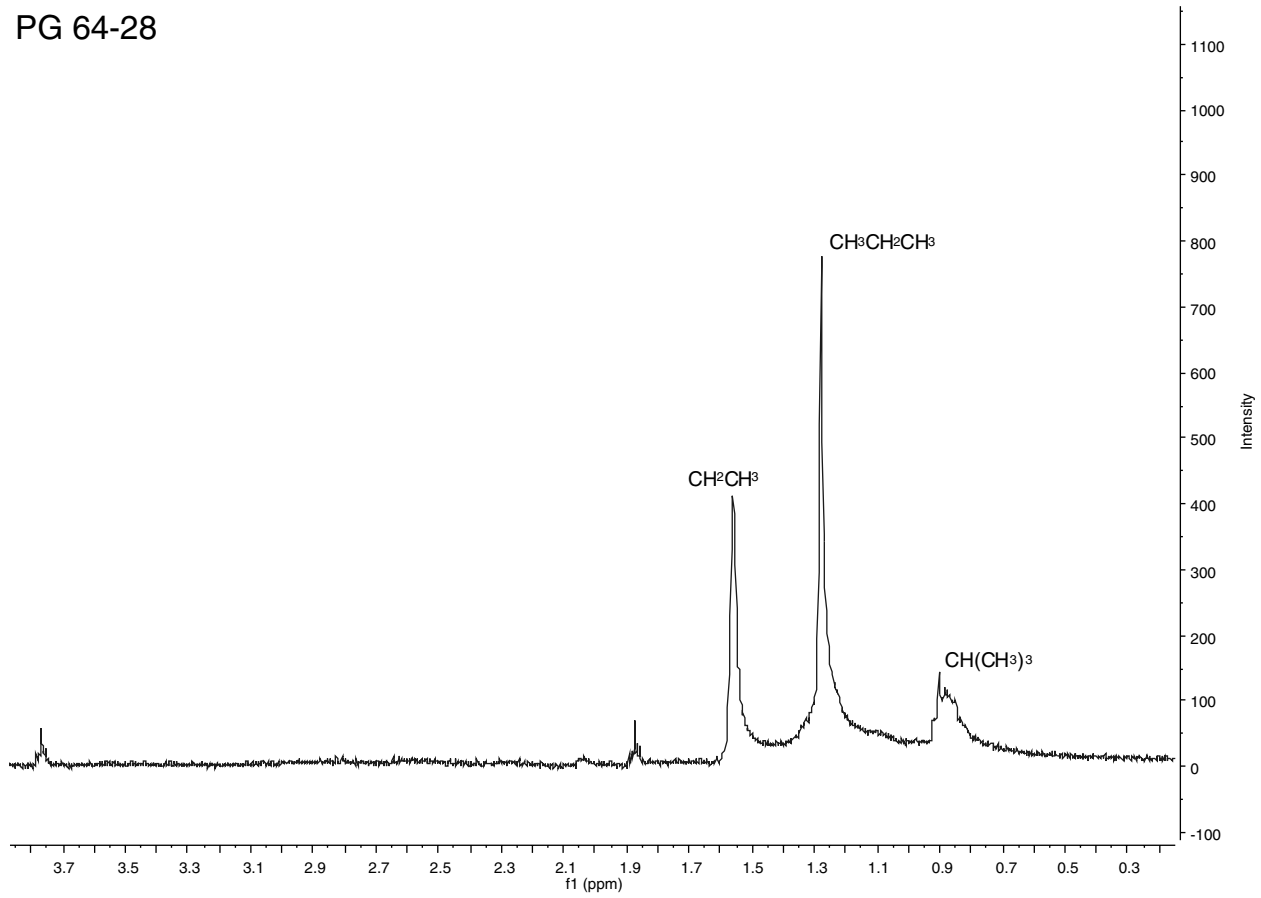

Figure M.19. NMR spectrum for PG 64-28 asphalt binder.

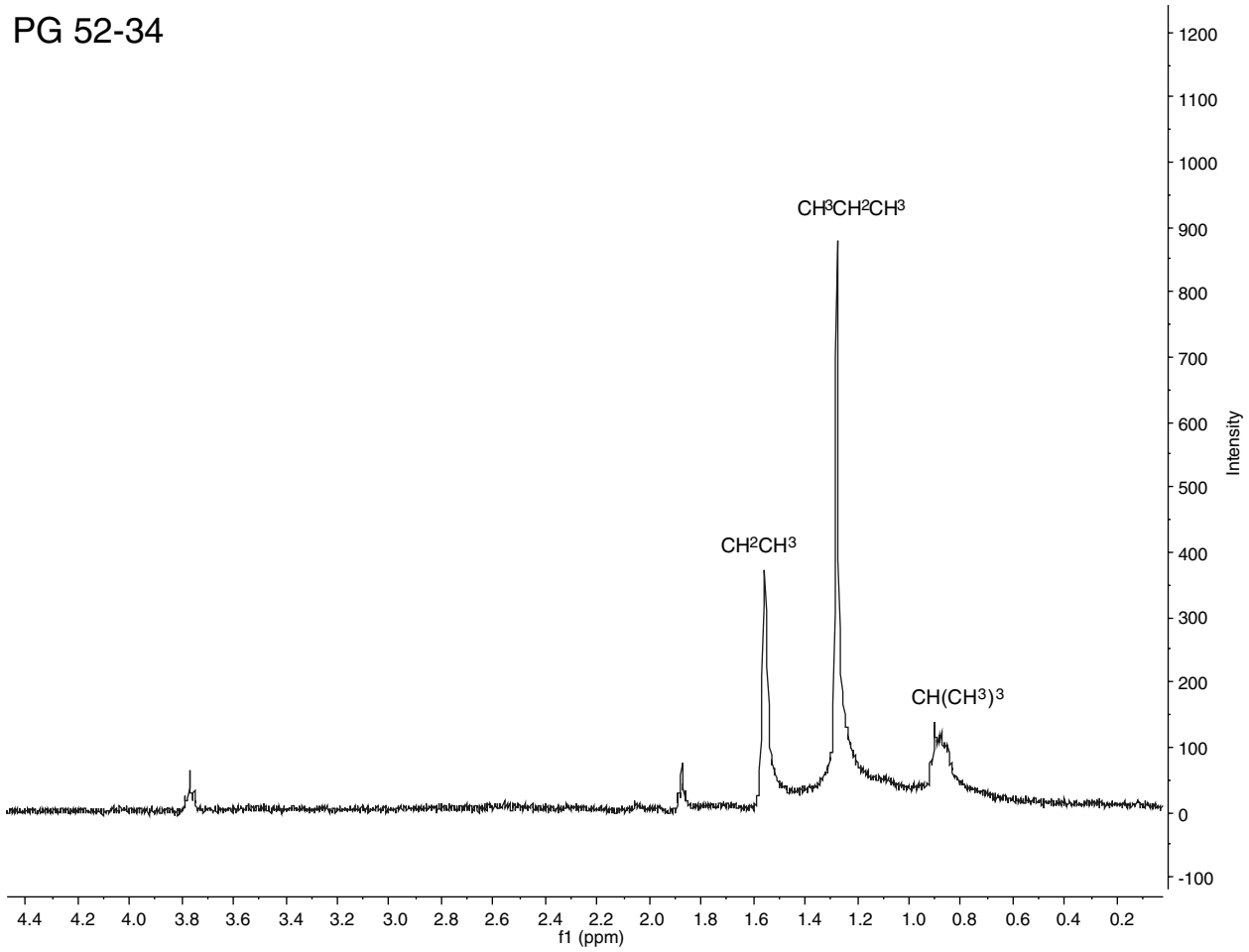

Figure M.20. NMR spectrum for PG 52-34 asphalt binder.

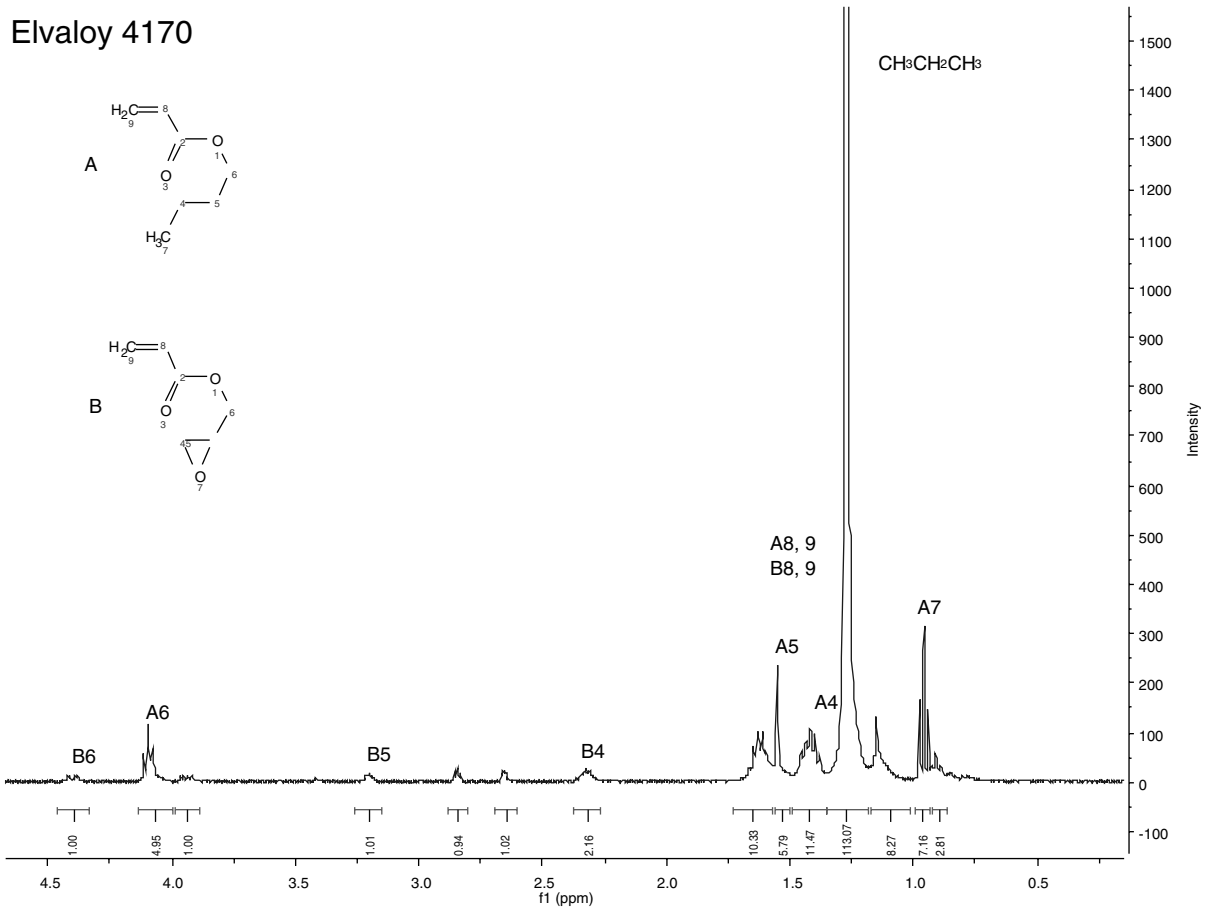

Figure M.21. NMR spectrum for Elvaloy 4170.

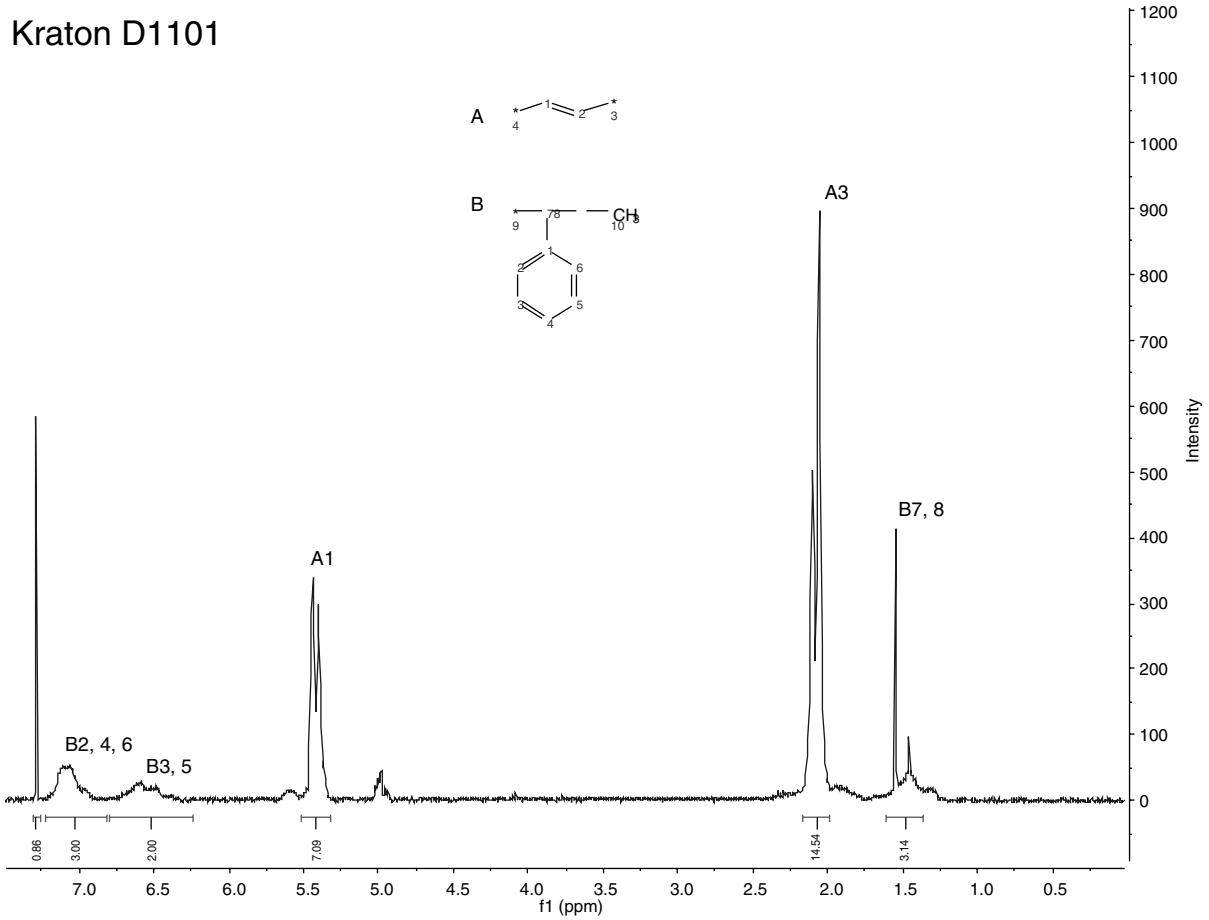

Figure M.22. NMR spectrum for Kraton D1101.

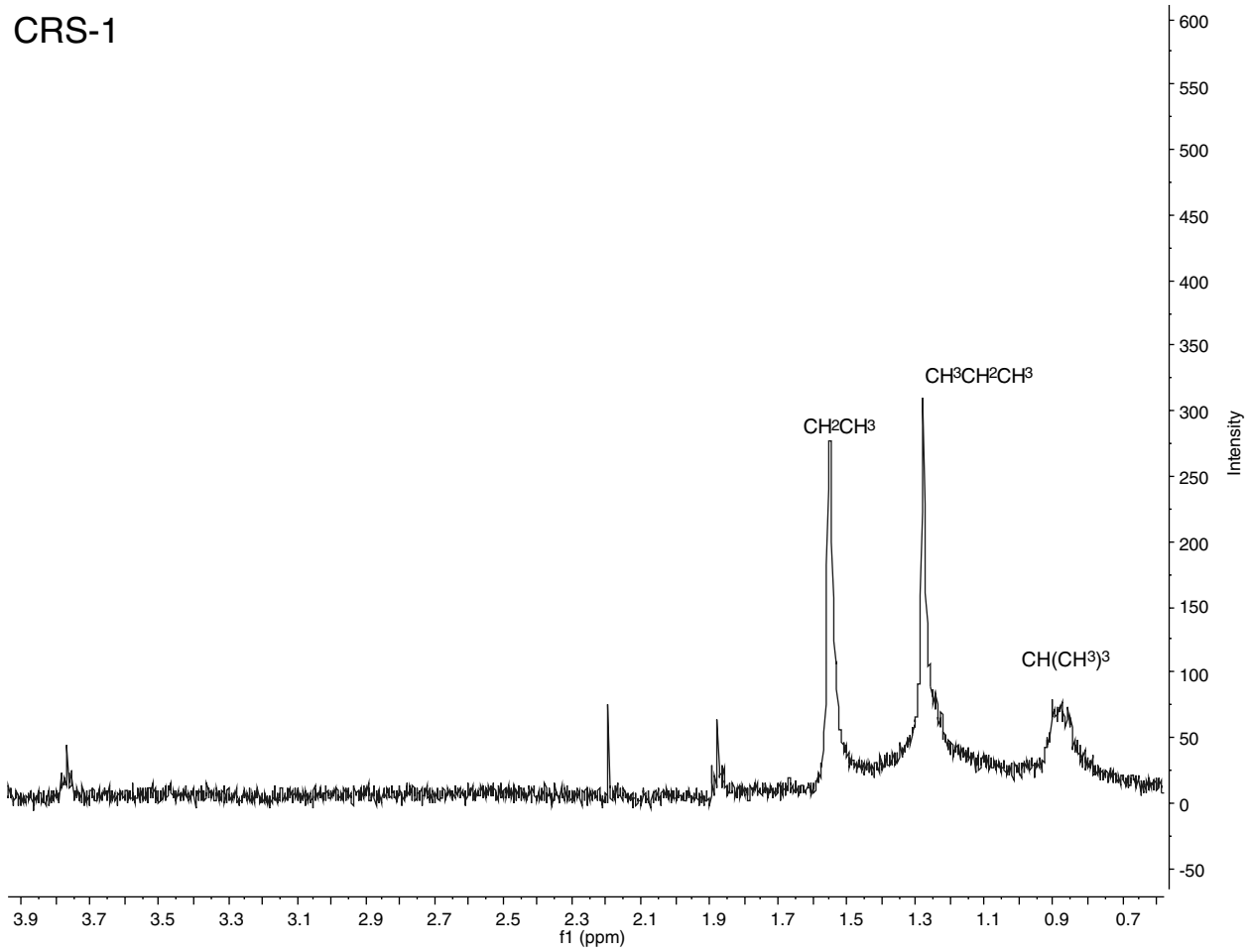

Figure M.23. NMR spectrum for CRS-1 asphalt emulsion.

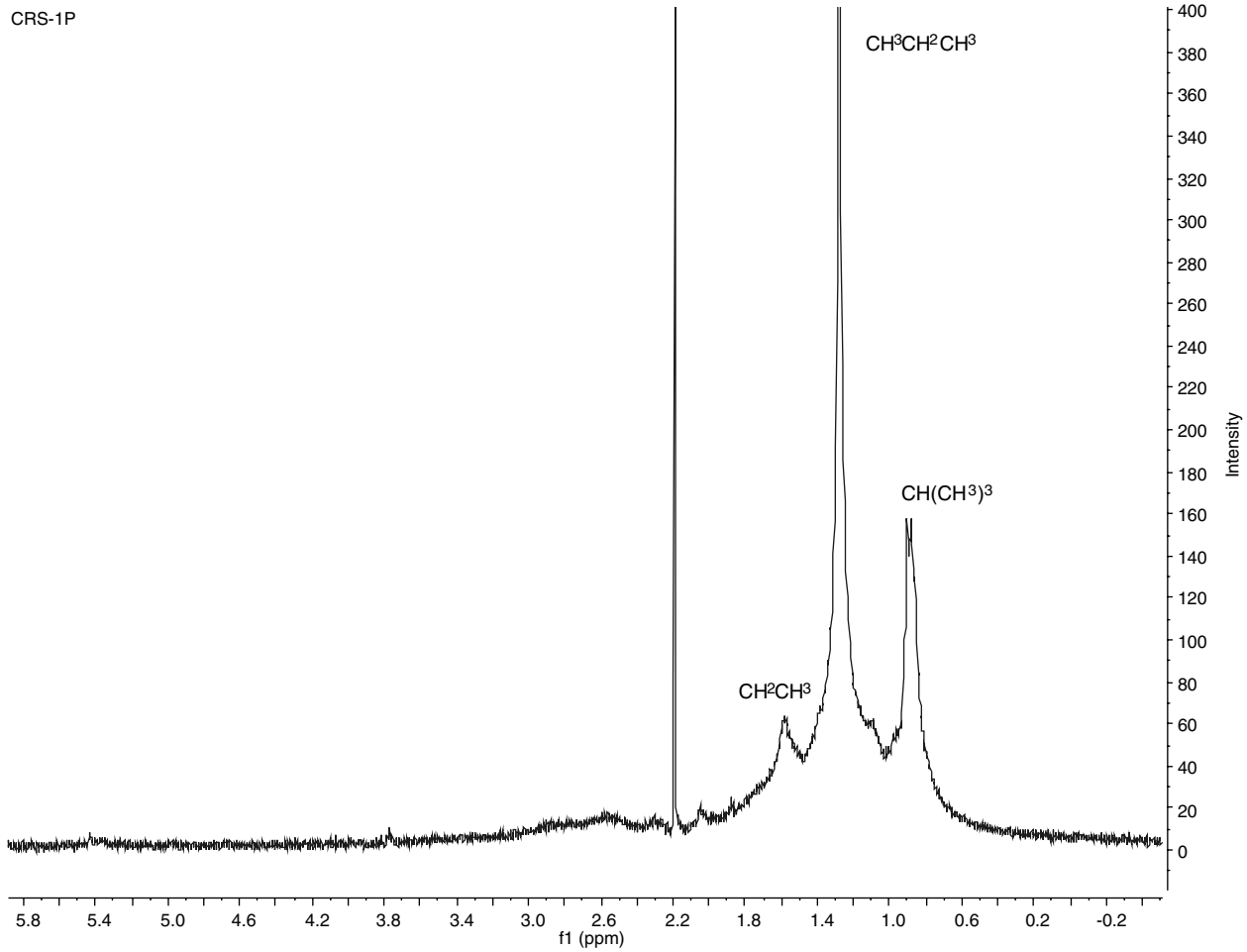

Figure M.24. NMR spectrum for CRS-1P asphalt emulsion.

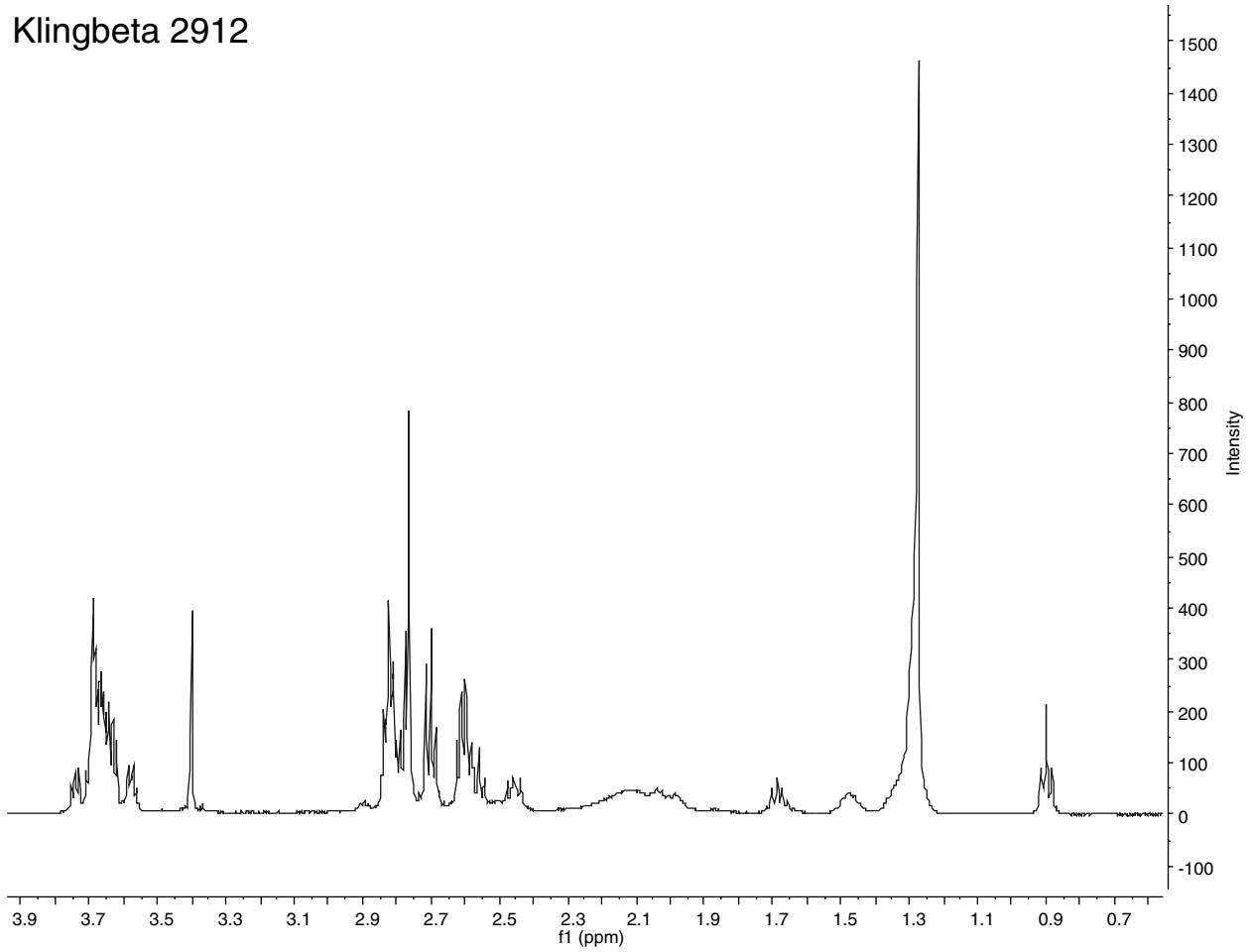

Figure M.25. NMR spectrum for Kling Beta 2912 antistripping agent.

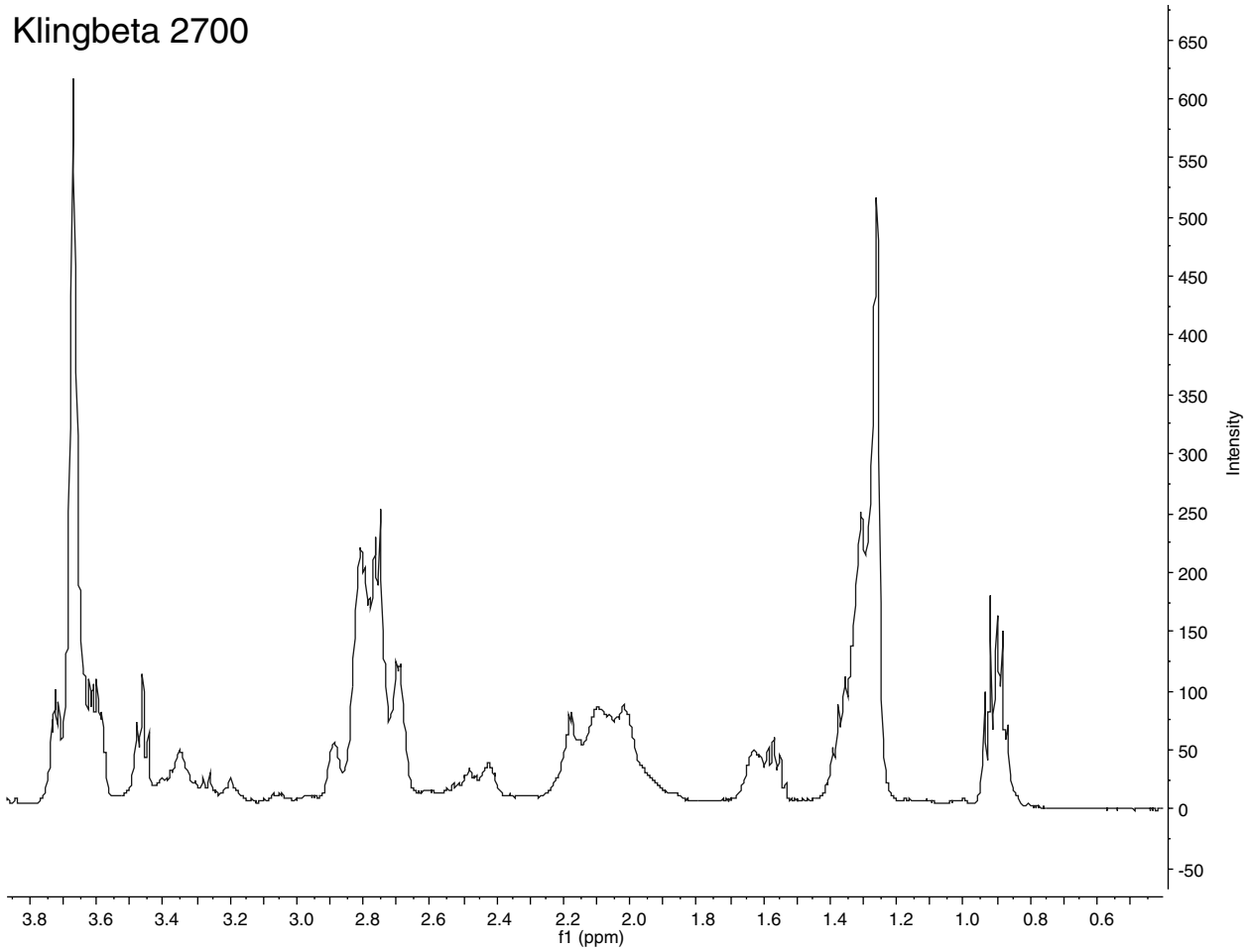

Figure M.26. NMR spectrum for Kling Beta 2700 antistripping agent.

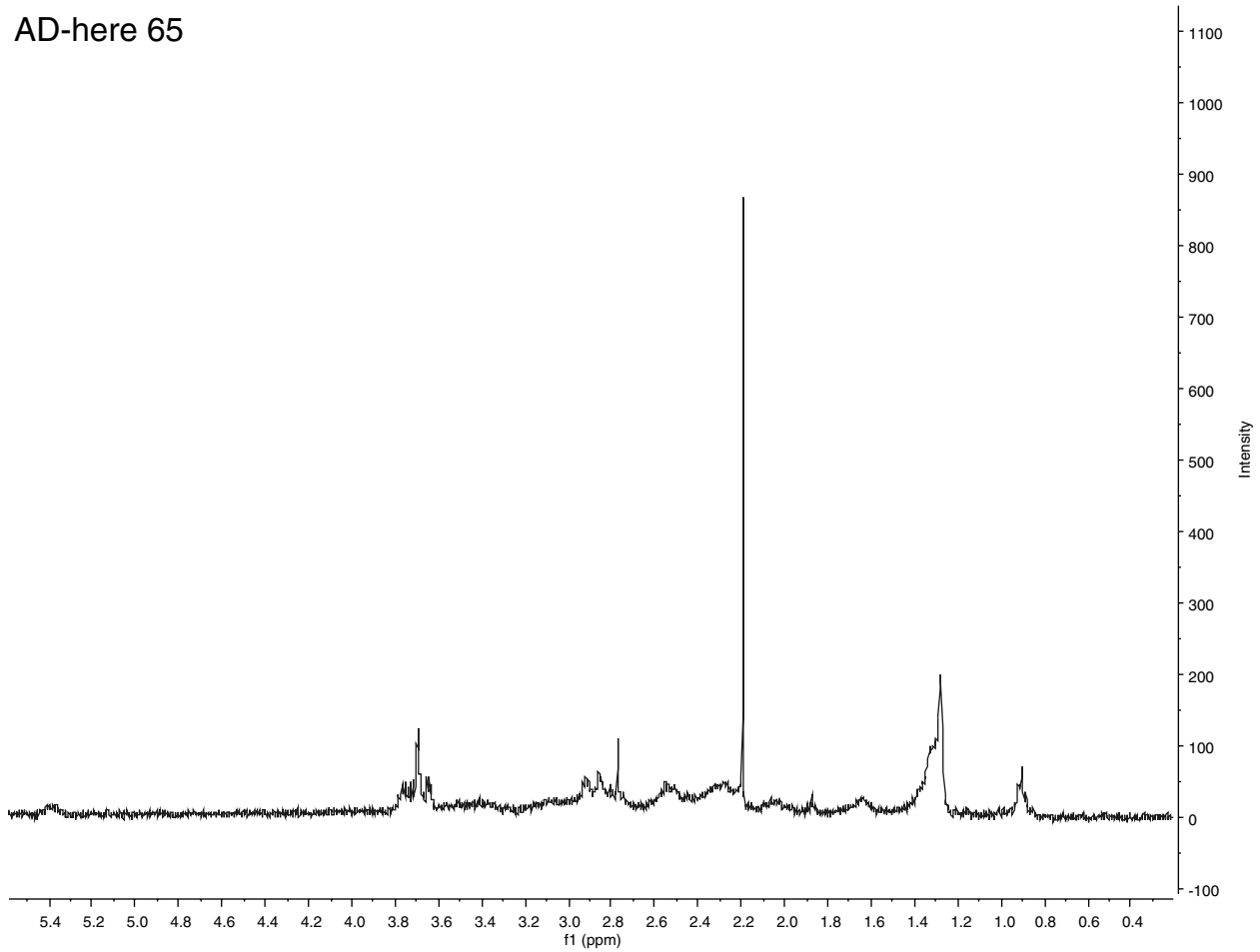

Figure M.27. NMR spectrum for AD-here 65 antistripping agent.

APPENDIX N

Quantitative Analysis of ATR FTIR Spectra

Peak-to-Peak Ratio

Quantification of SBS in Polymer-Modified Asphalt Binders

Three replicate binder–styrene–butadiene–styrene (SBS) mixtures for each of the SBS concentrations (1%, 3%, and 6%) were prepared over 2 months and scanned by the Bruker attenuated total reflectance (ATR) Fourier transform infrared (FTIR) spectrometer. The calibration equation for the quantification of SBS content in asphalt binder was developed based on the peak-to-peak ratio approach. Such an approach considered individual ratios of an absorption peak at either 966 cm^{-1} (A966) or at 700 cm^{-1} (A700) to the major peaks for which absorbance value did not change (e.g., A2920, A2850, A1460, and A1380 cm^{-1}). The A966 and A700 absorption values are respectively associated with polybutadiene and polystyrene. Because the ratio apparently changed with increasing SBS content, it was possible to choose the best suited ratio value based either on 966 cm^{-1} or 700 cm^{-1}. To achieve the best fit, the individual ratios of the two SBS-associated peaks were regressed on SBS content as in the example below:

$$A966/A2920 = \beta_0 + \beta_1 C + e \quad \text{(N.1)}$$

where

β_0, β_1 = regression coefficients,
C = polymer content, and
e = error.

In the first stage of the regression analysis, it was found that higher than 3 wt% polymer modification of binder resulted in significant deviation from linear trend expected by the Beer-Lambert law, as shown in Figure N.1. In addition, the variability in ATR measurements increased dramatically with change in SBS concentration from 3 wt% to 6 wt%. Therefore, 6 wt% SBS-modified samples were excluded from the analysis. When zero to 3 wt% modification was considered and outliers were removed from the data set, a similarly high goodness of fit was respectively achieved for both polystyrene and polybutadiene by using peak ratios A700/A2920 and A966/A2920 as predictors for polymer content C. Figure N.2 shows calibration trends along with trendline equations, goodness of fit (R^2), and standard error (SE).

Based on the R^2 values, it is suggested that the peak-to-peak ratio is a viable approach to quantification of styrene–butadiene polymers in asphalt binders. The main reason for variability in the ATR measurements is assumed to be nonuniformity of polymer-modified binder samples because of the differences in mixing procedures between replicate batches (e.g., time and temperature).

Valley-to-Valley Band Integration and Normalization

Oxidation of Polymer-Modified Binders and RAP

To quantify oxidation-related changes in the infrared (IR) absorption, band areas were computed using the following systematic procedure:

- Step 1. Collect the spectra as absorbance values (A) versus wave number ($\tilde{\nu}$). An absorbance value at each wavelength is calculated by dividing the measured absorbance value by the wavelength.
- Step 2. Apply atmospheric and water compensation and rubber-band baseline correction using default Bruker OPUS 6.5 software settings. The software calculates baseline as a frequency polygon, consisting of 64 baseline points. The "rubber band" is stretched between the spectrum end points, as it follows the spectrum minima (Figure N.3).
- Step 3. Smooth the spectrum line using the Savitzky-Golay algorithm (using a 10-point averaging interval and a third-order polynomial).

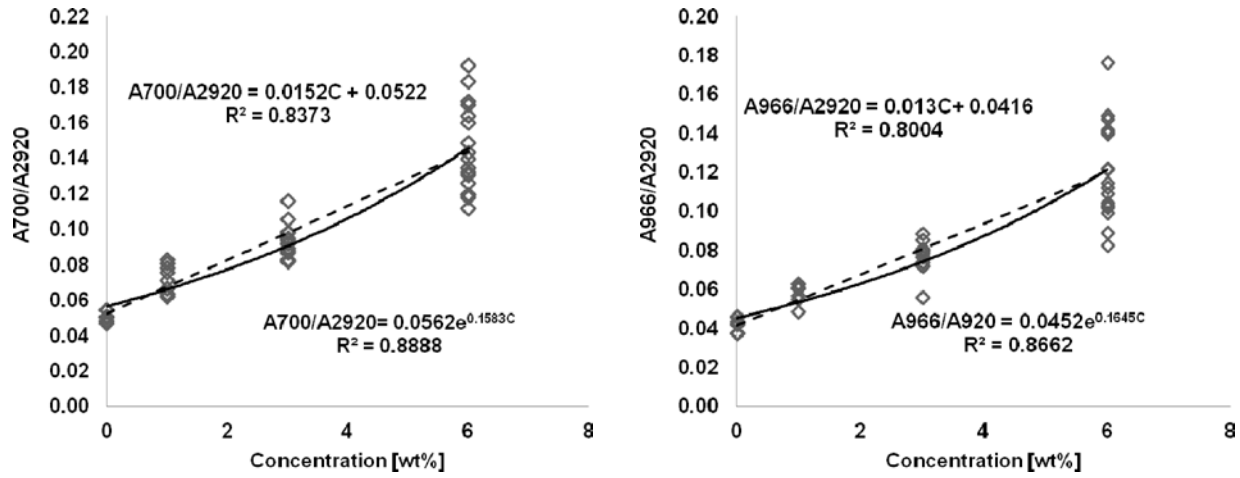

Figure N.1. Regression plots for peak ratios with all samples included.

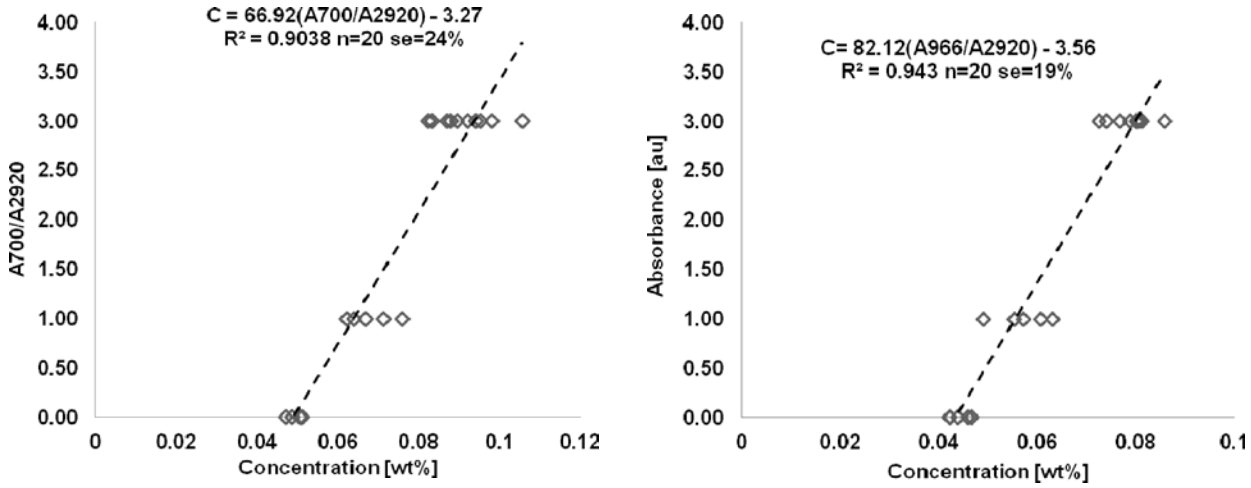

Figure N.2. Calibration equations for SBS concentration based on peak-to-peak ratios.

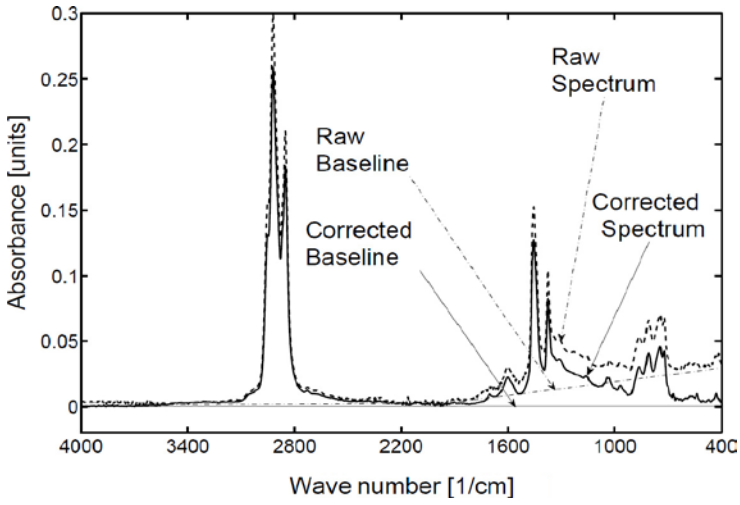

Figure N.3. Illustration of the rubber-band baseline correction.

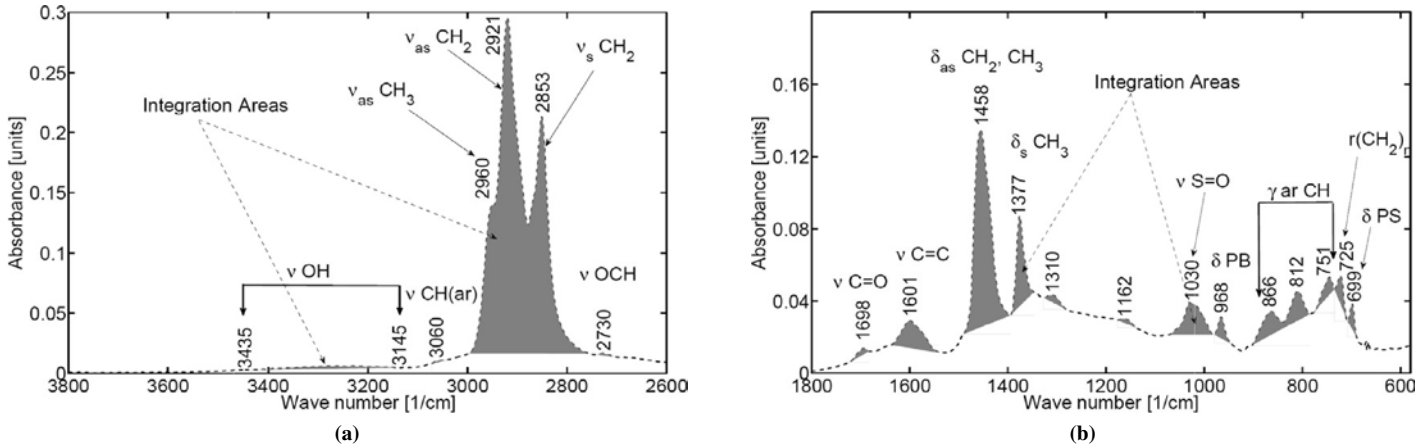

Figure N.4. Identification of bitumen components on FTIR spectrum in (a) region between 3,800 and 2,600 cm^{-1} and (b) fingerprinting region between 1,800 and 600 cm^{-1}.

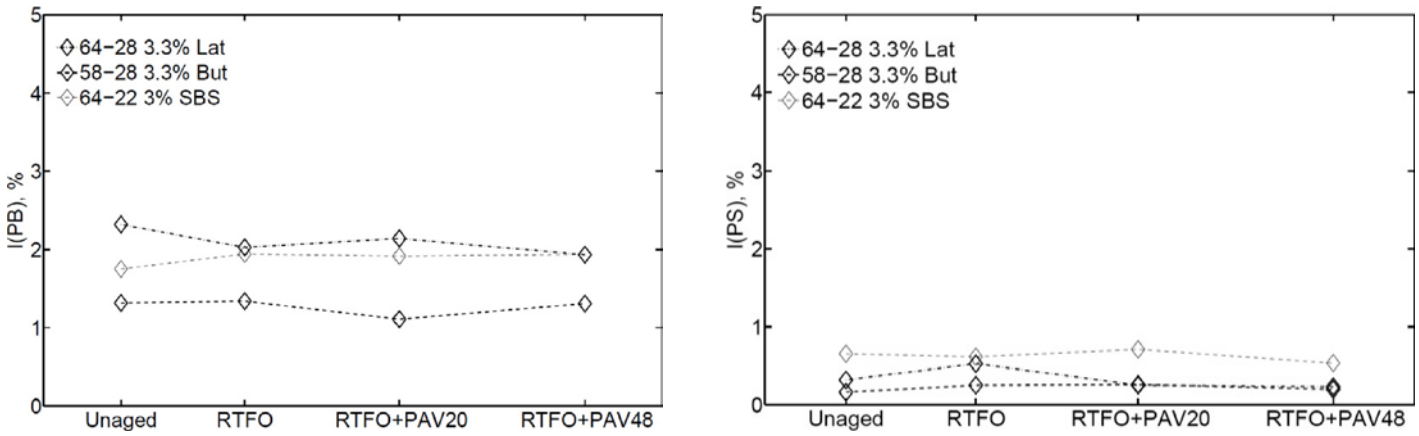

Figure N.5. Comparison of I_{PB} and I_{PS} between aged binders modified with 3 wt% of SB polymers.

- Step 4. Extract absorption peaks using a second-derivative approach.
- Step 5. Assign the extracted peaks to chemical functionalities in the bitumen sample (Figure N.4).
- Step 6. Compute band areas ($AR_{\tilde{\nu}}$) using valley-to-valley integration (Figure N.4).

The above procedure was automated using computational code developed in MATLAB 7.6.0 environment.

The $AR_{\tilde{\nu}}$ values were normalized to the total sum of all band areas ($\Sigma AR_{\tilde{\nu}}$), and the indices[24] for the aromatic, oxygen-containing, and polymer-related absorption bands were computed as follows:

- Aromaticity Index $I_{AR} = AR_{1600}/\Sigma AR_{\tilde{\nu}}$
- Carbonyl Index $I_{CO} = AR_{1700}/\Sigma AR_{\tilde{\nu}}$
- Sulfoxide Index $I_{SO} = AR_{1030}/\Sigma AR_{\tilde{\nu}}$
- Hydroxyl Index $I_{OH} = AR_{3400-3100}/\Sigma AR_{\tilde{\nu}}$
- Polybutadiene Index $I_{PB} = AR_{968}/\Sigma AR_{\tilde{\nu}}$
- Polystyrene Index $I_{PS} = AR_{700}/\Sigma AR_{\tilde{\nu}}$

The changes in the above indices over the aging cycle served as indicators of the oxidation rate and polymer degradation, as discussed in the following text.

The change in polybutadiene and polystyrene index values served as an indicator of the change in polymer content during accelerated aging by rolling thin-film oven and pressure aging vessel procedures. No statistically significant changes in polymer-related indices (I_{PS} and I_{PB} for polystyrene and polybutadiene content, respectively) throughout the aging cycle were found in this study (see Figure N.5). Note that the polymer content ranged between zero and 3.3 wt%. Such an outcome appears to be in line with the previous studies that reported swelling or degradation of SB-based polymers at concentrations higher than 4 wt%.

APPENDIX O

Quantitative Analysis of GPC and NMR Data

Quantitative Analysis of GPC Results

Polymer-Modified Asphalt Binders and Hot-Mix Asphalt

The chromatogram of the asphalt binder modified with styrene–butadiene–styrene (SBS) (Figure O.1) showed SBS peaks at an earlier elution time (15 to 19 min, as highlighted by the red box on figure) than asphalt binder (25 min). Figure O.2 shows a normalized chromatogram of SBS peaks that became larger as the amount of SBS increased. The peak areas for 1% SBS, 3% SBS, and 6% SBS were calculated and divided by the peak area corresponding to neat PG 64-22 binder. The peak area ratios for 1%, 3%, and 6% SBS were 0.00087, 0.0044, and 0.0085, respectively, which indicates a linear relationship with an $R^2 = 0.99$ (Figure O.4).

After the GPC method successfully identified the SBS component of the polymer-modified binder prepared in the lab, the SBS-modified PG 64-22 binder was mixed with aggregates to prepare three polymer-modified hot-mix asphalt (HMA) samples with concentrations of 1%, 3%, and 6% SBS, respectively. After the HMA mix was prepared, the binders were extracted from the HMA using D-chloroform solvent and injected into the GPC column. Figure O.3 shows a blown-up chromatogram for extracted SBS-modified binders with an obvious increase in the SBS-related peak area with increased amounts of SBS. The SBS-related peak areas for 1% SBS, 3% SBS, and 6% SBS were normalized to the area under the peak corresponding to a neat PG 64-22 binder and yielded values of 0.0011, 0.0020, and 0.0055, respectively.

Figure O.4 compares the normalized peak area values for SBS-modified binders and their corresponding mixes. The linear trends presented in the figure show high correlation for both binders and HMA mixtures.

In conclusion, GPC chromatogram can be used not only to qualitatively assess the presence of polymer modifiers but also to quantify the polymer content in asphalt binders and HMA mixtures.

RAP–Containing Asphalt Binders and HMA

Evaluating the oxidation level in recycled asphalt pavement (RAP)-containing asphalt binders and HMA mixes was an important part of the Phase 2 experimental design. Initially, RAP-modified binder blends were produced by mixing neat PG 64-22 binder with the RAP binder extracted from the RAP supplied by Tilcon-Old Castle Company from two separate stockpiles located in Manchester and Waterbury, Connecticut, which are denoted by TLCM and TLCW. Figure O.5 shows GPC chromatograms of the neat PG 64-22 and two RAP-modified blends. The shoulder seen in the figure suggests a minor peak for the component with a higher molecular weight eluting after 21 min, as opposed to the main peak corresponding to the main component (neat binder) eluting after 25 min. A higher molecular weight may indicate the presence of oxidatively cross-linked material resulting from the oxidation of RAP.

The next step was to quantify the amount of RAP added to the virgin HMA mix based on an analysis of the GPC chromatograms of the HMA mixes prepared with different RAP contents. For this purpose, samples of HMA mixes with concentrations of 0%, 10%, 20%, 30%, 40%, 50%, 60%, and 80% RAP were prepared. The binders were extracted from the resulting mixtures and the extracted components were injected into the GPC column. Figure O.6 shows a blown-up chromatogram of the RAP-modified HMA samples at elution times ranging from 21 to 22 min. The shoulder, located at an approximate elution time of 21 min, seems to be increasing with the increase of RAP. The deconvolution of GPC spectra into separate RAP (21.7 min) and virgin binder (24.8 min) peaks is illustrated in Figure O.7.

Figure O.8 shows the relationship between the RAP content and the area ratio of the RAP peak relative to the binder peak. The trend in Figure O.8 shows a large spread of values

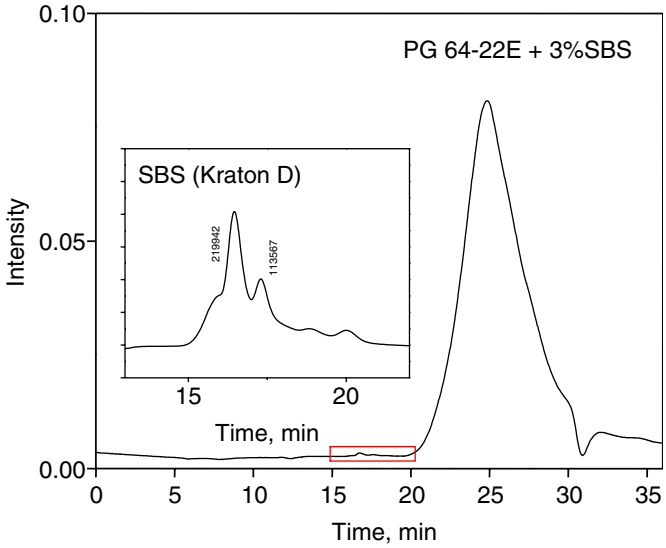

Figure O.1. GPC chromatogram of PG 64-22 binder modified with 3% SBS.

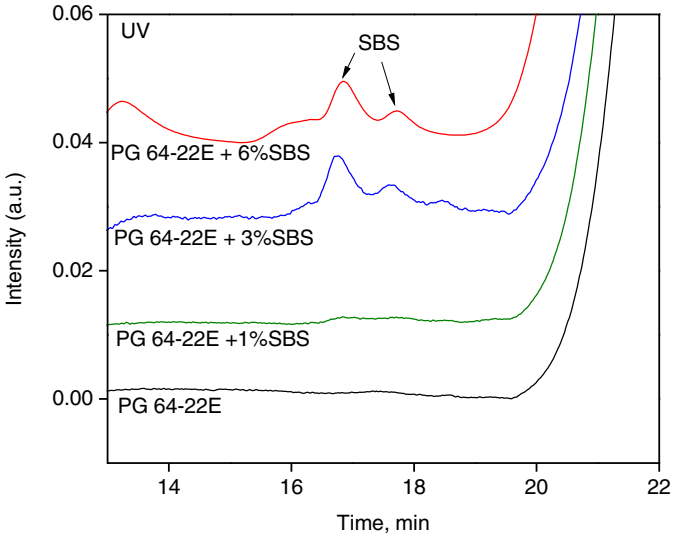

Figure O.2. Close-up of GPC chromatogram of normalized SBS peaks for PG 64-22 binders modified with 1%, 3%, and 6% SBS.

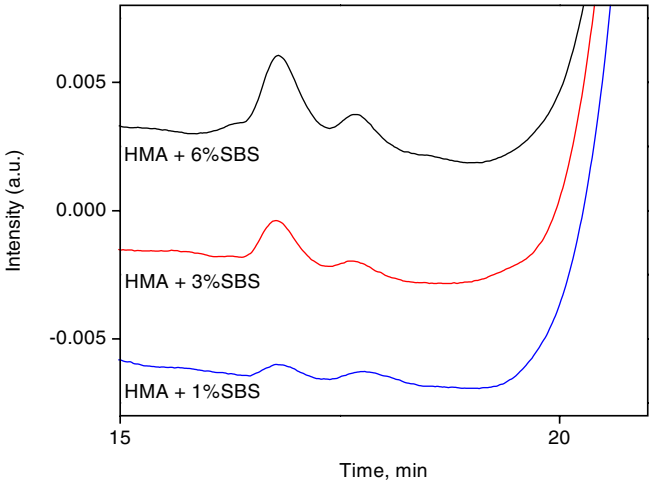

Figure O.3. Zoomed GPC chromatogram of normalized SBS peaks for 1%, 3%, and 6% SBS-modified HMA mixes.

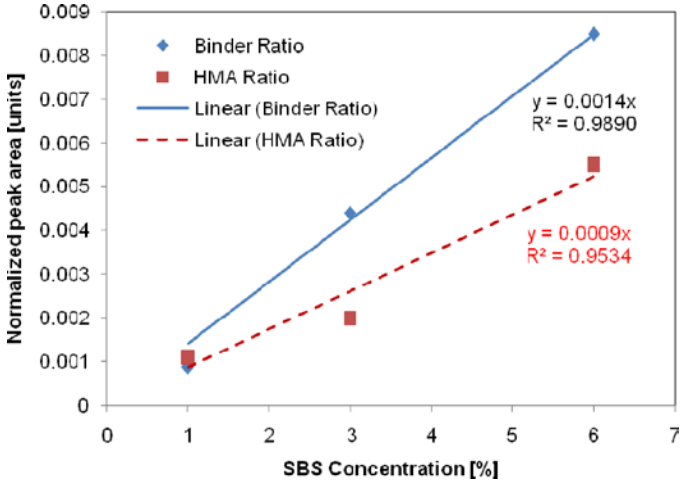

Figure O.4. Linear relationship between SBS concentration and GPC peak area.

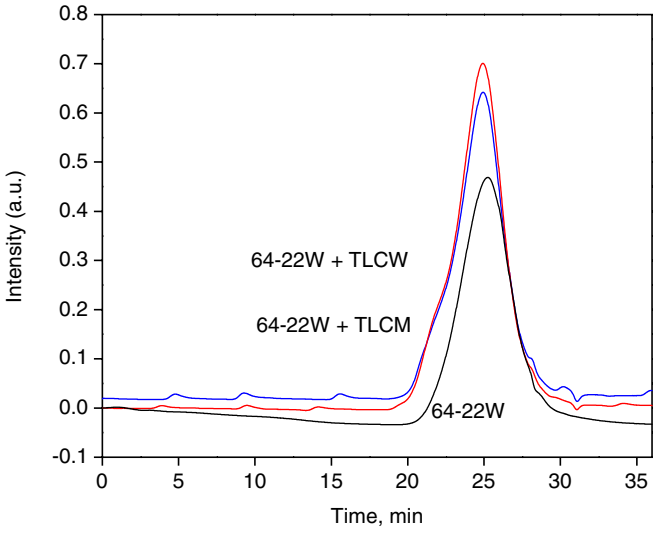

Figure O.5. GPC chromatogram of RAP-modified asphalt binder blends.

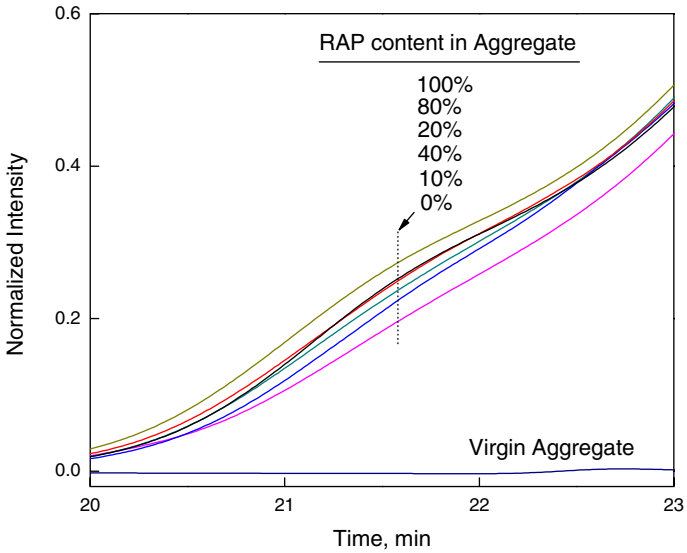

Figure O.6. Blown-up chromatogram of RAP-modified HMA samples.

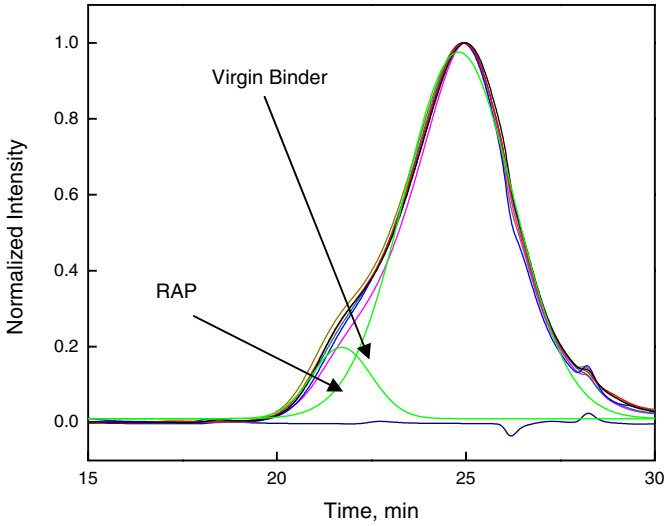

Figure O.7. Deconvolution of GPC peaks for binder extracted from RAP-modified HMA mixes.

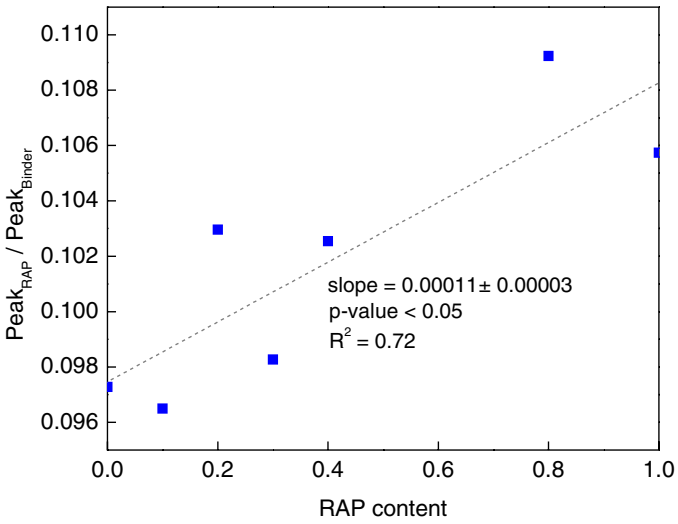

Figure O.8. Effect of RAP content on GPC peak area values. The blue boxes are markers for the data points.

around the trend line with a fairly low correlation ($R^2 = 0.72$) between the RAP content and GPC peak area values. This may be explained by the nonuniform distribution of oxidized RAP particles within the HMA sample or by the variability in the properties of RAP obtained from different paving projects.

Quantitative Analysis of NMR Results

Polymer-Modified Asphalt Binders and HMA

Initially, the nuclear magnetic resonance (NMR) chemical shifts were obtained for pure SBS to identify peaks that were unique for this polymer and to verify its formula (Figure O.9).

Figure O.9 shows two prominent peaks, located at 2.1 ppm and 5.4 ppm, related to the butadiene component of SBS and a sharp peak at 1.4 ppm associated with the terminal methyl of styrene. These peaks were used to identify the presence of SBS in the polymer-modified PG 64-22 binder and HMA mix produced with this binder.

Three samples of SBS-modified PG 64-22 binder with 1%, 3%, and 6% SBS content were dissolved in D-chloroform and analyzed in a Bruker DRX 400 NMR system. Figures O.10, O.11, and O.12 show NMR spectra for these samples. The integration values of the butadiene protons (peaking at 2.1 ppm) and those of the aliphatic protons of virgin binder (peaking between 1.5 and 1.2 ppm) are both reported at the bottom of the plot. Table O.1 summarizes the ratios of these values for 1%, 3%, and 6% SBS concentrations. The results

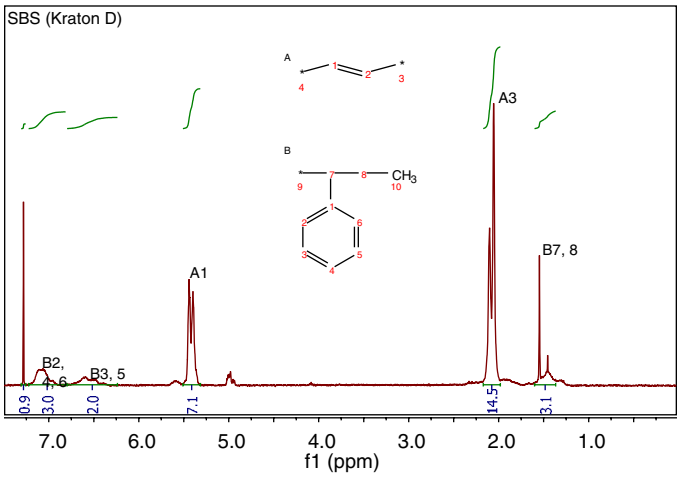

Figure O.9. NMR spectrum and chemical composition of Kraton D1101 SBS.

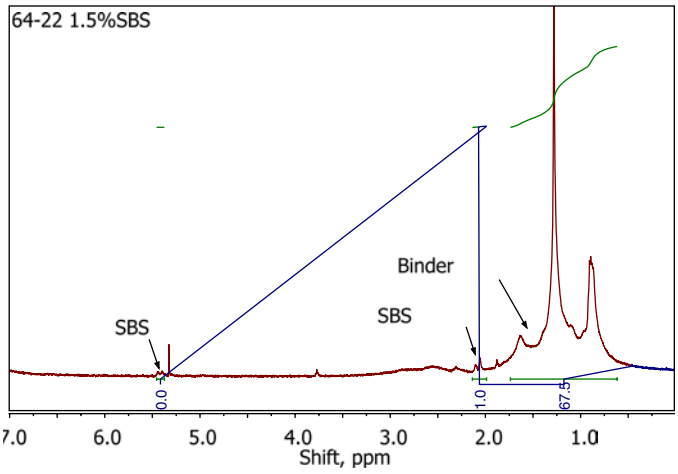

Figure O.10. NMR spectrum for 1.5% SBS-modified PG 64-22 binder.

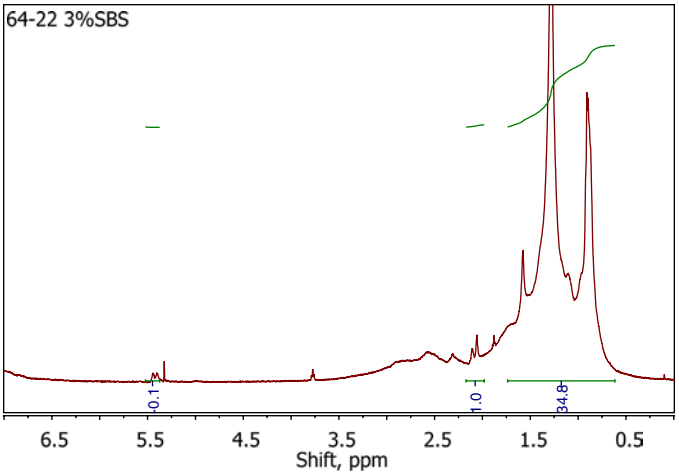

Figure O.11. NMR spectrum for 3% SBS-modified PG 64-22 binder.

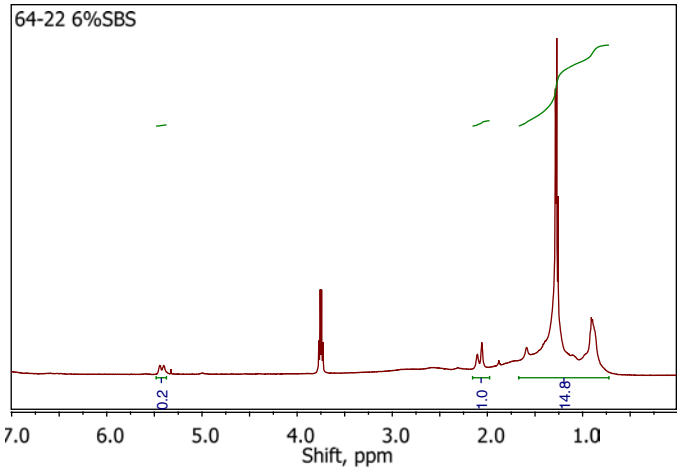

Figure O.12. NMR spectrum for 6% SBS-modified PG 64-22 binder.

clearly show that NMR yields the correct ratio of SBS concentration in samples prepared in the lab with small deviations that can be attributed to the variability associated with sample preparation. Tracking down the source of this variability was not possible because of time and expenditure issues related to using the stationary NMR equipment to repeat the experiment.

The SBS-modified binders were used to produce HMA mixtures from which the binder was then extracted and evaluated by the NMR system. The integrated ratios of the butadiene peak to the virgin binder peak were deduced from the NMR spectra and compared with the actual SBS concentration, as summarized in Table O.2. The absolute error values for the extracted binder presented in the table indicate a level of accuracy similar to that of the virgin binder. Furthermore, the error does not exceed 1%, which corresponds to the level of reliability achieved with the Fourier transform infrared method.

Although portable NMR devices were not available for evaluation in this study, it seems reasonable to assume that, in the future, NMR spectroscopy can be used in the field for both the qualitative and quantitative analysis of polymer-modified binders and asphalt mixtures.

RAP-Containing Asphalt Binders and HMA

NMR spectroscopy proved to be successful not only for the identification of hydrocarbons but also for the identification of oxygen-containing functional groups based on a chemical shift in the neighboring hydrogen atoms. Therefore, the NMR system was used for the analysis of RAP-containing asphalt binders and HMA mixtures. Figure O.13 shows the NMR spectra of an RAP-modified binder blend with a characteristic peak at 3.8 ppm corresponding to the CH group attached to carbonyl (C=O). Figure O.14 shows the NMR spectra of a 20% RAP-containing HMA mix where the peak assigned to the RAP at 3.8 ppm is hardly detectable. The attempts to establish a correlation between the amount of oxygen and the RAP content in mixes have not yet been successful. Therefore, it can be concluded that, while the increased

Table O.1. SBS Concentration in Binder as Measured by NMR

SBS Content as Prepared in Laboratory (%)	Integration Ratio SBS–Binder	SBS Content as Measured by NMR (%)	Absolute Error (%)
1	1:67.5	1.48	0.48
3	1:34.9	2.87	–0.13
6	1:14.8	6.76	0.76

Table O.2. SBS Concentration in Extracted Binder as Measured by NMR

SBS Content as Prepared in Laboratory (%)	Integration Ratio SBS–Binder (%)	SBS Content as Measured by NMR (%)	Absolute Error (%)
1	1:118.6	0.84	0.16
3	1:39.1	2.56	–0.44
6	1:20.0	5.00	–1.0

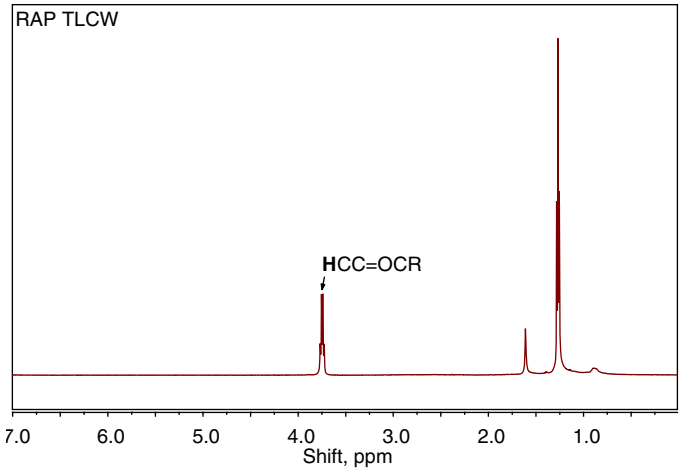

Figure O.13. NMR spectrum for RAP-modified binder blend.

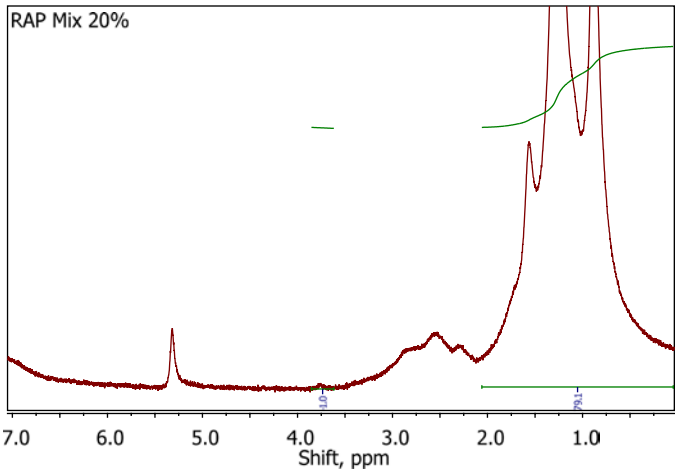

Figure O.14. NMR spectrum for 20% RAP-containing HMA mixture.

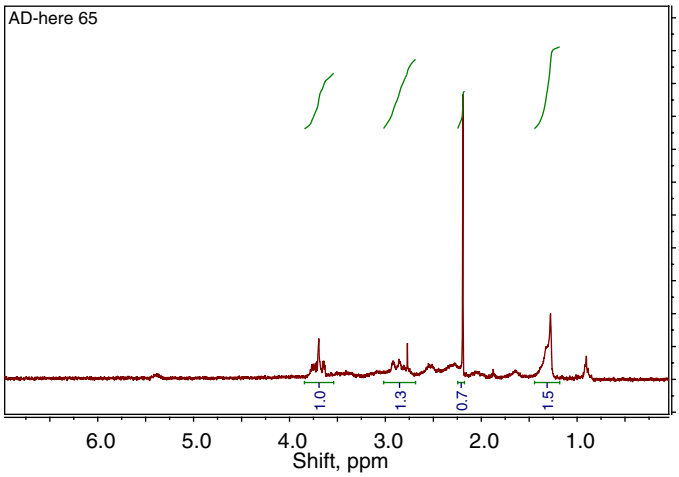

Figure O.15. NMR spectrum for AD-here LOF 65 antistripping agent.

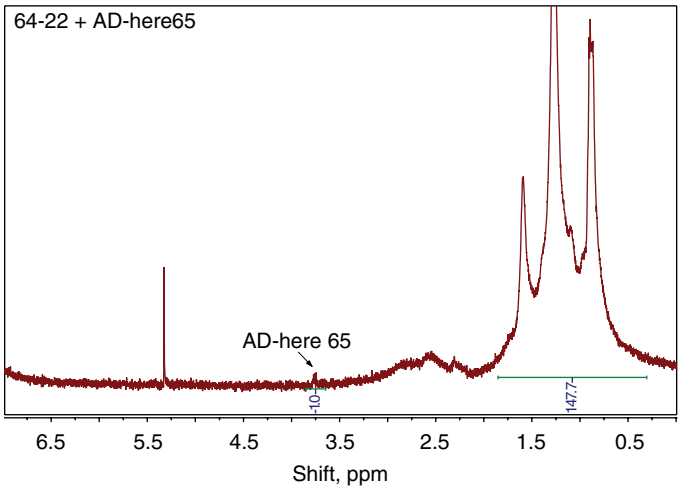

Figure O.16. NMR spectrum for PG 64-22 binder with 1% of AD-here LOF 65.

presence of oxygen-containing functional groups can be tracked using NMR, it can be only done qualitatively given the available data.

Binders with Antistripping Agents

The NMR method proved to be useful for identifying the presence of antistripping agents in asphalt. To verify this, the NMR spectra of pure antistripping agents were first obtained to identify the characteristic peaks (Figure O.15). Next, a sample of virgin PG 64-22 binder with an addition of 1% antistripping agent was prepared and tested. The resultant NMR spectra (Figure O.16) showed the characteristic peak at very low intensity. The team concluded that because of the extremely low concentration of antistripping agents used in the industry (0.25% to 1% of weight), quantifying the amount of these additives using the NMR method does not seem practical.

APPENDIX P

Reliability of Spectroscopic Measurements

Repeatability and Reproducibility of FTIR Spectra

Evaluating the repeatability and reproducibility of the results produced by the portable Fourier transform infrared (FTIR) equipment was necessary before making any recommendations for the further use of this equipment in the field study in Phase 3. Therefore, these parameters were evaluated in Phase 2 as discussed in the following text.

The results of the first round of testing showed that repeatability of FTIR results for pure materials and components and simple compounds (i.e., those materials that can be easily "fingerprinted") was not an issue. Therefore, the second round of testing in the repeatability and reproducibility study concerned composite materials, such as structural coating systems, pavement markings, portland cement concrete with admixtures, and polymer-modified binders. All of the aforementioned products were prepared in the laboratory according to the proportions summarized in Table P.1. More details on the results for particular materials from Table P.1 are provided in this appendix.

Reproducibility Study on Structural Coatings and Pavement Markings

All epoxy-based paint samples were first mixed using the component proportions prescribed by the manufacturer. Next, a ready mixture was placed on a metal pad with dimensions of 4 in. by 4 in. and allowed to dry for 24 h. The samples were tested by three operators independently using a Bruker attenuated total reflectance (ATR) FTIR spectrometer. Each operator tested five probes from one sample of each of the three test materials (Carbozinc 859, Scotchkote, and Epoplex LS50).

The FTIR spectra were obtained for each probe and analyzed in terms of repeatability and reproducibility. The repeatability was measured by the coefficient of variation (COV) in the absorbance of the primary components (major peaks) between the probes produced by one operator. The reproducibility was evaluated by COV in mean absorbance between the independent operators who tested the same material. Tables P.2 and P.3 show an example of within and between variations for Carbozinc 859 structural paint.

It was noted that the variation in the pressure applied to a sample placed on the ATR crystal before scanning significantly affected the absorbance values obtained for spectra of Epoplex LS50. This was not an issue for Carbozinc 859 and Scotchkote, which could be explained by the fact that Epoplex produced a thicker and less flexible film than Scotchkote. The stiffer film prevented full contact between the sample and ATR crystal, which interfered with the spectra. This observation should be reflected in developing a test procedure for pavement markings.

Repeatability and Reproducibility Study on Portland Cement Concrete with Admixtures

This study concerned the repeatability of FTIR scanning of wet portland cement concrete (PCC) samples prepared with air entrainer (Air 200) and retarder (Retarder 75), separately. Three replicate tests were done for each mixture and the variation in absorbance of major peaks (primary components) was evaluated. Tables P.4 and P.5 show an example of within (repeatability) and between (reproducibility) variations of PCC ready mix with the addition of air entrainer.

Repeatability Study on Polymer-Modified Asphalt Binders

The polymer-modified asphalt binders (PMABs) were produced by adding Kraton linear styrene–butadiene–styrene (SBS) in concentrations of 1%, 3%, and 6% to the Nu-Star PG 64-22 neat binder (PG 64-22 East). PMABs were produced by adding a designated amount of SBS to a binder

Table P.1. List of Materials Tested by Attenuated Total Reflectance FTIR in Reproducibility and Repeatability Study

Material Category	Brand/Material Name	Composition	Material State	Test Objective
Structural coatings	Carbozinc 859	2Part A : 1Part B:10 Filler 1Part A : 1Part B	Powder	Reproducibility study
	Scotchkote	1Part A : 1Part B	Solid	Reproducibility study
Pavement markings	3M White	100% Ready	Liquid	Reproducibility study
	Epoplex LS50 Yellow	2Part A : 1Part B	Solid	Reproducibility study
Portland cement concrete with admixtures	Lafarge Type 2 cement/ local aggregates/ Air 200/Retarder 75	8.0% Water 17% Cement 31.9% Stone 35.2% Sand 0.2% Air 200	Wet mix	Repeatability study
	Lafarge Type 2 cement/ local aggregates/ Retarder 75	8.0% Water 17% Cement 31.9% Stone 35.2% Sand 0.3% Air 200	Wet mix	Repeatability study Reproducibility study
Polymer-modified asphalt binders	PG 64-22 modified by Kraton SBS	PG 64-22 East + 1% SBS PG 64-22 East + 3% SBS PG 64-22 East + 6% SBS PG 64-22 West + 1% SBS PG 64-22 West + 3% SBS PG 64-22 West + 6% SBS	Viscous solid	Repeatability study

within the first 2 min followed by high-shear mixing (with a speed of about 4,500 rpm) at a temperature of 180°C to 195°C for 2 h. Three samples from each batch were scanned by a Bruker ATR FTIR spectrometer and the variability in the absorbance of major peaks (primary components) was analyzed (see Table P.6).

The values of COVs in Table P.6, when compared with mean concentration values, clearly indicate an increase in variability with a decrease in the concentration of primary component (major band). In addition, one can notice that the variation in major band concentration associated with SBS (e.g., 966 cm^{-1} and 700 cm^{-1}) increases from 7% to 13% at 1% SBS content to 23% to 24% at 6% SBS content. This phenomenon needs to be further investigated, because it may affect the results of the quantitative analysis of the chemical composition of polymer-modified binders. For the moment, this phenomenon can be attributed to the higher level of variability observed in absorbance bands of small concentrations or to the nonuniform distribution of the polymer network inside the binder phase.

Table P.2. Within Variation of Major Band Absorbance for Paint Carbozinc 859

Major Bands (cm^{-1})	Operator 1			Operator 2			Operator 3		
	Mean Concentration	SD	COV (%)	Mean Concentration	SD	COV (%)	Mean Concentration	SD	COV (%)
825–830	4.30	0.84	20	4.79	1.21	25	4.58	0.93	20
1,115–1,120	3.76	0.65	17	3.33	0.79	24	2.06	0.28	14
1,180–1,185	4.65	0.75	16	4.54	0.23	5	4.09	0.77	19
1,235–1,240	15.32	1.29	8	16.37	0.48	3	15.48	3.24	21
1,285–1,290	5.98	0.49	8	5.03	0.45	9	5.36	0.53	10
1,455–1,460	5.27	0.56	11	4.30	0.19	4	4.73	0.14	3
1,505–1,510	12.73	1.13	9	12.20	0.40	3	12.64	0.87	7

Table P.3. Between Variation of Major Band Absorbance for Paint Carbozinc 859

Major Bands (cm^{-1})	Mean Concentration	SD	COV (%)
825–830	4.56	0.99	22
1,115–1,120	3.05	0.57	18
1,180–1,185	4.43	0.59	13
1,235–1,240	15.72	1.67	11
1,285–1,290	5.46	0.49	9
1,455–1,460	4.77	0.30	6
1,505–1,510	12.52	0.80	6

Table P.5. Between Variation of Major Band Absorbance for PCC with Air 200

Major Bands (cm^{-1})	Mean Concentration	SD	COV (%)
505–515	24.48	3.95	17
595–605	4.63	1.42	37
665–675	2.33	0.68	29
875–885	1.76	0.34	20
925–935	3.23	0.62	20
1,115–1,125	17.32	3.02	17
1,445–1,455	1.52	0.55	39
1,640	30.25	3.09	10

Comparison of Portable and Stationary FTIR Results

The evaluation of the spectroscopic equipment in Phase 2 included a verification of FTIR results obtained with the portable device (Bruker ALPHA ATR FTIR) by repeating the tests for all materials on the stationary equipment available in the Institute of Material Science at the University of Connecticut (Nicolet Magna 560 transmission FTIR). Two main differences in the procedures should be pointed out:

1. Technological concept. On the one hand, portable FTIR uses the principle of ATR, which measures changes that occur in an internally reflected infrared beam when it comes in contact with a sample placed directly on the infrared (IR) window. On the other hand, the transmission IR measures the IR energy that passes through a sample when it is placed in the transmission window located between the source of IR radiation and the detector.
2. Sample preparation. Regardless of the state of material (liquid, solid, or powder), no sample preparation was made for the portable ATR cell, whereas for transmission FTIR testing, a sample was prepared as a thin film and put between two potassium bromide (KBr) disks.

Although a different number of scans were performed on a sample by the portable and stationary spectrometers (16 scans and 24 scans, respectively), the resolution of the scans was similar (1.9 cm^{-1} and 1.4 cm^{-1} for portable and stationary FTIR, respectively). Also, the IR spectrum of the sample was analyzed in the same frequency region between 4,000 cm^{-1} and 400 cm^{-1}. Therefore, it was initially assumed that a direct comparison of the spectrograms obtained with the portable and stationery FTIR equipment was possible. However, the analysis of the portable and stationary spectra revealed that they yielded different absorbance values for the same sample, yet at the same frequency. This is explained by the difference in path length. The path length of the IR window

Table P.4. Within Variation of Major Band Absorbance for PCC with Air 200

	Batch 1			Batch 2			Batch 3		
Major Bands (cm^{-1})	Mean Concentration	SD	COV (%)	Mean Concentration	SD	COV (%)	Mean Concentration	SD	COV (%)
505–515	25.69	0.25	1	25.94	2.83	11	21.81	8.78	40
595–605	4.30	0.74	17	6.14	0.77	13	3.46	2.76	80
665–675	2.12	0.37	18	2.70	1.06	39	2.18	0.62	29
875–885	1.82	0.31	17	2.07	0.34	16	1.40	0.38	27
925–935	3.13	1.06	34	3.32	0.18	5	3.24	0.63	21
1,115–1,125	16.02	1.78	11	19.34	5.01	26	16.61	2.28	14
1,445–1,455	1.72	0.13	7	1.62	0.74	46	1.21	0.78	65
1,640	33.70	2.23	7	24.53	1.35	5	32.51	5.69	18

Table P.6. Summary of Variation of Major Band Absorbance for PG 64-22 Binder with Different SBS Concentrations

Major Bands (cm^{-1})	Batch 1 (1% SBS)			Batch 2 (3% SBS)			Batch 3 (6% SBS)		
	Mean Concentration	SD	COV (%)	Mean Concentration	SD	COV (%)	Mean Concentration	SD	COV (%)
2,960	2.00	0.02	1	2.02	0.02	1	1.93	0.05	3
2,921	36.64	0.15	0	36.48	0.37	1	35.54	0.53	1
2,853	14.28	0.05	0	14.31	0.11	1	13.94	0.13	1
1,703	0.47	0.05	11	0.45	0.16	36	0.39	0.11	29
1,601	1.51	0.02	1	1.52	0.02	1	1.53	0.03	2
1,458	22.92	0.27	1	22.67	0.12	1	22.38	0.34	2
1,377	7.48	0.09	1	7.41	0.06	1	7.48	0.11	1
1,310	0.54	0.02	3	0.64	0.09	15	0.65	0.10	15
1,162	0.60	0.08	14	0.58	0.07	12	0.55	0.07	12
1,031	1.00	0.18	18	0.79	0.09	12	0.68	0.04	6
968	0.84	0.11	13	1.37	0.18	13	1.90	0.44	23
866	2.28	0.07	3	2.37	0.13	6	2.55	0.02	1
815	4.19	0.02	0	4.07	0.15	4	4.05	0.22	6
751	1.03	0.04	4	1.05	0.01	1	1.03	0.03	3
725	1.10	0.02	2	1.05	0.05	5	1.07	0.04	4
699	0.08	0.01	7	0.39	0.05	12	0.61	0.15	24
431	0.61	0.05	8	0.67	0.03	5	0.66	0.01	2

varied significantly because of the nonuniform thickness of samples in the KBr pellets, while in ATR reflectance mode, the path length was set to a constant value of 1 μm.

Because the path length of transmission IR samples remained unknown, it precluded a quantitative comparison of the concentrations of different functional groups as yielded by the two spectrometers. However, it was found that the stationary FTIR (Nicolet Magna 560) identified absorbance peaks at the same wavelengths as the portable ATR FTIR (Bruker ALPHA). Therefore, it was logical to conclude that the portable spectrometer was able to identify the unique spectra corresponding to the chemical composition of all tested materials at the same level of quality as the stationary device. Examples of the analysis for liquid and solid samples are provided below to justify this conclusion.

Liquid Sample

Figure P.1 shows the fingerprinting region of the IR spectra for Part A of Carbozinc 859 structural coating system with major absorbance bands as identified by the ATR and stationary IR spectrometers. One can observe that the major bands identified by the ATR match those identified by the stationary IR at exactly the same wavelengths. In addition, the stationary IR spectra clearly show much higher absorbance values, which indicates that a longer path is followed by the IR beam through the thickness of sample (as was mentioned in a preceding paragraph, the ATR path length is only 1 μm).

Solid Sample

The major absorbance bands as determined by the ATR and stationary IR for styrene–butadiene rubber (SBR) latex-modified PG 52-34 binder are compared in Figure P.2. The binder was chosen to illustrate the commonality and discrepancies between the results of the two devices when used for the identification of complex mixture, such as a polymer-modified binder. At the first glance, one can see that the major aliphatic bands at ~2,960, ~2,920, ~2,850, ~1,460, and ~1,380 cm^{-1} are equally identified by the two methods. The aromatic bands at ~1,600 and between ~870, ~815, ~755, and ~724 cm^{-1} also do not show any discrepancy between ATR and IR spectra in terms of absorbance intensity. A small but significant difference in spectra (see "Region of difference" in Figure P.2) can be identified around ~1,542 and 1,508 cm^{-1},

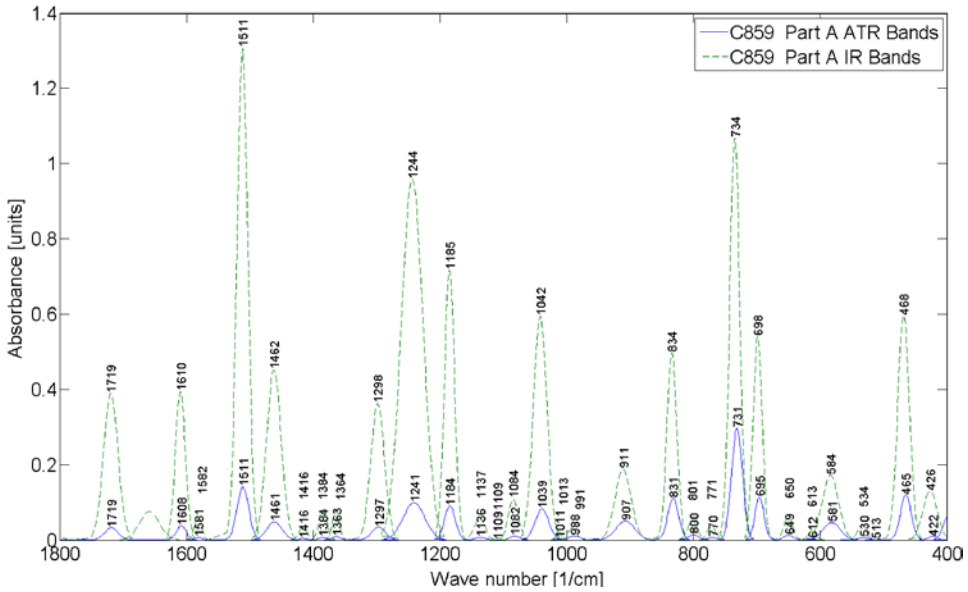

Figure P.1. Comparison of major absorbance bands identified by ATR and IR spectrometers for Carbozinc 859 Part A.

where the stationary IR identifies a small amount of nitrate ($-NO_2$), while the portable ATR ignores these bands. One significant difference shown is the amount of carbonyl (>C=O) at ~1,739 cm^{-1}, which was measured by the ATR to be at a much greater amount than by the stationary IR (minor peaks at ~1,773, 1,736, and 1,700 cm^{-1}). The discrepancy in identifying nitrate and carbonyl are most likely connected to the difference in sample preparation and environment during the testing, rather than to the composition of binder. Nevertheless, both portable and stationary spectrometers are able to identify even a small (1.5 wt %) amount of the polymer added to a binder (SBR latex band at ~970 and ~1,230 cm^{-1}).

In summary, it is concluded that the portable ATR FTIR spectrometer is capable of producing at least the same quality of IR spectra as a stationary IR spectrometer.

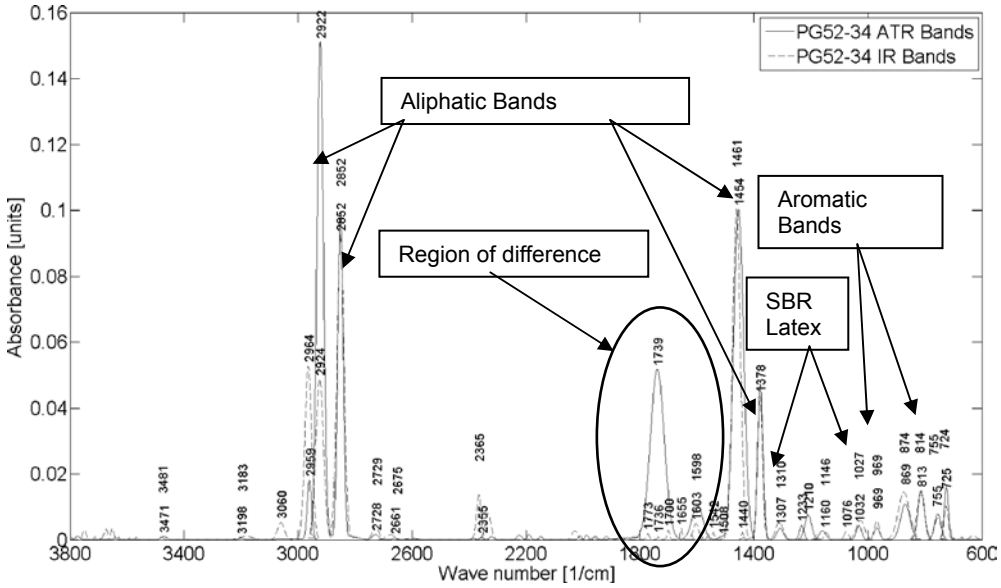

Figure P.2. Comparison of major absorbance bands identified by ATR and IR spectrometers for PG 52-34 1.5% SBR latex-modified binder.

Variability in X-Ray Fluorescence Results

A two-phase approach was adopted for all materials. Single measurements were first employed to establish proof of concept, that XRF can yield measurable results for each material. When an element was detected in prominent concentrations that would not likely have interferences from other field materials and were significantly higher than the method detection limit, XRF was considered a promising quality assurance/quality control (QA/QC) method. In the next step, 10 measurements were obtained for each material in order to determine the precision of the method.

It should be noted that, although XRF spectra are generated through software, the user does not see them unless explicitly requested, nor does the user have access to the spectrum manipulation to generate data. XRF calibration is a complex process that is performed at the production facility to which the user has no access; one simply performs the measurement and gets a summary table with the quantitative results (element concentrations in mg/kg for the soil mode and in wt % for the mining mode). Therefore, only quantitative results are provided in this report, as generated by the equipment software.

The portable XRF device owned by the team was deemed to be successful to different extents in the evaluation of structural coatings, pavement markings, curing compounds for PCC, portland cement, and aggregates. Therefore, only the testing results for the aforementioned material categories are discussed.

Structural Coatings

Scotchkote 3M

Table P.7 shows the ingredients of this product according to its material safety data sheets (MSDS). XRF can measure the titanium content of this material as the most likely candidate to conduct QA/QC.

Table P.7. MSDS-Based Composition of Scotchkote 3M

Ingredient	C.A.S. No.	Wt%
Di(4-Hydroxyphenol) Isopropylidene Diglycidyl Ether-Di(4-Hydroxyphenol) Isopropylidene Copolymer	25036-25-3	55–75
Quartz silica	14808-60-7	10–20
Potassium aluminosilicate	1327-44-2	5–15
Mica-Group minerals	12001-26-2	5–15
Titanium dioxide	13463-67-7	1–10
Cyanoguanidine	461-58-5	1–10
C.I. pigment green 7	1328-53-6	1–10
4,4′-Isopropylidenediphenol	80-05-7	0.1–1

Table P.8. XRF-Measured Composition of Scotchkote 3M Materials Tested with Soil Mode

Metal Detected	Part A (mg/kg)	Part B (mg/kg)
Cl	698 ± 40	n.d.[a]
K	192 ± 13	596 ± 176[b]
Ca	n.d.[a]	280,721 ± 2,716
Ti	n.d.[a]	108,161 ± 1,079
Fe	n.d.[a]	18,332 ± 177
Co	n.d.[a]	128 ± 27
Cu	n.d.[a]	87 ± 5
Zn	n.d.[a]	7 ± 2
Sr	12 ± 1	56 ± 1
Zr	32 ± 1	n.d.[a]
Mo	39 ± 1	n.d.[a]
Sb	31 ± 9	n.d.[a]
I	50 ± 6	n.d.[a]
Ba	n.d.[a]	1,468 ± 74

Note: Materials were tested with soil mode.

[a] n.d. = not detected.

[b] Standard deviations represent the instrument error.

This material is supplied by the manufacturer as two separate components: (a) Part A is a clear gel substance and (b) Part B is a green emulsion. These components were tested separately. Table P.8 shows the concentrations of metals detected in both Parts A and B.

Based on the results, the gel material appeared to be an organic substrate type of material. Part B was likely representative of the actual mixed coating. The Ti concentration in Part B was found to be 10.8% by weight, with an instrument-based error of 0.1%. This corresponds to a TiO_2 concentration of 18.9%. This far exceeds the TiO_2 concentration cited in the MSDS; however, the MSDS refers to the final emulsion, not Part B alone. Based on the results, it was concluded that XRF is a useful method for conducting QA/QC of Scotchkote 3M and further testing was initiated on the mixed product. Three separate mixes were prepared according to the manufacturer's instructions, as shown in Table P.9.

Table P.9. Mixing Design for Scotchkote Testing

Mix	5	10	20
Part A	5.0 g	10.0 g	20.0 g
Part B	6.65 g	13.3 g	26.6 g

Table P.10. Replicate XRF Results for Scotchkote 3M Tested with Both Modes

	Soil Mode (mg/kg)				Mining Mode (wt %)	
Sample ID	**K**	**Ca**	**Ti**	**Fe**	**Ti**	**Fe**
Scotchkote 20-1#	484 ± 109	134,115 ± 1,096	62,209 ± 530	11,206 ± 90	7.04 ± 0.11	1.62 ± 0.02
Scotchkote 20-2#	<LOD	137,183 ± 1,114	63,812 ± 540	11,372 ± 91	7.25 ± 0.11	1.67 ± 0.02
Scotchkote 20-3#	<LOD	137,684 ± 1,134	63,627 ± 546	11,402 ± 93	7.25 ± 0.11	1.64 ± 0.02
Scotchkote 20-4#	<LOD	133,303 ± 1,082	61,642 ± 522	10,999 ± 88	7.19 ± 0.11	1.65 ± 0.02
Scotchkote 20-5#	417 ± 109	138,639 ± 1,129	64,091 ± 543	11,405 ± 92	7.17 ± 0.11	1.72 ± 0.02
Scotchkote 10-1#	529 ± 109	136,325 ± 1,111	62,860 ± 534	11,242 ± 91	6.62 ± 0.10	1.58 ± 0.02
Scotchkote 10-2#	388 ± 106	134,688 ± 1,085	62,232 ± 523	11,160 ± 89	6.67 ± 0.10	1.57 ± 0.02
Scotchkote 10-3#	646 ± 110	136,432 ± 1,107	63,546 ± 537	11,226 ± 90	6.71 ± 0.11	1.59 ± 0.02
Scotchkote 5-1#	444 ± 111	141,321 ± 1,160	65,039 ± 556	11,631 ± 94	6.62 ± 0.10	1.58 ± 0.02
Scotchkote 5-2#	606 ± 110	137,357 ± 1,113	63,574 ± 537	11,252 ± 90	6.60 ± 0.11	1.62 ± 0.02
Average	**502**	**136,705**	**63,263**	**11,291**	**6.91**	**1.62**
SD	**97**	**2,339**	**1,023**	**172**	**0.29**	**0.05**

Note: LOD = limit of detection.

Several replicates of each mix were investigated for both the error associated with preparing different mixes and the variability within a single mix. Samples are named accordingly (i.e., Sample Mix # – Replicate #). Additionally, one mix was prepared when the mining mode calibration was available to test the difference between the two modes, since the Ti content was in the range of both calibrations. The results are shown in Table P.10. Trace metals are not shown. Standard deviations for each measurement are generated by the XRF equipment and are based on counting statistics. The overall average and standard deviation of the 10 measurements are calculated at the bottom of the table. Data are given in the units provided directly by the XRF (mg/kg for soil mode and wt % for mining mode).

The average Ti concentration was 6.33% with the soil mode and 6.91% with the mining mode, so that both calibrations yield reasonable results. These values correspond to 10.55% and 11.5% TiO_2. This is in agreement with the upper TiO_2 content provided by the manufacturer. The standard deviation was 1.6% of the average value and very close to the instrument standard deviation. Thus, repeatability of the experiment and the accuracy of the method are considered very high. Other elements, such as Ca and Fe, also had very consistent measurements and low standard deviations. The Fe concentration measured by both modes was again close: 1.4% by the soil mode and 1.6% by the mining mode. Thus, XRF is considered to be a highly suitable method for the QA/QC of Scotchkote material, with only one caveat: the TiO_2 content range provided by the manufacturer is extremely wide (1% to 10%), which would let dilutions of the epoxy go undetected if the entire range were considered to be within tolerable limits. It is recommended that more stringent criteria be developed for such materials.

The team attempted to determine the Ti concentration independently by sending samples out to Alamo laboratories for an evaluation of the total metal digestion and inductive coupled plasma/optical emission spectrometry, but the reported Ti concentrations were extremely low (129, 132, and 108 mg/kg for triplicate samples). It is clear that Ti recovery with the total digestion method is extremely poor and thus not reliable.

Carbozinc 859

This material was received in three parts. One part was described as a zincfiller and was a gray fine powder. The other two parts, designated Parts A and B, were a clear yellow liquid. The mixture of the three produced the spreadable coating. The zinc content of the material is cited to be 81% ± 2% in dry film by the product specification sheet. Thus, Zn is the target compound of interest for the XRF device. Table P.11 shows the mix design for the Carbozinc product. Only the mining mode was employed, because the high Zn concentration precluded the use of the soil mode for this material. Results for major elements (Zn and Fe) are shown in Table P.12.

Table P.11. Mix Design for Carbozinc 859

	1	2	3
Part A	1.591 mL	3.182 mL	4.773 mL
Part B	0.909 mL	1.818 mL	2.727 mL
Zinc filler	6.67 g	13.34 g	20.01 g

Table P.12. Replicate XRF Results for Carbozinc 859

Sample ID	Zn (wt %)	Fe (wt %)
Carbozinc 1-1	72.06 ± 0.12	1.67 ± 0.02
Carbozinc 1-2	73.73 ± 0.13	1.66 ± 0.02
Carbozinc 1-3	74.54 ± 0.13	1.71 ± 0.02
Carbozinc 2-1	77.39 ± 0.13	1.67 ± 0.02
Carbozinc 2-2	71.86 ± 0.12	1.65 ± 0.02
Carbozinc 3-1	77.57 ± 0.13	1.69 ± 0.02
Carbozinc 3-2	75.12 ± 0.13	1.61 ± 0.02
Carbozinc 3-3	73.61 ± 0.13	1.64 ± 0.02
Carbozinc 3-4	73.06 ± 0.13	1.62 ± 0.02
Carbozinc 3-5	73.91 ± 0.13	1.65 ± 0.02
Mean	**74.28**	**1.66**
SD	**1.96**	**0.03**

Table P.13. Replicate XRF Results for Epoplex White and Yellow Paints

Sample ID	LS50 White Ti (wt %)	LS50 Yellow Ti (wt %)
1	30.88	5.44
2	30.59	5.14
3	30.26	5.26
4	30.38	5.30
5	30.85	5.24
6	30.42	5.22
7	30.20	5.21
8	29.82	5.12
9	29.85	5.15
10	30.73	5.27
Average	**30.40**	**5.23**
SD	**0.38**	**0.09**

The average Zn content was 74.3%, which is in reasonable agreement with the 81% quoted in the MSDS, given that the XRF was measured for the wet paint and not the dry film (drying of the paint will have a concentrating effect on the Zn content). The results were again very consistent within and across the mixes, with the standard deviation being lower than the equipment accuracy. Thus, XRF is deemed a suitable QA/QC method for metal-based coating systems, such as Carbozinc 859, as long as a consistent Zn content of the wet emulsion is established.

The independent analyses of Zn by acid digestion and inductive coupled plasma performed by Alamo Analytical yielded 66.1%, 67.4%, and 61.5% for triplicate samples. These are slightly lower in comparison to the XRF data; however, it is unclear what the acid digestion recovery rates are at these high concentrations.

Again, it is recommended that if XRF is to be used for the QA/QC evaluation of metal-based paints in the field, then it is necessary to first establish the QA/QC criteria for the product in laboratory conditions using the same method. At high metal concentrations, different methods have different levels of recovery. In order to have a sound basis for comparison, it is recommended that the same method be used by the central DOT laboratories to develop QA/QC criteria for the selected materials.

Pavement Markings

Two pavement marking brands by Epoplex were evaluated in Phase 2 (LS50 White and LS50 Yellow). The MSDS of these materials cites a TiO_2 content of 18% to 25% in the white pigment, making Ti the element of interest for XRF analysis. The remaining components are polymers, glass beads, and silica, all of which do not have a significant metal content that can be identified by a portable XRF. Both paints were tested with the mining mode because of the anticipated high Ti content. Table P.13 shows the resultant replicate concentrations of Ti for both LS50 White and LS50 Yellow.

The TiO_2 content of the white pigment was 50.7%, significantly higher than the MSDS value. The yellow pigment TiO_2 content was 8.7%, also not within the quoted range. Both sets of measurements were very consistent, with the overall standard deviation being close to the instrument resolution. This indicates that XRF is a suitable method for QA/QC of the two Epoplex paints. The main issue is the establishment of the appropriate QA/QC criteria, given that the MSDSs do not provide accurate information to use as criteria for QA/QC. It is therefore recommended that individual DOTs establish criteria for each type of material approved for field use before implementing XRF-based QA/QC procedures. Again, the acid digestion method conducted by Alamo had extremely poor recovery rates and could not be used for comparison.

Aggregates

Two aggregates were tested using XRF: the sand and the gravel used to produce PCC samples in other experiments. Both materials had low concentrations in most elements, so they were tested in the soil mode. Mining mode results are provided only for Fe, which had a higher concentration. The replicate results are shown in Tables P.14 and P.15 for the sand and stone, respectively.

Table P.14. XRF Results for Sand

Sample ID	K	Ca	Ti	Cr	Mn	Ba	Pb	Fe	Fe (wt %)
Sand 1#	16,956 ± 272	11,239 ± 170	1,732 ± 61	26 ± 5	473 ± 10	212 ± 16	17 ± 2	17,110 ± 157	4.51 ± 0.04
Sand 2#	8,528 ± 207	23,249 ± 302	2,881 ± 84	30 ± 6	933 ± 16	192 ± 20	15 ± 2	33,035 ± 324	4.31 ± 0.04
Sand 3#	13,163 ± 244	8,612 ± 151	1,131 ± 60	31 ± 6	591 ± 12	195 ± 17	15 ± 2	27,295 ± 258	4.35 ± 0.04
Sand 4#	8,745 ± 205	15,310 ± 220	2,771 ± 81	35 ± 6	1,461 ± 21	184 ± 20	12 ± 2	34,968 ± 337	4.50 ± 0.04
Sand 5#	9,317 ± 212	23,739 ± 303	4,394 ± 99	37 ± 6	979 ± 16	238 ± 22	9 ± 2	31,065 ± 300	4.43 ± 0.04
Sand 6#	11,134 ± 226	18,984 ± 251	3,757 ± 89	33 ± 6	1,040 ± 16	221 ± 20	15 ± 2	29,787 ± 282	4.38 ± 0.04
Mean	**11,307**	**16,856**	**2,778**	**32**	**913**	**207**	**14**	**28,877**	**4.41**
SD	**3,275**	**6,240**	**1,216**	**4**	**352**	**20**	**2.9**	**6,340**	**0.08**

Note: All results are in mg/kg except last column, which shows Fe results for mining mode.

Both materials exhibited significantly higher variability in their composition than all previous materials tested by XRF. This is expected because aggregates are natural materials. In the case of aggregates, XRF is likely to be used more as screening tool, rather than as a QA/QC tool. For example, it may be used to assess whether there is heavy metal contamination in the delivered materials. It is theoretically possible to characterize aggregate materials that originate from a particular place and then screen the material in the field; however, the higher material variability precludes the use of XRF to establish strict QA/QC criteria for ubiquitous elements such as K, Fe, or Ca. For example, the Ca concentration in the stone varied from 10,000 to 50,000 mg/kg in the six replicates tested. This may be attributed to the varied distribution of bulk minerals such as calcite and feldspars.

Portable Versus Stationary X-Ray Diffraction

X-ray diffraction is used to determine the crystal structures of materials; thus, it can only be applied to solid samples that are expected to be of a crystalline nature. Therefore, XRD is generally applicable to inorganic materials; it may also be applied to limited organic applications, such as pharmaceuticals and polymers in pure form. However, the complex nature of asphalts does not make them amenable to XRD analysis, especially for QA/QC purposes. Therefore, the team decided to include only the following materials in the scope of Phase 2: portland cement, mineral aggregates (sand and stone), and the mixed portland cement concrete. The analysis of the XRD results for these materials is discussed below along with a qualitative and quantitative comparison of portable and stationary XRD testing.

Portland Cement

The Lafarge cement was run in triplicate with the Bruker instrument. Two of the samples were run without corundum at low resolution to provide a comparison with the portable Terra instrument and one sample was run with corundum at high resolution (HR) for quantitative analysis. Figure P.3 shows an overlay of the four diffraction patterns shown with offset for better visualization.

The figure illustrates that the major observed peaks were the same for the three patterns, indicating the same qualitative

Table P.15. XRF Results for Stone

Sample ID	K	Ca	Ti	Cr	Mn	Ni	Ba	Fe	Fe (wt%)
Stone 1#	17,410 ± 325	16,749 ± 257	4,363 ± 105	56 ± 7	259 ± 10	75 ± 10	285 ± 23	19,340 ± 207	3.63 ± 0.04
Stone 2#	26,295 ± 422	9,782 ± 185	3,768 ± 99	41 ± 7	336 ± 11	46 ± 10	293 ± 23	23,522 ± 251	3.63 ± 0.04
Stone 3#	20,854 ± 485	59,757 ± 926	2,830 ± 133	42 ± 11	884 ± 23	<LOD	544 ± 36	51,288 ± 710	3.57 ± 0.04
Stone 4#	16,765 ± 290	10,996 ± 180	3,493 ± 85	29 ± 5	166 ± 7	27 ± 8	246 ± 19	12,571 ± 126	3.59 ± 0.04
Stone 5#	14,063 ± 276	20,480 ± 285	3,002 ± 84	28 ± 6	354 ± 10	29 ± 9	210 ± 19	18,143 ± 187	3.63 ± 0.04
Stone 6#	14,556 ± 274	26,061 ± 332	3,916 ± 100	99 ± 8	1,048 ± 18	61 ± 11	323 ± 24	42,451 ± 416	3.62 ± 0.04
Mean	**17,867**	**22,087**	**3,138**	**44**	**446**	**48**	**297**	**24,483**	**3.62**
SD	**4,365**	**17,645**	**1,238**	**27**	**370**	**20**	**120**	**16,671**	**0.03**

Note: All results are in mg/kg except last column, which shows Fe results for mining mode.

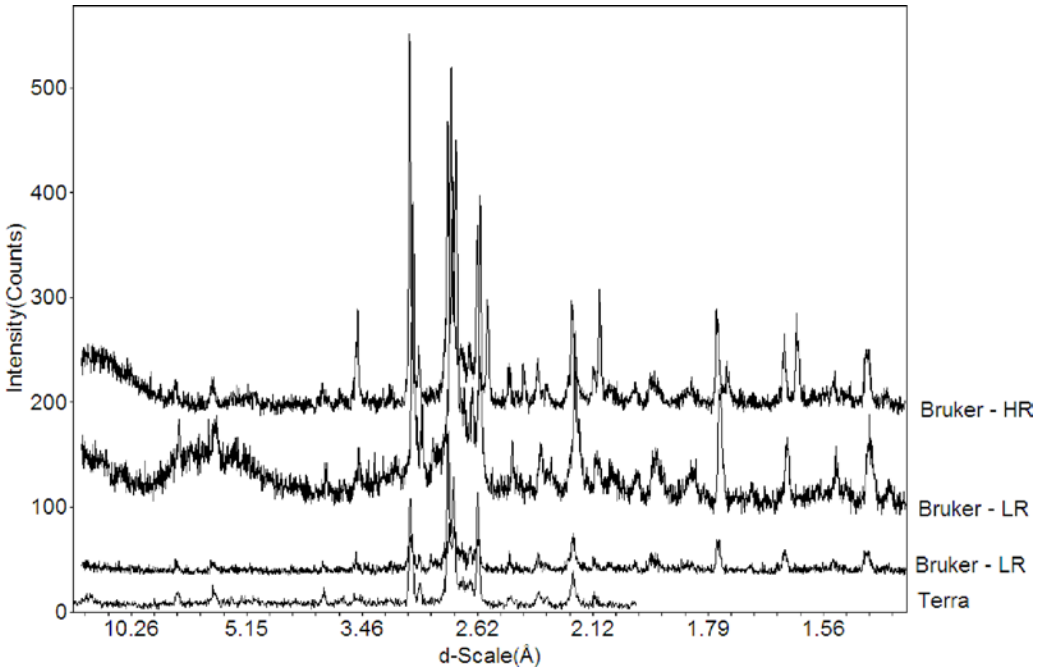

Figure P.3. Overlay of four XRD patterns obtained for Lafarge portland cement.

composition. However, the background and peak intensity of the various peaks differed, indicating variability in the quantitative distribution of the different phases. The signal-to-noise ratio was also different. The Bruker instrument provided a better resolution, even at low resolution, in comparison to the Terra equipment. Terra also has a limited range of *d*-spacings, which is why the respective pattern is truncated. This does not, however, limit the phases to be identified in soils and cements, because common phases have their major peaks in areas above the *d*-spacing of 2 Å, which is the approximate lower limit of Terra. Overall, Terra was able to qualitatively capture all of the phases that Bruker did at both low and high resolution.

To gauge the extent of the variability in the relative intensities of the identified phases, quantitative analysis was performed for all four patterns excluding corundum. This provides a relative distribution of the identified phases, but not an absolute quantity. Still, the variability in the relative distribution is indicative of the overall variability in the quantitative results. Table P.16 shows the relative quantitative results for the three samples obtained with the Bruker instrument

Table P.16. XRD Quantitative Results for Lafarge Portland Cement

Mineral	Formula	Bruker 1 with Amorphous (%)	Bruker 1 (%)	Bruker 2 (%)	Bruker 3 (%)	Terra (%)
Alite	$3CaOSiO_4$	36.8	48.5	52.5	54.6	62.9
Belite	$2CaOSiO_4$	14.5	19.1	23.7	23.0	10.0
Tricalcium aluminate	$3CaOAl_2O_3$	3.8	5.0	4.1	3.1	5.3
Brownmillerite	$4CaOFe_2O_3Al_2O_3$	7.3	9.6	9.2	9.1	11.1
Calcite	$CaCO_3$	3.4	4.5	4.1	2.7	na[b]
Periclase	MgO	2.6	3.4	n.d.[a]	2.2	2.5
Anhydrite	$CaSO_4$	1.6	2.5	2.4	n.d.[a]	n.d.[a]
Bassanite	$CaSO_40.5H_2O$	5.9	7.8	4.1	5.3	8.2
Amorphous	na[b]	24.2	na[b]	na[b]	na[b]	na[b]

Note: Amorphous by definition does not have a formula.

[a] n.d. = not detected.

[b] na = not applicable.

and the Terra XRD pattern, as well as the quantitative results for the first sample when the amorphous content was included in the analysis.

The results showed that the low-resolution (LR) Bruker samples yielded results that were reasonably close to the high-resolution (HR) sample. However, it should be noted that this was partly because an experienced user performed the quantitative analysis. One significant difference of the LR samples was that the peaks of the four major cement phases were less resolved than those of the HR sample. This requires manual manipulation of the software parameters to avoid artifacts of the Rietveld model that is applied to perform quantitative analysis. Thus, more experience is required to do these manipulations than is required by the HR sample that offers sharper peaks with improved resolution.

The absolute quantification using the Bruker instrument with corundum yielded very good agreement between the theoretical composition of Type 1 portland cement and the observed results. A typical composition is approximately 65% alite, 15% belite, 7% tricalcium aluminate, and 8% brownmillerite. The only differences from the anticipated composition were that the tricalcium aluminate concentration was slightly underestimated and the alite–belite ratio was a bit lower; however, the latter fluctuates and is still within the expected range. The main reason for these differences is the peak overlap between the major peak of tricalcium aluminate and secondary peaks of the dominant silicate phases. The goodness of fit was 1.3; any value below 1.4 is considered an excellent refinement (*1*). Figure P.4 shows the theoretical and calculated patterns with the residual (difference) pattern between the two displayed at the top.

The results from the Terra instrument exhibited the same trends as the Bruker samples, with some differences for the major silicate phases. Even though the alite and belite concentrations were closer to the ideal 65% and 10%, the brownmillerite content was overestimated. Overall, it is possible to see that Terra predicted the anticipated portland cement composition with reasonable accuracy given the limitations of the portable instrument (lower 2θ resolution and signal-to-noise ratio). An abnormal behavior was observed in the statistics of the quantitative analyses. The goodness-of-fit R/E provides an estimation of the agreement between the model and the actual pattern; a goodness of fit of 1 indicates an ideal refinement. In this case, a value of less than 1 was obtained when the background intensities were included in the R/E calculation, which suggests that the signal-to-noise ratio was too low to perform this type of analysis. One could, however, judge the quality of the fit by observing the difference pattern (Figure P.5). The residual pattern is noisier because of the low signal-to-noise ratio, but there are no significant spikes that would indicate a poor fit between the actual and calculated pattern.

The Lehigh portland was also run in triplicate with the Bruker instrument. This time it was observed that the LR sample (2.4-s dwell time) yielded a very poor pattern, so the two additional samples were run at a higher resolution (6- and 15-s dwell time). Table P.17 summarizes the results for both the stationary Bruker and the portable Terra XRD systems.

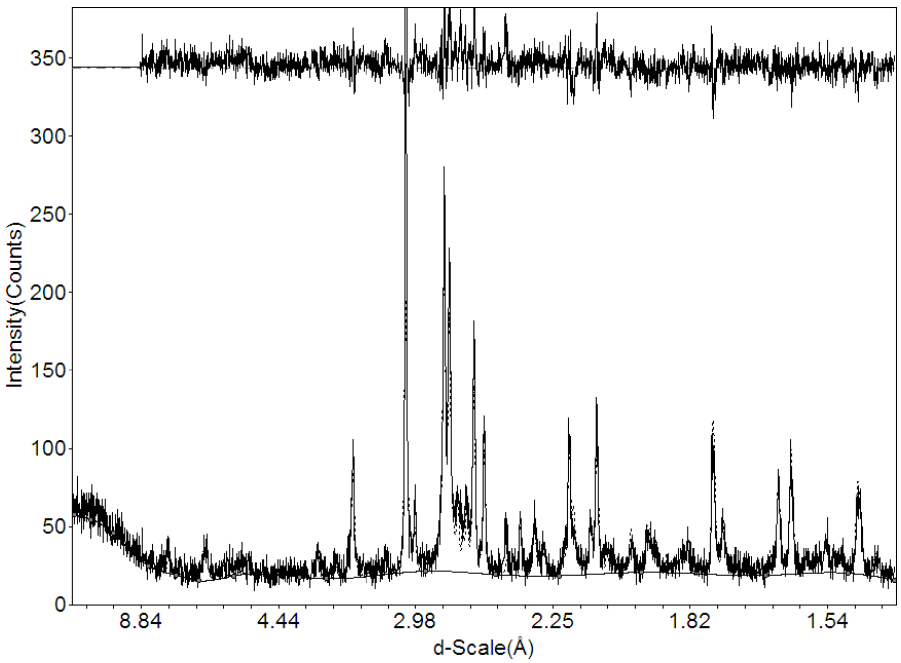

Figure P.4. Theoretical, calculated, and residual (difference) XRD pattern for the Bruker HR Lafarge sample.

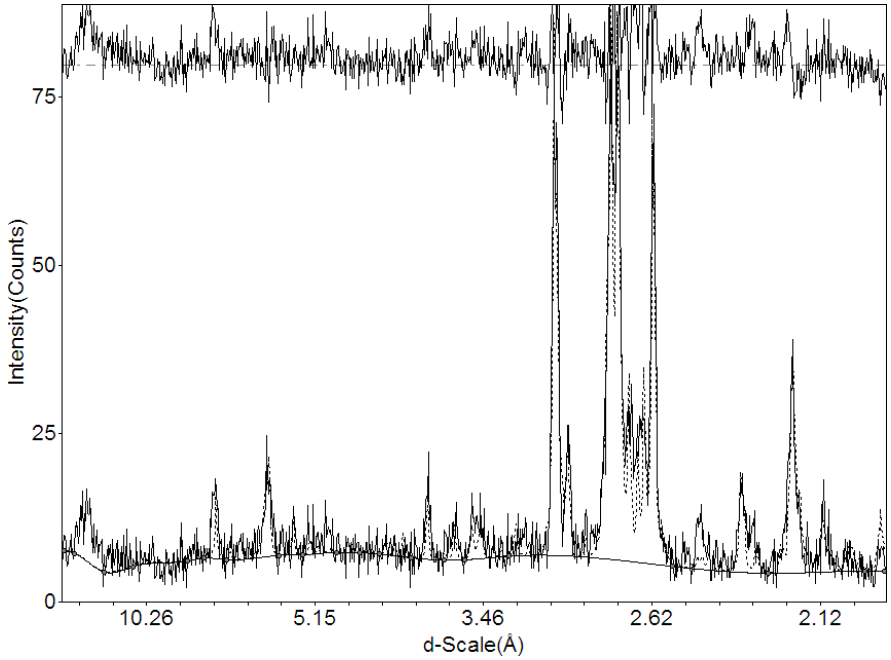

Figure P.5. Experimental, calculated, and residual (difference) (top) XRD pattern for Lafarge cement obtained with the portable Terra instrument.

The exact same trends were obtained with the Lehigh cement as with the Lafarge cement. Again, both portable and stationary instruments yielded reasonable agreement with the expected mineral concentrations. The alite–belite ratio and brownmillerite content were higher in the Terra pattern. It is not known which composition is closer to the real one because this information is not provided by the manufacturer. For QA/QC purposes, one could safely conclude that these samples were typical Type 1 portland cement using either data set because no impurities were observed and the calculated concentrations were reasonably close to the anticipated ones. With the Rietveld method, it is not possible to expect accuracy greater than 1% to 5%. The major obstacle in successfully performing this analysis is training users to use the software in a manner that avoids curve fitting and produces physically meaningful results. A round-robin study by the Internal Union of Crystallography found that user inexperience was a major source of error in quantitative analysis, exceeding absolute 5% error (*2*).

The conclusion of the analysis of portland cement clinkers was that it was possible to utilize XRD for QA/QC of the materials. The stationery equipment provided better results in terms of resolution, especially when longer scanning times were employed, but the portable equipment was also successful in identifying all major phases qualitatively. The quantitative analyses yielded some discrepancies between the stationary and

Table P.17. XRD Quantitative Results for Lehigh Portland Cement

Mineral	Formula	Bruker 1 (%)	Bruker 2 (%)	Terra (%)
Alite	$3CaOSiO_4$	56.3	53.3	62.6
Belite	$2CaOSiO_4$	22.1	24.2	11.3
Tricalcium aluminate	$3CaOAl_2O_3$	3.6	4.9	3.2
Brownmillerite	$4CaOFe_2O_3Al_2O_3$	8.2	7.4	12.7
Calcite	$CaCO_3$	4.7	4.3	n.d.
Periclase	MgO	n.d.	n.d.	n.d.
Gypsum	$CaSO_42H_2O$	1.2	1.3	2.6
Bassanite	$CaSO_40.5H_2O$	3.9	4.6	7.5

Note: n.d. = not detected.

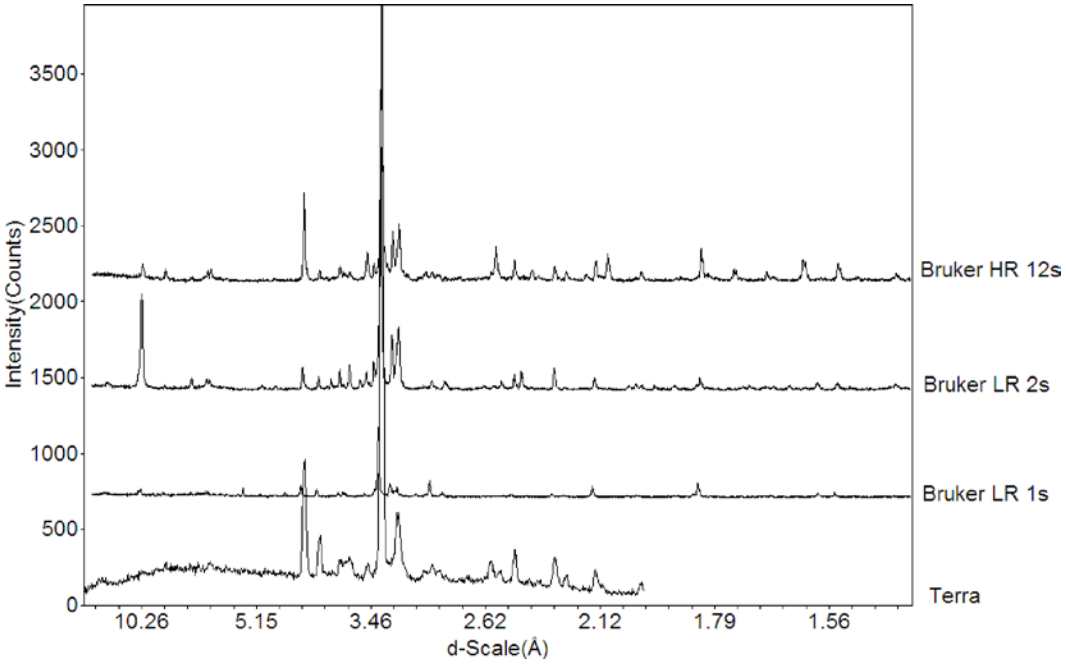

Figure P.6. XRD patterns obtained for sand with Bruker and Terra instruments.

portable equipment but remained within reasonable error. The major obstacle would be that software statistics showed that the signal-to-noise ratio of the Terra equipment was too low to trust the numerical goodness of fit. The difference pattern has to be used as guidance for the success of refinement.

Aggregates

Sand was first scanned at low dwell times (1 s and 2 s) and patterns of relatively good quality were obtained. Figure P.6 compares the LR Bruker patterns with the HR pattern obtained at 12-s dwell time and the Terra pattern. The 1-s pattern clearly had a higher detection limit and poorer resolution, with the minor peaks being obscured by the high-intensity quartz peak. There were also a few peaks that were not observed in any of the other patterns and could not be identified; this suggests variability in the sand composition. For these reasons, the 1-s pattern was not quantified, but qualitative results are included in Table P.18. The 2-s pattern was improved in terms of resolution, but the pattern was dominated by an albite (feldspar) peak that was clearly not representative of the bulk composition because quartz is the dominant sand mineral observed in other patterns. Therefore, only qualitative results are shown in Table P.18.

In the Terra pattern, only quartz and albite were detected. Consequently, quantitative results could not be accurate without the use of an internal standard; the concentrations of the phases that did not show up in the pattern were distributed

Table P.18. XRD Quantitative Results for Sand Aggregate

Mineral	Formula	Bruker HR, 12 s (%)	Bruker LR, 1 s (%)	Bruker LR, 2 s (%)	Terra (%)
Quartz	SiO_2	48.9	Yes[a]	Yes[a]	73.9
Albite	$NaAlSi_3O_8$	20.2	No[b]	Yes[a]	26.2
Microcline	$KAlSi_3O_8$	13.2	Yes[a]	No[b]	No[b]
Phlogopite	$KMg_3(Si_3Al)O_{10}(OH)_2$	15.2	Yes[a]	Yes[a]	No[b]
Cordierite	$MgAl_4Si_5O_{18}$	2.4	No[b]	No[b]	No[b]
Amorphous	na[c]	<1	na[c]	na[c]	na[c]

Note: Amorphous does not have a formula.
[a] Yes = Mineral detected.
[b] No = Mineral not detected.
[c] na = not applicable.

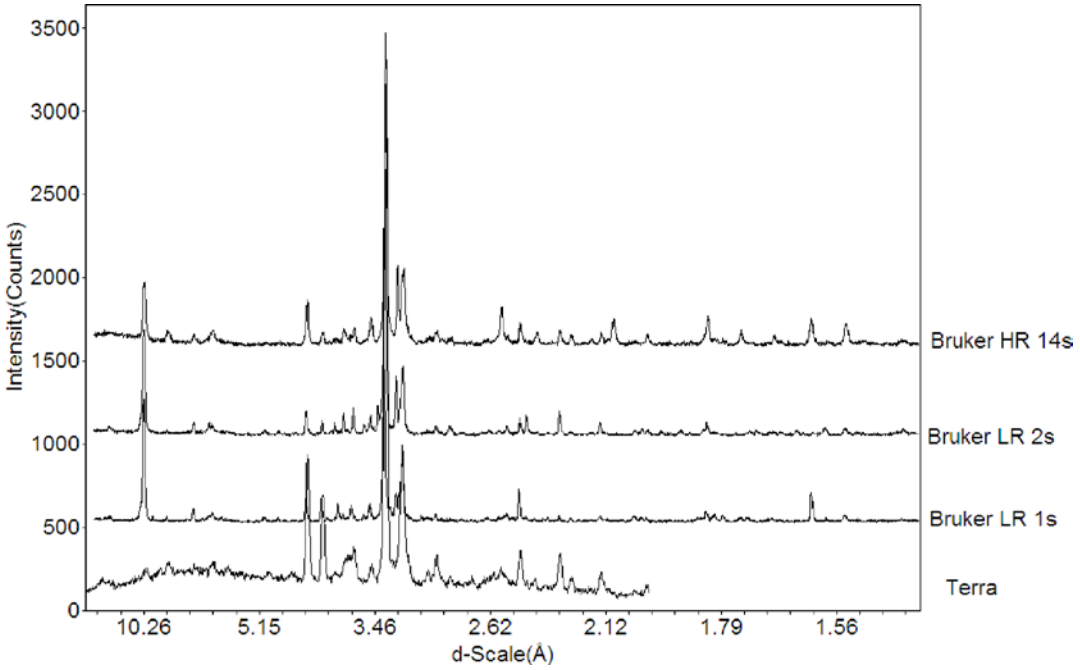

Figure P.7. XRD patterns obtained for stone with Bruker and Terra instruments.

between the two identified phases. Thus, the error was not associated with the fitting itself; Figure P.6 shows that the obtained fitting was quite good. Rietveld analysis itself is a relative method when an internal standard is not used. The more insensitive the equipment, the higher the error will be in the absence of an internal standard. In this case, Terra turned out to be quite insensitive, failing to capture the mica (phlogopite) and microcline that were captured by the Bruker LR samples.

Several XRD patterns were also obtained for the stone aggregate, with dwell times ranging from 1 s to 14 s. It was observed that the LR Bruker patterns had enough resolution for all of the phases, except one trace mineral, to be identified. The quantitative results, however, were of lower quality, with higher noise and lower goodness-of-fit values. The relative intensities of the various minerals again exhibited some variability (Figure P.7), as evidenced by the quantitative results shown in Table P.19. It appeared that Terra was only able to identify two major phases, missing several peaks, including a pronounced mica (phlogopite) peak. As with the stone, this caused a large error in the relative quantification results because of the redistribution of all unidentified phases to the identified ones.

To sum up, the quantitative XRD analysis of aggregates was only found to be meaningful as a screening tool to examine the mineralogy of aggregates originating from different sources. The natural variability of these materials prohibits the application of strict QA/QC criteria (and there is no reason

Table P.19. XRD Quantitative Results for Stone Aggregate

Mineral	Formula	Bruker HR, 14 s – Amorphous (%)	Bruker HR, 14 s (%)	Bruker LR, 1 s (%)	Bruker LR, 2 s (%)	Terra (%)
Quartz	SiO_2	37.9	40.8	26.1	27.4	64.0
Albite	$NaAlSi_3O_8$	29.0	31.2	32.6	25.7	36.0
Microcline	$KAlSi_3O_8$	4.8	5.2	12.7	5.3	n.d.[a]
Phlogopite	$KMg_3(Si_3Al)O_{10}(OH)_2$	15.0	16.1	17.2	34.0	n.d.[a]
Chlorite	$(Mg,Al)_6(Si,Al)_4O_{10}(OH)_8$	4.0	4.3	11.4	7.7	n.d.[a]
Cordierite	$MgAl_4Si_5O_{18}$	2.2	2.4	n.d.[a]	n.d.[a]	n.d.[a]
Amorphous	na[b]	7.1	na[b]	na[b]	na[b]	na[b]

Note: Amorphous does not have a formula.

[a] n.d. = not detected.

[b] na = not applicable.

for strict mineralogical criteria). If quantitative XRD is used as a screening tool, it is recommended that HR patterns are obtained. The portable XRD equipment (Terra) was very limited in the qualitative identification of phases, showing only two of the six phases present in each sample. This is perceived as a significant shortcoming for screening purposes and its further use in field applications of aggregate screening is not recommended with its current capabilities.

Portland Cement Concrete

Three concrete mixes were tested by XRD to investigate whether the relative proportion of ingredients could be determined. Table P.20 shows the mix design for the three mixes. The samples were obtained after setting and hardening for at least 3 days and were dried out. This was done to ensure that the degree of hydration would be similar in the different samples. Testing fresh cement paste with this method is challenging because drying and pulverization are necessary. Quick-drying methods, such as freeze drying, were considered but the manufacturer of the freeze driers available for the project did not consider the application to cement suitable for this equipment. Thus, abruptly halting hydration to obtain representative mineralogy as a function of progressive hydration state is not considered feasible for field conditions.

An alternative avenue that could be pursued would be to infer the amount of aggregate used by tracking the contents of its mineral compounds that are not present in portland cement (e.g., quartz). However, the quantitative analyses of the aggregates showed that there were several common minerals at high quantities [quartz, albite (feldspar), and phlogopite (mica)], which had substantial variability. Isolating the sources of each mineral turned out to be a difficult task. Nevertheless, the quantitative XRD analysis was performed to investigate whether any useful trends could be identified. All Bruker spectra were obtained at high resolutions (14-s dwell time) and used corundum as an internal standard to maximize the quality of the results. A subsample from concrete mix 1 was sent to inXitu for analysis with the Terra instrument.

Figure P.8 shows the XRD patterns of concrete obtained with the Bruker and Terra instruments, while Table P.21 summarizes the quantitative composition of PCC mix samples. The identified phases in the patterns obtained with the Bruker instrument included all the main minerals found in the two aggregates (quartz, albite, phlogopite, microcline), as well as residual alite

Table P.20. Summary of PCC Batch Proportions

Batch	1[a]	2	3
w/c	0.5	0.45	0.45
Design water	8.3%	7.6%	8.3%
Type 2 cement	16.6%	23.7%	18.4%
Batch water	8.7%	7.9%	8.7%
Stone	34.7%	41.1%	34.6%
Sand	40.0%	26.8%	38.2%
Admixture	0.0%	0.43%	0.07%
Admixture name	None	ADVA 190	Air 200
Total	100.00%	100.00%	100.00%

[a] Control.

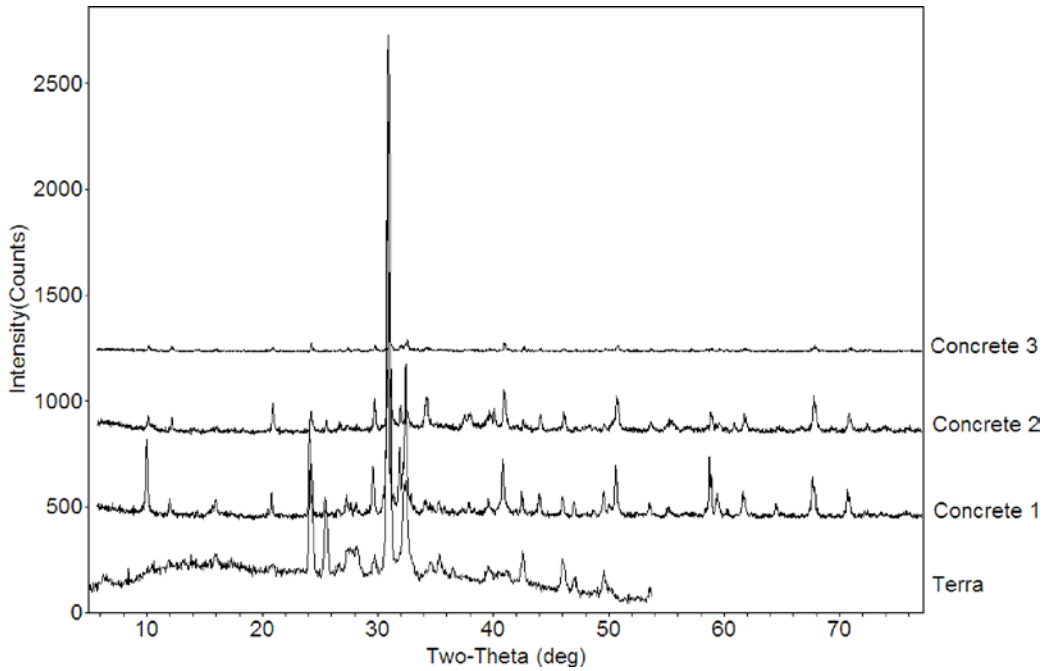

Figure P.8. XRD patterns of concrete obtained with Bruker and Terra instruments.

Table P.21. XRD Quantitative Results for Three Concrete Mixes

Mineral	Formula	Bruker Concrete 1 (%)	Bruker Concrete 2 (%)	Bruker Concrete 3 (%)	Terra Concrete 1 (%)
Quartz	SiO_2	26.4	18.8	21.4	58.8
Albite	$NaAlSi_3O_8$	14.2	9.8	15.7	41.2
Microcline	$KAlSi_3O_8$	5.0	4.1	n.d.[a]	n.d.[a]
Phlogopite	$KMg_3(Si_3Al)O_{10}(OH)_2$	3.6	11.4	10.1	n.d.[a]
Calcite	$CaCO_3$	n.d.[a]	7.8	7.0	n.d.[a]
Portlandite	$Ca(OH)_2$	1.4	4.3	2.8	n.d.[a]
Alite	$3CaOSiO_4$	1.3	10.7	n.d.[a]	n.d.[a]
Cordierite	$MgAl_4Si_5O_{18}$	3.3	nq[b]	nq[b]	n.d.[a]
Amorphous	na[c]	44.9	33.1	43.0	na[c]

Note: Amorphous does not have a formula.

[a] n.d. = not detected.

[b] nq = detected but not quantified due to low content.

[c] na = not applicable.

in two of the samples. They were calcite as a cement constituent and portlandite as a new phase derived from the hydration of portland cement. Only quartz and albite were identified by the Terra instrument; thus the stone, sand, and concrete samples were qualitatively identical based on the results obtained with the portable Terra instrument. The inability of the Terra instrument to distinguish between different materials is a major shortcoming. Thus, the portable XRD device is not considered mature enough to be taken into the field.

Based on the mix design shown in Table P.20, the composition of the concrete on a dry weight basis is 43.8% sand, 38% stone, and 18.2% portland cement. It is known from cement chemistry that hydrated portland cement contains approximately 30% portlandite. On the basis of a cement content of 18%, it would follow that hydrated concrete would contain a maximum of 5.4% portlandite. The detected concentrations ranged from 1.4% to 4.3%. One could jump to the conclusion that concrete sample 1 did not have sufficient portland cement. However, there are several reasons that portlandite could be lower, including carbonation and sample variability. Moreover, the accuracy of quantitative XRD analysis decreases with decreasing concentrations of portlandite and, when the concentration drops below 5%, uncertainty becomes quite significant. Therefore, it would be necessary to conduct at least triplicate analyses for each sample. The resources this would require are significant in terms of XRD running time and subsequent analysis.

The quartz content of the sand and stone were estimated at 48.9% and 37.9%, respectively. With these concentrations, it would follow that the expected quartz content in concrete would be 35.8%. This was not the case in any of the analyzed samples, which yielded lower quartz concentrations. This is attributed to a combination of error sources, such as the error of the method for both the individual aggregates and concrete samples, natural sample variability (which can be great), and mixing efficiency. On the basis of these findings, it is not recommended to proceed with field testing for the quantitative XRD analysis of concrete samples.

Conclusions and Recommendations on XRD

Qualitative and quantitative XRD analyses are useful methods for evaluating a material's composition and are widely applied in areas such as materials science and portland cement production, where material variability is extremely limited. The investigation of heterogeneous materials, such as natural aggregates and concrete, showed that it is not practical to apply this method in the field for QA/QC purposes. Good quantitative results require significant running time and effort in the lab, and the only portable equipment available in the market provided results of insufficient quality for either a qualitative and quantitative analysis of these three materials. Quantitative XRD was found to work for portland cement clinker (where it is already applied), but there are no major issues with the quality of clinker in the field. Interaction with people from the industry at the workshop showed that the portland cement and water contents of concrete are the major QA/QC issues; however, quantitative XRD cannot be used toward these issues. It is therefore recommended that XRD is not pursued for field testing in Phase 3.

References

1. Young, R. A. The Rietveld Method. Oxford University Press, New York, 1995.
2. Scarlett, N. V. Y., I. C. Madsen, C. Manias, and D. Retallack. On-line X-ray Diffraction for Quantitative Phase Analysis: Application in the Portland Cement Industry. *Journal of Powder Diffraction*, Vol. 16, No. 2, 2001, pp. 71–80.

APPENDIX Q

Field Verification Results

This appendix summarizes the activities and testing results from Phase 3 of the R06B project titled "Evaluating Applications of Field Spectroscopy Devices to Fingerprint Commonly Used Construction Materials." The appendix describes the Phase 3 objectives, followed by descriptions of the scope of work and experimental protocol. The example results of spectroscopic testing in the field are presented next. In addition, preliminary conclusions are briefly discussed.

Phase 3 Objectives and Scope

The main goal of Phase 3 was to verify the applicability of portable equipment identified as successful in Phase 2 to the testing of construction materials in field conditions at a level of quality that satisfies current quality assurance/quality control (QA/QC) criteria. Effectively, the following were the objectives for field experiments in Phase 3:

- Conduct field testing to demonstrate that the spectroscopic techniques recommended in Phase 2 can be transferred to field application.
- Document all test procedures and protocols for the successful techniques and applications.
- Recommend reasonable modifications to the equipment for improved implementation of the technologies.

Table Q.1 summarizes project types, locations, and labor and equipment details for the field experiments conducted in Phase 3.

Equipment, Field Settings, and Testing Protocols

Compact ATR FTIR Spectrometer

The Fourier transform infrared (FTIR) testing of all materials listed in Table Q.1 was done by the Bruker ALPHA spectrometer equipped with a single-reflection diamond attenuated total reflectance (ATR) accessory. This instrument was recognized as most successful in both fingerprinting pure compounds and chemicals and for qualitative evaluation of the chemical composition of complex composite materials. The only modification needed for field conditions was an external high-capacity battery with adapter cord supplied by the manufacturer. Typically, the ATR spectrometer was set in the trunk of a minivan and connected to a laptop and an external battery. No issues with power supply were detected during field trips. Furthermore, the ATR spectrometer was able to produce field spectra of the same precision and accuracy as laboratory spectra. It should be noted, however, that when the temperature was out of recommended range (18°C to 35°C), a longer warm-up period was required (up to 15 min versus 7 min standard).

The ATR sampling mode was used for substances in liquid, thin film, or powder form, such as paints, chemical admixtures to portland cement concrete (PCC), asphalt binders and emulsions, and cement mortars. To obtain spectra for those materials, several drops of a liquid or approximately 0.5 g of a solid were placed on the ATR sampling plate and 24 co-averaged scans were collected at a resolution of 4 cm^{-1}. In the case of thin films and powders, pressure was applied to the sample to ensure full contact with the ATR prism surface. The main issue with ATR testing of hot-mix asphalt (HMA) was relatively high (up to 30%) standard deviation from the mean of five replicates, mostly attributable to variability in particle size and material composition. The pulverized HMA and portland cement samples, however, did not yield variation higher than 15% of the mean.

During field experiments, it was helpful to analyze the binder component of the HMA mixes using dichloromethane (DCM) extraction. The DCM was found to be a more reactive, faster evaporating, and less toxic alternative to the AASHTO-standardized trichloroethylene solvent. The DCM extraction procedure included shaking 1:3 HMA–DCM

Table Q.1. Scope of Work for Phase 3

Location/Contractor	Project Type	Material Category	Sampling Method[a]	Equipment	Labor
Mansfield Depot, CT	NA	Structural coatings	Scraping dry paint (solid) Fresh paint (liquid)	Bruker ATR FTIR	Team technician
East Hartford, CT, Connecticut DOT	HMA paving/ marking	Pavement markings	Scraping dry paint (solid) Fresh paint (liquid)	Bruker ATR FTIR InnovaX XRF RTA Raman	Team technician
Mansfield Depot, CT	NA	Epoxy adhesives	Dried compound (solid) Fresh compound (liquid)	Bruker ATR FTIR	Team technician
Buckland St., Manchester, CT (site), East Granby (PCC plant), CT, Tilcon Connecticut, Inc.	Precast PCC slab casting	PCC with admixtures	Fresh PCC (paste) Fresh admixture (from the plant)	Bruker ATR FTIR, RTA Raman	3 Team technicians Site QC personnel
New York DOT, Oldcastle Precast Plant, Avon, CT	Precast wall block casting	Curing compounds for PCC	Before curing (liquid) After curing (dry)	Bruker ATR FTIR RTA Raman	Team technician Site QC personnel
I-84 eastbound, north of Exit 36, Middletown, CT, All States Asphalt Group	HMA Paving	Polymer-modified asphalt binders and mixtures	Fresh mix from the truck Extracted binder solution	Bruker ATR FTIR (binders)	Team technician
Route 160, Rocky Hill, CT, All States Asphalt Group	Novachip seal paving	Polymer-modified asphalt emulsions	Before breaking (liquid)	Bruker ATR FTIR	Team technician Site QC personnel
Route 89, Mansfield Center, CT	Rubberized chip seal paving	Polymer-modified asphalt binders	Binder from the truck Coated aggregate from the truck Binder from the road	Bruker ATR FTIR	Team technician
New Haven, CT Gateway Terminal, All States Asphalt Group	NA	Antistripping agents	Antistripping agent from tank Antistripping-modified binder	Bruker ATR FTIR	Team technician

Note: NA = not available; DOT = Department of Transportation; HMA = hot-mix asphalt; ATR = attenuated total reflectance; FTIR = Fourier transform infrared; XRF = X-ray fluorescence; RTA = Real-Time Analyzers; PCC = portland cement concrete; QC = quality control.

[a] See Appendix I for details.

solution for 1 to 2 min and filtering the solution through the regular two-layer tissue paper. To collect ATR spectra, several drops of the solution were placed on the ATR prism and left for 2 min to allow the DCM to evaporate completely. Next, the ATR absorbance spectrum was collected in the same fashion as the rest of liquid materials.

Portable XRF

The portable Innov-X Alpha X-ray fluorescence (XRF) analyzer owned by the team was used for testing traffic paints in field applications. Exchangeable alloy, soil, and mining measurement modes allowed for the detection of typical heavy metal concentrations in both liquid (laboratory tested) and solid (in situ tested) paint samples. To obtain concentration quantities, cured pavement markings were tested by applying the XRF instrument to the surface and collecting data over 90-s time intervals. Liquid paint samples were collected from the tank and tested in the laboratory (on arrival from the field) in their as-received state by placing 15 to 30 g of each sample in an XRF sample holder.

Compact Fourier Transform Raman Spectrometer

Field measurements of Raman spectra of traffic paints, curing compounds, and chemical admixtures to PCC were recorded using Real-Time Analyzers Inc.'s (RTA's) Fourier transform Raman spectrometer operating at 1,064-nm laser excitation at 500 mW. Resolution was set at 8 wave numbers (cm^{-1}) for all collections. Collection was performed using RTA's FTR software operating in continuous collection mode. A 5-m steel-jacketed fiber optic probe was used for collection. Given the potential interference of ambient light, spectral analysis consisted of first evaluating those contributions and determining the appropriate background removal techniques to yield spectra consistent with those of controlled laboratory conditions.

Initial evaluation of field conditions as they pertain to safety for outdoor laser operations was performed. While the Raman spectrometer is not in collection mode, the laser shutter is always closed to ensure safe handling and to minimize potential exposure. Only when the probe tip has been securely

applied to a sampling surface is the laser shutter opened. Additional precautions regarding safe handling of lasers for outdoor operation can be found in the approved American National Standard Institutes publication, ANSI Z136.1 (2007). Certain materials may require modifications to the nominal hazard zone (NHZ) calculations for use in transportation specific applications. All personnel within the NHZ must be made aware of the operation of the laser, advised of the potential hazards, and provided with proper safety control measures. For instance, the light reflected by any material with increased specular or diffuse reflectance may damage eyes of an operator. Other circumstances may arise in field conditions that could increase the likelihood of laser exposure and it is advised that operators be well versed in the safe operation and handling of laser equipment. For the current study, operators were equipped with Occupational Safety and Health Administration–approved eyewear and no additional personnel were present. More details on Raman measurements and sample handling are provided in this appendix.

Field Test Description and Results

Epoxy Coatings and Adhesives: ATR

Objectives:	Fingerprinting (verification of chemical composition) of fresh and dried epoxy samples
Team operators:	Iliya Yut
Field operator:	Not available (NA)
Equipment:	Bruker ALPHA ATR
Test date:	September 23, 2011
Location:	CAP Lab, Mansfield Depot, Connecticut
Contractor:	NA
Project type:	NA
Material collected:	Carbozinc 859 and Scotchkote (epoxy structural coatings) and Ultrabond 1100 (epoxy adhesive)—individual components
Sample type:	Liquid (freshly mixed compounds), thin films (dried structural coatings on the metal surface), solids (adhesives)
Ambient temperature:	23°C

Three types of epoxies were evaluated by the Bruker ALPHA ATR spectrometer to investigate the feasibility of fingerprinting their chemical composition in situ: (1) three-part, organic, zinc-rich epoxy coating system (Carbozinc 859), (2) fusion-bonded epoxy (Scotchkote), and (3) two-part high-strength epoxy bonding adhesive (Ultrabond 1100). The primary objective of the experiment was to obtain a signature spectrum for each material under the field conditions in Phase 3. The signature spectra obtained in Phase 3 were compared with those from the preliminary testing in the laboratory (Phase 2). In addition, changes in the ATR spectra of the applied epoxies during the drying process were analyzed.

Because of Connecticut Department of Transportation (DOT) limitations, the research team did not obtain access to any site projects involving bridge construction. Instead, the samples for Phase 2 testing were fabricated by mixing ingredients in accordance with manufacturer's instructions and applying the coating to a metal plate. Nevertheless, all epoxy samples were tested using the same equipment setup as for the other materials (i.e., the ATR spectrometer was set in the back of a van and the external battery was used).

Figure Q.1 compares the ATR spectra of the two Scotchkote samples collected during laboratory (Phase 2) and field

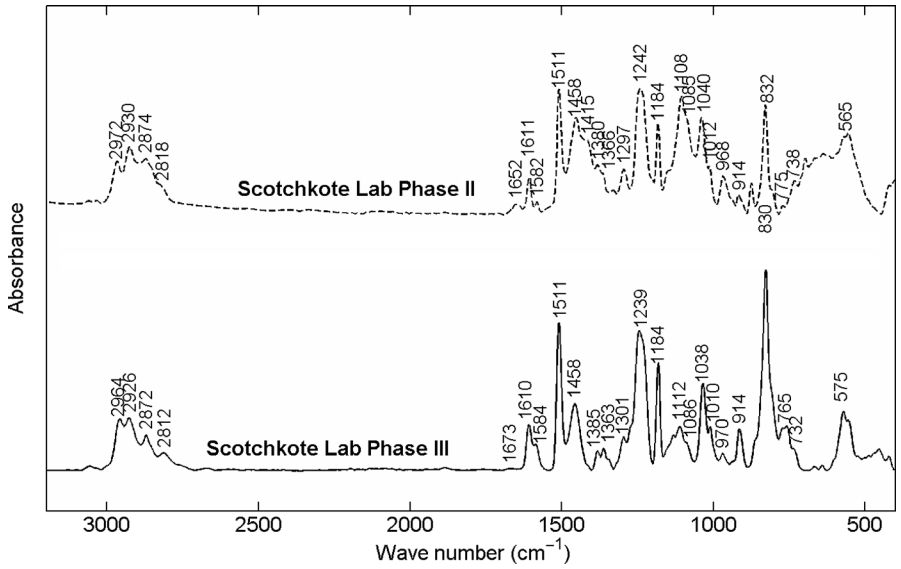

Figure Q.1. Comparison of the ATR spectra of Scotchkote epoxy coating samples collected in Phases 2 and 3.

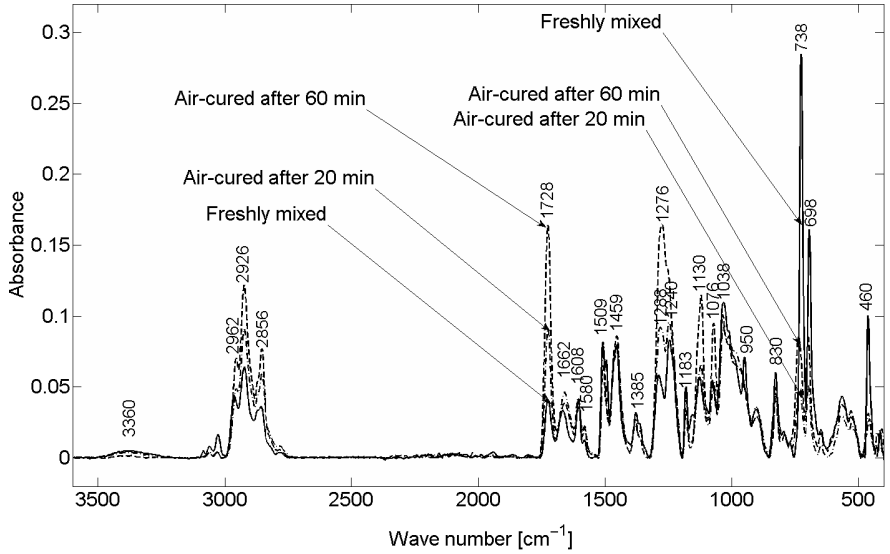

Figure Q.2. Change in the ATR spectra attributable to curing of Carbozinc 859 epoxy coating system.

(Phase 3) stages. Note that two different Bruker ALPHA ATR instruments of the same model were used to obtain the material spectra 18 months apart between testing events. One can confidently see the absence of any visible differences between the laboratory and field sample based on the location of the characteristic peaks shown in Figure Q.1. Similarly, a perfect match between the laboratory and field samples was found for the Carbozinc 859 coating system.

Once the freshly mixed epoxy coating was applied to a metal plate, ATR spectra of the material scraped from the plate surface were collected immediately and after 20 and 60 min, respectively. The three spectra shown in Figure Q.2 indicate the evaporation of toluene solvent by a drastic decrease in the infrared (IR) absorbance at 738 and 698 cm^{-1}, and the hardening and oxidation of the epoxy base by an increase in the absorbance at 1,728 and 1,276 cm^{-1}. Nevertheless, the presence of epoxy resin can be tracked even after an hour of air-curing, as evident by the IR absorption peaks at 1,662, 1,608, and 1,580 cm^{-1}.

Similarly to the epoxy structural coatings, the laboratory and field samples of the Ultrabond 1100 adhesive bonding system are superimposed in Figure Q.3. Once again, all characteristic peaks from the lab sample produced in Phase 3 are located within 5 cm^{-1} wave number from those in the sample

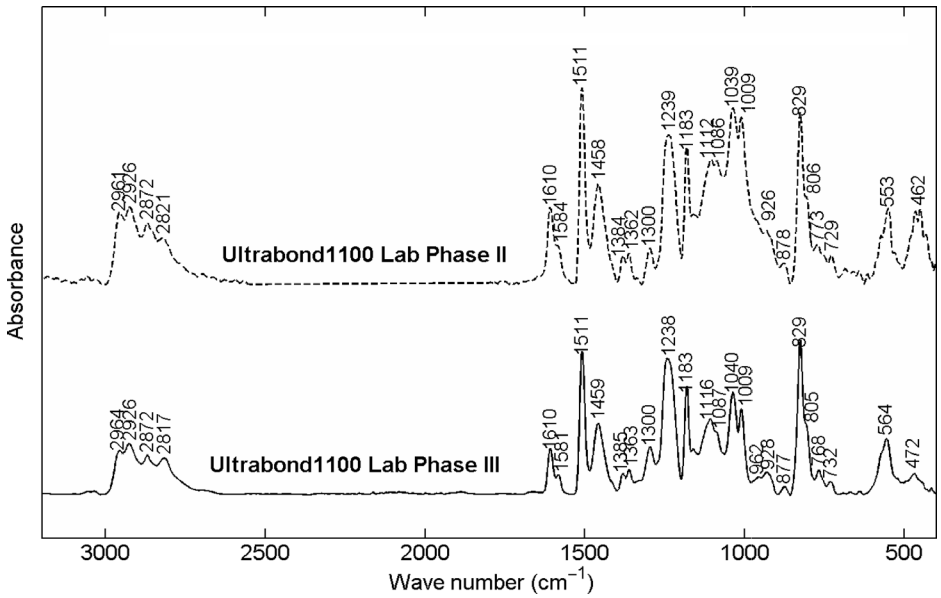

Figure Q.3. Comparison of the ATR spectra of Ultrabond 1100 epoxy adhesive samples collected in Phases 2 and 3.

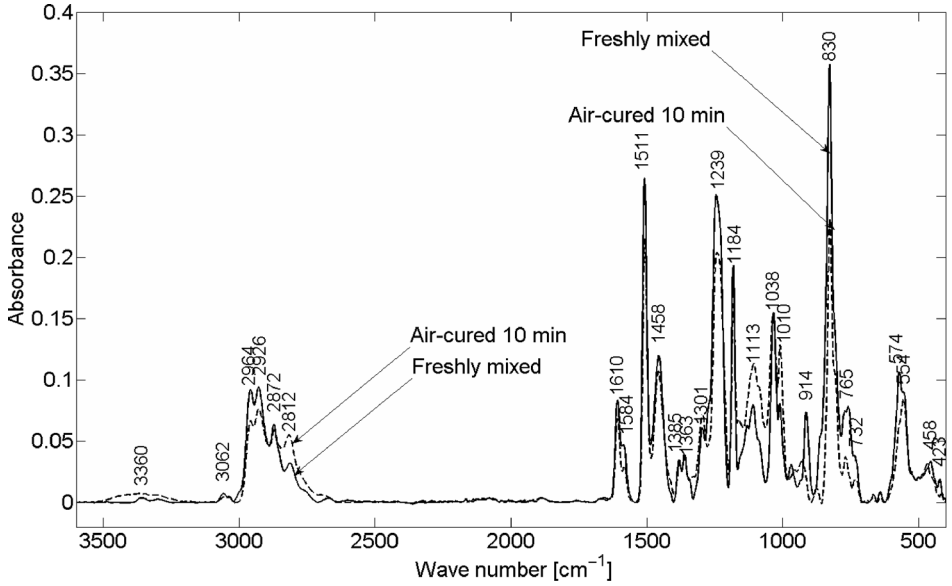

Figure Q.4. Change in the ATR spectra attributable to curing of Ultrabond 1100 epoxy adhesive.

tested in Phase 2 18 months earlier by a different instrument. Figure Q.4 shows that the adhesive can be positively identified within 10 min (onset time) from the moment of application.

Traffic Paints: XRF

Objectives:	Quantification of elemental composition of traffic paints (see example in Figure Q.5)
Team operators:	Chad Johnston
Field operator:	NA
Equipment:	Innov-X Systems XRF
Test date:	September 14, 2011
Location:	East Hartford, Connecticut
Contractor:	Connecticut DOT District 1 Pavement Marking Department
Project type:	Test of white and yellow pavement markings
Material collected:	White and yellow Ennis Fast Dry waterborne traffic paints
Sample type:	Liquid paint samples collected directly from paint applicator truck (lab analysis) and painted lines (field analysis)
Ambient temperature:	22°C

The concentrations of selected elements in Ennis white and yellow traffic paints are presented in Table Q.2 and Table Q.3, respectively. Three separate measurements were recorded for each paint strip. Each individual measurement has instrument-determined error values (±) that are element specific. The average elemental concentrations and standard deviations were computed for all sample types. Both white and yellow traffic paints are composed of greater than 10% Ca. This open-ended result is likely attributable to the high Ca signal that apparently saturated the XRF detector at 10% detection. The Ca is likely in the form of $CaCO_3$, which is added as a pigment extender for TiO_2. Thus, if one can assume that all of the Ca in the samples is in the form of $CaCO_3$, this translates to a $CaCO_3$ concentration of greater than 25%. The white paint contains an average of 64,772 ppm Ti, which is twice that of the yellow paint, which averaged 27,717 ppm Ti. This is attributed to the higher requirement of the white pigment, rutile. Titanium concentrations in the field test correspond to a TiO_2 content of 11% and 5% in white and yellow paints, respectively. The yellow pigment may be organic based (e.g., Yellow 65), which is undetectable via XRF, or iron (Fe) based (e.g., Fe-oxide). This latter possibility is supported by the average Fe concentrations of 769 and 3,100 ppm detected in white and yellow paints, respectively.

Measurements of the asphalt (i.e., the unpainted pavement surface) (see Table Q.4), and fresh white and yellow paint samples (Tables Q.5 and Q.6, respectively) were collected to evaluate possible interference with the road markings by the underlying substrate. XRF measurements in the field and fresh paint samples in the lab should yield comparable results, and, if not, a likely possibility would be the unwanted signal contribution from the pavement. This possibility arises because of the complexity of X-ray penetration depth, which ranges from micrometers to millimeters. Thus, if

Figure Q.5. Device calibration (*top left*), white paint testing (*top right*), zoom on XRF instrument (*bottom left*), and image of XRF result screen (*bottom right*).

incident X-rays penetrated beyond the paint layer into the asphalt, the measured data may not accurately reflect the true elemental composition of the paint, rather some unknown combination of the paint and the pavement. The results show slightly increased K, Fe, and Ti concentrations in the field versus the laboratory, which could be attributable to the asphalt. Alternatively, the discrepancy may be because the lab samples were fresh and thus had higher moisture content than that of the dried marking in the field. Water is undetectable via XRF but would still contribute to the overall mass and essentially dilute the concentrations of elements.

Table Q.2. Elemental Composition of White Traffic Paint Strip as Determined by XRF

Element	Sample 1		Sample 2		Sample 3		Average	
	Concentration (ppm)	±	Concentration (ppm)	±	Concentration (ppm)	±	Concentration (ppm)	SD
Ca	>10%	1%	>10%	1%	>10%	1%	>10%	na
K	4,791	448	5,668	394	4,811	383	5,090	676
S	ND	na	10,409	3,213	ND	na	10,409	na
Ti	62,051	1,207	65,260	1,045	67,005	1,071	64,772	2,988
Ba	587	102	770	87	818	89	725	142
Mn	ND	na	ND	na	ND	na	ND	na
Fe	669	22	794	20	843	20	769	106
Zn	24	4	18	4	ND	na	14	16
Sr	112	3	147	3	197	4	152	53
Zr	92	3	56	2	84	3	77	25

Note: ND = not determined.

Table Q.3. Elemental Composition of Yellow Traffic Paint Strip as Determined by XRF

Element	Sample 1		Sample 2		Sample 3		Average	
	Concentration (ppm)	±	Concentration (ppm)	±	Concentration (ppm)	±	Concentration (ppm)	SD
Ca	>10%	1%	>10%	1%	>10%	1%	>10%	na
K	5,109	333	4,170	308	4,208	306	4,496	614
S	ND	na	ND	na	ND	na	ND	na
Ti	27,774	467	27,894	457	27,484	448	27,717	295
Ba	343	54	224	52	315	52	294	81
Mn	ND	na	ND	na	ND	na	ND	na
Fe	3,803	59	2,644	42	2,854	45	3,100	718
Zn	79	5	78	5	77	5	78	1
Sr	168	3	156	3	144	3	156	15
Zr	90	3	90	3	96	3	92	5

Note: ND = not determined.

Table Q.4. Elemental Composition of Asphalt Adjacent to Paint Strips

Element	Sample 1		Sample 2		Sample 3		Average	
	Concentration (ppm)	±	Concentration (ppm)	±	Concentration (ppm)	±	Concentration (ppm)	SD
Ca	39,874	674	64,408	1,077	35,299	598	46,527	21,632
K	9,769	323	8,772	335	10,007	319	9,516	909
S	7,521	1,514	7,358	1,783	8,184	1,502	7,688	607
Ti	5,124	165	7,230	216	3,978	149	5,444	2,322
Ba	365	37	578	47	414	36	452	145
Mn	969	24	1,217	30	786	22	991	306
Fe	45,131	636	65,054	968	51,450	709	53,878	13,002
Zn	124	7	123	7	70	5	106	42
Sr	133	3	146	3	122	3	134	17
Zr	104	3	85	3	82	3	90	14

Table Q.5. Elemental Composition of White Traffic Paint as Determined by In-Lab XRF

Element	Sample 1		Sample 2		Average	
	Concentration (ppm)	±	Concentration (ppm)	±	Concentration (ppm)	SD
Ca	>10%	1%	>10%	1%	>10%	na
K	3,296	298	2,596	285	2,946	495
S	ND	na	ND	na	ND	na
Ti	49,598	755	48,818	735	49,208	552
Ba	624	71	795	71	709.5	121
Mn	ND	na	ND	na	ND	na
Fe	570	15	589	15	579.5	13
Zn	ND	na	ND	na	ND	na
Sr	121	3	123	3	122	1
Zr	39	2	35	2	37	3

Note: ND = not determined.

Table Q.6. Elemental Composition of Ennis Yellow Traffic Paint as Determined by In-Lab XRF

Element	Sample 1		Sample 2		Average	
	Concentration (ppm)	±	Concentration (ppm)	±	Concentration (ppm)	SD
Ca	>10%	1%	>10%	1%	>10%	na
K	2,819	256	3,086	261	2,953	189
S	ND	na	ND	na	ND	na
Ti	21,505	359	22,000	366	21,753	350
Ba	369	46	316	46	343	37
Mn	25	6	ND	na	13	18
Fe	2,177	35	2,248	36	2,213	50
Zn	62	4	70	5	66	6
Sr	127	3	133	3	130	4
Zr	86	2	91	2	89	4

Note: ND = not determined.

Traffic Paints: ATR

Objectives: Fingerprinting of the traffic paint samples in the field (see example in Figure Q.6)
Team operators: Iliya Yut
Field operator: NA
Equipment: Bruker ALPHA ATR
Test date: September 1, 2011
Location: East Hartford, Connecticut
Contractor: Connecticut DOT District 1 Pavement Marking
Project type: Test white and yellow line marking
Material collected: Ennis waterborne Fast Dry paint (white and yellow)
Sample type: Liquid from tank, thin film from surface (freshly painted and old)
Ambient temperature: 26°C

Figure Q.6. Application of white paint (top left), sampling from the tank (top right), sampling from the surface (bottom left), and sample placed on ATR plate (bottom right).

The ATR spectra of Ennis Fast Dry white paint samples from tank, newly painted white line, and the old white line are compared in Figure Q.7. The waterborne vinyl acrylate structure of a liquid sample from a tank can be easily identified by the medium-wide water-associated (~3,400, ~3,250, and ~1,640 cm^{-1}) and strong sharp carboxylate-associated (~1,730 and ~875 cm^{-1}) absorption bands. Note that the evaporation of water can be tracked by observing significant reduction in the intensity of the OH vibrations in the freshly painted white line (about 15 to 30 min after application). Consequently, no water can be detected in the old paint several months after application. The waterborne polyacrylic paint in discussion can definitely be fingerprinted by matching multiple peaks in the region between 400 and 1,800 cm^{-1} to a library spectrum as shown in Figure Q.8.

PCC and Chemical Admixtures: ATR

Objectives:	Fingerprinting of chemical admixtures and verification of their presence in a PCC sample (see example in Figure Q.9)
Team operators:	Chad Johnston, Alexander Bernier, Russell Duta
Field operator:	Site Foreman
Equipment:	Bruker ALPHA ATR
Test date:	July 11, 2011
Location:	Park-and-Drive facility, Buckland Street at Buckland Hill Drive, Manchester, Connecticut
Contractor:	Tilcon Connecticut Inc. (East Granby PCC Plant)

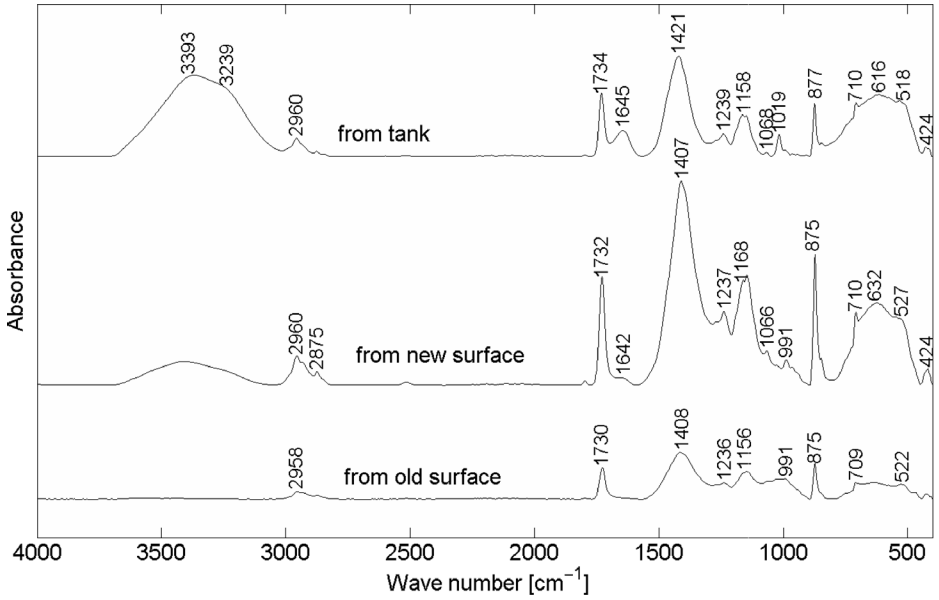

Figure Q.7. Comparison of the ATR spectra of Ennis Fast Dry white paint sampled from tank, freshly applied white marking, and old white line surface.

Project type:	Precast PCC slab casting
Material collected:	PCC, set-accelerating, air-entraining, and high-range water-reducing admixtures
Sample type:	Solid (fresh PCC from cast), liquid (chemical admixtures from plant)
Ambient temperature:	33°C

The ATR spectra of air-entraining, high-range water-reducing (HRWR), and set-accelerating admixtures are shown in Figures Q.10 through Q.12, respectively. Each figure superimposes spectra of three samples for each admixture:

1. Sample from the vendor's container during the laboratory testing in Phase 2,
2. Sample collected from a PCC plant and tested in the field (Phase 3), and
3. Sample collected from a PCC plant and tested in the laboratory on return from the field (Phase 3).

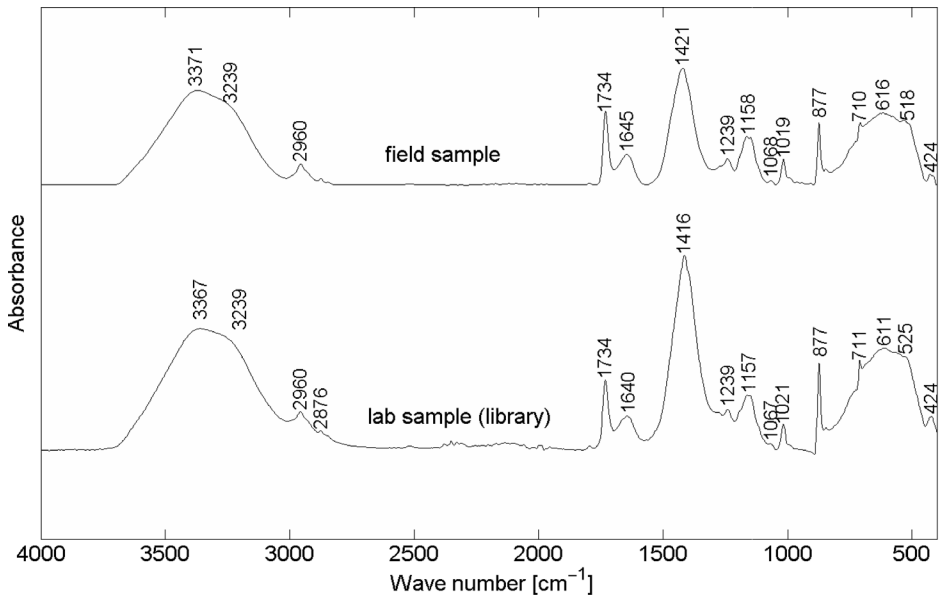

Figure Q.8. Matching ATR spectrum of Ennis Fast Dry white paint to a library spectrum.

Figure Q.9. Pouring of PCC into a slab mold (*top left*), sampling PCC (*top right*), placing PCC sample onto ATR plate (*bottom left*), and sampling of chemical admixture (*bottom right*).

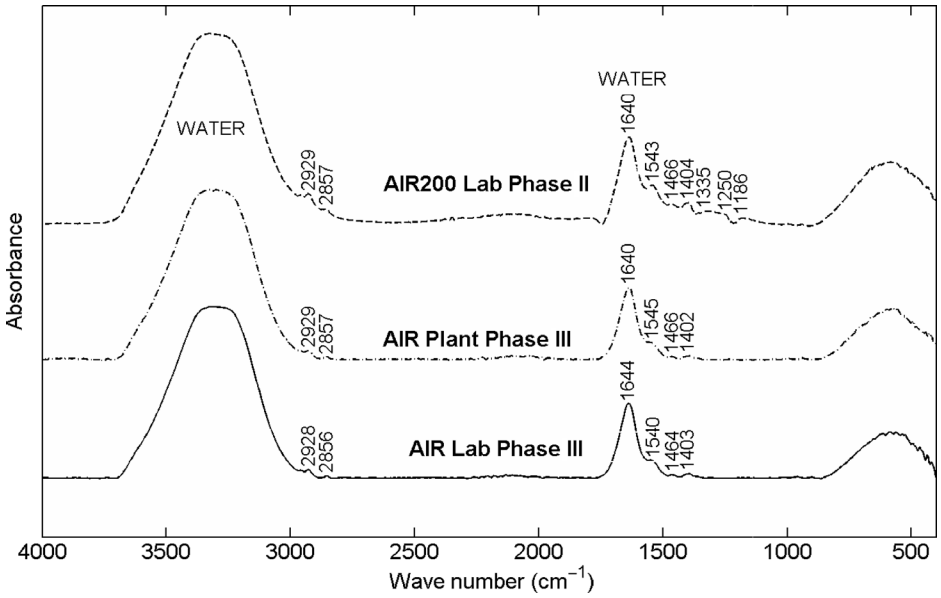

Figure Q.10. Fingerprinting of air-entraining chemical admixture.

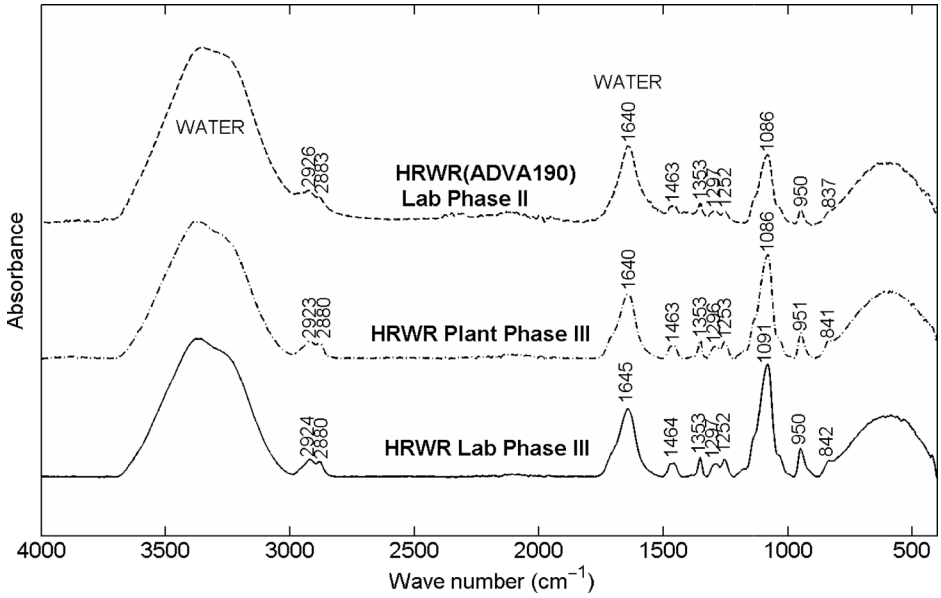

Figure Q.11. Fingerprinting of high-range water-reducing chemical admixture.

The characteristic absorption peaks associated with the tall oil component of the AIR chemical (2,929, 2,857, 1,543, 1,466, and 1,402 cm^{-1}) can be easily identified on each spectrum in Figure Q.10. On the basis of the analysis of spectra shown in Figure Q.11, the HRWR admixture collected from the plant (vendor is unknown) can be positively identified as ADVA 190, which was supplied by W. R. Grace & Co. for preliminary laboratory testing in Phase 2. The nonchloride SicaSet accelerator (NCL in Figure Q.12) can be distinguished from Accelguard 80 chemical by the presence of the thiocyanate-related band at 2,070 cm^{-1}, which is absent in Accelguard 80. Note that the calcium nitrate component in both admixtures (required by the ASTM standards) is identified by the prominent peak at about 1,330 cm^{-1} with a distinctive shoulder at 1,420 to 1,410 cm^{-1}.

It should be noted that two different Bruker ALPHA ATR instruments were used to perform FTIR testing in laboratory and in the field. Nevertheless, the very precise identification of the characteristic absorption peaks for all admixtures in discussion (within 5 cm^{-1} wave number) was possible. Thus,

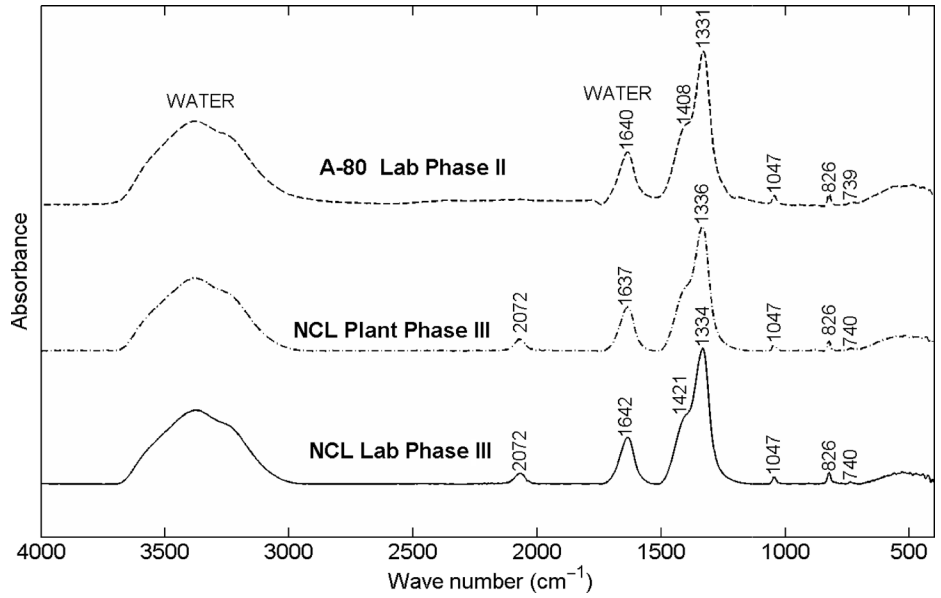

Figure Q.12. Fingerprinting of nonchloride set-accelerating chemical admixture.

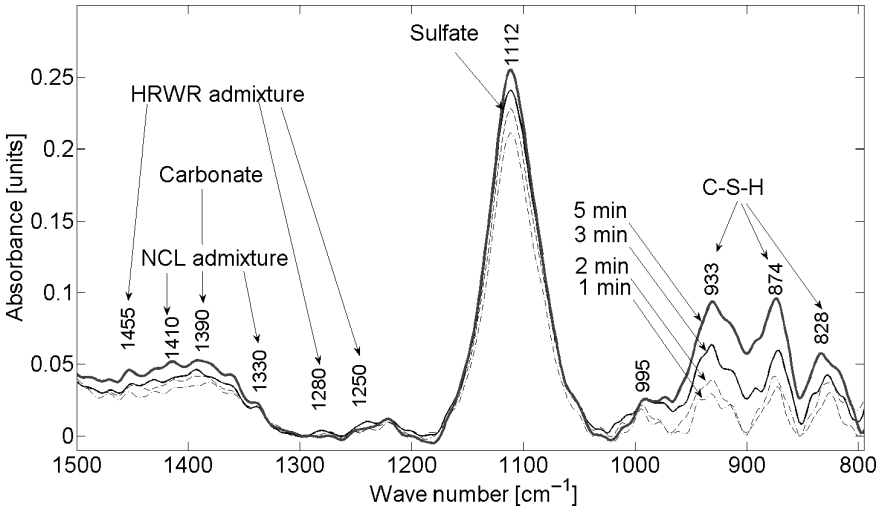

Figure Q.13. ATR spectra of hydrated PCC sample with HRWR and NCL admixtures.

it can be concluded that the FTIR spectra of chemical admixtures for PCC can be standardized without concern for precision and accuracy of the measurements.

One of the objectives of the FTIR testing of PCC was verification of the admixture's presence in a fresh PCC mix. The preliminary results in Phase 2 indicated this task as a very challenging one, primarily because of usually very low (less than 1% by weight) concentration of the admixtures. However, in knowing that HRWR chemicals preserve rate of hydration, the presence of HRWR can be verified by the relatively strong IR absorption peaks at 933, 874, and 828 cm^{-1} associated with formation of the primary hydration product [calcium–silicate–hydrate (C-S-H)], as shown in Figure Q.13. A closer look at the zoomed-in spectra in the region between 1,500 and 1,300 cm^{-1} reveals relatively weak but visible peaks associated with admixtures. For instance, the three peaks at 1,455, 1,280, and 1,250 cm^{-1} can be related to the presence of HRWR, while the two peaks at 1,410 and 1,330 indicate presence of NCL accelerator.

Curing Compounds: Attenuated Total Reflectance

Objectives:	Fingerprinting and verification of presence on the PCC surface (see example in Figure Q.14)
Team operators:	Iliya Yut
Field operator:	PCC plant technician
Equipment:	Bruker ALPHA ATR
Test date:	September 1, 2011
Location:	Avon, Connecticut
Contractor:	Oldcastle Precast
Project type:	In-plant precast foundation block manufacturing
Material collected:	TAMMSCURE curing compound
Sample type:	Liquid from container, powder from freshly covered PCC surface, powder from dried PCC surface
Ambient temperature:	23°C

Figure Q.15 superimposes the ATR spectra of the pure chemical (TAMMSCURE curing compound), the sample scratched from the freshly covered PCC surface, and the sample of dried PCC surface. Each spectrum represents an average of three replicate probes from each sample. It is obvious from Figure Q.15 that characteristic peaks (2,938, 2,856, 1,455, and 1,374 cm^{-1}) associated with hydrocarbon resin and aliphatic naphtha components of TAMMSCURE (see material safety data sheets) can be tracked on the ATR spectra of both freshly covered and dried PCC surfaces to which the curing compound have been applied.

Figure Q.16 compares ATR spectrum of TAMMSCURE tested from the dispenser in the plant with the spectrum of Sealtight from the manufacturer's package tested in the laboratory. An identical location of the peaks at 2,926, 2,851, and 1,455 cm^{-1} on both spectra indicates their similar chemical composition (emulsified hydrocarbon resin). However, the low intensity of those peaks relative to the water-associated bands centered around 3,400 and 1,650 cm^{-1} on the TAMMSCURE spectrum suggests higher water content (dilution) in the field application of this material. A sample collected in the plant and tested a day later in the laboratory yielded an ATR spectrum identical to that of its original condition.

Polymer-Modified Hot-Mix Asphalts: ATR

Objectives:	Verification of polymer presence and quantification
Team operators:	Chad Johnston and Iliya Yut

Figure Q.14. Equipment setup (*top left*), pure TAMMSCURE sampling (*top right*), surface sampling (*bottom left*), and sample on ATR plate (*bottom right*).

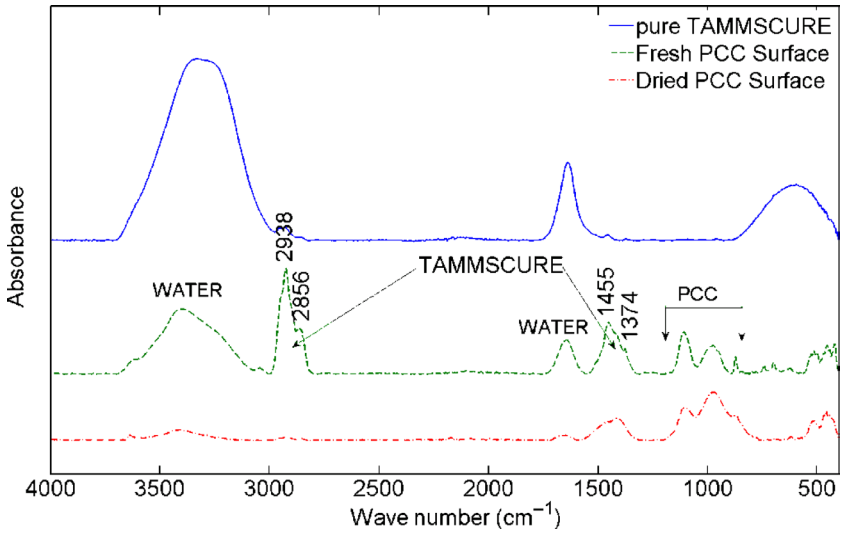

Figure Q.15. ATR spectra of TAMMSCURE curing compound before and after application to a PCC surface.

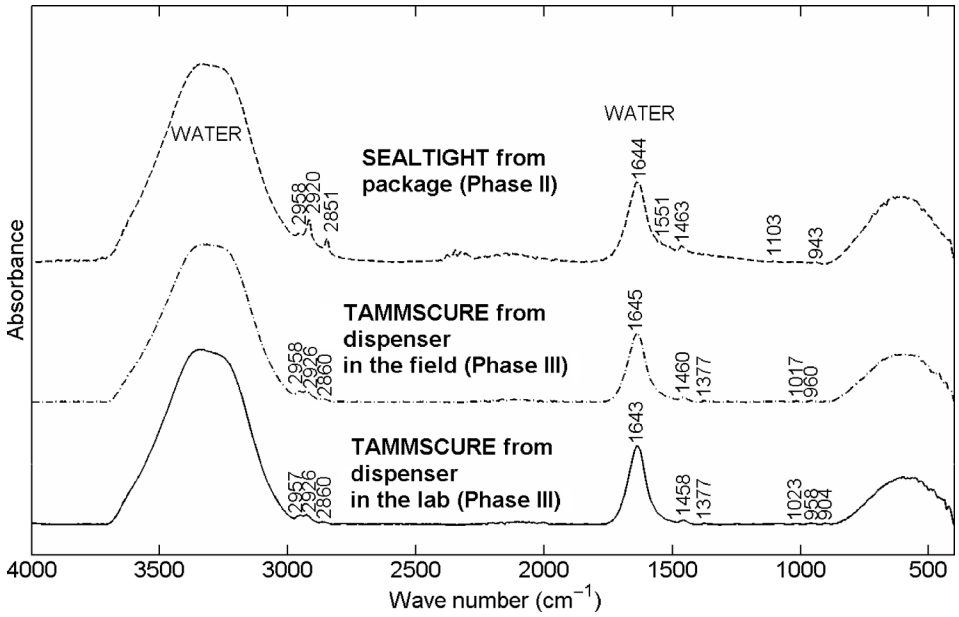

Figure Q.16. Comparison of the field TAMMSCURE and laboratory Sealtight ATR spectra of curing compound.

Field operator:	NA
Equipment:	Bruker ALPHA ATR
Test date:	August 16, 2011
Location:	Farmington, Connecticut, I-84 Eastbound, North of Exit 36
Contractor:	All States Asphalt Group
Project type:	2-in HMA overlay with styrene–butadiene–styrene (SBS)-modified PG 76-22 binder
Material collected:	HMA mix from paver, tack coat from pavement surface
Sample type:	Solid HMA and liquid tack coat (emulsion)
Ambient temperature:	28°C

Note: The project took place at night (9:00 p.m.) and no photos were taken.

Figure Q.17 presents the normalized (to 2,920 cm^{-1} peak value) ATR spectra of two samples taken from the paver within 15 min of each other (two separate trucks unloaded). One can see that absorption peaks of the two samples are matching, which suggests they have identical chemical

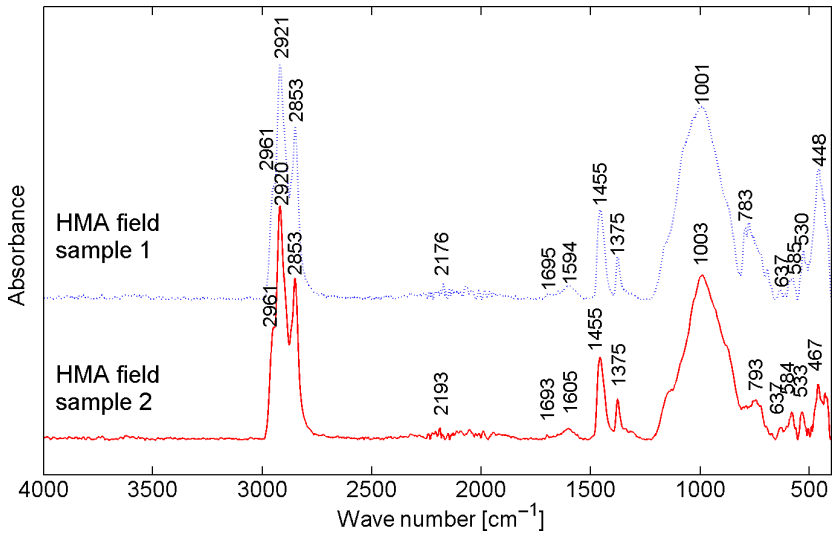

Figure Q.17. ATR spectra of HMA field samples.

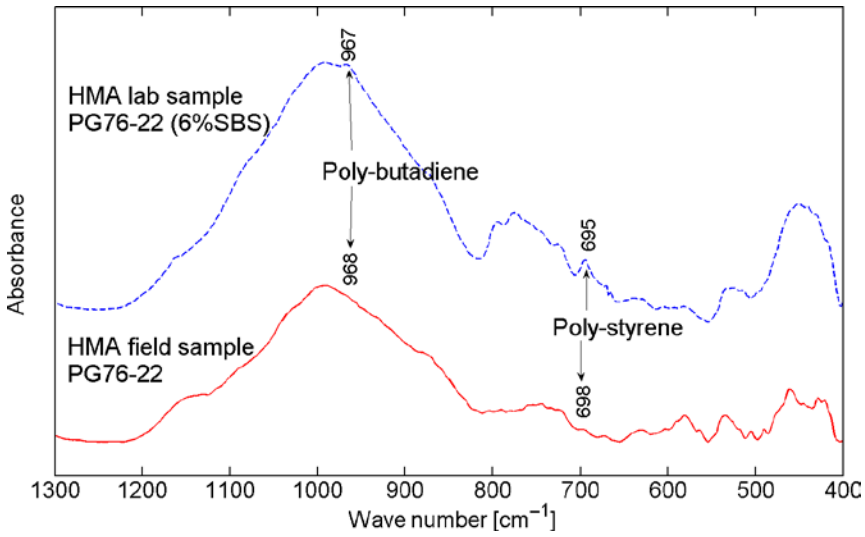

Figure Q.18. Zoom on SBS-associated absorption bands in laboratory and field samples of polymer-modified HMA.

composition. The peak at about 2,180 cm^{-1} indicates the presence of carbon dioxide from entrapped hot air. In addition, minor oxidative hardening resulting from mixing and placement of the HMA can be detected by the peak at about 1,700 cm^{-1}. The rest of the peaks are associated with the binder (2,961, 2,921, 2,853, ~1,600, 1,455, and 1,375 cm^{-1}) and filler and aggregates (~1,000, 793, 637, 585, 530, and 467 cm^{-1}). A closer look at the ATR spectrum in Figure Q.18 allows for the identification of weak but not negligible peaks associated with the presence of SBS polymer in the PG 76-22 binder.

Figure Q.18 compares the ATR spectrum of the SBS-modified HMA sample collected from the field with that of a sample mixed in the laboratory. A close look at the two spectra allows for identifying weak but not negligible peaks associated with presence of SBS polymer in the PG 76-22 binder. It should be noted that the polybutadiene peak at 967 cm^{-1} is likely to be obscured by the strong and wide band centered around 1,000 cm^{-1} that is associated with the silicate component of the aggregates. Furthermore, the peak near 700 cm^{-1} can be associated with quartz presence in silicious aggregates rather than with polystyrene-related IR absorptions.

Therefore, quantification of SBS content in the fresh mix appears to be impractical for two reasons. First, the weight percent content of the polymer compared with the mix sample weight is extremely low (around 0.002 wt %), which makes identifying the SBS peaks a very challenging task. Second, the polymer content is usually governed by a binder grade specification. Therefore, it appears logical to verify polymer content in an extracted binder sample as discussed in the next section.

Identification of Polymer in Asphalt Binder Extracted from HMA–ATR

Objectives:	Verification of polymer presence
Team operators:	Iliya Yut
Field operator:	NA
Equipment:	Bruker ALPHA ATR
Test date:	May 23, 2011
Location:	Rocky Hills, Connecticut, Route 160 Westbound
Contractor:	All States Asphalt Group
Project type:	Novachip seal
Material collected:	SBS-modified HMA mix from paver
Sample type:	Liquid (1:3 stabilized DCM solution)
Ambient temperature:	23°C

Special Sample Preparation

About 5 g of HMA passing No. 16 (1.18-mm) sieve size were added to 15 mL of stabilized DCM for spectroscopic applications, manually shaken for 2 min, and then left for 15 min to allow sedimentation of suspended filler particles. The liquid phase of the solution was probed by pipetting two to three drops on the ATR sampling plate. The ATR spectra of the sample were collected twice: immediately and within 1 to 2 min from the moment of placement.

Results

Figure Q.19 compares the ATR spectra in the fingerprinting region (1,800 to 400 cm^{-1}) of a DCM-extracted PG 76-22 binder sample obtained immediately and 1 min after placing the sample on the ATR plate. It is shown that the only three

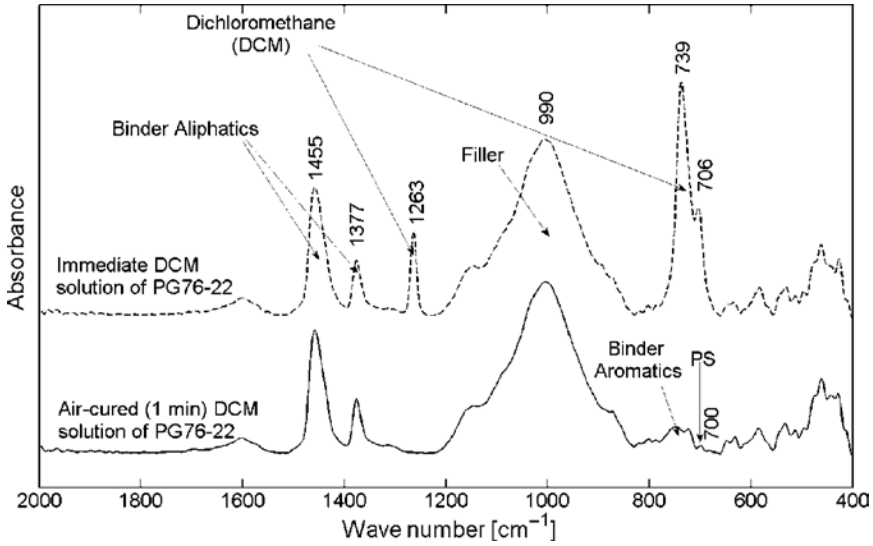

Figure Q.19. Identification of SBS polymer in asphalt binder PG 76-22 extracted from HMA.

characteristic absorption peaks attributed to DCM, which are at 1,263, 739, and 706 cm^{-1}, do not interfere with characteristic peaks of the aliphatic component of the binder (1,455 and 1,377 cm^{-1}) or with the absorption of filler particles. However, the DCM solvent peaks do obscure the signal from the aromatic hydrocarbons (860 to 725 cm^{-1}) and, if present, from the polystyrene component of the SBS polymer (expected around 700 cm^{-1}). When sample is allowed to cure for 1 min, the solvent evaporates completely, making it possible to identify both binder aromatics and the SBS-related peak.

Polymer-Modified Asphalt Emulsions—ATR

Objectives:	Verification of polymer presence (see example in Figure Q.20)
Team operators:	Chad Johnston and Iliya Yut
Field operator:	John DaDalt
Equipment:	Bruker ALPHA ATR
Test date:	May 23, 2011
Location:	Rocky Hills, Connecticut, Route 160 Westbound
Contractor:	All States Asphalt Group
Project type:	Novachip seal
Material collected:	CRS-2 polymer-modified emulsion, ready-coated seal stone.
Sample type:	Liquid emulsion, solid-coated stone particle
Ambient temperature:	15°C

Figure Q.21 superimposes the ATR spectra of the polymer-modified emulsion CRS-2 in two states: (1) sampled from the tank and (2) applied to stone aggregate (Novachip seal technology). The two main emulsion components are easily identified by strong and wide water bands centered around 3,300 and 1,640 cm^{-1} and doubled aliphatic binder peaks at about 2,920, 2,850, 1,455, and 1,375 cm^{-1}. The SBS additive can be detected by two characteristic peaks at 967 and 700 cm^{-1} associated with polybutadiene and polystyrene, respectively. The spectra of the Novachip stone coated by the CRS-2 emulsion clearly indicate the absence of water after the emulsion breaks on the aggregate. Note that the wide band at 1,600 cm^{-1} is associated with the aromatic carbon skeleton of the binder. In regard to the polymer, the polybutadiene peak is obscured by the signal from silicate component of the aggregate (990 cm^{-1}); however, the SBS presence can still be verified by a weak yet distinctive peak at about 695 cm^{-1}.

Figure Q.22 compares the ATR spectra of two polymer-modified asphalt emulsions tested in the laboratory and in the field by two separate Bruker ALPHA ATR spectrometers. Note that practically no difference in chemical composition of the two samples is indicated. However, the higher water content in CRS-1P relative to CRS-2 can be deduced by the significantly lower intensity of the absorption bands associated with the aliphatic binder. Nevertheless, the presence of polymer is clearly indicated by the SBS-related peaks at 966 and 695 cm^{-1}.

Antistripping Agents—ATR

Objectives:	Fingerprinting and verification of antistripping presence in asphalt binder
Team operators:	Iliya Yut
Field operator:	NA

Figure Q.20. Sampling emulsion (top left), Novachip application (top right), ATR testing setup (bottom left), and sample placement (bottom right).

Equipment:	Bruker ALPHA ATR
Test date:	September 9, 2011
Location:	New Haven Gateway Terminal, Connecticut
Contractor:	All States Asphalt Group
Project type:	NA
Material collected:	AD-here Regular
Sample type:	Liquid
Ambient temperature:	25°C

To identify the type of antistripping agent, a trip to the storage facility was undertaken and a sample of the AD-here chemical was collected and tested using the ATR spectrometer under in situ conditions. The obtained absorbance spectrum was compared with that of a previously collected sample of AD-here LOF 65 antistripping agent, as shown in Figure Q.23. It is easily observed that the field sample yields stronger absorption bands at 2,925, 2,854, and 1,459 cm^{-1} and significantly lower absorption at wave numbers associated with

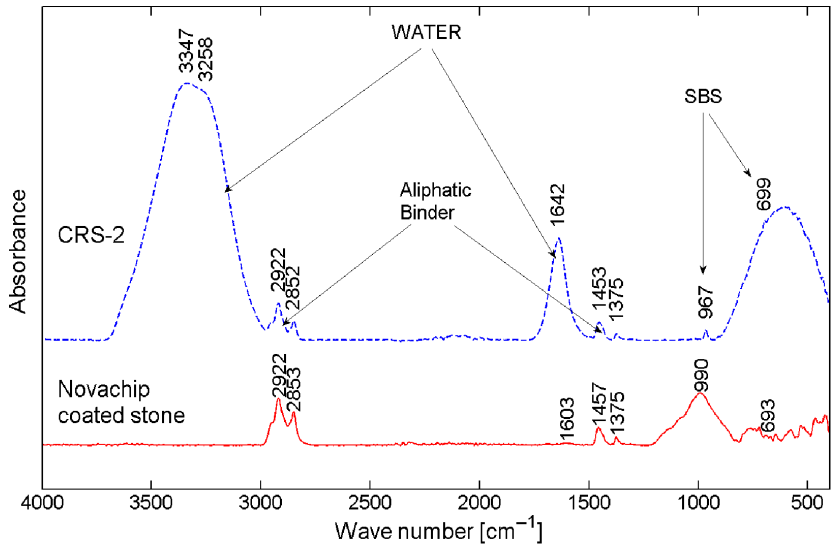

Figure Q.21. ATR spectra of pure emulsion from tank (CRS-2) and Novachip coated aggregate.

amido- (1,650 to 1,550 cm^{-1}) and amino- (2,813, 1,130, and 1,070 cm^{-1}) functional groups. Such a result suggests that the field sample may be contaminated with asphalt binder or, alternatively, diluted by an aliphatic solvent to reduce the viscosity of the antistripping agent.

An additional objective of this study was to identify the presence of an antistripping agent in an asphalt binder. Because no similar field projects were available at the time, a modified binder was produced by mixing nonmodified PG 64-22 binder with the AD-here chemical obtained from a storage facility. Because of the low concentration of the antistripping agent and very similar chemical structures of AD-here and PG 64-22 binder, it was not possible to positively identify the presence of the additives in the ATR-tested sample.

RTA's Raman Results

Samples previously identified as having sufficient Raman scattering were chosen to test the applicability of Raman analyses in the highway construction field environment. Six samples from the previous set were chosen from the Phase 1

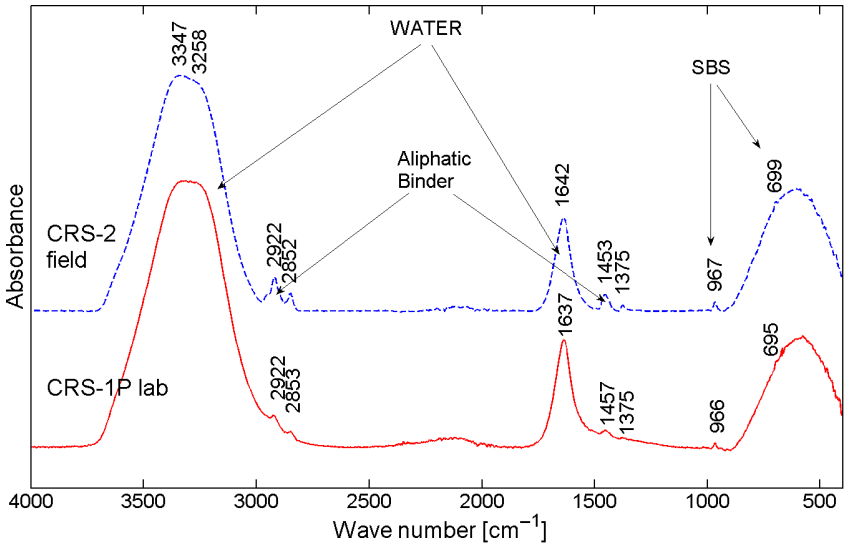

Figure Q.22. ATR spectra of polymer-modified emulsions.

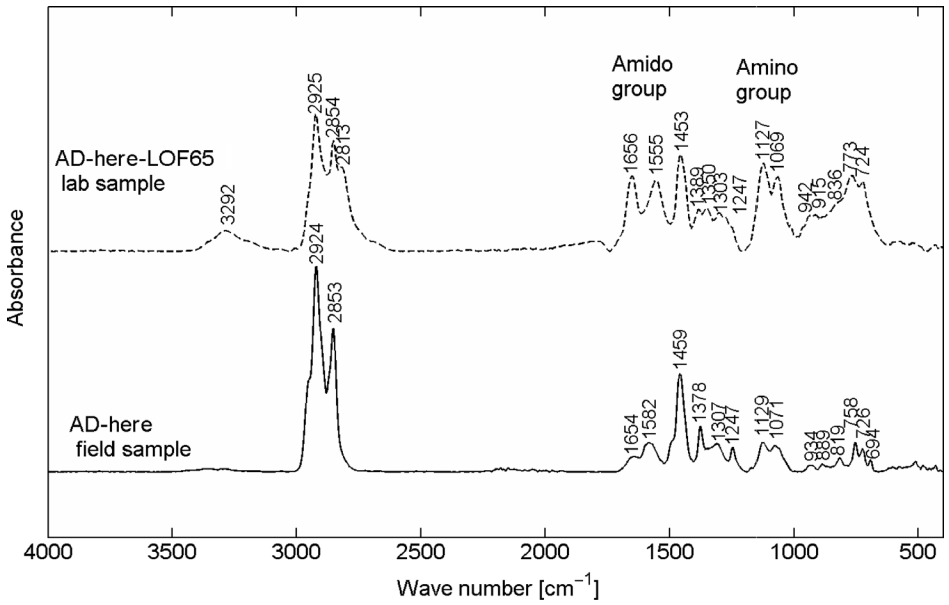

Figure Q.23. Comparison of the two AD-here antistripping samples with different chemical compositions.

library, namely, the existing white and yellow line pavement markings, TAMMSCURE curing compound, and the following PCC chemical admixtures: Accelguard 80 (A-80), air-entrainer Air 200, and Retarder R75. Additionally, field-specific conditions were measured to allow for corrections to the spectra. The detector used has a range of 1,064 to 1,700 nm to track Raman shifts from the excitation at 1,064 nm. This region also corresponds to natural ambient near-infrared light and, as such, additional measurements aid in the removal of stray light contributions. To simplify measurement collection, a continuous mode was used and sample collection times were logged accordingly and later matched up with the appropriate sample.

Given the potential interference of ambient light, spectral analysis consisted of first evaluating those contributions and determining the appropriate background removal techniques to yield spectra consistent with those of controlled laboratory conditions. Figure Q.24 shows the Raman spectra of a sample

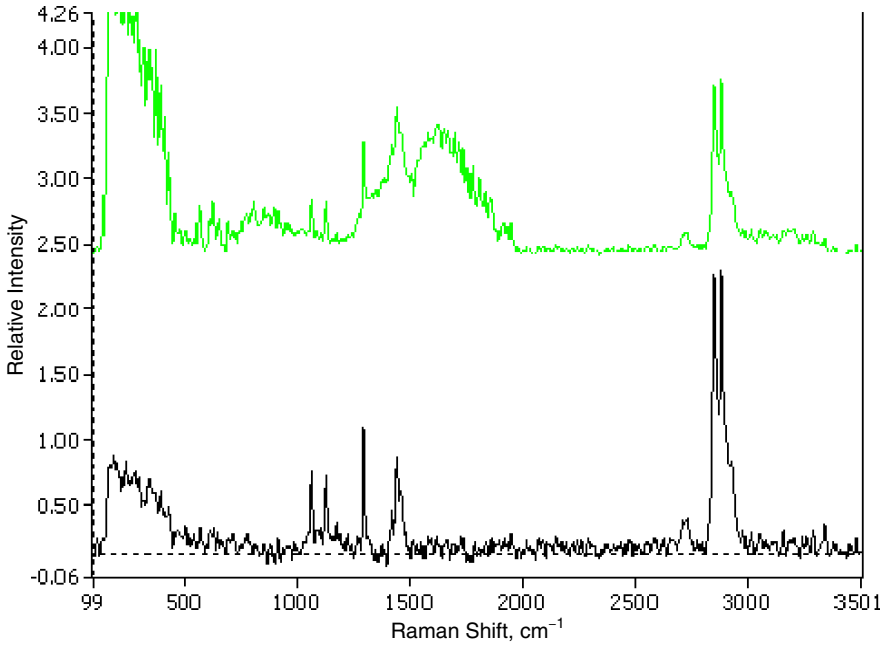

Figure Q.24. RTA's portable Raman analyzer.

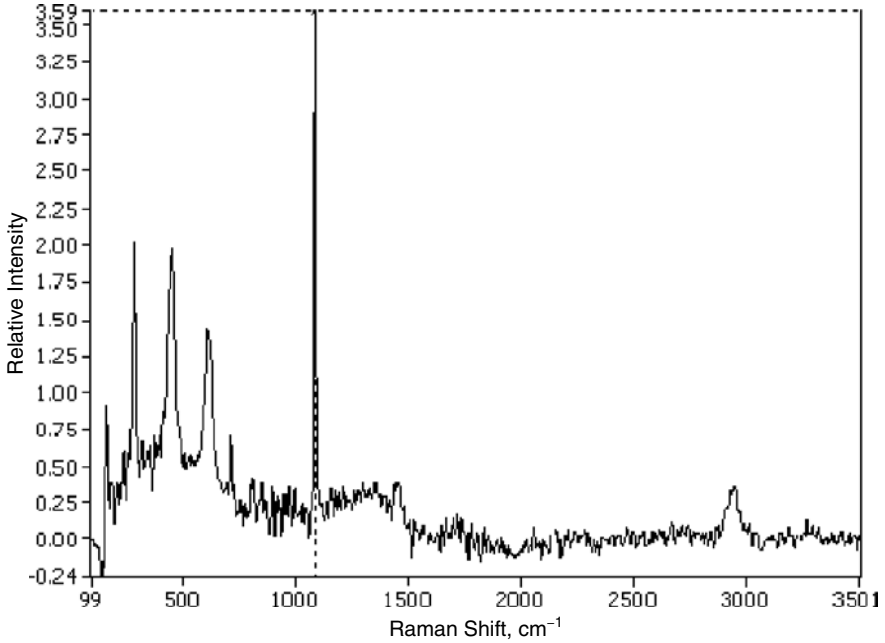

Figure Q.25. White paint measured on glass corrected to remove fluorescence and ambient light contributions.

of TAMMSCURE before (top) and after (bottom) removal of the contributions from ambient light. TAMMSCURE Raman spectrum recorded in the field (top green trace) shows contributions from ambient light (broad band from 1,400 to 2,000 cm^{-1}). The bottom trace shows the corrected spectrum calculated using RTA's Raman Vista advanced calculator and subtraction of background. Other spectra are shown with corrections only (see Figures Q.25 through Q.30), with spectra calculated on the basis of selections from the continuous scanning, and subsequently averaged before doing a baseline, fluorescence, or ambient light removal if necessary. Table Q.7 summarizes the results of Raman testing in terms of successful identification of maximum characteristic peaks and signal-to-noise ratios for the materials in discussion.

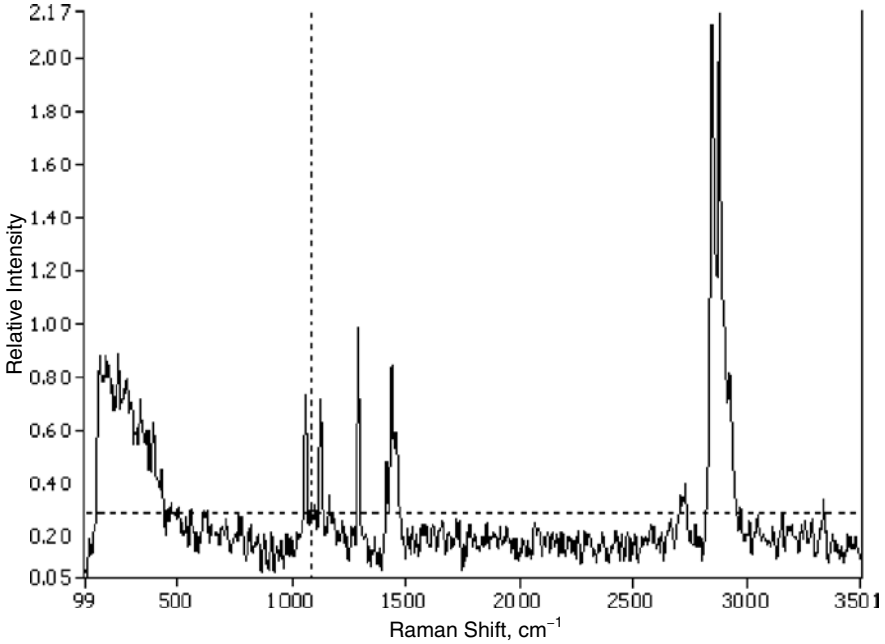

Figure Q.26. Yellow paint measured on glass corrected to remove fluorescence and ambient light contributions.

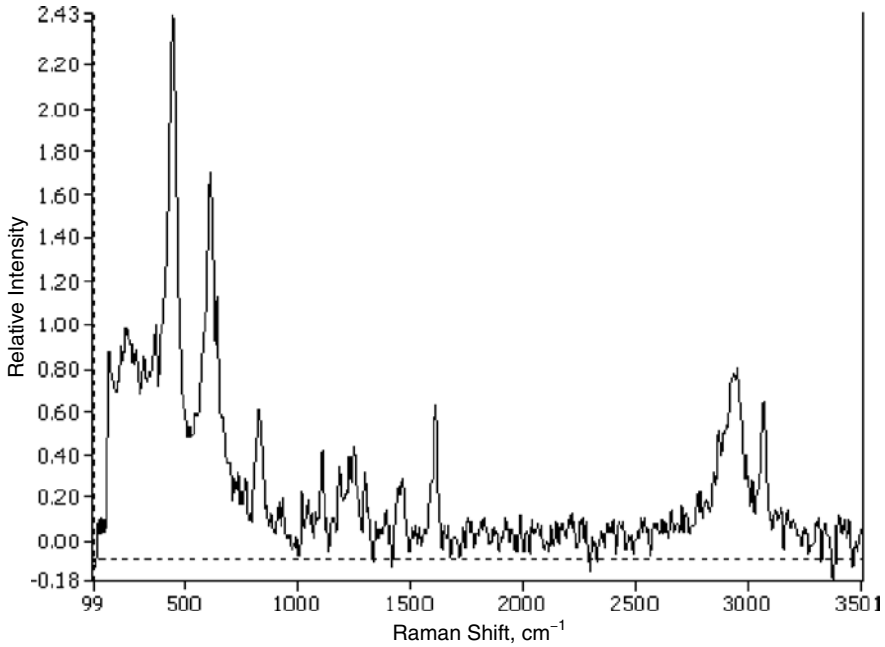

Figure Q.27. White paint (old) corrected to remove fluorescence and ambient light contributions.

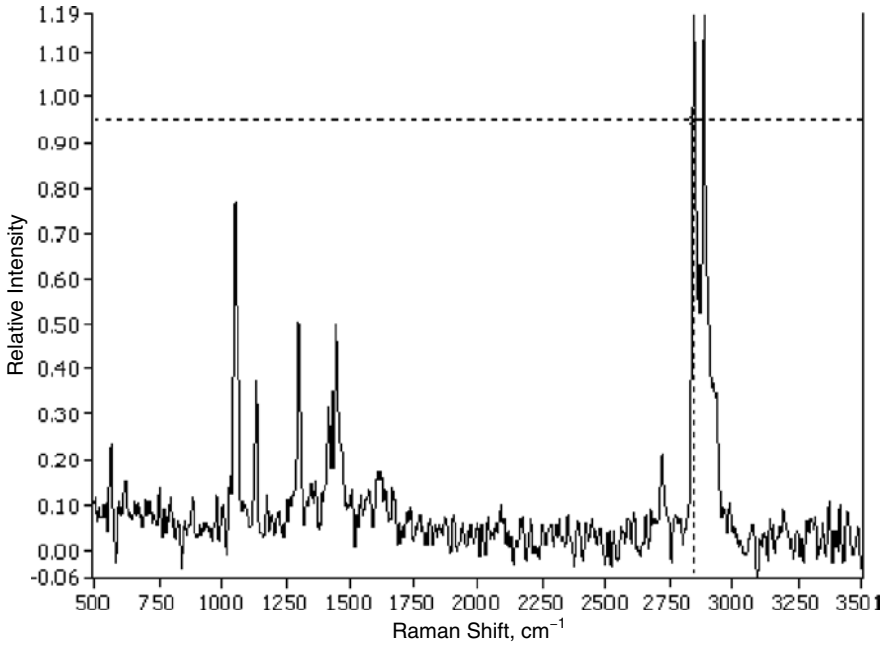

Figure Q.28. A-80 spectrum averaged for three collections (12 equivalent scans, no background subtraction necessary).

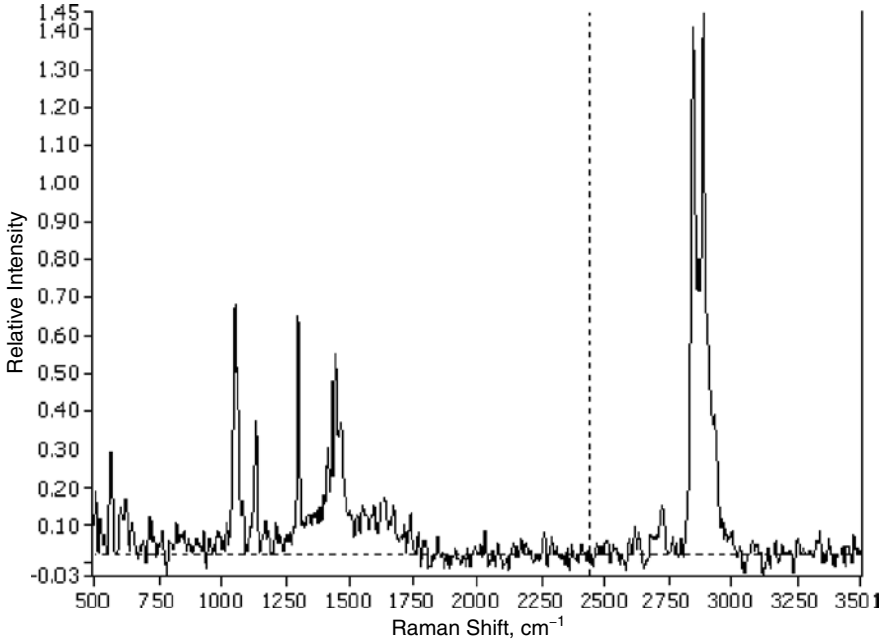

Figure Q.29. Air 200 spectrum averaged for 20 scans (five spectra measured at four scans, no background subtraction necessary).

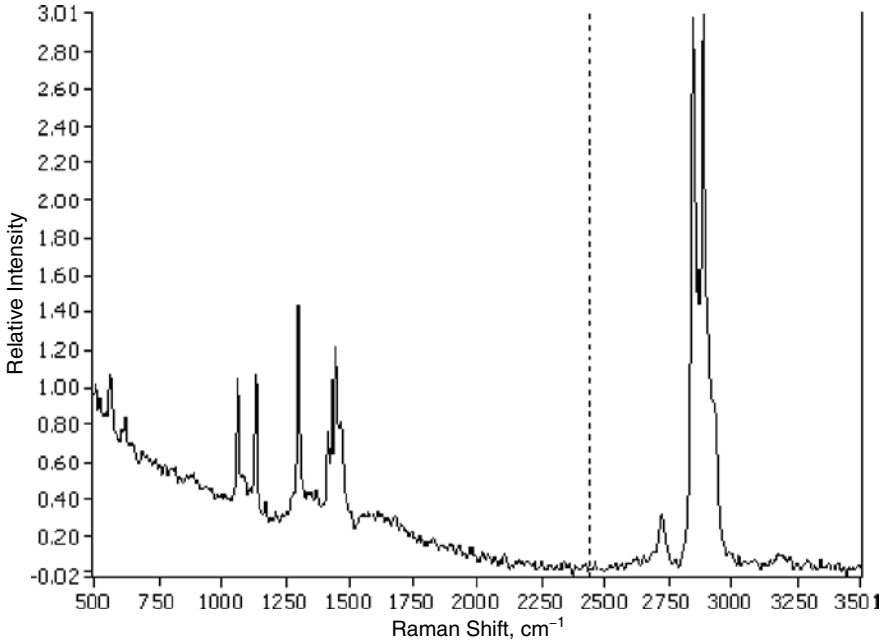

Figure Q.30. R75 spectrum averaged for 40 scans (10 spectra measured at four scans, no background subtraction necessary).

Table Q.7. Raman Spectral Results and Signal-to-Noise Ratio Calculations

Material Category	Sample ID	Success (Yes/No)	Relative Signal Intensity	Wave number Peak (cm^{-1})	Noise (SD)	Signal-to-Noise Ratio
Field-tested material	White paint	Yes	4.00	1086	0.0435	85
	Yellow paint	Yes	1.00	1295	0.036	27
	TAMMSCURE	Yes	1.19	1,110	0.0116	8
	A-80	Yes	1.29	2,843	0.040	0.71
	Air 200	Yes	na	na	na	na
	Retarder R75	Yes	na	na	na	na
	White paint strip (old)	Yes	2.43	443.4	0.058	46

Note: na = not applicable.

Preliminary Conclusions

On the basis of the results presented, it can be concluded that, predominantly, the experiments conducted in the field (Phase 3) verified the methodology and reproduced the results similar to those in the laboratory phase. Specifically, the compact ATR spectrometer, handheld XRF instrument, and RTA's Raman analyzer were successful in the identification of chemical structure, or fingerprinting, of both simple and complex organic compounds such as epoxy coatings and adhesives, curing compounds, and waterborne traffic paints. Furthermore, such complex composite material as PCC yielded meaningful ATR absorbance spectra, which allowed for the identification of chemical admixtures in fresh mix samples, provided their concentrations were higher than 0.5 wt %.

Verification of polymer presence in asphalt binders and emulsions was possible using the ATR spectrometer. Although identification of polymer in an HMA mix presented a challenge, the fast binder extraction procedure in the field using DCM solvent appeared to be a feasible alternative to direct evaluation of polymer-modified HMA.

Related SHRP 2 Research

Nondestructive Testing to Identify Concrete Bridge Deck Deterioration (R06A)

Using Infrared and High-Speed Ground-Penetrating Radar for Uniformity Measurements on New HMA Layers (R06C)

Nondestructive Testing to Identify Delaminations Between HMA Layers (R06D)

Real-Time Smoothness Measurements on Portland Cement Concrete Pavements During Construction (R06E)

Assessment of Continuous Pavement Deflection Measuring Technologies (R06F)

Mapping Voids, Debonding, Delaminations, Moisture, and Other Defects Behind or Within Tunnel Linings (R06G)

Bridges for Service Life Beyond 100 Years: Innovative Systems, Subsystems, and Components (R19A)